Björn E. W. Nordenström

Biologically Closed Electric Circuits

CLINICAL, EXPERIMENTAL AND THEORETICAL EVIDENCE FOR AN ADDITIONAL CIRCULATORY SYSTEM

Nordic Medical Publications

Biologically Closed Electric Circuits

Biologically Closed Electric Circuits

CLINICAL, EXPERIMENTAL AND THEORETICAL EVIDENCE FOR AN ADDITIONAL CIRCULATORY SYSTEM

by

Björn E. W. Nordenström, M.D.
Professor of Diagnostic Radiology
Karolinska Institutet, Stockholm, Sweden

Nordic Medical Publications

This book may be obtained from
Nordic Medical Publications
Grev Turegatan 2, S-114 35 Stockholm, Sweden

Graphic Design by Jerk-Olof Werkmäster
Printed in Sweden by Almqvist & Wiksell, Uppsala 1983

ISBN 91-970432-0-6

FOREWORDS

To contribute a preface to this work of Björn Nordenström is an honour for a French-speaking colleague, but above all it is a great responsibility with respect to the international scientific community, because the opinions expressed in this preface have the potential of influencing the speed of diffusion, study, and acceptance of the extraordinarily original and fruitful ideas of this work. "Biologically Closed Electric Circuits" marks no less than a major point in the evolution of our understanding of biologic science.

Nordenström's theory offers important implications throughout the entire range of normal and pathologic physiology. With profound conviction, I dare assert that no vital process can be fully understood without considering this new electrophysiologic theory. A vast field of multidisciplinary research is opening before us. Numerous concepts which today are confused, including even chemotaxis, are here clarified.

Consider a collection of tissues, organs, interstitial fluid, blood vessels, lymphatic channels and excretory canals. Such tissues, e.g., vessels, were found to function as insulated electric "cables". Their contents of blood plasma conduct current effectively inside the relatively insulating vessel walls to join the conducting interstitial tissue fluid over the blood capillaries. Differences of electric potential (no matter whether created normally, pathologically or artificially) will create electric fields throughout the body. Current will flow preferentially in conducting pathways, inducing ionic and electroosmotic transports over both short and long distances. These transports will produce diverse biologic effects.

This idea, so simple and logical, is supported by numerous experiments in this work. As the course of experimentation progressed, Björn Nordenström found himself led beyond the concept of the biologically closed electric circuit to predict the existence in organisms of an electrical circulatory system—a system not only as complex as the circulation of the blood but also one which intervenes in all physiologic activities.

To the reader of this book I offer specific advice: begin by reading not only the summary Chapter I but also on pages 327–328 the 27 lines of Section G ("Physiological capacity of BCEC systems"), which will immediately stimulate one's interest in this new theory and incite a wish to deepen one's knowledge of it.

This work is very clear. I feel little need for lengthy considerations of its scientific merit, but I cannot resist emphasizing the fascinating and broad medical scope of this book, i.e., a new view on carcinogenesis and a therapeutic mode against cancer which theoretically offers possibilities against diverse inflammatory states, fractures, atheromas and neurologic complications of various diseases (e.g., hepatic coma). Moreover, this book offers new scientific bases which will reorient future research on a wide range of hitherto poorly understood processes, e.g, acupuncture, oral galvanism, meteorologic influences on human beings, types of adipose tissue, diverse secretory mechanisms, diurnal cycles and embryogenesis. This list of disparate functions leaves unmentioned many other applications. In particular, extrapolation of the theory at the intracellular level offers many possible consequences.

The coming years will see a wealth of experimentation derive from this new approach to electrophysiology. Its full importance is today impossible to appreciate. For example, disparities of findings noted heretofore between in vitro and in vivo work can now be assessed anew. The implications of Nordenström's theory appear far-reaching even beyond today's most enlightened suspicions.

Jacques C. Hauton, D.M. D.Sc.
Professor of Biochemistry
Institut National de la Santé
et de la Recherche Médicale
Université d'Aix-Marseille II, France
(translation from French,
John H. M. Austin, M.D.)

Biopotentials have fascinated me for many years, and when I found that small positive potentials existed on skin carcinomas relative to normal tissue I searched for an explanation, feeling that it was of fundamental importance.

It was my search for more information that led me to Björn Nordenström. The vast amount of material he had collected in searching for an explanation of the corona structures around a variety of pulmonary neoplasms and inflammatory lesions, surprised me.

This book is an account of his research and, as so often happens, it touches on fields beyond the original observations. The potentials, although small, which he measured in many tumours seemed to be a major factor in water transport, cell movement, etc. Reproducing these electrical conditions in vitro as well as in vivo produced histological evidence of cellular transformations, migration of cells and ions and transport of tissue water, indicating that electrical forces must be of fundamental importance to maintain, e.g., homeostasis.

The way in which the morphology of breast adipose tissue changes under the influence of small D.C. currents and, in particular, how the histology is so different according to the position of the tissue in the potential gradient, is convincing evidence of cellular changes brought about by electricity.

The extracellular fluid and its regulation we know is fundamental to controlling cell division. Ionic differences lead to potential differences in the body between cells and between one organ and another. Currents of the order of microamperes flow across the edge of wounds, and limb regeneration, even finger tip regeneration in children, has been reported to be connected to these currents.

The new concept of energy conversion in tissue over biologically closed electric circuits (BCEC) described in this book offers a unified theory even for such diverse phenomena as acupuncture and the effect of electromagnetic fields on man and increases our understanding of the mechanism of tumour growth.

The test of a good theory is if it indicates further experiments. The treatment of lung tumours by direct current was such an experiment which has produced positive results in those patients treated so far. This encouraging application alone justifies the concept of BCEC and should encourage us to seek further applications of this theory.

I once heard a Professor say that writing a book was like giving birth to a baby. This book took my friend many hours of toil, not only in its conception but in meticulous measurement and experimentation. The time, in my opinion, is ripe for a new look at the importance of electricity in biology and therefore I am sure that this is a book not "born prematurely".

Bernard W. Watson, Ph.D.
Professor of Medical Electronics
St. Bartholomew's Hospital
London, England

Progress in Natural Science, including Medicine, depends on the interaction between ideas and techniques. In this book both aspects are amply represented. I may venture that the superb X-ray technique of Nordenström revealed to him new structures around tumours in the lung and the breast which he calls the corona structures. In the search for their origin he made use of various techniques, which led to, e.g., a mapping of the electric potential distribution across tumours and normal tissues in vivo and in tissue models. This started a new train of ideas.

All the evidence pointed to the existence of local electric current flow on a *macroscopic* scale in living tissue. His overall conclusion is that the blood vessels, not excluding even the large ones, are current carrying cables which, in combination with other conducting tissue media as, e.g., interstitial tissue fluid, allow closed electric circuits to operate over *large* distances (Nordenström's nomenclature: BCEC, Biologically Closed Electric Circuits). One specific circuit particularly considered in this book is called VICC (Vascular-Interstitial Closed Circuit). The activation of such a circuit must lead to various physiological effects and possibly structural modifications.

Nordenström's new views may appear startling to most physiologists, who are familiar with the old ideas of local nerve circuits, injury potentials, electrotonus, etc, which appear in the traditional textbooks. An important distinction, however, is the question of dimensions and location. While the nerve events take place in domains with the magnitude of millimetres, Nordenström's BCEC represent electrogenic systems for long range selective transports of material and distant functional effects in the entire body beyond centimetric even to the metric range, i.e., between organs.

I will now comment particularly on two physiologic aspects related to Nordenström's concept of BCEC:

1. The electric current as a driving force for water movement, i.e., electroosmosis,
2. The energetics of the current flow.

For more than a century electric potentials and currents have been discussed as driving forces for *ions* in the body fluids, mostly relating to nerve and muscles. The fact that theoretically, electrical forces are involved in the transport of the universal solvent, water, has by and large been neglected. The enormous

literature on "fluid balance" and "oedema formation" is based mainly on purely colloid-osmotic concepts. This is paradoxical, because the fixed charges, located in the ionic structure of protein-lipid membranes of the body, ought to mediate a force moving the mobile solvent water, providing an electric potential field is present. This is certainly the case in most living membranes and is also shown by Nordenström in his profile mapping mentioned above. The complex nature of electroosmosis may be unfamiliar to medico-physiologists, but is explained in many of the informative illustrations in his book.

However, in spite of the theoretical probability of the importance of electroosmosis, the evidence for its significance in biological material has been scanty and inconclusive. The reason may be that the systems studied have been on the *microscopic* or cellular levels. The detection of small degrees of swelling and shrinkage indicating water-transfer is very difficult. Only recently, I. Tasaki and K. Iwasa reported, for the first time, such events during action potentials on isolated, unmyelinated nerve fibres, using a sophisticated mechano-optical device (Upsala J Med Sci *85*, 211–215, 1980).

At this "to be or not to be" stage of in vivo electroosmosis, Nordenström's new views on *macroscopic* systems may change the scenario radically. Nordenström deals with the loose, spongy lung (and breast) tissue, where the mechanical restriction to swelling–shrinkage is minimized as compared with more compact cellular assemblies. Here the BCEC systems have ample space to operate. An additional advantage is that the direct observation by X-ray or histological or local biochemical analysis (of water–fat ratios, etc) could be utilized.

The final results of numerous experiments, some with ingenious model systems, lead the author to the conclusion that *long* distance control of water shifts operates; this is identified tentatively as electroosmosis and/or electrophoretic effects. Most interesting with respect to electrophoresis are some illustrations of the massive accumulation of different blood cell elements in certain vascular areas, exposed to external current flow. These experiments must reactivate discussions on the process of leukopedesis. These citations may serve as examples of the many effects which are logical consequences of an acceptance of the principle of BCEC.

As implied above, the energetics of the electric current production is involved. Nordenström clearly realizes that this is a "big" problem. He distinguishes the energetic behaviour of, what he calls, ionars (collections of ions) from ergonars (collections of ergons, i.e., nonionic energetic components) in the release of electromotive forces and the modulations of conductivity of BCEC systems. Thus he approaches the riddles of biological current formation, i.e., the "fuel cells". This is indeed a crucial problem in electrobiology. The great variety of terms in the contemporary literature such as salt batteries, active transport, ion-pumps, metabolic potentials, channels, gates, etc bear witness to the fact that the links between metabolism and electric currents are only vaguely understood, at least at the present. It is therefore evident that many of the electrochemical steps in the generation of electromotive forces to drive BCEC systems have to be considered in the future. Nevertheless, the primary energetic prerequisite for transport of currents over BCEC channels, i.e., metabolic potential differences, are since long well established facts.

At this point I conclude my review of Professor Nordenström's great interdisciplinary work by turning back to its origin, the observations of new structures in pathological conditions and the following advances: electrochemical treatment of tumours, the thorough analysis of the mechanism of water transport, and many other consequences of biologically closed electric circuits, all fine achievements. The overriding implication is the realization that electric current can act on tissue structure formation and by virtue of that participate in regulation of cell function and tissue transformation. This has an impact for the future and is also a bridge between clinical and theoretical sciences.

Torsten Teorell, M.D.
Emeritus Professor of Physiology
University of Uppsala, Sweden

Many important discoveries have been made through further investigations of seemingly trivial features that may well have been generally observed, but neglected. Pulmonary radiography has undoubtedly been one of the most widely performed radiographic examinations over the years. When Björn Nordenström's curiosity led him to look into the mechanism behind the corona that can be radiographically demonstrated around pulmonary lesions, he encountered a hitherto unknown biological system.

The further evidence the author presents in favour of his concept of Biologically Closed Electric Circuits

(BCEC) is remarkable, and takes the reader on a fascinating and thrilling journey through the tissues of the human body in health and disease during which generally accepted ideas of pathogenetic mechanisms are challenged. Thus, fundamental tissue reactions such as fibrosis and scarring, thrombosis, pathological vascularization, leukocyte accumulation, etc are given alternative explanations to those generally accepted. Hitherto obscure and vividly debated reactions such as oral galvanism and the effects of acupuncture are explained.

The concept of BCEC is based not merely on sound speculations but is supported by careful and unconventional experiments. The author's long experience of close cooperation with pathological anatomists has made it easy for him to relate the concept of BCEC to structural tissue alterations. The book can, in fact, be regarded as *an alternative introduction into the field of pathological anatomy*.

A hallmark of a good book is a feeling of losing a good friend and stimulating company when you close it after having read its last page. This was my feeling when my reading of this book was over. I do not feel too sorry, however, because I will repeatedly go back to this new friend of mine to benefit from its rich source of stimulating ideas for further research.

Arne Ljungqvist, M.D.
Professor of Pathology
Karolinska Institutet
Stockholm, Sweden

ACKNOWLEDGEMENTS

I wish to acknowledge the considerable and valuable contributions which have been made by my co-workers, my research assistant Mr Jerker Olsson, and my secretary Miss Kerstin Ersson. Mr Olsson's technical skill, knowledge and endurance have been valuable assets throughout the project. Miss Ersson's organizing ability, patience, language proficiency, and capability to decipher the author's usually illegible manuscript have been important elements in the process of completion of the book.

Dr John Austin, M.D., Associate Professor of Clinical Radiology, Columbia-Presbyterian Medical Center, New York City, USA has revised the English grammar of the author's original manuscript. Dr Austin has spent a considerable time with the text and has gone through a great deal of trouble to correct the grammatical form without altering the intended meaning of the contents. His contribution has been invaluable. Dr Austin has also contributed with a glossary as a guide to possible readers without medical background.

A special thanks is directed to Mr Jaak Berendson of the Department of Applied Electrochemistry and Corrosion Science at the Royal Institute of Technology, Stockholm, for good advice and many stimulating discussions.

Valuable assistance has also been given by Mr Bo Tedner, Mr Hans Larsson and Mr Jan Bergholm of the Department of Medical Engineering, Karolinska Institute, Stockholm, Mrs Isa Schwartzkopf, Mrs Lilly Winberg and Mr Veijo Methonen of the Department of Photography, and the staff at the Department of Diagnostic Radiology, Karolinska Hospital, Stockholm.

Part of the work concerning the electrical activity of the liver was carried out during a 2 month period in 1971 at the Strong Memorial Hospital, Rochester, New York, USA. This was made possible by Professor Harry Fischer, Head of the Department of Radiology.

Without economic assistance this work could not have been completed. The author is deeply grateful for the generous support given by:

Mr Sten Persson, Initium AB, Stockholm
National Swedish Board for Technical Development, Stockholm
Tekniska Röntgencentralen AB, Stockholm
King Gustaf V's Jubilee Fund, Stockholm
Captain Arthur Eriksson's Fund for Medical Research, Stockholm
Torsten and Ragnar Söderberg's Fund, Stockholm
AB Astra, Södertälje

Finally, I like to thank the members of the staff of Almqvist & Wiksell Tryckeri AB, Uppsala, Mr Gösta Nyström, Mr Jerk-Olof Werkmäster and Mr Alf Hedlund for their personal interest and help in the production of this book.

Stockholm 1983

B. N.

CONTENTS

I. Summary

This book leads stepwise to the identification of a basic biologic concept: *energy conversion in tissue over biologically closed electric circuits* (*BCEC*). Originally, this line of research developed from the observation that some seemingly strange structures are radiographically sometimes apparent in vivo around masses in the periphery of the lungs. Because of an appearance similar to the corona of the sun, these morphologic alterations were called *the corona structures*. It will be suggested that these structures represent modifications of tissue over a BCEC system, shortly to be explained, activated by a nonspecific injury of tissue.

Injury to tissue represents a source of release of energy, which induces closed circuit transports over BCEC channels, leading in turn to structural modifications in tissue. These modifications are of considerable interest because they represent *a result of the process of healing*. Consequently, knowledge of BCEC mechanisms may increase our understanding of how tissues heal. Indeed, it will be shown that artificial activation of BCEC mechanisms can even lead to beneficial effects in disease. Therefore, the theoretical and practical importance of BCEC as a basic biologic concept has made it necessary to devote most of this book to the identification of such circuits, including their activation and their function.

BCEC systems are possible because tissues differ in conductance and structure. Several kinds of BCEC can therefore be distinguished. The circuit particularly identified and studied in this investigation is the *vascular-interstitial closed circuit* (*VICC*).

BCEC systems are activated not only by the release of energy in tissue injury but also by physiologic polarization of tissues. This finding opens many possibilities for new understanding of normal and abnormal function and structural development of tissue.

This summary will concentrate on principles which, in the opinion of the author, are capable of bringing some new light on a number of biologic problems which presently are poorly understood. The original observations which led to the description of the corona structures will therefore be treated here only briefly, because associated problems reflect only one specific instance of the general principle. On the other hand, the corona structures represent a set of specific facts from which the general principle of BCEC systems has been inferred. Anyone interested in a full insight into the principle of BCEC systems is advised, therefore, to review the chapters in which the corona structures are described and analysed.

Physicochemical potentials are central to the biokinetic mechanism to be described. The importance of a so-

called injury potential has long been known, for example, as a source of error in bioelectric measurements. Its possible role in "clinical" injury of tissue has been neglected to a remarkably large extent. Current research tends to concentrate on "local" biochemical reactions in different kinds of injury to tissue.

After the development in the 1960's of techniques for percutaneous needle biopsy of pulmonary masses, attempts were made to supplement the biopsies with recordings of *electric potentials in tissue*. Two types of electrodes were used. In one series of patients, mixed redox-diffusion potentials of pulmonary masses were measured by means of metal electrodes. In another series, diffusion potentials were measured over nonpolarizable electrodes. In both types of measurements it was found that focal pulmonary lesions, mostly malignant tumours and granulomas, *sometimes* show an electric potential in relation to surrounding tissue. It soon became apparent that mixed potentials of lesions may develop under certain circumstances. These potentials are, when present, reproducible for each individual lesion. They are inconsistent among lesions in terms of polarity, even when lesions which are histologically similar are compared. This unexpected finding was interpreted as follows.

Locally injured tissue can be regarded as a site which liberates catabolic energy. This energy gives rise to a physicochemical potential difference in relation to surrounding noninjured tissue. Such potential differences are, in all probability, the results of local injury in tumours, for example caused by spontaneous necrosis, haemorrhage or infection. By means of such local processes of degradation, different regions of tissue polarize in relation to each other. Polarizing regions of tissue therefore tend spontaneously to equalize their physicochemical gradients. It is also a well known physical fact that any spontaneous reaction induces opposing reactions. The total process then attenuates in a fluctuating fashion as entropy of the system increases. A series of in vitro experiments was performed, showing how this tendency of increasing entropy can be modified. Varying the influence of movable or fixed matrices was found to affect both the speeds of reactions and their "final" structural appearances.

The gradients of potential observed in vivo in pulmonary masses therefore appear to reflect instantaneous stages of fluctuating and attenuating differences of potential. Any attempts, therefore, to determine the "absolute" magnitude of the potential gradient, without knowledge of at least the age of the degrading process become of no or little value. Next, in vitro experiments were performed on spontaneously degrading blood during hypoxia, to simulate at least some of the conditions common to degradation in vivo of necrotizing tissue. In these experiments, diffusion potentials measured with Ag–AgCl electrodes were observed to fluctuate by 250 mV while pH varied between 6.5 and 7.5, which is ≈60 mV.

Determinations of tissue potentials in vivo of this kind are of rather limited value for even further reasons. Potentials of normal tissue, used as reference to a degrading tissue, can be anticipated to vary in different tissues as a function of their varying metabolic phases. Assuming the existence of a closed circuit system, the electric resistance of the circuit will determine both the rate of losses of potential (from a defined potential difference) and the rate of generation of the potential difference. Blood plasma and interstitial fluid are the anticipated conducting media of vascular-interstitial closed circuit (VICC) channels. The resistivity of each of these media is about 0.7 ohm-m. The numerous interstitial and vascular channels between a degrading tissue and its surroundings should then, in all probability, allow substantial leak of current through tissue. Moreover, the magnitude of potential difference indicates nothing about the important factor, the quantity of current transported.

Besides diffusion potentials, redox potentials must also be considered in the activation of BCEC systems. We will shortly return to these potentials, to which a separate chapter is devoted. For the time being, we may conclude that electric potential differences can be measured between degrading tissue of a tumour, infectious lesion or granuloma in relation to the surrounding and presumably normal tissue, both by means of polarizable metal electrodes and nonpolarizable Ag–AgCl electrodes. The "profiles of tissue potential" obtained are reproducible in each lesion, but show varying polarity among different lesions. This result has been interpreted as an effect of the age of the necrotizing process in an injured tissue, which can be expected to present a fluctuating potential difference.

It should be apparent that in a biologically closed electric circuit, such as a VICC, even small electrical gradients working over a long time may give rise to substantial transport of ions. BCEC must also be considered to function between normal regions of tissue or even between different organs under the influence of regional differences in metabolic activities. For example, normal dog liver showed, relative to peritoneal fluid, that slowly fluctuating potentials can be induced by epinephrine, isoprenaline, glucagon and Vamin® (an amino acid and electrolyte preparation for parenteral nutrition).

The release of energy of degrading tissue appears to be coupled to systems of selective ionic transport through BCEC channels. The energy transformation of healing represents in this view a continually changing, fluctuating and attenuating process of electric transport amongst tissues. Ebbs and flows of ionic transport are induced, securing an appropriately time-

dependent supply of anions and cations for the healing process. Healing is achieved when the injured tissue has equilibrated with its surroundings. This equilibrium means that both the injured tissue and the surrounding tissues have changed. The driving force in these events is therefore not confined exclusively to the injured tissue but also involves the physiologically fluctuating metabolic potentials of the surrounding normal tissue. The integrated function of physicochemical forces over BCEC is, in the author's opinion, important not only for understanding tissue healing but also for understanding normal functions of tissue and morphogenesis.

The morphologic basis for closed circuit transports includes selective pathways for flow of current in tissue. This property should be evident because different tissues and tissue fluids possess different resistivities. Differences in conductive properties are known for fat, bone, muscle, tissue fluid, blood, kidney, liver, lung and brain tissue. The possibility that certain materials and structures may function as electrically conducting branches of closed circuit systems in tissue does, however, not appear to have been previously considered. As an introduction to the identification of vascular-interstitial closed circuits (VICC) as one example of BCEC, the process of corrosion of metal in vivo was studied.

Two types of corrosion in vivo have been defined. *Uncomplicated corrosion* is the type of corrosion which occurs when a piece of iron is placed in salt water. The driving force derives from the relatively anodic and cathodic parts of the metal. Metal dissolves at the anode depending on closed circuit transport of ions in the water, redox reactions at the anode and cathode, and transport of electrons in the metal. Such a process now appears to be identifiable radiographically in vivo on the basis of changes in the metal surfaces and adjacent tissues. The second type of corrosion is called *complicated corrosion*. In this case, driving electrochemical potentials are created between an injured tissue (e.g., due to trauma, blood clots, necrosis, infection), adjacent noninjured tissue and the metal. Even this type of corrosion may be radiographically identified. The energy in this type of corrosion is channelized over closed circuits, which in part have to be located in the tissue. Among the tissues which might fulfil the requirements of a separated conductor, blood vessels were the first studied.

Direct measurements of resistivity of vessel walls in vivo on dogs showed that "large" blood vessels (i.e., visible to the unaided eyes) function as relatively insulating and electrically conducting "cables". The walls of vessels present an electric resistivity which is at least 200–300 times higher than the conducting blood plasma and surrounding interstitial fluid, each of which have a resistivity only slightly higher than that of physiologic saline solution. Blood plasma and interstitial fluid, moreover, connect electrically over the capillary membranes.

The vascular-interstitial channels have been tested directly in vivo in animal experiments which show that vessels constitute preferential pathways for electric current, within certain limits. Therefore, in addition to the property of serving as mechanical transport channels, the "*large*" *blood vessels also function as insulated, electrically conducting "cables"*. After vascular-interstitial closed circuits (VICC) are recognized, it will become apparent that other biologically closed electric circuits must also exist. Such circuits may include conducting media such as urine, peritoneal fluid, excretory material in ducts, etc., in various combinations with vascular or interstitial channels in tissues.

Consider a necrotic tumour, electrochemically polarizing in relation to surrounding normal tissue (Fig. I: 1). The vascular-interstitial closed circuit (VICC) consists of vascular and interstitial branches, electrically connecting the tumour and its surroundings.

This circuit is seemingly very simple. A closer look at its different parts will soon disclose its complexity (Chapter XII). Its function includes the requirement of at least two (but very likely numerous) interpositioned redox steps for each closed circuit. Such redox steps are anticipated to function as electrode-equivalent sites for transfer of electrons. There is no doubt that redox reactions take place in biologic material, but their location and the structure of such sites for BCEC systems have yet to be established. Experimental evidence is presented suggesting that the location of one type of such sites is adjacent to fibrous membranes.

Blood, flowing in vessels with electrically insulating walls, contains a conducting part in the plasma and a nonconducting part in the blood cells. The membranes of the erythrocytes add a high resistance and capacitance in series and parallel with the plasma, which is a relatively good conductor. The erythrocytes can be regarded as a movable matrix while the vessel walls function as a structural matrix. An increase of haematocrit or contraction of a vessel will consequently increase intravascular electrical resistance.

The conducting medium, the plasma, obtains its conducting properties by the presence of water, electrolytes and charged, complex molecules. These components are evidently prerequisites for the function of BCEC systems. Another group of compounds can also be recognized with equally important but different properties for the function of BCEC systems. These are the nonionic compounds, which modulate conductivity and are able to "save" their electric energy until conditions are suitable for its release. Some of the most important sources of energy are present in this group, e.g., oxygen and glucose. These considerations lead us

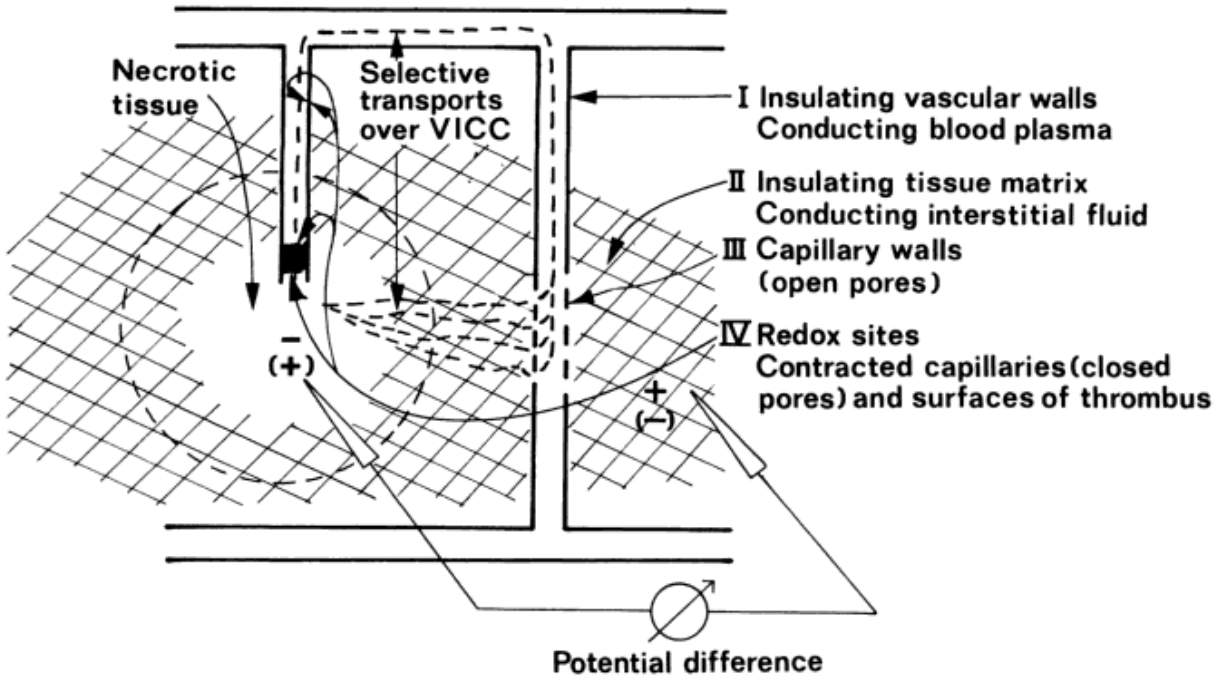

Fig. I: 1. Simplified principle of the vascular-interstitial closed circuit (VICC). Local processes of intratumoural degradation (e.g., necrosis, haemorrhage) create a driving, physicochemical "injury potential" between the tumour and surrounding normal tissue. Suggested sites of redox reactions of the circuit are indicated at the capillary membrane and vascular thrombus.

to the problem of activation and function of BCEC systems.

We may recognize that metabolically produced ions will appear temporarily within BCEC channels, as groups of ions. These groupings are possible as a result of diffusion and mechanical transport (circulation), differences in ionic mobility, gravity, influences of matrix properties, ionic recombinations, etc. A resulting and measurable difference of electrical potential (e.g., an injury potential) will become apparent. Such collections of separated ions giving rise to a net gradient of electric potential, compared with a "reference" tissue within a BCEC, are here tentatively called *ionars*. Two ionars of different ionic charges then represent a driving electromotive force of a BCEC system. The energy of an ionar couple depends, however, not only on its electric gradient. The total energy gradient is a composition of chemical, electric, volume-pressure and gravitational energies. Furthermore, the energy components are interdependent even as each is available for energy exchange. Chemical energy, for example, when exchanged between two reactants must be preceded by transports which take place in different steps. For instance, oxygen and glucose are transported in bulk in the blood stream over long distances before these compounds reach a working muscle. In the muscle, other steps of transport then follow, including selective transports. The vascular-interstitial closed circuit (VICC) serves as such a selective system of transport, although by definition it also is an integrated part of the mechanical system of indiscriminate bulk transport. Its closed circuit function depends consequently on the characteristics of the material transported. At the same time, *the superimposed driving electromotive force causing the closed circuit transports will also influence both "local" and distant chemical reactions* in the circuit. Such distant effects in VICC include elements of structural modification and selective distribution of materials *contributing to the maintenance of homeostasis*. The function of VICC with regard to their content of ionic and nonionic compounds will now be briefly reviewed.

The electric energy of ions and groups of ions (ionars) is immediately available, unlike the electric energy of nonionic compounds, e.g., oxygen and glucose. These energetic compounds are here named *ergons (Greek, ergon = work)*, analogous to ions. Collections of ergons are here called *ergonars*, analogous to ionars. The necessity of introducing these terms is a consequence of the closed circuit functions of BCEC systems.

Ergons are carriers of balanced electric charge, but under certain circumstances become electrically active. After activation they *obtain electronegativity in relation to their surroundings*. In this transformation the ergon is turned into an ion. Conversely, appropriate metabolic change of an ion may result in the creation of an ergon.

The existence and function of ergons appear to be a prerequisite for the existence of highly developed or-

ganisms, which require special systems such as circulation of the blood for transportation of energetic compounds. During transport, ergons "save" their electric energy, unlike ions, which are available instantaneously for electric interactions. Special couplings of oxygen to haemoglobin are known to exist. Oxygen is thereby prevented from starting immediate reactions with surrounding material, e.g., in the blood stream. The blood pigment packs the oxygen in a protective transport cover. This mechanism therefore functions to maintain the ergonic state of oxygen. The transport and storage of oxygen in the skeletal muscles of deep diving mammals is an extreme example of how efficiently this mechanism is utilized to preserve the ergonic character of oxygen.

Ergons as well as ions carry four energetic factors (chemical, electric, volume-pressure, gravitational). The interaction between the chemical and electric components of energetic compounds is treated theoretically and experimentally. Electrolytic experiments have been performed with water (an ergonar) and with water and a supporting electrolyte (KCl, an ionar) in the presence of a stabilizing matrix. These experiments illustrate important principles of interaction of ionars and ergonars in the activation of BCEC systems. The electric energy in ergons is available only after activation by their surrounding media. This principle is demonstrated experimentally in models in which electrolysis of the ergonar water produces proton and hydroxyl ionars as well as matrix-adsorbed hydrogen and oxygen ergonars. Such a driven system can actually then be turned into a self-driving system, in which the metal electrodes become activators for release of the electric energy of the ergonars.

The metal electrodes, providing the in vitro experiments with sites for redox reactions, should logically have their biologic counterparts within BCEC systems. The existence of redox reactions in biology is well established. A morphologic, organized structural analogue to metal electrodes in tissue is, however, still to be found. Several possibilities exist to localize such sites: one was attempted. When direct current was passed between flat platinum electrodes over tissue, *fibrous membranes were easily produced* at the electrode surfaces. In clinical medicine, fibrous tissue is known to develop around cardiac pacemaker devices and their electrode against the myocardium. Such fibrosis may eventually interrupt the current, because fibrous tissue is electrically insulating. One possibility for finding sites for redox steps may therefore be to look for locations of fibrous membranes. Many fibrous membrane structures are easily accessible, e.g., organ capsules, muscle fasciae and cerebrospinal dura, as well as less accessible, e.g., basement membranes, tissue septa and cellular membranes. In vivo experiments in dogs were therefore performed as follows: direct current was passed between one platinum electrode in the inferior vena cava and one in a glass cylinder (filled with 2M KCl in litmus-agar), placed against the exposed spleen or liver. *Depending on the direction of current flow, reversible litmus reactions were produced at the surface of the organ as at the surface of an interpositioned metal*. One possible explanation of these reactions may be that electrode-equivalent redox reactions have taken place at the organ surface. An alternate mechanism may be that metabolic products separated electrophoretically immediately under the liver surface. Whatever the mechanism, the experiments demonstrate that interphasic accumulation of material can be produced by leading direct current across the surface of an organ. Further studies on production of fibrous membranes in vitro by direct current support the theory that *fibrous membranes may be explained as interphase deposition of material* ("*electrode deposition*") *within BCEC systems*. When metabolic polarization of an organ, e.g., the liver, is asynchronous in relation to surrounding organs, ebb and flow transport of anions and cations should take place, leading to the development of fibrous membranes. The membranes can be expected to grow under the influence of the polarization current until the membrane becomes sufficiently thick to interrupt the current.

After this introductory description of the principle of BCEC systems, some specific observations and problems will be reviewed:

Water transport in a closed circuit has been devoted a full chapter. Prerequisites for electroosmosis are analyzed in in vitro and in vivo experiments. Four mechanisms of electric water transport are distinguished. Electroosmotic transport between electrodes has also been demonstrated in vivo in animals and in pulmonary parenchyma in man in connection with direct current treatment of inoperable lung tumours.

Effects on cells and tissues after application of direct current are described throughout this book in in vitro and in vivo studies. Specific reactions at the anodic and cathodic electrode surfaces are described, as well as induced field effects and electrophoretic effects. In in vitro electrophoresis of blood, red blood cells show laking of blood pigment around the anode, while pigment near the cathode accumulates in the centres of the red cells. Observations also suggest that anodic acidity and cathodic alkalinity may influence the polarity of the blood pigment. Thus, repelling and attracting of intracellular blood pigment have been observed. Moreover, haemoglobin may arrange in peculiar patterns in the erythrocytes. Many red blood cells were found actually to fuse into monstrous cell-like units, with strange arrangements of blood pigment.

Massive accumulation of leukocytes has been produced around the anode, when applied to dog mesentery and lung. It is suggested that the local attraction

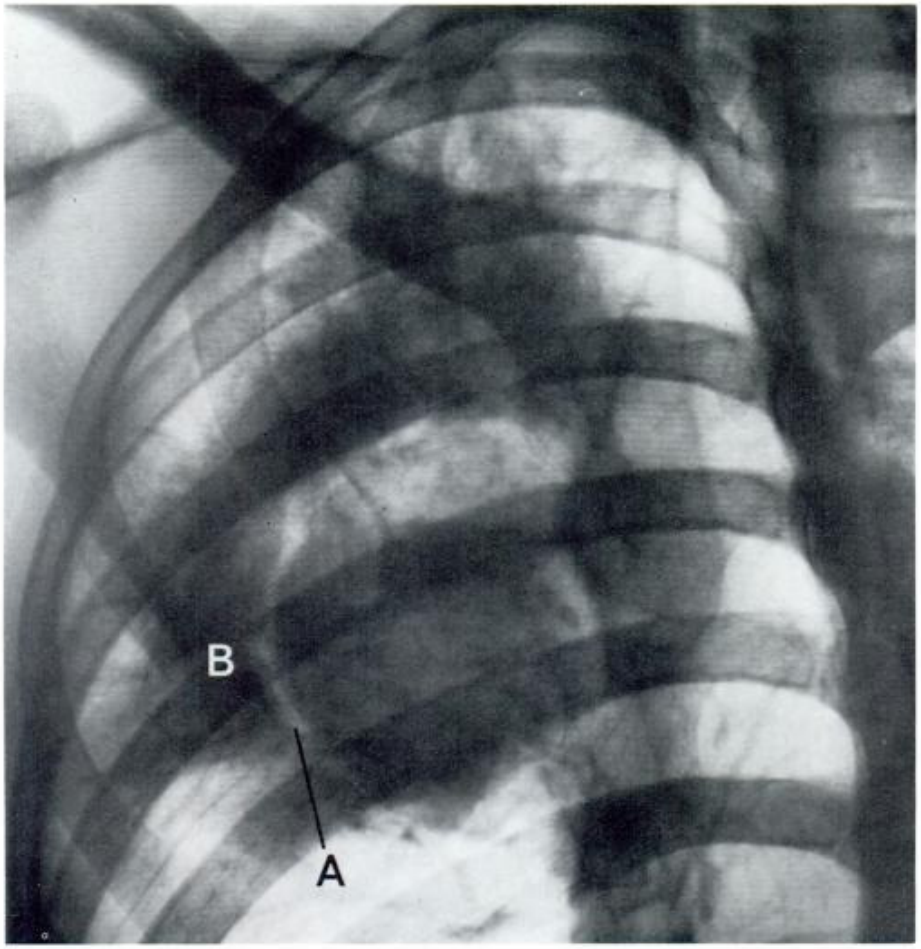

Fig. I: 2. Squamous cell carcinoma in the right upper lobe, surrounded by a 3 mm wide radiolucent zone separating the tumour from a superolateral, 2–3 cm broad, radiopaque zone. This radiograph from 1954, containing two of the corona structures (an "A" and "B" zone) became the impetus for the present study. Stasis, atelectasis, cancer growth or infection can not adequately explain the presence and appearance of the radiolucent and radiopaque zones.

of leukocytes (which carry a surplus of fixed electronegative surface charges) in tissue injury is caused by the driving electric force of the degrading tissue, during its electropositive phase over the VICC. This explanation represents a clearly definable mechanism for attraction of leukocytes in tissue injury as an alternative to the prevailing, but in many respects vague, concept of so-called chemotaxis. In vessels directing the blood flow toward the cathode, leukocytes are accumulated as a result of interference between blood flow and the cathodic field.

Thrombosis is also produced in the anodic field. Platelets, like other cells, are known to carry a surplus of electronegative charges. Accumulation of platelets may therefore also depend on electrophoresis in addition to other factors such as steric location and magnitude of charges. When a lesion in tissue polarizes spontaneously, the anodic phase may lead to microthromboses in capillaries in or near the lesion. The resultant focally decreased blood flow may contribute to local dystrophy of tissue. This mechanism probably contributes to the local "emphysema" which is sometimes seen around lung lesions. Local development of thrombosis around an anode will also cause blindly ending vascular pockets. Radiographic contrast media injected into the blood stream will then appear on angiography as the delayed "contrast enhancement" which is often seen around tumours.

The radiographic corona structures sometimes seen around lung tumours are described and analysed rather extensively as one example of an activated BCEC system causing structural modifications. The corona structures include a radiolucent "A" zone around a tumour, a radiopaque "B" zone outside the "A" zone (Fig. I: 2), radiating structures of various lengths extending from the surface of the tumour into surrounding tissue, and small arches, which connect to form arcades at the interface of the "A" and "B" zones. Furthermore, the corona structures include irregularly narrowed vessels and circumferentially displaced tissue structures, including vessels, around the tumour. These structural modifications can be explained as transformations of tissue in a polarizing BCEC system activated by degrading processes in the tumour. The corona structures could therefore be reproduced in in vitro and in vivo experiments.

Radiologic differential diagnosis of corona structures is also described and analysed. The radiopaque "B" zone mainly represents electroosmotic accumulation of water during an electropositive phase of polar-

ization of the tumour. The "B" zone can be distinguished from focal thickening of the pleura, atelectasis, neoplastic extension to the pleura and a previously undescribed finding called a pleural retraction pocket. This latter finding is produced by hydropenic retraction of fibrous radiating structures during anodic (electropositive) driving phase of the tumour. As overlying visceral pleura is retracted, an intrapleural pocket remains filled with pleural fluid. Further radiographic signs named lamellae and infiltrated strands are also described and analysed.

Radiographically observed corona structures are not specific for any kind of lung tumour, benign or malignant. This unexpected result led to consideration of the possibility that we here are encountering a more general biologic mechanism (which later on developed into the concept of BCEC).

Clinical and experimental studies of the corona transformation in lung tissue imply strongly that corresponding pathophysiological mechanisms ought to be found in other organs as well. To test this possibility, the human *female breast* was selected for study. Mammary structure and function obviously differ considerably from pulmonary structure and function. The breast has the additional advantage that it is easily accessible for in vivo radiographic-pathologic correlative studies.

Corona structures around breast cancers can be shown radiographically rather commonly. These structural changes are the same as those seen around lung tumours, including *"A" and "B" zones, arches and arcades, radiating structures, circular displacements* of tissue structures and *retraction of certain fibrotic components* within the radiating structures.

Electric potential measurements (with nonpolarizable Ag–AgCl electrodes over KCl bridges) were also performed, which showed that reproducible *potential differences could be demonstrated between tumour and surrounding tissue in certain instances of breast cancers*. Like lung tumours the polarity of the tumour was sometimes electronegative, sometimes electropositive, in relation to surrounding tissue.

Mammary tissue water in relation to fat was shown in in vitro and in vivo experiments to move from the anode toward the cathode in an electrically closed circuit. This movement produces radiographically detectable differences of attenuation between *hydropic and hydropenic fat tissue*.

Fat and water were then measured quantitatively in "A" and "B" zones after in vitro electrophoresis of dog fat tissue. High fat content and low water content appeared in "A" zones. High water and relatively low fat content were found in "B" zones. When electronegative fat is mobilized adjacent to the cathode in electrophoresis, it moves interstitially toward the anode and there enters the fat cells. This movement is, however, countered by that of fat from the anodic field, which obtains a reversed polarity under influence of anodic acidity. Eventually the moving fat boundaries will meet in the middle as a zone of cathodic and anodic fat. In vivo electrophoretic experiments in breast fat of dogs with quantitative determinations of relative fat and water content indicate that spontaneous development of radiographic *"A" and "B" zones around a breast tumour can be explained as in vivo electrophoretic transports over a BCEC*. Quantitative fat-water determinations around human breast cancers were found to support this hypothesis.

Circumferential structures around breast masses, which may be benign but are usually malignant, constitute a new radiographic sign, which should focus the physician's attention to a centrally located process which may be a carcinoma. These structures around a breast cancer are usually produced by realignment of interlobular fat septa. Sometimes peritumoural vessels are narrowed and positioned in a circular fashion, very similar to the findings seen around focal lesions in the lung. The mechanisms of these changes seem in principle to be the same for both lung and breast.

Radiating structures around breast cancers often contain both malignant cells and pathological vessels close to the tumour. Farther out in breast tissue the radiating structures contain fibrous tissue but not malignant cells. Some of the fibrous tissue is birefringent. Some of the nonbirefringent tissue is hygroscopic. A theory is presented, supported by in vitro experiments, that the *hygroscopic tissue elements in radiating structures shrink in the hydropenic "A" zone, producing skin retractions*. When the radiating structures reach close to the skin, these retractions contribute to lowering the local turgor pressure and facilitate the accumulation of tissue water in "*skin thickening*". The water, it is suggested, moves to this hydropic "B" zone as an electroosmotic transport of fluid from driving anodic to cathodic tissue within a spontaneously polarizing BCEC.

The well known *accumulation of white blood cells* both inside and around a carcinoma of the breast can readily be explained as an electrophoretic phenomenon. Experimental support for this theory is presented. When a tumour polarizes spontaneously (as by local necrosis or bleeding) and enters an electropositive driving phase, compared to its surroundings, the electronegative *white blood cells will accumulate electrophoretically* over VICC channels.

A pathologic finding, often recognized but hitherto unexplained, is a *red-yellowish zone* in the fat tissue around a malignant tumour. Similar changes of colour of breast fat have been produced electrophoretically in vivo in the dog and in vitro in human mammary fat tissue around the anode. It was also found that the so-called *atrophic fat tissue around breast cancers*, well

known to pathologists, occurs adjacent to the electropositive electrode in in vivo and in vitro electrophoresis.

Fibrous tissue commonly develops around carcinomas, by mechanisms previously poorly understood. Electrophoresis of normal fat tissue from human female breasts offers new approaches to the study of this phenomenon. The application of closed electric circuits was found to transform tissue and cell elements in breast fat tissue. Two types of new fibrous tissue were found to develop in vitro.

Anodic fibrous tissue appears microscopically to contain many fibroblast-like cells and large amounts of fibrous, partly birefringent, dense material. Irregular or circular arrangements of the fibres are often seen. This material appears to develop inside interstitial spaces at the time as fat cells loose their contents.

Cathodic fibrous tissue appears microscopically to form a delicate network (later it becomes more coarse) of partly birefringent material. It does not contain fibroblast-like cells. This tissue looks as if it develops by thickening of cell membranes while other parts atrophy. The intracellular material develops a reticular pattern of thin structures before it gradually disappears. Similar types of spontaneously developed fibrosis have also been found near cancers as regions of well-developed anodic and cathodic fibrosis.

Fibrotic tissue of different gross morphologic appearances can be produced. Thus, fibrous *membranes of anodic and cathodic types* can be produced by using flat electrodes. When these electrodes are provided with small protrusions, which lead to electrical edge enhancement, *radiating fibrous structures* develop. They can often be observed as thin fibrous streaks of irregular course between the electrodes in the in vitro specimen. Further variation of fibrotic tissue is obtained by changing the polarity of the electrodes. This switch has led to the development of mixed anodic and cathodic types of fibrous tissue.

Inside newly developed cathodic and anodic fibrosis, fat cells undergo remarkable transformations and develop structures which look like primitive ductal and vascular channels.

Under the influence of weak unidirectional direct current (a few microamperes during 2–5 weeks), human breast fat develops in the anodic field solid "*rods*" of an epithelial type of cells. The rods arrange themselves lengthwise in the fibrous tissue in *anodic groups* surrounded by a sheet of circular fibres, containing fibroblast-like cells. Eventually the groups develop each a central lumen. These structures, which are best developed close to the anode, have *an appearance very much like endogenously developed fibroadenosis in breast tissue.*

Close to the cathode, fat cells are simultaneously transformed into small "cells" with light cytoplasm and a dark point-like nucleus (haematoxylin-eosin). They arrange themselves in *cathodic groups* around a central fibrous material. This material extends with radiating structures between the "cells" to a circular fibrous enclosure (without fibroblasts). The cathodic groups of cells arrange themselves as cathodic *cores* in the direction of the newly formed cathodic fibrous tissue. Some of these cores lose their cells and leave a fibrous channel without cellular elements in its wall. Some cores gradually modify their cells and continue as anodic rods in the middle of the specimen. The light cathodic cells then gradually stain dark red-blue with haematoxylin-eosin.

Some cells in the cathodic field develop channel-like structures which have an appearance similar to endogenously developed pathological vessels.

The same type of cathodic channels, with an appearance of pathological vessels and anodic channels with fibrous walls containing fibroblast-like cells, could also be produced in normal, subcutaneous, human, abdominal fat specima. Further, in cathodic breast fat and abdominal fat, fibrous channels also develop without fibroblasts or cellular elements.

When bidirectional current was passed over breast fat, thin anodic channels were produced. They contained fibroblast-like cells in their walls.

The proposed existence of a *fluctuating potential arising after injury to tissue* is supported by in vitro experiments in which *microcalcifications were produced* in breast fat tissue. Fat removed from normal human breasts was exposed to direct current (e.g., 25 coulombs at 10 V). Anodic, intracellular, "bush-like" structures developed. They contained no calcium, but could be identified in microradiographs. At this point the current over the tissue sample was reversed. During this second phase, calcium precipitated in the bush-like matrix, which now had the histologic appearance of spontaneously developed microcalcifications in breast cancer.

Fat itself is a relatively poor electric conductor. The electric current over small specimens of fat tissue is therefore, after a few hours, usually in the range of a few microamperes. The time of treatment was therefore extended over weeks. During such long time periods, the current seems to protect the specimen from bacteriological decomposition.

Not only weak currents but also low energies of current are capable of modifying the structure of tissue, when the forces are allowed to act over a long time. Thus, the weak electric pulses around pacemaker devices and the intracardiac electrode can cause fibrous tissue to form, but only after relatively long periods of time. Such considerations may support the theory that metabolic polarization of tissues or organs should also be capable of producing substantial ionic transports over BCEC systems. Fibrotic tissues such as

tissue membranes and organ capsules may be the result. The studies presented suggest also that pathological conditions in which calcium precipitates in tissue, including healing of fractures by electric current (which has been attempted by previous researcher), need investigation in terms of BCEC.

The structural changes around carcinomas of the breast are remarkably similar to the structural changes around masses in the lung, despite the differences in basic morphology of the two organs. It has therefore been concluded that the biokinetic background for their development may essentially be the same. The central mechanism for such modifications of structure appears related to physicochemical polarization of tissues within biologically closed electric circuits.

Under the assumption that the BCEC systems represent a physiologic transport mechanism which influences normal functions, including healing, it seems reasonable to speculate that *artificial activation of BCEC systems offers the possibility of enhancing healing.*

Direct current used for therapeutic purposes (*electrochemical treatment*) raises many possibilities either for separate treatments with direct current or for combinations with other techniques.

Verified *cancers occasionally heal spontaneously*, according to well established reports in the literature. Several possible explanations have been advanced and also criticized. In addition to the commonly suspected immunologic or hormonal causes, it is suggested here that the mechanism of healing via the VICC system may be involved.

It is assumed that cancers, which develop internal necrosis, bleeding or infection obtain a release of catabolic energy which will activate their VICC system. This represents the start of a process of healing, including accumulation of leukocytes, production of fibrosis, microthromboses and other changes in the environment of the tumour. In *favourable cases*, such changes around the tumour may preclude its survival. More commonly, such changes should only slow the rate of neoplastic growth, because of insufficient release of energy for complete healing of all tumour tissue. An additional supply of energy to drive the VICC system is, however, possible over implanted electrodes connected to an external electric source of power.

The suggested mechanism of a natural, but rarely complete process of spontaneous healing of cancers and how this mechanism may be supported, formed the rationale for a series of electrochemical treatments of cancer.

A localized cancer may even offer rather favourable possibilities for therapy with direct current between implanted electrodes connected to an external source of DC power. After an earlier pilot study to introduce a *self-driving injury reaction* by local electrocoagulation of tumours, five patients with inoperable metastases in the lung were treated with *direct current*. This type of treatment represents, during treatments, an *externally driven system*. It offers the advantage that any magnitude of energy can be applied to activate the biologic circuits. The drawback is, however, that we still do not know enough about the mode of application to optimize the technique. As soon as the current is interrupted, a *self-driving system* will start in the tissues. The direction of current will now reverse, compared to the applied current. The tissues will take over the initiated process of healing.

Electrochemical treatments have now been further modified and applied in a trial series of 26 cancers in 20 patients. The study shows that some peripheral nonoperable lung tumours can be treated successfully in patients with poor cardiorespiratory or general condition. The tumour electrode is made anodic because cancer cells are generally considered to carry a surplus of fixed electronegative surface charges. In this way the tumour cells are kept attracted to the anode during treatment.

After treatment, 13 of the tumours gradually disappeared or decreased in size, usually during the first three or four months. One of these tumours later increased in size. Thirteen patients have died, five from multiple metastases, four from brain metastases, one each from bronchopneumonia, abuse of alcohol, myocardial infarction, and suicide. The treatments have been free of mortality. Complications (e.g., pneumothorax) have been minor.

Electrochemical treatment of tumours offers a new and promising therapeutic possibility. The technique of treatment, including the electronic equipment and electrodes, is, however, still far from optimized. Treatment of tumours with direct current might also be supplemented by chemotherapeutic compounds provided with a suitable charge. Experiments were performed which suggest that such a medium, after injection into the blood stream, might then become attracted electrophoretically to the tumour during application of direct current.

The treatment with direct current produces around tumours radiographically visible structural changes of an appearance which can not be distinguished from spontaneously developed *corona structures*. These changes include "A" and "B" zones, radiating fibrous structures, arches and arcades, and narrowing and circular displacement of vessels.

The formation of *new vessels in healing of injury* is still not well understood. Newly formed pathological vessels are often found inside and around malignant tumours. In vitro experiments on fat tissue have shown that application of direct current through an excised specimen is able to transform the tissue into *primitive channels*. It is anticipated, on the basis of these observations, that a spontaneous flow of current

over a BCEC system is likely to be a main factor in the development of tissue channels. Future research may disclose the role of an activated VICC system for the formation of new vessels.

As knowledge of BCEC mechanisms increases, other closed circuit therapeutic measures may become possible, e.g., healing of wounds, fractures and infections. The inconsistent results of previous attempts to improve healing of fractures by electric current is, in the opinion of the author, dependent on lack of knowledge about how the treatments should be coordinated with the physiologic mechanisms.

A large number of *chemicals, physical and biologic factors are capable of inducing cancer.* They all seem to have the capability, direct or indirect, of polarizing tissue. *A unidirectional activation of BCEC systems by weak currents over a long time will change the internal and external environment of cells. Surviving, modified cells still capable of multiplying may then possibly produce neoplastic tissue. It is suggested that activated BCEC systems, under certain circumstances, represent a common factor in carcinogenesis.*

An acceptance of the principle of BCEC systems leads logically to a number of interesting consequences. The last chapter of this book discusses some of these consequences. Thus, it will be seen that poorly understood events or even rather obscure phenomena such as acupuncture and oral galvanism may be explained on the basis of BCEC systems.

An important function of BCEC systems, not previously mentioned, must now be touched upon. Closed circuit electric transports are always associated with the creation of magnetic fields around each circuit. Such electromagnetic systems can be influenced by external electromagnetic fields, by the principle of superimposition. A flow of current in a BCEC system will consequently produce electromagnetic fields. Moreover, an external magnetic field moving in relation to BCEC circuits will produce a flow of current in the BCEC channels. *The BCEC system then can be seen to act as a receptor for external electromagnetic forces.* Such forces, both man-made and natural, are parts of our normal surroundings and within certain limits evidently well tolerated. A continuous separation of electric charges takes place in the atmosphere. When these collections of charges (ionars) move by winds, strong electromagnetic fields are created. Before thunderstorms, during certain winds such as the Föhn winds in Central Europe, and sometimes even during ordinary changes of weather, many organisms including human beings react in various ways. Headaches, hemicrania, epileptic fits, joint pains, increase in traffic accidents and the like are reported. From a physical standpoint the moving electromagnetic external fields must induce transport of current in the channels of BCEC systems. When these currents exceed physiologic tolerance, the organism will react. Such phenomena are most easily explained as a disturbance of homeostasis. An ordinary Faraday's cage will not protect against such interferences. The energy of activation of BCEC systems is tied to the moving magnetic fields. Their high power of penetration would probably require a chamber of steel with perhaps one inch thick walls for protection.

It is the hope of the author that the reader will proceed to read the following chapters, because this summary contains many shortcuts and simplifications.

II.
Radiographic detectability of corona structures

Clinical radiologic research based on large numbers of examinations is hampered by the fact that the quality of routine radiographs varies widely. This fact in turn may limit various aspects of a study. Not only do techniques of image production vary, but also interpretation and documentation of images are not standardized. For these reasons, the extraction of basic information about specific problems in diagnostic radiology is often difficult to collect and to present in statistically treatable terms. Furthermore, the collection of clinical radiologic information is frequently a discontinuous process influenced by personal interest, training, and trial and error. Improved examination technique increases knowledge, which in turn improves technique. This feedback makes clinical radiologic research a dynamic process. The statistical prerequisite of uniformity is therefore often very difficult to achieve in any large study.

Twenty-eight years ago the author was impressed by chest radiographs of a patient with a peripheral carcinoma of the lung and a peculiar pattern of air-filled lung separating peripheral "atelectasis" from the carcinoma (Fig. I: 2). In the next decade not one single additional case was recognized among several thousand patients with lung tumours. The explanation is not to be found simply in inadequate techniques of radiographic examination. It is mainly the result of lacking knowledge about what to look for. Radiologists' visual search patterns are of fundamental importance in diagnostic radiology. Improved visual search can lead to improvements not only of radiographic technique, but also to improved rates of detection of specific radiologic findings.

Similar situations, familiar to experienced radiologists, are probably infrequently appreciated by our non-radiological colleagues who have not been exposed to the almost impossible task of combining long-term research with standardization in radiologic technique and interpretation. So-called "routine technique" in chest radiography varies considerably between different institutions and different radiologists. So-called "special films", e.g., oblique chest radiographs, vary even more in technical quality. Also, radiographic quality has gradually improved over the past decades for a multitude of technical reasons.

With this background it is obvious that exact statistical figures over three decades of personal experience can not always be presented. Nevertheless, on the basis of personal experience of reviewing chest radiographs of more than 7 000 patients with tumours in the lungs, the author estimates that corona structures of the lung, described in 1969 (1), should now be recognized on

"routine" examinations in 20 to 30 per cent of patients whose tumours are peripheral to the hila and larger than approximately 2.5 cm.

Some technical radiographic and radiologic comments are now in order. So-called routine radiographs are often far from sufficient as a basis for proper clinical radiological research. One or two of the signs of corona structures may be detected on a single chest radiograph, but all the signs are rarely seen on one radiograph. Different projections and exposure techniques are often required. For reasons which will be described later, certain structural signs are sometimes completely lacking. A "good routine technique" is, however, essential for the preliminary detection of the radiographic signs. Some general remarks will, for that reason, be made on the author's technique of chest radiography.

The importance of oblique views in routine chest radiography is unfortunately seldom fully recognized. In our institution oblique views are included in the routine procedure for chest radiography, in addition to the traditional posteroanterior and lateral views. Any physician with experience in bronchography will immediately understand why the oblique views are of fundamental importance for a radiologic approach to structural analysis of the lungs.

In the lungs, only the central bronchi and the central pulmonary vessels are oriented predominantly in the sagittal and coronal planes. For structural analyses of the peripheral pulmonary parenchyma, oblique projections are very helpful (30°–40° to the left and to the right). Sometimes fluoroscopic examination may permit exact positioning and coning of the x-ray beam to optimize exposure technique.

Exposure time must be kept as short as possible to eliminate blur caused by motion. When exposure time exceeds 10 ms, motion blur often prevents the recognition of the radiating structures, arches and arcades. This motion blur is mostly caused by the pulsations of the pulmonary vessels and the transmitted pulsations of the heart. Exposure timers usually require prolonged exposure time, which is paid for by unnecessary motion blur. They also interfere with the use of shutters in chest radiography, which is even more serious with regard to image quality and dose reduction. Exposure timers can advantageously be omitted in chest radiography. Exposure time also can be reduced by elevating tube kilovoltage at the expense of filament current. 150–190 kVp has therefore been our standard in routine filming. At these energy levels a decrease in contrast will occur. This drawback is, however, counterbalanced by the reduced disturbing effect of the calcium of the ribs. The exposure time can in frontal and oblique views be kept at 1–6 ms at 300 mA current. Lowering of contrast by this technique is of obvious disadvantage for the recognition of density differences between the "A" zone and surrounding tissue. Radiographs obtained with relatively low tube tension improve contrast between the "A" zone and "B" zone but at the expense of considerable loss in resolution of detail.

Other radiographic technical considerations pertain to clinical radiologic study of small objects. X-rays are generated in a focal spot of a small but finite area, e.g., 0.3 by 0.25 mm^2. The size of the effective focal spot in relation to the size of the object is critical, as also is the homogeneity of the x-ray output. Variations of intensity from different parts of the focal spot may not only produce distortion of the image but actual false images, e.g., multiplication of structures in the radiograph.

A final radiographic point concerns those structures which produce lines as fine as threads in a radiograph. Is it really possible to see in the lung threadfine structures whose diameters are of the order of the diameter of a small focal spot, i.e., are considerably less than one mm? Is it not likely that for radiography to show such threadfine structures they must have an absorption coefficient considerably higher than the surrounding tissue? Perhaps these structures are shaped as thin sheets and are oriented tangentially to the beam?

In histological sections of lungs which in radiographs have shown threadfine structures, no calcium or other opaque material which could produce a marked increase in absorption has ever been reported. A dense absorber, however, is not a prerequisite for the production of radiographically visible, threadfine opacities. The material in these structures may have the same absorption coefficient as the material of surrounding lung tissue. The amount of material per unit volume in the threadfine structures may be greater than in the surrounding lung. Superimposition of a large number of threads may also produce such effects. The individual thread-structure might "drown" as an average increased density compared with the density of surrounding lung. If many small structures are randomly dispersed they will appear in the radiograph as a result of summation, which statistically can be expressed as a gaussian distribution. It is therefore important to recall that the images of the threads do not necessarily correspond to specific threads in the tissue. Instead, we see their statistical representation.

The biokinetic principles of structural development around lung lesions have also been studied in the female breast. These studies were performed as it seemed likely that the principles might be valid also in organs other than the lung. The female breast was selected because anatomically and physiologically it is very different from lung and because it offers suitable conditions for finely detailed radiographic studies.

The case material of breast tumours is selective. Mammograms from routine health examinations and

from patients with breast symptoms have been studied with regard to the possible existence of structural changes similar to those observed in the lung. No quantitative estimation of the structural changes has been attempted. It was found in a mixed material from several hospitals that strikingly similar structural changes can sometimes be observed around breast and lung cancers. The biokinetic mechanisms proposed to explain these similarities were then examined by different in vitro and in vivo studies in dogs.

The radiographic studies were made both with conventional radiographic breast examinations using compression of the breast and in certain cases xeroradiography without compression. Most of the "conventional" mammographies were made with "Diagnost M" (Philips/C. H. F. Müller), which is provided with a built-in six pulse generator. The tube potential has usually been 25–30 kVp, the rotating molybdenum anode has had a nominal 0.6 mm focal spot. To the beryllium window has been added a molybdenum filter. The focus-film distance has usually been 40 cm. The exposures have been made with an automatic exposure timer (Amplimat) and a mobile ionization chamber and light localizer. Standard craniocaudal, lateral and oblique projections have been available in all cases.

Sampling of cellular material for diagnosis and implanting of electrodes for measurements of electric potentials in breast tumours were made with a stereotaxic instrument, Mammotest (Tekniska Röntgencentralen AB, P.O. Box 50100, S-104 05 Stockholm, Sweden).

For the implantation of electrodes in lung tumours, a versatile biplane fluoroscopic unit was also developed, which is now available under the trade name of Angioscope (Siemens-Elema AB, Fack S-171 20 Solna, Sweden).

Reference

1. Nordenström, B.: New trends and techniques in roentgen diagnosis of bronchial carcinoma. In: Simon, M., Potchen, E. J., and Le May, M. (eds.): Frontiers of Pulmonary Radiology. New York, Grune and Stratton, 1969, p. 380.

III.
Corona structures around malignant and benign neoplasms in the lung

Despite the frequency of pulmonary neoplasms in contemporary radiologic experience, corona structures around these neoplasms have thus far not enjoyed adequate description. In this chapter it is attempted to correct this deficiency in radiologic analysis of lung tumours.

Previously, three of the corona structures have been reported, the "A" and "B" zones and the radiating structures (6). Once the author became aware of these characteristic appearances, their presence became detected around approximately 25 per cent of pulmonary masses larger than about 2.5 cm in diameter and peripheral to the hila. Additional corona structures are now found. Previous descriptions were incomplete.

To appreciate the analysis in this book of the functional and morphologic significance of the corona structures, their accurate description is essential. In this chapter, the most important radiographic coronal manifestations will first be described: the "A" and "B" zones, radiating structures, the arches and arcades, circular structure displacement and vascular narrowing. Other radiographically visible structures will then be described: lamellae, infiltrated strands, and retraction pockets. All of these structural changes will be seen in later chapters to represent interactions among specific pathophysiological events induced by the pathological tissue (see, e.g., Chapter XV).

As a preliminary example, Fig. III: 1 illustrates a centrally necrotic adenocarcinoma in the periphery of the right upper lobe. All the corona structures are usually not evident in a single radiograph. The radiographic signs may be quite subtle.

A. "A" zone

The "A" zone is radiographically seen as a halo or arcuate radiolucent area around all or a portion of an intrapulmonary radiopaque mass (Figs. III: 1–9). The "A" zone is less opaque than the surrounding pulmonary parenchyma. The width of the "A" zone ranges from 2 mm to 8 cm in the present material, but it is usually between 5 to 30 mm wide. The width often varies in different parts of the zone. The inner border of the "A" zone is limited by the surface of the tumour.

The outer border of the "A" zone is usually ill-defined (Figs. III: 2, 4, 5). In the periphery of the "A" zone, radiopacity frequently increases gradually until

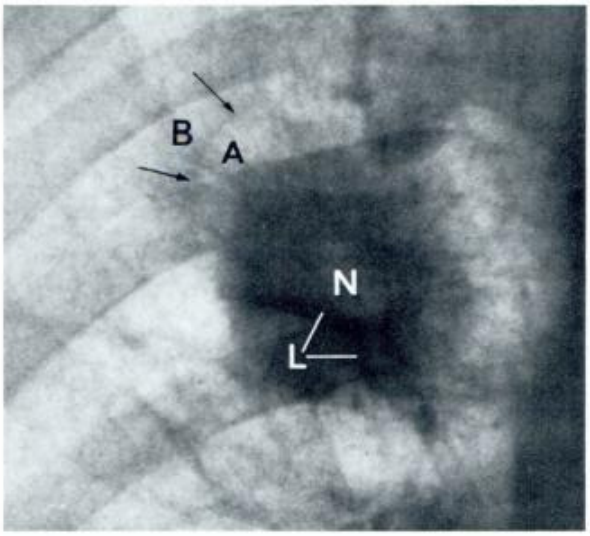

Fig. III: 1. Well differentiated adenocarcinoma of lung, frontal radiograph. A radiolucent, 1–2 cm broad, "A" zone (A) surrounds the tumour. The "B" zone (B) lies peripheral to the "A" zone, and is smaller and slightly more radiopaque. Histologically, the centre of the cancer was necrotic, evident on the radiograph as ill-defined, central radiolucency (N). Structures radiate from the tumour's surface. An opaque y-shaped band, here called a lamella (L), overlies the mass. At the sharp interface between the "A" and "B" zones, a 2 cm long arcade (arrows) is seen. Close inspection suggests it is formed by a number of tiny arches, each 1–2 mm broad.

Fig. III: 2. Poorly differentiated squamous cell carcinoma of the left lung, frontal radiograph. The tumour is surrounded by a radiolucent "A" zone, which is diffuse, irregular, and 0.5–1 cm broad. Its outer margin is indistinct.

Fig. III: 3. Squamous cell carcinoma, left upper lobe. (*a*) Left anterior oblique radiograph shows radiating structures, including lamellae (arrows). "A" and "B" zones are correspondingly labelled. (*b*) Left posterior oblique radiograph shows a 12 mm broad, radiolucent "A" zone (A). Along its superolateral portion a radiopaque "B" zone (B) has a well-defined margin against the "A" zone (arrowheads). Elsewhere the margin of the "A" zone is poorly defined.

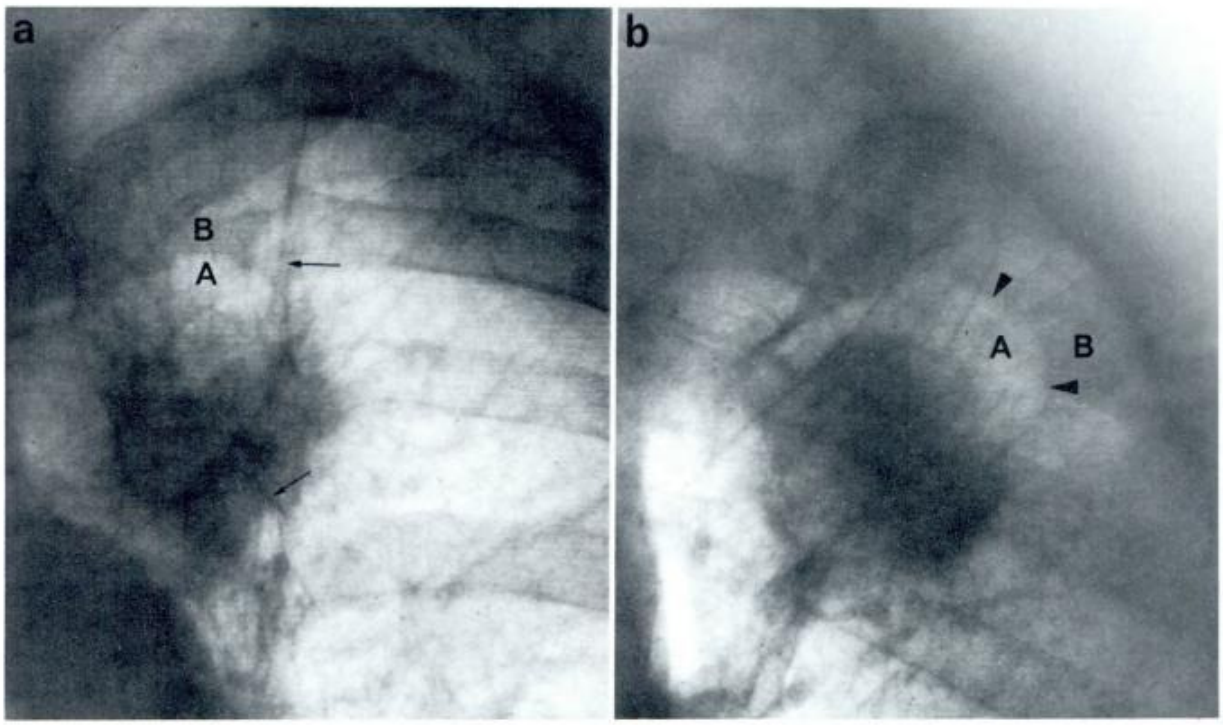

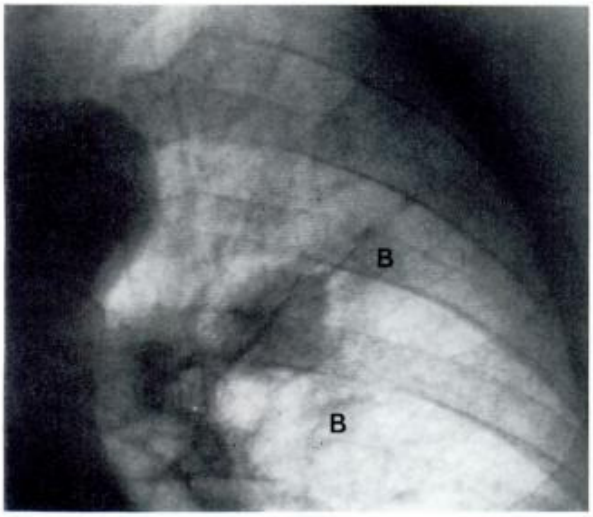

Fig. III:4. Small cell carcinoma, upper lobe, left lung, frontal radiograph. The "A" zone is about 5 mm wide. A "B" zone is seen as an irregular infiltration lateral to the tumour. The border between the radiolucent "A" zone and the radiopaque "B" zone is poorly defined.

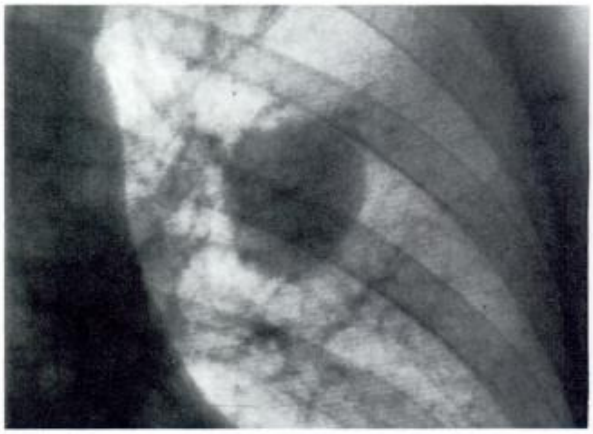

Fig. III:5. Carcinoma of breast, metastatic to the upper lobe, left lung, frontal radiograph. The tumour is surrounded by a faint, radiolucent "A" zone medially, inferiorly, and laterally. The periphery of the "A" zone is poorly defined.

it reaches the level of the surrounding lung parenchyma.

A sharp outer border of the "A" zone, on the other hand, is observed characteristically only against a "B" zone situated between the tumour and the periphery of the lung (Figs. I: 2, III: 1, 3, 9). Computerized tomography will occasionally be more sensitive than plain radiographs in detecting these changes (Figs. III: 8, 34).

No characteristic malignant cell type is associated with corona changes. *An "A" zone can be seen around different histological types of malignant tumours in the lung.*

For some time the author thought that an "A" zone was a radiographic sign of cancer. It is not so. An "A" zone can be found around some benign tumours as well as around primary and metastatic lung tumours of different types and degrees of differentiation. (As will be seen in the next chapter, corona structures may even develop around inflammatory lesions.) Two cases will now illustrate an "A" zone around a benign tumour.

In Fig. III: 6*a*, a hamartoma is seen surrounded by some discrete, 5–6 mm long, radiating structures and an irregular circle of vessels 4–5 cm in diameter. Six years later (Fig. III: 6*b*), a radiolucent zone, 5–12 mm broad, surrounds the tumour. This zone is indistinguishable from an "A" zone as seen around a malignant tumour. Confirmation of the marked radiolucency of the "A" zone is shown by a densitometric recording across the lung, the "A" zone and the tumour.

Another hamartoma (Fig. III: 7) is illustrated surrounded by a 1–8 mm broad "A" zone. A photographic "edge enhancement" and "Mach effect" (7, 11) as possible sources of error can be excluded in this case because of the irregular and variable width of the "A" zone. Furthermore, comparable differences of density, e.g., between ribs and lungs, do not show any edge enhancement artefacts in this radiograph.[1]

Computerized tomography may be more sensitive to "A" zone radiolucencies than plain radiographs. Fig. III: 8*a* shows a plain radiograph of a metastatic melanoma in the right upper lobe. No clear "A" zone can be seen around the tumour. In the computerized tomogram (Fig. III: 8*b*), on the other hand, the radiolucent zone is easily recognized, as well as circular deviation of vessels around the "A" zone.

[1] Evaluation of density differences in photographic films is subject to several errors: the so-called adjacency effects and Mach effects must be considered. The most common errors are the appearance of enhanced density along the edge of a dense area, known as the border effect, and decreased density outside the border effect, known as the fringe effect. The border effect is often referred to as the Mach line and the two effects together as the edge effect. They are partly produced during film development because the developer affects not only the surface of the film but also the emulsion. Horizontal diffusion of fresh developer within the emulsion enhances the developing process within a nearby area of higher exposure. On the other hand, the reactive products of development also diffuse in the opposite direction through the boundary of different exposure. Such reactive products tend to inhibit development in the less exposed side of the boundary. The edge effect occurs within a relatively restricted area adjacent to the boundary where the exposure gradient is steep; usually it is less than a millimetre wide. The visual analogue to the photographic border and fringe effects is called the Mach effect. Physiologically an intense stimulus of part of the retina results in a lower signal from adjacent retinal cells. This compensatory mechanism is called lateral inhibition. The intense signal is on the other hand enhanced. This visual mechanism enhances considerably the visual recognition of structures.

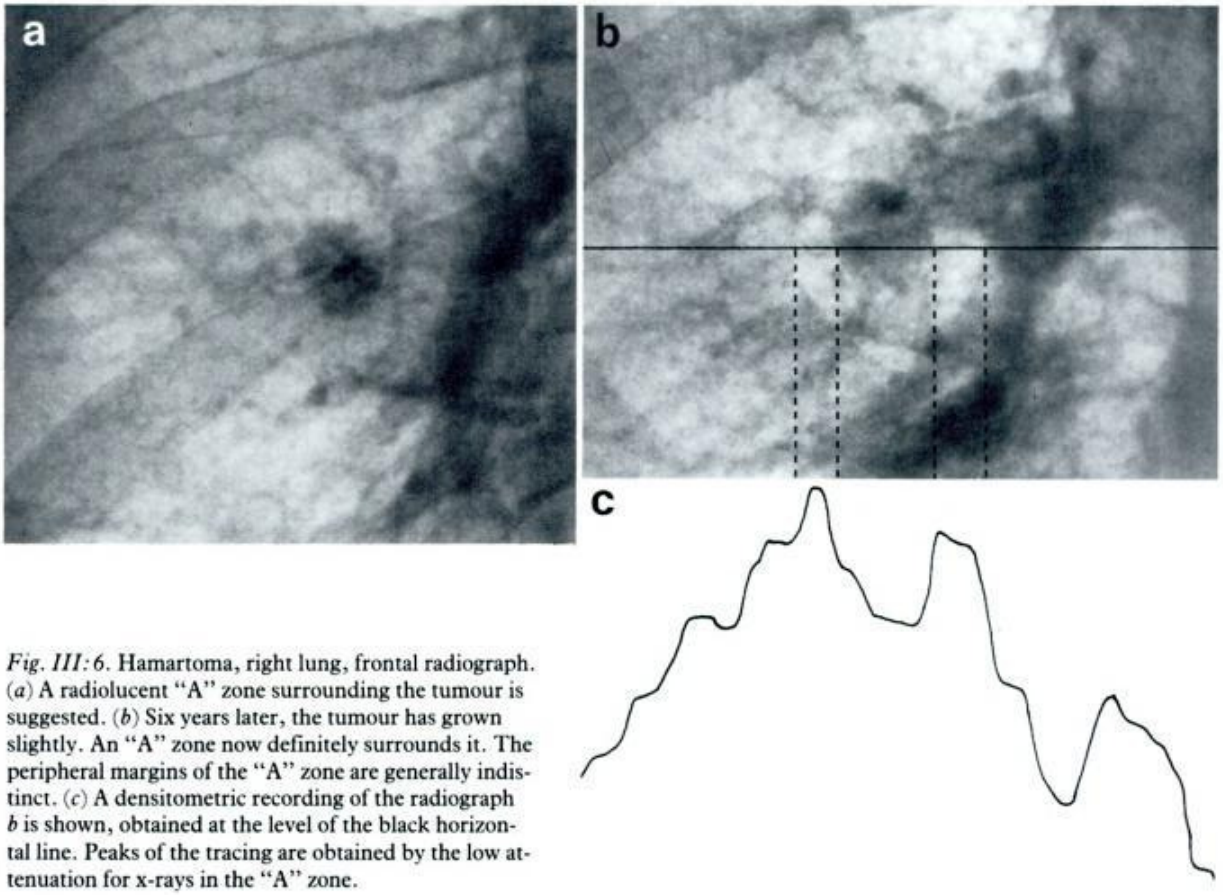

Fig. III:6. Hamartoma, right lung, frontal radiograph. (*a*) A radiolucent "A" zone surrounding the tumour is suggested. (*b*) Six years later, the tumour has grown slightly. An "A" zone now definitely surrounds it. The peripheral margins of the "A" zone are generally indistinct. (*c*) A densitometric recording of the radiograph *b* is shown, obtained at the level of the black horizontal line. Peaks of the tracing are obtained by the low attenuation for x-rays in the "A" zone.

Fig. III:7. Hamartoma, right lung, frontal radiograph. A narrow "A" zone of varying width surrounds the tumour. A pulmonary vessel (arrow) appears not to traverse the "A" zone.

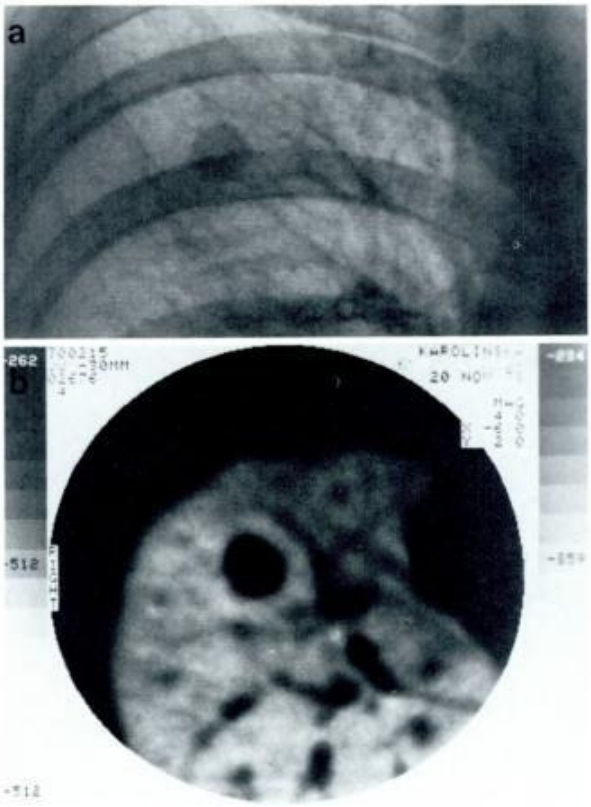

Fig. III:8. Pulmonary metastasis from an extrathoracic malignant melanoma. (*a*) Frontal radiograph, right upper lobe. No definite "A" zone is apparent. (*b*) Computerized tomography shows a radiolucent "A" zone around the tumour. Blood vessels appear deviated around the margin of the "A" zone.

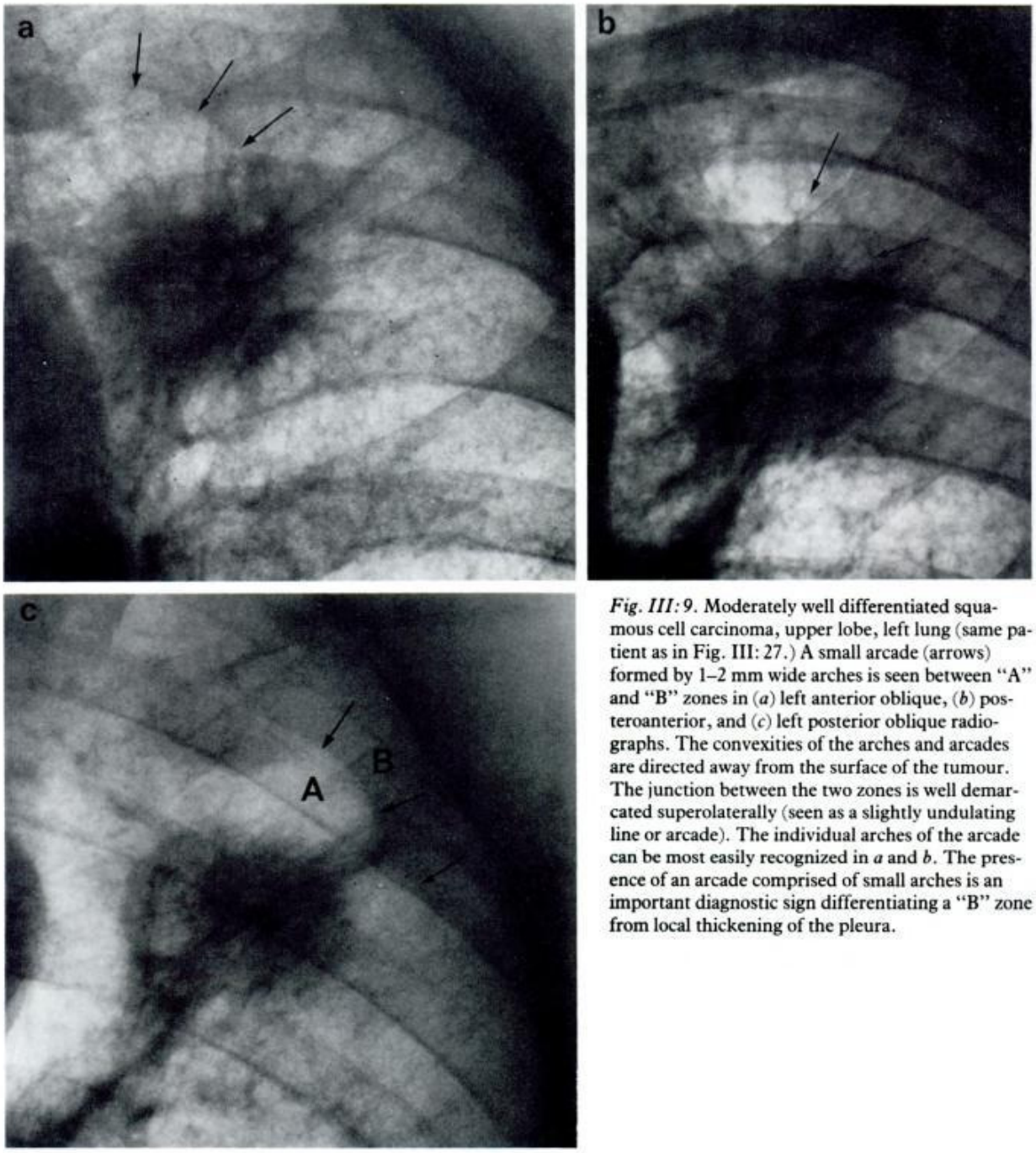

Fig. III: 9. Moderately well differentiated squamous cell carcinoma, upper lobe, left lung (same patient as in Fig. III: 27.) A small arcade (arrows) formed by 1–2 mm wide arches is seen between "A" and "B" zones in (*a*) left anterior oblique, (*b*) posteroanterior, and (*c*) left posterior oblique radiographs. The convexities of the arches and arcades are directed away from the surface of the tumour. The junction between the two zones is well demarcated superolaterally (seen as a slightly undulating line or arcade). The individual arches of the arcade can be most easily recognized in *a* and *b*. The presence of an arcade comprised of small arches is an important diagnostic sign differentiating a "B" zone from local thickening of the pleura.

B. Small arches and arcades

Before a general description of the different appearances of the "B" zone can be offered, specific description is appropriate for those parts of the interface of the "A" and "B" zones which are well defined, i.e., the arcades and small arches.

Wherever the "A" zone sharply borders the "B" zone, *small arches* characterize the interface. Each arch is from one to five mm wide. The convexities of these arches are always directed away from the lesion. The arches hang together in rows which are here called *arcades*. The arches and arcades often appear as a line or lines of increased radiopacity. Characteristic examples of small arches forming arcades between "A" and "B" zones can be seen in Figs. III: 1, 9, 10, 13.

Small arches forming a short arcade are seen in Fig. III: 9. In the left anterior oblique projection (*a*), the arcade (arrow) projects over the mid-part of the tumour, a moderately well differentiated squamous cell carcinoma. In the posteroanterior view (*b*), the arcade is seen superior and lateral to the tumour. In both *a*

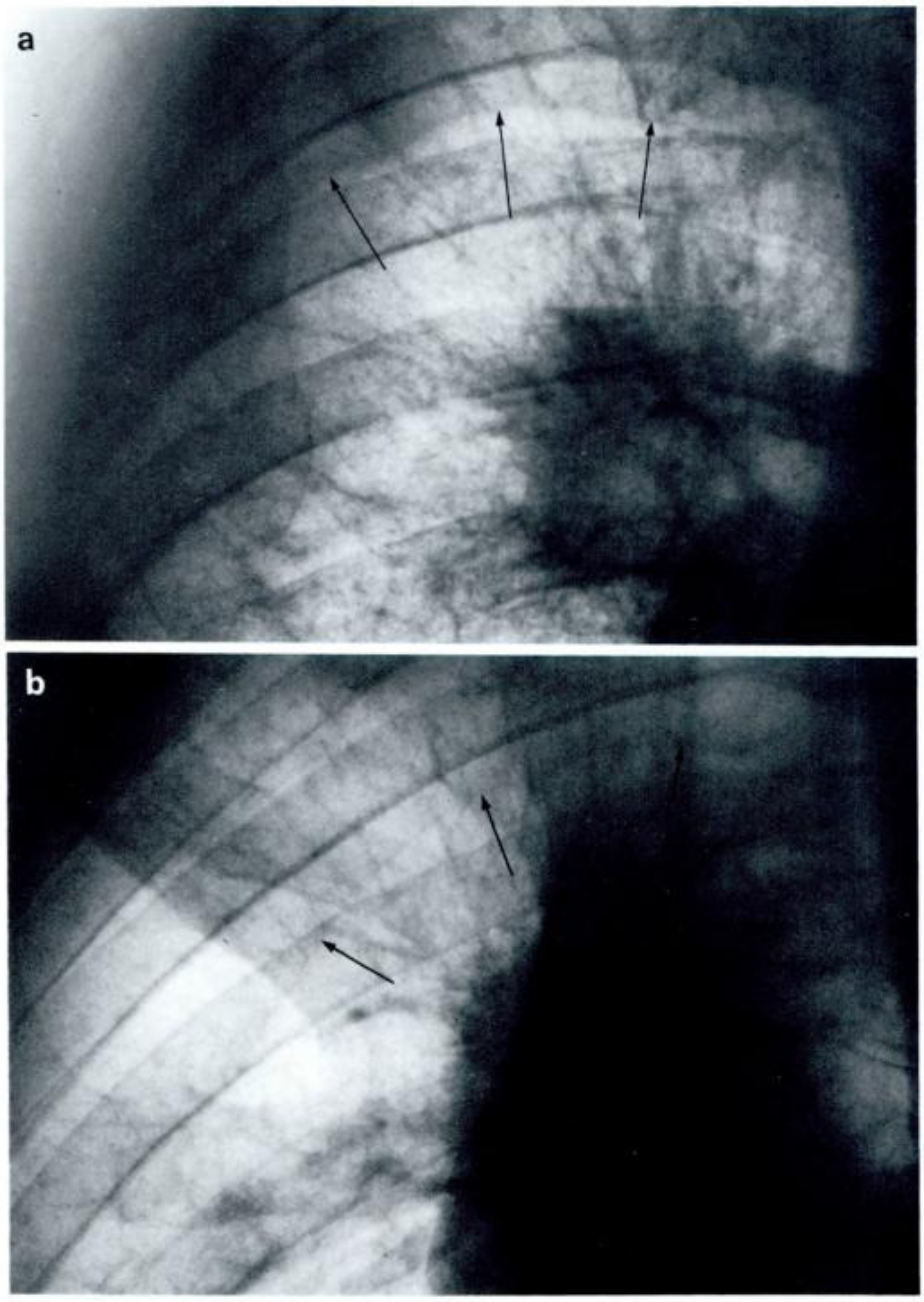

Fig. III: 10. Large cell carcinoma in the right lung of a 67-year-old man. Coarse structures radiate more or less perpendicularly to the surface of the tumour. They pass through the 2–4 cm broad "A" zone into the "B" zone. In a posteroanterior radiograph (*a*), the interface between the "A" and "B" zones (arrows) is seen as a slightly undulating line. In the right posterior oblique projection (*b*), the interface is seen as individual, small, 2–3 mm wide arches forming a 10 cm long arcade.

and *b* the convexities of the 1–2 mm wide arches are each directed away from the tumour. Some small radiating structures in *b* can also be seen in the "A" zone, ending at the edges where the small arches make contact with each other.

This tumour contains a cavity with some air and has an indentation in its inferior border (*c*). It is likely that the indentation represents partial collapse of the surface of the tumour. Such collapse may cause the formation of what are here called *lamellae*, which are seen either at the surface or projected over the tumour as opaque thick lines (see Section F on formation of lamellae).

This case also illustrates the importance of radiographic positioning of the patient for correct analysis of structures. Oblique projections in this instance aided differential diagnosis of the radiopacity here called the "B" zone. Distinguishing a "B" zone from local pleural thickening may be important clinically.

The small arches and arcades may be found seemingly far from a pulmonary tumour. A giant cell carcinoma, seen in the posteroanterior view (Fig. III: 10),

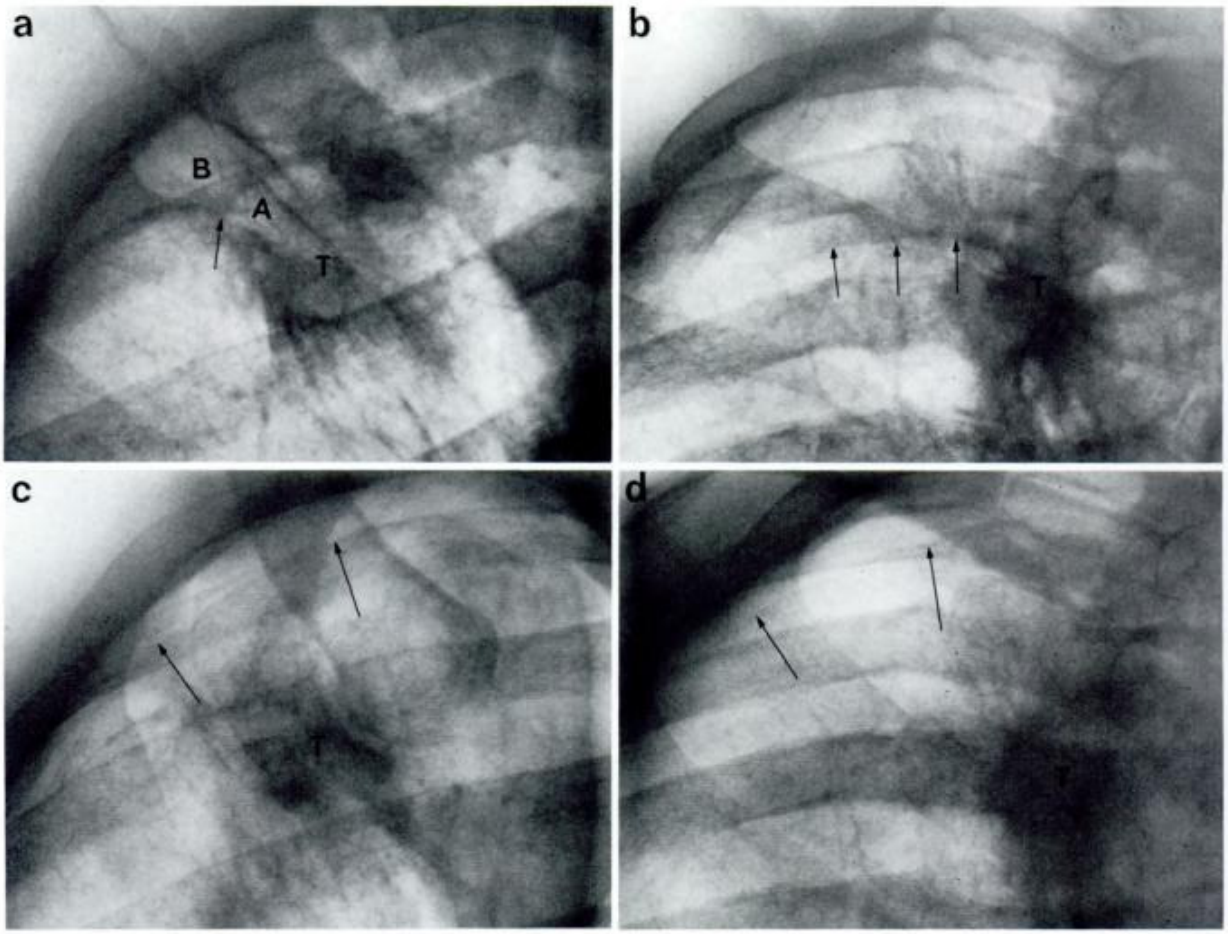

Fig. III: 11. Demonstration of disappearance of "B" zone and arcade after injection of air into the pleural space. Pleomorphic carcinoma (*T*) in a 61-year-old man. (*a*) "A" and "B" zones in a 15° right posterior oblique radiograph. The arcade, a biconvex interface, defines the superolateral margin of the "A" zone. The junction of the two convexities (arrow) appears retracted toward the tumour. (*b*) 20° right anterior oblique projection. Radiating structures are seen superior to the tumour. Arrows indicate the arcade. (*c*) and (*d*) Same projections as *a* and *b*, respectively, after insufflation of air into the pleural space. The pleural space is open, the "B" zone has disappeared, and the visceral pleura is normal (arrows). In this case, the disappearance of the "B" zone suggests that it was caused by a local fluid collection in the lung between the tumour and the pleura.

has a central air-filled cavity and rather coarse radiating structures which are arranged more or less perpendicularly in relation to the tumour surface. The radiating structures pass through a 4 cm broad "A" zone and deeply into a "B" zone. The interface between the "A" and "B" zones is well demarcated in Fig. III: 10*a* (arrows). In the right posterior oblique view (*b*), a projection is chosen which shows a row of small arches forming one slightly curved arcade. These arches each have a width of about 3 mm (arrows). The positions and clear definition of the interface between the "A" and "B" zones, as well as the passing of the radiating structures through the interface, indicate that the arcade is not caused by the interlobar pleura.

C. "B" zone, including its demonstration in a dog model

The "B" zone is a region of increased radiopacity peripheral to the "A" zone. Its opacity is greater not only than that of the "A" zone but also than that of normal lung. It often, but not always (see, e.g., Fig. I: 2), extends from the periphery of the radiolucent "A" zone to the pleura. A number of representative examples will be reviewed.

In Fig. III: 1 the "A" zone is very prominent, while the "B" zone appears only as a rather discrete radiopacity superolateral to the "A" zone. At the interface

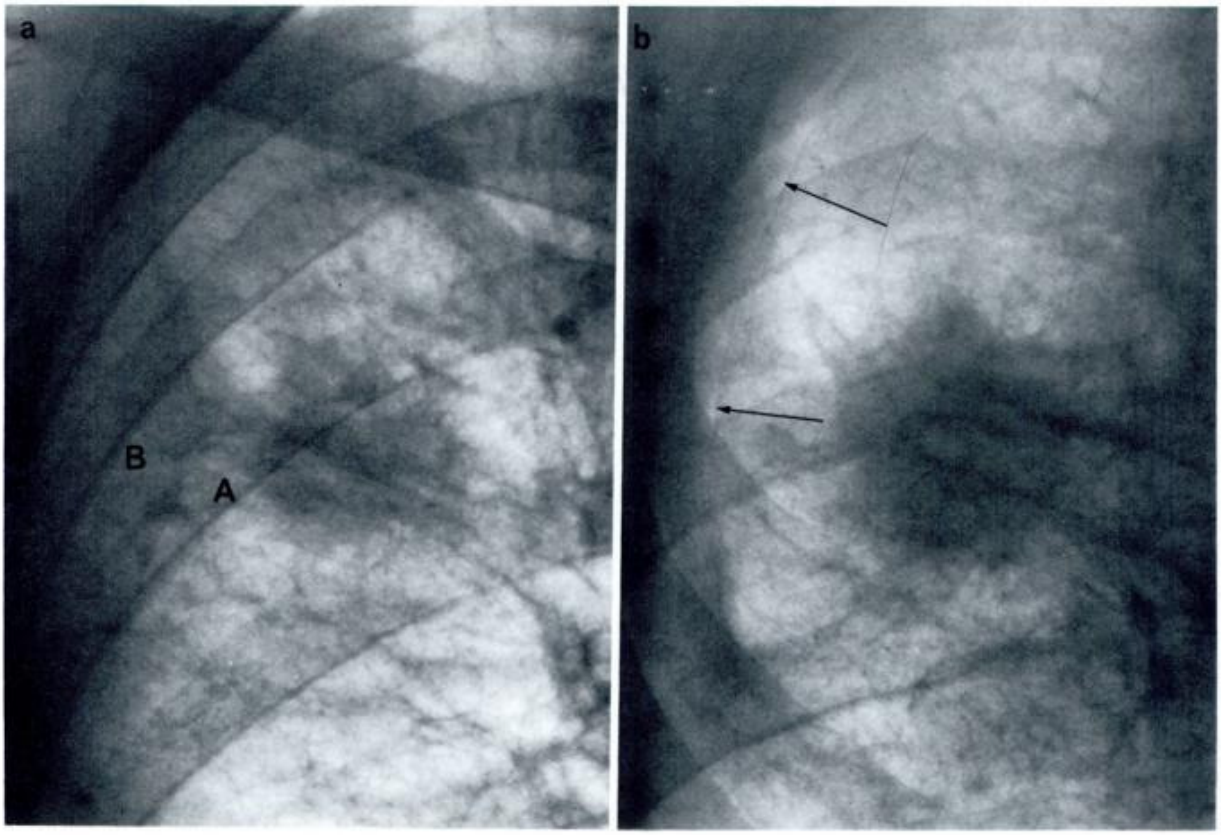

Fig. III: 12. Vanishing "B" zone after injection of air into the pleural space. (*a*) Squamous cell carcinoma in the right lung of a 68-year-old woman. Irregular, tiny, radiating structures and "A" and "B" zones are present. A "B" zone in broad contact with the pleura should not be misinterpreted as pleural thickening or extension of tumour into the chest wall. (*b*) After air was injected into the pleural space, the "B" zone disappeared. Normally thin visceral pleura (arrows) is evident medial to the air cap.

between the "A" and "B" zones a 2 cm long arcade is seen as a slightly undulating line.

The poorly differentiated squamous cell carcinoma in Fig. III: 3 is surrounded by a clearly visible "A" zone, particularly apparent in a left posterior oblique projection (*b*). The "B" zone is seen laterally to the "A" zone between the chest wall and the row of arches (arrowheads).

The "A" zone around the small cell carcinoma in Fig. III: 4 is only about 2 mm wide. Lateral to the tumour is also seen an irregular (5×1.5 cm) radiopacity which represents a "B" zone. The presence of an "A" zone between the tumour surface and this opacity (the "B" zone) is here of decisive importance for the differential diagnosis between a "B" zone on the one hand, and tumour, atelectasis, pleural thickening or bronchopneumonia on the other.

Whenever the increased radiopacity extends to the chest wall, thickening of the pleura becomes an alternate diagnostic possibility to a "B" zone, as in the moderately well differentiated squamous cell carcinoma in Fig. III: 9*c*. In such instances local pleural thickening will not show an opaque line of arches such as in Fig. III: 9*a–c*. A direct proof of the real character of this type of radiopacity can be presented as follows:

The pleomorphic adenocarcinoma seen in Fig. III: 11 shows a typical "B" zone in direct contact with the pleura (Fig. III: 11*a*). In another projection (Fig. III: 11*b*) the tumour is seen surrounded by some radiating thin structures. After air was introduced into the pleural space, the "B" zone disappeared (Fig. III: 11*c, d*, corresponding to Fig. III: 11*a, b*, respectively). The visceral pleura is thin and normal over the lung.

A similar case is shown in Fig. III: 12*a*. This squamous cell carcinoma shows irregular "pleural thickening" (B) lateral to the tumour. After air was introduced into the pleura (*b*), the pleural space is seen to be open, the visceral pleura appears normally thin, and the "pleural thickening" has disappeared.

Finally, a squamous cell carcinoma is seen in Fig. III: 13*a* surrounded by an "A" zone and a "B" zone. The inferior part of the "B" zone shows a sharp borderline. The upper border is unsharp and vanishes

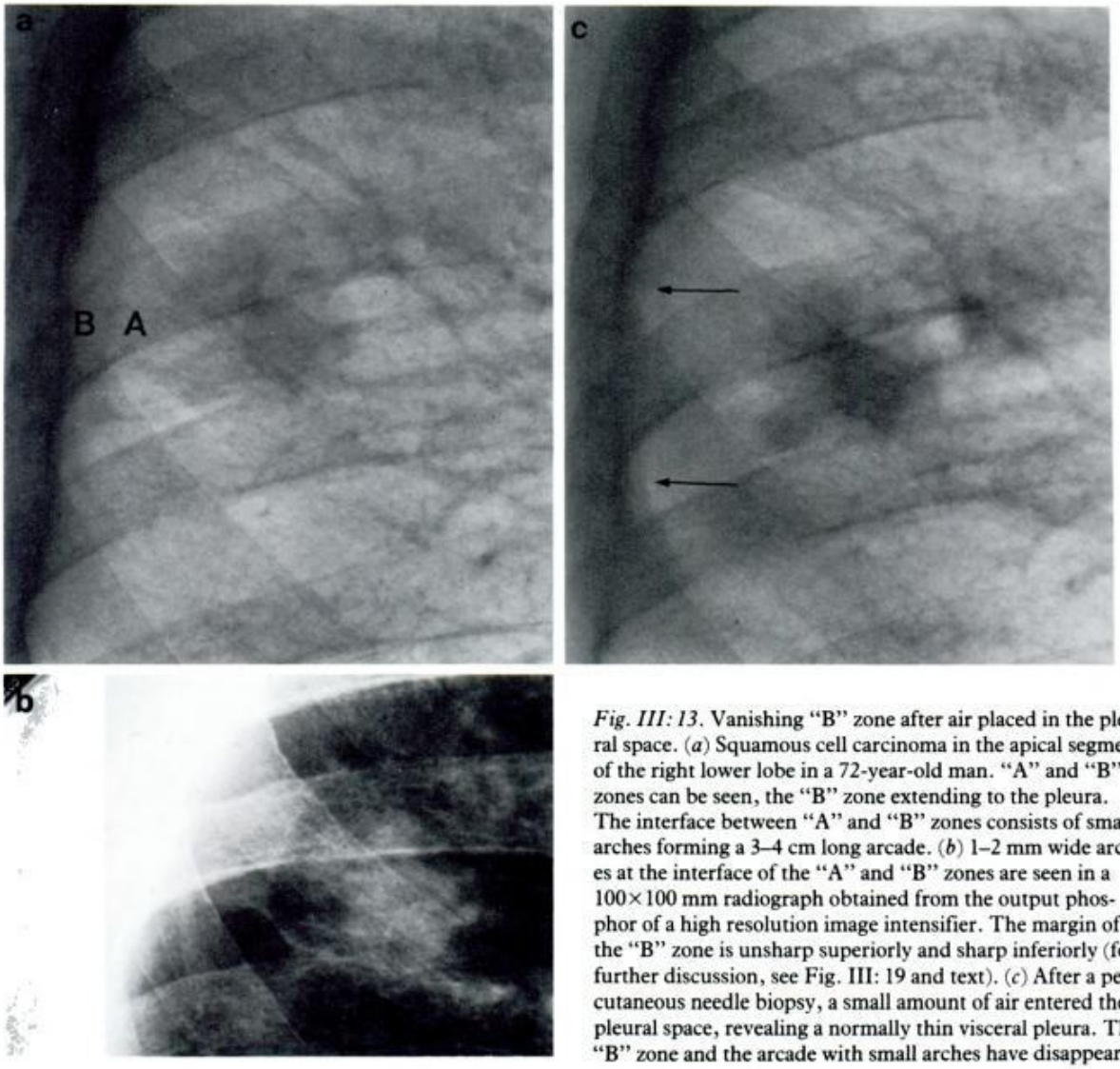

Fig. III: 13. Vanishing "B" zone after air placed in the pleural space. (*a*) Squamous cell carcinoma in the apical segment of the right lower lobe in a 72-year-old man. "A" and "B" zones can be seen, the "B" zone extending to the pleura. The interface between "A" and "B" zones consists of small arches forming a 3–4 cm long arcade. (*b*) 1–2 mm wide arches at the interface of the "A" and "B" zones are seen in a 100×100 mm radiograph obtained from the output phosphor of a high resolution image intensifier. The margin of the "B" zone is unsharp superiorly and sharp inferiorly (for further discussion, see Fig. III: 19 and text). (*c*) After a percutaneous needle biopsy, a small amount of air entered the pleural space, revealing a normally thin visceral pleura. The "B" zone and the arcade with small arches have disappeared.

diffusely. The small arches form an arcade between the "A" and "B" zones, not easily seen in Fig. III: 13*a*. Using a high resolution image intensifier it became possible to identify the small arches (Fig. III: 13*b*). After a small amount of air was introduced into the pleura, the "B" zone disappeared (Fig. III: 13*c*). The pleural space is seen to be free and the visceral pleura normally thin.

These examples indicate the practical importance of recognizing a "B" zone. Hazy radiopacity peripheral to a tumour does not necessarily represent the usually considered possibilities of pneumonia, atelectasis, pleural thickening or a direct overgrowth by the tumour. It may be caused by a "B" zone which disappears when the pleural space is opened.

Already these observations suggest the origin of the "B" zones. In some way tissue fluid must be involved. If increased fluid in lung peripheral to a tumour is caused by lymphatic stasis, then an early consequence of such stasis should be widening of the lymphatic channels peripheral to the tumour. An example of this possibility is suggested in Fig. III: 14. A rather large tumour is seen in the posterior basal segment of the right lower lobe. In pulmonary parenchyma distal to the tumour a "B" zone is seen, only 1–2 mm wide but 10 cm long. Irregularly non-branching structures are evident in the parenchyma between the tumour and the "B" zone. These structures are each a millimetre wide, linear, and have been interpreted as widened interlobular spaces (arrows), analogous to Kerley's B-lines (4). The radiographic appearance of this narrow "B" zone differs from that of a normal interlobar pleura. Comparison can also be noted superiorly in Fig. III: 14, where a portion of normal interlobar pleura between the middle and upper lobes is seen (*P*).

In experimental attempts to produce at least some of

Fig. III: 14. Large carcinoma in the lower right hilar region of a 52-year-old man. A 1.5 mm thick and 10 cm long "B" zone (B) is seen in the lung parenchyma 1–1.5 cm from the chest wall. Between the tumour and the "B" zone some nonbranching structures, each a mm wide, can be seen (arrows), interpreted as widened interlobar spaces due to stasis of lymph. Along the lateral chest wall and in the interlobar fissure (*P*) there is no evidence for an increased amount of pleural fluid.

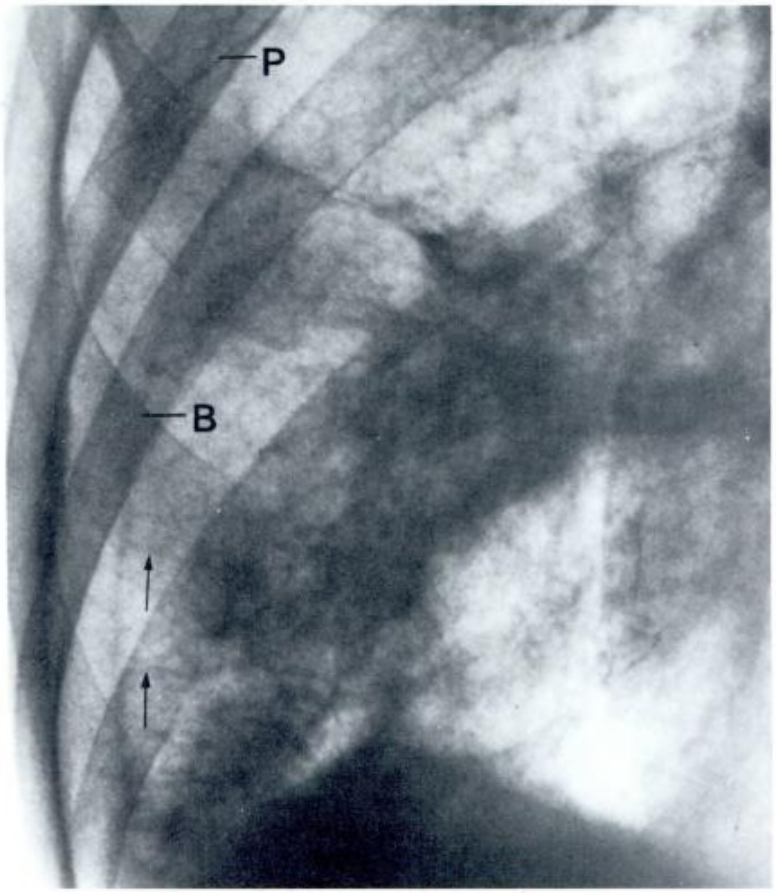

Fig. III: 15. Experimental demonstration of focal pulmonary oedema by an artificial "tumour" in a dog lung, and the subsequent disappearance of the oedema. (*a*) Lateral projection, anterior and cranial portions of a dog's chest. (*b*) After percutaneous injection of 1.5 ml of a polymerizing plastic material mixed with barium sulphate powder, an artificial radiopaque tumour was produced. (*c*) After three months an infiltration simulating atelectasis or thickened pleura was seen between the pleura and the plastic tumour. (*d*) The post mortem specimen showed no pleural thickening or infiltration in the lung corresponding to the infiltration seen in vivo. The infiltration has been interpreted as local oedema due to blocking of the draining lymph channels of the lung by the plastic "tumour". The occurrence and disappearance of the infiltrate in the dog, as in living patients, is further discussed in Fig. III: 16.

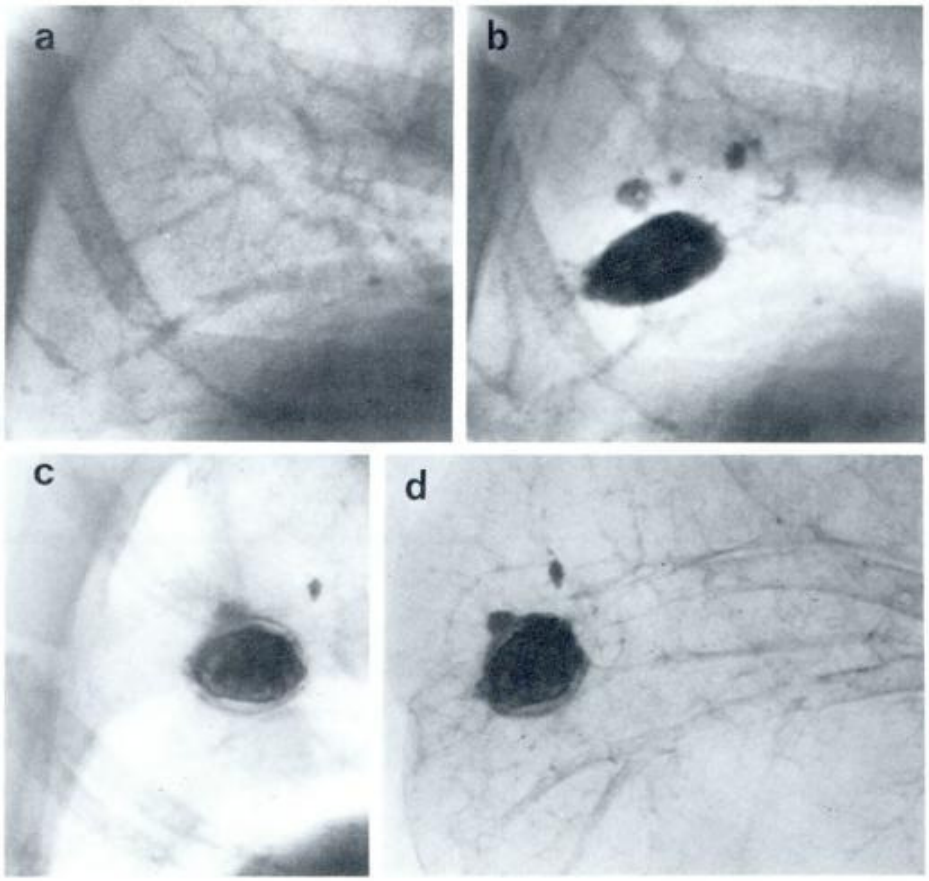

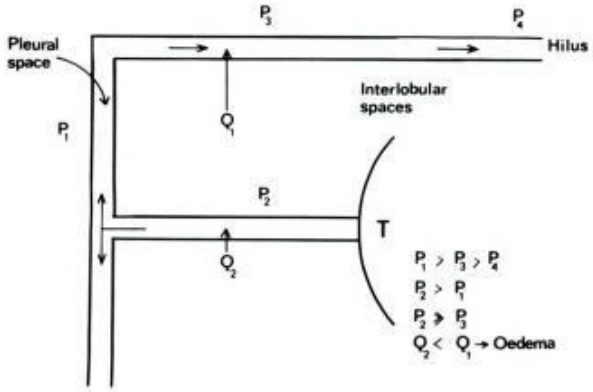

Fig. III: 16. Proposed mechanism for local oedema peripheral to a tumour in lung. A tumour (*T*) may obstruct some of the draining lymphatic channels and interlobular spaces between pleura and hilar lymph nodes. Local pressures (*P*) will change, altering flow of tissue fluid (*Q*). Oedema will occur between the pleura and the tumour. For further explanation, see text.

the radiographically observed changes, experiments were performed in ten dogs.

On the preliminary assumption that a tumour mechanically blocks lymph drainage, "tumours" were produced in the dog lungs by percutaneous injection of a polymerizing material (Crystic Tea® with an accelerator Butanox®) made of liquid plastic admixed with barium sulfate powder. After the injection of 1.5 ml into the lung parenchyma, the material formed a solid, radiopaque "tumour".

In Fig. III: 15 *a*, a lateral view is seen of a dog's anterior upper lobes before the injection. Fig. *b* shows the solid plastic "tumour" one hour after the injection. In Fig. *c*, three months later, the plastic "tumour" has shrunken and lies in a cavity. Between the "tumour" and the pleura is seen an infiltration simulating pleural thickening or atelectasis. The dog was then desanguinated under deep general anaesthesia. The removed lung did not show any changes in the pleura. The radiograph seen in Fig. *d* was taken after gentle inflation of the specimen. No thickening of the pleura, atelectasis or infiltration can be seen in the lung. At microscopic examination it was found that the plastic "tumour" was lying as a free body in a cavity which was outlined by a fibrous membrane. Otherwise no pathological changes were observed in the surrounding lung parenchyma or the pleura. In five of the ten dogs, radiographs revealed a "B" zone peripheral but not adjacent to the tumour, yet post mortem analysis showed no abnormalities in the apparently involved lung or pleura.

These experiments with plastic "tumours" in dog lungs have convinced the author that these "tumours" block the lymphatic drainage between the pleural space and the hilum, thereby producing local oedema by stasis. As soon as the pleural space is opened, whether in vivo or post mortem, fluid must leave the "B" zone due to retraction of the lung parenchyma

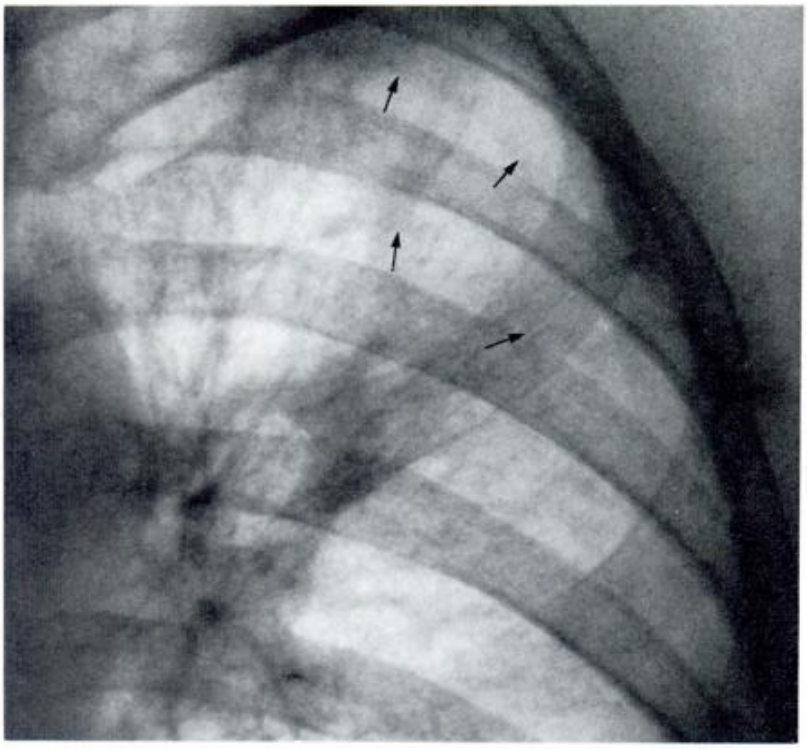

Fig. III: 17. Two incongruent "B" zones. Centrally located, cavitating carcinoma in a 63-year-old man. The two "B" zones (arrows) are thin, each about 2 mm wide and several cm long. For explanation, see Fig. III: 19.

and loss of the previously locally elevated turgor pressure in the lung. The pleural fluid is drained, at least in part, from the pleural space via the lymphatic channels in the interlobular and perivascular spaces toward the hilar lymph nodes and mediastinal lymphatic channels (2, 12).

The direction of flow from the pleural space into the interlobular lymphatics of the lung was earlier studied by the author in dogs by means of lipiodol injection into the pleural space. Lymphography in man later also showed (5) that after lipiodol was injected slowly into the azygos lymph node via a thin needle, respiration influenced its movement in the lymphatic channels of the mediastinum. During expiration the lymphatics are kinked and the flow of lipiodol decreased. During inspiration the lymphatics become stretched and the forward flow of lipiodol increased.

When a tumour grows in pulmonary parenchyma and blocks some of the lymphatics, stasis with local oedema can be expected to occur, as indicated in Fig. III: 16. A decreasing mean pressure gradient $P_1 > P_3 > P_4$ will be changed by a blocking tumour (T), so that the direction of emptying of tissue fluid in the blocked area will be altered. The pressure P_2 of the tissue fluid close to a blocked draining channel must be elevated above the pleural pressure P_1 before it can enter the blocked channel. This alteration suggests the flow of tissue fluid Q_2 diminishes. Fluid collects in the lung tissue and lymphatic channels between the tumour and the pleura.

In lung only partly within the blocked area or nearly freely emptying, less oedema can be expected. This consideration can explain why the border of the "B" zone is diffuse or fading in certain portions. A sharp borderline can, however, also be present in certain sites where the oedema extends toward obliterated interstitial spaces or interfaces between two pulmonary segments or lobes.

Wherever lymphatic collaterals are extensive in relation to the size of blocking mass, demonstrable lymphoedema may not be present. This consideration may explain the observed rarity of radiographic "B" zones

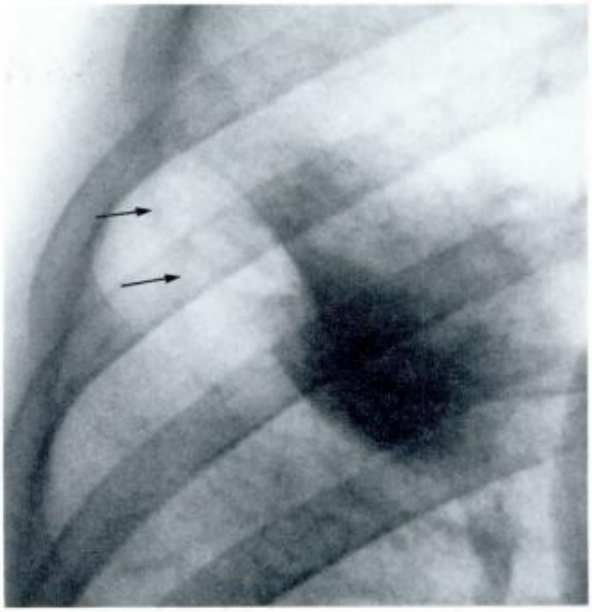

Fig. III: 18. Squamous cell carcinoma in a 76-year-old woman in the upper part of the right lung. Two arcades, each with small arches, appear as incongruent sectors of circles (arrows). For explanation, see Fig. III: 19.

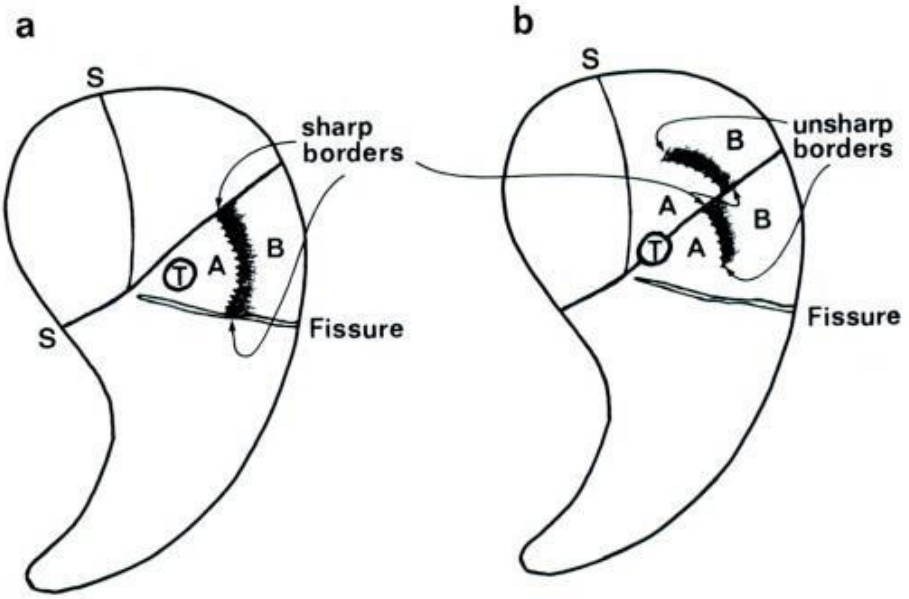

Fig. III:19. Diagrammatic explanation of Figs. III: 17 and 18. Transverse section through left upper lobe. (*a*) Tumour (T) located centrally in a segment, not involving segmental border (S) or interlobar fissue. Single "A" and "B" zones then develop. (*b*) Tumour growing over the interface (S) between two segments may give rise to two separate "B" zones. That part of the "B" zone which reaches segmental or lobar demarcation will end sharply. Otherwise it will appear unsharp (see also Fig. III: 13 *a*). Differences of distance between tumour and "B" zones may develop from differences of hydrostatic counterpressure in different parts of the lung vs. electroosmotic outflow of water from the tumour.

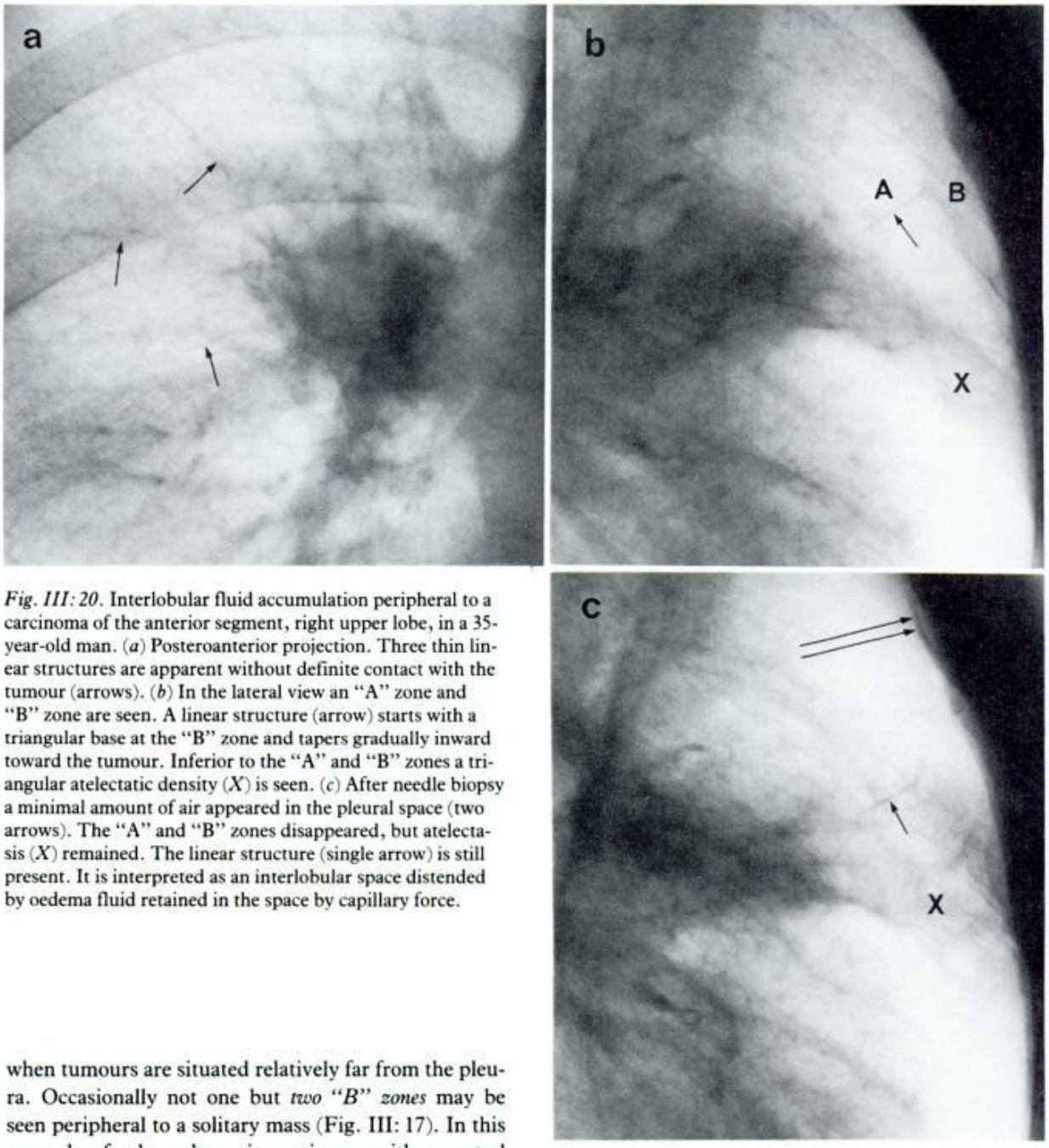

Fig. III: 20. Interlobular fluid accumulation peripheral to a carcinoma of the anterior segment, right upper lobe, in a 35-year-old man. (*a*) Posteroanterior projection. Three thin linear structures are apparent without definite contact with the tumour (arrows). (*b*) In the lateral view an "A" zone and "B" zone are seen. A linear structure (arrow) starts with a triangular base at the "B" zone and tapers gradually inward toward the tumour. Inferior to the "A" and "B" zones a triangular atelectatic density (*X*) is seen. (*c*) After needle biopsy a minimal amount of air appeared in the pleural space (two arrows). The "A" and "B" zones disappeared, but atelectasis (*X*) remained. The linear structure (single arrow) is still present. It is interpreted as an interlobular space distended by oedema fluid retained in the space by capillary force.

when tumours are situated relatively far from the pleura. Occasionally not one but *two "B" zones* may be seen peripheral to a solitary mass (Fig. III: 17). In this example of a bronchogenic carcinoma with a central air-containing cavity, the "B" zones are seen as two curved structures, about 2 mm thin and several cm long. Two arcades may sometimes appear as incongruent sectors of circles. Fig. III: 18, for example, shows a squamous cell carcinoma extending between the right upper and lower lobes with incongruent arcades between corresponding "A" and "B" zones.

When local lymphoedema is viewed as one of the important mechanisms for producing "B" zones, it is easy to explain the development of two "B" zones by only one tumour. This phenomenon probably depends on the location of the tumour in relation to segmental anatomy of the lung, schematically illustrated in a horizontal cross section of the left lung in Fig. III: 19. For instance, if a tumour (*T*) is centrally located in the anterior segment of an upper lobe (Fig. III: 19 *a*), the site of any local lymphoedema will be somewhere between the pleura and the tumour. Sharply demarcated borders may then develop against any limiting structure, e.g., the interlobar pleura or an interlobular septum. In Fig. III: 19 *b* the tumour is situated in two adjoining pulmonary segments. Such a location will cause local obstruction of lymph flow in different parts

of the segments according to differences in sizes of the segments, hydrostatic pressures, etc. Such differences explain why a "B" zone sometimes shows one sharp edge while the other may be unsharp and appears to vanish into the lung parenchyma.

The fact that the lymphoedema ("B" zone) does not extend to the edge of the tumour will be discussed rather extensively later on. Arches and arcades, radiating structures, displacements of tumour-surrounding structures, narrowing of vessels, as well as the formation of the "A" zones will be seen to relate to the development of pathological electric polarization which, under certain conditions, may occur in a tumour or tumour-like lesion.

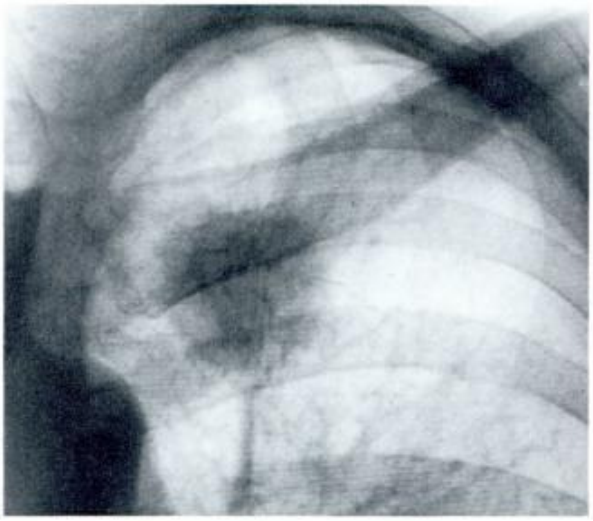

Fig. III: 21. Well differentiated squamous cell carcinoma in a 66-year-old man. Extremely thin, radiating structures make the tumour surface appear unsharp and "hairy".

D. Interlobular fluid accumulation

In the course of performing percutaneous needle biopsies of pulmonary masses surrounded by "B" zones, a frequent observation has been that the zones vanish totally (or nearly totally) whenever air enters the pleural space. Even small pneumothoraces induce this change.

The case shown in Fig. III: 20 (bronchogenic carcinoma, right upper lobe) is particularly instructive because it illustrates the effect of a small pneumothorax on the "A" and "B" zones and on three, thin, rather distinct, linear structures which appear separated from the surface of the tumour, as seen on frontal view (*a*). In the lateral view (*b*) one of these structures is seen to have a triangular or funnel-shaped base in the "B" zone and a line gradually tapering inward in the "A" zone (arrow). After needle biopsy of the tumour, a 2 mm broad pneumothorax (two arrows) appeared (*c*). Most of the "A" and "B" zones then disappeared, including the funnel-shaped base of the thin line, which still can be seen isolated from the centrally located tumour (single arrow). The density (*X*), inferior to the "A" and "B" zones and appearing to connect the tumour and pleura, has been interpreted as focal atelectasis not influenced by the pneumothorax. The thin line in the "A" zone has been interpreted as local fluid in an interlobular space on the basis of tapering shape, broad connection with the border of the "B" zone, and absence of contact with the tumour. The retention of the thin line in spite of disappearance of most of the fluid speaks for such an interpretation, because fluid in the interlobular space may be retained by capillary force.

E. Radiating structures

These structures, when present, emerge from the surface of the lesion and show a wide range of appearances. The radiating structures may be coarse or thin (Figs. III: 1, 3, 9–11, 21–27). Often they extend several centimetres out into the pulmonary parenchyma. Sometimes they are very short. Often they are unevenly

Fig. III: 22. Small primary adenocarcinoma in a 65-year-old man. Short, blunt, radiating structures emanate from the tumour.

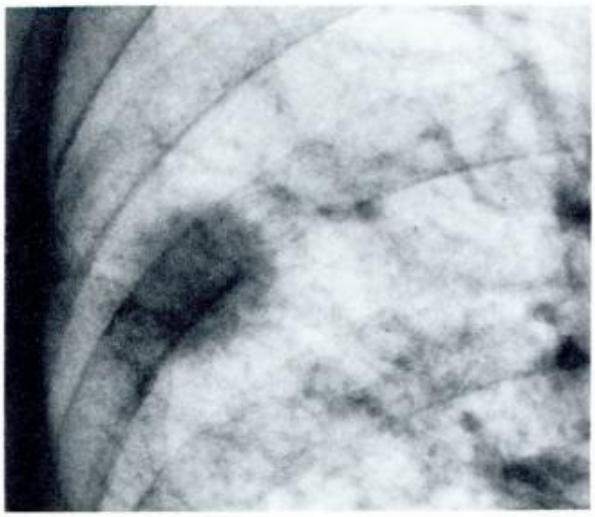

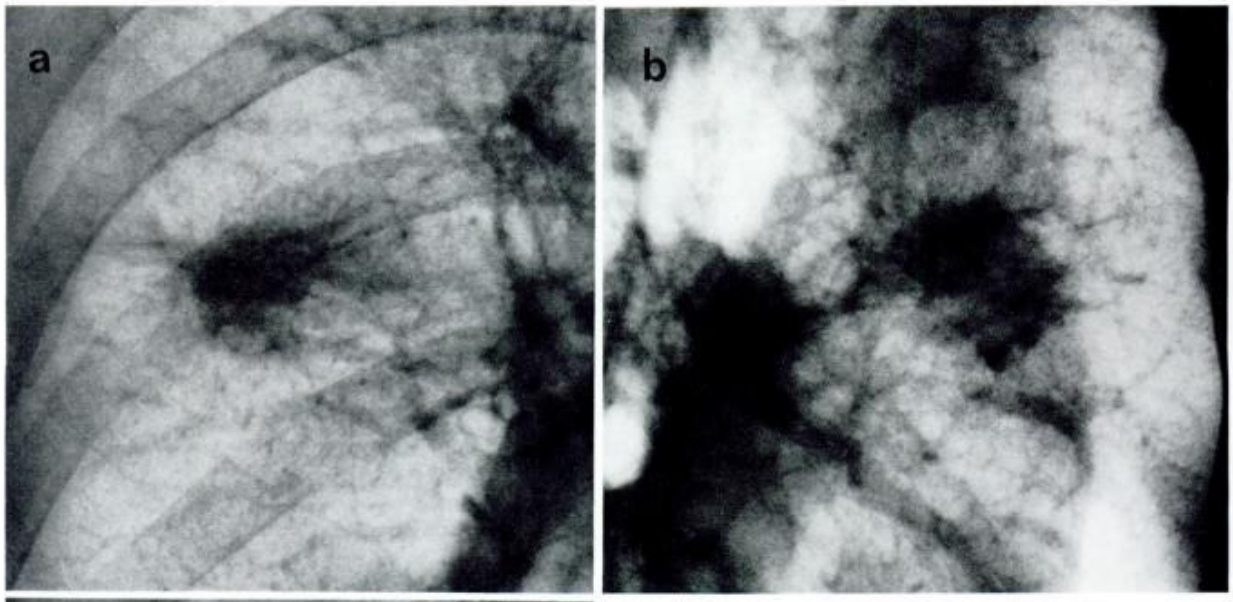

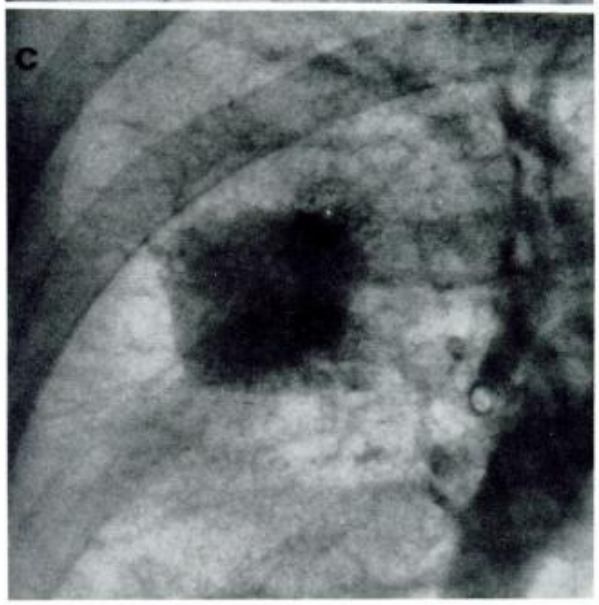

Fig. III: 23. Well differentiated squamous cell carcinoma in a 63-year-old woman. (*a*) Posteroanterior projection. Granular radiating structures surround the tumour. (*b*) Lateral projection. (*c*) Posteroanterior view one year later (the patient had refused treatment). In spite of expanding growth of the tumour, structures are still seen radiating from its surface.

Fig. III: 24. Metastatic breast carcinoma in an 82-year-old woman. Numerous, long, coarse radiating structures are oriented perpendicular to the surface of the tumour. No preformed channels in the lung, such as lymphatics, have this course.

Fig. III: 25. Metastatic adenocarcinoma in the left upper lobe of a 58-year-old woman. The tumour is adjacent to the pleura. Fine structures radiate more or less perpendicular to the surface of the tumour. Their courses diverge with respect to the hilum, whereas lymphatics and other preformed channels of the lungs have a convergent course. The direction of the radiating structures is therefore related mainly to the surface of the tumour and not to the underlying gross morphology of the lung.

Fig. III: 24

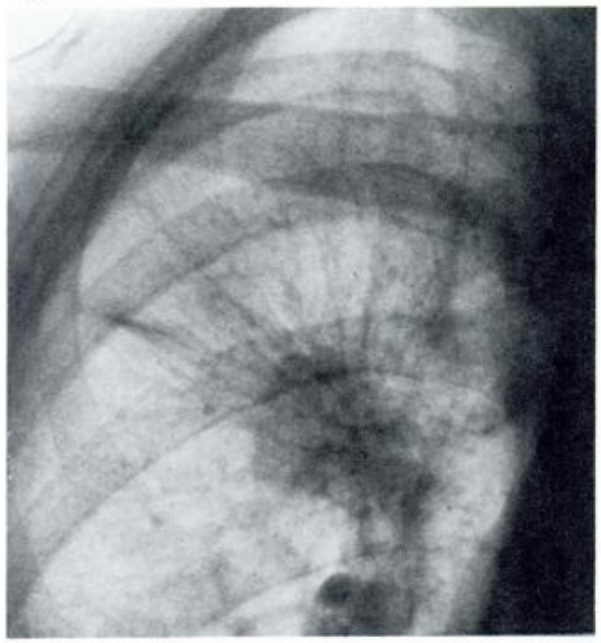

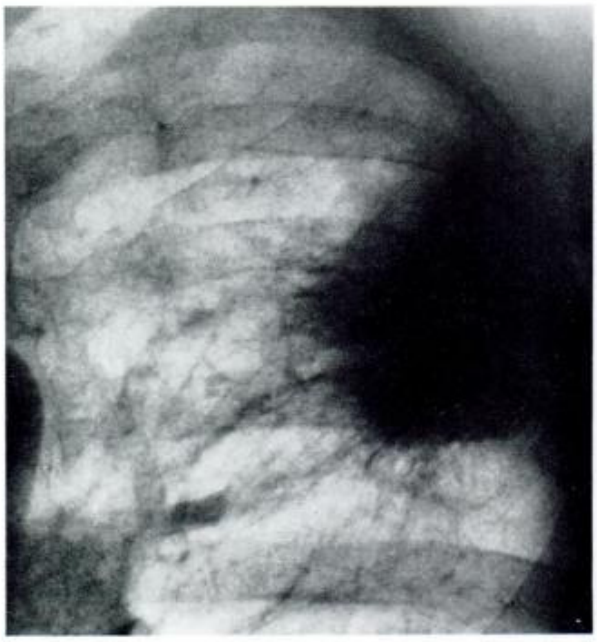

distributed around a lesion. Radiating structures are not necessarily seen when "A" and "B" zones are present (Fig. III: 2, 4–7, 18).

Radiating structures can be extremely thin. In Fig. III: 21 the surface of a well differentiated squamous cell carcinoma looks "hairy".

The structures can be very short and blunt (Fig. III: 22, a small primary adenocarcinoma). Note that this tumour is also surrounded by a 0.5–1 cm broad "A" zone.

Radiating structures occasionally appear discontinuous, so the periphery of a tumour may seem grainy (Fig. III: 23, a well differentiated squamous cell carcinoma). This case also illustrates the behaviour of the structures around a tumour as it grows. At initial presentation (Fig. III: 23 *a*, *b*), radiating structures and a certain displacement of vessels away from the tumour are evident. The patient refused treatment. One year later (Fig. III: 23 *c*), vessels are still displaced around the tumour and radiating structures remain perpendicularly arranged around its surface despite considerable growth of the tumour. Now a clearly visible "A" zone is also present. This case shows that both radial arrangement of structures around the tumour and the "A" zone have not developed as a result of tumour collapse or contraction, such as might be caused by internal necrosis with subsequent inward retraction of surrounding lung structures. As the tumour grew, so did the radiating structures.

Radiating structures can be numerous, long, and rather coarse (Fig. III: 24, metastatic breast carcinoma). They are consequently not a sign of primary cancer. They are arranged more or less perpendicularly to the surface of a tumour (Figs. III: 25 and 26).

An important feature of the radiating structures is that *their directions are generally independent of existing preformed channels in the lung*. The radiating structures develop perpendicularly to the surface of the lesion. No preformed channels such as lymphatics can explain the configurations seen in Figs. III: 21–26.

Tumour cells are sometimes seen histologically in the radiating structures close to the tumour surface (3). Often no tumour cells are present in the distal parts of the radiating structures, which consist of "fibrotic" material.

The independence of the radiating structures from existing morphologic channels of the lung can be seen especially well for tumours situated close to the pleura. For example, the tumour in Fig. III: 25 is situated in the left upper lobe close to the pleura. Radiating structures appear more or less perpendicular to the surface of the tumour. They diverge in relation to the hilum. Draining lymph vessels, on the other hand, mainly converge toward the hilum.

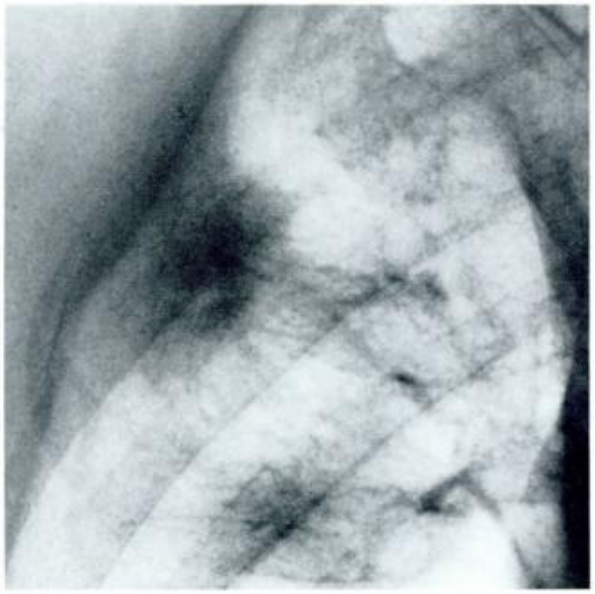

Fig. III: 26. Poorly differentiated squamous cell carcinoma in the right upper lobe of a 60-year-old man. The tumour, adjacent to the pleura, shows radiating structures at its surface. Their courses diverge, indicating that they are not following pulmonary lymphatic channels.

F. Coarse radiating structures: lamellae and infiltrated strands

Some radiating structures around pulmonary neoplasms often appear denser or thicker than neighbouring radiating structures. A representative example is seen in Fig. III: 27, projected over the tumour as a dense line. In Fig. III: 9 *a–c*, which represents different projections of the same case, at least two such structures are seen. They are typically seen at the edge, outside the tumour (Fig. III: 9 *a*) or projected over the tumour (Fig. III: 9 *a–c*), depending on the projection used. In Fig. III: 27 *a* of the same patient, a 10° left anterior oblique projection reveals two crossing, linear, dense structures projected over the tumour. The posteroanterior projection (Fig. III: 27 *b*), however, shows linear structures mainly separated from the tumour. The obliquely crossing linear structures are outside the tumour and extend through the "A" zone to the "B" zone (Fig. III: 27 *c*). In this projection the tumour also shows an air-containing cavity and an indentation on its inferior margin.

Central necrosis causing partial collapse of a tumour is known to occur from time to time. In such instances, structures close to the surface of the tumour

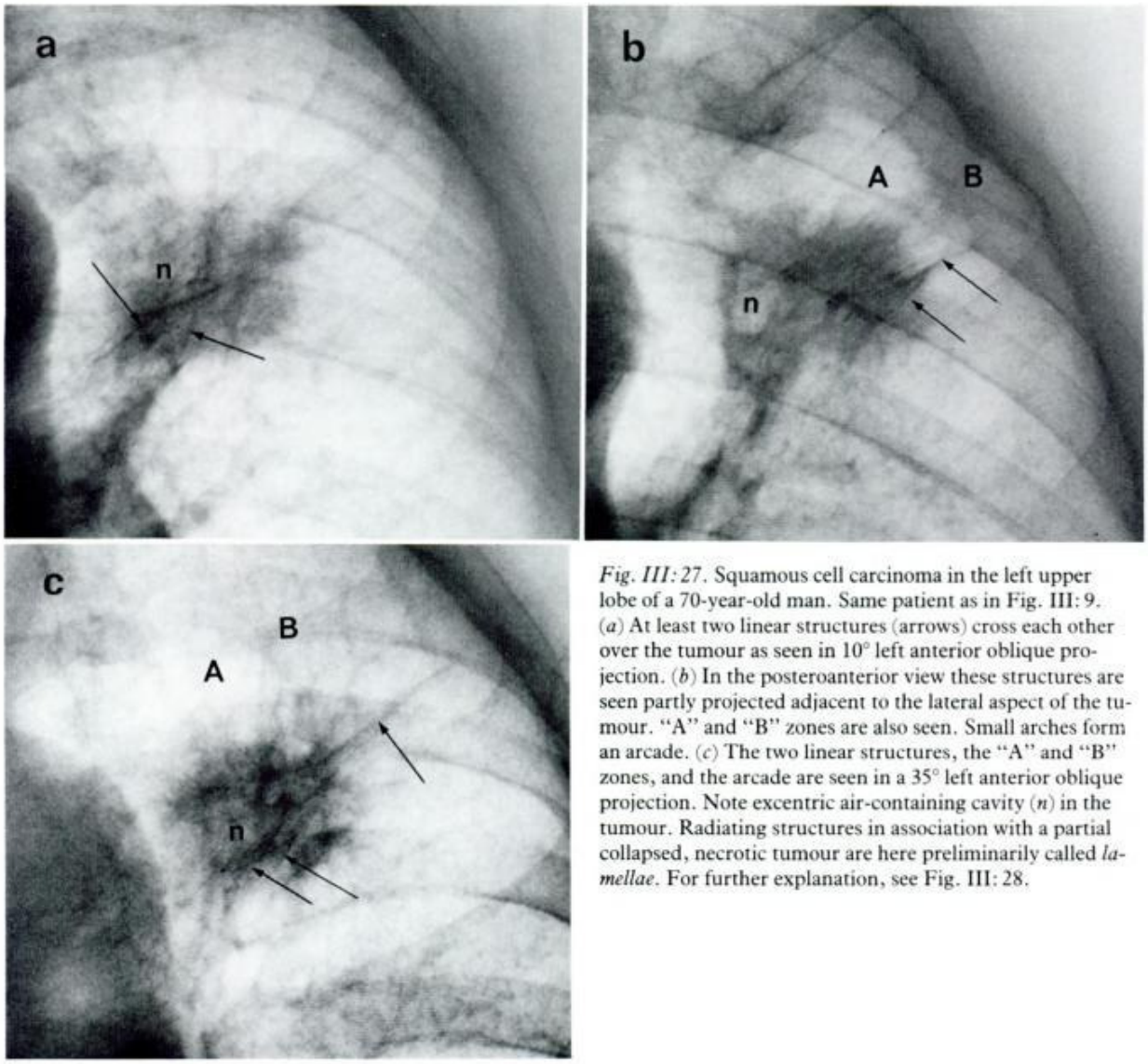

Fig. III: 27. Squamous cell carcinoma in the left upper lobe of a 70-year-old man. Same patient as in Fig. III: 9. (*a*) At least two linear structures (arrows) cross each other over the tumour as seen in 10° left anterior oblique projection. (*b*) In the posteroanterior view these structures are seen partly projected adjacent to the lateral aspect of the tumour. "A" and "B" zones are also seen. Small arches form an arcade. (*c*) The two linear structures, the "A" and "B" zones, and the arcade are seen in a 35° left anterior oblique projection. Note excentric air-containing cavity (*n*) in the tumour. Radiating structures in association with a partial collapsed, necrotic tumour are here preliminarily called *lamellae*. For further explanation, see Fig. III: 28.

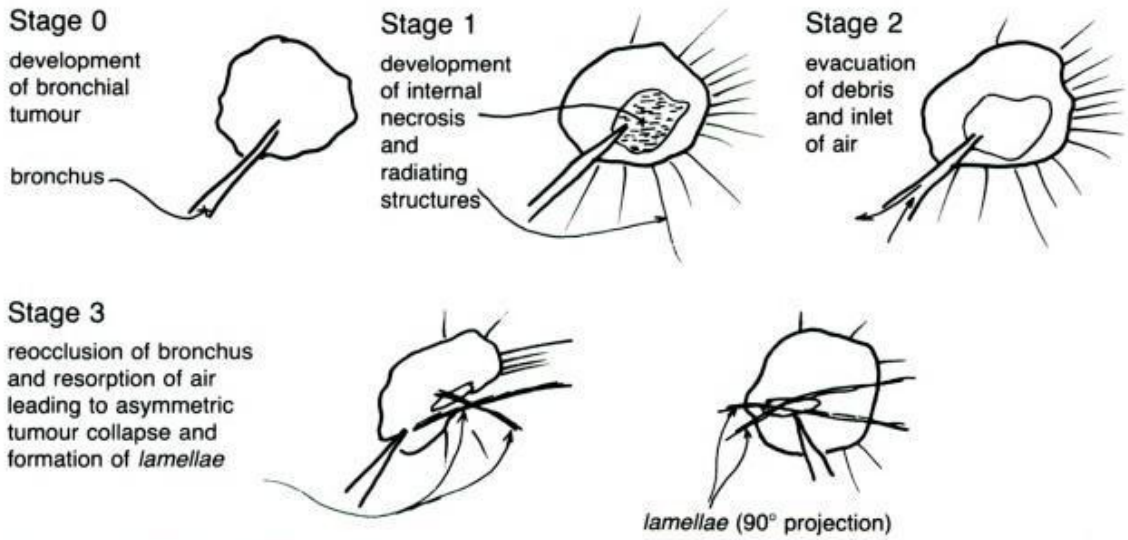

Fig. III: 28. Proposed principle of formation of *lamellae*. Stage 0: A bronchus enters a pulmonary mass. Stage 1: Excentric local necrosis develops in the tumour and thin radiating structures develop perpendicular to its surface. Stage 2: Necrotic debris leaves the tumour via the bronchus and is replaced by air. Stage 3: The bronchus becomes blocked, leading to resorption of the air in the tumour cavity. Asymmetric collapse of the tumour tissue will then produce local conglomeration of radiating structures in the surrounding lung tissue. *Lamellae* developed in this way may in certain projections appear as if they are crossing the tumour.

may undergo positional changes. Already developed radiating structures will then show partial displacements in relation to each other, as is interpreted to have been the case in Fig. III: 27. Fig. III: 28 summarizes this explanation of the pathogenesis of the dense linear structures:

A tumour (Stage 0) develops central necrosis and radiating structures into the surrounding pulmonary parenchyma (Stage 1). Necrotic material empties through the supplying bronchus and air enters the remaining cavity (Stage 2). When the bronchus later becomes blocked, presumably by growth of the tumour, the air resorbs and the tumour partially collapses. As a consequence, the radiating structures become displaced (Stage 3). This process gives rise to coarse, asymmetrical, dense, linear structures, which are here called *lamellae*. They appear in radiographs either at the edge of the tumour or appear as if they were crossing it.

Other mechanisms for the development of lamellae from radiating structures are also possible. For instance, altered water content or tissue atrophy may cause local changes in lung tissue. Local electroosmotic effects on the distribution of pulmonary water around a mass will later be presented as one of the integrated factors in the development of the radiolucent "A" zone (Chapter IX). Vascular effects, connected with the development of local tissue atrophy within the "A" zone, will be treated in Section G and in Chapter XIV. These effects, in brief, comprise field-induced changes on local blood supply around a locally polarized tissue within a closed electric circuit.

Partial displacement of structures in the lung is also known to take place in local emphysema. Such displacement is probably the case around the necrotizing, poorly differentiated, cavitary, squamous cell carcinoma seen in Fig. III: 29. In the selected left posterior oblique projection, five coarse and broadbased radiating structures can be seen perpendicular to the tumour surface. In this case the mass is clearly not collapsed, suggesting that the coarse radiating structures derive their shape and direction from emphysematous changes in the pulmonary parenchyma.

Coarse radiating structures can therefore develop around a tumour without any appreciable partial collapse of a necrotic centre. When emphysema is present in lung around a tumour, the structures may be called *infiltrated strands*. In this way a distinction may be suggested regarding the development of coarse radiating structures.

The idea has been forwarded in the literature (8–10) that "linear shadows" crossing a tumour is a diagnostic sign of malignancy. In the author's opinion, most linear structures which seem to cross a tumour are merely lamellae superimposed over it. Obliquities of radiographic projection are usually essential for proper appreciation of the linear changes. When a linear structure appears to cross through a tumour, it is likely that this structure is outside the tumour. There are virtually no reasons why a malignant tumour should develop a dense "linear structure" crossing through it.

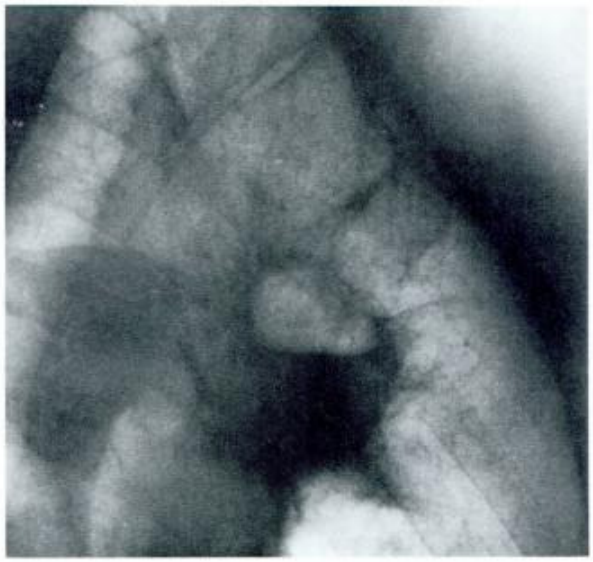

Fig. III: 29. Poorly differentiated squamous cell carcinoma in the left upper lobe of a 78-year-old man (left posterior oblique projection). A large cavity in the tumour contains air and fluid. Lung surrounding the tumour is irregularly emphysematous. Along the anterolateral aspect of the tumour, broad-based triangular structures radiate among emphysematous bullae. Although necrotic, the tumour has not collapsed. In such case the radiating structures may be called *infiltrated strands*.

G. Narrowing and circular displacement of vessels around lung tumours

The reader may already have noticed that vessels around some of the presented tumours are narrow, tapered and of irregular calibre. In addition the vessels seem to deviate in a circular fashion as if they were avoiding the tumour (Fig. III: 8). These radiographically observable structural changes will now be described in connection with the illustrated cases in Figs. III: 30–34.

A metastasis from a breast carcinoma (Fig. III: 30) shows circularly arranged, rather thick vessels which, on first glance, simulate an "A" zone. No clear radiographic evidence, however, of increased radiolucency

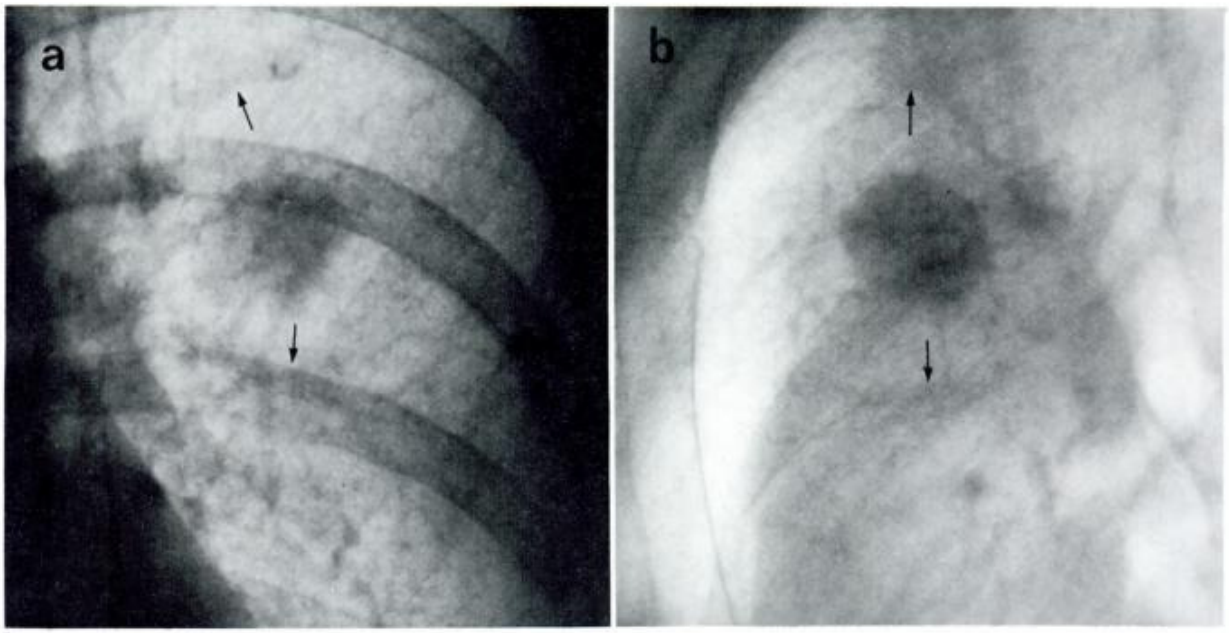

Fig. III:30. Circular displacement of vessels around a tumour. Metastatic breast carcinoma, anterior segment, left upper lobe, in a 53-year-old woman. (*a*) Posteroanterior projection. (*b*) Lateral projection. Circularly running vessels (arrows) are seen 1–2 cm from the surface of the tumour.

is evident in the area between the tumour surface and the circularly arranged vessels.

A poorly differentiated squamous cell carcinoma (Fig. III: 31) is seen in the anterior segment of the left lower lobe. Some vessels appear narrow, as seen superior to the tumour in the frontal view (*a*). In the lateral view (*b*), large vessels superior to the tumour appear displaced away from its surface. Anterior to the mass is a striking lack of small vascular branches. At least two fairly large vessels are considerably narrowed and

Fig. III:31. 47-year-old man. Poorly differentiated squamous cell carcinoma, anteromedial basal segment, left lower lobe. (*a*) Posteroanterior projection. Lung tissue close to the surface of the tumour shows absence of large vessels. (*b*) In the lateral view large vessels superior to the tumour are seen displaced away from its surface. Around the tumour are also seen locally narrowed, irregular vessels (arrows).

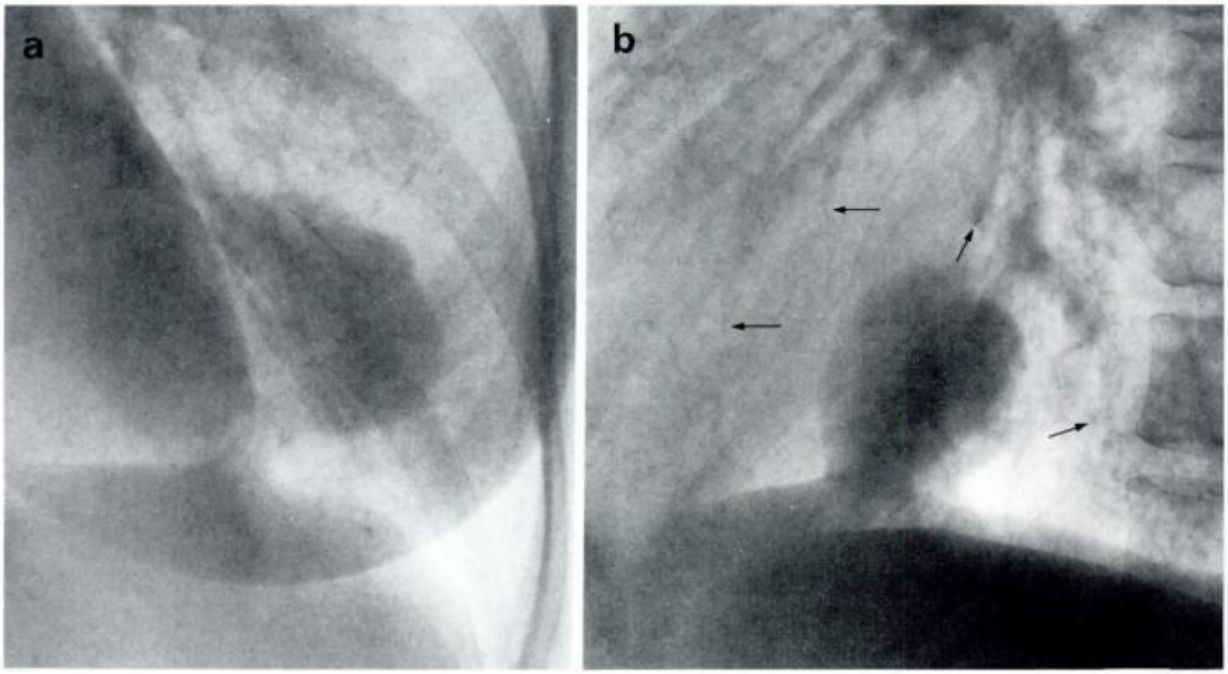

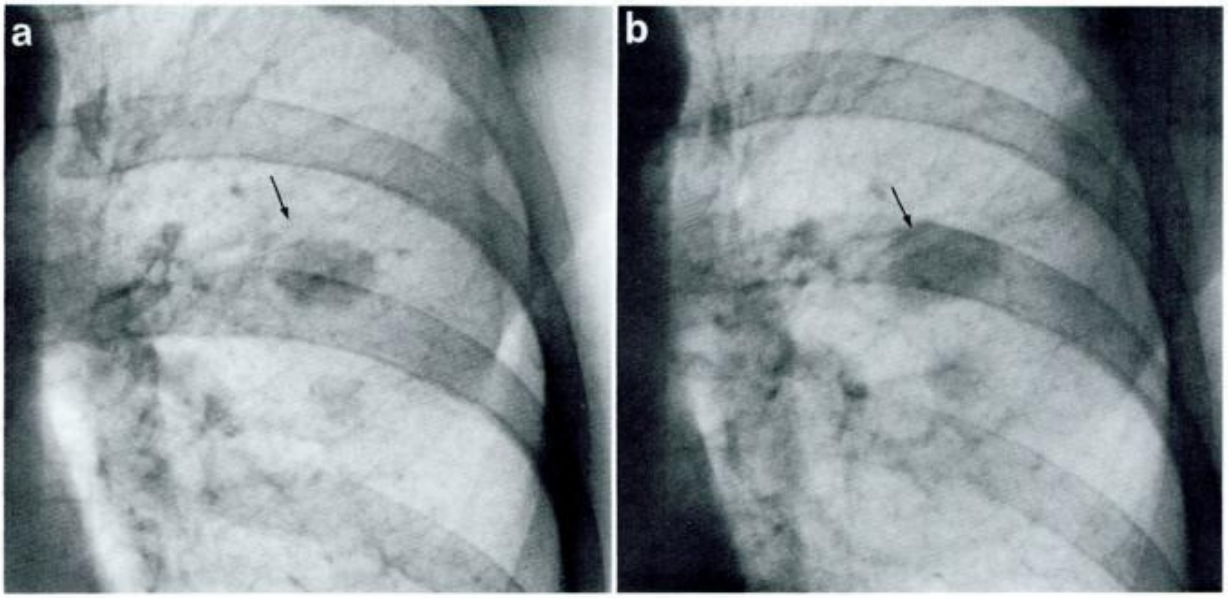

Fig. III: 32. Three metastases from carcinoma of the breast in a 55-year-old woman. (*a*) The largest tumour is surrounded by vessels (arrow). A translucent ring, 2–4 mm broad, surrounds the tumour. (*b*) Nine months later the tumours have grown. The large metastasis still shows a 2–4 mm avascular zone. The vessels superior to this zone are now stretched (arrow). Two vascular branches medial to the tumour have moved apart. The calibres of vessels appear decreased within a region of 5–6 cm diameter around the tumour.

peripherally irregular. By their slightly anterior deviation from the tumour they also give a visual impression of a radiolucent zone anterior to the mass. The average visual radiographic density, however, in this area is not clearly decreased.

The development of narrow, tapered, irregular and circularly displaced vessels is preferably studied by systematic inspection of radiographs from different times in the natural history of the tumours. For instance, in Fig. III: 32 three metastases from a breast carcinoma are seen in the left lung. The large central metastasis is surrounded by (*a*) circularly positioned vessels (arrow) and a zone, 2–3 mm broad, free of vessels. Nine months later (*b*) all three metastases have increased in size. The largest tumour has increased in length from 18 to 23 mm. The vessel above it (arrow) appears increased in length, as if this vessel had been stretched. Note that the distance to the tumour is unchanged. Another vessel, branching medial to the tumour, also undergoes progressive displacement of its branches away from the tumour during the observation period. A comparison of small vessels within 5–6 cm of the tumour also shows that a regional general narrowing of vessels has developed during the nine months interval.

Another example is illustrated in Fig. III: 33. Fig. *a* shows the left lung of a 46-year-old man in 1962. The vessels have smooth walls and ordinary course and calibre. Eleven years later (*b*), a small tumour is seen in the left lung. The vessels in the superomedial part of the lung seem to have the same calibre as in 1962. Some vessels already are tending to deviate away from the region of the tumour. Nine months later (*c*), the tumour has grown considerably. Radiating structures are now seen perpendicular to its surface. The vessels are particularly narrow in the lower lobe inferior to the tumour. The vessels also have irregular walls and are displaced away from the tumour, as compared with Figs. *a* and *b*. Only the large, central pulmonary artery and the vessels in the superomedial part of the lung have about the same calibre in the three different examinations. A semiaxial projection (*d*), from the same time as Fig. *c*, shows clearly a circular deviation of a narrow vessel superior to the tumour.

The displacement of vessels is often difficult to observe in ordinary plain films. Fig. III: 34 *a*, for example, shows a squamous cell carcinoma in the posterior basal segment of the right lower lobe. Arrows here point to a radiolucent zone medial to the tumour. In a computerized tomogram, however (Fig. III: 34 *b*), a zone one centimetre broad is easily recognized between the tumour and circularly displaced vessels. Later experimental demonstration (Chapter XIV) will show that the circular deviation and narrowing of vessels are likely to be caused by extensive thromboses and atrophy of the lung tissue around the tumour. This locally degenerated tissue is then passively distended by surrounding nonatrophied tissue.

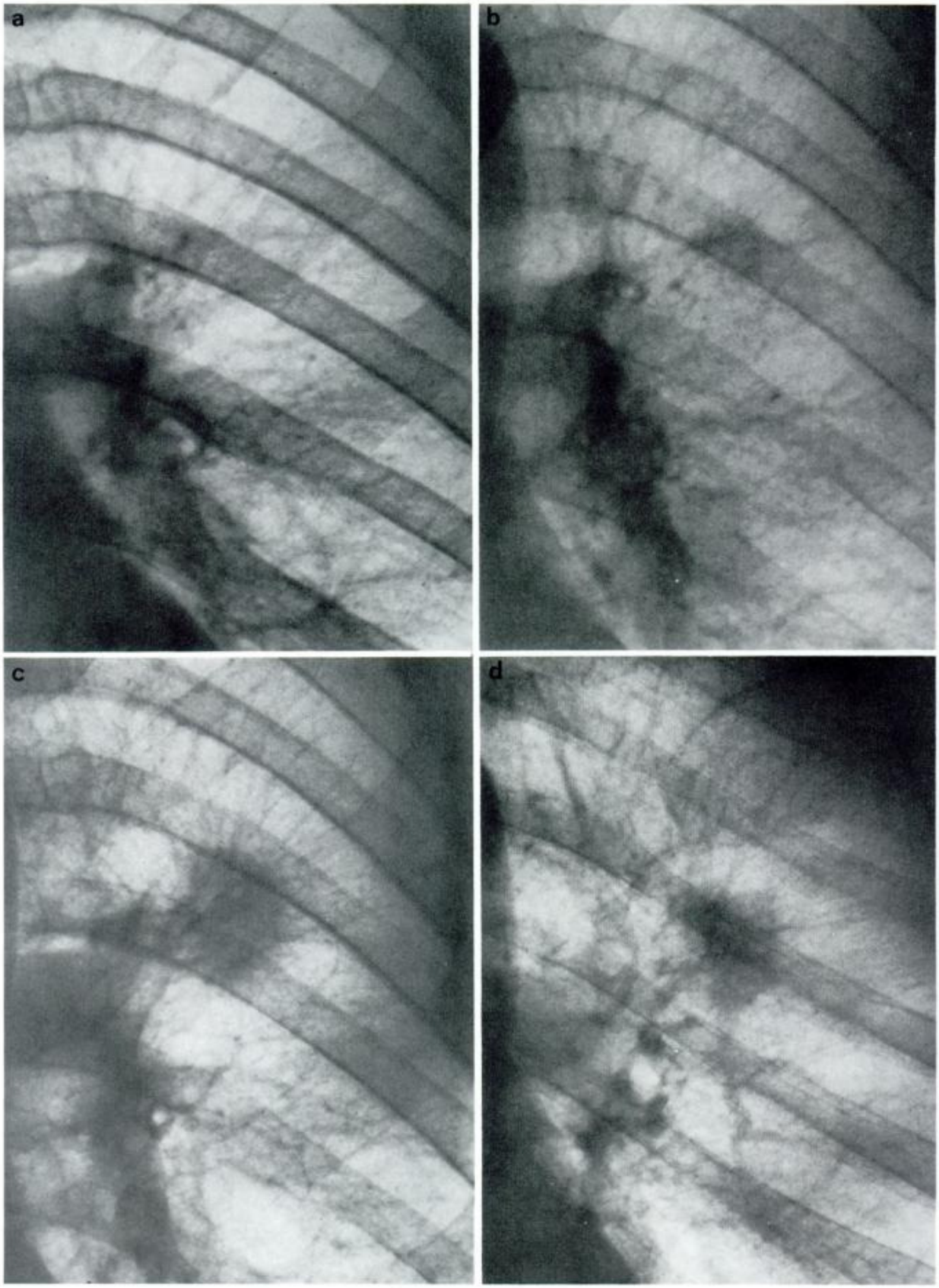

Fig. III:33. Gradual circular displacement and decrease in calibre of vessels surrounding a primary adenocarcinoma in the left upper lobe of a 57-year-old man. (*a*) Age 45. Vessels appear normal. (*b*) Age 56. A tumour, about 10 mm in diameter, is seen in the left lung. The vessels in the hilum and the medial part of the upper lobe have about the same calibre as seen in *a*. Around the tumour the vessels appear narrow. Within a 6 cm diameter they take a circular course. (*c*) Age 57. A radiolucent "A" zone appears around the tumour. Radiating structures are also seen. The vessels are now more narrow than in *b* and deviate in a circular fashion, particularly inferior to the tumour. (*d*) Age 57. Semiaxial projection shows narrowing and circular deviation of vessels superior to the tumour.

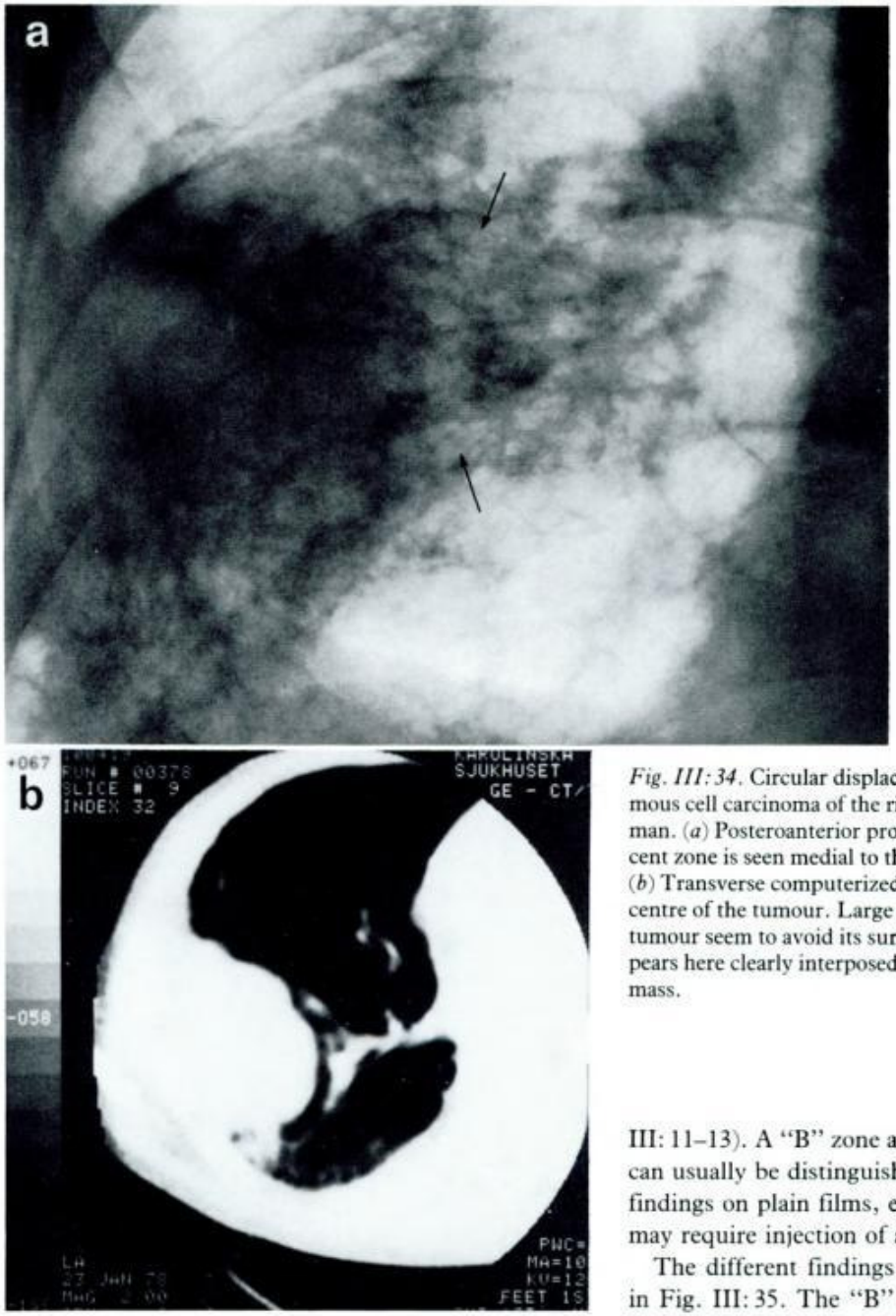

Fig. III: 34. Circular displacement of vessels around a squamous cell carcinoma of the right lower lobe in a 68-year-old man. (*a*) Posteroanterior projection. A barely visible radiolucent zone is seen medial to the carcinoma (arrows). (*b*) Transverse computerized tomogram at the level of the centre of the tumour. Large pulmonary vessels medial to the tumour seem to avoid its surface. The radiolucent zone appears here clearly interposed between the vessels and the mass.

H. Differential diagnosis: "B" zone, pleural thickening and "retraction pocket". Pathogenesis of local retraction of lung and pleura

That a "B" zone can easily be distinguished from atelectasis by the injection of a small amount of air into the pleura has previously been shown (Figs. III: 11–13). A "B" zone and a density of pleural origin can usually be distinguished on the basis of radiologic findings on plain films, even though conclusive proof may require injection of air into the pleura.

The different findings are schematically illustrated in Fig. III: 35. The "B" zone (*a*) has broad, diffuse, hazy, ill-defined, intrapulmonary borders except where it reaches an anatomic borderline, such as a segmental or interlobar septum, where the margin is sharp. An arcade of small arches can often be demonstrated. The "B" zone disappears after injection of air into the pleura (*b*). Locally thickened pleura (*c*) is usually irregular. Its distal ends usually taper. The pleural space is often obliterated so that local pneumothorax is impossible (*d*). A "retraction pocket" (*e*) is characterized by linear strands which connect with a funnel-shaped density continuous with the convex margin of the lung. After air is injected into the pleural space (*f*), the density may completely disappear. The lung tissue is then seen to be limited by persisting local retraction of the visceral pleura.

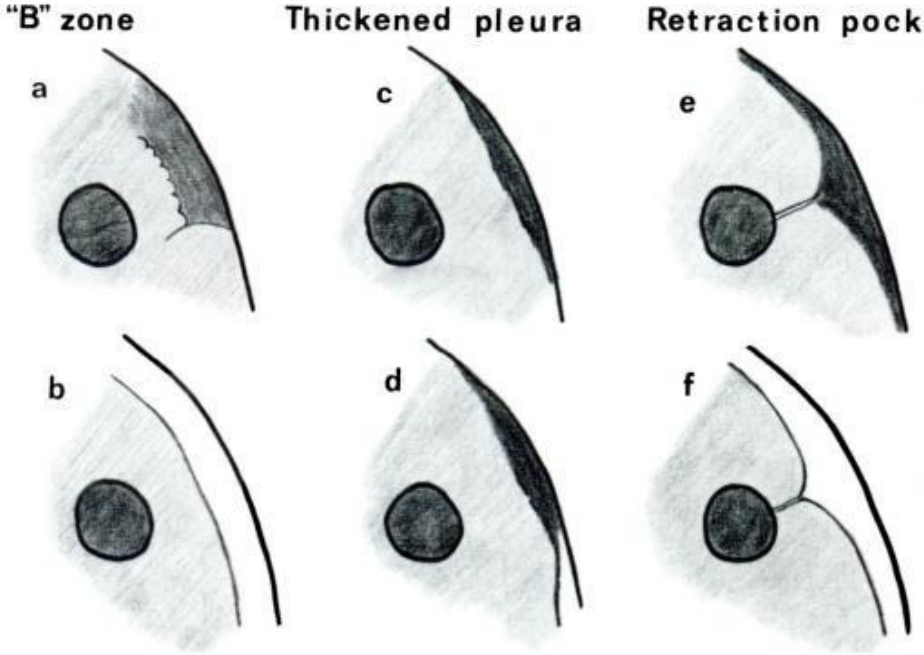

Fig. III: 35. Differential diagnosis of local "pleural thickening". A "B" zone (*a*) disappears when (*b*) air has entered the pleural space. (*c*) True local pleural thickening. The pleural space is obliterated, corresponding to the thickening. It does not open when (*d*) air enters the pleural space. (e) Visceral pleura retracted toward a tumour by shrinking fibrous strands (radiating structures). A *retraction pocket* of the pleura allows local accumulation of pleural fluid. This fluid disappears after (*f*) the injection of air into the pleura, but the retraction of the lung tissue persists.

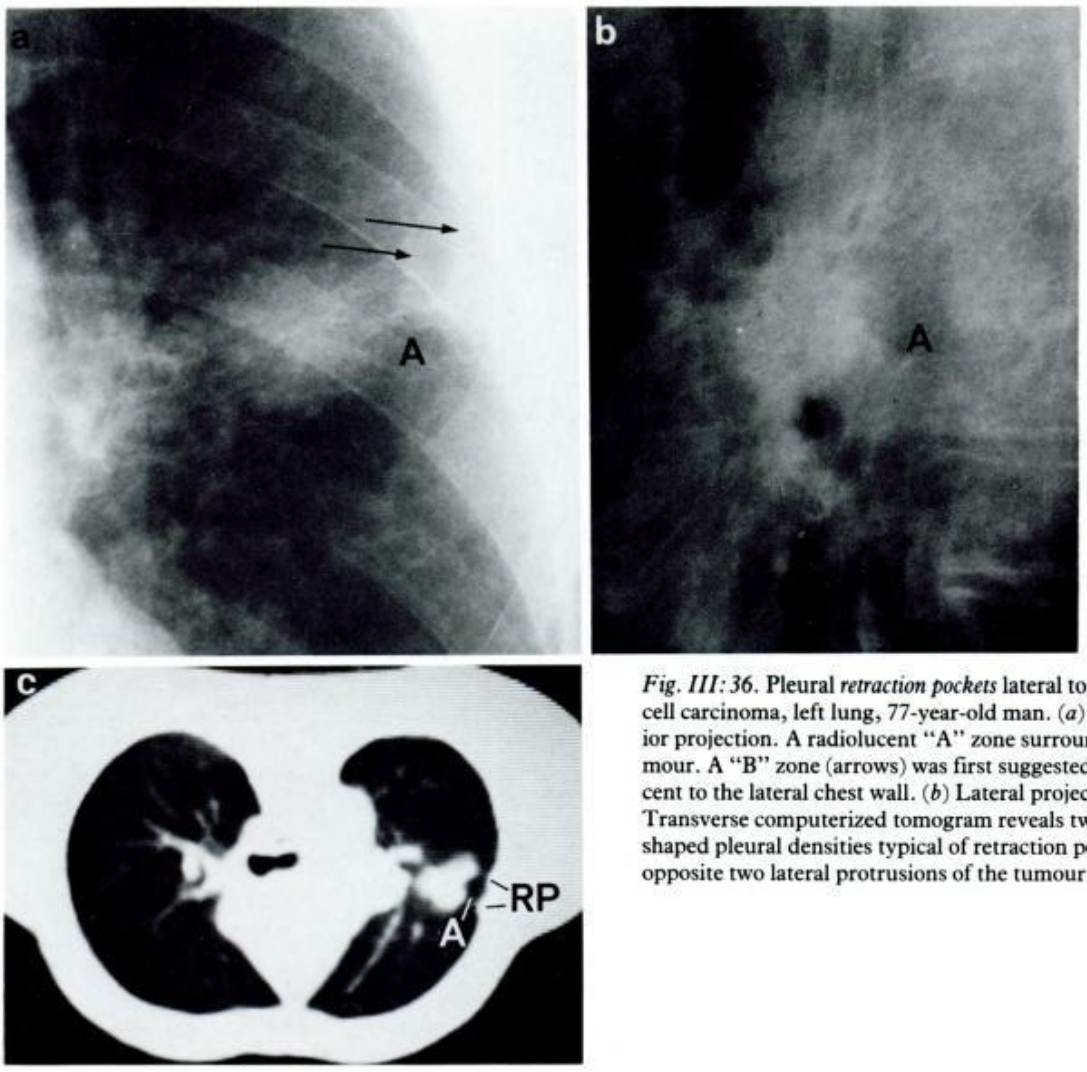

Fig. III: 36. Pleural *retraction pockets* lateral to a squamous cell carcinoma, left lung, 77-year-old man. (*a*) Posteroanterior projection. A radiolucent "A" zone surrounds the tumour. A "B" zone (arrows) was first suggested in lung adjacent to the lateral chest wall. (*b*) Lateral projection. (*c*) Transverse computerized tomogram reveals two funnel-shaped pleural densities typical of retraction pockets (*RP*), opposite two lateral protrusions of the tumour.

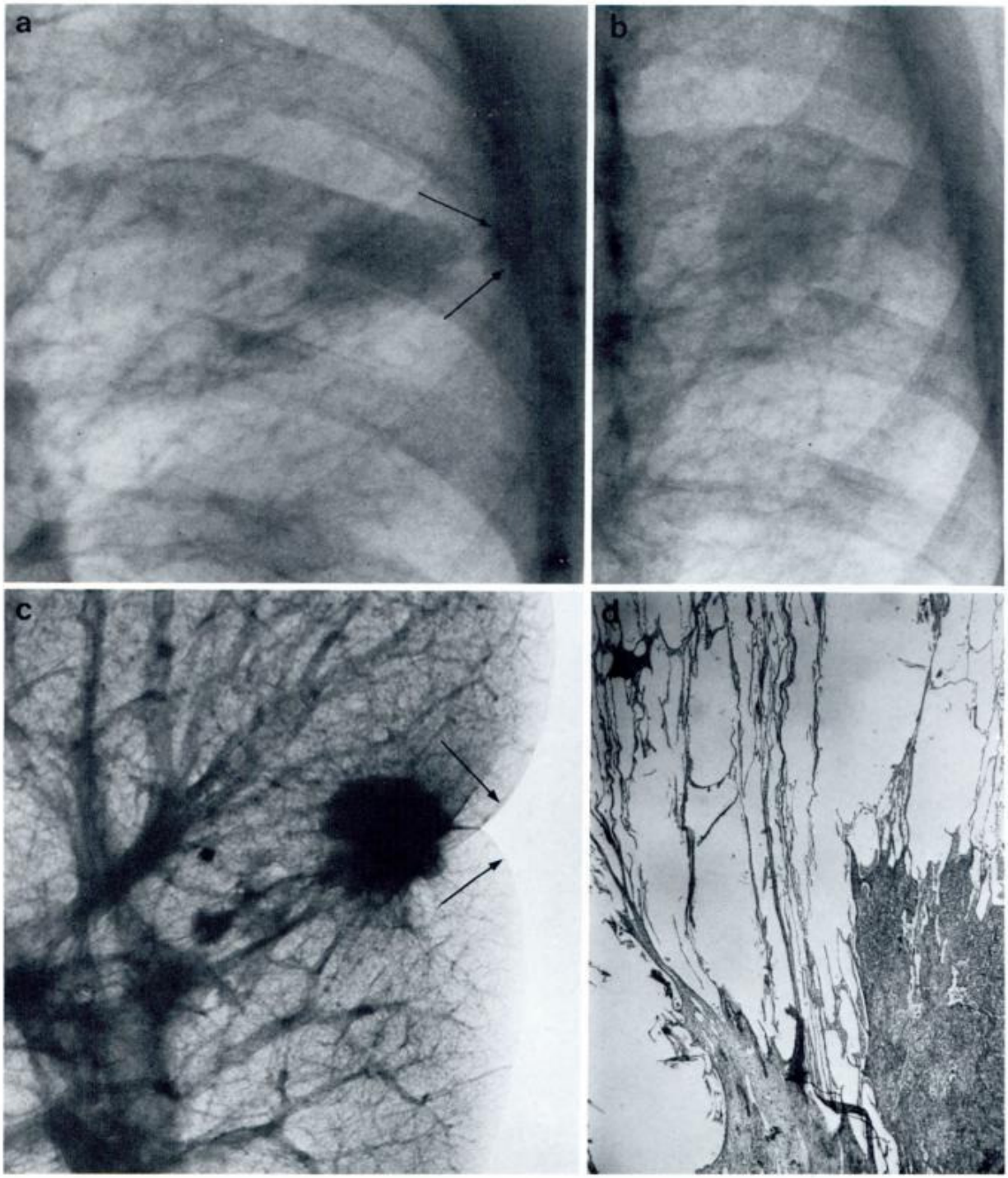

Fig. III: 37. Pleural retraction pocket (arrows) adjacent to an adenocarcinoma in the left upper lobe of a 69-year-old man. (*a*) Posteroanterior and (*b*) oblique radiographs. (*c*) Postmortem radiograph of the left upper lobe, distended by negative external pressure. Numerous small radiating structures surround the tumour but are not visible in the in vivo radiographs *a* and *b*. One of these radiating structures extends to the retracted funnel-shaped surface of the lung. (*d*) Histological section of some of the radiating structures reveals fibrotic strands and neoplastic cells in their bases. The development of this structural combination is discussed later (Chapters IX: E and XVI: J). It depends on a mechanism which will be shown to be responsible also for the development of so-called skin thickening in breast cancer.

The radiographic appearance of what is here named a retraction pocket is illustrated in Fig. III: 36. Posteroanterior (*a*) and lateral (*b*) projections show a squamous cell carcinoma in the left lung surrounded by a radiolucent "A" zone. Two funnel-shaped pleural densities are situated laterally, indicated by arrows in the posteroanterior view. Some linear tissue structures are also seen between the tumour and the funnel-shaped structures. A computerized tomogram (*c*) shows that the two funnel-shaped structures connect with the pleura and point opposite two protrusions of the tumour. These pleural changes show the radiographic appearance typical of retraction pockets.

Retraction pockets are also illustrated (Fig. III: 37 *a*, *b*) near a moderately well differentiated adenocarcinoma. In this case, extremely thin radiating structures were not seen in the plain radiographs. The lung, slightly inflated in a postoperative radiograph (*c*), shows the thin radiating structures and the retracted lung tissue between the tumour and the pleura. In a histological section (*d*), some of the small radiating structures are seen. They contain some vessels and tumour cells close to the tumour mass. Far out in the lung parenchyma the radiating structures consist of only "fibrous" tissue.

A preliminary explanation for the development of a retraction pocket can now be proposed.

Retracted lung tissue between a tumour and the pleura is often easily recognized. Fibrotic radiating structures from the surface of a tumour also are often easily recognized. It is well known that scar tissue shrinks slowly after its initial formation (1). This phenomenon can most easily be explained as a process of dehydration of a material with hygroscopic properties. The radiating structures around carcinomas of both lung and breast often contain a mixture of different fibrotic materials. Some of these materials are also birefringent (1) and show different degrees of tortuosity in relation to other adjacent fibrotic materials. The solubility in water of different fibrous tissues in the body is known to vary considerably (1). For instance, the predominant material of tendons is collagen, which is insoluble in water, unlike other fibrotic tissues. Variations in the degree of stretching and relaxation of radiating structures may therefore be produced by variations of water content of different fibrous materials. It will be shown in Chapter IX that the remaining prerequisite for local hygroscopic stretching and shrinking in radiating structures–local variations of their water content–is also present. Furthermore, it will be shown in Chapter XVI that the retraction pockets in the lung correspond to so-called skin thickening and retraction of the skin in cancer of the breast.

References

1. Asthbury, W. T.: In: Mercer, E. M. (ed.): Keratin and keratinization. New York, Pergamon Press, 1961, p. 255.
2. Cordier, G., Papamiltiades, M., and Cedard, C.: Les lymphatiques des bronches et des segments pulmonaires. Bronche 8: 8, 1958.
3. Dahlgren, S., and Nordenström, B.: Transthoracic needle biopsy. Stockholm, Almqvist & Wiksell, 1966.
4. Kerley, P.: In: Shanks, S. C., and Kerley, P. (eds.): A textbook of x-ray diagnosis, 2nd ed. London, Lewis, 1951, pp. 404, 414.
5. Nordenström, B.: Transjugular approach to the mediastinum for mediastinal needle biopsy. Invest. Radiol. 2: 134, 1967.
6. Nordenström, B.: New trends and techniques in roentgen diagnosis of bronchial carcinoma. In: Simon, M., Potchen, E. J., and Le May, M. (eds.): Frontiers of pulmonary radiology. New York, Grune & Stratton, 1969, p. 380.
7. Remy, J.: Die Wichtigkeit der Bildqualität bei der Auswertung von Schirmbildaufnahmen. In: Stieve, F.-E. (ed.): Bildgüte in der Radiologie. Stuttgart, G. Fischer Verlag, 1966, p. 249.
8. Rigler, L. G.: The roentgen signs of carcinoma of the lung. Amer. J. Roentgenol. 74: 415, 1955.
9. Rigler, L. G.: The earliest roentgenographic signs of carcinoma of the lung. JAMA 195: 655, 1966.
10. Rigler, L. G.: An overview of cancer of the lung. Seminars in Roentgenol. 12: 161, 1977.
11. Stieve, F.-E. (ed.): Bildgüte in der Radiologie. Stuttgart, G. Fischer Verlag, 1966, p. 380.
12. Trapnell, D. H.: The peripheral lymphatics of the lung. Brit. J. Radiol. 36: 660, 1963.

IV.
Corona structures around inflammatory lesions, including those of silicosis

Corona structures of different malignant and some benign neoplasms have thus far been presented. In fact, the author originally described a "corona maligna" (1) and believed for years that the different radiologic signs reported here were observed only around malignant tumours. It was therefore of considerable interest when a tuberculous granuloma was found which also showed several of the corona structures.

This rather large tuberculoma, first observed in 1967, is shown in Fig. IV: 1 *a*. Situated in the middle lobe of the right lung, it shows an "A" zone, radiating structures, some lamellae and deviation of the vessels in the surrounding lung parenchyma. Needle biopsies were performed on four different occasions because of the suspicion of malignancy. Neoplastic cells were never found. The biopsies revealed only necrotic material and chronic inflammatory cells suggestive of a tuberculous granuloma. Chest radiographs over an 8 year period did not change. Tuberculin skin test was positive. The diagnosis of tuberculoma was actually presumed rather than absolutely proven, but the evidence provides virtual certainty that the mass was inflammatory and not neoplastic.

A pneumothorax, about 3 cm broad, developed in 1969 after one of the needle biopsies (Fig. IV: 1 *b*). The pleural space is open and the visceral pleura locally thickened. The lung is irregularly collapsed. The tuberculoma contains an air cavity and is surrounded by an "A" zone. In contrast to observations of most malignant lung tumours, the "A" zone remained almost unchanged in spite of partial collapse of the lung. An explanation of this phenomenon could be that this particular case represents a pathologic condition in the lung which has persisted relatively unchanged over several years, resulting in a more or less permanent structural rearrangement of the tissue.

Fig. IV: 1 *c* shows the lesion in 1971 when no air was present in the pleura. The cavity of the lesion had resorbed, to be replaced by a concavity in the superolateral part of the lesion and the formation of a lamella in the adjacent pulmonary parenchyma. The radiolucent "A" zone around the lesion is apparent. Vascularity is possibly reduced in the "A" zone.

A verified tuberculous granuloma is illustrated in Fig. IV: 2. Situated in the apical segment of the right lower lobe, this lesion shows an "A" zone, a "B" zone and some radiating structures. Irregular dense opacity is caused by pleural calcification, presumed to be unrelated to the corona changes.

Corona structures can also be seen around a mycetoma within a large central air-containing cavity (Fig.

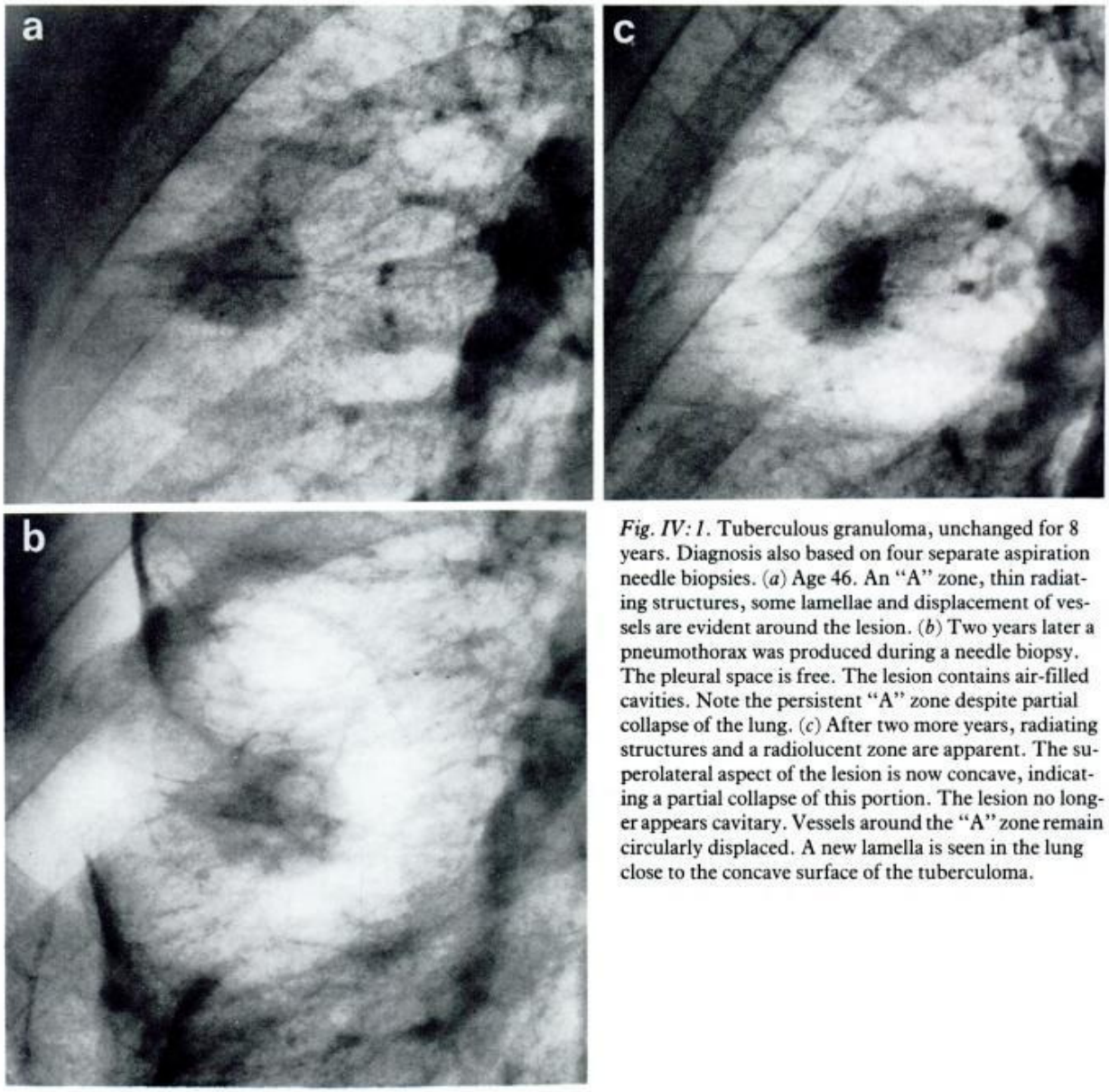

Fig. IV: 1. Tuberculous granuloma, unchanged for 8 years. Diagnosis also based on four separate aspiration needle biopsies. (*a*) Age 46. An "A" zone, thin radiating structures, some lamellae and displacement of vessels are evident around the lesion. (*b*) Two years later a pneumothorax was produced during a needle biopsy. The pleural space is free. The lesion contains air-filled cavities. Note the persistent "A" zone despite partial collapse of the lung. (*c*) After two more years, radiating structures and a radiolucent zone are apparent. The superolateral aspect of the lesion is now concave, indicating a partial collapse of this portion. The lesion no longer appears cavitary. Vessels around the "A" zone remain circularly displaced. A new lamella is seen in the lung close to the concave surface of the tuberculoma.

IV: 3). The lesion is surrounded by rather coarse radiating structures and narrow irregular vessels, some of which are circularly displaced around the lesion (arrows).

Finally, silicotic granulomas are illustrated in the right and left upper lobes (Fig. IV: 4 *a*, *b*). Both show radiating structures and "A" and "B" zones.

The different malignant and benign tumours in Chapter III and the various non-neoplastic, inflammatory lesions in this chapter all share several corona changes. The possibility of a common denominator behind these similarities will therefore be discussed in the following chapter.

Reference

1. Nordenström, B.: New trends and techniques in roentgen diagnosis of bronchial carcinoma. In: Simon, M., Potchen, E. J., and Le May, M. (eds.): Frontiers of pulmonary radiology. New York, Grune & Stratton, 1969, p. 380.

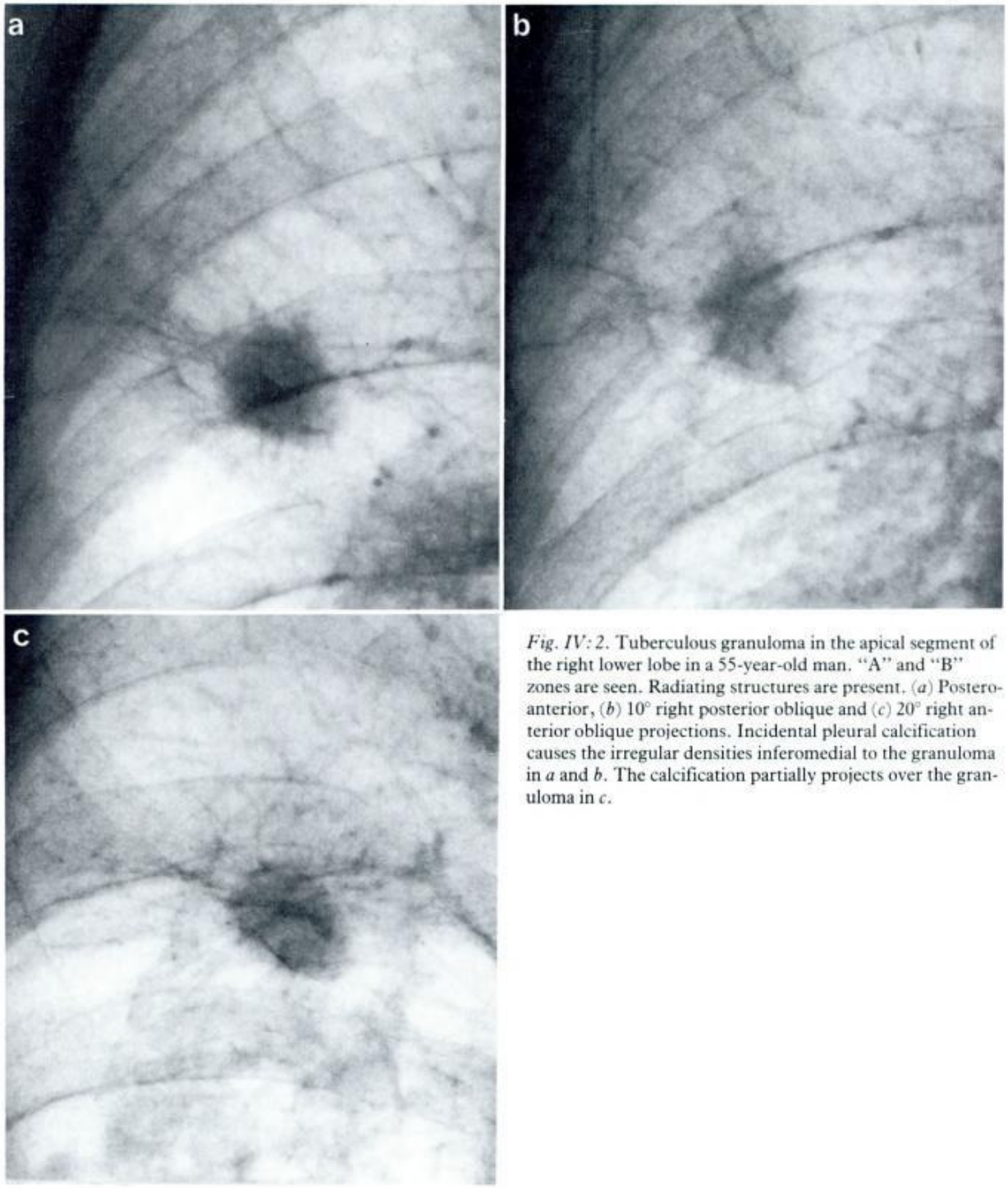

Fig. IV: 2. Tuberculous granuloma in the apical segment of the right lower lobe in a 55-year-old man. "A" and "B" zones are seen. Radiating structures are present. (*a*) Postero-anterior, (*b*) 10° right posterior oblique and (*c*) 20° right anterior oblique projections. Incidental pleural calcification causes the irregular densities inferomedial to the granuloma in *a* and *b*. The calcification partially projects over the granuloma in *c*.

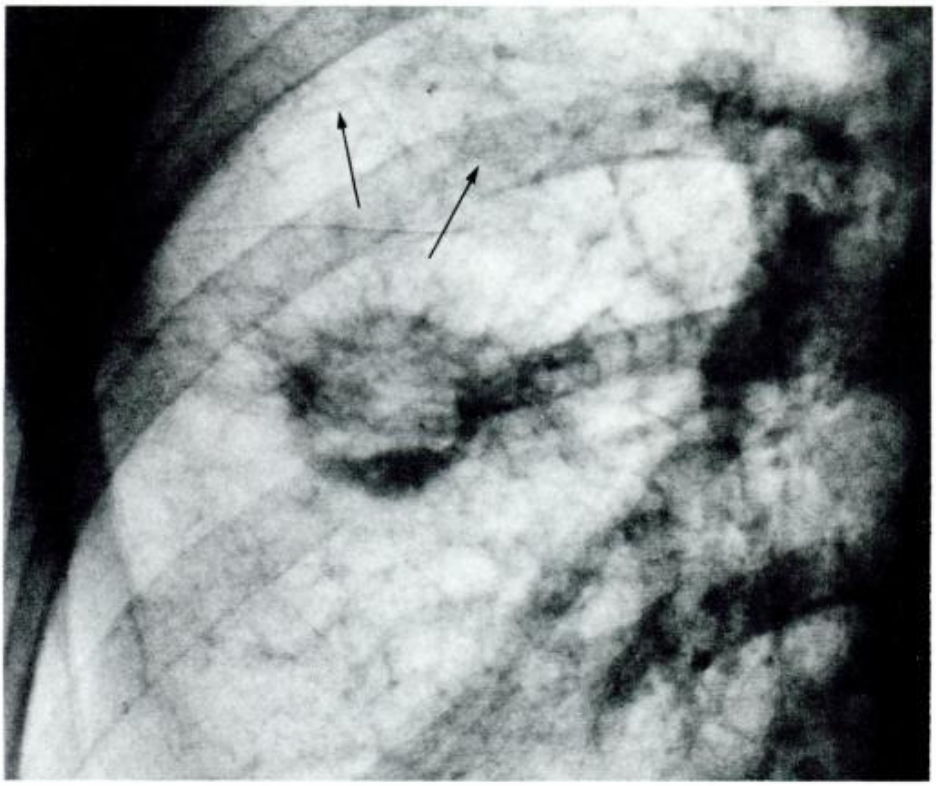

Fig. IV: 3. 60-year-old woman. Mycetoma (Mycobacterium III) of the middle lobe showing central air-filled cavity and radiating structures. The surrounding lung parenchyma contains some narrow and circularly displaced vessels (arrows).

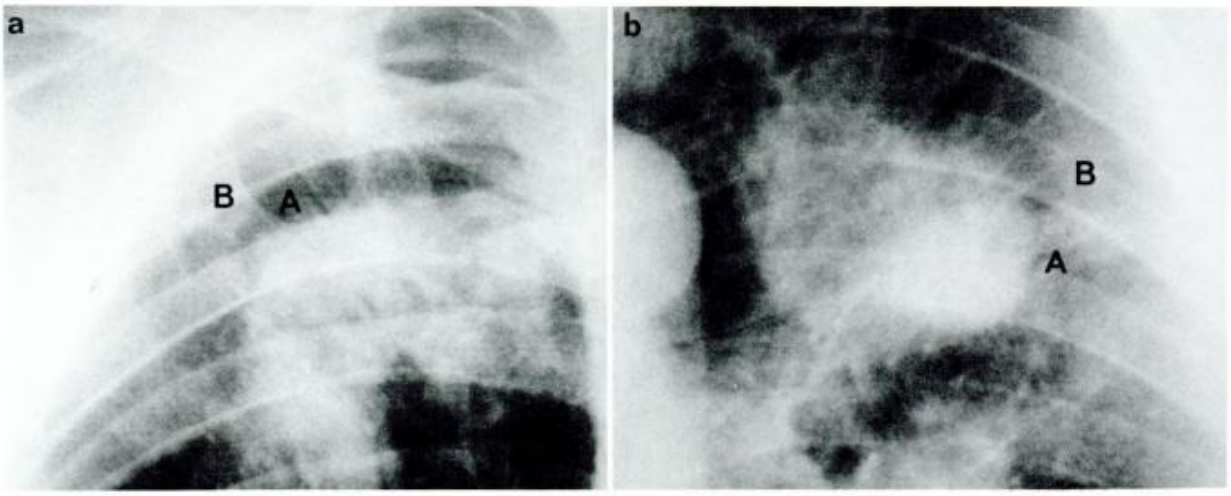

Fig. IV: 4. 70-year-old man. Silicotic granulomas in the right (*a*) and left (*b*) upper lobes. Radiating structures and "A" and "B" zones surround the lesions.

V.
Discussion of the radiological observations of corona structures

The existence of corona structures around a variety of pulmonary neoplasms and inflammatory lesions has been described in the previous two chapters. The morphologic and pathophysiologic background of these structural changes is in many ways confusing and may appear difficult to explain.

No direct correlation has been found with the histological type or degree of cellular differentiation of the tumours. The structural changes–here called "A" and "B" zones, arches and arcades, radiating structures, narrowing and displacement of vessels–may or may not be present in squamous cell carcinomas, adenocarcinomas, oat cell carcinomas or mixed cell carcinomas, in primary as well as in metastatic tumours. The structural changes have occasionally also been observed in the presence of different inflammatory lesions. Finally, some of the changes have been observed around hamartomas.

The structures are often very delicate and therefore may be difficult to recognize. As discussed in Chapter II, special attention is required for the technique of the radiographic examination. So-called "routine" frontal and lateral views of the lungs are not always sufficient for radiological identification and evaluation of the signs.

The "B" zone around malignant tumours has been found to disappear whenever air is introduced into the pleural space. This evidence strongly suggests that the "B" zone is fluid, locally collected in the lung tissue, probably due to the mechanical blocking of lymphatic channels between the pleura peripheral to the mass and the hilar lymph nodes. Supporting this assumption is the finding that it was possible to produce such a fluid collection in the lung in dogs after the placement of an artificial "tumour" of plastic material in the pulmonary parenchyma.

The experiments in dogs are equivalent to the situation in patients in regard to the mechanical effects of a real tumour or tumour-like lesion. A tumour in a patient may be expected to block the draining lymphatic channels between the pleura and the hilum, resulting in lymphatic stasis. Indeed, it would seem reasonable to expect frequent local accumulation of fluid in the parenchyma peripheral to a pulmonary mass. Such a mechanism is also capable of explaining the disappearance of the "B" zone in the dog experiments and in patients after some air is introduced into the pleural space. For these same reasons it can now also be understood that the "B" zone has not been observed in postoperative specimens examined by qualified pathologists. As soon as the mechanical conditions which exist in situ are changed, e.g., by the opening of

the pleural space, some of the prerequisites for the presence and demonstration of local oedema ("B" zone) will disappear.

A consequence of this discussion is also that a "B" zone peripheral to a pulmonary cancer should not be misinterpreted as malignant extension to the pleura, local bronchopneumonia, local pleural thickening or atelectasis. The "B" zone appears to be a harmless oedema and by no means a contraindication to operative removal of a tumour.

Recognizing the radiographic signs which identify a "B" zone is of evident practical importance. The following radiographic signs should be looked for:

1) A pulmonary opacity between a tumour or tumour-like lesion and the pleura.

2) Interposition of a radiolucent "A" zone between the lesion and the zone of increased opacity.

3) A sharp borderline in the shape of small arches forming an arcade.

4) The outer contours of the opacity appearing either to "vanish diffusely" into the adjacent lung or to end in a well demarcated line shadow such as interlobar pleura or an intrapulmonary septum.

5) The presence of enlarged interlobular spaces extending between a tumour and the pleura.

6) Disappearance of the opacity after injection of air into the pleural space.

Whenever an "A" zone can be seen between the surface of a mass and a peripheral, local increase in pulmonary opacity ("B" zone), neoplastic overgrowth or atelectasis can be excluded as possible causes of the "B" zone.

It has been pointed out that a "B" zone, which means lymphoedema due to local stasis in the periphery of the lung parenchyma, may be present in the absence of a definite "A" zone. In this situation, the only absolutely conclusive proof of the presence of a "B" zone is the sign of disappearance of the "B" zone lymphoedema after injection of air into the pleural space. The explanation, however, that "B" zones are caused by local pulmonary oedema does not entirely explain their location. Between the pleura, the "B" zone, and the blocking lesion, an "A" zone may be interpositioned, which also needs explanation.

Other signs requiring explanation are the formation of arches and arcades at the interface between the "A" and "B" zones, the existence of radiating structures, and the observed narrowing and displacement of vessels in the lung parenchyma near a pulmonary lesion. These vascular changes may seem difficult to understand, and can be tied to some earlier observations in this field.

In 1946 and 1951 Marchal and Marchal (3, 4) reported diminished pulsations in the lung parenchyma around malignant tumours. They made this important observation by means of direct fluoroscopy with a photocell between the subject and the screen. They considered these diminished pulsations to be a sign of malignancy. The observations of decreased pulsations around the tumours are in agreement with the author's observations of a decrease in calibre and irregular contours of the pulmonary vessels around the tumours.

Roentgen densitometry was also applied by the author in 1954 (5, 6) in studying the effects of balloon occlusion of pulmonary arteries. These studies showed that the occlusion of a central pulmonary artery causes a considerable decrease in calibre of the pulmonary vessels and a decrease in the blood pressure and blood volume in the lung distal to the occlusion. Bronchial arterial blood then shunts into the occluded pulmonary arterial branches distal to the level of obstruction. These branches then contain blood of higher arterial oxygen saturation than simultaneously obtained systemic arterial blood. The presence of such arterial blood in a pulmonary artery should, according to the well known experiments by von Euler and Liljestrand (2), cause local vasoconstriction. It should also be noted that in studying specimens of lung tumours, we have found (1) that thrombosis is often found in the vessels around malignant tumours.

From this discussion it is evident that several factors may be responsible for the radiologically observed structural changes (corona changes). Because these changes are very often seen together, it is likely that they depend on one or several common factors which are present under certain conditions.

The examples of inflammatory lesions as well as neoplasms may allow us to conclude that "A" and "B" zones, radiating structures, arcades, lamellae, deviations and narrowings of adjacent vessels are by no means specific to the histologic type of lung tumour. These structures can be found in association with a wide variety of benign and malignant tumours as well as with different tumour-like inflammatory lesions such as granulomas.

This finding does not mean that the reported radiologic signs are not specific. In fact, as will be seen, they are actually a very specific manifestation of a constellation of biokinetic and mechanical events which may occur in several pathological conditions in the lung (as well as in other organs). These events will further be discussed as they occur in experimental models. Next it is appropriate to turn to some of the electrical properties of the lung and pleura.

References

1. Dahlgren, S., and Nordenström, B.: Transthoracic needle biopsy. Stockholm, Almqvist & Wiksell, 1966.
2. von Euler, U. S., and Liljestrand, G.: Observations on the

pulmonary arterial blood pressure in the cat. Acta Physiol. Scand. 12: 301, 1946.
3. Marchal, M. M.: De l'enregistrement des pulsations invisibles du parenchyme pulmonaire ainsi que des pulsations cardiovasculaires par la cinédensigraphie. Arch. Mal. du Coeur 39: 345, 1946.
4. Marchal, M. M., and Marchal, M. T.: Nouvelle méthode de ciné-densigraphie étalonnée permettant le diagnostic différentiel du cancer du poumon. Comptes rendus des séances de l'Academie des Sciences 233: 458, 1951.
5. Nordenström, B.: Temporary unilateral occlusion of the pulmonary artery. Acta Radiol. Suppl. 108, 1954.
6. Nordenström, B.: Pulmonary circulation time. Acta Radiol. 41: 209, 1954.

VI.
Electric potentials in normal lung, pleura and liver and in focal pulmonary lesions, including bronchogenic carcinoma

A. Preliminary studies

1. Introduction

The possibility that pulmonary tumours sometimes may polarize electrochemically in relation to surrounding tissue is investigated in this chapter.

The variety of pathological conditions in which the described radiological signs have been found suggests that the signs are dependent on some common factors. Internal bleeding and necrosis, for instance, must be considered as phenomena common to various neoplasms and tumour-like inflammatory lesions.

Autolysis characterizes necrosis. Cellular elements are destroyed. Molecules are split. The result is entirely new physical and chemical conditions in the involved regions. Their relation to the surrounding tissues have here been studied by means of electrophysiological techniques.

This chapter describes a study of electric potentials of the lung and pleura in 27 dogs and in 119 patients with various pulmonary lesions. Supplementary experimental studies on electric potential of the liver and the effect of short circuiting subcutis (15 dogs and 3 rabbits) are also included. This latter part of the study was carried out to facilitate the evaluation of possible influences of reference tissues.

2. Procedures

An obstacle in the studies of patients was to obtain permission to introduce electrodes for the measurements. For ethical reasons the procedures had to be carried out as a compromise between the generally accepted techniques of needle biopsy for cytologic diagnosis and optimal techniques for measuring electric potentials. In a first series, polarizable metal electrodes were used and in a second series nonpolarizable Ag-AgCl electrodes in KCl bridges.

Stainless steel electrodes for the measuring of bioelectrical events have been used by Grundfest, et al. (6). They developed stainless steel microelectrodes by mechanical sharpening and electropointing. Careful analyses of the electrical properties of different metal electrodes have been performed by Weinman and Mahler (19) and of stainless steel electrodes by Geddes, et al. (5). The advantages and limitations of stainless steel electrodes are therefore well known.

The technique of percutaneous transthoracic needle biopsy for sampling of cellular material from the lung is now well established (3, 10, 11) and accepted in many institutions as a routine procedure in selected patients.

The diameter of the stainless steel biopsy needles is 0.9–1.0 mm. Their length is 16 cm. Nonpolarizing

electrodes, however, with these dimensions and a combined capability to sample cytologic material for clinical diagnosis could not be obtained. Stainless steel biopsy needles were modified so as to become electrodes for preliminary measurements of mixed electric potentials in the lung. The needles were coated with an insulating layer of Teflon, 0.1 mm thick. Despite the fact that increasing needle thickness is accompanied by an increased likelihood of complications, mainly pneumothorax, this very slight increase in thickness of the needles was considered acceptable. The insulation at the tip of each needle was scratched off so the steel could make contact with the tissue. The needles were in the preliminary series connected to an electrocardiographic amplifier. Later, nonpolarizable electrodes were used connected to a DC amplifyer (Grass Polygraph).

Electric potentials were then measured between a grounded subcutaneous reference electrode, also of stainless steel, and the exploring electrode, inserted percutaneously under local anaesthesia and fluoroscopic control into the lung (8). The exploring electrode was moved manually as evenly as possible from the chest wall through the lung tissue into the actual lesion. The electric potential difference was traced continuously. Cellular material from the lesion was aspirated by attaching a syringe to the hub of the needle-electrode. Several insertions were usually made through the walls of the lesion in order to check the reliability of the tracings and to sample representative cellular material.

After a series of 22 normal dog experiments, it was found that a reproducible tissue profile of electric potentials of the normal lung of the dog could be rather easily identified with this technique. With this background, a preliminary study on patients was begun.

3. Case material

Electric potentials of pulmonary lesions were measured in 107 patients.

The groups shown in Table VI: 1 were studied, the verification being based on cytologic, bacteriologic and postoperative histologic examinations.

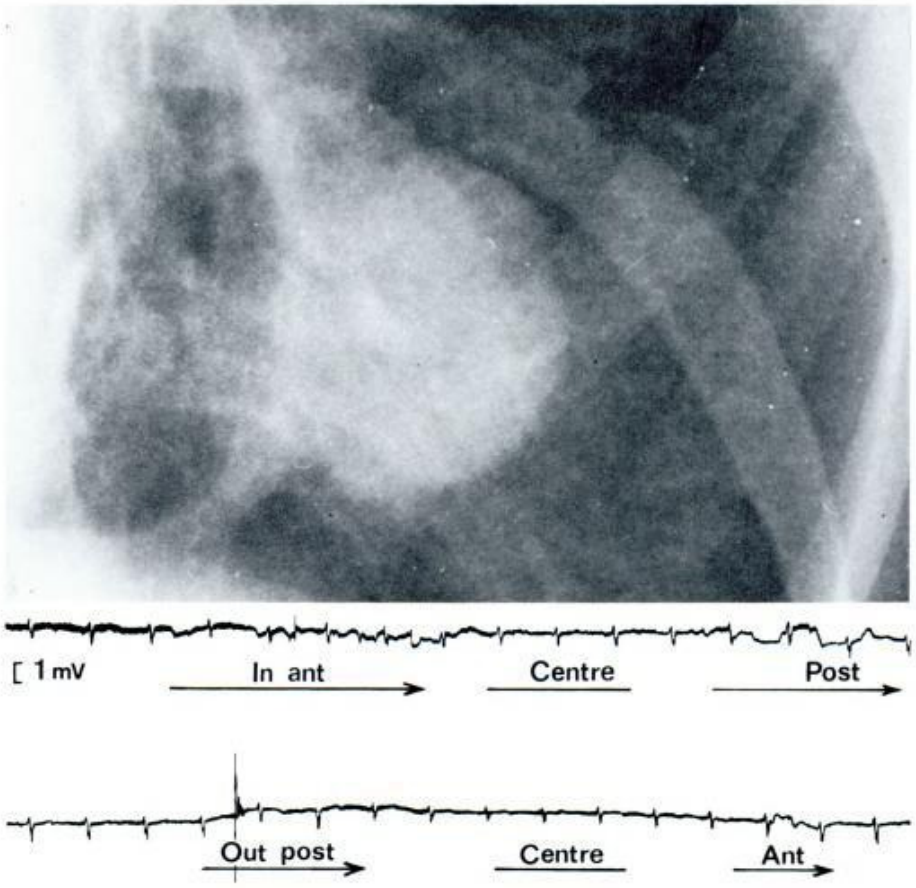

Fig. VI: 1. Absence of significant potential difference between tumour and surrounding lung. Poorly differentiated squamous cell carcinoma in the left lower lobe of a 55-year-old woman. On insertion of the needle electrode into the tumour (In ant), as it lay within (Centre) and as it passed through the posterior wall (Post), only small irregular deflections of the electric potential and regular electric fluctuations from the heart were recorded (upper tracing). On withdrawal of the electrode (bottom tracing), similar small deflections were recorded from the posterior wall of the mass (Out post), in the centre (Centr) and from the anterior wall (Ant).

Table VI: 1

Benign tumours (neurilemmoma 3, cysts 2)	5
Inflammatory lesions (pleuroma 3, tuberculoma 9, fibrous tuberculous tissue 11, chronic non-specific inflammation 11, mycetoma 2)	36
Metastases	12
Bronchogenic carcinomas	47
Diagnosis not proved	7

4. Results

(*a*) Repeated insertion and removal of the exploring electrode revealed a spatial pattern of potential, the "electric potential profile of tissue", usually reproducible for each lesion.

(*b*) Malignant tumours of similar size, location and histological type may show completely different patterns of electric potential.

For example, Figs. VI: 1 and 2 show the radiographs and tracings of potential from two poorly differentiated squamous cell carcinomas, each 4×5 cm in size (frontal projection), located in the left and right lower lobes, respectively, of two different patients.

The left-sided tumour (Fig. VI: 1) showed no definite or reproducible changes of potential at its surfaces or inside the mass in comparison with the adjacent pulmonary parenchyma.

The right-sided tumour (Fig. VI: 2) showed a very distinctly positive surface potential. The upper curve shows the tracing on a single slow insertion and retraction of the electrode. The lower curve shows repeated insertions and retractions, performed about three times more rapidly.[1] The bottom tracing shows the exposure markings (Exp) during simultaneous cineradiography (50 frames/sec) with the roentgen beam perpendicular to the axis of the needle-electrode. A rough correlation could be obtained in this way between the positions of the electrode point in the tissue

[1] The repeated insertion of the needle is part of an accepted technique for aspiration biopsy (3). As continuous negative pressure is applied in the needle, repeated insertions through the tumour surface produce a packing of potentially diagnostic cells into the needle from different parts of the tumour. The tracings of electric potential and the sampling of cell material were, however, made separately.

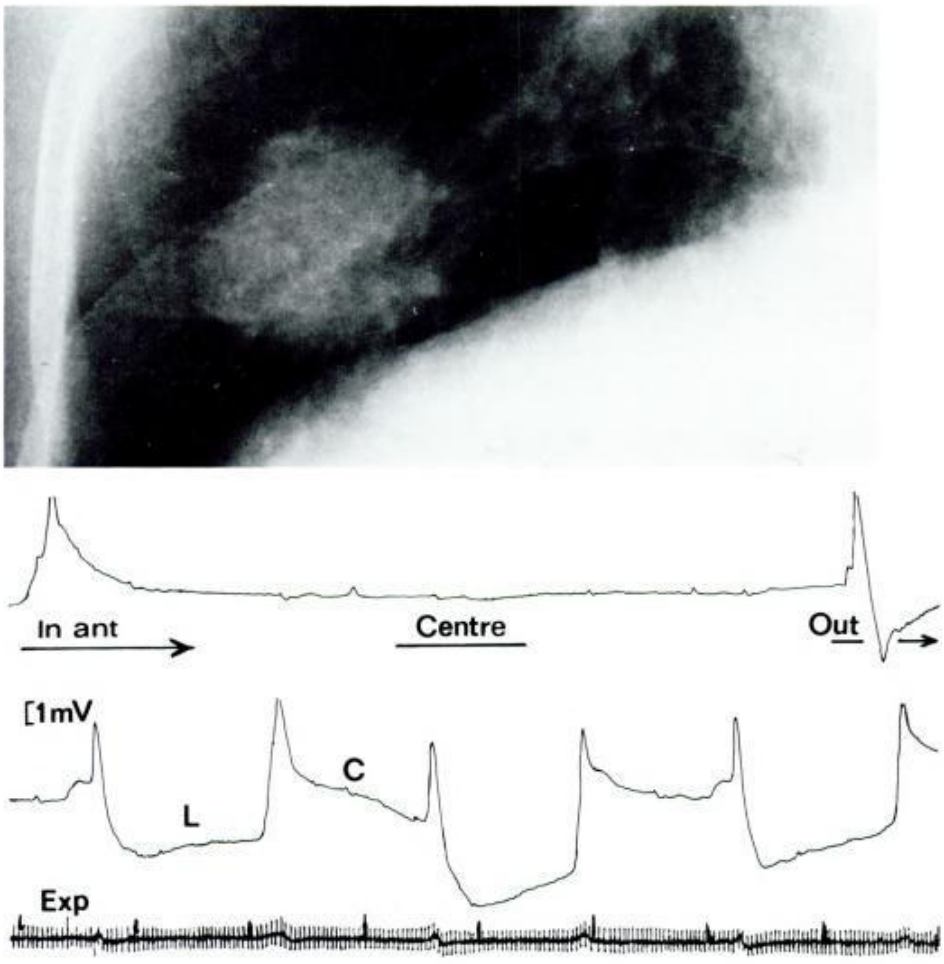

Fig. VI: 2. Electropositive tumour in lung. Poorly differentiated squamous cell carcinoma in the right lower lobe of a 74-year-old man. Positive electric potential was obtained in relation to surrounding lung tissue as the electrode entered the tumour (In ant), lay within it (Centre), and was removed (Out). These findings were constant both on one slow insertion and retraction of the electrode (top tracing) as well as on more rapid and repeated manoeuvres (middle tracing). *C* = inside the tumour; *L* = lung. Bottom tracing shows exposure markings at cineradiography (frame frequency, 50/sec) for the identification of the electrode tip in the tissues and its correlation with the tracings of potential.

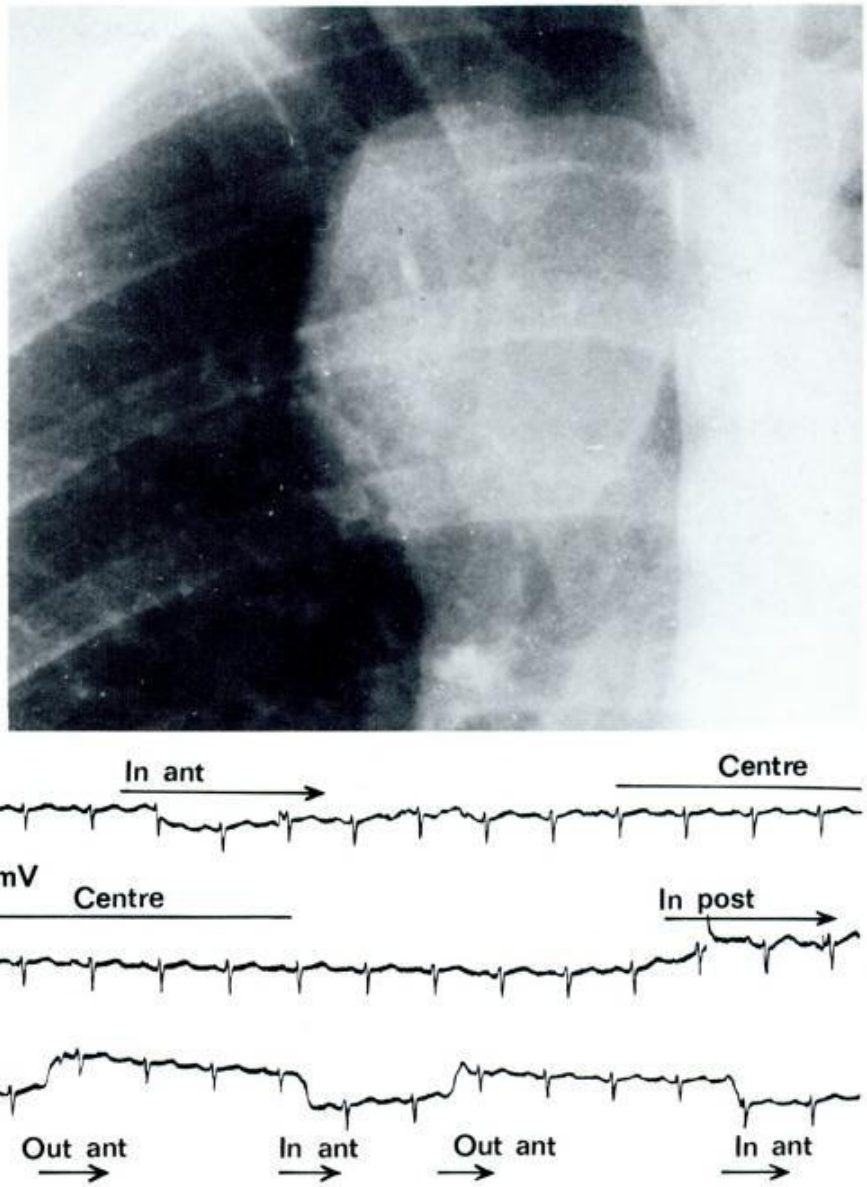

Fig. VI: 3. Electronegative tumour in lung. Metastatic melanosarcoma in the right upper lobe of a 57-year-old woman. Internal necrosis was found on aspiration of cellular material. A negative potential was present inside the tumour compared with the surrounding lung tissue, shown upon slow anterior insertion (In ant) and further passage through posterior wall (In post) of the exploring electrode (top tracing continues in the middle tracing). The same profiles of tissue potential were obtained upon more rapid, repeated insertions and retractions of the electrode (bottom tracing).

and the different parts of each tracing of electric potential.

(*c*) Regions of damaged tissue showed locally negative or positive potentials in relation to the surrounding lung tissue. This correlation was obtained by sampling the cells of these regions through the needle electrode. In fact, this finding appeared to be useful in the selection of suitable sites for biopsy. When the combined biopsy electrode-needle was inserted into a tissue in which potential was negative or positive, as compared with the surrounding tissue, the sampled cell material was usually necrotic and therefore cytologically nondiagnostic.

Such a case is illustrated in Fig. VI: 3, which shows a large metastatic melanosarcoma in the right upper lobe. It appeared to be extensively necrotic on needle aspiration biopsies from five sites. The electric potential profile of the tissue showed small but distinctly negative deflections inside the tumour compared to surrounding lung tissue. One slow insertion to the centre of the tumour and out through the posterior wall is seen in the top and middle tracings in Fig. VI: 3. Repeated insertions and retractions of the electrode through the anterior wall of the tumour are shown in the bottom tracing.

(*d*) Negative surface potentials and elevated internal potentials were also encountered in malignant tumours. A similar type of electric potential profile of tissue was also encountered in local infections.

(*e*) A positive surface potential and negative internal potential were also observed in granulomas. A tuberculous granuloma, for example, is seen in postero-

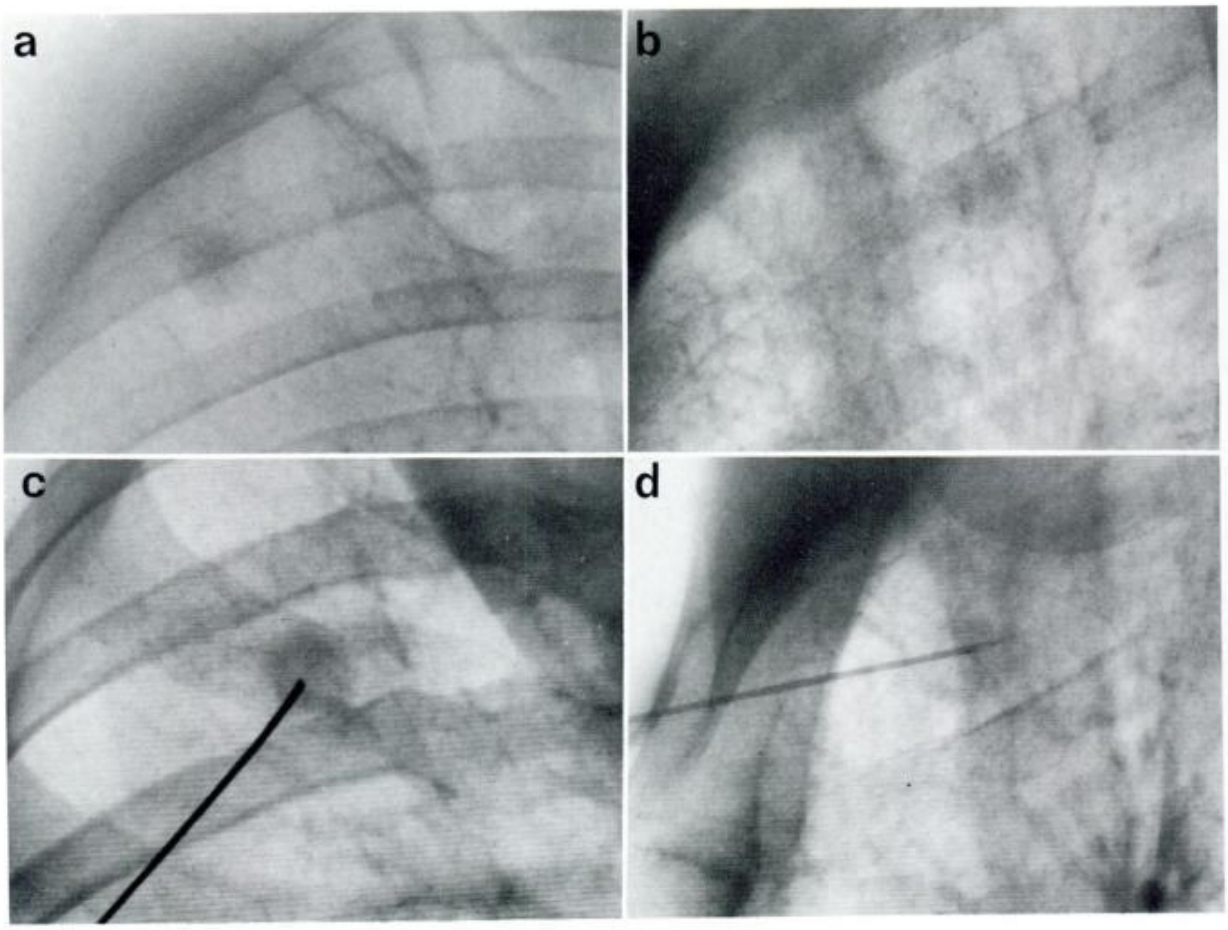

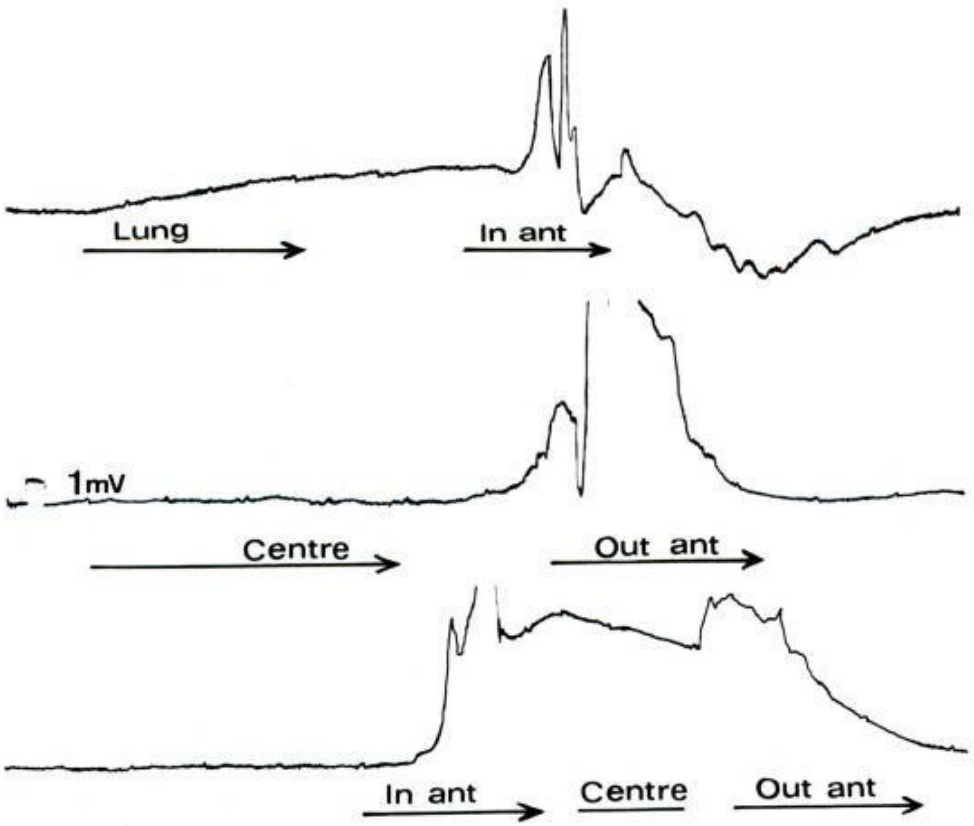

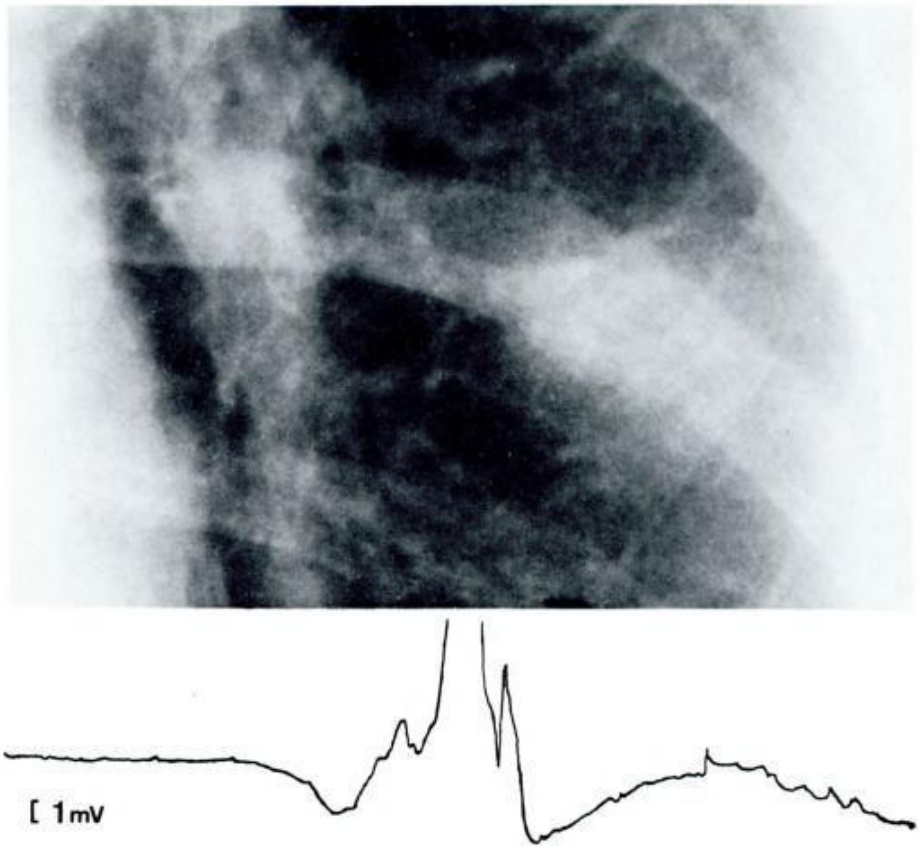

Fig. VI:5. Electric potential between inflammatory lesion in the lingula and surrounding lung in a 50-year-old man. A negative potential was obtained at the periphery of the lesion, and a positive potential inside the lesion as the exploring electrode entered the lesion and then was retracted into the lung parenchyma.

anterior and lateral views in Fig. VI: 4 *a* and *b*. Vessels around the lesion appear circularly displaced. Fig. VI: 4 *c* and *d* show the needle electrode inside the lesion. Positive fluctuations of potential were seen when the needle-electrode entered the lesion. The positive surface potential was then followed by a deeply negative potential inside the mass. When the electrode was retracted from the centre to the surface of the lesion, a new positive potential deflection appeared (middle tracing). When these two manoeuvres were combined rapidly (bottom tracing), i.e., insertion to the centre and immediate retraction, a combination of the top and middle tracings was obtained.

A "reversed" profile of tissue potential was also observed occasionally, as in the nonspecific inflammatory lesion seen in Fig. VI: 5. As the needle electrode was inserted and then retracted, the corresponding tracing showed a negative deflection with the "exploring" electrode at the periphery and a positive with the electrode inside the tumour. The inflammatory lesion seen in Fig. VI: 6 also gave rather consistently small negative deflections of potential when the needle electrode was passed through its anterior and posterior margins, as shown in the three tracings.

(*f*) Both malignant tumours and inflammatory lesions showed, to a large extent, similar types of profiles of electric tissue potential. They also showed considerable variation among individual patients, although each lesion revealed a consistent pattern of fluctuations of potential on repeated tracings.

The magnitude of the differences of potential could never be predicted beforehand. In 20 (19%) of the 107 cases, positive or negative potential differences exceeded 12 mV, compared with surrounding normal tissue. In eleven cases (10%), potentials of 30 to 50 mV were observed. No significant potential difference was found in 20 cases. In 56 cases the potential profile of tissue showed multiple small positive and negative deflections.

The variability of the different types of potential

Fig. VI:4. Electropositive surface potential of a tuberculoma in relation to surrounding lung tissue. Right upper lobe of a 42-year-old woman: (*a*) posteroanterior and (*b*) lateral views, (*c*) and (*d*) biopsy electrode in lesion. When the electrode entered the lesion (top tracing, In ant) a positive surface potential was observed. Upon retracting the electrode from the centre of the lesion into lung anterior to it (middle tracing, Out ant), a new positive potential was obtained. Upon reinserting the electrode into the lesion and immediate pulling it back into the lung parenchyma, a summation of the individual top and middle tracings was obtained (bottom tracing).

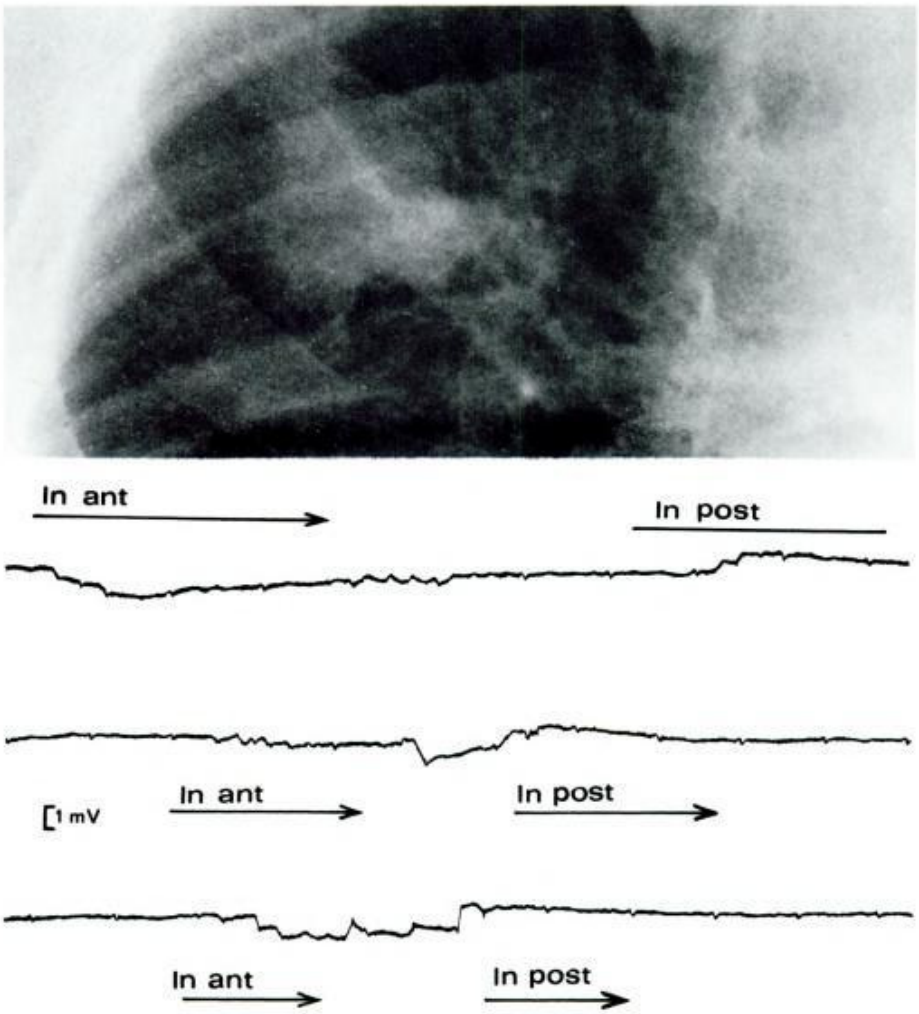

Fig. VI:6. Slightly negative electric potential inside a nonspecific pulmonary inflammatory lesion in a 58-year-old man. Each of the three tracings depicts an electronegative lesion, compared to surrounding lung.

differences illustrated above appeared initially to be unexplainable. The reproducibility of the fluctuations of the tissue potential in the individual cases indicates, however, that specific differences of electric potential do sometimes exist between lesions in the lung and surrounding tissue. No attempts have been made thus far to determine "absolute values" of such potential differences because their functional effects, in terms of flow of electric current (a main topic of this book), depend not only on the generation of potential gradient but also on the characteristics of existing circuitries and times of current flow.

As will be seen in later chapters, electric polarization of tissues, giving rise to electric transports, fits into a logical explanation for the development of structures and various functions.

Before reporting these studies, however, we should briefly discuss possible sources of local polarization of tissue. Local changes of the physicochemical potential, e.g., at the surface and inside a lesion as compared with surrounding normal tissue, can be expected to develop in two principal ways: (*a*) by the "normal" metabolism of the actual pathologic process, or (*b*) additionally, by a "complicating" pathologic process, i.e., local necrosis, bleeding or infection.

In the case of "normal" pathologic metabolism, tissue-specific physicochemical potentials might be expected. The electric potential, however, appears most unlikely to permit differential diagnosis of normal and pathologic tissues.

In the case of a degrading process in a normal tissue or tumour, the total physicochemical potential can be expected to change as an injury potential. In this view it is understandable why tissues such as malignant tumours very often, but not always, show electric polarization as a consequence of the internal bleedings or local necrosis common to neoplastic tissues. The "accidental" local development of necrosis, bleeding, infection or similar factors is probably the most likely background for the development of local electrochemical changes in malignant tumours.

To investigate the accumulation of local charge, e.g., at the surface of certain lesions, the local effects of short circuiting of normal tissue were assessed.

Studies were performed first in normal subcutaneous tissue of the dog, then in human pulmonary masses found to have an elevated electric surface potential in relation to surrounding normal tissue. Finally, experiments were performed to charge and discharge tissues.

Table VI: 2

Stability characteristics	Average zeta potential (millivolts)
Maximum agglomeration and precipitation	0 to +3
Range of strong agglomeration and precipitation	+5 to −5
Threshold of agglomeration	−10 to −15
Threshold of delicate dispersion	−16 to −30
Moderate stability	−31 to −40
Fairly good stability	−41 to −60
Very good stability	−61 to −80
Extremely good stability	−81 to −100

B. Short circuiting of different parts of normal subcutaneous tissue

The possible influences of local differences of charge in tissues require some considerations of the characteristics of colloids.

When in aqueous suspension of low ionic concentration, practically all organic and inorganic colloids are electronegative in the pH range of 5 to 10 (14). The zeta potential in such systems (see also Fig. X: 8) varies generally between −14 to −34 mV. Proteins with zeta potential values less negative than −14 mV are usually unstable. Stability characteristics of colloids are presented in Table VI: 2 as a function of their zeta potentials, according to Riddick (14).

Proteins of living tissue also fall into these categories, although as pH decreases they become less electronegative. Even the average level of electric potential of living tissue maintains a net negative charge, usually well below the threshold values for colloid agglomeration and precipitation (14). Within a tissue, levels of electric potential can be expected to vary. Hypothetically, then, experimental levelling of the densities of ionic charge among different regions of a tissue should be expected to alter the normal electrochemical environment and most likely interfere with usual tissue functions. This hypothesis was tested in the subcutis of three normal dogs in the following way:

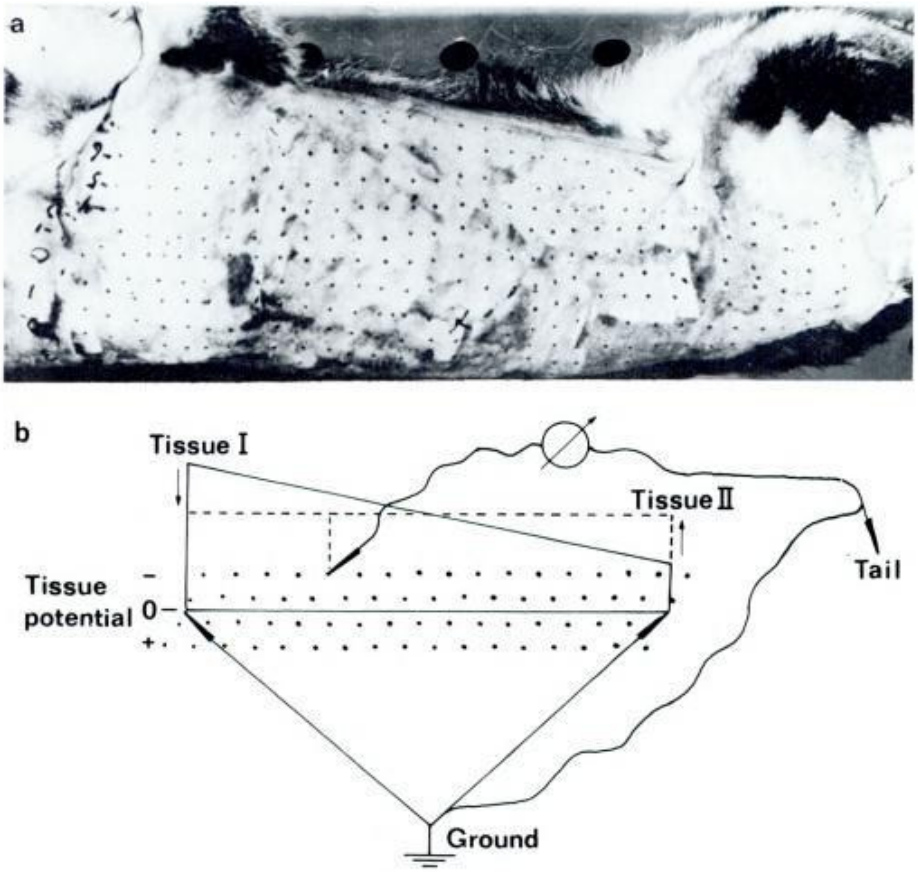

Fig. VI: 7. Short circuiting of different parts of the subcutis of a dog. (*a*) The right side of a dog was shaved and a regular pattern of ink dots were placed on the skin. (*b*) Two regions of tissue of different potential (I and II) were connected with each other by an external wire (over ground). The conducting electrolytes in the interstitial fluid complete a closed circuit, allowing a levelling of the assumed differences of tissue potential. The resultant levelling is recorded as changes in the local electric potential under each dot in relation to a distant, grounded reference tissue (subcutis of the tail).

Table VI: 3. *Deflections of potential (in mV, numerically negative) in the subcutis of the dog pictured in Figs. VI: 7 and 8*

Grounded sites of short circuit of the subcutis are indicated by *X*. For explanation, see text

					70	75	70	70	65	70	70	70	60	60	55	55	50	45	40	40	35	32	30	30	28	25	35	25	30	
				50	45	45	50	50	45	55	50	50	52	52	50	50	52	50	50	55	60	55	52	55	70	65	70	75	75	
			60	65	65	70	65	70	55	60	60	55	55	75	70	75	80	70	70	75	60	75	75	75	55	40	40	40	35	40	
		52	50	52	50	48	45	48	45	44	46	52	50	52	50	55	50	48	50	45	45	45	35	30	32	35	35	32	42	32	
	52	52	48	46	45	48	48	50	50	52	52	50	48	45	45	50	44	48	42	44	50	38	35	32	32	38	30	24	40	20	X
X	05	12	15	20	20	18	22	24	25	25	25	24	22	10	15	20	22	22	23	25	24	25	24	26	18	25	24	22	25	26	
	32	30	30	28	30	28	28	30	30	28	26	30	28	32	32	30	30	28	30	25	22	24	24	25	24	26	24	22	20	16	
	15	20	18	22	24	24	28	28	30	30	30	28	28	35	38	35	34	34	32	30	35	36	32	30	32	32	42	38	34	38	
		40	38	40	40	35	32	30	32	30	32	38	35	35	34	34	36	36	38	32	30	30	28	25	28	25					
		25	40	25	28	25	30	28	28	30	32	28	34	30	32	35	38	40	40	38	38	40	42	48							

Each animal was anaesthetised with an intravenous injection of sodium pentobarbital. One side of the chest and abdomen was shaved. 275 to 300 dots were made with ink to form corners of squares 2 cm apart all over the shaved skin (Fig. VI: 7 *a*). Different parts of the subcutis were then connected to each other over a common ground (Fig. VI: 7 *b*). The electric potential of the subcutis corresponding to each of the ink dots was then determined versus a distant grounded reference electrode in the animal's tail.

Electrodes of mechanically stable steel were used to permit perforation of the skin. The potential difference between each measuring point and the reference electrode was determined with a Brush DC-potential instrument (Mark 220, input impedance 10 megohms). One examiner inserted the exploring electrode while the numerical readings of the potential differences were read and noted by assisting examiners. Insertions of the electrode were made in a transverse scanning mode at each of the skin dots. Care was taken to introduce the exploring electrode into the space between the subcutis and the fascia of underlying muscle, without entering the muscles. This placement was most easily achieved by a slight lifting of the

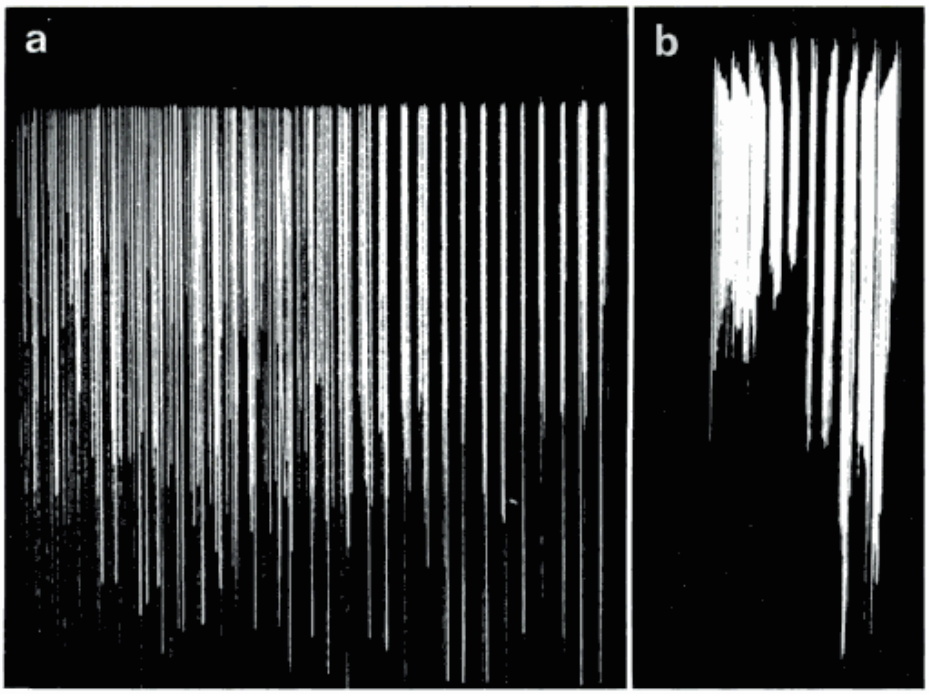

Fig. VI: 8. Three-dimensional display of electric potentials in the subcutis of a dog, as represented by corresponding lengths of hanging white strings. The upper ends of the strings represent zero, so that each individual tracing in the experiment represents a negative value in comparison to the reference electrode. Fig. *a* shows a longitudinal view and *b* a cephaled view, which means the short side of the display of strings. Two sites of the subcutis were short circuited (indicated by *X*, in Table VI: 3). As seen in *b*, a "tunnel" of low values of potential is present between the two short circuited sites.

Table VI: 4. *Deflections of potential (in mV, numerically negative) in the second part of the experiment in the subcutis of the dog in Figs. VI: 7 and 9*

Grounded short circuit sites of the subcutis are indicated by *X*. For explanation, see text

					X											X											
					40	25	40	48	48	42	46	35	38	32	38	35	35	45	42	48	50	50	50	55	50	65	60	
				40	38	36	28	38	48	45	46	45	35	35	30	45	32	32	42	42	48	50	50	52	50	50	60	60	
			28	40	36	35	30	35	40	45	46	40	36	35	32	42	30	30	42	45	47	55	55	55	50	55	60	60	
		42	28	40	40	30	30	38	40	45	42	38	40	32	35	38	30	36	40	45	42	50	50	55	50	55	55	70	55
	42	40	30	40	40	30	32	40	38	48	42	40	40	32	32	42	26	38	42	46	42	55	55	50	50	60	50	70	52
	40	45	32	38	40	30	28	38	38	48	48	40	42	42	32	40	24	35	40	42	40	55	55	52	52	70	55	70	52
	42	42	32	38	40	30	30	36	40	50	42	40	40	35	36	42	28	35	40	40	42	60	55	50	50	55	50	70	55
	50	42	36	40	40	30	32	35	38	48	50	40	40	35	35	40	24	36	38	42	40	60	55	52	50	60	55	65	55
		45	38	42	40	30	32	30	40	45	46	40	42	32	38	35	22	38	36	40	40	55	60	55	45	60			
		42	40	42	40	28	30	30	40	40	48	42	40	32	38	40	20	40	38	40	40	60	75	70					
						X													X								

skin as the needle electrode was introduced. The readings were made immediately on entrance of the electrode into the subcutis. The sites of tracings of potential and their corresponding readings were correlated at the conclusion of each experiment.

In the dog seen in Fig. VI: 7 *a*, points in the subcutis of the right shoulder and hind leg were short circuited over ground for 30 minutes. Measurements of potential were then made during the following 20 minutes of continued short circuiting between each of 276 recording sites and the reference electrode. After the numerical tracings were recorded (Table VI: 3), they were displayed as three-dimensional histograms (Fig. VI: 8). Each histogram was made simply by colouring pieces of white wool strings with dark ink so that the uncoloured parts corresponded to the actual readings of potential. The strings were then hung in a pattern corresponding to the sites and values of each reading.

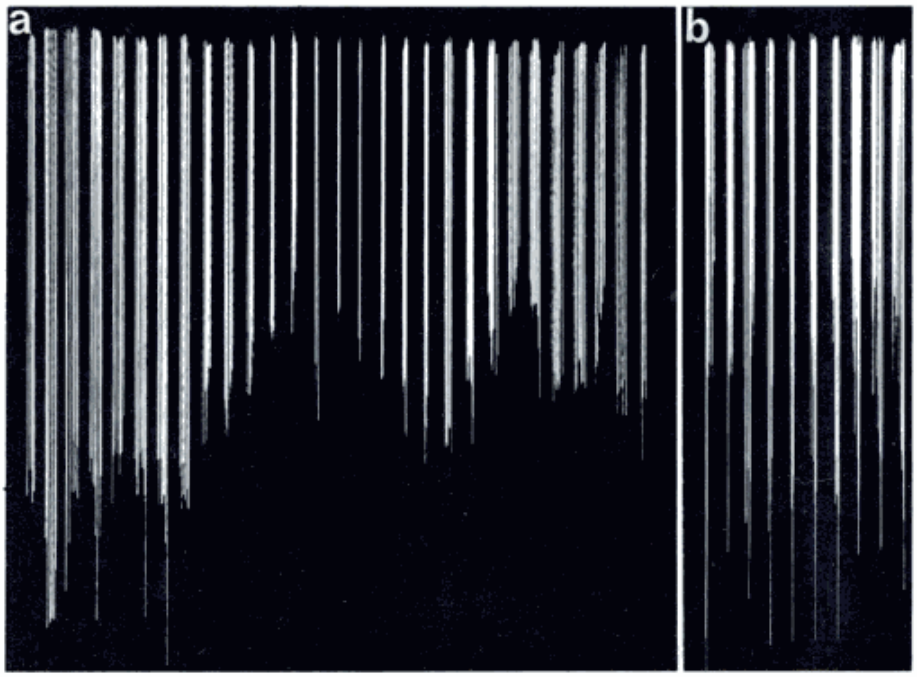

Fig. VI: 9. Three-dimensional display of electric potentials of the subcutis in the second part of the experiment on the dog in Fig. VI: 7 *a*. Fig. *a* represents a longitudinal view and *b* a cephaled view. For the previous 30 minutes, two short circuits of the subcutis were made perpendicular to the short circuiting represented in Fig. VI: 8. The positions of the short circuited sites are indicated in Table VI: 4 by *X* markings. Two new "tunnels" (*a*) of low potentials are present between the two pairs of short circuiting sites. For explanation, see text.

Table VI: 5. *Deflections of potential (in negative mV, except as indicated by a + sign) when many grounded sites were short circuited in the subcutis over the area of shaved skin*

Same dog as pictured in Figs. VI: 7 and 10. For further discussion, see text

				10	12	10	8	5	4	2	1	+5	+6	+1	+5	+14	+2	+2	2	0	0	2	0	+2	7	4	5	4	+4	0
		10	10	4	10	8	5	5	5	2	0	+4	+8	2	+4	+15	+2	+1	0	+2	0	2	+2	0	6	3	4	1	+2	0
8	8	10	12	5	6	6	10	6	8	2	5	+4	+5	0	+4	+2	+3	+2	+5	0	0	0	+5	0	6	5	4	2	+2	0
8	10	10	12	8	10	5	8	6	8	2	6	+4	+5	0	0	+2	+4	+2	0	0	0	2	+5	1	4	6	4	3	0	0
8	10	8	12	10	10	6	4	8	8	+8	5	0	0	0	10	+5	+6	+3	0	1	+2	0	+6	5	4	5	4	4	0	4
8	10	10	12	10	6	6	2	8	5	+8	2	0	2	0	+4	+5	+6	+3	2	1	0	+2	2	5	4	5	+8	5	0	6
12	8	10	10	10	10	8	2	10	5	+5	2	1	4	0	+4	+6	+6	+5	+2	0	2	+4	+10	6	4	12	20	6		4
20	5	18	10	10	12	8	4	8	5	+6	2	4	1	2	+3	+5	0	+5	0	0	0	+2	+2	4	8	5	12	5		
15					5	8	5	8	10	+4	4	4	0	0	+3	+8	+8	+4	0	0	+4	0	+5	4	8	+10	12	15		
5								8	0	0	0	5	0	0	+7	+9	+7	+4	+2	+2	+8	2	+8	4	4	+10	10	4		
10								5	0	0	+4	4	+1	0	+7	+10	+8	+4	+2	+8	+12					+5	0	4		

The three-dimensional display of the readings is then seen in two photographs taken at right angles (Fig. VI: 8). The distribution and magnitude of the numerical values represent negative millivolts. The electrically short circuited sites of the subcutis are indicated by (*X*) in Table VI: 3. A "tunnel" of relatively less negative values of potential than in the surrounding subcutis was found to bridge the two electrically connected sites (*X*) in the subcutis.

A second part of the experiment was performed one hour after the previous short circuit connections had been removed. Four new sites in the subcutis were grounded, two anteriorly and two posteriorly along the midportion of the long side of the examination area. The short circuit was again maintained for 30 minutes. Thereafter, the electric potential was measured between each of the 276 sites and the reference electrode, as above. The results of this part of the experiment are seen in Fig. VI: 9, while the corresponding numerical values of potential and sites of grounded short circuit connections appear in Table VI:4. Two new "tunnels" of lowered negative values of potential have appeared somewhat obliquely across the middle of the area of examination, corresponding to the regions between the sites of the short circuits.

A third part of the experiment on the same dog was

Fig. VI: 10. Three-dimensional display of electric potentials in dog subcutis after short circuiting of the subcutis across many sites. Potentials were measured between the exploring electrode and a grounded subcutaneous reference electrode (in the tail). As seen in Table VI: 5, very small negative and even positive potentials were obtained. The zero level is here indicated by small pieces of white plastic tubing. Fig. *a* represents a view of the long and *b* a view of the short side of the display of strings.

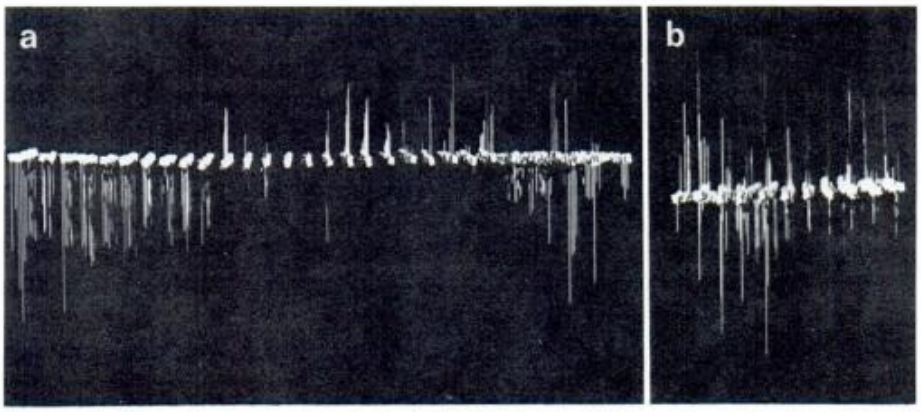

performed after additional short circuiting of the subcutis across many sites (Fig. VI: 10, Table VI: 5). In this situation the potential differences were found to be either slightly negative or even positive. In the display seen in Fig. VI: 10 the zero level is represented by small pieces of plastic tubing on the strings. At autopsy, examination of the subcutis revealed only a few minor blood stains but no large haemorrhages. Similar results of the three parts of the experiment were also found in the two other dogs tested.

The experimental results in these 3 dogs indicate that the average level of potential of normal subcutis may be changed by external short circuiting of two or more regions of the tissue. The effects of such a measure are mostly regional and localized, as might be expected, to the tissue most immediately between the electrodes. As illustrated in Figs. VI: 8 and VI: 9, which were performed in the same animal, a recovery of the levels of potential took place between the first two parts of the experiments. This capability shows that the produced changes may be reversible.

These effects on subcutaneous electric potentials indicate that electrical transport developed preferentially in the tissue between the short circuited electrodes. This difference of potential then appeared to tend to equalize after 30 minutes in a closed circuit. A change of the distribution of electrical charges between electrodes can therefore be anticipated to influence function of the tissues near the electrodes, resulting in a change in an electropositive direction of electronegative potentials between the electrodes. This finding may be regarded as an interference with the electronegative potential normally generated physiologically in the tissue. In Chapter XVIII, these experimental results will be utilized to explain acupuncture.

C. Induced levelling of the electric potential of pulmonary lesions

When an exploring nonpolarizable Ag–AgCl electrode or polarizable metal electrode is moved through the lung into a focal lesion, reproducible profiles of electric potential are usually obtained in relation to a grounded reference electrode in the subcutis. Impedance of the recording instrument must be sufficiently high, (>10 megohms. See also Fig. XIII: 9).

When a recording instrument of "low" impedance (e.g., 1–2 megohm) is used, current can be demonstrated to leak through the instrument, thereby diminishing the potential difference of the tissues. Fig. VI: 11 shows such a tracing of potential while the exploring electrode touched many times against the surface of a bronchogenic carcinoma which had an elevated surface potential. The grounded reference electrode was positioned subcutaneously about 25 cm from the lesion. Large deflections of potential are seen on the left side of the tracing at the beginning. The amplitudes of the deflections then diminish, as seen on the right side of the tracing.

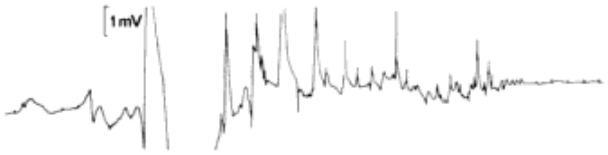

Fig. VI: 11. Local discharge of a bronchogenic carcinoma with elevated surface potential in relation to surrounding lung over a low impedance (2 megohm) voltmeter. Grounded reference electrode in the subcutis. The tip of an exploring electrode was moved repeatedly against the surface of the tumour. The surface potential of the tumour was initially elevated but progressively decreased as current leaked through the recording instrument.

A similar experiment in tracing the profile of electric potential in tissue is illustrated in Fig. VI: 12, when picking movements were made with the exploring electrode against different parts of the surface of a tuberculous granuloma. Large fluctuations of the electric potential were seen initially at various parts of the surface of the lesion (top tracing). During a second series of picking movements of the electrode against the surface (bottom tracing, left) and then a third series of picking movements (bottom tracing, right), the average amplitude of the deflections decreased. The lowering of amplitudes was larger between the first and second than between the second and third series of picking movements.

An experimental analogue to this study will be pre-

Fig. VI: 12. Local discharge of a tuberculous granuloma with elevated surface potential in relation to surrounding lung. Grounded reference electrode in the subcutis. Repeated contact of the tip of the exploring electrode against the surface of the granuloma showed initially large potential differences (upper tracing). Later, these diffferences diminished in amplitude (on left and right of lower tracing). For further discussion, see text.

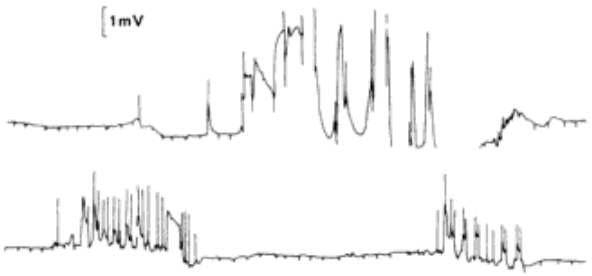

sented in Chapter XIII, Fig. 9, where the leak of current through a low impedance recording system has been studied and utilized for similar purposes.

The experimental levelling of the surface potential of a lesion in relation to a reference tissue can be most easily explained as a closed circuit discharge of tissues which may be regarded as a conglomeration of biogalvanic cells. If this hypothesis is correct, then it should also be possible experimentally to charge and discharge specific tissues or regions of tissue.

D. Experimental charging and discharging of tissue

Testing of the clinical observations on local discharge of a tissue was carried out in five dogs in the following way (see also charging of tissue in tumours of patients in Chapter XVII).

A 1.8 mm thick catheter was introduced via a femoral vessel into the lumen of the aorta or the inferior vena cava of the anaesthetized animal (sodium pentobarbital). A platinum electrode was inserted into the catheter, which was irrigated continuously with physiologic saline solution. The abdomen was surgically opened. Another platinum electrode was directly placed against tissues of various organs, e.g., mesentery. A direct current potential of predetermined magnitude was applied between the electrodes for one to several minutes. The potential difference between the two electrodes was then measured with a millivoltmeter immediately after interruption of current flow. The electrodes were then short circuited over a microamperemeter in parallel with the millivoltmeter. The values of current and potential were then read at regular intervals and plotted against time.

These experiments revealed in the 5 dogs that in vivo an artificial electrical charging and discharging of a tissue was easily demonstrated.

Thus, in the experiment illustrated in Fig. VI: 13 a potential of 23 volts at an initial current of 6.5 mA was applied between the aorta and a mesenteric electrode in a dog. After 15 minutes, a potential of 1.8 V was measured between the electrodes. The electrodes were then connected to each other over the microampere meter. The current-time integral of the discharge is illustrated in Fig. VI: 13. The initial values are not included because initial discharge was very rapid.

Fig. VI: 13. Artificial electric charging and discharging of living tissue of a dog. One platinum electrode was placed against the mesentery and one in the lumen of the aorta via a femoral catheter. A 23 volt potential, giving initially 6.5 mA current, was applied between the electrodes for 15 minutes. 1.8 volts were then measured between the electrodes. The current flow between the electrodes was then read by means of a digital microamperemeter in parallel with the voltmeter. The initial part of the discharge took place very rapidly between the cessation of applying potential to the electrodes and the first measurement. Initial current values are therefore not included.

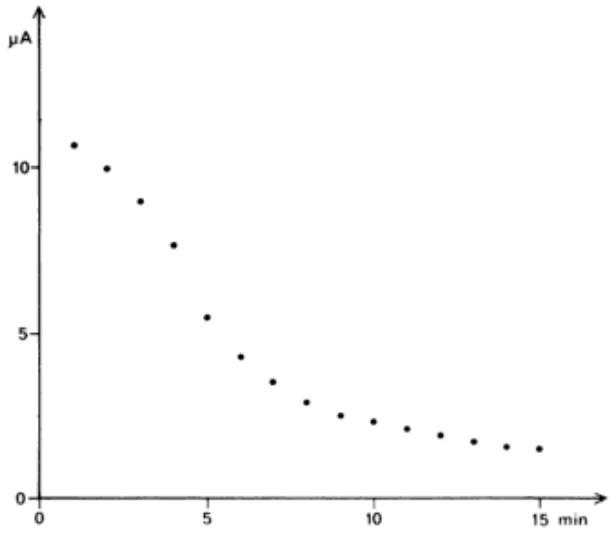

Differences of electric impedance and ionic concentration in different tissues allow local variations of electric charges. These charges can be artificially changed when the tissues are electrically connected to each other over electrodes and an external conductor. Thus, short circuiting between tissue regions of different electric potentials can level that potential difference. Moreover, when an external source of direct current is connected into the circuit, an artificial local charging of tissues can be obtained. Different tissues such as fat, muscle, viscera, bone, blood, interstitial fluid, cell membranes, etc., are also known to have different resistivities (see Chapter XII). It is therefore logical to regard tissues as composed of numerous galvanic cells with different capacity. A tumour or granuloma with an electric potential in relation to the surrounding tissues should therefore contain a surplus of cations or anions in relation to surrounding tissue. Why and how such ionic separations occur in vivo is another problem, which will be considered later.

E. Control studies of electric potentials of normal and pathological tissues

At this stage of experimentation the existence of electric potential between a pulmonary lesion and surrounding lung was checked with a modified technique. This part of the study was performed in a group of

fifteen patient-volunteers. In these studies nonpolarizable Ag–AgCl electrodes with KCl–agar bridges were used. The electric potentials of normal lung, pleura and liver in dog will be described as a background to discussions of integrated influences by "reference" tissues.

1. Electrodes, recording of potentials, and techniques of cell sampling

Nonpolarizable *Ag–AgCl electrodes* with KCl bridges were used in order to explore the possibility that diffusion potentials participate in the development of the observed electric potentials of lung lesions.

Silver strings, 155 mm long and 0.25 mm thick, were each soldered to electrical cables. The site of soldering was protected with Araldite® and a plastic tube. The strings were polished and chemically cleaned (CCl_4 15 minutes, 1 M HNO_3 2 minutes, 10% $(COOH)_2$ 5 minutes). The surfaces of the silver strings were then coated with a layer of Teflon (954-103) in liquid suspension. The Teflon was allowed to dry with the string in a vertical position. The string was then placed in an oven for 5 minutes at a temperature of 260°. In this manner two Teflon layers were applied to the surface of the string. The distal 5 mm of the Teflon layers were then scratched off the string and the surface polished and cleaned chemically as described above. A chloride layer was applied to the 0.04 cm^2 of silver surface (0.9% NaCl solution, current of 0.4 mA between the string and an equally cleaned silver plate, duration 50 seconds).

Electrodes manufactured in this way were then kept in the dark in a 2 M KCl solution. Their electrical cables were connected to each other and to a carbon rod, which was also placed in the KCl solution, as recommended by Cooper (2). Because carbon is slightly cathodic with respect to silver-silver chloride, a small chloriding current was maintained. Electrodes treated in this way show good electrical stability, comparable to what has been reported by Cooper (2) and Geddes and Baker (4).

Salt bridge carriers were manufactured from hard radiopaque Teflon tubes, Teflon coated cannulas (1.2 mm thick), or in dog experiments, glass capillaries. They were filled with 3 M KCl solution in 2% agar.

Cytological sampling followed by electric potential studies was performed through hard Teflon tubes. These tubes (165 mm long, 1.5 mm thick) were provided with a plastic three-way stopcock and an indwelling, 1 mm thick, biopsy cannula. Each tube was inserted under local anaesthesia in the skin through a 3 mm incision. The tube was advanced under fluoroscopic control to the edge of the lesion. Cytologic material was then sampled by means of a screw needle, 0.55 mm thick, inserted through the cannula into the tissue, according to the technique previously described by the author (11). After removal of cellular material, a new needle was inserted through the plastic tube and advanced to the distal wall of the lesion, where again cellular material was sampled.

The lumen of the plastic tube was then filled with the sterile agar–KCl solution, which shortly before was made liquid by placing the agar–KCl bottle in boiling water. The Ag–AgCl electrode was introduced into the plastic tube with the proximal part secured in the hub of the stopcock. Care was taken not to introduce air bubbles, both when filling the tube with the KCl–agar material and when inserting the electrode.

A corresponding, grounded, reference electrode was also introduced into the subcutis of the chest wall.

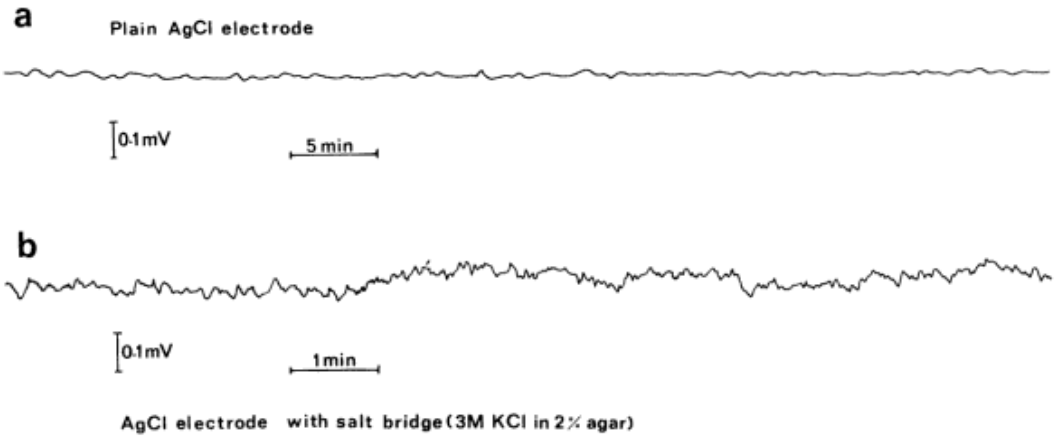

Fig. VI: 14. Stability tests of Ag–AgCl electrodes in 0.9% NaCl. (*a*) Drift of 6 microvolts during a 30 minute period. Fluctuations < ±10 microvolts. (*b*) Same electrodes in 0.9% NaCl with interconnected 3 M KCl-agar bridges. Potential drift of 100 microvolts during a 30 minute period. Fluctuations < ±40 microvolts.

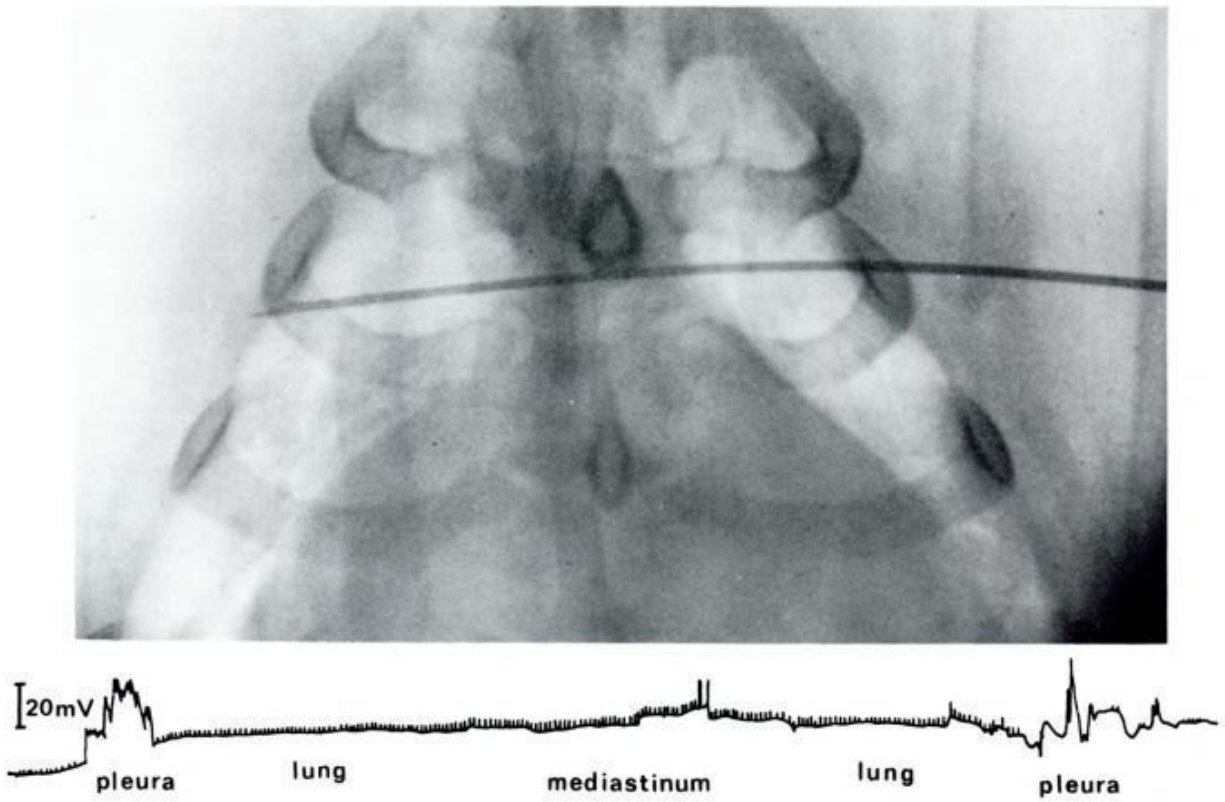

Fig. VI: 15. Profile of electric potential of tissue through the chest of a dog in relation to subcutaneous grounded reference electrode. Anteroposterior radiograph. Needle electrode was inserted from the left side through the chest, anterior and superior to the heart. While the exploring electrode was removed, 30 mV positive potentials are seen when the electrode traversed the left and right pleurae. Two positive tissue potentials are also seen upon traversing the mediastinum. Small regular "spikes" represent a superimposed electrocardiogram. These are of lower amplitude in the chest wall than in the lungs.

Electric potential of the tissues was recorded during withdrawal of the exploring electrode. When recordings were made during cineradiography (frame speed 50/sec), the position of the electrode was determined by comparing the cine frames with the markings of the frame exposures on the same chart paper as the electric potentials.

The impedance of the recording circuit was usually in the kiloohm range. The input impedance of the recording instrument (Grass Polygraph direct current recorder) is 10 megohms.

Stability of the electrodes was tested repeatedly and found entirely satisfactory (Fig. VI: 14).

After primary amplification of the input signal, the outgoing signal was fed back into parallel-coupled, secondary amplifiers. This arrangement permitted separate treatment of amplification and filtering of individual tracings, which appeared necessary because the actual tissue potential profiles could not be predicted.

In instances when the tissues were fibrotic or otherwise hard, salt bridges of higher mechanical stability than the Teflon tubes were used. Biopsy needles, 1.2 mm thick, were then coated with double Teflon layers on their inside and outside surfaces in the same way as the Teflon coating on the electrode surfaces. Salt bridges within these needles have shown excellent mechanical stability but preclude use of these needles for combined cytologic sampling and studies of electrical potential. On the other hand, several tracings of electric potential can be made during insertion and withdrawal of the instrument.

2. Electric potentials of pleura and lung

The preliminary studies of electric potential of lung revealed certain characteristics of the profile of electric potentials of two specific tissues. These profiles could be identified as related to specific structures by means of high speed cineradiography.

The electric potential of pleura and lung, studied in 22 dogs, appeared as follows. Tracings were made with the polarizable stainless steel electrodes and with the nonpolarizable Ag–AgCl electrodes provided with a salt bridge in a glass capillary.

In Fig. VI: 15, a frontal view is seen of the thorax of a dog with the exploring, Teflon-coated, polarizable, stainless steel electrode inserted through the anterior and superior part of both lungs. The noninsulated tip of the electrode is situated in the soft tissues of the right thoracic wall. The grounded reference electrode is positioned in the subcutis of the left side of the thorax but is not seen in the radiograph. The exploring electrode was pulled as evenly as possible out of the chest as electric potential was traced continuously.

A series of positive fluctuations of potential differences appeared in the chest wall or the pleura. The section of tracing corresponding to lung shows a relatively even level of potential. A superimposed electrocardiogram shows very small fluctuations in the chest wall compared with the lung, where the amplitudes also increased as the tip of the electrode moved toward the heart.

The potentials of chest wall-pleura were further investigated. When the electrode was passed through the pleura in a dog, positive fluctuations of potential are seen in Fig. VI: 16 before (upper tracing) and after (lower tracing) the introduction of some air into the pleural space. When the electrode was introduced and removed, about 20 mV positive deflections of potential were seen at the site of contact between pleura and chest wall. After some air was put into the pleural space, the electrode was introduced and pulled out, but slowly. This tracing shows a large positive deflection of potential before the tip of the electrode reached the air-filled pleural space. When the retracted tip reached the air in the pleura, rapid oscillations occurred due to the open circuit. At the touch of the visceral pleura these oscillations disappeared. The potential in the lung was approximately the same as observed previously in the chest wall. Positive deflections of potential of the type that occur on traversing the parietal pleura were not observed from the visceral pleura in dog or man.

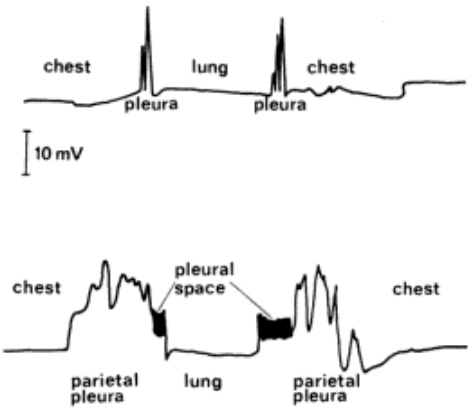

Fig. VI: 16. Demonstration of electric potential of pleura in dog. As the exploring electrode passed between the chest wall and lung, about 20 mV of potential difference was recorded, corresponding to the pleura (upper tracing). When air was present in the pleural space (lower tracing), the same manoeuvre shows that the potential difference is related to the parietal pleura. As the electrode is inserted or withdrawn through the air-filled pleural space, an open circuit is created, causing rapid oscillations. Stainless steel electrodes.

In Fig. VI: 17 a control study is shown of the electric potential of pleura and lung in the dog, using the same recording equipment and the nonpolarizing Ag–AgCl electrodes inserted into glass capillaries filled with KCl–agar. The grounded reference electrode was positioned in the subcutis of the right chest wall. The exploring electrode was inserted from the opened abdominal cavity through the diaphragm into the lung close to the costophrenic sulcus. The glass capillary could then be moved repeatedly from the lung to the pleurae and chest wall. As in previous studies, positive deflections of potential were obtained at the contact with the inner surface of the chest wall. These deflections, corresponding to the parietal pleura, have a magnitude of about 20 mV in relation to the pulmo-

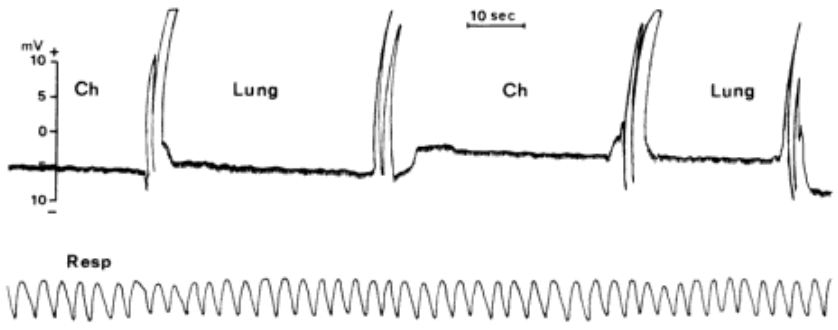

Fig. VI: 17. Electrical potentials at the pleura, upon four insertions and retractions of a Ag–AgCl electrode in a thin glass capillary with KCl agar salt bridge. Grounded reference electrode of the same construction was positioned in the subcutis of the chest wall. *Resp* = pneumotachygraphic recording of respiration. The exploring electrode was inserted from the abdominal cavity through the diaphragm into the lung, and then moved from the lung to the chest wall (*Ch*) and back. Each movement to and from the parietal pleura caused two deflections of potential. These pleural potentials were used in the studies of tissue potential profiles of pulmonary masses to localize the tip of the exploring electrode.

nary parenchyma. The potential deflections of the pleura were present in all the twentytwo dogs and are also detectable in man (see Fig. VI: 21).

After repeated needlings in the same place, the tissue profile of electric potential of the lung sometimes varies slightly, which may result from small haemorrhages in the track of the electrode. The superimposed electrocardiogram usually shows a lower amplitude in the chest wall than in the pulmonary parenchyma.

Discussion. Agostoni (1) published in 1972 an extensive physiologic review of the pleura, including 268 references. From this source and further search of more recent literature, it appears that pleural electrophysiology has not been a subject of previous study.

No attempts have been made here to evaluate the functional significance of the positive potential of the pleura. It seems possible, however, that the mechanism for in vivo development of membranes and organ capsules which is proposed in Chapter XII is also valid for the development of the fibrous pleural membranes.

The distinctive electrical changes observed upon inserting and retracting an electrode through the chest wall and the lung have become a helpful landmark for topographic localization of the electrodes during tracing of electric potentials of normal and pathological lungs.

The thickness of an air layer in the pleura can easily be measured directly with an exploring needle electrode. The electrode is slowly pulled out from the lung. When an open circuit with high frequency disturbances is observed, the external position of the needle in relation to the skin is noted. After further retraction of the needle, the circuit will close when the parietal pleura is reached. Assuming the needle was approximately perpendicular to the pleural surface, the distance the needle was pulled across the open circuit indicates the thickness of the air layer in the pleura.

3. Fluctuating "demand potential" of a "reference tissue" (liver)

Considerable technical difficulties were encountered in the study of normal variations of pulmonary electric potentials in vivo. To investigate the possibility that such variations might be caused by outside events, e.g., metabolic changes in an organ or "reference" tissue, any organ or tissue might be studied. The liver, more easily accessible than the lung, was chosen for these studies.

The experiments shortly to be described suggest the concept that physicochemical potential of a normal tissue changes during different phases of its metabolic activities. These changes represent what might be called physiological "demand potentials" (see further Chapter XII).

As previously stated, a tissue may be regarded as composed of multiple galvanic cells of variable charge. During different functional states they may be charged or discharged. In such events the nervous system may integrate metabolic activities and the functions of ignition and balancing. Individual cells and grouped populations of cells may then, by their "physicochemical, metabolic demand potential", influence their surroundings. Accordingly, demand potentials may be traced to partial functions within a cell, a whole cell, a group of cells or a seemingly arbitrary large part of a "tissue region" such as an organ. It follows that a recording of an electric demand potential of a tissue also depends on geometry, size and location of the electrodes. These relationships include the integrated electro(-physico)-chemical potentials of the tissue components around the "exploring" electrode, around the "reference" electrode and interconnected

Fig. VI: 18. Electrical potentials from the gastric and hepatic parenchyma of a 24 kg dog. The potentials were measured in relation to a grounded sponge, soaked in saline solution in the abdominal cavity. (*a*) Rhythmic fluctuations of potential from the liver. Their frequency is similar but their amplitude lower and of a slightly different pattern than that of the stomach. These rhythmic fluctuations are independent of respiration and of cardiac electrical activity. The maxima of the fluctuations of potential of the liver and the stomach varied from (*a*) out of phase to (*b*) almost in phase. Low or high amplitudes of the fluctuations of gastric potential were not accompanied by corresponding changes of amplitude in fluctuations of hepatic potential. Rhythmic fluctuations of hepatic potential have not been previously described.

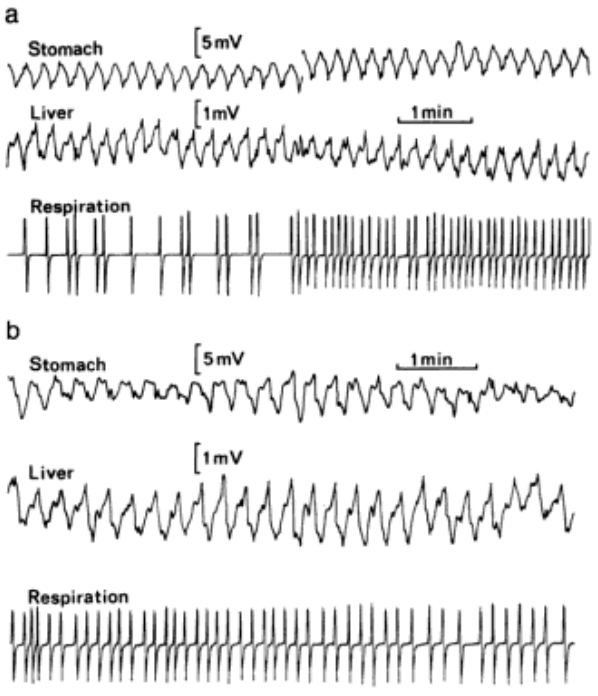

conducting tissues. A short report has previously been presented on this problem by the author (9).

In 18 experiments (15 dogs, three rabbits), laparotomy was performed. An Ag–AgCl electrode was placed under the hepatic capsule through a polyethylene tube (2 mm thick, filled with 3 M KCl solution in 2% agar). The grounded reference electrode was placed either in the subcutis or connected to a sponge sheet soaked in 0.1 M KCl solution and placed in the abdomen between the stomach and liver. An exploring electrode was also placed under the serosa of the stomach, which is known to produce rhythmic fluctuations of potential, induced by the nervous system (7, 12–13, 15–18). Respiration was recorded as pressure changes in a corrugated rubber tube, slightly stretched and tied around the lower part of the chest.

Fig. VI: 18 shows representative electric potentials of dog liver and stomach, compared to a grounded subcutaneous electrode.

These experiments revealed rhythmic fluctuations of electric potential from the liver, usually at a frequency of 3–5 per minute. The fluctuations, previously undescribed, were not produced by respiration, cardiac activity or bowel movements. Sometimes these fluctuations were almost synchronous with those of the stomach (Fig. VI: 18 *b*). Sometimes they were asynchronous (Fig. VI: 18 *a*). The waxing and waning pattern from the stomach is interpreted as an interference phenomenon of superimposed transmitted impulses. The electric potential fluctuations in the stomach are known to be of neurogenic origin (7, 12–13, 15–18). As in the stomach, fluctuations of potential in the liver parenchyma are probably also of neurogenic origin. Most likely they represent secretory electric impulses to the organ. The hepatic electric potentials could be altered by pharmacological agents. In the experiment illustrated in Fig. VI: 19, one electrode was inserted into the liver and one connected to a grounded sponge sheet soaked in 0.1 M KCl between the liver and the stomach. After intravenous injection of pharmacological agents as morphine, epinephrine, glucagon, histamine, antihistamine and others, different changes of amplitude were produced in the rhythmic fluctuations of hepatic potential. Previously undescribed slow waves of electric potential were also produced (Fig. VI: 19). Epinephrine drove the potential in a downwardly positive direction (note relatively low amplification and slow speed of the recording). The time-voltage integral is roughly dose-related. Isoprenaline gave a slow wave in the electronegative direction, while glucagon and the amino acid nutrition compound Vamin® also produced electropositive deflections. Usually the 3–5 per minute fluctuations changed their frequency and amplitude after administration of the agents which produced the slow waves.

Other organs, e.g., pancreas and kidney, have also shown fluctuations of electric potential similar to those shown in the liver. The rhythmic 3–5 per minute potential fluctuations and the accompanying slow potential wave, artificially induced by different metabolically active agents, represent examples of "demand potentials" of a normal tissue. It is evident that "demand potentials" of any tissue will influence gradients of potential in relation to locally injured tissue as well as to adjacent, but differently activated, normal tissues.

4. Electric potentials of pulmonary carcinomas

In these studies the electric potentials were recorded with the Grass Polygraph DC instrument and the described Ag–AgCl electrodes. Thus, a technique different from the preliminary was used.

Difficulties were encountered in obtaining a sufficiently large number of patients for detailed analysis of tissue polarization in different lung lesions. Permission

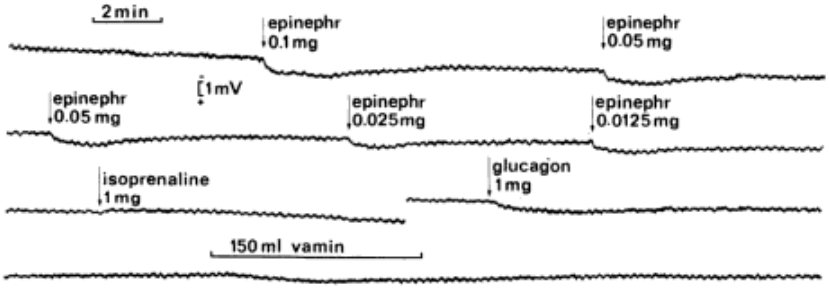

Fig. VI: 19. Electrical activity in a dog liver, recorded in vivo with Ag–AgCl electrodes over KCl bridges. An abdominal reference electrode was grounded. The rhythmic electrical fluctuations of the liver show a frequency of about 4.5 per minute. Intravenous injections of different pharmacological agents were each followed by a slow electrical wave, also previously undescribed. The time-voltage integral of these waves was found to be dose-related, within certain limits.

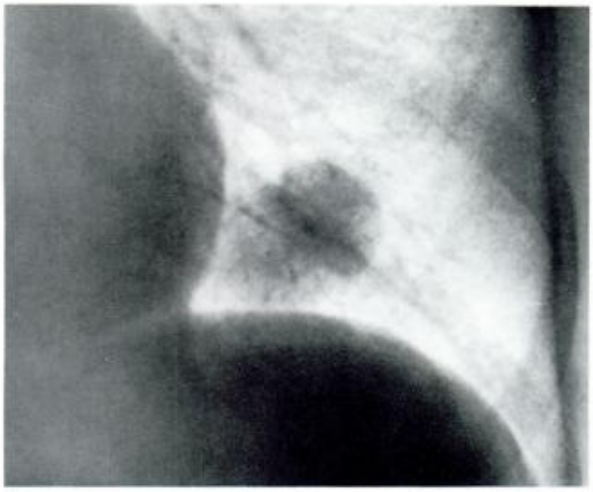

Fig. VI: 20. Poorly differentiated myosarcomatous metastasis in the left lower lobe of a 63-year-old woman. Cellular material was obtained via a needle through a percutaneously inserted plastic tube. The tube was next advanced through the tumour into the lung tissue and filled with 3 M KCl in 2% agar. An Ag–AgCl electrode was then introduced into the tube. During retraction of the electrode, with bridge, the electric potential was recorded (Fig. VI: 21) against a corresponding grounded nonpolarizable electrode introduced into the subcutis of the chest wall.

nowadays must be obtained from a patient only after it has been explained that the procedure is part of a research program and not exclusively to his or her own benefit. In twelve patients from whom permission could be obtained, the actual technique of examination has given essentially the same main information as was obtained in the preliminary study: tumours in the lung do sometimes (8 patients) show an electric potential difference in relation to surrounding lung parenchyma. This potential difference is sometimes electropositive, sometimes electronegative in relation to a grounded subcutaneous reference electrode.

A poorly differentiated myosarcomatous metastasis in the lung is seen in Fig. VI: 20. The tumour was surrounded by an "A" zone, 2 cm broad. Two tracings of electric potential were simultaneously obtained from the tumour (Fig. VI: 21). Filters of different frequency were used. The tracings show from left to right the electric potential difference in lung behind the tumour, then differences of about 5 mV of potential in three portions of the tumour, a region of increased amplitudes of ecg fluctuations in the "A" zone and lowered ecg amplitudes in the "B" zone, an electropositive "pleural spike" and finally the potential of the chest wall. It should also be noted that in at least one part of the tumour the electric potential was negative in relation to that of the surrounding lung.

The appearance of a higher amplitude of the superimposed ecg in the "A" zone compared with the "B" zone is of certain interest. As will be seen later (Chapter XVI), it is possible to produce "A" and "B" zones experimentally. A tracing of the electric potential across such zones during the production of superimposed pulses simulating an ecg can also produce the sudden change of amplitude between the "A" and "B" zones.

This phenomenon can be explained as a change of conductivity depending, for instance, on differences in ionic composition or concentration between the "A" and "B" zones. The "A" and "B" zones seem in this way to be characterized by bioelectrical correspondences to their radiographic appearances.

Fig. VI: 22 illustrates a squamous cell carcinoma

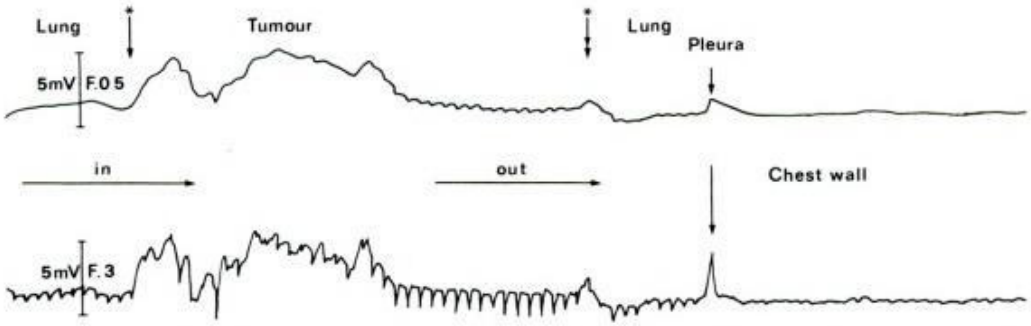

Fig. VI: 21. Electric potential profile through the lung and the tumour shown in Fig. VI: 20. Two simultaneous tracings obtained with different amplifications and cut-off filters. When the exploring electrode was retracted from the lung behind the tumour, small electrocardiographic (*ecg*) fluctuations can be seen superimposed on the left in the lower tracing. Upon entering the tumour surface (↕), the electrode revealed a positive electric potential. Compared to the levels of potential in the surrounding pulmonary parenchyma, a region of relatively negative potential can be seen inside the tumour. When the electrode entered the "A" zone of the lung, increased ecg fluctuations are seen until the "B" zone (↕) was entered, where the magnitude of ecg fluctuations is approximately halved until the pleura was reached. After the exploring electrode traversed the pleura (↓), the ecg fluctuations from the chest wall are relatively very small.

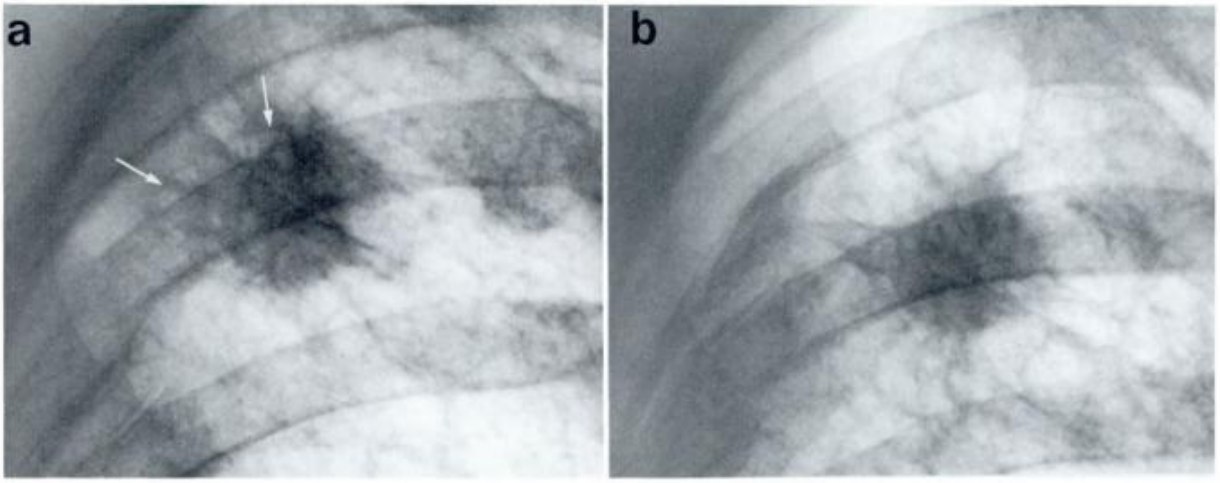

Fig. VI: 22. Squamous cell carcinoma, right upper lobe of a 64-year-old woman. (*a*) Posteroanterior projection. The tumour is surrounded by a radiolucent "A" zone. Irregular structures are at the surface of the tumour. An arcade (arrows) is suggested at the edge of the "B" zone. (*b*) Shallow right anterior oblique projection after needle biopsy. A 1.5 cm pneumothorax is present. The pleura is thin and the pleural space open. The "B" zone has partly disappeared. See also Fig. VI: 23.

surrounded by a radiolucent "A" zone. Arrows in Fig. VI: 22 *a* indicate a row of small arches at the interface between an "A" and "B" zone. Fig. VI: 22 *b* shows the tumour and the surrounding parenchyma after the development of a pneumothorax 1.5 cm broad. The electric potential difference was measured between the inserted exploring electrode and the grounded reference electrode in the subcutis. The exploring electrode was then slowly pulled out. During this retraction of the electrode, the exact position of the electrode tip was determined by cineradiography (Fig. VI: 23). At the posterior and anterior parts of the tumour the tracing reveals an electropositive deflection of potential in relation to the surrounding lung. The interior of the tumour, on the other hand, shows a relatively electronegative potential.

Fig. VI: 23. Electric potentials in the tumour shown in Fig. VI: 22. (*a*) Posteroanterior view of tumour and electrode. (*b–d*) Lateral views of tumour and electrode with corresponding parts of the recordings of electrical potential. Elevation of electrical potential is seen in the posterior and anterior parts of the tumour in relation to both surrounding lung and the interior of the tumour. Grounded reference electrode in subcutis.

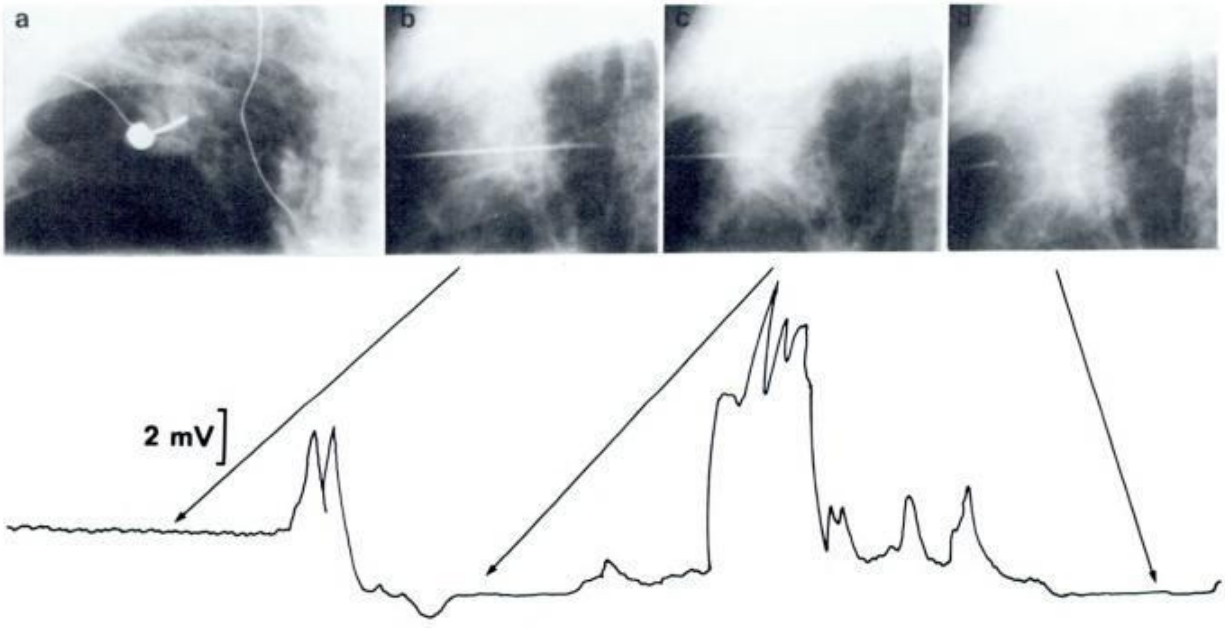

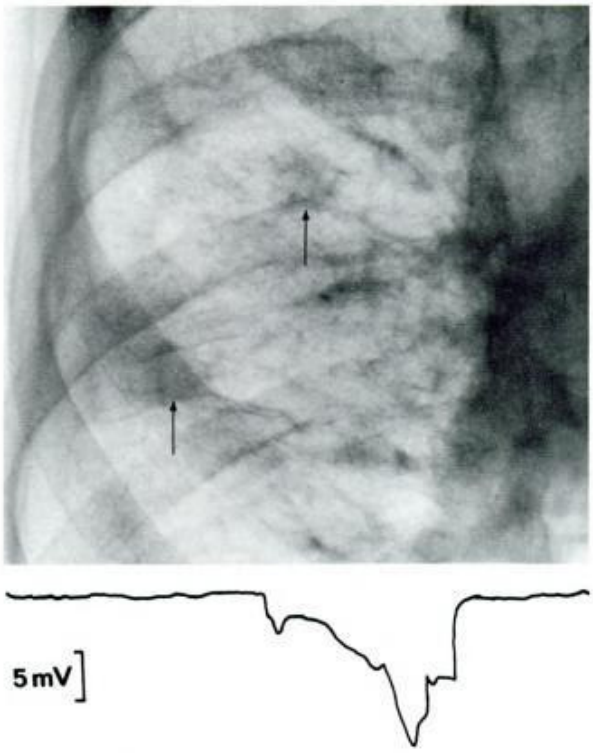

Fig. VI: 24. Two inflammatory granulomas (arrows) in a 56-year-old man. The electric potential of the upper lesion shows a 15 mV negative deflection in relation to the surrounding lung.

Fig. VI: 24 shows two pulmonary nodules in the right lung of a patient who was referred for diagnostic needle biopsy. The exploring needle electrode was inserted through the upper of the two lesions (diameter 1.5 cm). Tracings of potential were obtained, revealing a 15 mV negative potential difference in relation to the surrounding lung. Two samplings of cells were taken from the upper and three from the lower lesion. Histologically the material from all samplings showed macrophages, some inflammatory cells and tissue debris, but no neoplastic cells. The cytologic results indicated that the lesions were inflammatory granulomas.

Electric potential differences also were found in nonneoplastic pulmonary masses (30 of 36 patients, 84%) (see Section A. 3).

F. Summary and conclusions

These studies of electric potentials, especially in different pulmonary lesions in relation to a grounded reference electrode in the subcutis of the chest wall, have revealed:

1) Repeated insertion and retraction of the exploring electrode usually produced reproducible differences of potential between the lesion and the surrounding lung. This has been the case with polarizable metal electrodes as well as with nonpolarizable electrodes.

2) In certain neoplasms and inflammatory lesions, the potential of the periphery of the lesion was elevated or lowered in relation either to the surrounding lung or to the centre of the tumour. In other lesions no potential difference was present between the lesion and the surrounding lung in comparison with the reference electrode. These findings have shown no correlation to the cellular type or bacteriologic nature of the lesion.

3) The cause for this seeming disparity has been suspected to depend on the presence or absence of local tissue injury. When regions in a lesion showed potential differences (positive or negative) in relation to the surrounding lung, sampled cytologic material was often necrotic and therefore unsuitable for specific diagnosis. Statistical proof of such a correlation is hampered by many predictable and unpredictable variables and would therefore require a very large material, which is yet not available.

4) The complex but reproducible appearances of the electric potentials in different lung lesions allow only preliminary assumptions about their possible origin. Neoplasms and granulomas frequently develop spontaneous bleeding or necrosis, a finding common in any case material. Such local injuries should have electrophysiological correspondence in an electric injury potential (a well established concept). The occasional finding of polarized lesions in the lung appears to support this assumed correlation. Discussion in subsequent chapters of physicochemical polarization of injured tissue will provide explanations for variations of electric polarity of the lesions and their relation to structural modifications inside and outside lesions.

The idea is advanced that different regions in cells and tissues can be regarded as conglomerations of galvanic cells of different capacity and charge. Thus, short circuiting of different parts of normal subcutis in the dog produced marked local decrease of electronegative potential. The application of an external direct current between two subcutaneous electrodes produced marked local accumulation of charges in the tissues, which discharged relatively slowly after a short circuit was established. This finding led to studies of spontaneous electric activity in other organs. These studies are of principal interest because normal metabolism in the tissue surrounding a lesion should influence the internal physicochemical gradients between the tissues. More easily accessible tissues than the lung were therefore selected for these studies.

5) Rhythmic fluctuations of potential in dog livers (frequency about 3–5 per minute, amplitude about 1

mV) were measured against a grounded reference electrode in the abdomen or subcutis. These fluctuations of electric potential have not been described previously, except for a preliminary report (9), and most likely are of neurogenic origin. After intravenous injection of pharmacologic agents (epinephrine, histamine, isoprenaline, glucagon and others) dose-related waves of slowly changing potentials could be induced. These findings, also previously undescribed, show how a normal tissue apparently may develop electric potential gradients in relation to a surrounding tissue. It is suggested that the rhythmic endogenous waves of the liver represent neurogenic potentials which trigger metabolic events of the organ, e.g., secretion. The superimposition of rhythmic potentials and slow potential waves then represent a "demand potential" in the organ. The appearance of such demand potentials can be expected to depend on factors including size and shape of activated tissue, size, shape and location of the electrodes.

6) Parietal pleura, but not visceral, demonstrates a high "spike" of positive potential (15–20 mV) when an exploring electrode is passed through the chest wall into the lung. This spike was found to be a reliable landmark in studying the electric potentials of pulmonary lesions.

7) Electrocardiograms superimposed on the tracings of the lung tissue potential profile show higher amplitude in the "A" than in the "B" zones. The explanation for this finding depends not simply on spatial location of the electrodes but also on differences of conductivity between these zones.

8) The metabolic activities of lung, stomach, liver and probably many other tissues may vary local electrical charge, here identified by the presence of waves of slowly changing potential. Furthermore, local injury in an organ will produce a local accumulation of charges ("injury potential"), e.g., by diffusion of ionic products of decomposition. A potential is then created between the injured tissue and the surrounding noninjured tissues, each possessing their own metabolic potentials. This concept is important because the differences of potential between injured and surrounding noninjured tissue, in the author's opinion, provide the energy necessary to drive the processes of healing.

The existence of physiological polarization of tissues or organs should, however, also lead to the development of normal structural modifications. With the latter possibility in mind, the presence of well-defined spikes of electrical potential, such as described for the pleura, are of interest. As illustrated in Fig. VI: 25, well-defined potential differences are also observable when the exploring electrode passes the peritoneal membrane and liver capsule and the reference electrode is positioned in the subcutis of the abdominal wall. Associated problems will be treated in Chapter XII, where a mechanism for development of membranes is outlined.

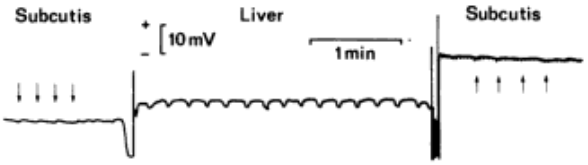

Fig. VI: 25. Tracing of potential of abdominal wall and liver in dog. The exploring electrode was inserted from subcutis through abdominal wall into liver and back to subcutis. A grounded reference electrode was placed subcutaneously. A negative and then positive deflection was obtained between the subcutis and the liver parenchyma, showing regular fluctuations of potential (frequency about 4–5 per minute). In the subcutis smaller fluctuations of the same frequency are seen (arrows), presumably transmitted from the liver. On retraction, electrode passes an air gap between the liver and the abdominal wall. The hepatic capsule showed a positive deflection of potential.

The information collected in this chapter is preliminary but indicates that electro(-chemical) energy gradients may be identified between different tissues. These gradients appear to express differences of local metabolic activities of normal tissue or differences between normal and injured tissue. The utilization of such energy gradients depends largely on the suggested system of selective transport of material which is here called biologically closed electric circuits (BCEC). This system will be particularly considered in Chapter XII. Chapter XIII outlines the driving energy of this system. An understanding of the function of BCEC systems requires, however, further studies of its components, which will be presented in Chapters VII–XI.

References

1. Agostoni, E.: Mechanics of the pleural space. Physiological Reviews 52: 57, 1972.
2. Cooper, R.: Storage of silver chloride electrodes. EEG Clin. Neurophysiol. 8: 692, 1956.
3. Dahlgren, S., and Nordenström, B.: Transthoracic needle biopsy. Stockholm, Almqvist & Wiksell, 1966.
4. Geddes, L. A., and Baker, L. E.: Chlorided silver electrodes. Med. Res. Eng. 6: 33, 1967.
5. Geddes, L. A., Da Costa, C. P., and Wise, G.: The impedance of stainless steel electrodes. Med. Biol. Engng. 9: 511, 1971.
6. Grundfest, H., Sengstaken, R. W., Oettinger, W. H., and Gurry, R. W.: Stainless steel microneedle electrodes made by electro-pointing. Rev. Sci. Instr. 21: 360, 1950.
7. Mond, R.: Über die elektromotorischen Kräfte der Magenschleimhaut vom Frosch. Pflügers Arch. Ges. Physiol. 215: 468, 1926/1927.
8. Nordenström, B.: Electric potentials in pulmonary lesions. Acta Radiol. Diagn. 11: 1, 1971.
9. Nordenström, B.: Electric potential fluctuations in the liver. IRCS 2: 1666, 1974.

10. Nordenström, B.: New instruments for biopsy. Radiology 117: 474, 1975.
11. Nordenström, B., and Sinner, W. N.: Needle biopsies of pulmonary lesions. Fortschr. Röntgenstr. 129: 414, 1975.
12. Quigley, J. P., Barcroft, J., Adair, G. S., and Goodman, E. N.: The difference in potential across gastric membranes and certain factors modifying the potential. Am. J. Physiol. 147: 67, 1946.
13. Rehm, W. S.: Evidence that the major portion of the gastric potential originates between the submucosa and mucosa. Am. J. Physiol. 147: 69, 1946.
14. Riddick, T. M.: Control of colloid stability through zeta potential. New York, Zeta-Meter Inc., 1720 First Avenue, New York, N.Y. 10028, 1968.
15. Sarre, H.: Beziehungen des Eigenpotentials der Magenschleimhaut des Warmblüters zur Salzsäuresekretion. Z. Biol. 95: 135, 1934.
16. Swyngedauw, J.: Sur l'existence d'une différence de potentiel variable entre la bouche et l'estomac au cours de la sécrétion gastrique. Compt. Rend. Soc. Biol. 98: 1431, 1928.
17. Swyngedauw, J.: Variations du potentiel développé dans la muqueuse gastrique au cours de la sécrétion. Compt. Rend. Soc. Biol. 98: 1433, 1928.
18. Swyngedauw, J.: Evolution du potentiel d'un estomac à jeun. Compt. Rend. Soc. Biol. 99: 796, 1928.
19. Weinman, J., and Mahler, J.: An analysis of electrical properties of metal electrodes. Med. Elect. Biol. Eng. 2: 299, 1964.

VII.
Spontaneous development of a fluctuating injury potential in tissue

The incidence of necrosis in pulmonary cancers is difficult to estimate. According to Byrd et al. (2), cavitation develops in approximately 10 per cent of primary pulmonary neoplasms. Found almost exclusively in squamous cell carcinomas, cavitation is rare in undifferentiated and alveolar cell carcinomas (3, 5). Because necrotic material is not always replaced by air which is radiographically evident in cavitation, the 10 per cent value probably represents a low estimate for the incidence of necrosis in pulmonary neoplasms. In the author's experience, adenocarcinomas and metastatic cancers in lung may also be necrotic, but the lung tumours which are most frequently necrotic are definitely primary squamous cell carcinomas.

The low incidence of cavitation in such highly malignant tumours as undifferentiated bronchogenic carcinomas is difficult to explain. One possible explanation would be that such cancers tend to obstruct central bronchi by rapid and continuous overgrowth so that endobronchial evacuation of the necrotic material is seldom possible.

Rapid growth of a malignant tumour is generally thought to cause imbalance between nutritional supply and demand, leading to necrosis. Compression or invasion of an artery supplying the tumour may also produce necrosis. Erosion of a nutrient vessel also may produce internal bleeding and thereby increase internal pressure, inducing necrosis. A thrombus in a blood vessel in a lung cancer may be regarded as a metabolically isolated tissue which will be subject to autolytic changes.

Injury of tissue may be produced by circulatory, metabolic, mechanical, chemical and electrical factors, heat or radiation. From a physical point of view, any of these sources can produce an electrical injury potential.

Consider hepatic autolysis as an example of necrosis. Almost no light microscopic changes can be seen during the first six hours (1). Thereafter, cell membranes gradually disintegrate and nuclei start to show pyknosis. Mitochondria then begin to swell and vacuoles appear in the cytoplasm (11). After about 24 hours karyolysis is observed. After 48 to 72 hours most cells are necrotic. Electron microscopically, changes can be observed soon after hypoxia. Saladino and Trump (13), studying slices of mouse liver, observed the earliest autolytic changes in mitochondria after a mere 5 minutes of hypoxia.

When lack of oxygen injures a tissue, lysosomes liberate soluble hydrolytic enzymes (7). These enzymes are most active in an acidic environment, spread into different parts of the cell, and reach a maximum

intracellular concentration after 3 to 4 hours (7). Lysosomal enzymes appear to be of central importance in proteolytic degradation of cells, a point recently stressed by Marzella (12). After lysosomal enzymatic digestion is established, other cellular enzymes are then continually liberated in the tissue (1, 10, 14).

Hydrolases initiate lysosomal action in the liver of starved rats exposed to carbon tetrachloride, according to De Duve, et al. (8). The soluble hydrolytic enzymes are released across the lipoprotein membrane of the lysosome in a primary attack which appears to derive from ischaemic injury to the centre of the lysosome. In addition to the release of lysosomal hydrolases, autolysis is accomplished also by acid phosphatases, cathepsin, β-glucuronidase, acid ribonuclease and acid desoxyribonuclease (8, 9).

Studies in organs other than the liver further indicate that the liberation of lysosomal enzymes is one of the earliest reactions in the development of autolysis (12).

In its early stages, autolysis includes an increase in tissue weight and then an accumulation of intracellular calcium. Dawkins, et al. (6) have attributed the increase in weight to an osmotic effect. This osmotic weight increase is also an indication of the ongoing destruction of molecules, which as a physical process can be characterized as a catabolic liberation of energy.

As cells die, they lose their metabolic functions and become more acid in reaction (4). They change their permeability characteristics for ions and macromolecules. Influx of water swells their protoplasm. Granular bodies appear. Cytoplasm and nuclei coagulate and disintegrate into debris (4).

The studies of electric potential of lung tumours and granulomas (Chapter VI) revealed that potential gradients of varying magnitude and polarity may be present in lung lesions, relative to a surrounding reference tissue. These gradients may be electronegative, electropositive or even zero. Usually, reproducible profiles of potential could be obtained from any particular kind of lesion.

No correlation could be found between the tissue profiles of electric potential in different tumours of corresponding size, location or histologic type. The variability of the profiles of potential among different tumours (and sometimes in different parts of the tumours) nullified attempts at quantitative correlation. Empirically, however, it became evident eventually that necrotic material could be obtained by aspiration biopsy from most of the polarizing lesions.

This preliminary empirical information was next turned into directed research attempting to explain the finding of inconsistent electrical potential in histologically similar lesions. Tumours are known sometimes to contain internal bleeding or necrotic regions of varying extent (2, 3, 5). These changes are a form of injury to tissue, which should produce electrochemical injury potentials. Necrosis or haemorrhage may well explain why a tumour of particular histologic type, size and location presents electric polarization in relation to surrounding noninjured tissue in one patient while a seemingly corresponding tumour in another patient does not show such changes.

Furthermore, focal autolysis in a lesion might be expected to cause local variations in electrochemical potential. Age of the locally degrading process may also be a factor. Controlled research on these problems would be extremely difficult to carry out in vivo in the lung. As focal internal haemorrhage in a lesion is very probably involved in the process of polarization, blood was chosen as a readily accessible tissue to study in attempting to explain the possible origin of electrical polarization of lung lesions.

A. Degradation of blood

The development of local necrosis in a surviving subject is not restricted to hours or a few days. The whole process may be found to modify the tissues during months or even years. In the present in vitro experiments, the spontaneous degradation of blood during hypoxia was studied over the relatively long time periods of one to eight weeks. These studies were arranged to simulate, at least approximately, the spontaneous degradation of clotted blood inside a tumour.

Fresh human blood was studied under sterile conditions with regard to spontaneous pH and changes of electric diffusion potential (Fig. VII: 1). Twenty to 50 ml of fresh sterile blood were placed in a sterile collodium bag which was suspended in a jar containing 1 000 ml of circulating Ringer's solution at 37°C. Three Ag–AgCl electrodes with KCl bridges and three pH electrodes were placed through holes in a rubber stopper, fitted to the bag opening. A grounded reference (Lazaran) Ag–Ag Cl electrode with KCl bridge was inserted in the Ringer's solution. The surface of the blood and the Ringer's solution was covered with a 2 cm thick layer of sterile liquid paraffin to prevent contact of air with the fluids. The entire apparatus was then kept inside a sterilized plastic cover.

The pH of the blood and its change of diffusion potential in relation to the grounded reference electrodes were recorded intermittently during the experimental periods, which varied from one to eight weeks. Experiments on six different samples of human blood and two samples of dog blood were performed. Samples of the blood were taken at different times to confirm bacteriologic sterility.

The results of these studies showed that pH of the blood decreased rapidly during the first days (Fig.

VII: 2). The three separate pH electrodes showed some internal differences despite careful calibration before the experiments. Control calibrations after the experiments usually showed some differences among the electrodes, particularly after they had been immersed in the blood over several weeks. These disparities probably are a function of different adsorptions of various proteins on the glass surface of the electrodes, an unavoidable aspect of the experiment.

A spontaneous lowering of the pH during the first days took place equally in human and in dog blood.

Measurements of pH and simultaneous electric potential of diffusion in the blood in relation to the Ringer's solution are illustrated in a representative example in Fig. VII: 3. The diffusion potential of the blood showed considerably greater fluctuations than the pH. The changes of potential spanned as much as 200 mV during the first days and 250 mV between the maximum and minimum fluctuations during the experiment. The pH fluctuated in this experiment about one pH unit (equivalent to 61.54 mV at 37°C). The arrow "sterile" shows the time when a sample of blood was taken for bacteriological culture. This sample was sterile. Some hours after the sampling, the pH and the electric potential showed large fluctuations. A new blood sample taken 8 days later showed the growth (*X*) of nonfermenting, gram-negative, aerobic rods.

Early development of acidity in the spontaneously degrading blood has been a constant finding in these experiments. Initially, the corresponding electric diffusion potential has shown large electropositive fluctuations. Later, a varying pattern of fluctuations of pH and diffusion potential has been observed, including a tendency toward increasing stabilization. Inlet of air or infection of the blood has always disturbed this tendency immediately.

These experiments have been performed to obtain information about electrical changes of blood degrading over a relatively long period of time. It is apparent that control of the experimental conditions could be improved, e.g., with regard to glucose level and oxygen content of the blood at the beginning of the experiments. Deviations from in vivo conditions apply in these experiments also to several other variables, e.g.,

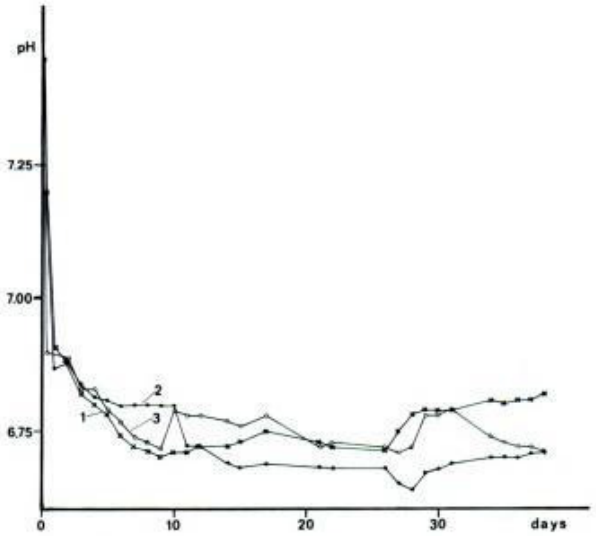

Fig. VII: 2. Spontaneous changes of pH in degrading human blood (without citrate or heparin) during 40 days. Initially, pH lowered rapidly. Tracings are from each of the three electrodes.

Fig. VII: 1. Apparatus for determination of pH and electric diffusion potential of spontaneously degrading blood. A collodium bag is filled with blood (1) without citrate or heparin and suspended in Ringer's solution (2) circulating at 37°C. Three pH electrodes (3) and three Ag–AgCl electrodes (4) (one of each illustrated) pass through a rubber stopper (5) and are immersed in the blood. A grounded Lazaran reference electrode (6) is placed in the Ringer's solution. A covering thick layer of liquid paraffin (not illustrated) prevents contact of air with the blood and Ringer's solution. A stirrer (7) circulates the Ringer's solution.

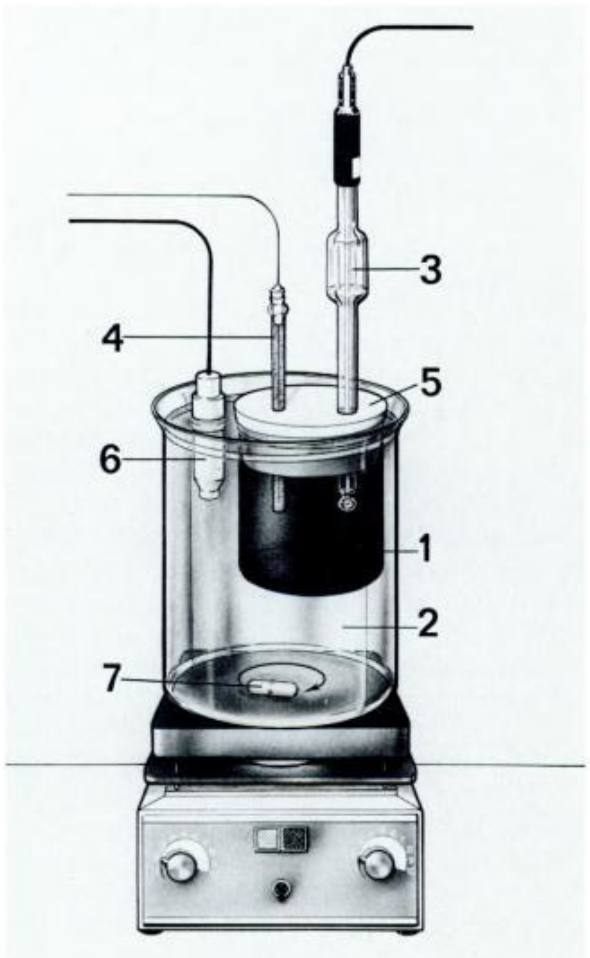

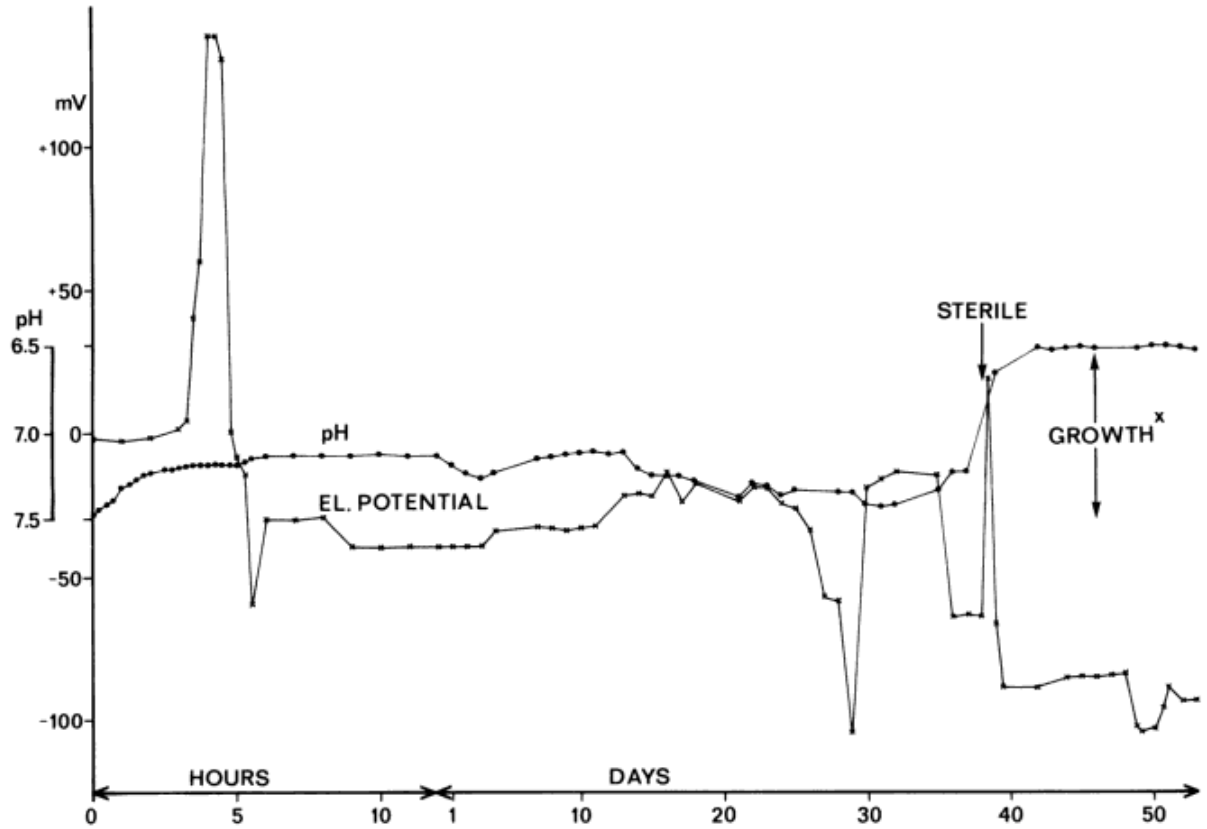

Fig. VII:3. Spontaneous fluctuations of pH and electric diffusion potential of spontaneously degrading human venous blood. The fluctuations of the "total" diffusion potential are considerably more pronounced than the changes of pH. The early electropositive and electronegative fluctuations of the diffusion potential cover a span of about 200 mV. The last sterile bacteriological test sample was obtained after 40 days. After this sampling, the pH and electric potential suddenly moved in an electronegative direction. New sampling of the blood showed bacterial growth (gram-negative aerobic rods), presumably caused by bacterial contamination during the previous sampling.

composition of the surrounding medium and the simulation of a tumour barrier by the semipermeable collodium membrane. Furthermore, immersion of electrodes for several weeks in blood causes apposition of material on their surfaces, which must disturb their sensitivity. Besides the pH and the difference of "total" diffusion potential, redox potentials should also be studied in this way, but were not included in the present initial study. In performing an experiment on hypoxic degradation of blood we have, however, already by definition, this important additional factor in mind. So far we may limit ourselves to conclude that the actual experiments support the view that the spontaneous hypoxic degradation of blood includes a focus of electric "injury" polarization in relation to a "normal" surrounding medium. Evidently this is also a dynamic process characterized by considerable electrical fluctuations in the early phases, followed by eventual attenuation as the reactions drive toward equilibrium.

B. The fluctuating electrochemical potential of an injured tissue

The spontaneous changes in electric potential of hypoxic blood can be regarded as a degrading molecular process in which an electrochemical injury potential develops. This process is catabolic; it liberates energy. Its progress in one direction will, as in all spontaneous reactions, induce counter-reactions. Eventually this combination will lead to a fluctuating attenuation toward equilibrium. The actual electric (physicochemical) potential should therefore vary depending on the phase of development of the degrading tissue.

This mechanism may explain the observed variety in electric potentials of lung tumours in vivo.

Cell death is known to be accompanied by a series of events in which the lysosomes play an important role. Lysosomal liberation of different enzymes leads to decomposition and splitting of cellular molecules. The

necrotic mass may liquify by the action of hydrolytic enzymes.

Energy produced by the degrading processes now becomes of particular interest. To explain the changes of electrical activity and pH illustrated in Fig. VII: 3, the following synthesis of known facts may be offered.

Many well-known chemical reactions participate in the early production of acidity in autolysis. During hypoxia, oxidation of glucose to CO_2 and water will deplete locally available resources of oxygen. Continued glucolysis will proceed as anaerobic production of lactic acid, a main compound responsible for local tissue acidity. Experiments of Gallagher, et al. (9) suggest that one of the first manifestations of tissue injury is a loss of ATP. As oxygen levels in autolysing tissue progressively diminish, the Krebs cycle decreases in quantitative importance. As ATP diminishes, the ATP-ADP system turns into an irreversible hydrolytic reaction,

$$ATP + H_2O \rightarrow ADP + \text{phosphate} + H^+ + \text{energy}.$$

The initial phase of low pH (Fig. VII: 3) only represents a minor part of the early electropositive potential difference between degrading blood and a surrounding reference medium. A multitude of reactions are known to take place in autolysis of tissue (9, 15). It is, however, here beyond the intentions or even necessary to discuss many of the complex, possible series of biochemical events described in autolysis. It may be sufficient to establish that degrading tissue develops an early electropositive transient phase which is partly caused by acidity.

The early acidity (Fig. VII: 2) is evidently explainable as a statistical, intermediate phenomenon between the production and disappearance of acidic products by diffusion, migration and recombination.

Because protons among all ions possess the fastest rates of diffusion and a high tendency to recombine with counterions, the relative loss of protons is probably the leading reaction in the events which subsequently drive the tissue in an electronegative direction. The tendency of the degrading blood to change from electropositive to electronegative is further enhanced by hypoxic production of anions, e.g., phosphate ions, which gradually appear as ATP undergoes hydrolysis. Other sources for the production of phosphate ions are phosphocreatinin, phosphoarginine and polymetaphosphate. An accumulation of phosphate ions is of particular interest for the eventual development of calcifications in tissue injury.

When degrading tissue turns electronegative, different cations will be attracted to the accumulating anions. In particular, Ca^{++} and Mg^{++} will be attracted to the accumulating phosphate ions and should precipitate as calcium and magnesium phosphate when the appropriate isoelectric regions for these compounds have been reached. In this way the development of apatite, which is the most common calcium-containing salt deposited in injured tissue, can be explained. As apatite forms and anions then become depleted, the overall reaction might then be anticipated to drive again in the electropositive direction.

An overview now must consider the observed electrical events as applying to a large number of ions of different sizes, electrical charges, concentrations and specific activities. Thermal factors, pressure, gravity, externally superimposed electromagnetic fields, convection, diffusion and local circulation must further interact with this behaviour. One factor which will be particularly considered in this work is the effect of *biologically closed electric circuits* between a pathological injured tissue and the surrounding normal tissue, electrochemically polarizing against each other.

It is easy to understand that a local injury of any kind represents a region with a level of entropy, which under the influence of factors, such as those mentioned above, must drive toward a higher level. After the injury has healed macroscopically, a pseudo-equilibrium is reached (as further transformations of tissue will take place, but at a slow rate). The differences in speed and intensity of the partial reactions during different stages of their development can be anticipated to result in a fluctuating but attenuating sum of the partial reactions. This perspective gives an explanation for the sometimes electronegative, sometimes electropositive polarity of an injured tissue in relation to its surroundings. The injured tissue presents different phases in its development. As a consequence of this view, it can be seen that sampling of material for measurements of electric potential (and chemical analysis) of injured tissue is rather meaningless unless the results are related to the momentary phase of the natural history of the injury.

Thus far the presentation has mainly been concerned with electrical factors in tissue polarization, while concentration-activity, pressure-volume and gravity have as yet received only passing mention. The important chemical forces will next be briefly discussed (Chapter VIII), followed by an experimental demonstration of interactions between electrical and chemical forces (Chapters X, XI).

References

1. Berenbom, M., Chang, P. I., Betz, H. E., and Stowell, R. E.: Chemical and enzymatic changes associated with mouse liver necrosis in vitro. Cancer Res. 15: 1, 1955.
2. Byrd, R. B., Miller, W. E., Carr, D. T., et al.: The roentgenographic appearance of squamous cell carcinoma of the bronchus. Mayo Clin. Proc. 43: 327, 1968.

3. Byrd, R. B., Miller, W. E., Carr, D. T., et al.: The roentgenographic appearance of small cell carcinoma of the bronchus. Mayo Clin. Proc. 43: 337, 1968.
4. Cameron, G. R., and Spector, W. G.: The chemistry of the injured cell. Springfield, Ill., Charles C. Thomas Publ., 1961.
5. Chaudhuri, M. R.: Primary pulmonary cavitating carcinomas. Thorax 28: 354, 1973.
6. Dawkins, M. J. R., Judah, J. D., and Rees, K. R.: Factors influencing the survival of liver cells during autolysis. J. Path. Bact. 77: 257, 1959.
7. De Duve, C., and Beaufay, H.: Tissue fractionation studies. 10. Influence of ischaemia on the state of some bound enzymes in rat liver. Biochem. J. 73: 610, 1959.
8. De Duve, C., Wattiaux, R., and Baudhuin, P.: Distribution of enzymes between subcellular fractions in animal tissues. Advan. Enzymol. 24: 291, 1962.
9. Gallagher, C. H., Judah, J. D., and Rees, K. R.: Enzyme changes during liver autolysis. J. Path. Bact. 72: 247, 1956.
10. Gössner, W.: Untersuchungen über das Verhalten der Phosphatasen und Esterasen während der Autolyse. Arch. Path. Anat. 327: 304, 1955.
11. Holle, G., Burkhardt, R., Arndt, S., and Blödorn, M.: Über manometrische, histochemische, histologische und phasenoptische Befunde bei ischämischer Hypoxydose. Virchows Archiv 327: 150, 1955.
12. Marzella, L.: Studies on mechanisms of intracellular degradation with special reference to lysosomes. A biochemical and electron microscopic study. Thesis, Dept. of Pathology, Huddinge Hospital, Huddinge, Sweden, 1979.
13. Saladino, A. J., and Trump, F.: Ion movements in cell injury. Am. J. Pathol. 52: 737, 1968.
14. Wahi, P. N., Tandon, H. D., and Bharadwaj, T. P.: Acute carbon tetrachloride hepatic injury. Acta Path. Microbiol. Scand. 37: 305, 1955.
15. Van Lancker, J. L.: Molecular and cellular mechanisms in disease. Berlin, Springer, 1976.

VIII.
Concentration-dispersion forces

A brief review of intermolecular physical behaviour

Present knowledge of concentration and dispersion forces is incomplete in many respects (7, 11). Still, their importance can often be recognized, even if only indirectly. This chapter offers a short survey of these forces. Some physical models will be presented in Chapters IX and X. Implications of these models will then be illustrated in further experimental studies of structural development in vivo (Chapter XI).

The concentration-dispersion forces are long-range or short-range (3, 4), depending on the presence or absence of exchange of electrons among molecules. Long-range forces are of three main types: electrostatic, induction and dispersion (2, 3, 5). The short-range forces are of two main types: overlap repulsion (van der Waals' forces) and fixed-charge electrostatic forces. They all constitute extremely complex, interacting variables, even in relatively "simple" and uniform systems such as water. These forces, still obscure in many respects, are of fundamental importance to the physical behaviour of matter.

The interactions of concentration forces constitute a basis for understanding the development of structure in normal and pathological tissues. The structural changes around the pulmonary and mammary lesions presented in this book may be regarded as induced by local degeneration of tissue, a rather specific situation in which these forces come into play. Before some of these aspects of structural development of tissue are considered, physical aspects of concentration and dispersion forces will be briefly surveyed (3, 6–10, 12–16).

The interaction between two particles or molecules A and B may be written as a potential energy function U_{AB}. The force between A and B depends on their separation d and the spatial orientation of their polar moments, which may be induced or permanent. Between A and B the force F_{AB} is written:

$$F_{AB} = \pm\frac{kAB}{d^{\exp}}$$

where the function is negative when the net force is attractive and positive when the net force is repulsive (4). The constant k is specifically determined by AB, and the exponential function of d by the rotational or stationary potential energy of particles.

For an infinite separation of particles the U_{AB} approaches zero. When two particles approach each other within a distance of, e.g., some molecular diameters, the U_{AB} is either positive, zero, or negative. For most particles the observed value is negative, as in condensing water, or zero, as in clustered water molecules with a finite volume. The low compressibility of ice shows

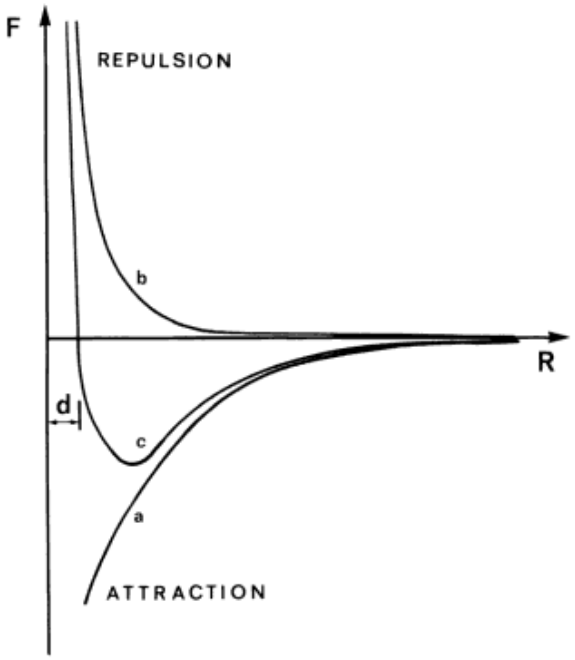

Fig. VIII: 1. Besides "ordinary" electrostatic forces, attractive and repulsive forces of the van der Waals' type are important for structural development. F = force; R = distance dependence of potential energy; d = distance between two particles. Van der Waals' forces are both (a) long-range attractive and (b) short-range repulsive. The relationship of force F and distance d is expressed as the resultant force c, i.e., $a+b$, represented by the curve $c=k/d^7$, where k is a constant that depends on the particles. At any distance shorter than d, the repulsive force increases rapidly, which prevents matter from collapsing.

that when values of d are less than those for which U_{AB} is zero, the U_{AB} rapidly increases in positive value. This positive potential energy function counteracts the possibility of collapse of matter.

The principle is illustrated in Fig. VIII: 1, showing the well known distribution curve of resultant potential energy (c), composed of attractive (a) and repulsive (b) forces. Such forces vary experimentally and theoretically for different kinds of matter and their degree of purity (4). For instance, different kinds of carbon (such as coal, graphite, and diamond) present a wide range of internal cohesion. Fixed angulation or rotation of particles also influence the resulting forces.

In a system of many particles it is assumed that most but not all of the concentration forces are pairwise additive (3).

Among the three types of so-called long-range forces, *electrostatic forces* (I) are either repulsive or attractive. They also are pairwise additive according to the principle of superposition (simple addition) of the fields. Electrostatic forces dominate large separations. In the case of *dipole-induced dipoles* (II), however, the forces are not pairwise additive. They arise by the interactions of the permanent electrical moments of particles. The long-range *dispersion forces* (III) are exclusively attractive and pairwise additive. These forces are also called *concentration forces* (9, 10, 11).

Thus, long-range forces acting upon several particles can be written as a sum of the individual electrical forces and dispersion (concentration) forces, when consideration is given to the spatial orientations and rotational moments of the participating particles. Derivation of the contributions of the long-range forces to U_{AB} have been given by Hirschfelder, et al. (6), as follows:

I) The long-range electrostatic forces may be written as a series

$$U \text{ electrostatic} = U\mu\mu + U\mu_Q + U_{QQ} + \ldots$$

where each partial term is a potential energy function of separation, orientation, as well as electrical moments of the particles (see also Fig. X: 2). $U\mu\mu$ represents the potential energy function of the electrical charges μ^+ and μ^- of a $\mu\mu$ dipole. It may be described by the function $(\mu^2/d^3)\, f$, where f is a function of angulation and d the distance between the two charges. $U\mu_Q$ is a similar function between the neighbouring and attracting opposite charges of the $\mu\mu$ dipole and another dipole of charges Q^+ and Q^-. U_{QQ} is the similar function for the QQ dipole. Likewise, all other combinations of dipoles in the given collection of particles are added into this electrostatic series. The values of $U\mu_Q$ and U_{QQ} are much smaller than $U\mu\mu$. They fall off, according to Margenau (11), proportionally to d^{-4} and d^{-5}, respectively, whereas $U\mu\mu$ is proportional to d^{-3}.

II) The long-range *induction forces* produce balanced net forces between particles without additive effect on surrounding matter (3). Their importance for structural development within a given field should therefore depend to a large extent on the dielectric properties of the material in which induction takes place.

III) The third type of long-range forces, the *concentration forces* (dispersion, London–van der Waals, cohesive adsorption forces), are believed to arise as a specific dipole effect on a particle by electron movement in an adjacent particle. Thus London (9, 10) has shown that the overall energy function U_{disp} may be written as a series of exclusively additive terms proportinal to $-k/d^6$ for each pair of particles. The concentration forces can be determined but require knowledge of the particular wave function for ground and excited states of the electrons. Formulas for their calculation have been developed (8, 10, 13, 15).

The counterbalance of the negative long-range attractive forces is the repulsive short-range van der Waals' forces. These forces rapidly increase their dominance within distances of approximately 3 Å. This effect depends on the increasing repulsion caused by overlap of the electronic charge clouds of particles

as they move closer to each other (11, 12). This repulsive potential energy is described by a term proportional to e^{-pd} or d^{-n} where p and n are constants (n varies between 9 to 24) (3).

A potential function for overlap repulsion between water molecules was described by Kamb (7) in the form

$$U_{\text{repul}} = A^* \left(\frac{\sigma}{d}\right)^n,$$

where $\sigma = 276 \times 10^{-8}$ cm ("collision diameter" of the molecules). Two pairs of coefficients and exponents were derived: $A^* = 2.7$ kcal molufe^{-1}, $n = 10$ and $A^* = 4.0$ kcal mol^{-1}, $n = 9$ for ice of two different energy contents.

Interatomic forces and short-range molecular forces are known to be integrated into the combined or hybrid movements of orbital electrons around atoms of a molecule (3, 4). Two electrons move with opposite spins in each orbit around the molecule, producing internal bonds of the molecule within certain sections. The variations in electron density of certain sections of the orbits allow interactions between adjacent molecules. When external forces have vanished, this mutual process produces an equilibrium configuration of the participating nuclei. The short-range repulsive forces must then be balanced by an electrostatic attractive charge. This attraction is limited to the binding regions of the molecule, whereas all other regions tend to separate the molecules. A specific molecular orientation takes place at the binding sites. The balance of the forces involved in the binding follow the Hellmann–Feynman rule (3, 4), which states that the forces acting on the nucleus of a separated molecule are the sum of the electrostatic forces arising from the other nuclei and the force derived from electronic charge density.

In the discussion on physicochemical potential, the chemical potential contains the activity component a_j. The influence of this factor is not simply a matter of concentration of j. The "total activity" of solute j is related to both its concentration and other energy components, which are included as an activity coefficient, γ_j:

$$a_j = \gamma_j c_j.$$

The activity coefficient is usually synonymous with the electric characteristics of solute j and differs for charged particles in water solution by their electrical charge from the activity being caused only by the concentration. This variation was recognized by Debye and Hückel (1) who also found that, as the concentration increases, the electrical fields of the ions interfere increasingly with each other. Consequently, local accumulations of a species of ions of varying concentration will interact different internally and with surrounding reactants. The activity factors for ions in solution also vary by their different net electric charge in relation to the activity of surrounding media. In addition, thermal factors, pressures, gravity and external electric fields will, of course, also influence ionic dispersion. In a local region around any ion, the electric forces influence the movement of other ions. As concentration increases, the distance between ions decreases, which facilitates ion-ion interactions.

The presented view of ionic potential has its correspondence in the molecular potential of certain biologically active nonionic compounds. Associated problems are particularly considered in the presentation of the ionar-ergonar concept of energy exchange over biologically closed electric circuits (Chapter XIII), an important prerequisite for the utilization of their biologically stored electrical energy.

This condensed survey of some characteristics of molecular and particulate forces of attraction and repulsion may on first impression seem far distant from problems of structural modification in biological material. It is not so. These forces constitute important partial functions in a complicated system of many interacting forces, all of which must be considered in order to understand related problems.

Some of these functions will next be shown in studies of movement of water in organized tissue (Chapter IX) and then of the behaviour of particles, i.e., nonorganized corpuscular elements (Chapter X).

Gross morphologic development of tissue is complicated particularly by the superimposition of both variable and more stable interacting components. Among these components, convection, diffusion, and tissue matrices constitute important factors. To this group belongs also a hitherto overlooked, important component: biologically closed electric circuits.

References

1. Debye, I. P., and Hückel, E.: Zur Theorie der Elektrolyte I. Phys. Zeitschr. 24: 185, 1923.
2. Edsall, J. T., and Wyman, J.: Cit. in Biophysical chemistry, Vol. 1. New York, Academic Press, 1958.
3. Eisenberg, D., and Kauzmann, W.: The structure and properties of water. Oxford, Clarendon Press, 1969.
4. Feynman, R. P., Leighton, R. B., and Sands, M.: The Feynman lectures on physics. New York, Addison–Wesley Publ. Co., 1964.
5. Hamaker, H. C.: The London-Van der Waals attraction between spherical particles. Physica 4: 1058, 1937.
6. Hirschfelder, J. O., Curtiss, C. F., and Bird, R. B.: Molecular theory of gases and liquids. New York, Wiley, 1954.
7. Kamb, B.: In: Rich, A., and Davidson, N. (eds.): Structural chemistry and molecular biology. San Francisco, Freeman, 1968.
8. Kirkwood, J. G.: The dielectric polarization of polar liquids. J. Chem. Phys. 7: 911, 1939.
9. London, F.: Zur Theorie und Systematik der Molekularkräfte. Z. Phys. 63: 245, 1930.

10. London, F.: The general theory of molecular forces. Trans. Faraday Soc. 33: 8, 1937.
11. Margenau, H.: Van der Waals forces. Rev. Modern Physics 11: 1, 1939.
12. Margenau, H., and Myers, V. W.: The forces between water molecules and the second virial coefficient for water. Phys. Rev. 66: 707, 1944.
13. Muller, N.: Concerning structural models for water and chemical-shift data. J. Chem. Phys. 43: 2555, 1965.
14. Rowlinson, J. S.: The second virial coefficients of polar gases. Trans. Faraday Soc. 45: 974, 1949.
15. Slater, J. C.: Introduction to chemical physics. New York, McGraw-Hill, 1939.
16. Stockmayer, W. H.: Second virial coefficients of polar gases. Chem. Phys. 9: 398, 1941.

IX.
Water

Electroosmotic transport over closed electric circuits

In Chapters III–V it is indicated that tumours in the lung may produce local accumulation of fluid (a "B" zone) between the pleura and the lesion, due to blocking of draining pathways between the pleura and the hilum. The fluid accumulation in the lung is often seen separated from the surface of the tumour by another zone, which shows radiographic signs of decrease in fluid content (an "A" zone). The existence of the two zones may be explained as a result of local lymphoedema produced by stasis and an electroosmotic process. Electroosmotic transport of water in tissue will be described in this chapter as a function of biologically closed electric circuits (BCEC).

A. Movement of water into necrotic tissue

Early stages of autolysis of a tissue include increased weight of the tissue and accumulation in it of calcium (21, 32). Conway and McCormack (18) showed that the freezing point depression of autolyzing tissue increases rapidly, indicating an increased osmotic pressure. Furthermore, direct measurements of ionic concentrations in injured tissue indicate that the increased weight and swelling are caused mainly by a net uptake of water, sodium and chloride (45, 59).

When hypoxia induces injury of tissue, proteolytic enzymes are released (32). Molecular degradations ensue, thereby increasing the osmotic properties of the injured tissue (63). Water then enters the tissue. Locally increased fluid pressure should also contribute to a further progression of the necrosis.

Water content of mammalian tissues may also increase during hypoxia, without permanent damage to cells (2, 81). It has been suggested (63) that the intracellular fluids are hypertonic and that respiration governs water balance of tissue because energy is expended for active transport of water out of the cells.

Increased content of water in necrotic neoplasms can also be expected for other reasons. Consider the case of fixed negative charges in the matrix of a tumour barrier (defined as the viable tissue surrounding a necrotic centre) and the presence of a closed electric circuit containing a gradient of electric potential over the barrier. Electroosmotic flux of water should then take place toward the cathodic tissue. Such a biologically closed electric circuit (BCEC) and its activation will be described in Chapters XII and XIII. For the moment, we will assume only that BCEC systems exist and investigate the consequences of such a mechanism on transport of water in tissue. In the case a tumour is

electropositive in relation to the surrounding tissue, an outward flow of water, away from the tumour, should take place. This effect should then be detectable radiographically as a hydropenic "A" zone and the displaced water, if locally accumulated around a tumour, as a hydropic "B" zone. Conventional radiographic techniques, however, are not capable of identifying a local increase in water content inside a tumour with a cathodic centre.

B. Intercellular space and movement of water through tissue

An important effect of forces of attraction and repulsion in tissue is connected with the existence of intercellular spaces. These forces balance each other, leaving a distance d open (Fig. VIII: 1). The rapidly increasing component of repulsion force therefore prevents adjacent cells from achieving "absolute contact".

It is easy to understand that the space d should be of considerable importance for the functions of cells and tissues. Physically, a space must be present between individual cells. Biologically, a space sufficiently large to allow water and solutes to pass between the cells is an obvious prerequisite for cellular functions. Current belief is that the adhesive bonds generally maintain intercellular distances of no greater than 5 Å and that the repulsive forces maintain intercellular distances of no less than 3 Å (7, 15, 20). The size of a water molecule has been found to be 0.9572 ± 0.0003 Å (7, 8). The vibrational state does affect the dimensions of the water molecule, but only slightly (22, 40). Passage of water molecules between cells is therefore physically possible. *The space d is indeed a space of life.*

A further possibility is that passage of water molecules between cells may open further the intercellular space for new molecules, the attraction forces between adjacent cells having lessened. Whatever the mechanisms may be to modify the space d, it is obviously a large enough space to permit the entrance of water.

C. Fixed surface charges on cells

Bernstein (9, 10) proposed in 1902 the "membrane theory" on the basis of the Nernst-Planck concept of the liquid junction potential (see Chapter XIII). He thereby identified fundamental physical characteristics of molecules and cells. Diffusion potentials across membranes and electrical phenomena of living cells and tissue became to a certain extent explainable.

Bethe and Toporoff (11) next pointed out, in osmotic studies, that the direction of deviation of the concentration potential from the liquid junction potential correlates with the electrokinetic charge of a membrane.

Teorell (82, 88) formulated in the 1950's his "fixed" charge theory, that ionic membranes have two Donnan equilibria and one net diffusion potential. Meyer and Bernfeld, (57) in particular, and later many others (17, 24, 37, 38, 43, 44, 55, 56, 66–69, 71–74, 77, 79, 80, 93) have further extended the basic concept of fixed charges of membranes and their many important functions in biology. For example, fixed surface charges are considered to exist on the surface of both plant and animal cells (1, 36, 90–92). Large molecules of organic substances containing a polar part are often arranged periodically in so-called pseudocrystallinic aggregates (15). Such aggregates are present in cellulose, wood, silk and cotton wool, as well as in many animal proteins (3, 29). Some of these aggregates are in the form of surface-coating lipoproteins with a micelle structure. The polar parts of these molecules at the cell surfaces are thought to act as fixed surface charges (27). The water-absorbing properties of many substances are also considered to depend on the fixed charges of the absorbing material. Cotton wool, which has a large surface per weight, may absorb as much water as 25 times its weight (3).

The surfaces of cells are known to carry fixed electropositive and electronegative charges (92). A surplus of negative charges almost always characterizes the surfaces of cells (1, 92). Two adjoining cells electrostatically attract each other at certain sites where the fixed charges have opposite polarity (1, 4, 36, 38, 50, 75, 91). These charges are important for the mechanical strength of tissue. Fixed surplus charges are also important constituents in the structural prerequisites for transmembranous and regional transport of water in interstitial tissues (61, 75, 94).

D. Liquid water: structure and energy

Before we can discuss electroosmosis adjacent to lung lesions, some physical properties of water must be reviewed (26, 42, 44, 62, 77). The structural features of liquid water depend largely on its ability to form bonds by combinations of the molecular orbits of electrons of its hydrogen and oxygen atoms. Liquid

water also appears in polymers that possess a varying degree of vibrational characteristics (7, 8).

In ice, representing the lowest energy level of water, hydrogen-bonded clusters of water molecules form tetrahedrons (26). As energy content in liquid water increases, the numbers of tetracoordinated bonds decrease. Thus triple, double and unbonded water molecules appear progressively as energy increases to the level of vapour, which represents the highest level of energy content (60, 75). The difference in energy between the levels for the tetrabonded and unbonded water molecules is estimated to be 2.7 kcal/mole. Brownian and vibrational movements of water molecules constitute an important part of their total free energy content.

Because a water molecule possesses a permanent dipole moment, it will orient itself within an electric field, i.e., liquid water is "structured" in a way similar to what takes place in the formation of ice (60). An augmentation of the dipole moment will also develop when the molecule is exposed to an electric field.

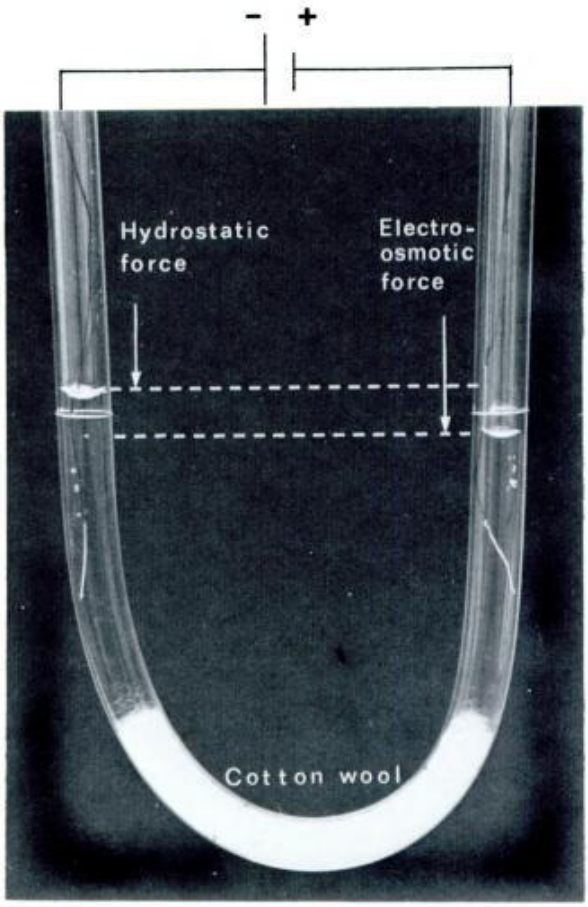

Fig. IX: 1. Electric transport of water. Cotton wool is packed in the lower part of a U-shaped glass tube, which is partly filled with water. Two clean platinum electrodes are immersed in the water. When an electric potential difference is applied between the electrodes, water is moved in the "capillaries" of the wool from the electropositive to the electronegative side of the system. An equilibrium is obtained between opposing electroosmotic and hydrostatic forces.

E. Electroosmosis: transport mechanisms Types I–IV

The mode of water transport in electroosmosis is known to a certain extent (44, 70, 77).

Transport of water by use of fixed charges on cellular surfaces can be demonstrated in the following experiment (Fig. IX: 1). Cotton wool is packed in the lower part of a U-shaped glass tube, forming "capillaries". A matrix now exists of spaces or channels among the cotton fibres. Water is poured into the tube. Two clean platinum electrodes are immersed in the water. When an electric potential is applied between the electrodes, water moves from the positive to the negative side of the system until an equilibrium is obtained between the electroosmotic and hydrostatic pressures. This flow of water, against a hydrostatic pressure, may be regarded as a primitive form of "active transport" (defined as transport against an energy gradient), for which the presence of suitably sized capillaries lined with fixed charges is just as essential as the applied electric field. Such transport of water (electroosmotic water transport of what may be called Type I) can be assumed to take place without concomitant electrolysis of water molecules. In a simplified version, Fig. IX: 2 illustrates this electroosmotic transport of Type I.

1. Type I electroosmosis

When an applied electric field is strong enough to break up clustered water molecules, a field orientation or "structuring" of the molecules will take place. Simultaneously, the molecules and dielectric components of the matrix will increase their dipole moments. The dimensions of the matrix of "capillaries" are also important. Lined with fixed charges, the capillaries must be small enough to prevent hydrostatic return. Under these conditions, water will move in the capillaries in a predictable way.

Negative surface charges of the capillaries will push some of the oriented molecules (Fig. IX: 2, site *X*) and pull some of them (site *Y*). Vibrational and rotational movements of the water molecules can still take place in irregular capillary channels (77). Certain molecules will be transported along the matrix secondary to the motion of the molecules in sites *X* and *Y*. The presence or absence of net electrostatic forces on a molecule of water in the matrix largely depends on the

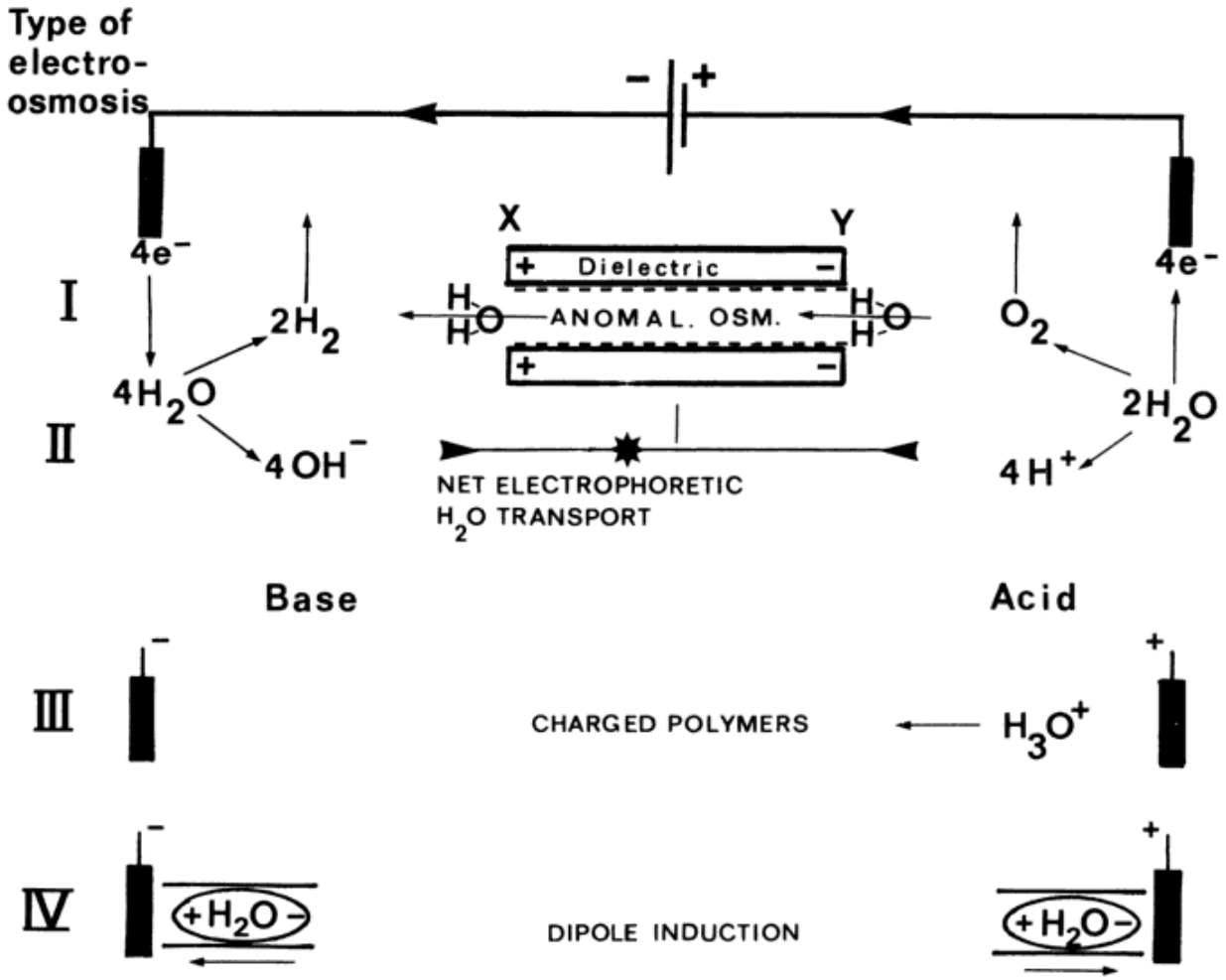

Fig. IX: 2. Electroosmotic water transport. Four mechanisms can be identified. *Type I* transport requires fixed electric charges on the surfaces of the dielectric matrix (e.g., cotton wool). These charges are negative in cotton wool and tissue, leading to a net movement of water molecules from anode to cathode. The energy for this transport is suggested to derive from the applied electric field transforming the energy of the water molecules. The transformations include breaking of clustered water molecules, and reduction of their vibrational and rotational molecular movements. A net movement of water is produced by electrostatic interaction between the dielectric matrix and aligned water molecules. *Type II* transport is electrophoretically linked and requires a closed electric circuit but no fixed surface charges on the dielectric "capillary" walls. When water is ionized, the different speeds of migration of ions and their recombination create a net transport of water. *Type III* transport is cationic. It is based on the fact that cations adsorb water molecules, but anions do not. The cations therefore selectively carry water molecules in a closed circuit. This type also includes transport of ionic polymers of water. *Type IV* electroosmosis (induction-adsorption) takes place in matrices close to an electrode and does not require fixed surface charges on the "capillary" walls. Water molecules undergoing dipole induction by the electric field are transported (adsorbed) to an adjacent charged electrode surface, irrespective of its polarity. The "capillaries" of the matrix may be thought of as mechanical rectifiers.

location of the fixed negative charges in relation to the actual charge distribution of the water molecules. During transport in the matrix, the dipoles of the molecule and the fixed charges are exposed to synchronously fluctuating forces from their electrical fields, depending on their spatial locations in relation to each other. A different dipole moment of the field-oriented water molecules is also to be expected depending on their location in the positive or negative side of the superimposed electric field.

The direction of water flow in electroosmosis is determined by the polarity of the surplus of fixed charges of the capillaries (C), within a defined electric field.

$$E^- (\overleftarrow{C^-}) E^+$$

or, $$E^- (\overrightarrow{C^+}) E^+$$

Sollner (77) studied electroosmosis through a typical unoxidized collodium matrix membrane of high porosity. Thereafter he oxidized the same membrane with heparin, which is electronegative, and prepared an-

other membrane with protamine, which is electropositive. An electroosmotic flow was then obtained for a 10^{-3} M KCl-water solution (current intensity, 0.1 mA/cm^2) as follows:

Unoxidized collodium membrane	+2840 mm^3/100 cm^2/hour
Oxidized collodium membrane	+4640 mm^3/100 cm^2/hour
Protamine collodium membrane	−4380 mm^3/100 cm^2/hour

The rate of transport of water depends on several factors: magnitude of the electric field over the pores, the membrane porosity (number and size of pores), and the magnitude, density and geometry of fixed charges. As voltage increases over the electrodes, movement of water will increase. A similar effect can be obtained by placing the electrodes closer to the matrix, due to the increase of intensity of the electric field.

The size of the "capillary" channels also may be critical. If the channels are too large, hydrostatic pressure will cause water to return. This effect may reduce the difference between the fluid levels or may even lead to no difference at all.

2. Type II electroosmosis

The mechanisms of "electroosmotic water transport" are complex. It is easy, for example, to recognize that water can also be transported as a result of electrolysis followed by migration of protons and hydroxyl ions and their recombination. In such instances semipermeable membranes or capillary channels need not be charged (Fig. IX: 2). The membranes or channels then act simply as a mechanical hindrance to convection.

In Type II electroosmosis, diffusion and electrophoretic migration of participating ions in an applied electric field determine where the recombined water molecules will be found. The transport mechanism of the migration derives from the mobility of ions. Proton movement, for instance, is defined as $36.2 \cdot 10^{-4}$ cm^2 V^{-1} s^{-1} at strong dilutions and 25°C; the corresponding value for hydroxyl ions is $20.7 \cdot 10^{-4}$ cm^2 V^{-1} s^{-1} (41). Their distance of recombination into water can then be expected to be $\frac{36.2}{36.2 + 20.7}$ or about ⅔ of the interelectrode distance from the electropositive electrode. This value is, however, also modified by different adsorption properties of ions in a matrix as well as by gravitation. (We will here refer to Fig. XIII: 7 which, besides serving a different purpose, also illustrates Type II electroosmosis.) In this experiment a 10 volt DC potential was applied between two platinum electrodes on litmus paper soaked in water. By electrolysis of water, protons are produced at the anode and hydroxyl ions at the cathode. The ions migrate in the electric field and recombine to form water. Due to differences of mobility of the ions, a net transport of water will occur toward the cathode (see Fig. IX: 2). Gravity considerably influences the position of the recombination zone, an effect which can easily be observed by slight tilting of the electrolytic specimen. Water transport of this kind (electroosmosis, Type II) increases in importance as voltage increases and is, in fact, a special case of electrophoresis. In the conventional view of electrophoresis, transport of electrons in the electrical cables requires a corresponding electrical transport in the water. This transport has been explained as depending on proton jumps on water molecules (26), after their ionization at the electrode surfaces. However, electrolysis of water can be induced immediately on applying a potential difference over water, despite the fact that water is a good electrically insulating medium. Some dissociation of water is evidently present for an initial ionic flow of current, but other mechanisms may also be involved. Dielectric induction and structuring of water molecules adjacent to the electrode surfaces can, for instance, be regarded as the initial prerequisite for redox reactions at the electrode surfaces. Water molecules are thereby oriented in an optimal way to consume electrons from the cathode and to donate electrons to the anode. The reaction products then diffuse and migrate in the electric field. This mechanism is compatible with the relatively slow transport of OH^- and H^+ ions in the direction from the electrode surfaces to the zone of recombination, which should be a barrier of resistance for the passage of protons and hydroxyl ions.

3. Type III electroosmosis

Another of the mechanisms of electroosmotic water transport depends on differences in behaviour of cations and anions (Fig. IX: 2). It is known that cations may become hydrated, but not anions (41). When ions migrate in the electropositive part of an electric field, cations should then carry water molecules adsorbed on their surfaces. A corresponding adsorption and transport by anions should not occur in the opposite direction. The resulting net electrophoretic water transport might then be looked on as a primitive form of "mediated" transport. A release of transported water molecules from the carrier can even be predicted when the aggregate enters a region of high pH.

4. Type IV electroosmosis

Finally, an electroosmotic partial function may be distinguished (Fig. IX: 2). Within a matrix, which does not need to be lined with fixed charges, strong dipoles

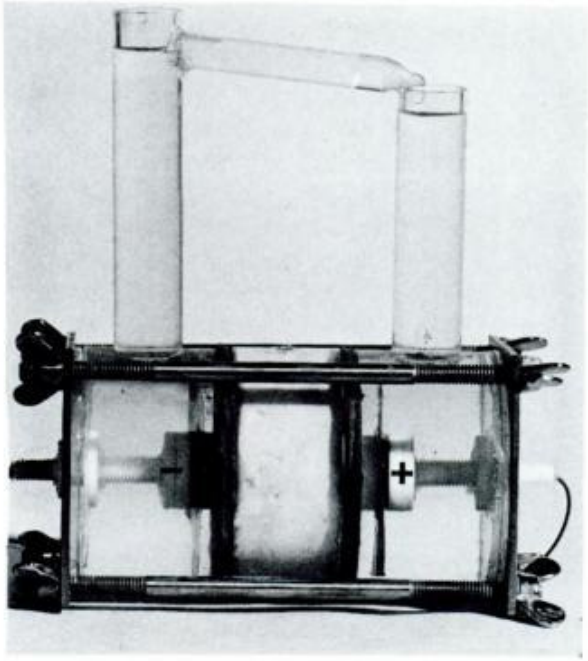

Fig. IX:3. Apparatus for circular electroosmotic transport of water. The electroosmotic chamber consists of two perforated plastic (perspex) plates. Cotton wool is compressed between the plates. On the other side of each plate is a platinum electrode and a vertical tube. The tops of the vertical tubes are connected by a slightly tilted tube. The apparatus is filled with water up to the level of the lower end of the tilted connector. Positive voltage is applied to the right electrode and negative to the left one. Electroosmotic flow of water will then take place from the right to the left chamber. Increased hydrostatic pressure of the elevated left column of water will be limited by the flow of water from the left to the right vertical tube over the slightly tilted tube. The circular movement of water will then be seen as a dripping of water from the "mouth" of the tilted tube. This flow will continue for a while. Then it will slow and stop spontaneously, despite maintenance of the voltage over the electrodes.

Fig. IX:4. Pressures in electroosmotic transport of water: The tilted connecting tube in the apparatus shown in Fig. IX: 3 has been replaced by a pressure transducer in the left vertical tube. Upon application of a 20 volt DC potential between the electrodes (left negative, right positive) a rapid rise in pressure (phase *a*) was followed by a slow rise (phase *b*). Two minutes later, when the electric potential generator was turned off, the pressure rapidly diminished (phase *c*). Phase *a* is thought mainly to be caused by Type I electroosmosis, and phase *b* by continued electrophoretic water transport (mainly Types II and III electroosmosis). The remaining pressure (*d* minus *c*) is produced by gas formed in the left chamber. The electrophoretic water transport during phase *b* is caused by pressure *c* minus *a*.

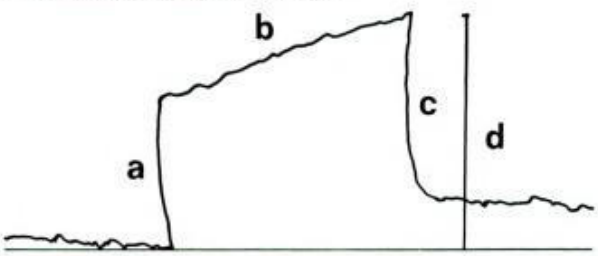

may be induced in the molecules close to a charged electrode. These inductions will cause a net attraction force (adsorption) of water to any charged electrode, regardless of its polarity. The matrix in this Type IV electroosmosis serves then as a rectifier for the transports.

F. Two distinguishable pressure variables in electroosmotic transport of water

One critical question is whether appreciable electroosmotic water transport can occur at voltages low enough not to create electrolysis of water. Different opinions have been presented in the literature on this problem (76).

Helmholtz (39) found electrolysis of water to start at about 1.64 V. Bartoli (6) found the value to be 1.23 V. Part of the movement of water during electrolysis in electroosmosis is then connected with the formation of H_3O^+ and its polymers (corresponding to Type III electroosmosis). In search of further insight into the mechanisms of electroosmosis, the behaviour of water in terms of transport pressures was assessed experimentally.

1. Experimental methods and results

An electrophoretic apparatus was constructed as shown in Fig. IX: 3. It consists of a chamber and two platinum electrodes, each attached to electrical cables. Between the electrodes, various materials can be placed under compression between two perspex plates with multiple holes. Vertical tubes are connected with the right and left parts of the apparatus. A slightly tilted tube connects the tops of the vertical tubes. In the arrangement shown in Fig. IX: 3, the electrophoretic matrix consists of compressed cotton wool. When, for instance, 10 volts are applied between the platinum electrodes, the right one positive and the left negative, water will flow through the cotton from right to left. This flow results in a return of water from the left to the right side through the slightly tilted tube, appearing as dripping of water from the mouth of the tilted tube.

The degree of compression of the cotton wool, the distance between the electrodes, and the potential difference each were found to influence the transport of water. These influences were seen as differences in numbers of drops of water per unit time. The rate of water transport was not found to be constant. It

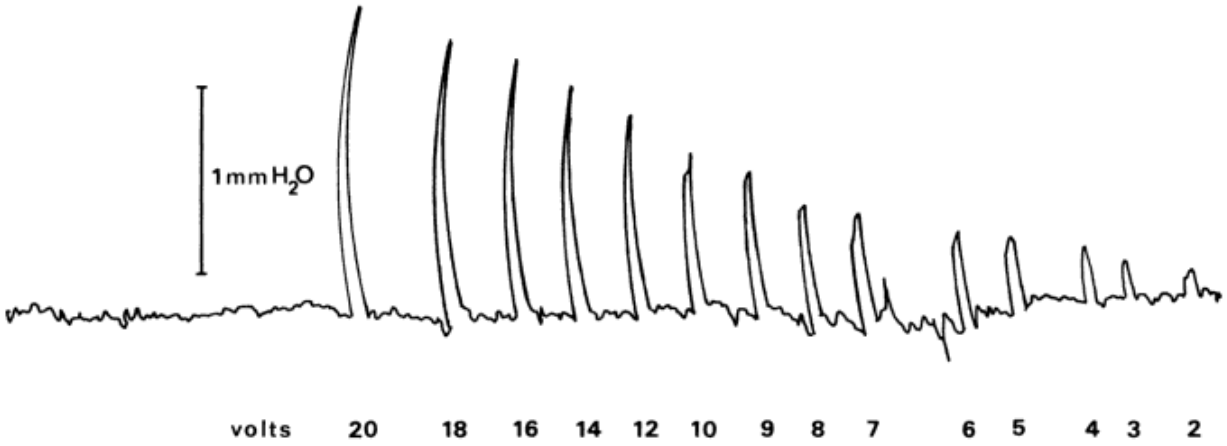

Fig. IX: 5. Pressures in electroosmotic transport of water when fourteen DC pulses of one second each were applied. The rapid pressure phase returned to the initial level of pressure after each of these short pulses, indicating that remaining effects of ionization and gas formation must have been minimal.

reaches a maximum after some time, depending on voltage, then decreases and eventually stops completely. This change in water transport is associated with formation of gas at the electrodes, which also elevates the free fluid levels in both vertical tubes. The temperature of the water will simultaneously rise, the more rapidly as voltage is elevated. After transport of water has stopped, renewed transport can be obtained by elevation of the electric potential between the electrodes. The water will then start to flow with increasing speed, again reaching a maximum and then retarding until it again stops.

These preliminary observations were further studied by removing the tilted communicating tube and connecting a pressure transducer (Statham P23 DC) to the left or right vertical tube, which was closed by an airtight stopper of low compressibility. The apparatus was filled with water, replacing all air pockets. The pressures were recorded by means of a Grass 7 B Polygraph.

When a constant potential of 20 V was applied between the electrodes for 2 minutes, two components appeared in the changing pressures obtained from the electronegative side of the system (Fig. IX: 4). Initially, pressure increased rapidly (phase *a*) and then it rose slowly and steadily (phase *b*). When the voltage was switched to zero, the pressure diminished immediately (phase *c*), which is larger than the initial elevation of pressure (*a*). The new base level of the pressure was elevated, at the value *d* minus *c*.

In the next experimental variant, the values of (*a*) and (*c*) were the same during a consecutive series of 14 applications of square voltage pulses of one second duration each (Fig. IX: 5). The voltage pulses varied from 20 down to 2 V (Grass S88 stimulator). The magnitudes of the initial *a* pressures were directly proportional to the applied voltages (Fig. IX: 6).

Intermittent applications of 20 V for 2 minutes each, separated only by turning the applied voltages off and then immediately on, gave results which are shown in Fig. IX: 7. The slow phase now steadily built up the pressure in the system. Ionization causing the formation of gas, visible on the electrodes as bubbles, is the probable main source of this increase. The insert in Fig. IX: 7 shows the increasing total pressure (*d*) of the system. At the same time, the rapid phase (*a*) also shows increasing values with each repeated application of 20 V. This effect is possibly a consequence of increasing ionization of water, which should relatively enhance Type III electroosmosis.

Fig. IX: 6. Electroosmotic transport of water: hydrostatic pressures increase during a series of one second pulses of increasing voltage. The pressures were proportional to the potential differences between the electrodes (voltages ranged between 0.4 and 20 volts). The relationship suggests linear correlation.

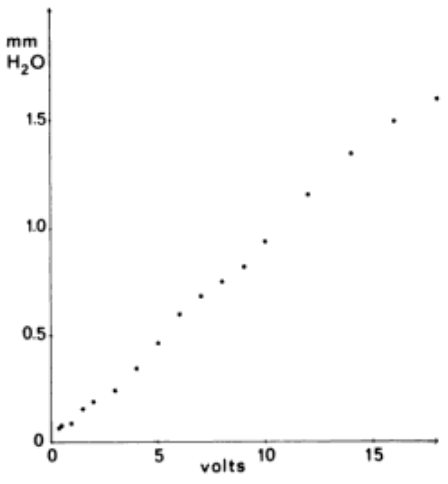

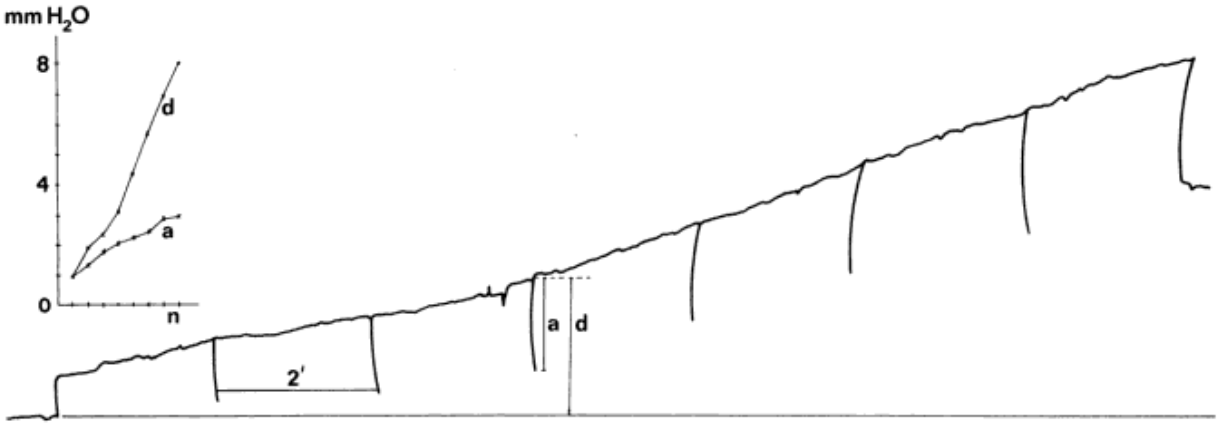

Fig. IX: 7. Electroosmotic transport of water: pressures increase during intermittent applications of 20 volts for periods of 2 minutes each. The slow pressure phases caused the pressure in the system to increase continually, an effect due mainly to gas, forming as a consequence of ionization. Such events can also explain the progressive increases of the rapid pressure phases (*a*). The insert shows the relation at two minute intervals (*n*) between the total pressures (*d*) in the system and the rapid pressure phases (*a*).

2. Discussion of pressure changes and electric transport of water

It is now apparent that two separate phases of pressure changes are integrated in electroosmotic water transport.

The slow, continuous pressure phase is obviously connected with ionization and the formation of gas in the system. This phase is not easily recognized at low voltages with pulses of up to 20 V of 1 sec duration. Gas formation and consequently also ionization are not particularly prominent with this mode of application of voltage.

The rapid pressure phase is easily observable at low and high voltages and immediately on the application of a voltage difference between the electrodes. Voltage pulses between 0.4 to 20 V and of 1 sec duration each have shown linear correlation with the pressures, implying that they may be extrapolated to zero. These findings have not been described previously.

The gradual increase in magnitude of the rapid pressure phase on repeated applications of voltage shows that this phase also is partly coupled to the mechanism of the slow continual pressure phase and most likely to Type III electroosmosis.

In the author's opinion, the rapid pressure phase in these experiments corresponds mainly to the transport process which is sometimes called anomalous electroosmosis (77), while the slow and rapid pressure phases are both included in what is usually called electroosmosis. It seems questionable to make a distinction between anomalous osmosis and electroosmosis, because each includes all four types of transport mechanisms. The internal relative importance of the Type I–III mechanisms for net transport of water changes as ionization increases. According to the pressure measurements, the rapid pressure phase is an instantaneous electric field effect which is most clearly demonstrated upon application of short pulses of voltage.

The "low" voltages, e.g., 10–20 V between the electrodes, are "high" compared with what can usually be expected in biologic situations. Still, extrapolation of the rapid pressure phase with short voltage pulse suggests that electroosmosis also can occur over very low voltages between the electrodes. This observation is of interest, because it suggests that small gradients of potential should also be able to include transport of water. The amount of water transported may even be large when the forces are allowed to work over a long time.

A more critical problem is that proof has not yet been put forward, demonstrating in tissues any channelizing mechanism which could function as a closed electric circuit in vivo. Such a circuit is a prerequisite for electroosmosis. Chapters XII and XIII are devoted to this problem.

So-called anomalous osmosis, known since its first description by Dutrochet in 1835 (25), has been much studied (5, 34, 35, 46–51, 70, 78). Graham suggested that anomalous osmosis is a special kind of osmosis (33). Bartell and Loeb (5, 52–54) have suggested that spontaneous electroosmosis occurs whenever electrolytes, but not non-electrolytes, diffuse across a charged membrane.

A double layer of high field strength on the surface of cells, including vascular endothelium, is normally about 10^6 to 10^8 volts per centimetre (64). These electric fields are caused by fixed cellular charges which correspond in vivo to the fixed surface charges in vitro in the cotton wool experiments. The magnitude and direction of anomalous osmosis directly de-

pend on the fixed charges of membranes (77). Depending on the polarity of these charges, as well as the concentration differences across the membrane, anomalous osmosis may be positive or negative.

In the author's opinion, all transport of water via a closed electric circuit is *electroosmosis*. This transport comprises four integrated but different mechanisms (Fig. IX: 2). These may be characterized as follows:

Electroosmosis of Type I seems to be almost synonymous with previous descriptions of "anomalous (electro) osmosis". It is characterized by its dependence on a surplus of fixed negative or positive charges in "capillaries". Type I electroosmosis may therefore also be described as *fixed charge electroosmosis*. Its field-induced rapid change of pressure correlates directly with the magnitude of the voltage applied over the matrix.

Electroosmosis Type II does not require fixed charges in the matrix. It involves electrolysis of water, diffusion and migration of H^+ and OH^- ions and their recombination into water as a special case of electrophoretic transport. Type II electroosmosis is characterized by the slow elevation of pressure, which is not directly proportional to the magnitude of the voltage applied over the matrix. Type II electroosmosis may also be described as *electroosmosis by ionic recombination*.

Type III electroosmosis is closely related to Type II electroosmosis. Its mechanism is based on ionic hydration (77) but applies only to cations. Cations therefore carry water and water polymers from the electropositive to the electronegative part of the electric field. This function may therefore be looked on as a primitive form of mediated transport. Type III electroosmosis may also be described as *cationic electroosmosis*.

Lastly, a *Type IV electroosmosis* may be recognized. It takes place in a matrix close to charged electrodes, which by induction produce a net attractive force on nearby water molecules. In Type IV, no fixed charges are necessary in the matrix. The water molecules will always move to the adjacent charged electrode regardless of its polarity. Type IV electroosmosis may also be described as *field-induced osmosis* and should be regarded as a special case of Type I electroosmosis. In Type IV electroosmosis the charged electrodes include the functions of both the applied field and the fixed charges.

G. Transport energy in Type I electroosmosis

The driving force in anomalous osmosis (fixed charge electroosmosis) through cell membranes, according to Sollner (77), may possibly be the streaming potential which occurs as an electrolyte diffuses. According to this view, the streaming potential difference as a source for the driving force should require a closed circuit, which may exist but is not yet demonstrated. Other authors have suggested that the whole electroosmotic process can be explained as an electrophoretic transport of water (47–49, 58). This latter explanation is evidently oversimplied, because now two different phenomena of electric transport of water can clearly be distinguished by their pressure characteristics.

The energy of electroosmosis of the fixed charge type may possibly derive from the thermal energy of water. This consideration merits discussion.

According to Wagman et al. (89), and Cottrell (19), the following energies are associated with the formation of a molecule of water:

	kcal mol^{-1}
(1) Energy of formation from atoms at 0 K	−219.34
(2) Zero-point vibrational energy	13.25
(3) Electronic binding energy = (1) minus (2)	−232.59
(4) Enthalpy of formation at 25°C	−22.54
(5) Bond energy of O–H bond at 0 K = ½×(1)	109.7
(6) Dissociation energy of H–O	101.5
(7) Dissociation energy of H–OH = (1) minus (6)	−117.8

The free molecular energy of nonhydrolyzed water molecules is stored as vibrational and rotational movements. This energy could be available for Type I electroosmosis as follows: an electric field can be anticipated to restrict molecular movements. This restriction will lead either to (*a*) loss of energy to the surroundings, or (*b*) modification of kinetic energy from the previous vibrational and rotational movements into directed transport of the molecules, or (*c*) a combination of both possibilities.

The breaking of clusters of bonded water molecules (16, 30, 31) and their "structuring" by an electric field means that the amount of "available" free energy of the water is modified in some way. This energy, which is part of the total energy content of water, cannot spontaneously return to its initial equilibrium state unless the electric field is removed. Some reactions toward an increase of entropy are still possible, but toward a different stage of equilibrium, which in the presence of fixed surface charges in capillaries may lead to transcapillary electroosmotic transport of Type I.

The restriction of brownian movements of water molecules by an applied electric field might, theoretically, be reflected in a temperature change of the water. The effects of different water temperature on electroosmotic transports as well as different electrode

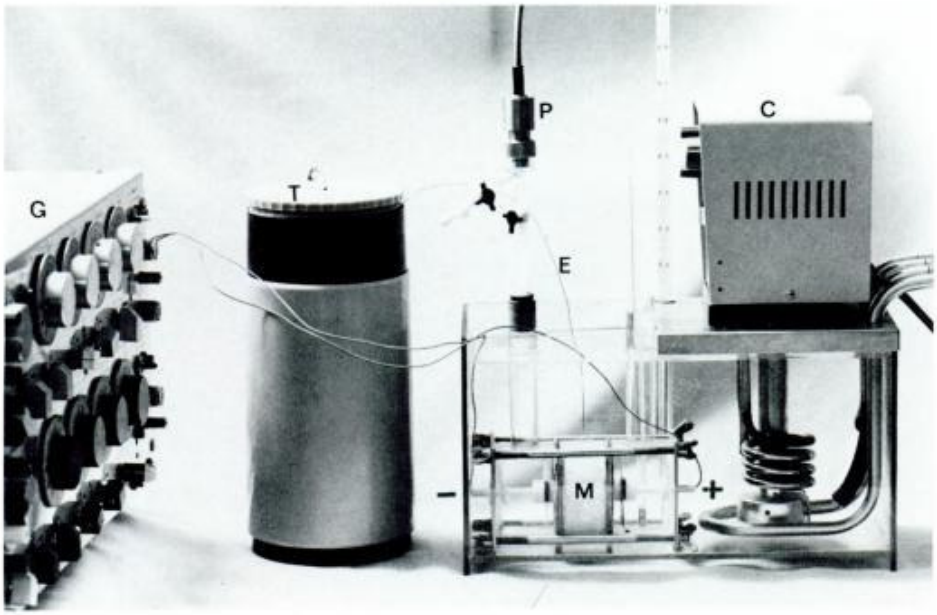

Fig. IX: 8. Electroosmotic transport of water: temperature effects. Temperature and pressure were recorded in the apparatus for electric water transport, immersed in a thermostat (*C*)-controlled water bath. A sensitive (0.01°C=1 mm deflection) electrothermometer (*E*) was placed in the cotton wool matrix (*M*). Matrix temperature was measured against a reference electrothermometer in ice water in a thermos flask (*T*). One second pulses of 10 to 40 volts were applied (*G*) over the matrix at equilibrated matrix temperatures against the thermostat water in ranges from +1°C to +50°C. The displacements of water were determined over the pressure transducer (*P*).

potentials on water temperature were therefore studied (Fig. IX: 8).

The temperature of water inside the matrix of "capillaries" (cotton wool) was measured with a sensitive (±0.01°C) electrothermometer (Philips Chromel Alumel Thermocoax). The electroosmotic apparatus was immersed in a thermostatically controlled water bath. A sensitive pressure transducer (Statham P23 DC) was connected to the branch of the electronegative side while a mercury thermometer for rough controls was inserted into the open opposite branch. The electrothermometer was positioned with its tip in the cotton wool matrix and its reference electrode in a thermos flask containing ice water. Single electric potential pulses of one second duration were produced by a square pulse generator. Pressure changes in the electronegative side of the system were amplified and recorded (Grass Polygraph Model 7B).

When stable temperature levels were applied to the external bath and measured inside and outside the apparatus, variations from +1°C to +50°C did not influence the electroosmotic pressure elevations as potential pulses of 10 to 40 volts of 1 sec duration each were applied over the electrodes.

At the same time, no elevation or depression of temperature was observed within the cotton wool matrix.

The range of water temperature in these experiments, +1°C to +50°C, includes most of the actual range of biologic temperatures. The absence of detectable influence of water of different temperatures on electroosmotic pressure as well as the absence of detectable temperature changes within the cotton wool matrix during electroosmosis suggest two possible explanations. First, the sensitivity of the pressure and temperature recording devices may have been too low, which is not very likely. Second and more likely, the transformation of the available free energy of water may correlate directly with the energy level of the applied electric field. This possibility is consistent with the previously described experimental results (Fig. IX: 6), showing a linear relation between applied electrode voltages and fixed charged (Type I) electroosmotic pressures. This explanation is in itself not particularly remarkable: isothermal reactions are commonly encountered in biology.

H. Experimental electroosmosis in dog and human lung tissue

Normal, fresh, peripheral lung tissue from 2 dogs and 2 humans after pneumonectomy were each carefully minced. The tissue materials were then washed repeatedly in water. Each specimen was placed under slight

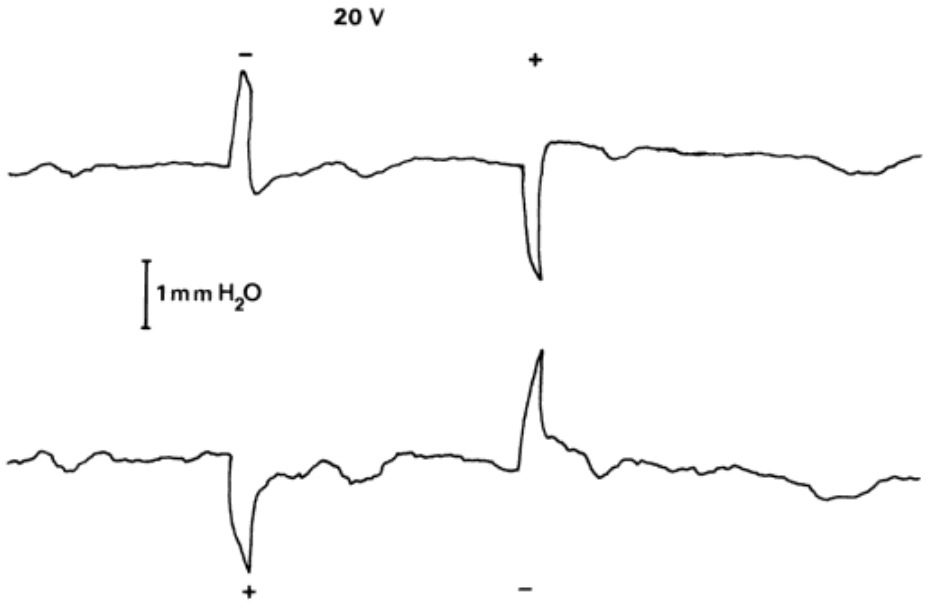

Fig. IX: 9. Electrophoretic transport of water: matrix of freshly minced tissue from the lung of a dog. Pressure elevation in the electronegative side (left upper) and corresponding lowering in the electropositive side (left lower) of the apparatus for electric water transport. Twenty volts for one second were applied across the electrodes. Reversed pressures were obtained when the polarity of the electrodes was reversed (right upper and lower pulses). Dog and human lung tissue each appear to allow electric transport of water in the same way as does compressed cotton wool. In this experiment traces of blood and electrolytes were present. Nevertheless, the rapid pressure phases were of approximately the same magnitude as those with a matrix of deionized water and cotton wool (cf. Fig. IX: 5).

compression between the perforated perspex plates in the electroosmotic apparatus (Fig. IX: 9). The apparatus was then filled with water. Voltage was applied between the electrodes. Pressure was recorded in the two water chambers.

These electroosmotic experiments revealed that human and dog lung tissue behaved in the same way as cotton wool.

From these experiments it is apparent (Fig. IX: 9) that short pulses through a closed electric circuit can induce similar rapid pressure gradients over fresh human and dog lung tissue and cotton wool. Electroosmotic water transport may possibly, therefore, also take place in the lung, e.g., as Type I electroosmosis (= fixed charge electroosmosis ≃ "anomalous osmosis"). Such a possibility, however, warrants some further considerations.

I. Electroosmotic flow of water: local displacement of water in the formation of "A" and "B" zones around a tumour

Many studies have estimated the possible importance of electroosmosis in biology (14, 20, 23, 25, 26, 28, 34, 35, 46, 65, 70, 77, 85). A small electroosmotic movement of water toward the negative pole in the large cells of *Nitella* was found by Blinks and Airth (13, 14) but only at potential differences of 1–2 V, which they considered to be 20 times greater than common biological levels.

An exceedingly small electroosmotic flow has been demonstrated in *Nitella* by Fenson and Dainty (28), but they concluded the flow was too small to be of physiological significance. 20 mm^3 H_2O/coulomb was transported by electroosmosis. The physiological current across the membrane by ion transfer is about 10^{-7} A/cm^2, which should allow a water flow of only 2×10^{-6} H_2O cm^{-2} sec^{-1}.

According to these calculations, electroosmotic flow should have minimal if any significant function in biology. Further information in the literature suggests otherwise. Sawyer, et al. (64), state that transverse streaming potentials or pressure equivalent electroosmosis (65) exist as a result of pumping of positively charged ions and water (compare Type III, cationic electroosmosis) through the negatively charged "Swiss cheese" pores of blood capillary walls. A pressure drop of as much as 100 mm Hg is then maintained across at most a few microns of intima. The electric double

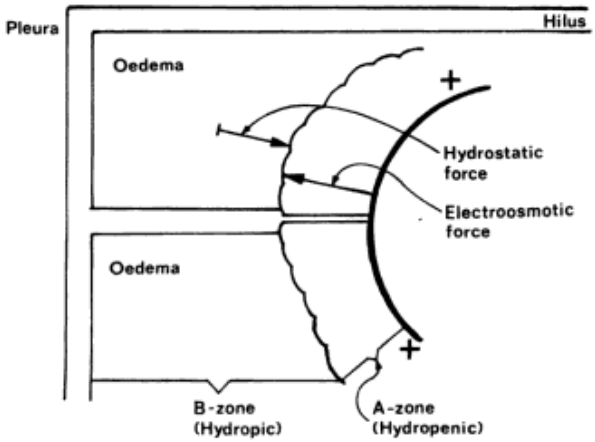

Fig. IX: 10. A tumour in the lung obstructs lymphatic flow toward the hilum by blocking some of the interlobular spaces. Oedema then develops in the tissue between the tumour and the pleura. Electroosmosis will move water away from the tumour, in the presence of a closed electric circuit between an electropositive tumour surface and a relatively electronegative, surrounding pulmonary matrix of narrow channels lined with fixed negative charges. An equilibrium is obtained between the electroosmotic pressure and the elevated hydrostatic turgor pressure. The outward displacement of water will produce a radiopaque "B" zone, which may also be called a hydropic zone. The displaced water will be replaced by increased quantity of air in the alveoli, contributing to the radiolucent (hydropenic) "A" zone.

layer at the vascular interface and at the surfaces of the cells within the walls presents a surprisingly high field strength. It approaches 10^6 to 10^8 volts per transmembranous cm (64). As indicated by Teorell (83–86) and others, certain cellular functions can be explained by assuming electroosmotic transmembranous water transport. Thus, pressure-volume changes in cells might be coupled to transmembranous concentration changes of flow and to a postulated closed circuit electric transport over the cell membrane, producing electroosmotic flow. In this way an electrochemical-mechanical system could be described which may have a biological correspondence (87).

The polarity of the net surface charge of cellular surfaces has been reported to be almost exclusively electronegative (4, 12, 36, 92). One curious exception are spirochaetes, which carry a positive net surface charge (1).

Previous investigators of electroosmosis in biology have dealt with these problems in connection with transmembranous water transport.

In the present investigations the possibility of interstitial water transport is of particular interest. The basic physical requirements for such a mechanism are narrow channels with fixed charges, a closed electric circuit and a driving electric potential gradient.

The network of intercellular spaces forming such channels ("capillaries") in lung tissue appear to possess the capacity to produce electroosmosis, according to the in vitro experiments here presented. Because most mammalian cells are provided with a surplus of fixed negative surface charges, it can be anticipated that the electroosmotic water transport is partly mediated by these surface charges of the cells, analogous to the case with cotton wool. This possible Type I mechanism of electroosmosis does not exclude the presence of other mechanisms of electroosmosis in tissue.

The assumption that electroosmotic water transport is likely to produce "A" and "B" zones around different lung lesions still requires an electric potential gradient in a closed electric circuit. Chapter VII suggests that a possible energy source for activation of such a circuit is local degrading of tissue due to injury, bleeding, local necrosis, infection, etc. Chapter XII will present the structure and Chapter XIII the principle of activation of such a closed circuit. This circuit will be seen to permit an understanding not only of electroosmosis in tissue but also of several aspects of structural development and function.

For the time being, we may preliminarily assume that the prerequisites exist for electroosmotic water transport. Fig. IX: 10 illustrates some consequences in the lung. A tumour blocks the interstitial channels which normally carry fluid centrally from peripheral lung and the pleural space. Stasis results and fluid collects between the tumour and the pleura. Let us also assume that an electric field is superimposed between the electropositive tumour and the surrounding parenchyma and that the interstitial spaces are lined with a surplus of fixed negative charges. Furthermore, let us assume that a closed electric circuit exists between the tumour and the surrounding tissue.

Given these prerequisites, water must move through the tissue away from the surface of the tumour. The hydrostatic (turgor) pressure and the electroosmotic pressure must then equilibrate. A hydropenic "A" zone and a hydropic "B" zone will form.

The author has attempted to determine the actual water content in the "A" and "B" zones in human lungs after pneumonectomy and in animals post mortem. These attempts have been unsuccessful in demonstrating changes in water content in lung peripheral to tumours, despite radiologic demonstration in vivo of the two zones. This negative result is readily explained by the fact that the mechanical changes on opening the chest will modify the pressure conditions which allow tissue water to be retained in the hydropic zones. As has radiographically been shown earlier, the "B" zone, representing local accumulation of fluid in tissue, disappears immediately after the introduction of air into the pleural space.

(In the female breast "A" and "B" zones also may

develop around carcinomas. In such cases it has been possible to demonstrate a difference in water content between the "A" and "B" zones. These studies are reported in Chapter XVI.)

Later we will return to the problem of local electroosmotic water transports in vivo, in connection with therapeutic polarization of tissues (Chapter XVII). At this point, however, it is now appropriate to consider the corpuscular effects of chemical concentration forces and superimposed electric fields.

References

1. Abramson, H. W.: Electrophoresis of cells and proteins. New York, Hafner Publ. Co., 1968.
2. Aebi, H.: Elektrolyt-Akkumulierung und Osmoregulation in Gewegsschnitten. Helv. Physiol. Acta 11: 96, 1953.
3. Asthbury, W. T.: Fundamentals of fibre structure. Oxford, Univ. Press, 1933.
4. Bangham, A. D., and Pethica, B. A.: The adhesiveness of cells and the nature of the chemical groups at their surfaces. Proc. Roy. Phys. Soc. Edinburgh 29: 43, 1960.
5. Bartell, F. E.: Membrane potentials and their relation to anomalous osmosis. In: Mathews, J. H. (ed.): Colloid symposium monography. Dept. Chem., Univ. Wisconsin, Madison, 1: 120, 1923.
6. Bartoli, A.: Über die Zersetzung des Wassers durch eine schwächere electromotorische Kraft als die des Daniell'schen Elementes. Beibl. Ann. Physik 2: 566, 1978.
7. Benedickt, W. S., Gailar, N., and Plyler, E. K.: The vibration-rotation spectrum of D_2O. J. Chem. Phys. 21: 1301, 1953.
8. Benedickt, W. S., Gailar, N., and Plyler, E. K.: Rotation-vibration spectra of deuterated water vapor. J. Chem. Phys. 24: 1139, 1956.
9. Bernstein, J.: Electrobiologie. Braunschweig, Friedr. Vieweg u. Sohn, 1912.
10. Bernstein, J.: Zur elektrochemischen Grundlage der bioelektrischen Potentiale. Biochem. Z. 50: 393, 1913.
11. Bethe, A., and Toporoff, T.: Über elektrolytische Vergänge an Diaphragmen. Z. Physik. Chem. 89: 597, 1915.
12. Bikerman, J. J.: Physical surfaces. New York, Academic Press, 1970.
13. Blinks, L. R.: The relations of bioelectric phenomena to ionic permeability and to metabolism in large plant cells. CSHSOB 8: 204, 1940.
14. Blinks, L. R., and Airth, R. L.: Electroosmosis in Nitella. J. Gen. Physiol. 41: 383, 1957.
15. Brandenberger, E., and Epprecht, W.: Röntgenographische Chemie. Basle, Birkhäuser, 1960.
16. Buijs, K., and Choppin, G. R.: Near-infrared studies of the structure of water. I. Pure water. J. Chem. Phys. 39: 2035, 1963.
17. Caplan, S. R., and Mikulecky, D. C.: In Marinsky, J. A. (ed.): Ion exchange. Vol. I. New York, Dekker, 1966, p. 1.
18. Conway, E. J., and McCormack, J. I.: The total intercellular concentration of mammalian tissues compared with that of the intercellular fluid. J. Physiol. 1: 120, 1953.
19. Cottrell, T. L.: The strengths of chemical bonds. London, Butterworths, 1958.
20. Dainty, J., Croghan, P. C., and Fenson, D. S.: Electroosmosis, with some applications to plant physiology. Can. J. Bot. 41: 953, 1963.
21. Dawkins, M. J. R., Judah, J. D., and Rees, K. R.: Factors influencing the survival of liver cells during autolysis. J. Path. Bact. 77: 257, 1959.
22. Dennison, D. M.: The infra-red spectra of polyatomic molecules. Part II. Rev. Mod. Phys. 12: 175, 1940.
23. Dick, D. A. T.: Cell water. London, Butterworths, 1966.
24. Dray, S., and Sollner, K.: A theory of dynamic polyionic potentials across membranes of ideal ionic selectivity. Biochem. Biophys. Acta 21: 126, 1956.
25. Dutrochet, R. J. H.: De l'endosmose des acides. Ann. Chim. Phys. 60: 22, 1835.
26. Eisenberg, D., and Kauzmann, W.: The structure and properties of water. Oxford, Clarendon Press, 1969.
27. Epprecht, W.: Grundlagen der Kristallstrukturbestimmung. In: Schinz, H. R. (ed.): Lehrbuch der Röntgendiagnostik. 6 Aufl., Band I. Stuttgart, G. Thieme, 1965, p. 78.
28. Fenson, D. S., and Dainty, J.: Electroosmosis in Nitella. Can. J. Bot. 41: 685, 1963.
29. Frank, H. S., and Evans, M. W.: Free volume and entropy in condensed systems. J. Chem. Phys. 13: 507, 1945.
30. Frank, H. S., and Wen-Yang, W.: III. Ion-solvent interaction. Structural aspects of ion-solvent interaction in aqueous solutions: a suggested picture of water structure. Disc. Faraday Soc. 24: 133, 1957.
31. Frank, H. S.: Covalency in the hydrogen bond and the properties of water and ice. Proc. Roy. Soc. London A 247: 481, 1958.
32. Gallagher, C. H., Judah, J. D., and Rees, K. R.: Enzyme changes during liver autolysis. J. Path. Bact. 72: 247, 1956.
33. Graham, T.: VII. The Bakerian Lecture. On osmotic force. Phil. Trans. Roy. Soc. London 144: 177, 1854.
34. Grim, E., and Sollner, K.: The contributions of normal and anomalous osmosis to the osmotic effects arising across charged membranes with solutions of electrolytes. J. Gen. Physiol. 40: 887, 1957.
35. Grim, E., and Sollner, K.: True anomalous osmosis in multisolute model membrane systems. J. Gen. Physiol. 44: 381, 1960.
36. Haydon, D. A.: The surface charge of cells and some other small particles as indicated by electrophoresis. Biochim. Biophys. Acta 50: 457, 1961.
37. Helfferich, F., and Ocker, H. D.: Ionenaustauscher-membranen in bi-ionischen Systemen. Z. Physik. Chem. 10: 213, 1957.
38. Helfferich, F.: Ion exchange. New York, McGraw-Hill, 1962.
39. Helmholtz, H.: Studien über electrische Grenzschichten. Ann. Phys. Chem. 7: 337, 1879.
40. Herzberg, G.: Molecular spectra and molecular structure. 2nd ed. New York, Van Nostrand, 1950.
41. Hägg, G.: Allmän och oorganisk kemi. 4th ed. Uppsala, Almqvist & Wiksell, 1966.
42. Kavanue, J. L.: Water and solute-water interactions. San Francisco, Holden-Day, 1964.
43. Kedem, O., and Katchalsky, A.: Permeability of composite membranes. Trans. Faraday Soc. 59: 1918, 1963.
44. Lakshminarayanaiah, N.: Transport phenomena in artificial membranes. Chem. Rev. 65: 491, 1965.
45. Leaf, A.: Maintenance of concentration gradients and regulation of cell volume. Ann. N. Y. Acad. Sci. 72: 396, 1959.
46. Loeb, J.: The influence of electrolytes on the electrification and the rate of diffusion of water through collodion membranes. J. Gen. Physiol. 1: 717, 1919.
47. Loeb, J.: Influence of the concentration of electrolytes on the electrification and the rate of diffusion of water through collodion membranes. J. Gen. Physiol. 2: 173, 1920.
48. Loeb, J.: On the cause of the influence of ions on the rate of diffusion of water through collodion membranes, I. J. Gen. Physiol. 2: 387, 1920.
49. Loeb, J.: On the cause of the influence of ions on the rate of diffusion of water through collodion membranes, II. J. Gen. Physiol. 2: 563, 1920.
50. Loeb, J.: The reversal of the sign of the charge of membranes by hydrogen ions. J. Gen. Physiol. 2: 577, 1920.
51. Loeb, J.: The reversal of the sign of the charge of collodion membranes by trivalent cations. J. Gen. Physiol. 2: 659, 1920.
52. Loeb, J.: The origin of the potential differences responsible for anomalous osmosis. J. Gen. Physiol. 4: 213, 1922.
53. Loeb, J.: Electrical charges of collodion particles and anomalous osmosis. J. Gen. Physiol. 4: 463, 1922.
54. Loeb, J.: Cataphoretic charges of collodion particles and

anomalous osmosis through collodion membranes free from protein. J. Gen. Physiol. 5: 89, 1922.
55. Mackie, J. S., and Meares, P.: The diffusion of electrolytes in a cation-exchange resin membrane. Proc. Roy. Soc. London Ser. A: 232, 498, 510, 1955.
56. Mackie, J. S., and Meares, P.: The sorption and diffusion of ethanol in a cation exchange resin membrane. Disc. Faraday Soc. London 21: 111, 1956.
57. Meyer, K. H., and Bernfeld, P.: La perméabilité des membranes. IX. La perméabilité ionique des membranes inhomogènes. Helv. Chim. Acta 28: 980, 1945.
58. Meyer, K. H., and Sievers, J.-F.: La perméabilité des membranes. I. Théorie de la perméabilité ionique. Helv. Chim. Acta 19: 649, 1936.
59. Mudge, G. H.: Electrolyte and water metabolism of rabbit kidney slices: Effect of metabolic inhibitors. Am. J. Physiol. 167: 206, 1951.
60. Némethy, G., and Scheraga, H. A.: Structure of water and hydrophobic bonding in proteins. I. A model for the thermodynamic properties of liquid water. J. Chem. Phys. 36: 3382, 1962.
61. Nobel, P. S.: Introduction to biophysical plant physiology. San Francisco, W. H. Freeman, 1973.
62. Partington, J. R.: The composition of water. London, Bell, 1928.
63. Robinson, J. R.: Osmoregulation in surviving slices from the kidneys of adult rats. Proc. Roy. Soc. B 137: 378, 1950.
64. Sawyer, P. H., Stanczewski, B., Ramsey, Jr., W. S., Ramasamy, N., and Srinivasan, S.: Electrochemical interactions at the endothelial surface. J. Supramol. Structure. New York, Alan R. Liss Inc., 1973.
65. Sawyer, P. N., and Harshaw, D. H.: Electroosmotic characteristics of canine aorta and vena cava wall. Biophys. J. 6: 653, 1966.
66. Scatchard, G.: Ion exchanger electrodes. J. Am. Chem. Soc. 75: 2883, 1953.
67. Scatchard, G.: General introduction. Disc. Faraday Soc. 21: 27, 1956.
68. Schlögl, R.: Elektrodiffusion in freier Lösung und geladenen Membranen. Z. Physik. Chem. (N.F.) 1: 305, 1954.
69. Schlögl, R.: The significance of convection in transport processes across porous membranes. Disc. Faraday Soc. 21: 46, 1956.
70. Schlögl, R.: Zur Theorie der anomalen Osmose. Z. Physik. Chemie (N.F.) 3: 73, 1955.
71. Schlögl, R.: Stofftransport durch Membranen. Darmstadt, Steinkopff, 1964.
72. Schmid, G., and Schwarz, H.: Zur Elektrochemie feinporiger Kapillarsysteme. Z. Elektrochemie 55: 295, 1951.
73. Schmid, G., and Schwarz, H.: Zur Elektrochemie feinporiger Kapillarsysteme. Z. Elektrochemie 55: 684, 1951.
74. Schmid, G.: Zur Elektrochemie feinporiger Kapillarsysteme. Z. Elektrochemie 56: 35, 1952.
75. Scheraga, H. A.: Protein structure. New York, Academic Press, 1961.
76. Sokolow, A. P.: Experimentelle Untersuchungen über die Elektrolyse des Wassers. Ann. Physik u. Chem. 58: 209, 1896.
77. Sollner, K.: The electrochemistry of porous membranes, with particular reference to ion exchange membranes and their use in model studies of biophysical interest. J. Macromol. Sci.-Chem. A 3: 1, 1969.
78. Sollner, K., Carr, C., and Abrams, I.: The structure of the collodion membrane and its electrical behaviour. III. The base exchange properties of collodion. J. Gen. Physiol. 25: 411, 1942.
79. Spiegler, K. S.: Transport processes in ionic membranes. Trans. Faraday Soc. 54: 1408, 1958.
80. Staverman, A. J.: Non-equilibrium thermodynamics of membrane processes. Trans. Faraday Soc. 48: 176, 1952.
81. Stern, J. R., Eggleston, L. V., Hems, R., and Krebs, H. A.: Accumulation of glutamic acid in isolated brain tissue. Biochem. J. 44: 410, 1949.
82. Teorell, T.: Transport processes and electrical phenomena in ionic membranes. Progr. Biophys. Biophys. Chem. 3: 305, 1953.
83. Teorell, T.: On oscillary transport of fluid across membranes. Acta Soc. Med. Upsalien. 62: 60, 1957.
84. Teorell, T.: Transport processes in membranes in relation to the nerve mechanism. Exp. Cell. Res. Suppl. 5: 83, 1958 a.
85. Teorell, T.: Rectification in a plant cell (Nitella) in relation to electro-osmosis. Z. Phys. Chem. 15: 385, 1958 b.
86. Teorell, T.: Oscillatory electrophoresis in ion exchange membranes. Arkiv Kemi 18: 401, 1961 a.
87. Teorell, T.: A biophysical analysis of mechanoelectrical transduction. In: Loewenstein, W. (ed.): Handbook of sensory physiology. Vol. 1. Berlin–Heidelberg, Springer-Verlag, 1971, p. 292.
88. Teorell, T.: Non-linear transport and oscillations in fixed charge membranes: some possible biological implications. In: Sélégny, E. (ed.): Charged gels and membranes II. Dordrecht, Holland, Reidel Publ. Co., 1976, p. 205.
89. Wagman, D. D., Evans, W. H., Holow, I., Parker, V. B., Baily, S. M., and Schumm, R. H.: National Bureau of Standards. Technical Note 270-1, 1965.
90. Weiss, L., and Levinson, C.: Cell electrophoretic mobility and cationic flux. J. Cell Physiol. 73: 31, 1969.
91. Weiss, L.: Biophysical aspects of initial cell interactions with solid surfaces. Fed. Proc. 30: 1649, 1971.
92. Weiss, L.: Studies on cellular adhesion in tissue culture. IX. Electrophoretic mobility and contact phenomena. Exp. Cell Res. 51: 609, 1968.
93. Wyllie, M. R. J.: Ion exchange membranes. I. Equations for multi-ionic potential. J. Phys. Chem. 58: 67, 1954.
94. Zimmerman, M. H., and Brown, C. L.: Trees: structure and function. New York, Springer-Verlag, 1971.

X.
Corpuscular movement and structural development

Effects of molecular and electric field forces

Part of the mutual attraction of biologic cells depends on the presence of electronegative and electropositive charges on their surfaces (12, 21, 36). Electronegative charges dominate, causing cells to move to the anode during electrophoresis. Mutual attractions of adjoining cells take place at charge sites of opposite polarity. Superimposed electric fields can influence this electrostatic adhesion in a tissue (1, 27).

Red and white blood cells and platelets normally repel each other by their negative surface charges (20, 37). They also are repelled by normal vascular intima, which is negatively charged (28, 29). Toxic or mechanical injury to the intima can reverse its charge, leading to deposition of blood cells on the injured vessel wall (26, 30, 31, 32). These effects are considered, at least in part, to result from forces of electrostatic attraction and to constitute an important part of coagulation.

In addition to electrostatic forces, so-called molecular attraction and repulsion forces also influence cellular adherence (as briefly surveyed in Chapter VIII). The normal forces of molecular attraction between blood cells are relatively weak. In organized tissues, such as bone and muscle, these forces are relatively strong (18, 35).

Forces of attraction and repulsion among neoplastic cells are often abnormal and considered an important risk factor for tumour spread (22). This risk may even be enhanced by certain anions, including heparin (2, 4, 10, 11, 13, 14, 34). The forces of attraction and repulsion are therefore important for the behaviour of cancers, e.g., metastatic seeding via the blood stream and local spread into the tissues surrounding a malignant tumour (12). This and the following two chapters will show experimentally in vitro how the effects of molecular and superimposed stationary electric field forces compete to produce several of the radiographically observed modifications of structure around tumours. A demonstration follows of how such effects can be produced in vivo in the dog (Chapters XI, XIV) and in man (Chapters XVI and XVII).

The radiographically observed structural changes which have been described around lung masses are caused not only by displacement of water. Very distinct radiating structures, more or less linear, have a different origin. In every living tissue there are various kinds of nonorganized cells such as blood cells and subcellular material such as fragments of dying cells, macromolecules, etc. Electrical and molecular forces influence their movements, qualitative transformations and structural adaptations to their environment.

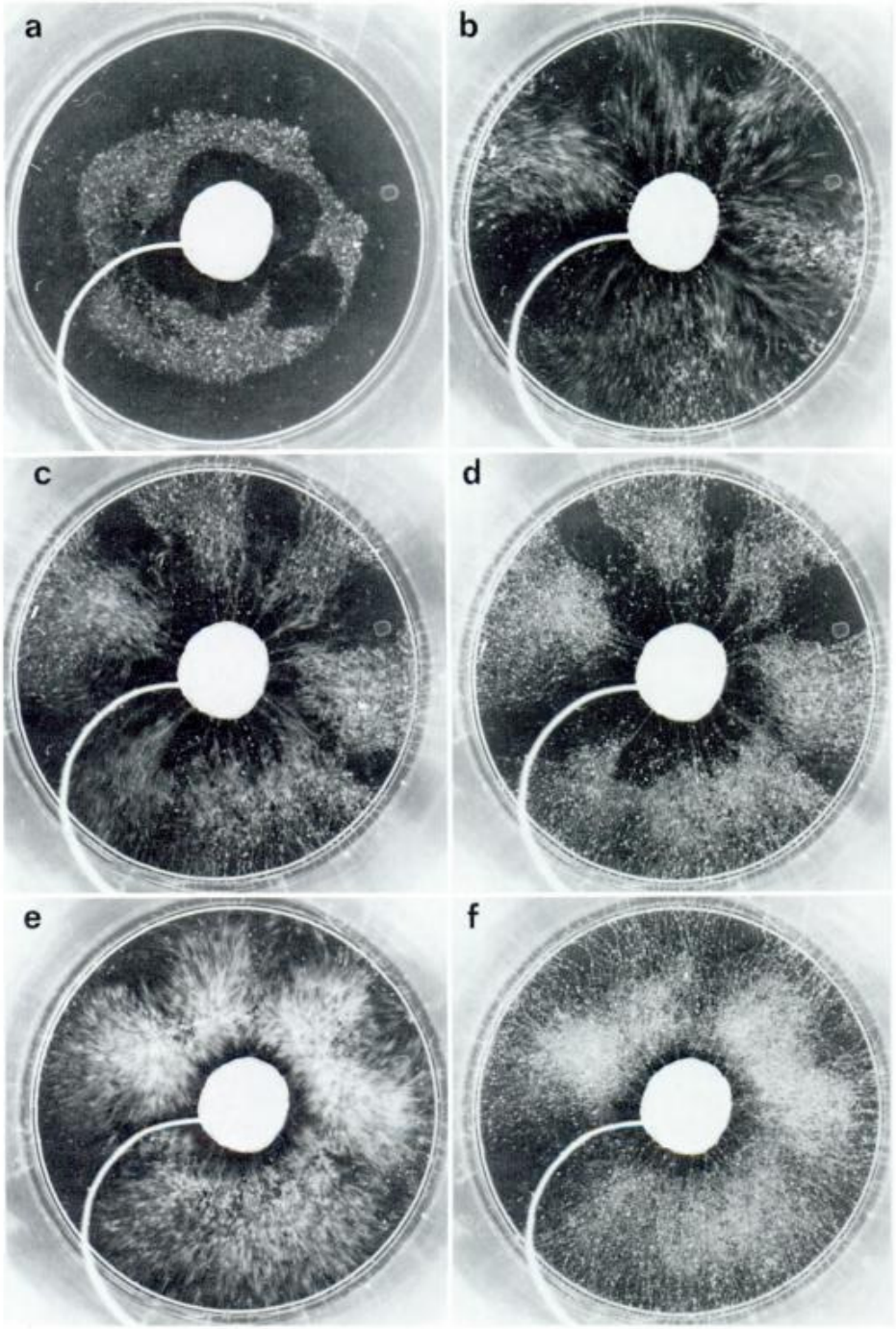

Fig. X: 1. In vitro production of radiating structures, arches and "A" and "B" zones. Light transillumination photographs of a glass jar. An aluminium ball with a slightly irregular surface (small protruding edges) is glued to the bottom of the inside of the jar. The ball and aluminium foil lining the inner surface of the jar are each connected by cables to a DC potential generator. Liquid paraffin is poured into the jar to the level of the middle of the ball. (*a*) Short circuit of terminals. Dielectric semolina grains sifted onto the liquid surface have arranged themselves as a ring between the aluminium terminals. (*b*) Five second exposure during application of 1.5 kV potential. The semolina grains have started to move in the electric field. (*c*) Ten seconds later, the grains are arranged in radiating structures around the ball with preference for the protruding edges (electric field enhancement). (*d*) Ten seconds after *c*. Grain movements have stopped, showing radiating structures, a halo or "A" zone, a higher concentration of grains outside the halo (a "B" zone) and small "arches" forming an "arcade" at the interface between the "A" and "B" zones. Note that each "arch" is supported at the base by two radiating structures. (*e*) More grain sifted *unevenly* on the paraffin (continued 1.5 kV potential between terminals). The local groups of grains within the "B" zone in *d* now act as concentration foci. Molecular forces compete with the electrostatic forces of the applied field and attract the new semolina grains toward the concentration centra. (*f*) 20 seconds after *e*. State of equilibrium. Density of the "B" zone has increased. Size of the "A" zone has decreased.

A. Experimental model: molecular forces and a superimposed electric field combine in vitro to form corona structures

Radiating structures, arches and "A" and "B" zones can be shown in vitro as follows: a piece of aluminium foil was shaped into a small ball, 2.5 cm in diameter. Its surface was made slightly irregular (Fig. X: 1). It was connected to an electric cable and glued to the centre of the bottom of a glass jar, 11 cm in diameter. The inner wall of the jar was covered with a thin aluminium foil connected to another cable. The jar was filled with a layer of liquid paraffin one cm deep. The cable of the aluminium ball was then connected to one terminal of an electric DC generator and the cable from the periphery of the jar to the second terminal. An electric potential ranging between zero and 1.5 kV could be applied between the ball and the periphery. The jar was placed over a light box, permitting transillumination with cold light. A camera was mounted above the jar for photography.

The jar (Fig. X: 1 *a*) is seen from above after both the periphery and the central ball have been grounded. Some semolina grains, which are dielectrics, have been sifted onto the surface of the paraffin. The grains all float on the surface and move together as a ring around the ball (exposure duration, 5 seconds each, Fig. X: 1 *a–f*). When a 1.5 kV positive (or negative) potential is applied between the ball and the periphery, the semolina grains start to move rapidly (Fig. X: 1 *b*). The movements are demonstrated by their motion blur. About 15 and 25 sec after the application of 1.5 kV potential, the grains form radiating structures perpendicular to the ball surface (Fig. X: 1 *c–d*). Varying distances separate the radiating structures of grains. Between them appear small "arches", which together form an "arcade". Each "arch" is supported at its base by radiating structures. The radiating structures and arches combine to give a picture similar to that of the flat, inner surface of a divided citrus fruit (Fig. X: 1 *c–d*). A zone similar to the "A" zone is seen as a "halo" around the ball. The regions with higher concentration of grains correspond to the "B" zone. A new photograph (Fig. X: 1 *e*) was obtained shortly after some more semolina grains had been sifted *unevenly* over the surface. The potential of 1.5 kV was kept unchanged. Nearly all grains are seen to move again to achieve a new "final" equilibrium (Fig. X: 1 *f*).

If the positive 1.5 kV potential on the ball is switched to a 1.5 kV negative potential, the position of the structures does not change, indicating that the switch does not induce any mechanical moment.

The structural developments in this experiment result from interaction between molecular forces of the semolina grains and cellular redistributions caused by the superimposed electric field.

B. Molecular and electrostatic forces in the development of "A" and "B" zones

After the central ball and periphery were given the same ground potential, semolina grains sifted onto the surface of the liquid paraffin moved together to form a ring between the ball and the periphery (Fig. X: 1 *a*). This movement occurs as a result of the forces of internal molecular attraction among grains (see Chapter VIII). Localization of the grains has produced "A" and "B" zones around the ball. Had no metal ball been present in the centre of the jar, the grains would have produced a circular plate in the centre. The presence of the ball in the centre constitutes a "foreign body" in the system, which breaks the internal attraction forces in a radial direction. This vector of radial force therefore tries to make the doughnut-shaped ring as thin as possible. This tendency is counteracted by a vector of circular force. Under these circumstances a "noncorpuscular" "A" zone and a "corpuscular" "B" zone must develop.

From this part of the experiment it is important to realize that structural development creating "A" and "B" zones can occur in ways other than as a result of electroosmotic movement of water (see Chapter IX). Actually, it is not even necessary to assume that the central ball (or in vivo a tumour) is polarized compared to its surroundings.

According to the laws of electrostatics, flux from the surface of a charged body is proportional to its total charge. Moreover, the electric field is a gradient of a potential which declines as the square of the distance from the body. The circulation of the field is zero.

When the central ball and periphery are grounded, the first semolina grains sifted onto the liquid paraffin surface move immediately together to form a ring, as described. When a potential difference is produced between the ball and the periphery of the jar, the location of the grains is disturbed immediately. Under the influence of the created electrostatic field, dipole moments are induced in the grains. These moments orient their long axes along the steepest gradient of the field, i.e., radially in these experiments. The tendency of accumulation will produce one maximum locus

close to the ball. A second maximum locus, but of lower magnitude, is created at the periphery of the jar. Initially, grains close to the charged ball will accelerate toward it, while simultaneously those close to the periphery will move in the opposite direction toward the wall of the jar. A minimum (zero) is present somewhere between the two terminals in the place where the grains had previously formed a "B" zone.

The total electric field is therefore a plus-minus potential gradient with an imaginary circulation of the field equal to zero. In an intermediate zone adjacent to the zero equipotential, where the applied electrostatic field is weak, the attraction (concentration) forces (15) of the grains will be powerful enough to influence their internal arrangements. When the local concentration of grains is high, they will even produce dense groups or nuclei, which then compete with each other and the applied field forces. In this way the irregular "B" zone accumulation is created as seen in Fig. X: 1*f*.

The position of the zero potential in the applied field is governed by the distance between the terminals and the magnitude of the charge per surface unit of the terminals. Because the ball is smaller than the periphery, the zero equipotential will be positioned closer to the periphery than to the ball.

C. Edge enhancement and radiating structures

The basic situation just described is modified by the irregular surface of the ball. Protrusions of edges on the surface of a charged body will always enhance the electric field at such points. This fact was utilized in constructing the artificial "tumour". Small protruding edges, simulating the irregular surface of a tumour, were all over the surface of the crumpled piece of aluminium foil.

A smooth, polished, spherical ball in the centre would present a "smooth", "homogeneous", outwardly decreasing strength of the electric field. No clearly visible, linear arrangement of grains could then develop. The irregular surface of the central ball, however, makes linear developments possible.

Small corpuscles, such as semolina grains, located in the vicinity of the charged central ball will therefore be attracted initially to protruding edges of the ball. Single grains touching the surface of the ball or the peripheral terminal will then rebound (they really bounce back), be reattracted, and so on in an oscillatory way until they are adsorbed at the surface. Eventually, grains near the ball settle on its protruding edges. The external field of the ball now starts at the distal part of these grains. Deposition of grains will concentrate at the edges rather than between protrusions. This concentration of grain at the edges results in a growing accentuation of the edge effect (Fig. X: 2*a*).

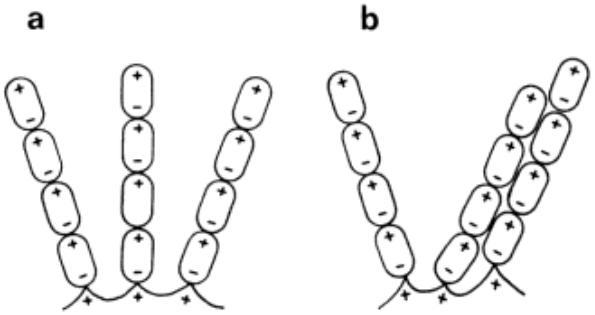

Fig. X: 2. Development of radiating structures. (*a*) Radial apposition of grains by induced dipole moments in dielectric corpuscular elements. Lateral repellent forces stabilize the radiating structures. (*b*) Lateral apposition of grains produces stabilization by both dipole-induced attraction and long-range forces of molecular attraction. Enhancements of the electric field at protruding edges determine the positions of the radiating structures.

D. Stabilizing effects on radiating structures

The apposition of dipole-induced grains into radially directed chains is stabilized by lateral repellent forces between induced equipotential charges of the grains (Fig. X: 2*a*). These repellent forces counteract the forces of attraction. A sidewise stabilizing effect on radiating structures may also be produced by different degrees of sidewise dipole-induced forces of opposite polarity. Long-range molecular attraction forces eventually produce an additional, sidewise mechanical stabilization (Fig. X: 2*b*).

In this way linear structures are produced in the experimental model, forming visible "field lines" or "radiating structures".

E. Development of "arches" and "arcades"

The peripheral ends of the radiating linear structures border the bulk of semolina grains by a series of small "arches", which are convex outward (Fig. X: 3). Adjacent arches originate on each side of the same radiating structure. The individual arches hang together in a row ("arcade").

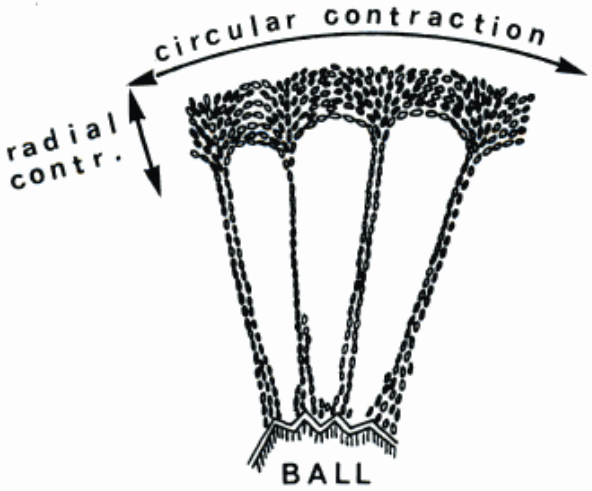

Fig. X:3. Formation of small arches. Edge enhancement of the irregular surface of the central ball creates variations in intensity of the electric field around the ball. Captured semolina grains form radiating structures, developing from the edges, in turn forming supporting pillars for the small arches. Attraction forces among the bulk of grains contribute to forming the arches. A circumferential vector acts as a force of concentration to diminish cross-sectional diameter of the ring of grains around the ball. A radial vector of concentration acts to expand the ring.

The presence of these structures may therefore in part be explained as a result of variations in intensity of the applied field, due to the uneven surface of the central ball. In part the effect also is due to the competitive forces of molecular attraction among semolina grains.

The forces of molecular attraction can be divided into two vectors. (Consider for a moment the experiment as planar, the grains floating in one layer on the liquid paraffin.) One vector (Fig. X: 3) is circular and tries to move the grains closer to the central ball. The other vector is radial, acting to expand the circle. Both vectors contribute to the formation of the arches.

A stabilizing effect for the bulk of semolina grains probably can also be ascribed to the arches and radiating structures. The main bulk of semolina grains contracts as a result of their forces of internal attraction. As grains interact they obtain a position of equilibrium between long-range forces of attraction and short-range forces of repulsion. This equilibrium is modified at the inner edge of the circularly arranged mass of grains by the attraction forces of grains localized at the attachments of the radiating structures.

In this view the circular arrangement of the main bulk of semolina grains, leaving a relatively free zone ("A" zone) around the central ball, may be looked on as a special case of a complete arch, i.e., a ring. The small arches at the inner border of the ring can be regarded as incomplete rings. Their appearance as arches or semicircles depends on summations of molecular and electrostatic forces. Edge enhancements of the central ball not only make the surrounding electrostatic field inhomogeneous, but also initiate the production of radiating structures.

F. Inertness and matrix functions

Interacting molecular and electrostatic forces can readily and efficiently be influenced by matrix structures. The effect of an artificial matrix on corpuscular movements will be illustrated in the following experiment.

A plastic mosquito net stretched over a circular frame was placed on a surface of liquid paraffin in a glass jar, which in turn was placed on top of a light box. An aluminium ball was placed in a hole in the centre of the net. The ball was connected by a wire to a DC generator. The grounded periphery of the jar was connected to the other terminal.

Horse hair in pieces 0.5–1.0 mm long was cut by an electric razor and strewn over the net and liquid surface. The ball was charged to a 0.7 kV potential relative to the periphery. The jar was then subjected to vibrations from a small electric motor. The pieces of horse hair then oriented themselves in a pattern of radiating structures within the mosquito net matrix

Fig. X:4. Effect of a matrix on the development of radiating structures in an electric field. A plastic mosquito net was stretched over a frame and placed on a surface of liquid paraffin. Pieces of horse hair, cut with a razor, were sifted over the surface as a 0.7 kV potential was applied between the central aluminium ball and the periphery. Moments of inertia were overcome by subjecting the jar to vibrations. The hairs then oriented themselves in a radial direction in the squares of the matrix. Dipole induction by the applied electrical field produces this result.

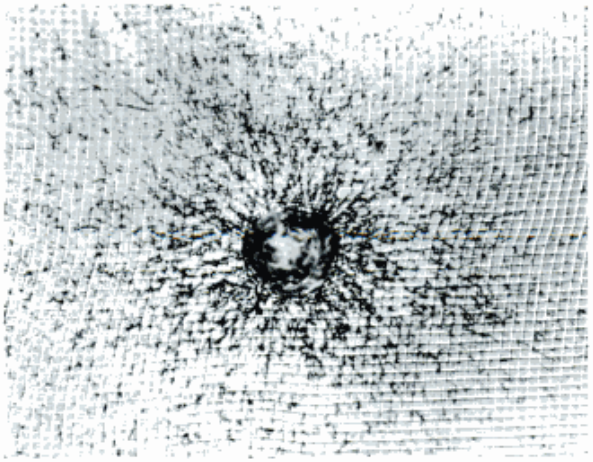

(Fig. X: 4). After the voltage generator was switched off, the pattern remained.

The experiment illustrates the creation of a modified structural pattern by positional change of small pieces of horse hair under the influence of an applied electric field and vibrations. The latter served the purpose of reducing the restrictive effects of the narrow spaces of the matrix and the moment of inertia of the small horse hairs. In vivo, corresponding effects may be induced by different kinds of physicochemical energies, including mechanical effects by tissue matrices and movements of tissues.

G. Energy potential of corpuscular distribution

A "Type I" electroosmosis was suggested in Chapter IX. Its transport energy was explained partly as a transformation of available free energy (e.g., vibrational and rotational movements of the water molecules).

In a static system the degree of randomness of distribution of participating reactants represents one source of free energy (19). In the experiments with semolina grains this energy potential was created by sifting the grains onto the liquid surface. Depending on how evenly or unevenly the grains were distributed, different distributions of energy and patterns of "final" equilibria were created.

As an instance of matrix interference, an aluminium ball was fixed on the bottom of a jar filled with liquid paraffin up to the level of the middle of the ball (Fig. X: 5). No voltage difference was applied between the ball and the periphery of the jar in this experiment. Semolina grains were then sifted as evenly as possible over the liquid surface. After about 10 seconds, the pattern of structure obtained represents a stage "close to equilibrium". The ring of grains around the ball has here the appearance of a net.

Fig. X: 5. A special case of "matrix" interference. Aluminium ball glued to the bottom of a jar and partly surrounded by liquid paraffin. Semolina grains were sifted as evenly as possible over the whole surface. After about 10 seconds and close to a visible cessation of movement of the grains, they present a "net"-like structure (5-second exposure). The fixation of the ball constitutes a special case of matrix interference by restricting free participation of the ball in the reactions. This restriction influences indirectly the development of the surrounding structural pattern.

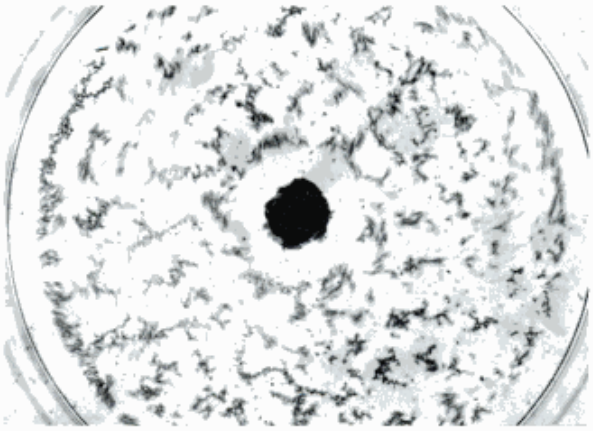

One of the interacting factors, the centrally located metal body, is immobile in this experiment. This fixation constitutes a mechanical restriction on free participation of the ball and can be considered as a special case of matrix interference. Were the ball allowed to float on the surface, a completely different pattern of equilibrium would be created. In this and in similar ways, the spontaneous reactions can be made to undergo different experimental modulations. Depending on the initial energy potential, as determined by the degree of randomness of distribution, the system will produce different patterns of equilibria in its drive to increase entropy. How the interacting forces determine initial motion and final equilibrium in these reactions is a problem closely related to statistical mechanics.

An example of transient, modulated interactions within such a system is shown in Fig. X: 6. Saline solution was poured into a glass jar to a depth of 2 cm. Underneath the jar a layer of air and a thick glass plate served as a heat protective system between the jar and a cold light source, which was used only during short periods of transillumination for photography. Carbon particles covered with dextran (Charcoal radioimmunoassay particles, Schwarz/Mann, Orangeburg, New York) were distributed irregularly on the surface.

The particles of different charcoal preparations behaved differently on the surface of the salt solution. Some sank to the bottom, others floated as rather firm conglomerations. One preparation of particles, however, floated as an evenly dispersed layer, unwetted on the fluid surface. Such a layer of charcoal particles was spread on the liquid, covering about half of the total surface. Energy was then supplied to the system by a brief and rapid stirring. A shellacked aluminium ball, about 1 cm in diameter, was dropped in the middle of the jar. The ball floated easily on the surface of the salt solution. A glass cover was placed on top of the jar to prevent disturbances by external air motion.

Immediately on contact of the ball with the fluid, nearby particles moved away from the ball, creating a "halo" free of particles around the ball. The ball then started to accelerate toward one of the largest concentrations of particles. During this movement a persisting zone free of particles was present in front of the ball, which by its movement divided and stirred the grouped carbon particles. As the ball decelerated, the

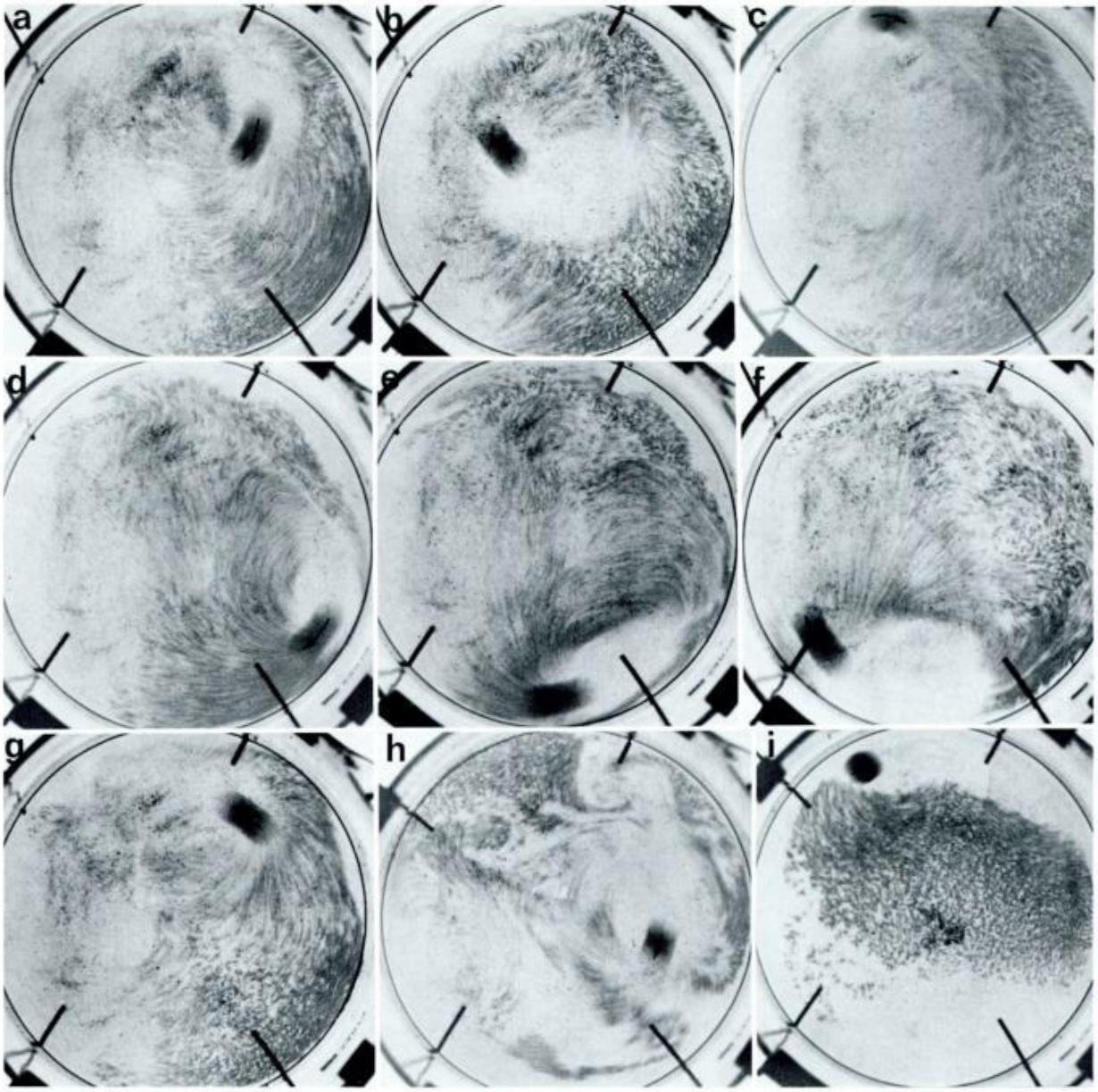

Fig. X:6. Reactants mutually delaying spontaneous equilibrium. Dextran-coated carbon particles floating on the surface of saline solution were stirred briefly, producing an uneven distribution. A shellac-painted, light aluminium ball was dropped in the jar. Motion blur (5-second exposures) indicates movements of the ball's motion. The drive toward equilibrium of the system is disturbed by continuous interactions of the reactants. Areas of high concentration of particles easily attract the ball, which then moves them apart by its moment of inertia. The stirring effect of the ball then creates new attraction centres of concentrated particles, and so on. Reaching equilibrium in the system is thereby considerably delayed. Figs. *a* and *b* show the ball initially near the centre of the jar. Fig. *c* shows the ball bumping against the wall of the jar. Figs. *d–h* show the ball progessively moving in circles at a speed of about one turn per minute. The ball was still moving 17 hours after the start of the experiment, at a rate of one circular turn close to the wall of the jar in 3 minutes (Fig. *i*). Experiments of this kind must be carefully protected from interferences by external forces (temperature, air motion, etc.).

particles formed new concentration centres, one of which was strong enough to attract the ball. The ball again accelerated, split this concentration centre and stirred the particles. In this way, eventual equilibrium of the system is considerably delayed.

Initially, the ball mostly crossed the centre of the jar, tending to split the carbon layer in two parts (Fig. X:6*a*, *b*). The ball accelerated regularly toward the largest group of grains. Sometimes the ball bounced off the wall of the jar (Fig. X:6*c*). Gradually over the next hour a more circular pattern of movements developed (Fig. X:6*d–f*). Splitting of the particulate groups decreased but considerable stirring of the carbon particles remained.

For the next two hours the ball circulated with a speed of about one circular turn per minute. After 17 hours it still was circulating at a speed of about one turn in three minutes. The ball then followed rather closely the periphery of the jar, without touching it. The carbon particles formed a more nearly uniform mass than earlier (Fig. X: 6 *i*).

The gradual extinction of the reaction in this experiment was thus remarkably slow compared with, for instance, the experiment illustrated in Fig. X: 5.

An essential point in experiments of this type is that very small changes may considerably influence the reaction. In this experiment many factors are involved: concentration of the salt water (which influences the water potential), physical characteristics of the ball (size, weight and shape), size and shape of the glass jar in relation to the quantity of reactants, dielectric properties of the materials, the initial distribution of the grains and positioning of the ball, etc.

The seemingly simple experiment illustrated in Fig. X: 6 is in fact very complicated. If we knew the forces, resistances and initial particle distribution we should, at least theoretically, be able to determine particle motion and "final" particle distribution (which has to be defined). This is all in reality an extremely complicated task, even if the basic principles are known. Some general remarks may, however, be offered.

Consider a large number of interacting corpuscles (e.g., semolina grains) and assume that the force between any two of the corpuscles depends only on their distance of separation. As the corpuscles approach each other, long-range attraction forces will cause them to accelerate, overcoming friction and moments of inertia. As the corpuscles become very close, e.g., within a few Å, short-range forces will increase rapidly until the corpuscles repel each other and bounce at the collision.

When many corpuscles (n) interact, the potential energy is the sum of all the energy pairs, which can be represented by a well-known exponential function:

$$n_{(E)} = n_{\text{total}}\, e^{-E/kT}$$

where $e^{-E/kT}$ is the Boltzmann factor, k the Boltzmann constant $= 8.617 \times 10^{-5}$ electron volts/corpuscle, T = absolute temperature and E the energy of each corpuscle (5).

As corpuscles collide, energy is randomly gained or lost by individual molecules. A randomly dispersed large number of corpuscles therefore presents a potential of very complicated patterns of energy exchange, movements and "final" equilibrium.

The situation is further complicated by the presence of one or several bodies which differ from the bulk of reacting elements in size, mass, degree of friction or fixation to the surroundings, electrical properties, temperature, etc. The sum of all the deviating factors of such a body makes it more or less "foreign" to its surroundings. These factors and the degree of initial randomness of corpuscular distribution will influence the "final" spatial state and the time it takes to reach such an equilibrium.

H. Structural effects of molecular concentration forces

To what extent do molecular forces and superimposed electric field forces each contribute to the development of experimental corona structures? What biologic conditions may be so represented?

In the experiment shown in Fig. X: 1 *a*, when both the ball and the periphery of the jar were short circuited, an "A" zone free of semolina grains and a "B" zone with accumulated grains were produced. After the application of 1.5 kV between the ball and the periphery, a new equilibrium was created after some time (Fig. X: 1 *b–f*), showing permanent, radiating structures and small arches and arcades at the interface between the "A" and "B" zones.

At first glance, the creation of a superimposed field may seem to be necessary to create radiating structures and arcades. There is, of course, no doubt that the superimposed strong electric field is highly capable of producing these structures in a short time. However, energy levels of 1.5 kV are biologic rarities. In certain species (Electrophorus, Torpedo, Malopterus, Raja and others), instantaneous levels as high as 600 V are known to be generated (24). Usually, however, potential differences are of the order of 0.1 V in biology (24). An often neglected component is time, which permits various small gradients to produce considerable effects. We will later return to this exceedingly important issue.

As yet, however, we have not sufficiently penetrated the role of concentration-dispersion forces in structural development. In the experiments, let us now consider the events between the sifting of grain onto the liquid surface and the state of equilibrium (Fig. X: 1 *a*) in which the grains form a ring at a distance from the central ball, creating "A" and "B" zones. These events will be illustrated in the following experiment, which slightly modifies the situation in Fig. X: 1 *a* in an informative way.

An "inert" metal, a stainless steel razor blade, was used (Fig. X: 7). Because a meniscus at the liquid-metal interface might disturb particle distribution, a sharply edged object was chosen to minimize possible meniscus effects. The sharp edges were also chosen

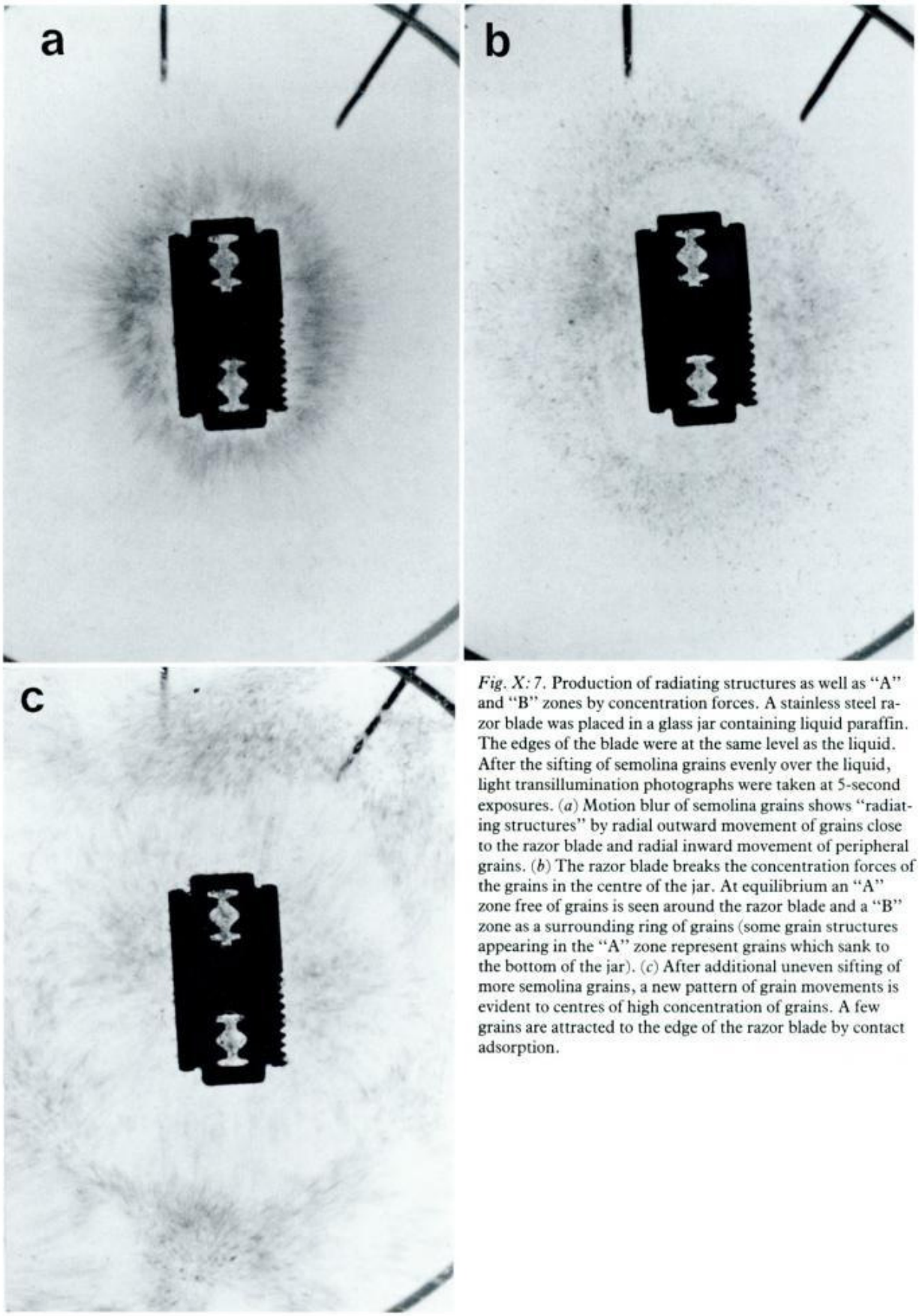

Fig. X:7. Production of radiating structures as well as "A" and "B" zones by concentration forces. A stainless steel razor blade was placed in a glass jar containing liquid paraffin. The edges of the blade were at the same level as the liquid. After the sifting of semolina grains evenly over the liquid, light transillumination photographs were taken at 5-second exposures. (*a*) Motion blur of semolina grains shows "radiating structures" by radial outward movement of grains close to the razor blade and radial inward movement of peripheral grains. (*b*) The razor blade breaks the concentration forces of the grains in the centre of the jar. At equilibrium an "A" zone free of grains is seen around the razor blade and a "B" zone as a surrounding ring of grains (some grain structures appearing in the "A" zone represent grains which sank to the bottom of the jar). (*c*) After additional uneven sifting of more semolina grains, a new pattern of grain movements is evident to centres of high concentration of grains. A few grains are attracted to the edge of the razor blade by contact adsorption.

because they might cause edge enhancement. To vary this effect locally, part of the blade was serrated with a file. The razor blade was fixed to the top of a 2 cm high rubber stopper in the centre of a glass jar, which was then filled with liquid paraffin up to the edges of the razor blade. By inserting wedges of wood under the jar and adjusting the amount of fluid, the surface of the fluid was brought to the horizontal plane of the edges of the blade. When a light beam was shined across the fluid-metal interface, no meniscus could be seen. Semolina grains were then evenly distributed over the liquid surface.

The photographs in Fig. X:7 were made with an exposure time of 5 seconds, shown by motion blur of the initial movements of the distributed grains (Fig. X:7*a*). They created a radiating pattern of movements, some of a distance even greater than the length of the blade. These radiating structures are produced by concentric movements of peripheral grains and centrifugal movements of those grains which were dispersed close to the razor blade. After about 10 seconds (Fig. X:7*b*) nearly all of the grains were concentrated at a certain distance from the edges of the razor blade, showing an equilibrium as a ring. An "A" zone, about one cm wide and almost free of grains, is seen between the inside of the ring and the edges of the blade. A few grains adhere to the edge of the blade (some blurred grains can be seen in the "A" zone, but these are heavy grains which sank initially to the bottom of the jar).

Some more grains were next distributed unevenly on the surface. An uneven pattern of grain movements was then created by concentrations of focally attracting grains (Fig. X:7*c*).

The first part of this experiment illustrates that the formation of a "halo" or "A" zone around the razor blade does not depend on a meniscus forming at the interface between the metallic edge and the fluid. It also does not depend on a superimposed electric field.

The "radiating structures" seen in Fig. X:7*a* are mainly produced by molecular concentration forces of inwardly and outwardly moving grains. The equilibrium distribution of the grains in Fig. X:7*b* shows an influence of the razor blade in the shape of the "A" zone, which roughly follows the shape of the blade. The razor blade acts by breaking up the attraction forces of the grains, which would otherwise form a mass without a hole in the centre. Only minimal distant electrostatic induction can take place through the interpositioned dielectric medium, the liquid paraffin. The NHE potential of +0.25 V of the chrome-steel is very weak in comparison with the long-range attraction forces of the grains. The electric field of the blade influences the surrounding media only within a distance of a few Å. Only a few single grains are therefore seen adsorbed to the edge of the metal. Even the serration of part of the metal edge does not visually alter the relations among the interacting forces.

When the supply of grains was uneven (Fig. X:7*c*), local areas with high concentration of grains competed with each other and the metal. Altered routes of movements of grains can be produced in this way.

In this section we have now seen that radiating structures and "A" and "B" zones can be produced simply by concentration forces without the application of a superimposed electric field.

I. Electrolytic double layers

Molecular concentration forces have been discussed in this chapter only in terms of the behaviour of semolina grains as morphologically visible, corpuscular, dielectric elements. These forces of molecular concentration act between charged or uncharged particles of any size. An example of these forces is the phenomenon known as electrostriction, which gives rise to a decreasing volume when an electrolyte solution becomes increasingly concentrated. Important effects also take place at the interphases between a charged body and charged particles in a solution. In an ionic milieu, electrical charges and concentration forces interact, leading to boundary phenomena which have been well studied in, e.g., colloid chemistry (6, 16, 25, 33).

We will therefore start with a short discussion of the interactions between a metal surface and an electrolyte.

Regardless of how "inert" a metal is made, polarization will occur at its surface when it is immersed in an electrolyte solution or it is implanted in living tissue. This polarization leads to the development of an electrolytic double layer. The structure of the electrolytic double layer was described by Helmholtz, Nernst, Gouy, Chapman, Stern and Freundlich (3, 7, 9, 17, 23, 33). It is now assumed, mainly on the basis of works by Stern (33) and Freundlich (7), that an equilibrium is obtained under the influence of electrostatic forces, concentration forces and specific adsorption forces. The theory further assumes that thermal motion modifies an outer, so-called diffuse, layer. Briefly, this equilibrium is described as follows:

Electrostatic attraction of ions in a solution at the surface of a charged body will create a thin, firm layer (Stern layer, inner Helmholtz layer) of counterions (Fig. X:8). This layer balances electrostatically the surface charge of the body. Just outside the inner firm layer, a mobile layer exists which is called the outer Helmholtz layer. In this layer, ions of the same polarity as those in the firm layer decrease in concentration (charge density) as a function of their distance from the particle. These ions are moving in relation to the

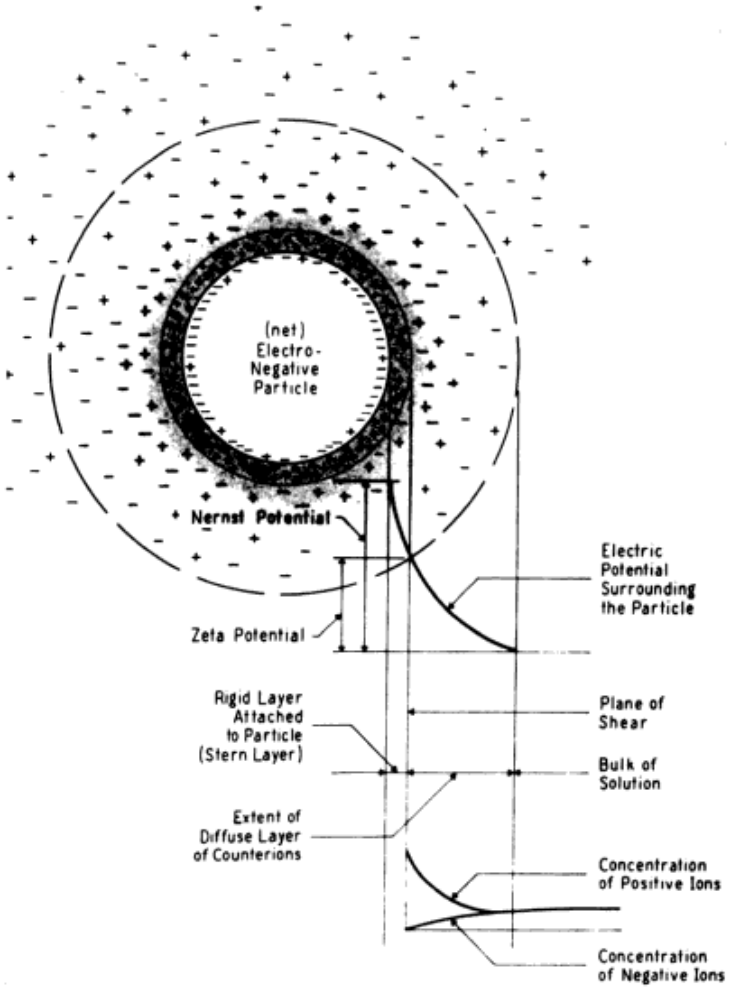

Fig. X:8. The zeta potential of a colloid. A net electronegative particle in a colloid will attract positive ions to its surface, balancing the charge of the particle. The concentration of ions in this firm layer will attract more ions of the same kind. This attraction can be considered as a specific type of adsorption which is stronger than the electrostatic attraction of counterions. In this way a "slipping potential plane" will be created of an outwardly decreasing number of electronegative ions. The potential gradient of the slipping plane constitutes the zeta potential.

firm layer due to their thermal energy. This outer part of the electric double layer is partly mixed with counterions, which increase outwardly in concentration until a zero potential region is reached where positive and negative ions appear in balance with each other. The counterions are, of course, also under the influence of thermal motion. The potential difference between the firm layers and the zero region constitutes the zeta potential of Freundlich (7). The enormous importance of this potential in biology and particularly for the stability of colloids has been stressed particularly by Riddick (25).

The interactions are, however, even more complex than as thus far presented. Consider the following example: A silver plate is placed in a 1.0 M $AgNO_3$ solution. Ag^+ will be attracted to the silver plate, which will become positively charged. NO_3^- will produce a negatively charged layer in the solution outside the positive layer. One may therefore anticipate that *some specific adsorption or attraction forces* exist between Ag and Ag^+, stronger than the electrostatic forces between Ag^+ and NO_3^-. In general, related or identical kinds of matter show some kind of preference for themselves. Thus iron "likes" iron, carbon carbon, etc. Another example of preferential attraction is the tendency of attraction between cations and water molecules, while anions do not present such tendencies. It is very likely that such preferences play a role in the formation of electrolytic double layers.

Fig. X: 8 illustrates how a colloid particle is built up around an electronegative nucleus. The nucleus attracts positive counterions from the surrounding medium to the extent that the particle's negative charge becomes neutralized. The concentration forces of the Stern layer then compete with the solution pressure and with the electrostatic attraction forces of the surrounding electronegative ions. The result is an outwardly decreasing concentration of positive and an inwardly increasing concentration of negative ions. These forces create the potential gradient outside the Stern layer which represents *the zeta potential.*

The spatial distribution of these interphase phenom-

ena is only a few Å, but nevertheless of considerable importance in the physiologic behaviour of cells and membranes.

Consider the present study of transformations of tissue around a centrally necrotizing tumour. The viable periphery constitutes a "tumour barrier", which is a special case of semipermeable "membrane". It is anticipated that its intercellular spaces function as a sieve for large macromolecules, cells, cellular fragments, etc. Such "corpuscular" elements, carrying fixed surplus charges, are available in the surrounding tissues. Factors important to developing transmembranous potential gradients in the cell should therefore also be important for transbarrier potential differences of a necrotizing tumour. Structural changes such as "A" and "B" zones, radiating structures, narrowing and displacement of vessels, arches and arcades are radiographically seen in vivo around lesions in an appearance, strikingly similar to what has been shown experimentally in vitro in this chapter. This remarkable similarity, however, can not be explained only as an effect of molecular forces. Adsorption to interpositioned matrices of a biologic tissue will, of course, interfere with concentration forces of movable particles. We may therefore postulate that other forces also are involved in these structural developments. A superimposed electric field is the only known force which can produce long distance structural effects through an existing tissue matrix. This possibility, however, requires the development of *electric polarization of tissue within a closed electric circuit*. From in vitro studies we are now ready to turn to experiments in vivo.

References

1. Abramson, H. A.: The cataphoretic velocity of mammalian red blood cells. J. Gen. Physiol. 12: 711, 1929.
2. Ambrose, E. J., Easty , D. M., and Jones, P. C. T.: Specific reactions of polyelectrolytes with the surfaces of normal and tumour cells. Brit. J. Cancer 12: 439, 1958.
3. Chapman, D. L.: A contribution to the theory of electrocapillarity. Philosophical Magazine 25: 475, 1913.
4. Coman, D. R.: Mechanisms responsible for the origin and distribution of blood-borne tumour metastases: A review. Cancer Res. 13: 397, 1953.
5. Diem, K., and Lentner, C. (eds.): Scientific tables, 7th ed. Basle, Ciba-Geigy, 1971, p. 228.
6. Donnan, F. G., and Harris, A. B.: Osmotic pressure and conductivity of aqueous solutions of congo-red, and reversible membrane equilibria. J. Chem. Soc. 99: 1554, 1911.
7. Freundlich, H.: Cited by Stern, O. In: Zur Theorie der electrolytischen Doppelschicht. Z. Electrochemie 30: 508, 1924.
8. Gileadi, E., Stanczewski, B., Parmeggiani, A., Lucas, T. R., Rangathan, M., Srinivasan, S., and Sawyer, P. N.: Antithrombogenic characteristics of cathodically polarized copper prostheses. J. Biomed. Mat. Res. 6: 489, 1972.
9. Gouy, M.: Électricité. Sur la constitution de la charge électrique à la surface d'un électrolyte. C.R. Acad. Sci. 149: 654, 1909.
10. Hagmar, B., and Boeryd, B.: Disseminating effect of heparin on experimental tumour metastases. Path. Europ. 4: 274, 1969.
11. Hagmar, B., and Norrby, K.: Evidence for effects of heparin on cell surfaces influencing experimental metastases. Int. J. Cancer 5: 72, 1970.
12. Hagmar, B.: Cell surface charge and metastasis formation. Acta Path. Microbiol. Scand. Sect. A. 80: 357, 1972.
13. Hagmar, B.: Influence of cell changes on the distribution of metastases from intravenously transfused tumor cells. In: Garattini, S., and Franchi, G. (eds.): Chemotherapy of cancer dissemination. New York, Raven Press, 1973, p. 261.
14. Hagmar, B., and Norrby, K.: Influence of cultivation, trypsinization and aggregation on the transplantability of melanoma B16 cells. Int. J. Cancer 11: 663, 1973.
15. Hamaker, H. C.: The London–Van der Waals attraction between spherical particles. Physica 4: 1058, 1937.
16. Haydon, D. A.: The electrical double layer and electrokinetic phenomena. In: Danielli, J. F., Pankhurst, K. G. A., and Riddiford, A. C. (eds.): Recent progress in surface science. New York/London, Academic Press 1: 94, 1964.
17. Helmholtz, H.: Studien über electrische Grenzschichten. Ann. Phys. Chem. 7: 337, 1879.
18. Humphreys, T.: Chemical dissolution and in vitro reconstruction of sponge cell adhesion. Develop. Biol. 8: 27, 1963.
19. Ingram, L. L., and Pardee, A. B.: Free energy and entropy in metabolism. In: Greenberg, D. M. (ed.): Metabolic pathways. 3rd ed., Vol. 1. New York, Academic Press, 1967, p. 2.
20. Marikovsky, Y., and Danon, D.: Electron microscope analysis of young and old red blood cells stained with colloidal iron for surface charge evaluation. J. Cell Biol. 43: 1, 1969.
21. Mehrishi, J. N., and Seaman, G. V. F.: Temperature dependence of the electrophoretic mobility of cells and quartz particles. Biochim. Biophys. Acta 112: 154, 1966.
22. Mehrishi, J. N.: Positively charged amino-groups on the surface of normal and cancer cells. Europ. J. Cancer 6: 127, 1970.
23. Nernst, W.: Die electromotorische Wirksamkeit der Jonen. Z. Physik. Chem. 4: 129, 1889.
24. Ottosson, D.: Nervsystemets fysiologi. Stockholm, Natur och Kultur, 1970.
25. Riddick, T. M.: Control of colloid stability through zeta potential. New York, Zeta-Meter Inc., 1968.
26. Sawyer, P. N. (ed.): Biophysical mechanisms. In: Vascular homeostasis and intravascular thrombosis. New York, Appleton-Century-Crafts, 1965.
27. Seaman, G. V. F., and Heard, D. H.: The surface of the washed human erythrocyte as a polyanion. J. Gen. Physiol. 44: 251, 1960.
28. Seaman, G. V. F., and Vassar, P. S.: Changes in the electrokinetic properties of platelets during their aggregation. Arch. Biochem. Biophys. 117: 10, 1966.
29. Seaman, G. V. F.: Surface potential and platelet aggregation. In: Brinkhous, K. M., et al. (eds.): Platelets, their role in hemostasis. Stuttgart, F. K. Schattauer Verlag, 1967, p. 53.
30. Sheppard, B. L., and French, J. E.: Platelet adhesion in rabbit arteries observed by scanning and transmission electron microscopy. Nature 225: 1054, 1970.
31. Srinivasan, S., and Sawyer, P. N.: In: Silverman, H. T., Miller, I. F., and Salkind, A. J. (eds.): Electrochemical bioscience and bioengineering. Princetown, New Jersey, Electrochemical Society, 1973, p. 17.
32. Srinivasan, S., Cahen, Jr., G. L., and Stoner, E.: Electrochemistry in the biomedical sciences. In: Bloom, H., and Gutmann, F. (eds.): Electrochemistry, the past thirty and the next thirty years. New York, Plenum Press, 1977.
33. Stern, O.: Zur theorie der electrolytischen Doppelschicht. Z. Electrochemie 30: 508, 1924.
34. Weiss, L.: The cell periphery. In: The cell periphery, metastasis and other contact phenomena. Amsterdam, North-Holland Publ. Co., 1967, p. 17.
35. Weiss, L.: Studies on cellular adhesion in tissue culture. Exp. Cell Res. 53: 603, 1968.
36. Weiss, L., Bello, J., and Cudney, T. L.: Positively charged groups at cell surfaces. Internat. J. Cancer 3: 795, 1968.
37. Weiss, L., Zeigel, R., Jang, O. S., and Bross, I. D. J.: Binding of positively charged particles to glutaraldehyde-fixed human erythrocytes. Exp. Cell Res. 70: 57, 1972.

XI.
Structural effects of an artificial tumour in dog lung

A. Experimental studies

To study modification of structure surrounding a tumour in the lung of a living animal, experiments were performed in which an artificial "tumour" was implanted in a dog. The "tumour" was constructed of radiographic density and internal structural appearance sufficient to be identifiable in radiographs (Fig. XI: 1). Two used, small, disc-shaped, mercury batteries were glued together, leaving a millimetre separating their contact surfaces. This separation made it possible to find comparable projections of the "tumour" in radiographs exposed during different examinations. An aluminium foil was wrapped around the glued batteries and shaped into a ball about 1 cm in diameter. The metal foil shielded completely any residual charge of the two batteries and served also as a support for two outer, electrically insulating layers of shellac. The insulating shellac thereby prevented tissue fluids from corroding the aluminium.

A thoracotomy, incising the right 6th intercostal space, was performed on a 40 kg dog. A small incision was then made in the posteromedial part of the apical segment of the right lower lobe. A small haemostat was inserted 2 cm into the lung tissue to create a small pocket, in which the artificial tumour was placed. No obvious bleeding appeared when the pocket was created. The pocket was then closed with two silk sutures. After the chest was surgically closed, air was aspirated from the pleural space. Radiographs taken immediately after surgery revealed no visible structural changes of the lung parenchyma lateral and anterior to the "tumour" (Fig. XI: 1).

When the completely recovered animal was examined 17 days later, chest radiographs showed a radiolucent zone around the "tumour" (Fig. XI: 2 *a*). Lateral to this zone the lung shows a zone of relative increase in x-ray absorption (arrow). The interface between the two zones shows also some arch-like formations. No air or increased amount of fluid was present in the pleural space. For comparison, the appearance of a "halo" around the same "tumour", examined before operation and surrounded by semolina grains on liquid paraffin, is seen in Fig. XI: 2 *b*.

A recording of the *tissue profile of electric potential* was then made in the same dog using Ag–AgCl electrodes and KCl bridges, as previously described (Chapter VI). The potential was recorded between a grounded subcutaneous electrode and the exploring electrode in the lung. Fig. XI: 3 shows the recording of potential as the exploring electrode was moved in

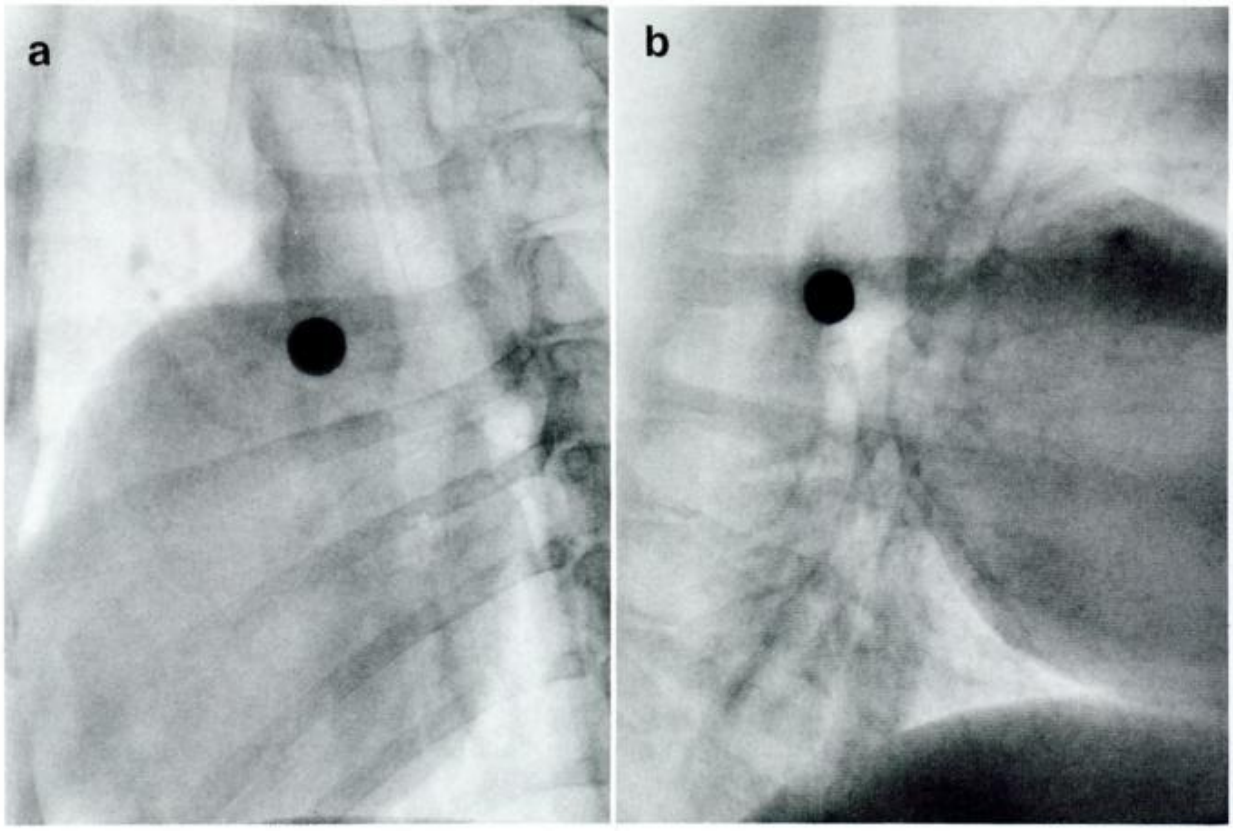

Fig. XI: 1. Effects of implanting an artificial "tumour" in the apical segment of the right lower lobe in a dog are illustrated in Figs. 1–8. The "tumour" consisted of two small mercury batteries glued to each other, 1 mm apart, to make the in vivo orientation of the "tumour" radiographically detectable. The batteries were wrapped in aluminium foil, which served as electric shielding. The surface of the foil was painted with two layers of shellac to prevent corrosion and insulate electrically the "tumour" from the surrounding tissue. (*a*) Anteroposterior and (*b*) lateral radiographs.

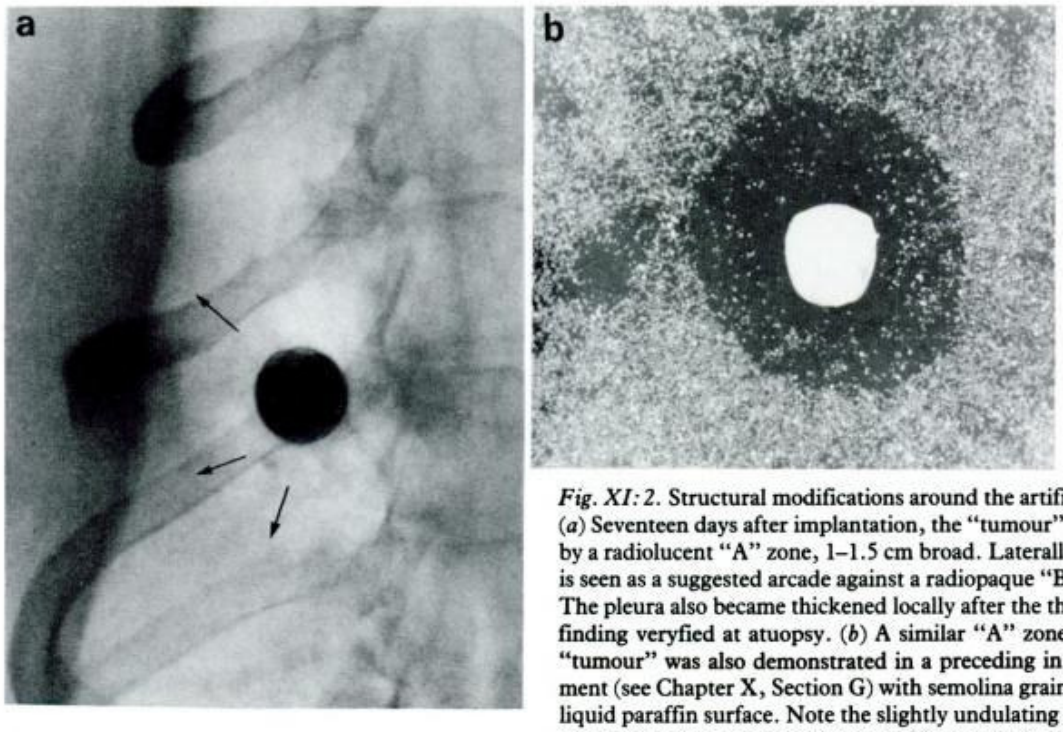

Fig. XI: 2. Structural modifications around the artificial "tumour". (*a*) Seventeen days after implantation, the "tumour" is surrounded by a radiolucent "A" zone, 1–1.5 cm broad. Laterally the interface is seen as a suggested arcade against a radiopaque "B" zone (←). The pleura also became thickened locally after the thoracotomy, a finding veryfied at atuopsy. (*b*) A similar "A" zone around the same "tumour" was also demonstrated in a preceding in vitro experiment (see Chapter X, Section G) with semolina grains sifted on a liquid paraffin surface. Note the slightly undulating edge (arcade) of the semolina grains at this stage of their structuring. Earlier phases of the same process are presented in Fig. XI: 6 *d*, *e* and the earliest phase in Fig. XI: 7 *c*.

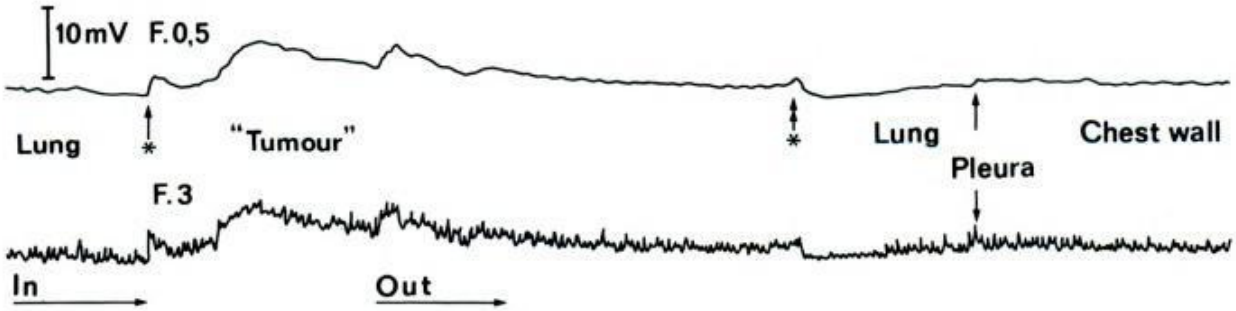

Fig. XI: 3. Two tracings of the profile of electric tissue potential, each with different cut-off filters. Two grounded Ag–AgCl electrodes with KCl bridges were employed, one placed in the subcutis. The exploring electrode was advanced to the artificial "tumour" and then pulled back to the chest wall. The DC tracing shows a positive surface of the "tumour" ($\overset{\uparrow}{*}$) in relation to the surrounding lung. $\overset{\updownarrow}{*}$ indicates the interface between "A" and "B" zones. ↕ indicates pleura. Compare also the measurements of electric potential shown in Figs. VI: 20, 21. The elevation of the electric potential of the "tumour" surface has been interpreted as caused by injured tissue adjacent to the "tumour" as a result of the implantation.

the lung to the "tumour" and then away from it. A potential difference of 8–10 mV was found between the "tumour" surface and surrounding lung on each of many recordings. The profile of tissue potential shows a pattern rather similar to that shown in the patient illustrated in Figs. VI: 20, 21.

The possibility of an air pocket around the "tumour" due to the operative procedure is excluded by these recordings. Fluoroscopic control permitted easy guiding of the electrode to the "tumour". If the probe had entered a pathologic air-filled cavity, an open circuit with high frequency oscillations should have been created. This possible finding never happened in any of the movements of the electrode in different directions to the "tumour".

The electrode caused some small haemorrhages in the lung parenchyma. These changes were seen radiographically as diffuse haziness and focal patchy radiopacities around the "tumour" in the parenchyma of the radiolucent zone (Fig. XI: 4).

The animal was then allowed to live for two more weeks for further studies. At fluoroscopy the "tumour" was seen oscillating with a frequency of about 100/min due to the transmission of cardiovascular movements. Also respiratory movements required some kind of control in order to avoid radiographic motion blur, which threatened to jeopardize the analyses of the pulmonary structures.

Motion blur in the radiographs was therefore controlled by means of intravenous injections of acetylcholine. A single dose of 0.25 mg/kg body weight produced respiratory and cardiac standstill for 4 to 12 seconds, followed by spontaneous recovery (1, 2). Fig. XI: 5 shows an ecg tracing of cardiac arrest induced for 6 seconds after the intravenous injection of 10 mg of acetylcholine in the dog 14 days after the experiment shown in Fig. XI: 3.

Now a *well-defined arcade* is seen at the interface between one radiolucent and one radiopaque zone, which can be identified as *"A" and "B" zones* (Fig. XI: 6 *a*). The orientation of the "tumour" corresponds to that in the radiograph *b* and photograph *c*. For comparison, the preceding study with semolina grains (*d, e*) shows a clear formation of arcades and even some incomplete *radiating structures*.

Fig. XI: 4. After insertion of the electrode, hazy and patchy radiopacities appeared in the "A" zone, interpreted as local accumulation of blood.

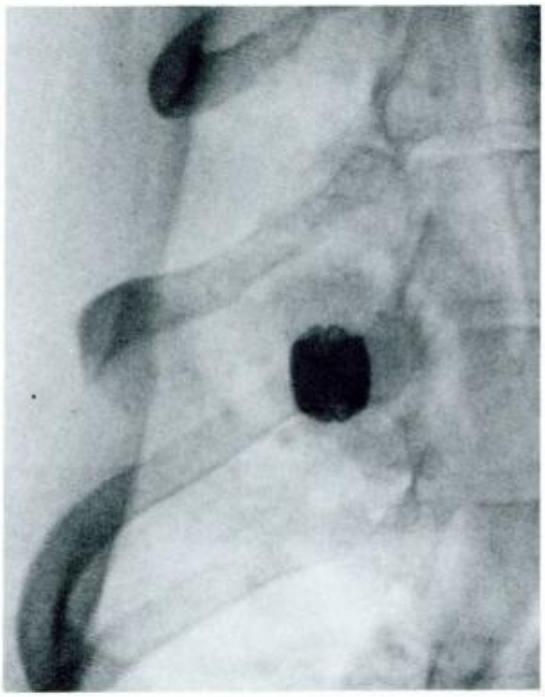

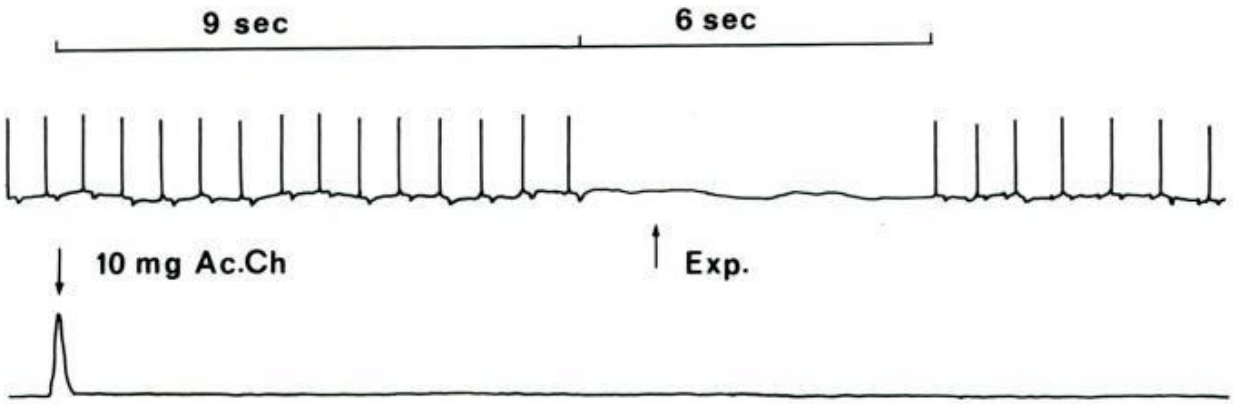

Fig. XI: 5. For optimal radiographic demonstration of structures in the living dog, temporary respiratory and cardiac arrest was induced in this case for 6 seconds, by intravenous injection of acetylcholine (0.25 mg per kilogram body weight). The simultaneous ecg tracing served as indicator of the period of time during which radiographic exposure avoided motion blur.

Fig. XI: 6. Arches and arcades around an artifical tumour in dog lung. Radiographs obtained during induced temporary respiratory and cardiac arrest (Fig. XI: 5). An interface between "A" and "B" zones can be seen as small arches form an arcade (arrowheads). Figs. *b* and *c* show the actual orientation of the artificial tumour. For comparison, a preceding in vitro experiment (*d*, *e*,-see also Figs. XI: 2, 7) with a "tumour" illustrates two phases in the formation of small arches and a circular arcade as an interface between the "A" zone (halo) and the "B" zone (the surrounding grains). Some faint linear radiating structures are also seen.

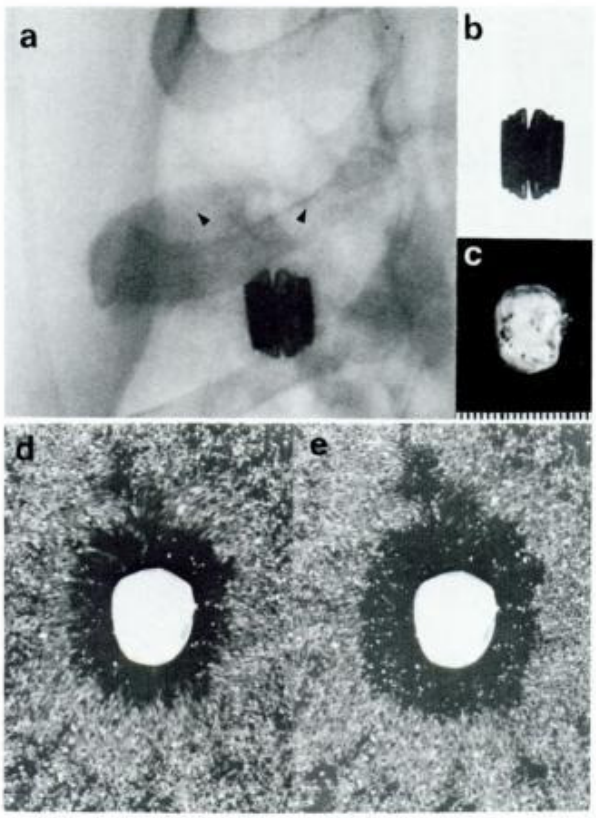

In certain projections (Fig XI: 7 *a*, *b*) some coarse radiating structures could also be seen of the local haemorrhage in the lung tissue produced during the recordings of potential two weeks previously. Some of these coarse structures can be seen extending from the "tumour" in a superolateral direction toward the pleura. Figs. *d* and *e* show the actual orientation of the "tumour" and *c* the similar movements of semolina grains in the preceding in vitro experiment.

Subsequent desanguination and necropsy of the dog showed a local pleural adhesion corresponding to the thoracotomy wound. No pleural or parenchymatous changes were seen corresponding to the "A" zone, as seen radiographically in vivo. After the lungs and the adherent part of the chest wall were removed, focal increased opacities, corresponding to the sites of the bleeding, were seen in radiographs of the slightly inflated lung parenchyma (Fig. XI: 8). No structural arrangements of the type seen in the radiographs in vivo could be found. Histologic examination of the lung revealed only some irregular infiltrations of blood in the lung parenchyma.

B. Discussion

The aluminium "tumour" in the animal experiment was painted with shellac in order to prevent any possible development of corrosive electric currents between the metal and the surrounding tissue. The metal itself, efficiently shielding the internal nucleus, would furthermore be expected to induce only a very weak, static, dipole-induced electric field on the external surface of the shellac. Electrostatic field effects around the tumour can therefore be expected to produce only minimal effects on the surrounding tissue very close to

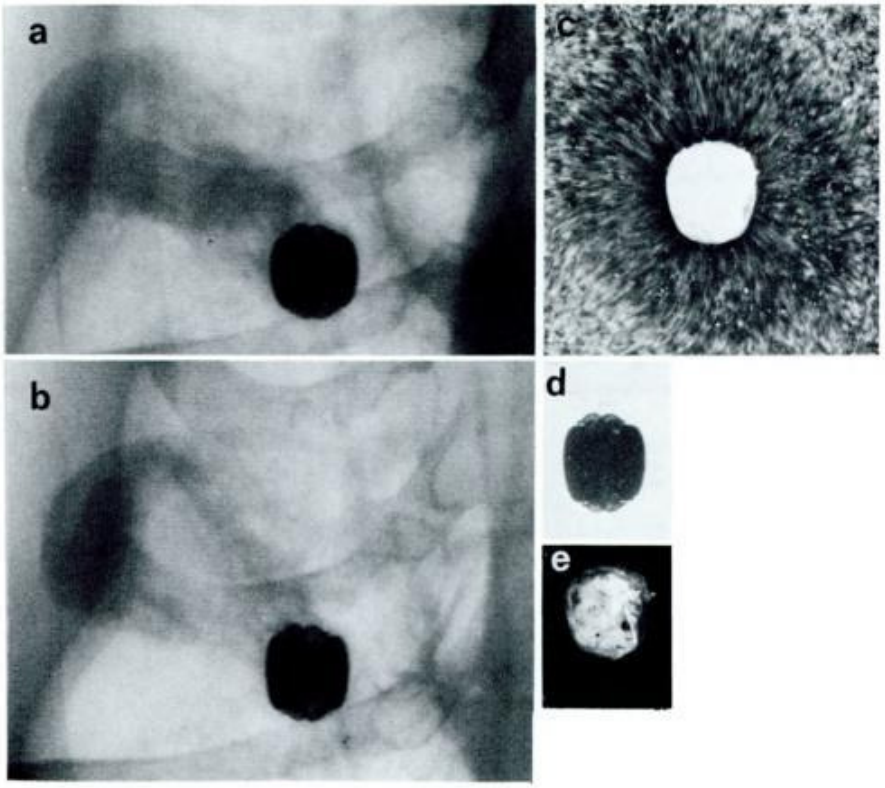

Fig. XI: 7. (*a, b*) Coarse radiating structures, representing rearranged blood, extend superolaterally from the "tumour" surface (two different radiographic projections). (*c*) A similar phase of radial movement of semolina grains is shown in a preceding in vitro experiment (see Figs. XI: 2, 6). The actual orientation of the "tumour" is shown in radiograph *d* and photograph *e*.

the shellac surface. The magnitude of such field effects should correspond to those produced at the edges of the razor blade experiment illustrated in Fig. X: 7. In spite of these precautions, "A" and "B" zones, arches and radiating structures all developed in vivo around this "tumour" in the lung. In the absence of a closed electric circuit (Chapter X), only concentration forces among small particles, e.g., semolina grains, can produce corona structures ("A" and "B" zones, arches and arcades, and even to some extent radiating structures). The hydropenic "A" and hydropic "B" zones caused by water displacement, however, cannot be produced simply by concentration forces. A closed electric circuit, as in the case of electroosmotic water transport (Chapter X), is a necessary requirement.

A closed electric circuit should also be necessary for the development of radiating structures extending two to three cm into a tissue matrix. The blood corpuscles outside the artificial "tumour" presented radiating structures, oriented against the "tumour". This result is an impossibility as a function only of the concentration forces of blood corpuscles. These forces, which were distributed unevenly to one side of the "tumour", should instead create their own concentration centres outside the "tumour". The only known force that can possibly produce radiating structures of the observed extensions and locations in the lung is a closed circuit

Fig. XI: 8. After desanguination of the dog, the lung and adjacent chest wall were removed en bloc. The radiograph shows the specimen after slight inflation of the lung. No structures are evident corresponding to "A" and "B" zones observed in vivo. Some irregular infiltrations around the "tumour" represent local blood. This experiment illustrates some of the critical discrepancies between an examination in vivo and at necropsy. In the lung the distension of the parenchyma in vivo by subatmospheric intrapleural pressures and by vascular perfusion pressures are of particular importance in structural analyses.

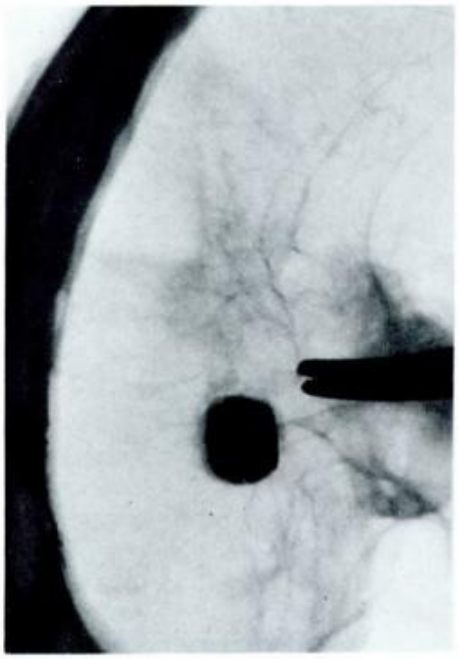

Fig. XI: 9. Postmortem radiograph of slightly inflated lung with multiple metastases from carcinoma of colon. Note faint radiolucent areas ("A" zone) around several tumours.

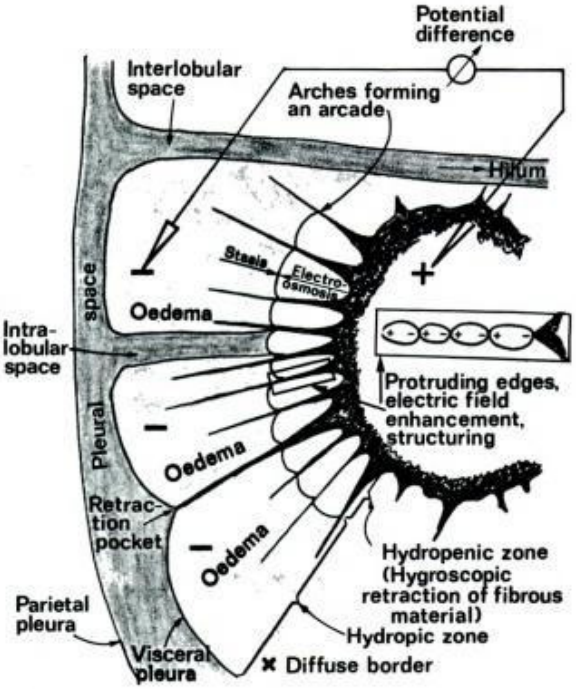

Fig. XI: 10. Factors producing corona structures around a tumour during an electropositive phase. Surrounding tissue is electronegative. Transport of material takes place over a postulated biologically closed electric circuit (BCEC). The tumour blocks the local flow of pleural fluid toward the hilum. Electroosmosis acts to prevent this fluid from moving near the surface of the tumour, giving rise to a perifocal halo, the "A" zone (hydropenic zone). The displaced tissue water produces increased opacity, a "B" zone (hydropic zone). At the interface between these zones hydrostatic turgor pressure and electroosmotic pressure balance each other. Small arches develop at the interface of the "A" and "B" zones. Electric edge enhancement at small protrusions of the tumour surface causes dipole induction in dielectric movable materials, which form radiating structures. Their hygroscopic material contracts in the hydropenic zone, contributing to the shape of the arches and to the production of retraction pockets in the pleura.

electric field. Nevertheless, we have already argued that the "tumour" itself, by virtue of its insulating shellac layer, is excluded from any closed circuit tissue channels. The only remaining possibility to explain the development of the radiating structures must be the creation of tissue injury during the implantation of the tumour. Tissue, including blood, adjacent to the implanted tumour should then have polarized electrochemically against surrounding noninjured tissue. In order to resolve our dilemma we are now forced logically to postulate that a closed electric circuit must exist between surrounding normal tissues and degrading blood and cell material adjacent to the "tumour".

The corona structures observed radiologically around the artificial "tumour" were disarranged or not evident after removal of the lung. This finding is not surprising. As soon as the chest is opened in any animal, the mechanical factors in the lung parenchyma are changed. The effects of subatmospheric pleural pressures, interstitial and intravascular fluid pressures, etc., are changed radically compared to the situation in vivo. These differences appear to explain why radiologic observations in vivo of structures in the lung (produced by fluid and movable cellular elements) are not readily recognized on histologic or radiographic examinations of removed lungs. This situation should hold at least when the pathologic condition has been present for only a relatively short period of biologic time, e.g., 2 weeks. Permanent fixations of the structural arrangement are, however, possible. Thus, faint radiolucent "A" zones are seen in Fig. XI: 9, which is a postmortem radiograph of a slightly inflated lung, containing many small metastases from a carcinoma of the colon (radiograph kindly submitted to the author by Dr. L. Kreel, Northwick Park Hospital, Harrow, Middlesex, England). Similar findings can also be seen in vivo in processes of long duration, e.g., a granuloma (Fig. IV: 1) even after a pneumothorax has been produced.

Factors contributing to the development of corona structures are reviewed in Fig. XI: 10. The tumour in this figure is represented as polarized electropositively in relation to surrounding lung tissue. The existence of a biologically closed electric circuit across polarizing regions of tissue is postulated in Fig. XI: 10. Note that protrusions on the surface of the tumour locally enhance the electric field. Under the combined influence of the forces within an activated closed circuit and of the physicochemical forces of ionic and nonionic movable materials in the tissue matrix, different structures will become produced or modified. One of the most characteristic modifications in the circuit is transport of water. Water moving in a closed electric circuit through a matrix of cotton wool or lung tissue was demonstrated in Chapter IX. Cotton wool and lung each carry a surplus of fixed electronegative charges, so water moves from anode to cathode. Such move-

ment will produce a hydropenic (radiolucent) "A" zone around an anodic tumour. Movement of water will also produce a hydropic (radiopaque) "B" zone outside the "A" zone when water moves against a hydrostatic pressure. Equilibrium is then created between the two opposing forces, giving rise to an interface, seen as a row of arches forming an arcade. The actual structural changes seen in radiographs are, however, created not only by water but also by movement and reorientation of charged or dielectric corpuscular elements, i.e., cells, cellular debris, macromolecules and electrolytes. Concentration forces also contribute to the development of radiating structures and arches (as well as nonhydropenic and nonhydropic "A" and "B" zones, respectively), as shown in vivo in this chapter. The radiating structures around tumours consist mainly of fibrous, partly hygroscopic, partly nonhygroscopic material. Within the hydropenic zone a local scar-shrinking effect may occur. Such a shrinking of a well-developed radiating structure extending to nearby pleura should then be able to produce a retraction pocket (see also Chapters III and XVI).

At this juncture it must be evident to the reader that for all components of corona structures to develop, particularly over distances of several centimetres, electric forces acting over closed circuits are a prerequisite. We have now arrived at a point central to the study of tissue transformation by local electrochemical polarizations between tissues. The introduction of this concept will make it easier to understand not only the corona structures but also phenomena connected with tissue healing and tissue development. In the next two chapters a mechanism will be described which permits extensive transformations of tissue over long periods of time at low voltage gradients. This mechanism will now be described as the biologically closed electric circuit (BCEC).

References

1. Arnulf, G., and Chacornac, R.: L'artériographie méthodique des artères coronaires grâce à l'utilization de l'acétylcholine; données expérimentales et cliniques. Lyon Chir. 54: 2121, 1958.
2. Törnell, G., and Nordenström, B.: Unpublished data, 1962.

XII.
Biologically closed electric circuits (BCEC)

When an electrolyte is brought in contact with a metal, an electric double layer will develop at their interface (26, 27). This interaction can be regarded as a structuring process, usually in a zone no thicker than a few Å. This restricted spatial extension of the electric double layer and of its surrounding diffuse layer, indicates that further explanation is required for the uneven distribution of material sometimes seen radiographically (Fig. XII: 1) within one to two millimetres adjacent to metallic fixation devices in tissue. Corrosion is one factor to consider. Associated events are always connected with electric transports over closed circuits between relatively anodic and cathodic sites. In tissue, such mechanisms should involve electric transports over the metal and conducting tissue channels and also include at least one anodic and one cathodic site of reaction. Multiple reaction sites of different kinds and their corresponding conducting channels will be seen shortly in a variety of combinations.

Corrosion of metallic devices in vivo will be described in this chapter as a radiographically detectable expression of closed electric circuits. A preliminary description will be offered of a dynamic interaction between tissue and metal during corrosion in vivo. A description will then follow of a mechanism in tissue which appears to be of importance for understanding the development of normal and pathologic structures in tissue. The mechanism takes place over what will be called biologically closed electric circuits (BCEC).

A. Corrosion in vivo

Corrosion is often encountered in vivo around metallic surgical implants. Often misinterpreted radiologically, the process is called "bone resorption" because the implant appears as if it were resting in a bony cavity containing a narrow (1–3 mm) space between the implant and a radiopaque line seemingly defining a cavitary wall (Fig. XII: 1).

The differential diagnosis between a real cavity in bone surrounding a loose implant and corrosion around a well-fixed implant is a very important clinical problem which has been largely ignored. A discussion of some of these problems at current levels of understanding has been presented by Frank and Zitter (18).

The electrochemical stability of a metal is given by its normal potential, related to the standard normal hydrogen electrode (NHE). The normal potentials of

Table XII: 1. *Normal potentials of metals and metal-blood potentials in relation to normal hydrogen electrode (NHE)*

Metal	Metal/Metal ion standard electrode potential (V, NHE)	Resting potential at metal-blood interface (V, NHE)
Mg	−2.375	−1.360
Al	−1.670	−0.750
Cd	−0.402	−0.050
Cu	+0.346	+0.025
Ni	−0.230	+0.029
Au	+1.420	+0.120
Pt	+1.200	+0.125

some metal-metal ion combinations and some metal-blood potentials are shown in Table XII: 1 (68).

Corrosion of a metal implant means that an electrochemical interaction with electrolytes in the surrounding tissue partially destroys the metal. Redox reactions take place, in which oxidation means delivery of electrons to the metal and reduction means acceptance of electrons by the tissue from the metal. The process of corrosion requires an anode, a cathode, an electrolyte and at least one closed circuit between anode and cathode.

Different "inert" metallic prostheses contain local differences in quality of the metal. Such local changes in metal, for instance, can be created by a hammer-stroke during surgery, producing a local "injury potential" in the metal. The varying potentials of the connected internal regions of a metallic prosthesis constitute its relatively anodic and cathodic parts. Surrounding electrolytes complete the electric circuit. Current will flow through such a galvanic "battery". The anodic (negative) or "active" part of the metal is the donor of electrons and becomes corroded (oxidized). The cathodic (positive) or "passive" (noble) parts of the metal form the electron acceptor and is the site of reduction. The cathodes do not corrode. Chemical analyses of bone tissue close to metal implants have been performed by Ferguson, Laing and Hodge (16), who found metal in the tissue in concentrations significantly higher than expected, despite the supposedly "noncorrosive" character of the metallic implant.

The dissolution of metal takes place at the anode:

e.g., $\text{Metal} \rightleftarrows \text{Metal}^{2+} + 2e^{-}$.

Metal ions will then either diffuse in the solution or combine with hydroxyl ions as a precipitate:

$\text{Metal}^{2+} + 2\text{OH}^{-} \rightleftarrows \text{Metal(OH)}_2$.

The solubility of hydroxides of different metals varies with ionic concentrations and values of pH in the tissue fluid (Fig. XII: 2) (65).

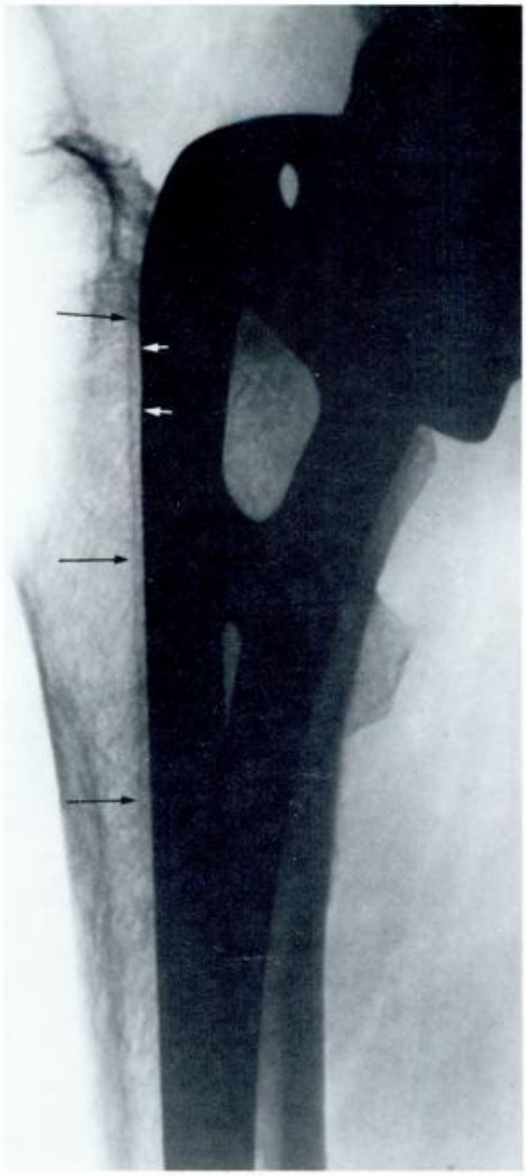

Fig. XII: 1. "Uncomplicated corrosion" between metal and bone, radiographically seen at the lateral aspect of a metal prosthetic implant in the hip. A radiopaque metal deposit lies parallel and 1–2 mm lateral to the shaft of the prosthesis (black arrows). The deposit appears farthest from the bone opposite a slightly irregular dent (white arrows). The distance between the surface of the metal and the metallic deposit in the bone is greatest in this region. Note that no "line" is present opposite the distal part of the prosthesis.

Corrosion requires a complete electric circuit. The corroded part of the metal (under the metal deposit) constitutes the anode, the noncorroded part the cathode. Tissue electrolytes represent the "external" ionic part of the electric circuit, the metal between the anode and cathode the electronic "internal" part of the circuit.

When resistivity of the "external" conducting medium is high, corrosion will usually be enhanced close to the transition zone between the anodic and cathodic parts of the metal. So-called general corrosion takes place at multiple microscopic anodic and cathodic sites, which even change their polarity in time. This effect will also lead to corrosion over a macroscopic surface.

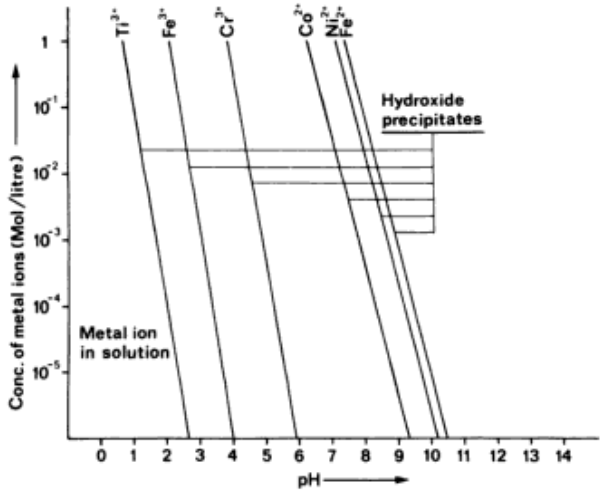

Fig. XII: 2. Solubilities of some metal hydroxides at different values of pH and ionic concentrations.

Tissue pH does vary to some extent, within physiological limits. For instance, arterial plasma is slightly more alkaline than arterial whole blood during physical exercise. When acid-base equilibrium is acutely disturbed, pH may fluctuate, during short periods, between 6.8 and 7.8 (18). Corrosion-dissolved metal in tissue is partly engulfed by histiocytes, macrophages and leukocytes and is eventually transported away or encapsulated in fibrous tissue. Metal ions may also be resorbed and produce general or local toxic effects. Local accumulation of metal precipitates is also considered to lead to aseptic necrosis (18).

Oxygen around the cathode is reduced, as follows:

$$\tfrac{1}{2}O_2 + H_2O + 2e^- \rightleftarrows 2OH^-.$$

The above explanation for in vivo corrosion is generally accepted, but in the author's opinion, incomplete in two respects: the sites of the driving force of the reaction and the transport channels.

It is likely that corrosion often originates from the differences between relatively anodic and cathodic parts of an implant, an internal phenomenon usually found in such devices. This process will here be called "uncomplicated" corrosion.

Regardless of local differences in quality of the implanted metal, local metabolic changes in the tissue in the vicinity of the implant also are a source of local electrochemical differences. Even an inserted nail should locally stress bone and theoretically produce local polarization as a piezoelectric effect. Pathologic changes such as local bleeding, aseptic necrosis or infection may create considerable differences of electrochemical potential between local regions in tissue and the metal. Such "polarizing" foci are of considerable clinical importance. They lead to what is here called "complicated corrosion", indicating the presence of a complicating reaction in the tissue.

Another source of energy can be found in the metabolic fluctuations of the physicochemical potential of the surrounding normal tissue. This source will influence both complicated as well as uncomplicated corrosion.

1. Ordinary "uncomplicated corrosion"

This type of corrosion is synonymous with the classical concept of corrosion, based on a closed circuit reaction between relatively anodic and cathodic parts of a metal in contact with an electrolyte.

A radiograph of a stainless steel prosthesis in the right femur 12 months after surgery is shown in Fig. XII: 1. The metal of this prosthesis is made of a material "as inert as possible", as are other similar fixation devices of metal. The prosthesis consists of iron combined with chromium, nickel and molybdenum (Table XII: 2 shows the complex composition of two types of common metal implants used in bone surgery).

The prosthesis was inserted into the femur without the use of any cement. A thin, slightly irregular "line", half a mm thick and about 10 cm long, is seen along the upper straight lateral part of the implant. The distal part of the line gradually disappears, so that no line is seen at the lower lateral part of the metal. The greatest width between the line and the implant

Table XII: 2. *Composition of materials*

Stainless Steel Type 316 S12	
Carbon	0.03% Maximum
Silicon	0.20 to 1.00%
Manganese	0.50 to 2.00%
Nickel	11.00 to 14.00%
Chromium	16.50 to 18.50%
Molybdenum	2.25 to 3.00%
Sulphur	0.03% Maximum
Phosphorus	0.04% Maximum
Iron	Balance
Cobalt Chrome Alloy	
Chromium	27.00 to 30.00%
Nickel	2.50% Maximum
Molybdenum	5.00 to 7.00%
Carbon	0.20 to 0.35%
Iron	0.75% Maximum
Silicon	1.00% Maximum
Manganese	1.00% Maximum
Cobalt	Balance

The table shown above is from British Standard 3531: 1968, "Metal Implants and Tools used in Bone Surgery".

corresponds to a shallow dent in the metal over a distance of about 2 cm.

A radiolucent zone around prosthetic metal in the skeleton often indicates that the metal is movable and lying more or less free in a cavity or bony canal. The implant shown in Fig. XII: 1, however, is not movable. The line which gives the impression of a radiolucent zone close to the metal is only a local change next to the superolateral two-thirds of the implant. The local deposition of metal corresponds only to a certain region of the metal without other signs of local changes in the bone. The metal may have its most intense anodic focus in the shallow dent in the metal, corresponding to the place where the radiopaque line in the bone is thickest and most distant from the metal surface.

The mechanism for this process of "uncomplicated corrosion" is suggested in Fig. XII: 3. The metal has in this instance one anodic and one cathodic part and is surrounded by the tissue and its electrolytes. The anodic part is electronegative due to accumulation of electrons in the metal from dissolving iron. Secondarily, electrons flow in the metal to the cathode. In the meantime, anions such as $(OH)^-$ in the electrolyte migrate to the anodic part of the metal.

The ionized iron then combines with hydroxyl ions to produce $Fe(OH)_2$ (and later on, probably $Fe_2O_3 \cdot nH_2O$), which forms the radiographic line close to the metal:

$$Fe \rightarrow Fe^{++}+2e^-,$$
$$Fe^{++}+2H_2O \rightarrow Fe(OH)_2+2H^+.$$

At the cathode, oxygen will be reduced and hydroxyl ions liberated:

$$O_2+2H_2O+4e^- \rightarrow 4(OH)^-.$$

The hydroxyl ions will then move in the tissue fluid toward the anode. They will, however, never reach the anode, as instead they combine with H^+ ions, which are moving toward the cathode, to become water.

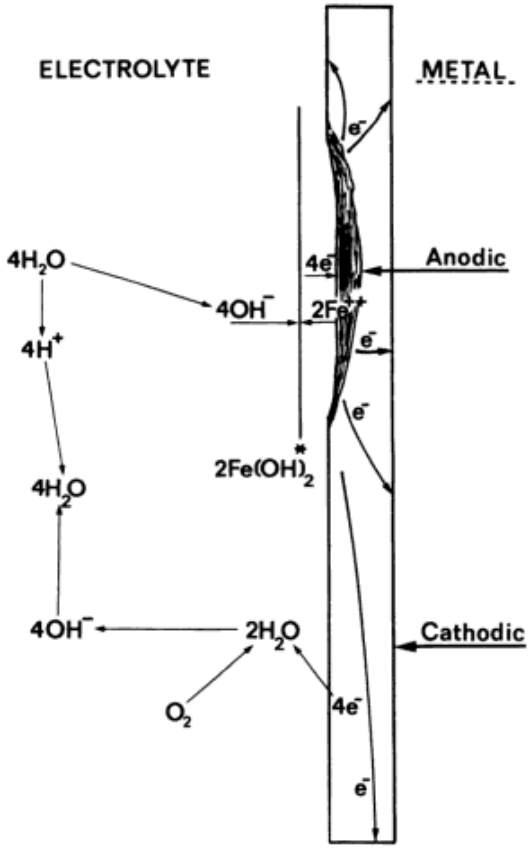

Fig. XII: 3. Schematic explanation of "uncomplicated corrosion". The driving force is found between relatively anodic and cathodic regions in the metal. The dissolved iron in the anodic region recombines with hydroxyl ions to form $Fe(OH)_2$ as a "line" (*) adjacent to the metal. No corrosion takes place in the cathodic, electron-donating metal.

2. Corrosion influenced by BCEC: "complicated corrosion"

The term "complicated corrosion" is introduced to indicate that the driving force of the corrosive process originates in pathologic tissue locally polarizing adjacent to a metal implant. Polarizing sites in the metal itself may then be absent or minimal.

Fig. XII: 4 illustrates a fixation of a hip fracture, in which corrosion probably originates from local electrochemical differences in different parts of bone surrounding the metal. Fig. XII: 4 *a* shows two screws (von Bahr) after surgical repair of a fracture of the medial aspect of the femoral neck. The screws are correctly aligned. The round margin of the head of the femur shows a smooth cortical contour. Trabeculae appear normal. Two years later, two different views (Fig. XII: 4 *b, c*) exposed during the same examination show a radiopaque line in bone around the more cranial screw in portions distal to the head. No corresponding radiopaque line is seen in bone along the other screws. Fig. XII: 4 *b* and *c* also show that the cranial screw is situated close to a fracture line (arrow) dividing the femoral head into two parts. The cranial fragment (left) shows an irregular bone-cartilage contour and irregularly calcified and decalcified regions, as in developing necrosis. The inferior part (right) of the femoral head shows normal bone, including the bone-cartilage contour. This patient complained of some pain in the hip, but no clinical signs of local infection were present. The presence of a radiopaque line in bone along only one of the two hip screws and outside

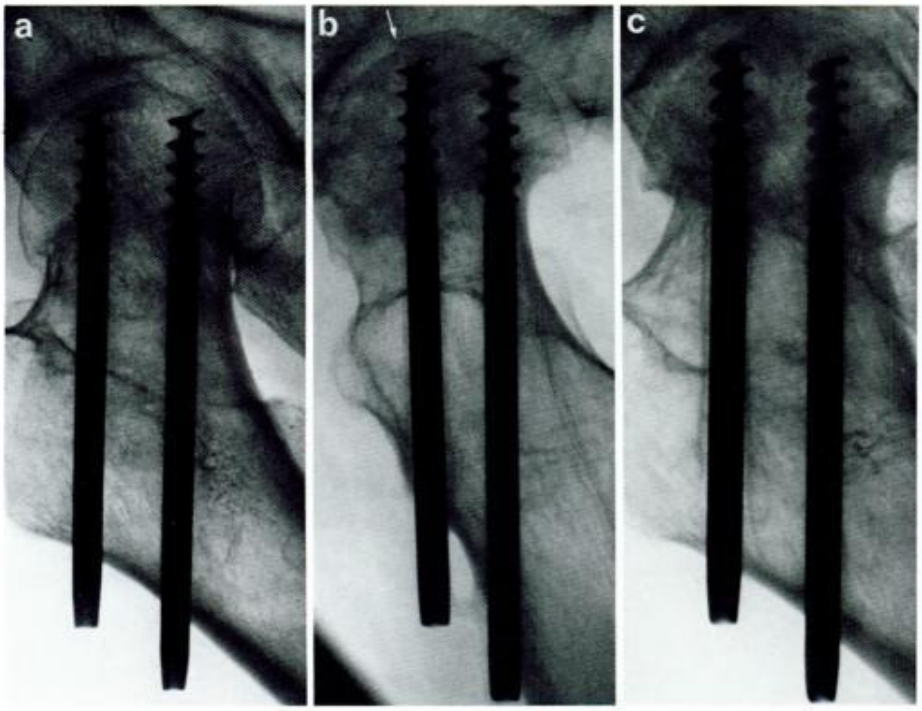

Fig. XII:4. "Complicated corrosion". Radiographic appearance of a human hip after surgery. (*a*) Two screws in position after operation for fracture of the femoral neck. Note normal bony trabeculae and the cortical margin of the femoral head. (*b* and *c*) Two projections of the hip two years after operation. The femoral head is split in two (cortical fracture, arrow). The cranial (left) part is necrotic. The bone-cartilage interface is irregular and bony structures are blurred and irregular. A metal deposit distal to the region of necrosis surrounds the cranial screw. No metal deposit is seen around the part of the screw which is in necrotic bone. No metallic line is present adjacent to the other screw.

Evidence in the text suggests that injured tissue in the necrotic part of the femoral head creates an electrochemical polarization ("injury potential") in relation to the metal and the normal tissue in the trochanter and neck. The screw constitutes one branch and the intercellular tissue fluid the other branch of an electrically closed circuit. Another closed electric circuit, coupled in parallel, is created by a vascular-interstitial connection between the injured and normal tissue (see also Fig. XII: 8).

the necrotizing fragment in the femoral head here suggests the development of "complicated corrosion". Fig. XII: 5 tentatively describes this corrosion process.

The fundamental characteristic of "complicated corrosion" is that the driving potential emerges between, e.g., a metal and a dynamically changing local process in tissue, from which catabolic energy is liberated. Such a process here localized to the lateral side of the femoral head (Tissue I) may be a result of hypoxic degradation of various components of injured bone tissue and accumulated blood. An adjacent prosthesis which consists of different metals may further influence the catabolic reactions by the various catalytic properties of the metals. The multitude of reactions involved in these processes are difficult to define for various reasons. Reactants and reaction products can, e.g., be anticipated to be exposed to modulations by selective transports within closed electric circuits. Some of the possible events in complicated corrosion will nevertheless be briefly discussed.

During an early phase of hypoxic degradation the tissue will become acid, mainly as a result of hypoxic degradation of glucose into lactic acid (38). Anaerobic glycolysis will further increase the amount of ATP which, by hypoxic hydrolysis, contributes to tissue acidity:

$$ATP + H_2O \rightarrow ADP + H^+ + energy + phosphate.$$

In previously reported experiments on spontaneous degradation of blood, an initial decrease of pH was observed (page 70). It has further been suggested that the first biochemical manifestation of tissue injury is a loss of ATP (37). Irrespective of its mode of development the initial acidity may explain the common radiologic observation of calciolytic areas in recently injured bone. It should be noted, however, that hydrolysis of ATP is used in Fig. XII: 5 only as one example of possible reactions which may contribute to make Tissue I initially acid and as one reaction capable to deliver phosphate ions, a necessary component for the eventual precipitation of apatite. Other sources for

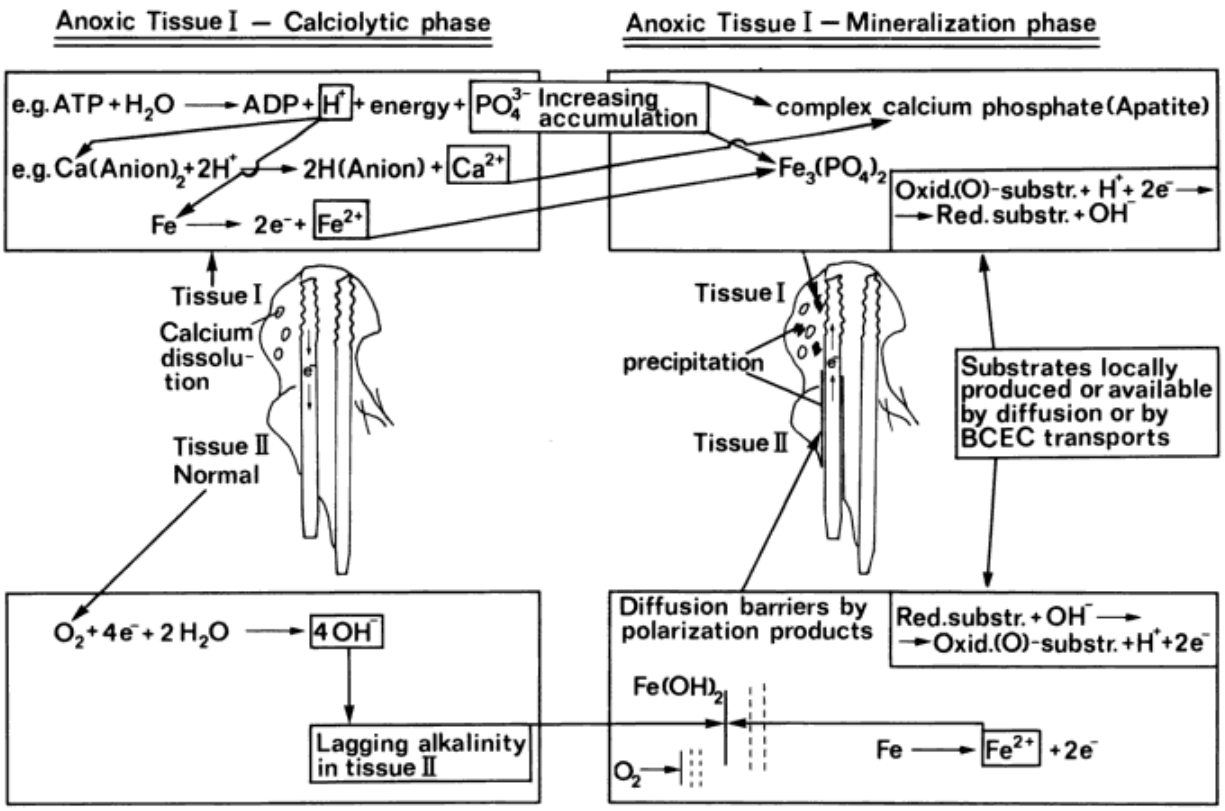

Fig. XII: 5. "Complicated corrosion", schematic illustration. No initially anodic and cathodic regions of metal are necessary in this type of corrosion. In time, the chemical activity of tissue fluids and tissue currents may secondarily polarize the metal. Injury to tissue, e.g., local necrosis or infection, releases electrochemical energy, which supplies the driving force. Acidity, produced in the "calciolytic phase" by the degrading Tissue I, dissolves calcium and iron ions, which then precipitate in the alkaline "mineralization phase" as complex calcium phosphate (apatite) and as $Fe_3(PO_4)_2$. Local sites of decalcification and calcium deposition are produced in Tissue I in this way. The precipitation "line" is produced as $Fe(OH)_2$ (and later, as $Fe_2O_3 \cdot nH_2O$) when there is a net dissolution of metallic iron in Tissue II. BCEC = biologically closed electric circuits.

production of phosphate ions as phosphocreatin, phosphoarginine and polymetaphosphate are even more likely to supply the tissue with substantial amounts of phosphate for a subsequent precipitation of apatite.

The initial acidic (calciolytic) phase of complicated corrosion can not lead to the development of a precipitation "line" as in uncomplicated corrosion because of extensive acidity in Tissue I. The decalcified areas further make the entire matrix irregular which should counteract the development of a regular "line" of precipitated $Fe(OH)_2$ and later Fe_2O_3. As long as the tissue is acid, calcium ions and dissolved ions from the implant and protons will spread by diffusion (and migration in the closed circuit) in the injured tissue:

e.g., $Ca(Anion)_2 + 2H^+ \rightarrow 2H(Anion) + Ca^{2+}$
$Fe \rightarrow Fe^{2+} + 2e^-$.

Because circulation is impaired to the damaged tissue (which in itself is likely to induce an hypoxic injury reaction), the surrounding tissue fluid is restricted in its ability to buffer the local reactions. Protons will, however, diffuse and migrate more rapidly than phosphate ions and eventually combine with hydroxyl ions, diffusing from Tissue II, to form water. Such consumption of protons may lead to an increasing accumulation of phosphate ions. During these events, electrons are produced in the metal adjacent to Tissue I, i.e., this part of the screw becomes electronegative. Electrons flow then to the relatively electropositive metal next to Tissue II. The metal then delivers electrons to the tissue oxygen. Tissue II is not hypoxic, so oxygen is available:

$O_2 + 2H_2O + 4e^- \rightarrow 4(OH)^-$.

Because the circulation of blood is relatively intact in Tissue II, the alkaline reaction there will, however, be counteracted to some extent by the buffering and circulation of tissue fluids. During a late stage of the development of complicated corrosion, the morphologic appearance of the tissues (Fig. XII: 4 *b, c*) gives a

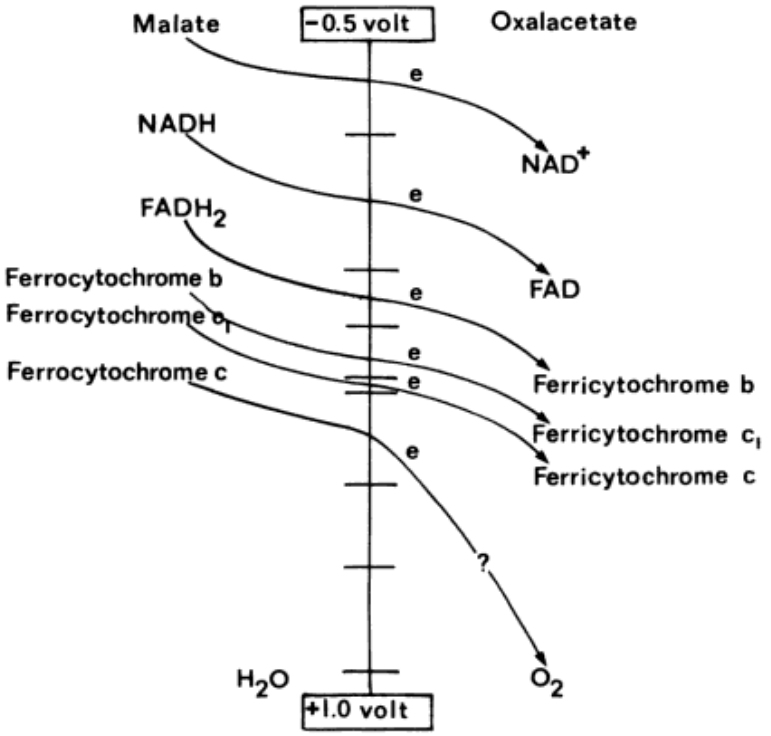

Fig. XII: 6. Sequence of reaction steps in terminal oxidation of cellular respiration (from Jordan).

hint to a drastic change of the tissue reactions: The anoxic Tissue I enters a phase of mineralization with irregular calcifications and the well oxygenized Tissue II shows a "line" of precipitation adjacent to the metal. These changes indicate that a reversal of flow of current must have taken place in the closed circuit.

The biochemical reactions leading to these changes seem to be at least as complicated as those of the calciolytic phase. Associated events will only be preliminary discussed as follows:

The increasing accumulation of phosphate ions in Tissue I drives it toward the mineralization phase (Fig. XII: 5, right side). The question now arises whether this suggested relative accumulation of phosphate ions in Tissue I is sufficient to reverse the overall electric polarity of the system. This question is critical: a change of polarity of the injured tissue must be a prerequisite for an inflow of cations such as calcium and magnesium. It is, however, from an energetic point of view unlikely that proton loss and phosphate accumulation alone should be sufficient to reverse the polarity of the injured tissue. This preliminary explanation of "complicated corrosion" does, on the other hand, not exclude the contribution of other biochemical reactions to such events. By diffusion or by closed circuit transports between Tissues I and II, oxidizing substances may accumulate in Tissue I. Similarly, reducing substances may accumulate in Tissue II. It is furthermore possible that these substances are also to some degree produced locally in Tissues I and II. Such events should also be included in a discussion of reversal of polarity between Tissues I and II.

Several possibilities exist to support biochemical reversal of the driving potential in the reactions. Electric potential fluctuating between an injured tissue and a noninjured tissue over a closed circuit will now be presented as a preliminary hypothesis. These considerations are based mainly on information on degradation of tissue collected by Lehninger (38), Wilson, Dutton and Wagner (81) and Jordan (30).

A large number of enzymes and substrates participating in degrading processes react with groups capable of acting as general acids or general bases, e.g., amino, carboxyl, sulfhydryl, phenolic hydroxyl and imidazole groups. However, an anodic phase of degrading tissue should not be able to enter a cathodic phase as a result of a single reaction. An alternative possibility might be that different reactions are superimposed on preceding phases of enzyme-catalyzed reactions, as the maximum velocity for each reaction takes place at different pH. In this way, sequences of electron-donating and electron-accepting enzyme reactions may produce fluctuations of the electric potential of the degrading tissue as the whole process drives toward equilibrium. Examples of such sequences are known, as in the electron transfer reactions of haemoproteins. Thus, Jordan (30) has described a redox potential cascade for the terminal oxidation chain of cellular respiration of the overall reaction:

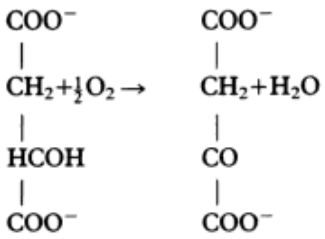

as shown in Fig. XII: 6.

Malate is not directly oxygenized in the presence of oxygen. The oxidation to oxalacetate occurs, however, rapidly via the intermediate steps shown in Fig. XII: 6. This leads to a potential difference of more than 1 V, even though the potential differences for successive steps are small. It is also known that exergonic reactions (with a negative standard-free-energy) may change, e.g., the oxidation of glucose to water and carbon dioxide ($\Delta G^{\circ\prime} = -686$ kcal mol^{-1}) into an endergonic esterification of glucose and phosphate to glucose G-phosphate and water, which presents a positive standard-free-energy change ($\Delta G^{\circ\prime} = 3.3$ kcal mol^{-1}). Such reactions may be generally expressed as:

Exergonic $A+B \rightarrow C+D+$energy (ΔG° negative)

Endergonic energy (ΔG° positive)$+E+F \rightarrow G+H$.

How sequences of oxidizing and reducing reactions may change the direction of electron flow, or to which individual step or steps of a sequence should be attributed such functions in necrotizing tissue, e.g., bone, is presently not predictable. These mechanisms appear also to depend to a large extent on the function of adjacent normal tissue.

Polarization products will also form at the cathodic metal surface during the calciolytic phase. This development should impair the diffusion of oxygen toward the cathode. It should also facilitate a reversal of the direction of electron flow.

The proposal of fluctuating and attenuating driving forces between Tissues I and II is based partly on the studies on injury potentials in tumours and spontaneously degrading sterile blood (Chapter VII), and partly on the physical fact that all known spontaneous reactions proceed in a fluctuating, attenuating fashion toward equilibrium. It is inconceivable, moreover, to assume that the induction of a degrading process in vivo should proceed under the influence of a unidirectional gradient of potential between the injured and surrounding normal tissue, simply because new distortions of the ionic compositions at the reaction sites would then be created. Acceptance of a fluctuating injury potential between Tissues I and II also makes it possible to understand many biologic transformations which otherwise are difficult to explain.

The early acidic phase of Tissue I is proposed to dissolve calcium in the bone matrix, hence this is here called the "calciolytic phase". Local decalcifications in bone are commonly seen radiographically after bone injury, e.g., trauma.

Direct evidence of a change of Tissue I from an acidic, "calciolytic phase" into an alkaline "mineralization phase" is encountered in the development of radiographically evident, irregular zones of calcification, appearing in previously decalcified bone. This mineralization may now be explained as a result of inflow of calcium and magnesium ions as a selective transport over the closed electric circuit under the influence of the now cathodic reaction of the tissue. Local phosphate ions, in the meantime, are lagging in the process of diffusion in the degrading tissue and are therefore available for recombination with calcium and magnesium ions into complex calcium-magnesium-phosphate salts as apatite. The development of decalcified and calcified regions, which are radiographically common in aseptic necrosis or other kinds of bone injury, now in principle can be explained. As will also be shown later (Chapter XVI), the same principle can be applied experimentally to produce microcalcifications in breast fat tissue.

How does iron now appear as a precipitation line in the normal Tissue II? First, we may anticipate that hydroxyl ions remain in Tissue II from the phase when this tissue was an electron acceptor. When the polarity changes so that Tissue I consumes electrons, Tissue II accumulates dissolving iron ions from the adjacent metal, which delivers electrons:

$$Fe \rightarrow Fe^{2+} + 2e^{-}.$$

Fe^{2+} ions then diffuse and migrate away from the metal surface to a region in Tissue II where the pH is favourable for the combination of Fe^{2+} with remaining hydroxyl ions, to form insoluble $Fe(OH)_2$ (and later, $Fe_2O_3 \cdot nH_2O$).

Local sites with increased x-ray attenuation in Tissue I are generally regarded as caused by deposition of calcium. It should not be surprising, however, if future analyses will show that these sites also include precipitated iron, dissolved during the acidic phase of Tissue I.

This preliminary description of "complicated corrosion" is simplified and incomplete in many respects. It probably represents only one of several possible explanations. Metal implants consist of different combinations of metals, two of which are presented in Table XII: 1. Dissolving of iron in stainless steels in active states is accompanied by similar reactions of chromium, nickel, molybdenum and manganese. Furthermore, one may expect that in the tissue fluid various compounds, not considered here, must also induce reactions with the implant.

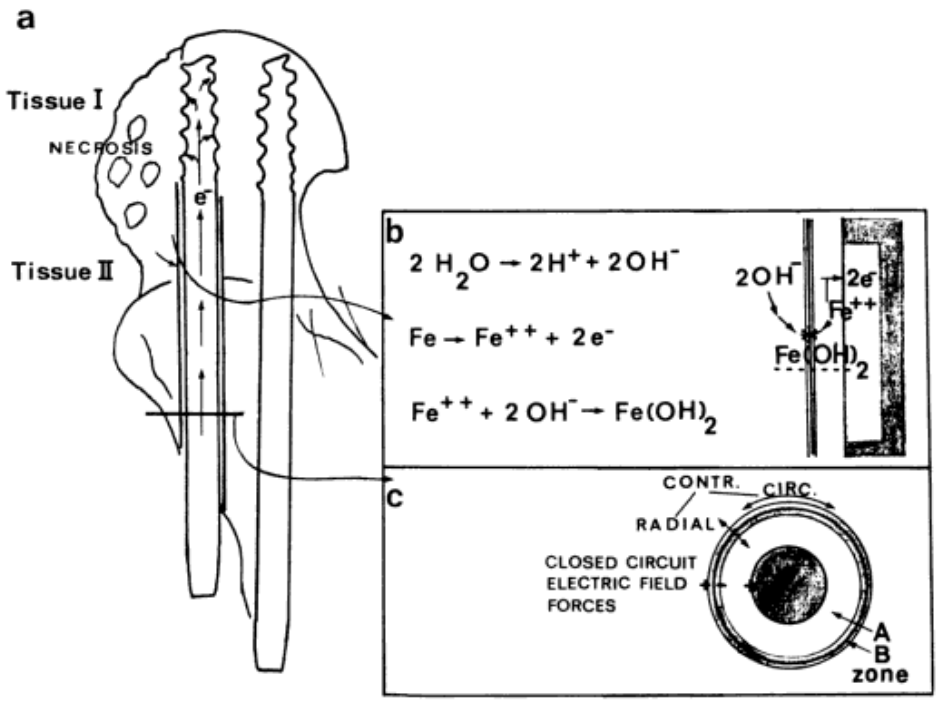

Fig. XII: 7. (*a*) Precipitation "line" produced adjacent to metal in the relatively normal Tissue II during its mineralization phase. (*b*) The necrotic Tissue I consumes electrons delivered from the metal adjacent to Tissue II as iron there dissolves. The Fe^{++} ions produced, then recombine with hydroxyl ions to form $Fe(OH)_2$. (*c*) In cross section, the iron precipitate forms an equilibrium deposit as a ring around the metal by the action of closed circuit electric field forces and concentration forces (= formation of "A" and "B" zones). See also Chapter X, Figs. 1, 7.

The characteristic appearance of metallic precipitation as a line structure in radiographs will now be considered.

3. The precipitation line

Dissolved metal has been chemically identified adjacent to metal in bony tissue by Ferguson, Laing and Hodge (16). Its constituent chemicals are most likely $Fe(OH)_2$ and $Fe_2O_3 \cdot nH_2O$.

During the mineralization phase of anoxic necrosis, the necrotic Tissue I consumes electrons from the metal (Fig. XII: 7 *a*). The dissolving metal adjacent to Tissue II donates electrons to the implant (Fig. XII: 7 *b*). A cross section of the implant (Fig. XII: 7 *c*) shows the precipitation of $Fe(OH)_2$ as a ring. Its development can most easily be explained like that of the "A" and "B" zones of semolina grains around a charged body (Fig. X: 1 *a*, 7 *b*). Closed circuit electric field forces compete with the radial, circular and longitudinal vectors of concentration forces (Fig. X: 3). The precipitate appears in cross section as a "B" zone separated by an "A" zone from the metal.

These zones also represent two different phases in which preferential adsorption and local concentration take place at their interface (the small arches and arcades previously described between the "A" and "B" zones around a lung tumour are also sometimes seen radiographically as a thin adsorption line of higher attenuation of x-rays than the surroundings). The line of $Fe(OH)_2$ or $Fe_2O_3 \cdot nH_2O$ in bone adjacent to a metal does, of course, not appear as arches but rather as one complete arcade, which is a circular ring (provided the metallic surface is circular and smooth). Only when small edges protrude from the metal can the precipitation line of the iron compounds be predicted to appear in the cross section as a line of small arches corresponding to the edges.

Alternative explanations also must be considered in the development of a precipitation line. Thus, metal in a passive state (e.g., stainless steel) is known to dissolve slowly in any oxygenized environment, leading to secondary diffusion and precipitation of metal hydroxide of low solubility. Such a mechanism is very likely to be involved in the events described, but only as a partially contributing mechanism. Other modifications of bone structures adjacent to the implant can also become induced as a result of toxic effects on cells by dissolved metals. Such injuries enhance conductivity of BCEC systems, leading to a gradual increase in intensity of all associated closed circuit reactions.

4. Dynamic factors in in vivo corrosion

The uncomplicated and complicated types of in vivo corrosion have thus far for didactic purposes been described as instantaneous stationary situations. Biologically, the actual condition must be different. It is even unrealistic to assume that uncomplicated or complicated corrosions exist as isolated phenomena. One

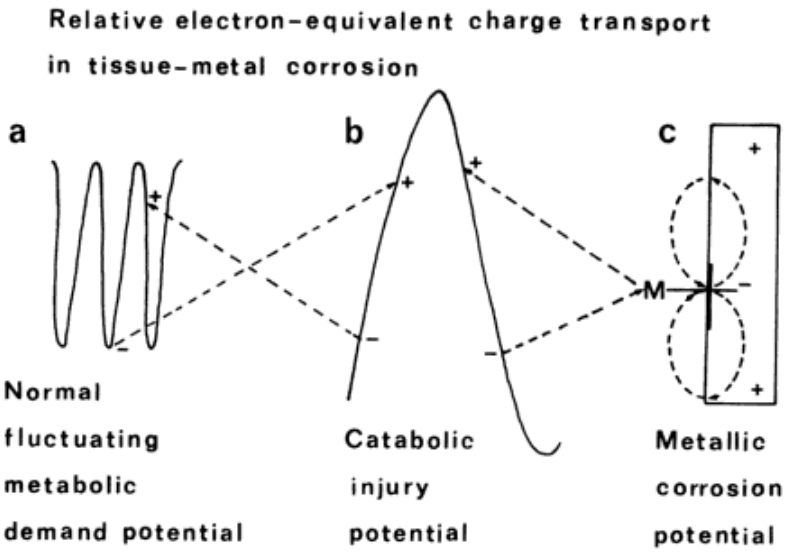

Fig. XII: 8. Relatively alternating polarity in corrosion. (*a*) Normal tissue, (*b*) injured tissue or (*c*) metal in tissue may be relatively electropositive or electronegative, depending on the actual time-related phases of fluctuating tissue potentials. Note the more rapid change of potential of normal tissue than of degrading tissue, which also presents larger amplitudes. Arrows indicate directions of increasing electropositive gradients between sites of reaction. The tissue sites representing the origins of the driving forces of the system can be anticipated to vary spatially during different phases of the fluctuations of the injury potential.

or the other type may more or less dominate. A third important factor will now be introduced: the modifying influence of surrounding normal tissue.

In the theoretical situation of "pure" uncomplicated corrosion, substances are produced at the sites of redox reactions. These materials lead to a local decrease of entropy, which in turn induce a new spontaneous drive toward an equilibrium.

In the theoretical situation of "pure" complicated corrosion, polarization in tissue represents the driving force, characterized by a catabolic, *fluctuating* injury potential. During the process of healing, however, the injured tissue will interact not only with the adjacent metal implant but also with the surrounding normal tissue, as in any other healing process. The modifying effects of the normal tissue are also characterized by its own normally fluctuating, metabolic demand potentials. These three partial components may influence each other in varying ways in an overall physicochemical corrosion reaction driving toward equilibrium. The dynamic interaction of such a system is outlined in Fig. XII: 8 in terms of relative polarity and direction of charge transports in tissue-metal corrosion. It may be seen that in certain phases any of the reactants may be anodic or cathodic. Locally decalcified and calcified irregular regions in necrotizing bone are now nearly ready to be linked to the described dynamic correlations between injured and surrounding noninjured tissue.

A practical message from this presentation is that a radiographic "line" adjacent to a metallic implant in bone is not necessarily a sign of poor fixation of the implant. It may be caused by relatively harmless uncomplicated corrosion. On the other hand, corrosion of an implant is not always synonymous with the classical "uncomplicated" example of relatively anodic and cathodic parts in the metal. Corrosion in living tissue, in the author's opinion, is quite complex and depends to a large extent on the activities of both pathologic and normal tissue adjacent to the metal.

In analyzing these events, the reader must recognize a recurrent issue: the radiographically visible, in vivo modifications of tissue structures are created by driving forces which are separated by long distances. Such conversions of energy over long distances can only take place in combination with electric transports over suitable conducting channels, i.e., biologically closed electric circuits.

5. Pathways for the electric current

To explain the morphologic background of biologically closed circuits is not simple, even in uncomplicated corrosion. The surface of an iron nail immersed in salt water, for instance, is in contact with the conducting salt solution. The redox reactions necessary for corrosion always require a closed circuit. It can be assumed that this circuit contains one branch within the metal, providing transport of electrons between the relatively anodic and cathodic sites. The electrolyte and water provide the other branch of the electric transport units. The water molecules, by their dielectric properties, then can be regarded as an insulating and channelizing but movable matrix for the solute.

In the case of complicated corrosion involving normal tissue, pathologic tissue and metal, as proposed in Fig. XII: 8, an explanation for closed circuit ionic exchange between normal and pathologic tissues has heretofore been lacking. One conducting branch is obviously formed by the electrically conducting interstitial fluid in the interstitial tissue channels. To complete the circuit, however, requires another branch. The following section deals with this problem.

B. A biologically closed electric circuit over vascular-interstitial conducting channels

This circuit will first be described on the basis of some preliminary observations:

Any vascularized part of the body can in principle contain this circuit. It contains five main components: 1. insulating walls of blood vessels, 2. conducting intravascular plasma, 3. insulating tissue matrix (possibly including lymph vessels), 4. conducting interstitial fluid, 5. electrical junctions for redox reactions.

An entirely new function is now ascribed to the vascular system. As will be seen, the walls of large blood vessels insulate electrically (within certain limits) the conducting medium of blood, i.e., plasma, from extravascular interstitial fluid, which also is conducting. One essential junction exists between plasma and interstitial fluid: the capillary membranes, which allow an exchange of water and electrolytes between the two fluid branches. The normal physiologic activities of cells, of a region of tissue or of an entire organ will present gradients of electric potential compared to surrounding or distant cells, tissues or organs containing different metabolic, physicochemical potentials. Given the presence of a biologically closed electric circuit, energy exchange will take place between such sites. Structural modifications and functional effects will follow. In a conventional sense the movement of fluids mechanically transports ions and other necessary materials to reaction sites in tissue. The existence of an additional pathway for energy exchange over a biologically closed electric circuit not only promotes

Fig. XII:9. Suggested biologically closed electric circuit in a lung with a necrotic tumour. One branch of the circuit is the plasma in blood vessels, the other is the interstitial fluid in the lung. The major driving force in the system is the local electrochemical difference between surrounding tissue and degrading tissue, e.g., necrosis inside the tumour. For simplicity, this example considers only the systemic circulation. For further discussion, see text.

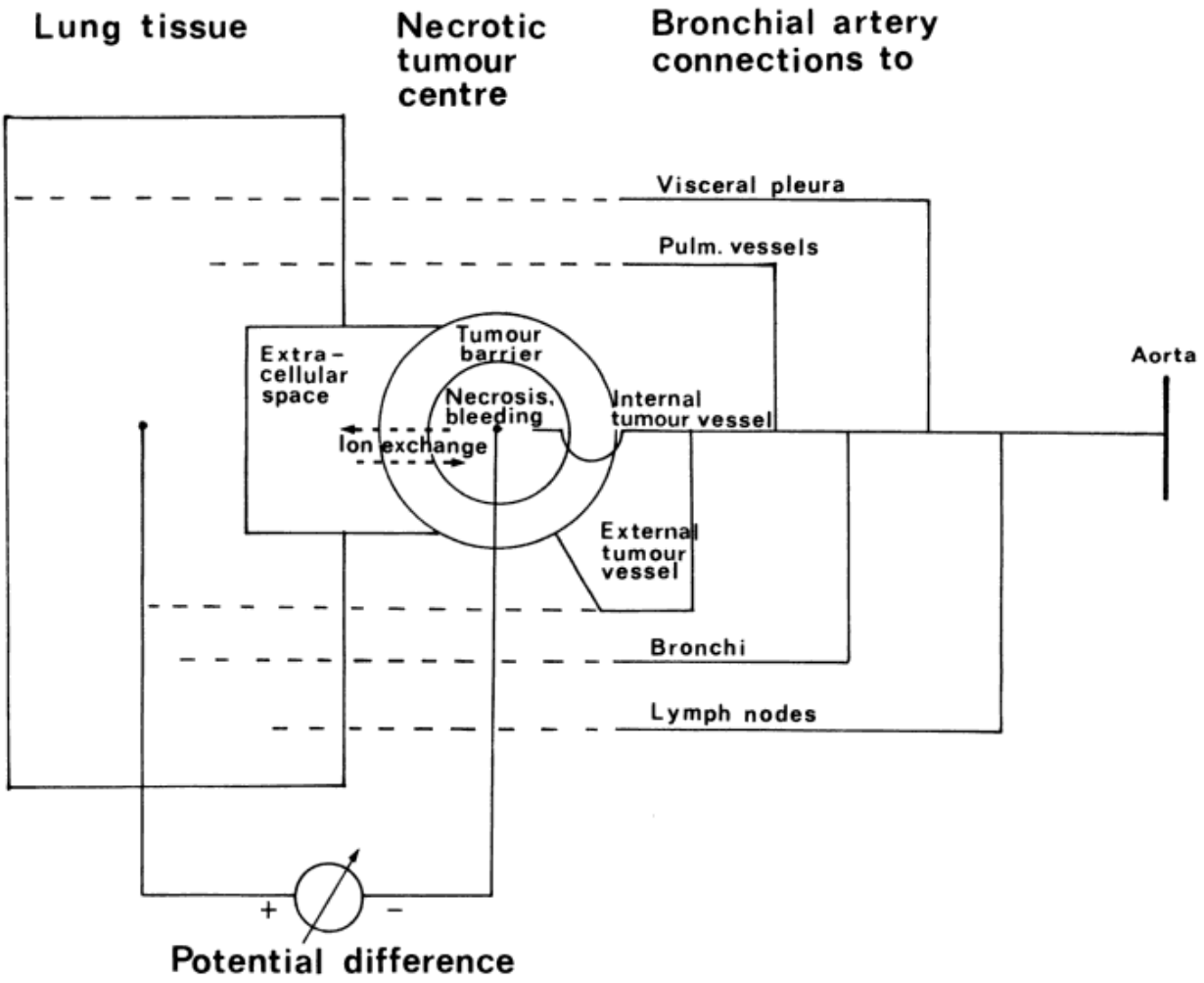

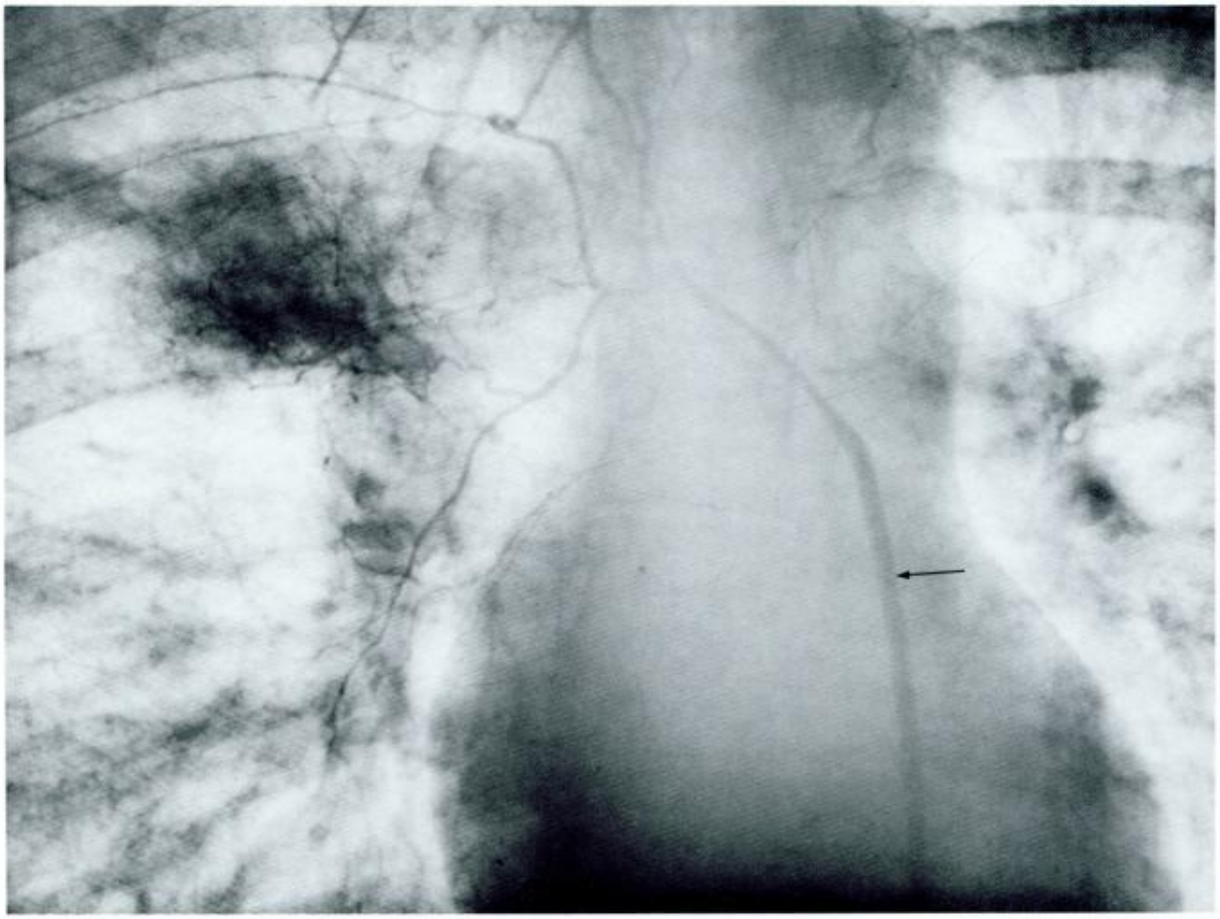

Fig. XII: 10. Bronchial arteriogram, outlining the arteries supplying a bronchogenic carcinoma and other bronchial structures in the right upper lobe of a 52-year-old man. A catheter (arrow) has been placed in the aorta with its tip in a right bronchial artery. Radiographic contrast fills numerous pathological vessels in the tumour as well as vessels supplying blood to tissues surrounding the tumour.

selective exchanges of ions but also permits reactions among distantly situated regions of tissue. In a closed circuit, energy exchange and reaction effects are possible at sites which are in the circuit but separated from the location of the driving forces of the system.

Given this introduction, the structure of such a circuit will next be described.

1. Structure of the vascular-interstitial closed circuit (VICC)

The principle of electric communications over bronchial arteries and interstitial fluid between a necrotizing lung tumour and adjacent lung is surveyed in Fig. XII: 9. It is understood that similar circuits also exist over bronchial veins, pulmonary arteries and veins and lymphatic vessels. The anticipated regions for ionic diffusion and redox transfer of electric charges are not indicated.

The bronchial arteries are of particular interest in the lung because they are nutritional vessels in bronchogenic carcinomas.

The distribution of the bronchial arteries can be studied by techniques developed by the author for infusing the bronchial arteries in dogs (42, 43) and man (44). Fig. XII: 10 illustrates a right bronchial arteriogram in a patient with a poorly differentiated squamous cell carcinoma of the right upper lobe. The right bronchial artery supplies numerous pathological vessels to the tumour. As the cancer grows, it may erode or thrombose the bronchial arterial branches which supply it, thereby causing local haemorrhage or necrosis. Usually the centre of a tumour is most subject to such dystrophic changes.

The living cells at the periphery of a tumour act as a "semipermeable" sieve or barrier between the surroundings and central necrosis in the tumour. This property may at first inspection not be quite obvious.

A prerequisite for continued life of any normal or pathological tissue is a functioning intercellular system of communicating channels for water, electrolytes, nu-

trients and wastes. The actual distance between cell surfaces in normal tissue has been estimated between 10 to 20 Å (3) or 100 to 200 Å, according to evidence from electron micrographs (15). The tissue matrix can therefore be considered as a kind of sieve.

Many neoplasms make a tissue firmer and denser than surrounding normal tissue. The sieve function of the individual interstitial channels of such tumours will therefore be increased compared to the channels in the surrounding normal tissue. Hence, the network of interstitial channels in a tumour potentially constitutes a relative barrier to interstitial flow, i.e., a "tumour barrier".

On both sides of a tumour barrier nonpermeable bodies may be found, i.e., macromolecules, cellular debris and fragments, and whole cells such as individual erythrocytes, leukocytes, thrombocytes, macrophages and tumour cells. Such units usually carry net electric charges. Consequently they will be transported electrophoretically in a closed circuit. Many such biological units may then be too large to pass through the intercellular spaces of an organized tissue. In this sense the intercellular sieve of a tumour acts as a barrier where material can be adsorbed or trapped by diffusion and closed electric transports.

2. Resistivity of tissue and body fluids

The conductances of different tissues have been determined by a number of investigators (19–21, 32, 55, 62, 63). It has long been known that living cells become polarized by electric fields, as is the case with dielectric materials. This property gives cells low resistance for high frequency currents and increasingly high resistance as frequency decreases. It also means in general that cells possess high resistance for DC currents.

The impedances of organ tissues have been determined in vivo by Schwan and Kay (64) to be too small to influence significantly common ecg tracings. In studies of impedance of various human tissue exposed to low frequency alternating currents (Table XII: 3), they found the following values for specific resistance (= resistivity) in situ:

Table XII: 3. *Resistivity of tissues, according to Schwan and Kay*

Resistivity Ωm	10cps	100cps	1 000 cps	10 000 cps
Lung	11.20	10.90	10.40	9.50
Muscle	9.65	8.80	8.30	7.60
Liver	8.40	8.00	7.65	6.85
Heart muscle	9.65	9.25	8.45	
Fatty tissue			15.00–50.00	

Table XII: 4. *Resistivity of tissue and body fluids, according to Kaufman and Johnston (Ωm)*

Specimen	Resistivity pre-biol. calibr.	Resistivity post-biol. calibr.
Lung, inspiration	7.66	7.44
Lung, superinflation	13.67	
Lung, deflation	4.01	
Muscle	7.11	5.75
Liver	6.72	5.06
Heart	2.24	2.07
Pericardium	4.34	4.05
Foot	22.05	18.08
Serum	1.78	0.98
Blood	2.30	1.75

The average resistivity of these tissues, about 10 ohm-m, may be compared with the resistivity of blood of only about one ohm-m, according to Schwan and Kay (64).

Measurements of tissue resistivity have often yielded widely ranging results, which Kaufman and Johnston have ascribed to great technical difficulties encountered in attempting to obtain such measurements in living tissues (32). They obtained the following average values for resistivity of human tissues (Table XII: 4), using pulses of 500 to 10 000 Hz. Note that the values of resistivity decreased ("post-biol. calibr.") at the end of the experiments.

Most determinations of resistivity in tissues have been made in vitro, a few in vivo. Galeotti noted differences before and after death (21) and Crile, et al., found that the resistivity of all measured tissues decreased with time after removal from the body (14).

Resistivity of walls of blood vessel, in the experiments shortly to be described (see Section 3, page 125), was shown to require in vivo conditions as well as great care to avoid damage to the vessel walls and to the vasa vasorum (otherwise, wall resistance rapidly decreased). Geddes and Baker have reviewed the electric properties of tissues (22). From this report, certain figures of tissue resistivity will be cited.

The resistivity of dog *cardiac muscle* has been found to differ by a ratio of 2.2 to 1 when measured parallel and transverse to the direction of the fibres (58). At average body temperature, low frequency resistivity for random orientation in canine cardiac muscle was estimated to be 7.5 ohm-m. In studies of *skeletal muscles*, the resistivities along and across the fibres also showed large differences.

In the *lung*, determinations of resistivity have been made in vivo by many authors (14, 21, 32, 34, 58). During maximum inspiration and expiration, the resistivity of lung tissue in the dog varied between 21.70 and 4.01 ohm-m (average mean, 12.75).

The resistivity of human *kidney* is about 1 ohm-m and for other mammals about 3.7 ohm-m (21, 28, 34, 45).

The *liver* shows at "low frequencies" and at body temperature a variable range of resistivity (5.9–11.0 ohm-m), average 8.2 ohm-m (28, 45, 58, 62).

Nerve tissue fibres show notable differences between transverse and longitudinal resistivities in cow, pig and rabbit brain (51).

Human *adipose tissue* shows resistivity values of 27.3 ohm-m at 200–900 MHz, and values of 28.80 ohm-m at low frequencies in canine fat (28, 58, 62).

Bone shows high resistivity. Hemingway and McLendon found a resistivity of 18.0 ohm-m in human bone (28) and Osswald average values between 37.0 and 62.0 ohm-m in cow and pig (45).

Different body fluids such as cerebrospinal fluid, bile, amniotic fluid and urine all contain electrolytes and have therefore considerably lower resistivity than cellular biological tissues. *Cerebrospinal fluid* has a resistivity of 0.64 ohm-m at 1 kHz, *bile* 0.59–0.76 ohm-m at 50 kHz, and *amniotic fluid* 0.49–0.65 ohm-m at 1 kHz. *0.9% saline solution* has a resistivity of 0.7 ohm-m at 20°C and 0.50 ohm-m at 37°C, both determined at 1 kHz (8, 22, 45, 62).

Resistivity of *blood* has been studied rather extensively (8, 14, 20, 21, 32, 34, 41, 45, 49, 56, 62, 67). The resistivity of human blood varies with haematocrit and temperature. Thus, 34.4% haematocrit gives a resistivity at 37°C of 1.38 ohm-m, and 1.80 ohm-m at a haematocrit of 56.4% (56). Kinnen, et al., found 1.55 ohm-m in dog blood at 41% haematocrit; Rush, et al., 1.60 ohm-m with 0.1 sec DC pulses (34, 58).

It is known that turbulence of blood diminishes its resistance. Thus, a resistivity of 1.54 ohm-m was reported (41) in flowing venous blood (at 120 kHz test current). For small densities of current, blood is equivalent electrically to a resistor in series with a capacitor (19, 20, 74). The specific capacity of blood in man is due to the red corpuscles and amounts to a few hundred picofarads, while the specific resistance is about 1.9 ohm-m at low frequencies. Extrapolated to infinitely high frequencies, the specific resistance of blood is 1.24 ohm-m (19). It has also been pointed out that the capacity of the blood corpuscles is independent of the frequency of the electric current, and that the capacity stays constant when the corpuscles are suspended in different media, as long as the shape of the corpuscles does not change (19). This indicates that the capacity represents a static property of a thin surface membrane of dielectric material. The high resistance of the blood cell is therefore due to its membrane, while the interior is highly conductive.

The resistivity of *human blood* at 37°C is 1.60 ohm-m and that of *plasma* 0.70 ohm-m, according to other studies (8, 19, 62). This value of specific resistance for plasma does not differ very much from that of physiological saline solution, which amounts to 0.72 ohm-m at 18°C (8). According to Rosenthal and Tobias (56), human blood plasma shows an average of 0.61 to 0.67 ohm-m at 1 kHz. Dog serum shows an average of 1.38 ohm-m at 1 kHz, according to Kaufman and Burger, who also found a resistivity of 0.65 ohm-m in cow plasma (8, 32). Fricke found that calf serum had a resistivity of 0.894 ohm-m at 87 kHz (19), which is comparable to that of saline solution and interstitial fluid.

There is no doubt that the cell membranes in organized tissue are responsible for the high specific resistances of different organs, including whole blood. The predominant conducting media in organs are found in their intercellular fluid, secretions and plasma. Plasma is in this respect almost comparable with physiologic saline solution.

The ionic and nonionic concentrations of blood are not constant. They vary, for instance, as a result of food intake, starvation, dehydration, acid-base alterations and other metabolic changes which can be assumed to change the conductivity of blood plasma and interstitial fluid. Local variations of water content in the tissue should also produce changes in conductivity (the sudden change in ecg amplitudes as an electrode is moved through a hydropenic "A" zone into a hydropic "B" zone in the lung may be explained by variations in water content; see also Figs. VI: 21, XVI: 16).

Previous determinations of resistivity of tissues have often regarded tissues as homogeneous "bulk" materials. Examples are the total effect of tissue impedance in electrocardiography or in electric accidents with large densities of current. The resistivity of one specific tissue now becomes important: the proposed hypothesis of vascular-interstitial conducting channels requires information concerning the resistivity of the walls of blood vessels.

3. Resistivity of the walls of blood vessels

A hypothetical picture of the physical and chemical properties of the arterial wall has been presented by Sawyers, et al. (60). The intimal surface of the vessel is composed partly of mucopolysaccharides containing sulfate and carboxylate groups. This chemical structure gives the intima, compared to blood, a net potential of -3 to -13 mV (59). This negative inner surface should therefore repel platelets, erythrocytes and other blood corpuscles, which also are negatively charged. Furthermore, the vessel wall should tend to adsorb positively charged ions. Any injury to the intima will locally make it positively charged and induce local thrombosis (59, 61). Thrombosis can also be produced by applying electrodes to the intima. Thrombi will be

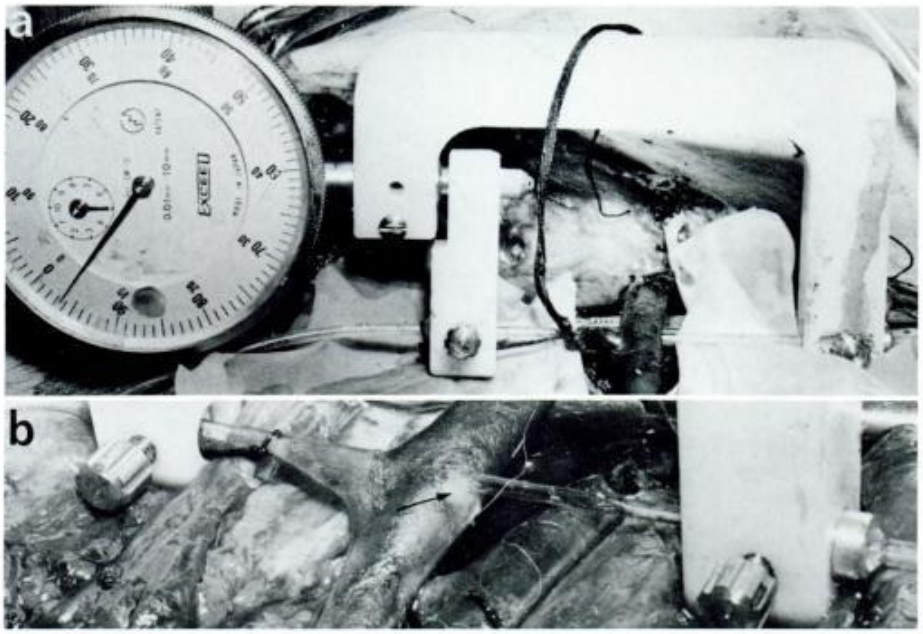

Fig. XII: 11. In vivo determination of resistivity of a blood vessel of a dog. (*a*) A glass tube has been inserted through a branch of the femoral vein. Another glass tube was placed opposite the first tube against the external wall of the vein. The distance between the tubes was determined by a spring-loaded measuring device, which also held the tubes. Separate pairs of platinum electrodes positioned in the glass tubes supplied current and measured the voltage difference across the vessel wall. Conducting fluid in the glass tubes is 0.9% saline solution. (*b*) Even slight but continuous pressure by the glass tubes may produce ischaemic injury at the vascular measuring site, here seen as a white spot (arrow).

produced only at the anode, while formation of clot is inhibited at the cathode (59, 61). The outer surface of vessel walls, meanwhile, is positively charged (60, 61).

The resistive properties of vessel walls will now be studied experimentally.

a) *Alternating current*

Resistivity was determined for the femoral veins and arteries of 5 dogs.

Anaesthesia (intravenous sodium pentobarbital) was administered through a catheter placed in the vein of a foreleg. The femoral artery and vein were surgically exposed. Two glass tubes (internal diameter 1.3 mm, external diameter 1.8 mm, surface area at the end of each tube 1.3267 mm^2) were each provided with two platinum strings, one ending 1.2 cm from the tip for measuring potential differences over the vessel wall and one 5.2 cm from the tip to supply current. One tube was inserted through a perpendicular branch of the vessel, allowing the tip of the tube to be placed against the opposite internal vessel wall. The other glass tube was placed at the corresponding place against the external vessel wall. The tubes were centered against each other and held in place with two plastic holders connected to a spring-loaded precision instrument for determining distances (accuracy ± 0.01 mm at a constant total pressure of 30 g) (Fig. XII: 11 *a*). The frictional resistance of the spring-loading branch was overcome by gently tapping on it with a pair of pliers. The tubes were filled with 0.9% NaCl solution.

The femoral artery and vein had to be freely dissected to apply the electrode tubes. Some damage to the vessel walls and vasa vasorum could not be entirely avoided. The duration of spring-loaded pressure on the glass tubes was kept as short as possible (circa 10 minutes) in order to minimize mechanical and circulatory injury to the vessel wall. Nevertheless, a small white spot, a sign of focal hypoxic injury, developed rather rapidly (after about 5 minutes) around the external glass tube (Fig. XII: 11 *b*).

The resistivities were determined by an automatic recording system for measuring biological impedances, developed and described by Tedner (73). The actual determinations of resistivity of the vessel walls and test liquids were carried out in cooperation with Mr B. T. Tedner (M.Sc.) and Mr H. Larsson (M.Sc.). In this system, a constant current of 10 μA is sent through the test object via the outer platinum electrodes in the glass tubes and an external reference resistor. The potentials developed between the measuring electrodes and over the reference resistor are then fed into two differential amplifiers via four high-impedance input amplifiers. The outputs from the differential amplifiers are connected to a network analyser system which

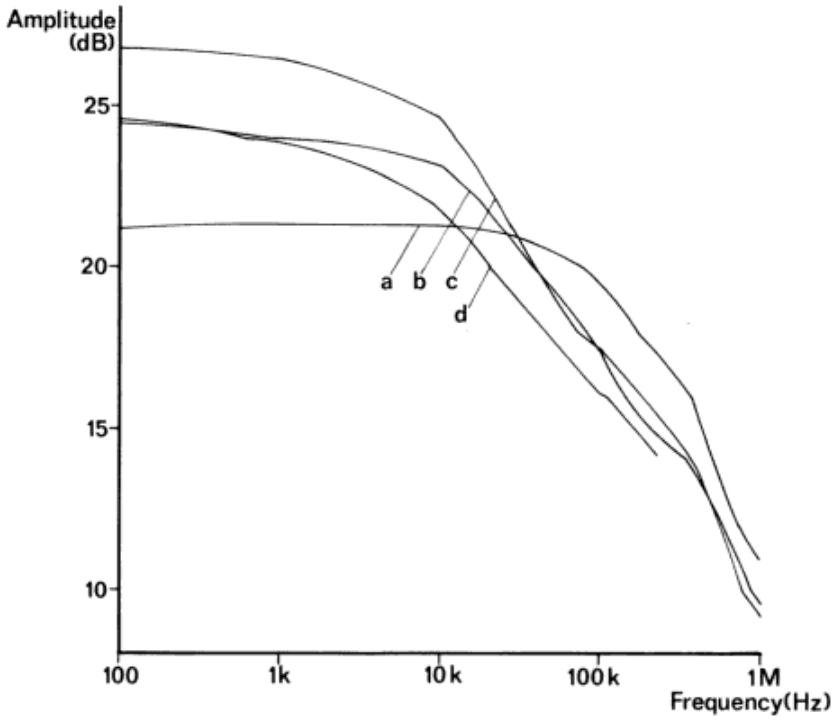

Fig. XII: 12. Amplitudes of potential drop across walls of blood vessels (dog) by alternating current of different frequencies. A 10 microampere constant current ranged in frequency from 100 to 1 MHz over (*a*) 0.9% NaCl, (*b*) wall of femoral vein, (*c*) wall of femoral artery, (*d*) wall of femoral artery after small local injury of the vessel. Each tracing consists of recordings from 160 discrete, logarithmically spaced frequencies. Samples for determination of resistivity were compared at 10 kHz. From these recordings impedance values and then resistivities were calculated.

measures amplitude ratio and phase angle between the inputs at a given frequency. This system consists of a digital synthesizer and a network analyser controlled by a calculator. The ratio between the two potentials is recorded. Because amplitude readings are obtained in decibels, the impedance is calculated from

$$Z = R10^{dB/20}$$

where Z is the impedance, R the reference resistance and dB the amplitude value determined by the analyser. The calculator is programmed to sweep automatically from one hundred Hz to one MHz at 160 logarithmically-spaced discrete frequencies. The resistivity ϱ of the vessel wall is then calculated according to the formula

$$\varrho = \frac{R_v A}{l}, \text{ where } R_v = Z - R_s$$

and l is the thickness of the vessel wall, A the internal cross-sectional area of the glass tube (1.3267 mm^2), R_v the resistance of the vessel wall and R_s the resistance of the column of saline solution between the measuring electrodes. R_v is determined by subtraction of R_s from Z, the total resistance. The measurements of the saline solutions were made at temperatures ranging from 23°C to body temperature, yielding resistivity values of 0.70 to 0.62 ohm-m at 1 to 10 kHz, which is in good agreement with earlier values from the literature (8, 22).

Fig. XII: 12 shows amplitude curves at different frequencies for (*a*) saline solution, (*b*) fresh vein and (*c*) fresh arterial walls in situ. An example (*d*) is also given of the effect on resistivity of an arterial wall in situ after the production of a visible local ischaemic tissue injury.

The amplitude curves in Fig. XII: 12 show a relatively rapid fall around 10 kHz, which is interpreted as caused by the lowering of the inductive resistance by high frequencies. Below 10 kHz the prominence of this effect decreases.

The resistivities of the femoral arteries and veins in 20 measurements of the 5 dogs were compared with the resistivity of 0.9% NaCl (0.62 ohm-m at 23°C). The immediate determinations of resistivities of the vessel walls, before obvious damage was produced by the glass tubes, showed values for the vein varying between 60 to 116 ohm-m at 1 kHz and 20 to 79 ohm-m at 10 kHz and 37°C. For the artery, values of 81–121 ohm-m were obtained at 1 kHz and 45–67 ohm-m at 10 kHz and 37°C.

The variations depended partly on the difficulties of measuring the thickness of the vessel walls, which varied between 0.03–0.05 mm for the vein and 0.10–0.15 mm for the artery. Two other factors were the injury necessitated by the dissection of the vessels free from surrounding tissues, which may have partly damaged the vasa vasorum, and the direct damage by the glass tubes. Values of resistivity decreased at the end of each examination. For example, examination of an artery which had a directly visible ischaemic region around the glass tube gave 36 to 54 ohm-m at 1 kHz and 8.0 to 11.5 ohm-m at 10 kHz (Fig. XII: 12 *d*).

The results of these examinations indicate clearly that the resistivity of femoral arteries and veins is of an

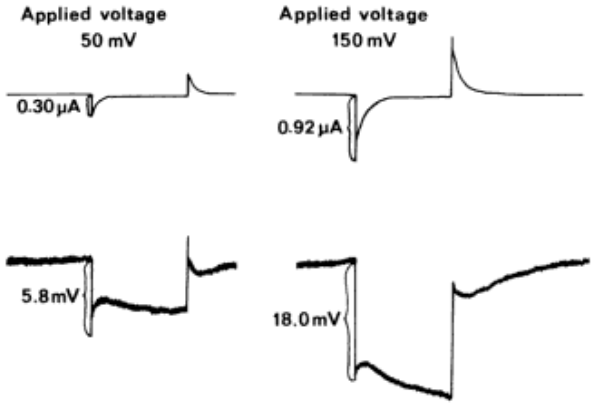

Fig. XII: 13. In vivo determination of resistivity to DC pulses across the wall of a dog's femoral artery. Method of Burger and van Milaan: amplitudes (μA) and potential differences (mV) when 50 and 150 mV pulses were applied (pulse duration: 0.5 second). The distortions in the tracings are caused by polarization of the electrodes. Initial deflections were used to obtain a relative measure of resistivity.

order at least 100 to 150 times higher than the resistivity of saline solution, which in turn is known to have roughly the same order of resistivity as blood plasma, serum and interstitial fluid.

b) *Pulsed direct current*

Resistivity studies with direct current are of considerable interest, as this type of current represents electric transports in vivo. Attempts were therefore made to study resistivity of blood vessels with a technique developed by Burger and van Milaan (8). In this way, information on the resistance of walls of large vessels in comparison to resistance of the intravascular conducting medium, the plasma, should be possible to obtain.

As in determinations of resistivity with alternating current, many sources of error can interfere in determinations of resistivity with direct current. It is evident that an application of DC pulses will ionize the test material and change its relative conductivity during each pulse. The applied potential will furthermore produce ionic separations, providing electromotive forces in the opposite direction. This effect means that the test current builds up a galvanic potential.

When potential difference is constant within certain limits, the degree of ionization is a dynamic event which initially increases exponentially the actual flow of current per unit time. This observation is well known since Julius Tafel (72). On prolonged application of direct current, different counteracting reactions will contribute to decelerate the current. Moreover, the same technical difficulties are encountered in both DC and AC determinations of resistivity of a vessel wall, i.e., geometric measurements of specimens and avoidance of injury to tissue.

These experiments were performed in five dogs, using the same type of preparation of femoral vessels and electrodes in glass tubes as was employed in the determinations of resistivity with alternating currents. A series of 10 DC pulses (0.5–1.0 sec duration each) was applied over 25, 50, 100 and 150 mV through the vessel wall in one direction and then in the opposite direction.

Polarization caused a distortion of the measured deflections of potential. It is therefore necessary to define how the measurements were obtained and the results analyzed.

Fig. XII: 13 shows tracings of measured currents and potential differences through the vessel wall during application of 50 and 150 mV potential pulses over the current-supplying electrodes. The distortions of these potentials are in principle easy to understand, despite the complicated nature of the underlying kinetic events.

For the actual measurements the high initial potential and peaks of current have been used. In the well known formula

$$R = \frac{l}{A} \cdot \varrho$$

R = resistance, ϱ = specific resistance, l = length, A = cross-sectional area. R is determined by the simultaneous measurements of voltage drop and current flow through the specimen.

In these experiments (as well as in determinations with alternating current) no clear difference could be observed when current was passed from outside to inside or vice versa.

Table XII: 5 presents the actual measurements and calculated resistivities of a dog's femoral artery in situ.

The resistivity of femoral veins was of the same order of magnitude as that of the arteries (resistivity of 0.9% NaCl gave values of 0.70 ohm-m at 23°C). The measured resistances to pulses of direct current through the walls of the femoral artery and vein were 200 to 280 times higher in these experiments than in those through 0.9% NaCl solution.

Table XII: 5. *Resistivity determinations of femoral artery of dog by means of direct current pulses*

Applied voltage (mV)	Current (μA)	Obtained voltage (mV)	Vessel wall resistance (kΩ)	Vessel wall resistivity (Ωm)
25	0.15	2.59	5.93	143
50	0.30	5.79	7.96	192
100	0.67	13.21	8.38	202
150	0.92	18.06	8.29	200

C. Observations of a preferential electric pathway in vessels and tissues

The experiments on resistivity of "large" vessel walls in relation to the relatively low resistivity of plasma and interstitial fluid indicate the possibility that electrochemical gradients in tissue may be levelled over the proposed VICC (vascular-interstitial closed circuit). If this hypothesis is correct, the vascular system must be acknowledged to possess a previously unrecognized function: *the large (i.e., macroscopic) vessels act as electrically conducting, insulated cables*. The vessel walls thus insulate one branch of the conducting media, the plasma, from its surroundings, except at its transcapillary junctions with the other branch, the interstitial fluid. This hypothesis of a conducting VICC will now be tested in different ways.

Consider an electric direct current, passing from the interior of a vessel to a distant region of tissue. After a sufficient quantity of current has flowed, certain morphologic (and presumably functional) changes should develop in the preferential pathways for the current. Such changes appeared to be the actual case in experiments in which the changes were examined by direct visual inspection, in vivo microscopy and histologic techniques. These experiments will now be presented.

1. Cathodic field

A catheter was passed from a femoral vein or artery into a pulmonary artery or the aorta, respectively, of each of 15 anaesthetized dogs. Through the catheter an arteriographic guidewire of stainless steel was passed, and its tip positioned 5 to 10 cm beyond the tip of the catheter. This guidewire was used as a cathode. A platinum string was used as an anode and placed percutaneously either in the lung tissue 3–4 cm from the pulmonary arterial cathode, or in the shoulder muscles or in an intraabdominal organ, 10 to 15 cm from the cathode in the aorta or inferior vena cava. Ten volts were applied between the electrodes and the quantity of current was measured in coulombs. Insulating properties of the aortic wall could be demonstrated at 10 volt potential difference with doses of current as large as 1 700 coulombs.

After the animal was sacrificed, the external wall of the aorta (Fig. XII: 14 *a*) was found to be oedematous and brown-black within a 3×2 cm area. The speci-

Fig. XII: 14. Demonstration of preferential pathway of current from the lumen of the aorta to the vasa vasorum in a dog, indicating electrical insulating properties of the aortic walls. Direct current (1 700 coulombs at 10 volts) was passed between an intraaortic cathode (stainless steel wire, extending 10 cm beyond the tip of a plastic catheter) and platinum anode electrode in the shoulder muscles. (*a*) External surface of aorta. Oedema and brown-black discolouration are seen in the adventitia in an area approximately 3×2 cm. Microscopically, the numerous vasa vasorum in this region were dark brown. (*b*) Inside the aorta, opened lengthwise. The brown vasa vasorum were found to be a branching network of twigs all supplied by a single dark brown artery (arrow) arising from the lumen of the aorta. The intraaortic cathode, which had been lightly touching the intima, caused a small ridge (white arrows) of focal oedema. This ridge passes close to the dark artery, which seems to have served as a preferential pathway for the electric current. The media between the injured intima and adventitia was not substantially injured (see Fig. XII: 16 *a*).

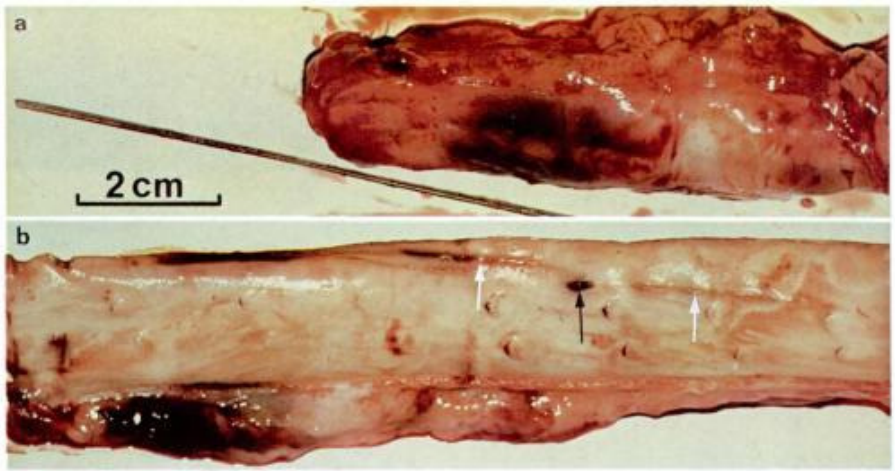

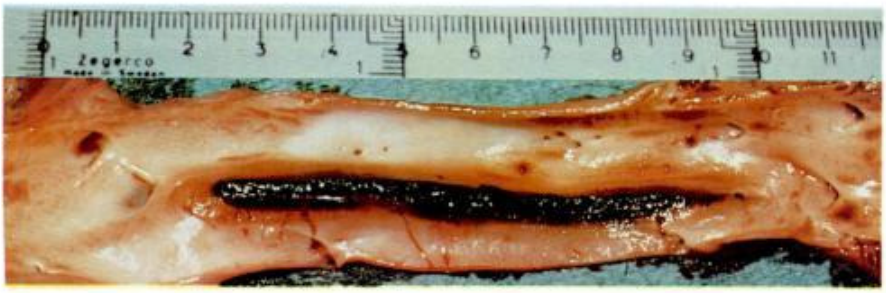

Fig. XII: 15. Serious injury provoked by direct current to the aorta in a dog. 500 coulombs at 10 volts were passed between the cathode, pressed against the aortic intima, and the anode in the shoulder muscles. All layers of the aorta were necrotic (see Fig. XII: 16 *b*).

men was then opened by a longitudinal incision (Fig. XII: 14 *b*). It showed only minimal injury macroscopically as a small ridge of oedema where the guidewire cathode had been in contact with the aortic wall (white arrows). This finding is a clear discrepancy from the widespread oedema and discolouration of the external aortic wall. A local dark spot (arrow) was also found, representing the orifice of an artery. By dissection, the artery was followed as a dark channel in a cranial direction to the discoloured section of the aorta, where it ramified into the dark brown vasa vasorum. In this case, the relatively minor intimal injuries at the site of the cathode and the widespread changes in the distribution area of vasa vasorum arising from a single artery appear to indicate a preferential pathway in this vessel for the flow of electric current.

A local, marked injury to the aortic wall can, on the other hand, also be provoked (Fig. XII: 15). In this case the stainless steel cathode was pressed firmly against the inside of the aortic wall while 500 coulombs at 10 volts potential difference were passed between the electrodes (intraaortic cathode and a platinum anode in the prostate gland of each of 3 dogs). Externally the aorta showed no discolouration or obvious oedema. Arteries arising locally from the aorta showed no discolouration.

Histologic sections of cathodic injuries to the aorta are illustrated in Fig. XII: 16. Fig. XII: 16 *a* shows the left part of the aortic specimen in Fig. XII: 14 *b*. Coagulation injury and oedema were found mainly in the outer part of the media and in the adventitia. Foci of dark amorphous material were interpreted as representing destruction of blood and walls of the vasa vasorum. Fig. XII: 16 *b* shows the severe cathodic injury seen in Fig. XII: 15 of the intima (left), media and adventitia at the site of direct contact of the electrode with the aortic wall.

Thrombosis was not seen at the metal surface of the cathode. As an electron emittor, the cathode does not corrode. Serious damage to the vessel wall appears to be avoidable if the electrode is kept away from the intimal surface. In the case illustrated in Fig. XII: 14,

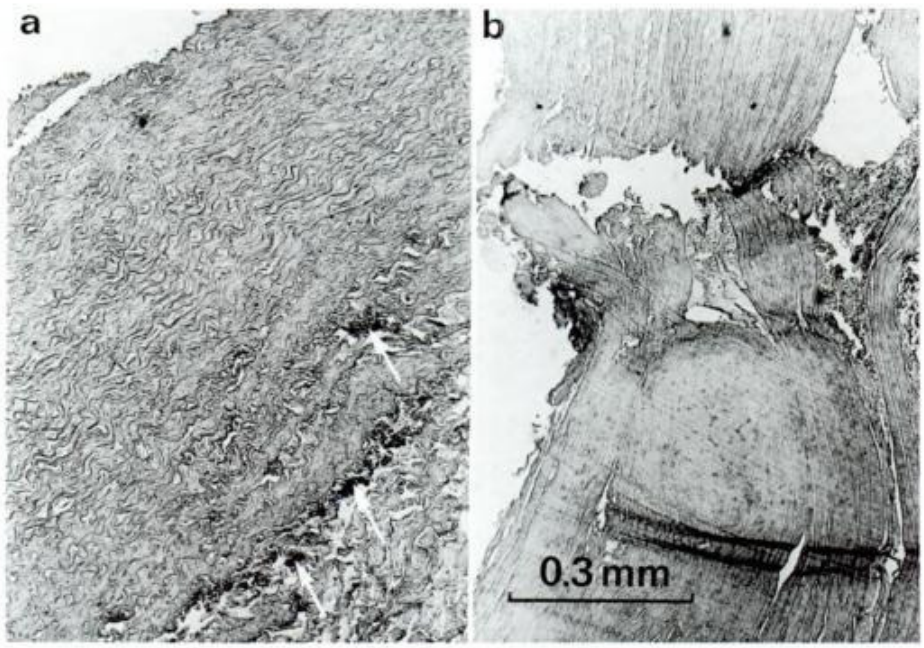

Fig. XII: 16. Injuries by direct current to the aortic wall: histologic sections. (*a*) Macroscopic injuries localized mainly in the peripheral layers of the aorta (left part of Fig. XII: 14 *b*). Foci of destruction of aortic wall tissue are seen (lower right) in the outer part of the media and in the adventitia, which were oedematous. In the injured part of the wall, foci of dark amorphous material are also present, interpreted as necrotic blood from the vasa vasorum.
b corresponds to the injury shown in Fig. XII: 15. Intima to the left. Marked coagulation necrosis extends through all the layers of the aortic wall. The specimen ruptured easily during histologic preparation. Scale same in each view.

the current produced only minor injuries to the intima close to the electrode.

In all the dogs, the experiments revealed that it was possible to pass direct current selectively over veins and arteries. This finding was possible with vessels of a calibre down to less than one mm in width and voltages up to 10 volts. As potential difference increases, the resistive properties of the vessel walls become increasingly critical. Although little detailed information has yet been obtained on these important correlations, at 40 volts electrode potential the prerequisites for selective transport in tissue seem, however, to be suspended (Fig. XVII: 14).

The experiments of this section suggest that veins and arteries can serve as selective pathways for electric current, even when generated at energies well above what is commonly encountered in biology.

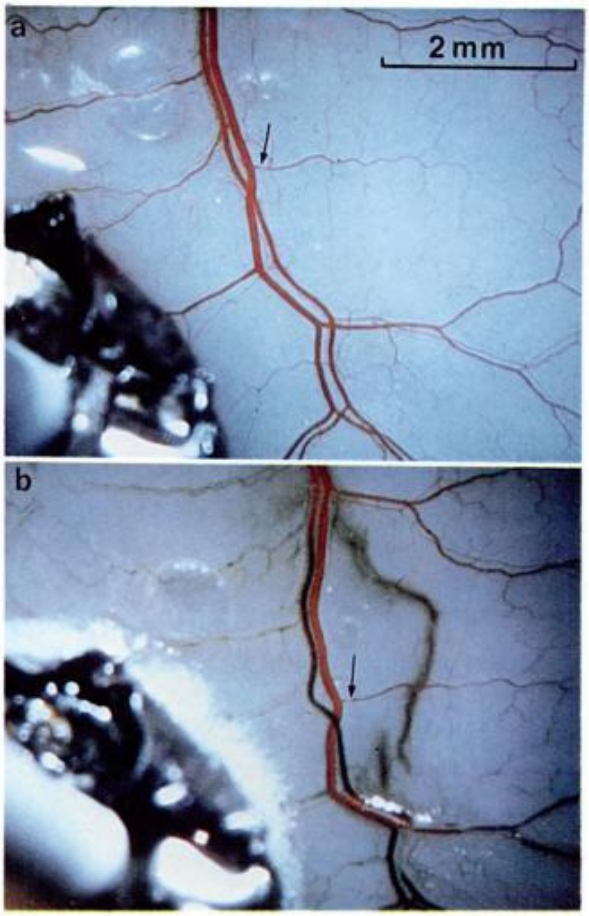

Fig. XII: 17. Intraarterial effects of the passage of direct current between electrodes in the aorta and mesentery of a dog. The aortic electrode is electronegative (cathodic). The mesenteric electrode is electropositive (anodic) and visible in the lower left corners of the illustrations. (*a*) Before passage of current. The large vessel is a vein and the adjacent vessel an artery. Note that a small venous branch is blocked just before entering the large vein (arrow). (*b*) After passage of current (one volt potential difference). Initial flow of current was 1.8 microamperes. Small arterial branches within a few minutes showed multiple contractions, diapedetic bleedings and formation of thrombi. After 75 minutes about 0.08 coulombs had passed and the large artery thrombosed and turned brown. Eventually the corresponding vein showed some discolouration (after about 3 hours). The venous branch, still blocked (arrow), reveals no discolouration or other change. Consequently, the electric current can be inferred to flow preferentially through the artery, which thereby constitutes a major channel of communication between the electrodes.

2. Anodic field

As destruction of tissue is easily produced by direct current in the anodic region, the studies of morphologic changes were performed mainly under direct microscopic observation of dog mesentery in vivo. The abdomen of each of 5 anaesthetized dogs was opened and several different sections of mesentery were used. These experiments revealed that a preferential pathway for the current could be recognized in macroscopically visible small arteries and veins even at electrode potential differences up to 10 volts. In these experiments, one electrode (anode) was placed gently against the mesentery and one electrode (cathode) was placed in the aorta. The selective pathway for the electric current will be illustrated in the following way:

In Fig. XII: 17, the edge of a 4×5 mm platinum electrode is seen to the lower left placed directly on a dog's mesentery. A constricted or thrombosed vein (arrow) is seen in Fig XII: 17 *a* before the application of one volt between the electrodes. The adjacent, slightly smaller vessel is the corresponding artery. Upon application of one volt between the electrodes, initial current of 1.8 microamperes passed through the circuit. Small arterial branches soon developed many regional contractions, the flow of blood became interrupted and thrombi formed around the anodic electrode against the mesentery. Diapedetic bleedings also appeared in multiple small areas.

After 75 minutes about 0.08 coulombs had passed between the electrodes. The blood in the large artery thrombosed and became brown. The blood in the corresponding large vein flowed as before, retaining normal colour (Fig. XII: 17 *b*).

The continued flow in the large vein could, of course, depend on supply of fresh blood from nonoccluded arterial branches and a washing out of venous thromboemboli. This explanation, however, appears unlikely because the blocked venous blood vessel branch (arrow) appeared unchanged even as the blood in the large artery turned brown. Blood was also flowing through the vein at the site where it crossed under the artery and even where it was positioned between the anode and the artery. After about 3 hours, venous

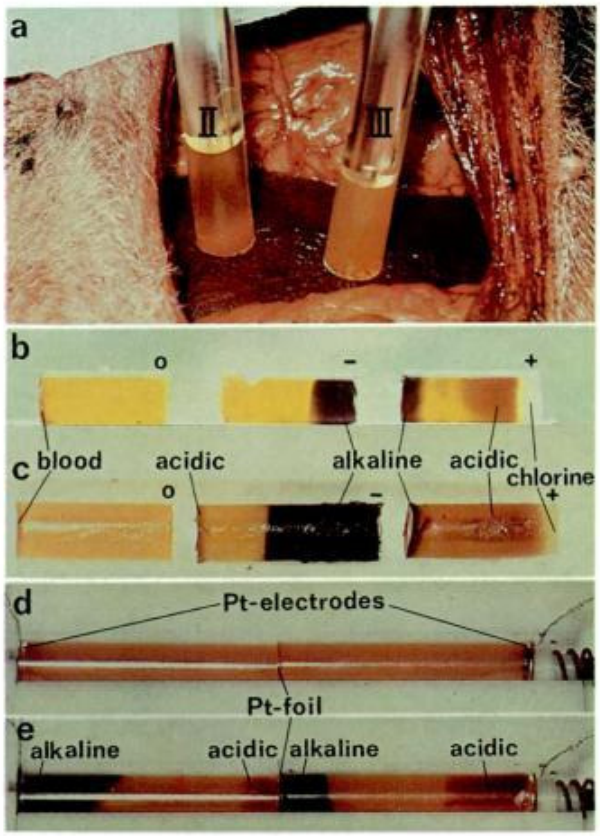

Fig. XII: 18. Demonstration of the same type of closed circuit reactions at the splenic surface of an anaesthetized dog (Figs. *a–c*) as at the surface of an interpositioned electrode material (platinum foil) in the circuit of an in vitro experiment (Figs. *d, e*). (*a*) Direct current is passed in vivo between one platinum electrode (I) in the inferior vena cava of a dog and one electrode (II) in contact with KCl-agar-litmus in a glass tube cylinder resting against the exposed spleen. A glass tube cylinder with KCl-agar-litmus (III) without an electrode is used to check spontaneous diffusion at the contact of the salt bridge and the organ. (*b*) Three specimens of the cylinders are shown with electrode attachments to the right, contact with spleen on left. *Right specimen:* electrode II anodic, after 10 volts and 5 coulombs. The agar cylinder shows a partially chlorine-bleached acid (red) reaction adjacent to the former site of the electrode and an alkaline (blue) reaction where the cylinder rested against the spleen. *Middle specimen:* electrode II cathodic, after 10 volts and 5 coulombs. Alkaline reaction is obtained adjacent to electrode II. *Left specimen:* no current, shows only some blood from the surface of the spleen. (*c*) The experiment performed as above, except with approximately 25 coulombs at 20 volts. *Middle specimen:* electrode II cathodic. A strong alkaline reaction is obtained adjacent to the electrode. A thin, bright red, acidic reaction is seen where the cylinder rested against the splenic surface. *Right specimen:* electrode II anodic. Bleaching and acidity are evident at the anode. The site of contact with the spleen is alkaline. *Left specimen:* no current, no litmus reaction. (*d, e*) Illustration of behaviour of a bipolar electrode (platinum foil) before (*d*) and after (*e*) applications of current between platinum electrodes. The same types of surface reactions, depending on direction of current, are created at the surfaces of the foil as at the surface of the spleen.

branches also thrombosed close to the electrode, but the tendency was clear for a considerably earlier brownish discolouration of the blood in the artery between the tissue electrode and the aortic electrode. Findings were similar in the other 4 dogs.

These experiments, like those of the previous section, suggest that electric current flows selectively in the blood vessel between an intravascular electrode and the region of an extravascular electrode. This selective electric transport in vessels was observed even when potential differences were as great as 10 volts between the electrodes and the vessel was only one mm in diameter.

The observations in the cathodic and the anodic areas each support the postulated principle that vessels function as electrically insulated cables with internal conducting properties.

D. Structuring of interfaces in BCEC systems: development of membranes and organ capsules

In tissue between metal electrodes, closed circuit electric transports are accompanied by polarization phenomena with deposition of material on electrode surfaces. For example, when direct current is applied between platinum electrodes in tissue, several kinds of material and structures can be identified at the surfaces of the electrodes. With this background, fibrous membranes, including organ capsules, basement mem-

Fig. XII: 19. In vitro electrophoresis of fresh dog liver tissue in the mid-part of a glass tube and KCl-agar-litmus on both sides of the tissue sample. Electrodes at the open ends of the glass tube. (*a*) Before direct current was applied, (*b*) after 20 volts, 0.35 coulombs, alkaline (left) and acidic (right) electrode reactions were obtained. To the right of the specimen the reaction was alkaline, to the left acidic. These reactions at the surfaces of a specimen are less obvious than the corresponding reactions in vivo illustrated in Fig. XII: 18.

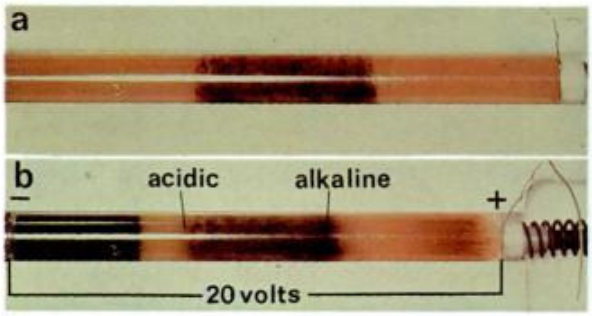

branes and cell membranes should be looked at anew. *Fibrous membranes* can actually be produced easily not only at electrode surfaces but also *between electrodes* in tissue, as will be shown in Chapter XVI. The principle of existence of a biologic equivalent to an electrode-electrolyte interface will now be presented.

Reactions at interfaces in BCEC systems can be anticipated to lead to a large variety of structural developments. To test the hypothesis that the development of fibrous membranes, e.g., intraabdominal organ capsules, may be a BCEC-induced phenomenon, the following experiment was performed in vivo in three dogs.

A platinum electrode (I) was inserted via a catheter from a femoral vein into the inferior vena cava of the anaesthetized animal (Fig. XII: 18). Another platinum electrode (II), shaped like a small disc, was placed in a glass tube (8 cm long and 0.8 cm wide) filled one-third full with a mixture of 0.9% KCl+2% agar-litmus. The abdomen of the animal was opened so that the tip of the agar-salt bridge of electrode II could be placed against the surface of the liver, the spleen or a kidney. Fig. XII: 18 *a* shows the exposed surface of the spleen with electrode II to the left and a "blank" bridge III to the right, without a platinum electrode. This salt bridge was used to check possible spontaneous diffusion at the contact between the bridge and organ surface. Current was then led between electrode II in contact with the test organ and electrode I in the inferior vena cava. Potential differences between 2 to 20 volts were tested between 10 to 30 minutes, each test with new salt bridges.

Fig. XII: 18 *b* shows the colour changes of KCl-litmus-agar cylinders after two experiments each with 10 volts potential difference applied for 15 minutes. To the right, after the electrode had been anodic (+), chlorine has partly bleached the otherwise acidic red electrode end of the cylinder. Its other end, which had been in contact with the splenic surface, shows a blue alkaline reaction. The middle cylinder shows this experiment after the electrode had been cathodic (−). The electrode end of the cylinder shows an alkaline reaction. The left salt bridge showed only some contamination of blood on the contact surface against the organ, but no litmus reaction.

The experiments were then repeated with 20 volts potential between the electrode in the inferior vena cava and the electrode with a salt bridge interpositioned against the splenic surface. The result is shown in Fig. XII: 18 *c*. The right cylinder shows in principle the same reactions as the right cylinder in Fig. *b*. The middle cylinder, however, shows an additional interesting reaction. The alkalinity at the cathode is accompanied by a bright, red zone of acidity, corresponding to the site of contact with the splenic surface. These findings were consistent in the three dogs studied, with application of the electrode bridges at different sites on the hepatic and splenic surfaces.

These studies also showed a clear tendency for an alkaline reaction of the salt bridge to be more easily produced at the organ surface than an acidic reaction. Furthermore, it was found that when electrode II was made anodic, the organ surface under the salt bridge shrank and became dry. When the electrode was made cathodic, a profuse flow of tissue water appeared around the bridge. These findings appear to represent an expression of electroosmotic water transport.

For comparison, Fig. XII: 18 *d, e* illustrates the development of redox reactions at the surface of an electron conductor, a platinum foil, positioned in the mid-part of a KCl-litmus agar cylinder when current is led through the cylinder between two platinum electrodes at either end. The same types of surface reactions are created on the inserted foil as were created on the surface of the spleen.

Electrophoretic experiments were also performed on fresh specimens of dog liver. Thus, Fig. XII: 19 *a* shows a liver specimen in the middle part of a glass tube with KCl-agar-litmus bridges and platinum electrodes before treatment. After application of 20 volts between the electrodes (Fig. XII: 19 *b*), blue and red colouring developed adjacent to the platinum cathode and anode. Corresponding to the interface between specimen and salt bridge, blue colouring developed on the anodic side and red on the cathodic side.

These reactions adjacent to biologic material should not be accepted without reservation as proofs of the existence of analogues to electrode reactions at the surfaces of various organs. Alkaline and acid compounds may, for example, have been produced by tissue metabolism. Under the influence of the applied electric potential between the electrodes, such compounds may have separated electrophoretically and therefore given the observed litmus reactions. It should be noted that these reactions were found to be more pronounced in vivo than in vitro. This finding is remarkable in that the in vivo experiments should be influenced by the buffering capacity and circulation of the tissue fluids.

The experiments do indicate, however, that interphase transports may take place within a closed electric circuit, including the surface of an organ. If biologically closed electric circuits become accepted as a biologic mechanism, the development of several important structural components, e.g., organ capsules and perhaps also basement membranes and other fibrous membranes, may become explained.

Let us anticipate for a moment that the functional activities of an organ such as the liver (Chapter VI, Fig. 19) cause it to polarize against a nearby structure, such as the abdominal wall. The abdominal muscles also produce metabolic polarization which should fluc-

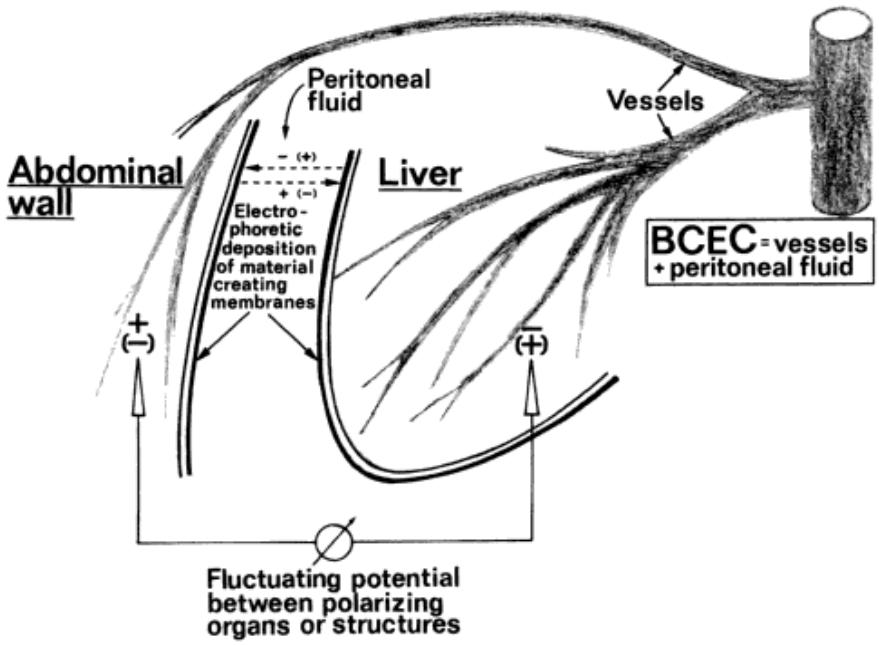

Fig. XII: 20. Suggested principle for development of biological membranes as organ capsules. Metabolic activities in nearby tissues or between adjacent organs create differences of potential, giving rise to a driving electromotive force through a biologically closed electric circuit (BCEC). Asynchronous times of polarization of adjacent tissues or organs account for ebb and flow transport. Materials then become deposited against electrode-equivalent surfaces of the circuit, or are deposited by trapping and surface adsorption in adjacent tissue matrices. When the membrane has obtained a certain thickness, the polarizing current may be anticipated to cease.

tuate in intensity, asynchronously in relation to the polarizations of other organs, including the liver. If such structural units are joined in a closed electric circuit, an electrophoretic interphase deposition of material from the organs and the fluids positioned between the structures should take place. This deposition is illustrated schematically in Fig. XII: 20. The asynchronicity of the metabolic polarizations of two adjacent organs, such as the liver and the abdominal wall, accounts for a two-way current. A kind of ebb and flow effect on material is thereby induced, which might be the prerequisite for a complete and suitable composition of the membranes of both organs. As material accumulates at polarizing organ surfaces or other structural interfaces, the polarizing current will diminish and eventually cease. Consequently, the thickness of the membranes should be determined by the driving force of the metabolic polarizations.

An "everyday observation" which may partly support this theory is the development of a fibrous capsule around cardiac pacemaker devices in the subcutis and around intracardiac pacemaker electrodes. In these instances part of the closed circuit is the wiring of the device and part is the electrically conducting material in the tissues. When the fibrous material has obtained a certain thickness, successful function of the pacemaker requires either the driving potential difference to be increased or one has to replace the pacemaker and the intracardiac electrode.

Circular membrane-like structures will also be shown (Chapter XVI) to develop from interphase deposition of material between "A" and "B" zones around polarizing breast cancers. Furthermore, it will be seen that such interphase structures can be produced by closed circuit transports between electrodes and against electrode surfaces in tissue. Mixed anodic and cathodic fibrous material produced in this way adjacent to platinum electrodes in tissue will be seen to be strikingly similar histologically to fibrous membranes which develop endogenously. It is important to point out, however, that mechanisms of adsorption of material to the surfaces of tissue matrices must be involved in these processes.

E. Capillaries and VICC

1. Biologic transfer of electrons

Long distance transport of material in biological systems is currently regarded as a function of mechanical transport mechanisms and diffusion. Long distance

transport of electric energy can be induced over cables by an electric source with electrodes inserted into living tissue or an electrolyte. The electrode surfaces and adjacent electrolyte then serve as conversion sites between electronic and ionic electric charges. How does this picture correspond to the possibilities of a BCEC system without obvious electrode surfaces?

First, there is no disagreement about the fact that short distance electron transfer takes place between molecules in biology as an expression of redox reactions. But the processes themselves are remarkable because most organic molecules behave as dielectrics. Bockris and Dražić (5) discussed the possibility of electronic charge transfer by rotation of such molecules, but rejected the possibility. Instead they referred to the fact that large protein and enzyme molecules are semiconductors, as pointed out by Szent-Györgyi (71). The high activation energy in semiconduction seemed, however, to make this mechanism unlikely until it was found that the protein cytochrome oxidase could give kinetic evidence of semiconduction (10, 11, 12). The activation energy of semiconduction of this enzyme molecule was also found by Straub (69) to be approximately equal to the activation energy of the enzymatic reaction catalyzed by the molecule. It has also been shown by Trukhan (75) that electron conduction within molecules may be considerably higher than conduction across interfaces between particles. This effect is explained as electronic tunneling or a microwave Hall effect on mobility of electrons (54).

As pointed out by Bockris and Dražić (5), a significant mobility of electrons can be understood in the case of many enzymes having conjugated double bonds (—C=C—C=C—). The resonance effect of excited electrons then produces huge orbitals along the chain.

In protein molecules without long conjugated double bonds but with cross-linked polypeptide bonds,

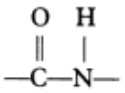

gives the following form of the chain

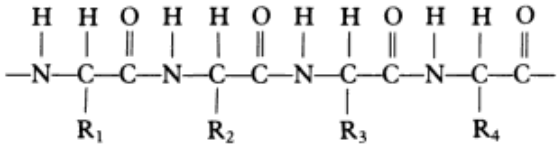

The orderly repetition of the peptide bond should then be able to produce an electronic conduction band, as in ordinary semiconductor crystals.

Another possibility is that the close connection between the electron-donating NH and electron-accepting CO groups may permit electron tunneling through the peptide chain (11).

Different other models have also been suggested (4, 23) which indicate the existence of different electron transport systems in biologic material involving intra- and intermolecular transfer of charges. Rosenberg (54), for example, has shown that wet crystalline haemoglobin is an electron conductor.

The reason for referring to the works above should be evident: the function of a BCEC, such as the VICC, will require an electrode-electrolyte analogue allowing regional transfer of electrons. Only in this way can the ionic conduction, transport and recombinations of a BCEC be activated and lead to purposeful biologic structuring and function.

Experimental studies of electron exchange systems between molecules represent one important approach to these problems. Another approach may be to look for possible reaction sites in organized living systems.

We are here particularly interested in the VICC. Where should redox-steps most likely be located in this circuit? The answer would probably be; somewhere in the capillary wall, as this serves as an intermediate partition for the exchange of material between blood and tissue.

2. The capillary wall

Gases, water, ions, and compounds of low molecular weight pass over the capillary membranes by diffusion, filtration and osmosis, according to prevailing opinions (24, 25). In these transports, transmural hydrostatic pressure differences, colloid osmotic pressures and concentration differences across the membranes play important roles. The endothelial cells themselves are permeable for lipophilic substances such as gases, but not for hydrophilic substances (53). The latter pass through the capillary walls through interepithelial spaces (82), called stomata, pores or leaky junctions. Another type of transport is called micropinocytosis or cytopempsis (29), in which small vesicles transport material through the endothelial cells (47). Morphologic studies and studies with radioactive tracers have led to the hypothesis that the vesicles may to some extent transport proteins and colloidal particles across the endothelium (7, 47). The function of the vesicles is, on the whole, not very well understood. Their function must also be distinguished from that of transport through the channels of the "leaky junctions" (82). Before we discuss an additional possible mechanism, electrogenic closed circuit transport over the capillary membrane, a short survey of the morphology of capillaries is necessary.

A lengthwise section of a capillary is illustrated schematically in Fig. XII: 21 *a*. It contains six layers (13). On the outside is the basement membrane. Between the basement membrane and the periphery of an endothelial cell is the so-called exoendothelial space.

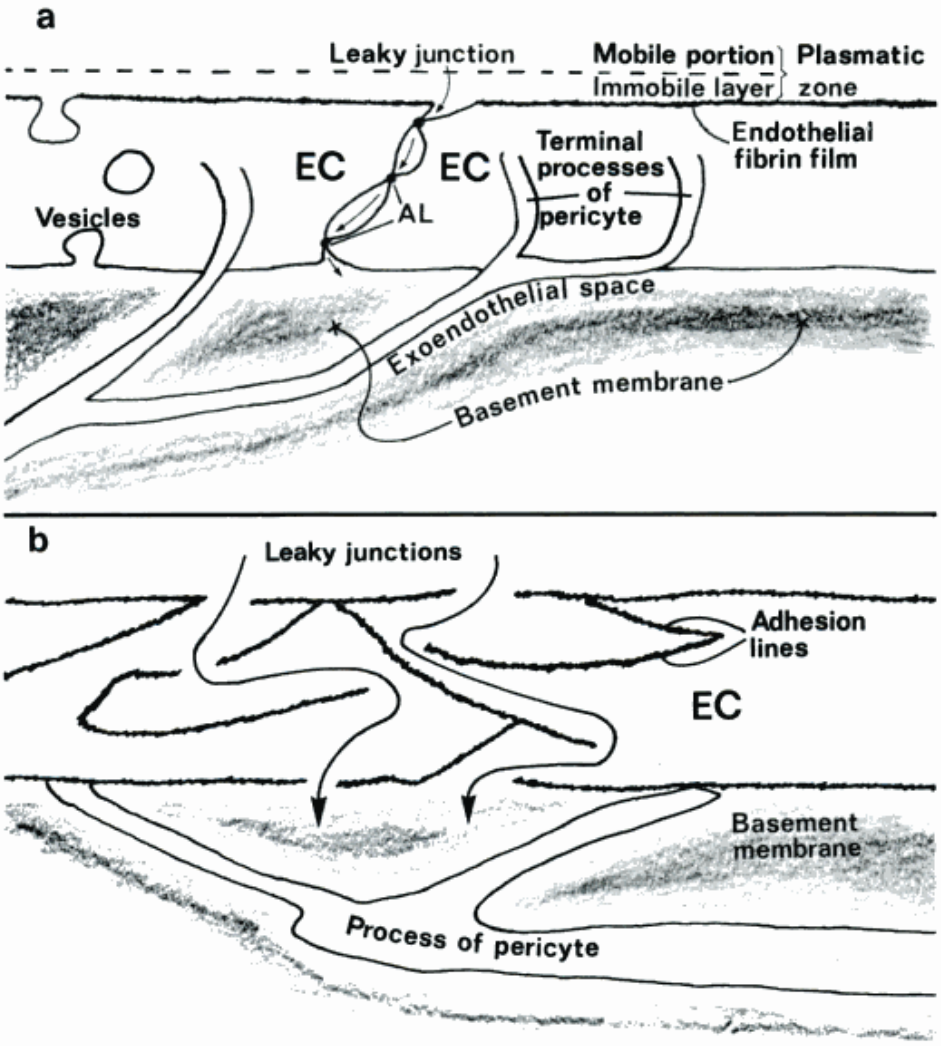

Fig. XII: 21. A capillary wall: schematic presentation, (*a*) lengthwise, and (*b*) crosswise sections. Six layers are recognized: basement membrane, exoendothelial space, endothelial cells (EC), endothelial fibrin film, immobile and mobile layers of the plasmatic zone. Adhesion lines (AL) between adjoining endothelial cells form leaky junctions for water, electrolytes and large molecules and probably also for blood cells in diapedetic transport. Additional mechanisms of transport include diffusion, filtration and pinocytosis (via vesicles) through the endothelial cell. The pericyte (see Fig. XII: 22) makes contact with some of the endothelial cells by ramifications of primary and secondary (terminal) processes. The endothelial cells measure in thickness about 1 μm. The thickness of the basement membrane is about 600 Å, which in actuality is much less than as depicted in the figure.

The endothelial cell has an endothelial fibrin film, which borders the lumen of the vessel. Next to the fibrin film is the plasmatic zone containing a layer of more or less immobile plasma and finally a mobile plasmatic portion (50).

In the walls of capillaires the endothelial cells make contact only at specific adhesion lines (82). According to this view, the nonadherent parts of adjacent epithelial walls form "leaky junctions". Such junctions (stomata), seen in a plane through the adhesion lines are shown in Fig. XII: 21 *b*. Tortuous distensible channels or clefts are formed in this way. Peroxidase, with a molecular diameter of 20 Å, has been found to pass through these channels, of a presumed cylindrical diameter of 90 Å (82). Even under normal conditions, white blood cells pass by diapedesis through stomata without rupturing their walls (35). Diapedesis takes place by means of pseudopods. Part of the leukocyte moves as an extension through a stoma, which widens. The content of the blood cell then "flows" successively through the stoma into the surrounding tissue. Transcapillary transport of red blood cells also takes place by diapedesis, mainly during venous stasis (35).

An interesting component of capillaries is the peri-

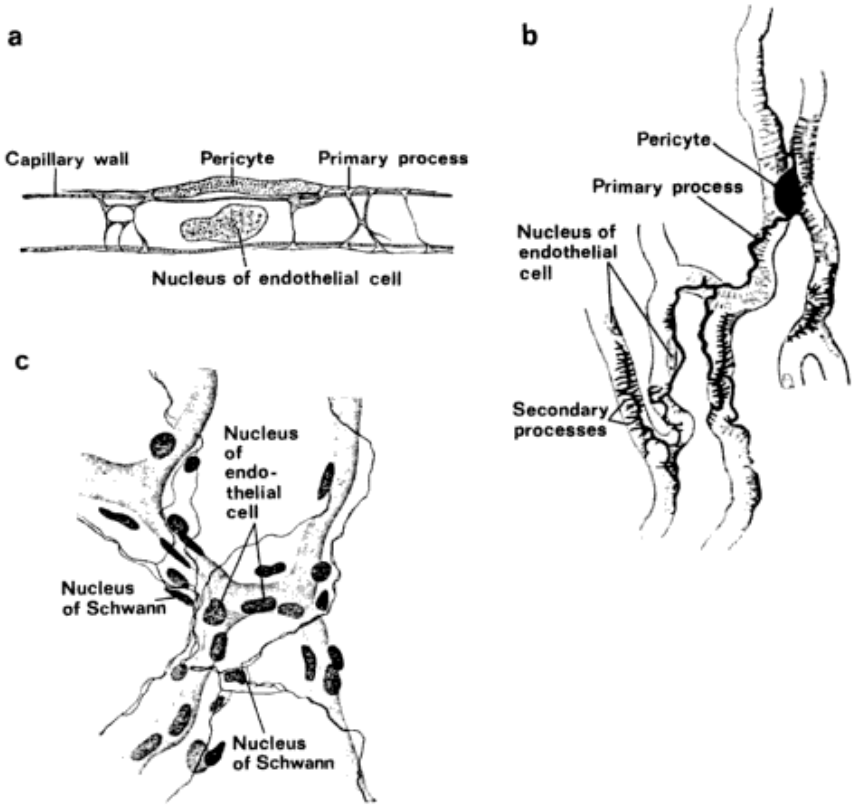

Fig. XII: 22. (*a*) The pericyte (after K. W. Zimmermann, 1923) is a cell located at scattered sites adjacent to capillary walls. (*b*) It usually gives off two primary processes along the vessels. Secondary processes are arranged perpendicularly to the length of the capillary and make contact at certain points with endothelial cells. The pericytes are believed to be part of the mechanism of contraction of the capillaries. Their distribution in intervals along the capillaries suggests that segmental capillary contractions are possible. Pericytes are also thought to possess some phagocytic activity. (*c*) The capillaries are also provided with a delicate network of nerve fibres, which make contact with the periphery of the capillary walls.

cyte, a cell known since 1873 (57). Its shape is described as an ellipsoid, usually with two main processes (Fig. XII: 22 *a*) (83). These processes follow the capillary in its longitudinal directions, giving off secondary processes in a crosswise direction around the vessels (Fig. XII: 22 *b*). The secondary processes make contact with the endothelial cells at certain points (78). The processes of pericytes are also described (35) to appear as intermediate forms of muscle fibres of veins and arteries.

Pericytes are described as involved in the mechanism of contraction of arterioles, venules and capillaries (36, 70, 76, 77). They may also have some phagocytic functions (40). Pericytes have now been found in all capillaries of mammals (78). They are remarkably few in the lung and in the capillaries of small animals such as the shrew, which has exceedingly thin capillary walls (78).

The basement membrane is of considerable interest in this connection. It consists of a collection of material outside the endothelial cells and forms a layer of irregular thickness. It is further separated from the endothelial cells by the so-called exoendothelial space (13). The distal extensions of the pericytic processes cross the basement membrane. A layer of the basement membrane of relatively low electron density (which seems to be identical with the exoendothelial space) has been described toward both the endothelium and toward an adjacent pericyte and its processes (39, 78). The blood capillaries are further provided with a fine reticulum of neurofibrils (Fig. XII: 22 *c*) located at the outer side of the endothelial tube (2, 35, 52).

The control of blood flow to a tissue region depends on pre- and post-capillary resistance (1). Precapillary sphincters (84) and arteriolar smooth muscle adapt their activity to the metabolism of the tissue and to signals from central sympathetic influences (2, 17, 52).

How does this picture of the structure and known functions of the capillaries fit with a presumed VICC, permitting selective closed circuit electrogenic transports of material between blood and tissues? At a first glance it may seem unlikely or even impossible to assume the existence of simultaneous redox reactions and closed circuit ionic transports in the presence of leaking pores of the capillary walls. Reversible redox sites adjacent to leaky junctions in the capillary wall should perhaps at the most permit small and rather inefficient circuits. For further insight into these problems, we will first turn to direct in vivo studies of the behaviour of small vessels and capillaries, exposed to electric fields.

3. Capillary reactions in electric fields

Direct in vivo microscopy and microphotography were performed of vessels of the mesentery of eleven dogs. One platinum electrode was gently placed against the mesentery, one was placed in the aorta and one in the inferior vena cava. Four possibilities to vary the electric field around the mesenteric electrode were then available. Direct current voltages of 100 mV, 1, 2 or 5 V were applied between the electrodes. The following results were obtained on microscopic in vivo inspection of small vessels (about 0.1 mm in diameter).

When the mesenteric electrode was electropositive or electronegative in relation to the electrode in the aorta or the vena cava, small arteries contracted immediately in various sites around the mesenteric electrode (Fig. XIV: 1 *a*) at each of the potential differences tested. Blood flow was then completely interrupted in many small arteries. Sometimes they suddenly opened and let the blood flow through. Some small arterial branches showed no contractions, while some showed diapedetic leaking of red blood cells (Fig. XIV: 16). In each of the combinations of polarity and voltages, small arteries were regionally nearly always empty of blood cells. Rarely, veins were slightly more narrow than the adjacent artery. Local contractions over relatively short distances were also seen in small arteries but occasionally also in veins (Fig. XII: 23).

The immediate regional effects of electric fields on calibre of small vessels of the mesentery were then extended to the study of arterioles, venules and capillaries.

A standard dose of 1.2 coulombs at 5 volt potential difference for 20–30 minutes was applied in the four combinations of polarity and electrode positions mentioned above. Platinum electrodes were used. The mesenteric electrode was a 4×4 mm plate gently positioned against the mesentery without causing tissue injury. The electrodes in the aorta and the vena cava were introduced through vascular catheters. A small glass partition was used as a support for the mesentery (plastic material was unsuitable as it easily produced spontaneous diapedetic bleedings). After 1.2 coulombs were applied, pieces of the mesenteries were excised, fixed in formalin, stained (haematoxylin-eosin) and examined microscopically.

The relative appearances of small arteries and veins, arterioles, venules and capillaries could now be inspected. While it is evident that results from instantaneous and prolonged exposure of vessels to electric fields may differ, the actual results are nonetheless informative.

In general, small arteries appeared empty and often very narrow compared to the accompanying relatively wide veins, which contained large amounts of granulocytes. This tendency was present in all four combinations of polarity and electrode positions (Fig. XII: 24). Around the mesenteric anode, granulocytes accumulated in veins in increasing number up to the electrode and even beneath it. Around the mesenteric cathode, an area of about 10–15 mm in diameter was completely free of cellular elements in the arteries and veins. Immediately peripheral to the cell-free zone, granulocytes were collected in veins in increasing amounts up to the cell-free zone.

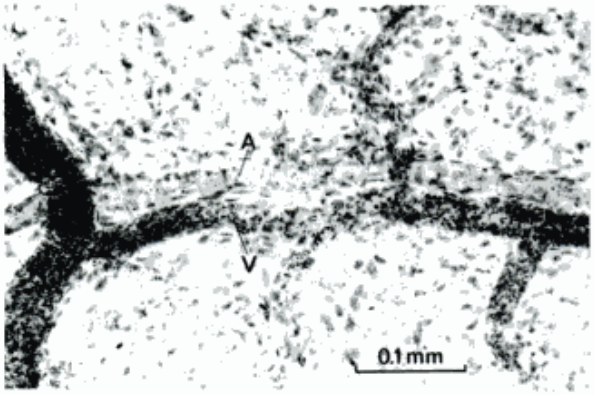

Fig. XII: 23. Regional contractions were commonly observed in small arteries (A) exposed to an electric field. Sometimes a small vein (V) appeared slightly narrower than the accompanying artery as seen in this figure. Mesentery of dog, haematoxylin-eosin.

The locations of granulocytes and the relative calibres of arterioles, capillaries and venules are illustrated in Fig. XII: 25. These studies showed a clear tendency in all four combinations of polarity and electrode position. The arterioles and arterial portions of capillaries were all narrow and empty of blood cells in regions of variable size. The corresponding venules and venous capillaries were wide and contained occasionally large amounts of granulocytes. These cells also appeared often in the interstitial tissue.

In three experiments in dogs, two 4×4 mm platinum electrodes were placed 2.5 cm from each other against the mesentery. These experiments showed the same tendency as the previous experiments with regard to the calibre of arterioles, capillaries and venules and to the local accumulation of granulocytes. Even after application of voltages between the electrodes of as little as 100 mV (10 μA, 30 minutes, 0.018 coulombs), granulocytes collected selectively in small veins, venules and venous capillaries (Fig. XII: 26).

4. Selective distribution of granulocytes in a closed circuit

How is it possible that granulocytes accumulate in veins, venules and venous capillaries when corresponding small arteries, arterioles and arterial capillar-

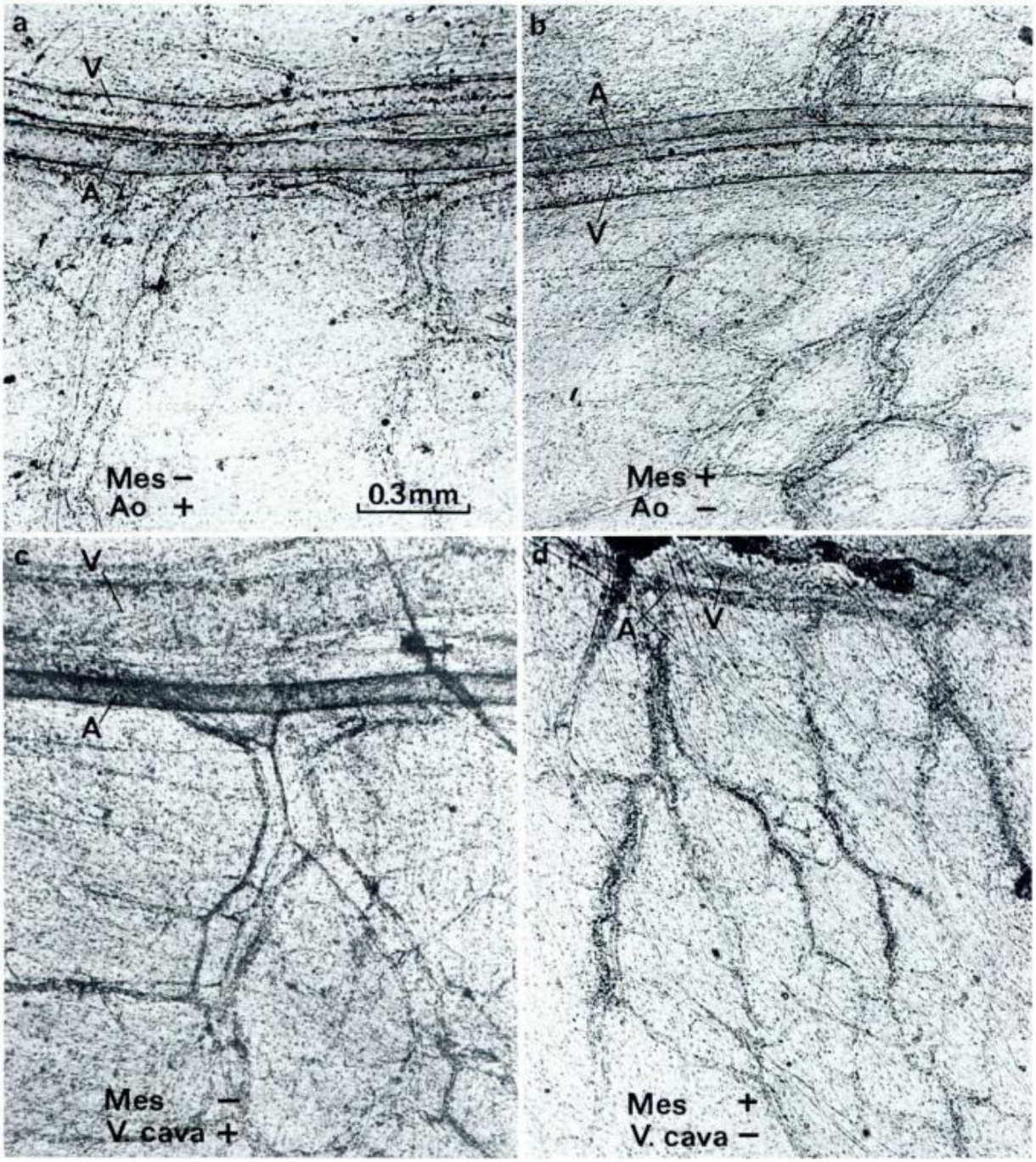

Fig. XII: 24. Overview of dog mesenteries with different electrode positions and polarities, each exposed to 1.2 coulombs at 5 V between the electrodes. In each of the electrode combinations small arteries were empty of blood cells. Small veins contained varying degrees of increased numbers of granulocytes outside a cell-free zone around the electronegative mesenteric electrode (*a* and *c*) and directly up to the electropositive mesenteric electrode (*b* and *d*). A = "small" arteries, V = "small" veins (approx. 0.1 mm in diameter). Mes = mesentery, Ao = aorta, V. cava = vena cava inferior. Scale same in each view. Haematoxylin-eosin.

ies are narrow and empty of blood cells? This problem is further considered in Chapter XIV, Sections I–K, where an alternative theory to so-called chemotactic accumulation of leukocytes and charged compounds in tissue is presented. A preliminary brief explanation will be given in this connection.

All mammalian cells, including blood cells, are known to carry a surplus of fixed electronegative charges on their surfaces (79). Under the influence of an electric field of suitable strength in relation to the charged cells, and considering the factors of cell size, steric characteristics of cellular charges and matrix

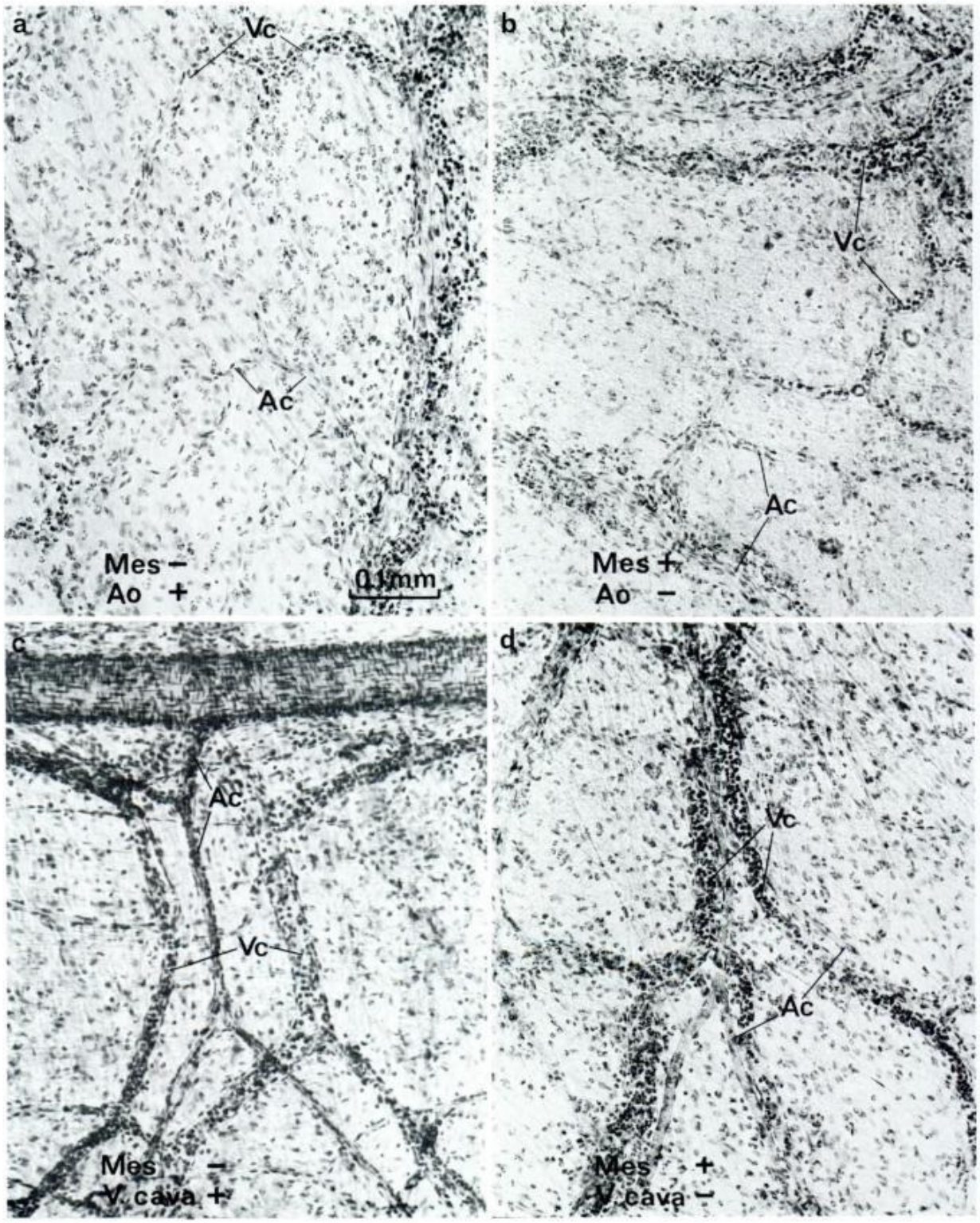

Fig. XII: 25. Distribution of granulocytes in four different combinations of electrode positions and combinations of voltages in dog mesentery. In each combination arterioles and arterial capillaries (Ac) are empty and narrow while the venules and venous capillaries (Vc) are relatively wide and contain granulocytes, some of which also appear in the tissue. Mes = mesentery, Ao = aorta, V. cava = vena cava inferior. Scale same in each view. Haematoxylin-eosin.

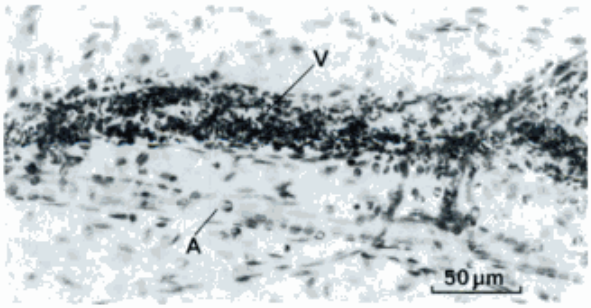

Fig. XII: 26. Mesentery of dog. Narrow small artery (A) is virtually empty of cells and widened small vein (V) contains selectively accumulated granulocytes peripheral to the zone free of cells around the cathode. Anode positioned on the mesentery 3 cm away from the cathode. 100 mV, 10 μA, 30 minutes, 0.018 coulombs. Haematoxylin-eosin.

properties of tissue, the charged cells will be attracted or repelled depending on the polarity of the electric field. *The electronegative granulocytes will consequently be attracted to an anode and repelled by a cathode like any charged particle in an electrophoretic process.* This process requires an activated closed electric circuit, which in the present experiments was created by an external source of electric power, cables, electrodes and the conducting media in the tissue. We are therefore still only simulating the existence of a BCEC in our experiments. This is one of the reasons we must wait until later (Chapters XIV, XVI) for discussion of how granulocytes can accumulate electrophoretically over an endogenous, activated closed circuit (the VICC).

The accumulation of granulocytes in vessels toward the anode, positioned against the mesentery, is readily explained as an electrophoretic attraction of the granulocytes. Around the cathode, however, electronegative particles and cells should be repelled. A cell-free zone was therefore also regularly observed around the cathode. Nevertheless, outside this zone large amounts of granulocytes accumulated in vessels (Fig. XII: 26). The mechanism of this phenomenon is explained in Chapter XIV (and illustrated in Fig. XIV: 18).

5. Mechanisms of regional contraction of arterioles and arterial capillaries

Is there any mechanism which can explain the local regions of field induced contractions of small arteries, arterioles and arterial capillaries while corresponding venous vessels are wide? The capillaries, small vessels arteries and veins are provided with nerve fibres which evidently offer one possibility for neurogenous impulses of contraction. Another or an associated mechanism may be connected to the pericytes, which furthermore are described to be involved in the contraction of capillaries. We may now focus our attention to the remarkable fact that pericytes are sparsely found in the lungs and in the vessels of very small animals (78).

Let us anticipate that the pericytes are involved in a mechanism of segmental small vessel contractions induced by electric fields of a closed circuit (identified as a VICC system). In this case pericytes should not cover the entire capillary net as this should jeopardize a segmental mode of contractions. Consequently, possibilities of modulating selective closed circuit, "long- or short-distance" electrogenic transports should not be possible (see also Fig. XII: 30 *a*). Small animals as the shrew (smallest mammal, weight 2 g) should need very few pericytes because their capillary membranes are exceedingly thin. The shrew may get along well simply by diffusion through the thin capillary membranes. The sparse extent of pericytes in the human lung is perhaps similarly explained. Gas exchange, the main function of the lungs, is sufficiently well covered by diffusion. There is consequently not a very large need in the lungs for an additional mechanism of long distance electrogenic transport.

6. Search for redox sites: possible origin of the basement membrane and the endothelial fibrin film

In attempts to find the sites for the necessary redox steps of the VICC, we must take a second look at the components of the capillary membrane. Certain details of interest are shown in electron micrographs (Figs. XII: 27–29), kindly placed at my disposal by Prof. E. R. Weibel, University of Berne, Switzerland (78).

The basement membrane is a structure about which little is still known of its origin and function. These membranes were recognized as early as 1848 by Kopf and Bowman. They are described as consisting of connective tissue elaborated by cells of mesenchymal origin (Descemet's membrane) or of ectodermal origin (the basement membrane of the lens) (37). Basement membranes are composed of an amorphous matrix, which contains a fine network of partially oriented fibres (37). Chemically, basement membranes contain various sequences of amino acids and carbohydrates. They also contain a low molecular weight glycoprotein and collagen (33) and antigenic protein (6).

Strangely enough, the basement membranes are described as covering the lumens of the anticipated channels of transport, the stomata and the places where vesicles must empty their content into the tissue (13, 48). However, an exoendothelial space (Figs. XII: 21, 27–29) is also described (13, 48), which could represent a space for escape of materials transported through the capillary walls.

Colloids of blood are normally excluded from the interendothelial clefts which are occupied by ground substance contiguous with basement membrane (40,

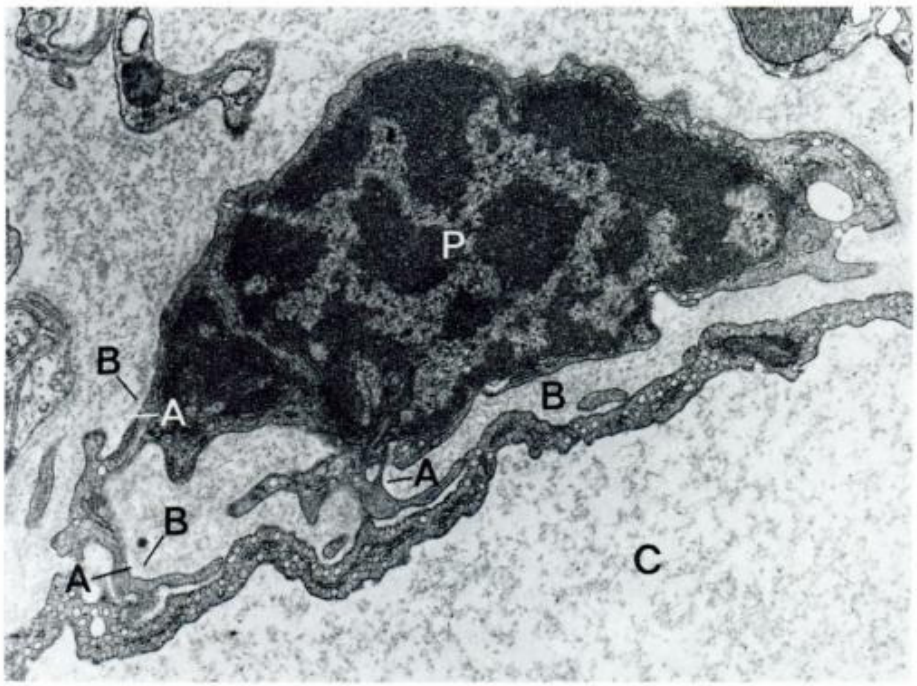

Fig. XII: 27. Electron micrograph of capillary (C) from rat cardiac muscle with pericyte (P). Magnification 20 500×. Basement laminae (B) surround the pericyte and the interstitial side of the endothelium. Note a zone of low electron density (A) between basement laminae on one hand and pericyte and endothelium on the other. It is suggested that the basement membrane represents an apposition of material and not primarily a structural element of the capillary wall.

Fig. XII: 28. Capillary of rat cardiac muscle. Magnification 18 700×. Observe a zone of low electron density (A_p) between endothelium and basement membrane (B) and another broader zone of low electron density (A_i) between endothelium and content of capillary. These findings suggest that similar forces may be involved in the creation of zones of low electron density such as shown for the creation of "A" zones in a contracting movable precipitate adjacent to a fixed "matrix" (see Figs. XII: 1, 4 and 7 and Chapter X). A pericyte process (P) is enframed (see also Fig. XII: 29).

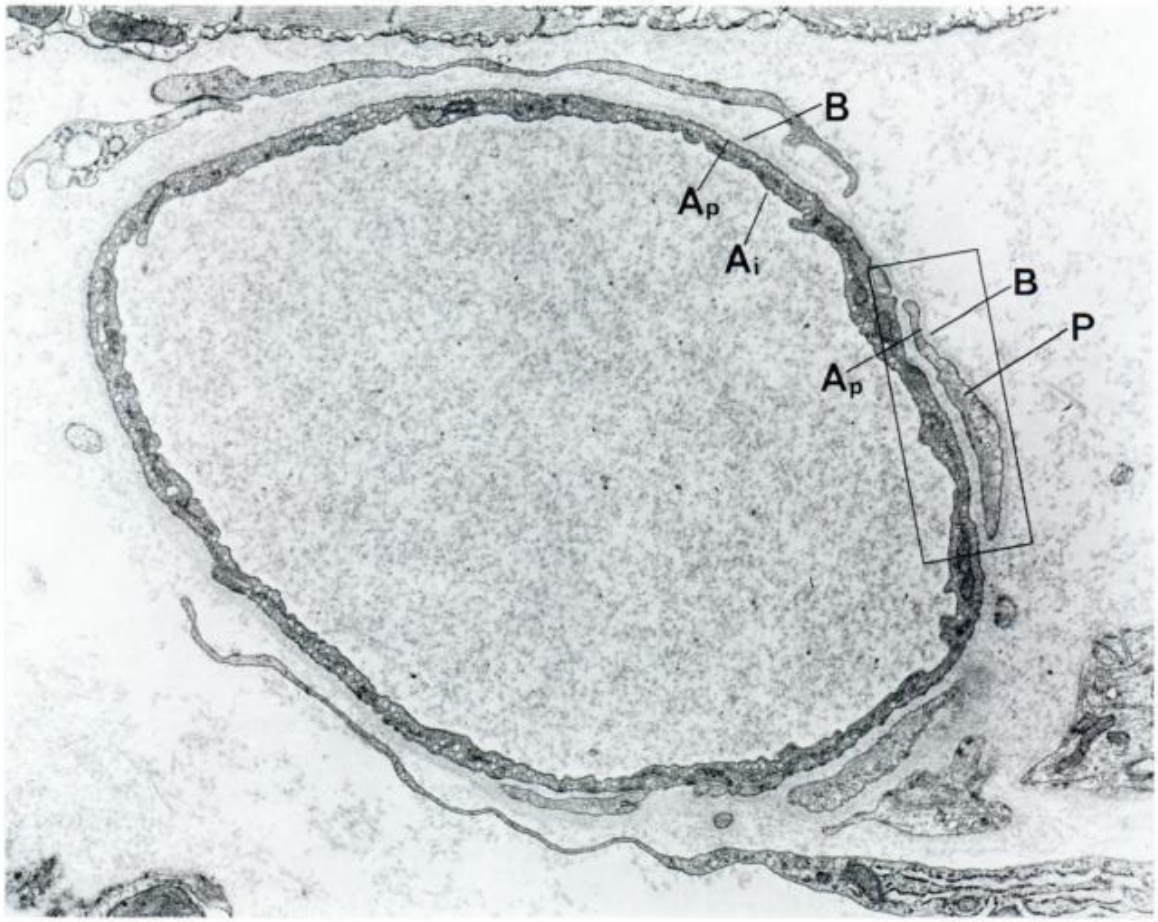

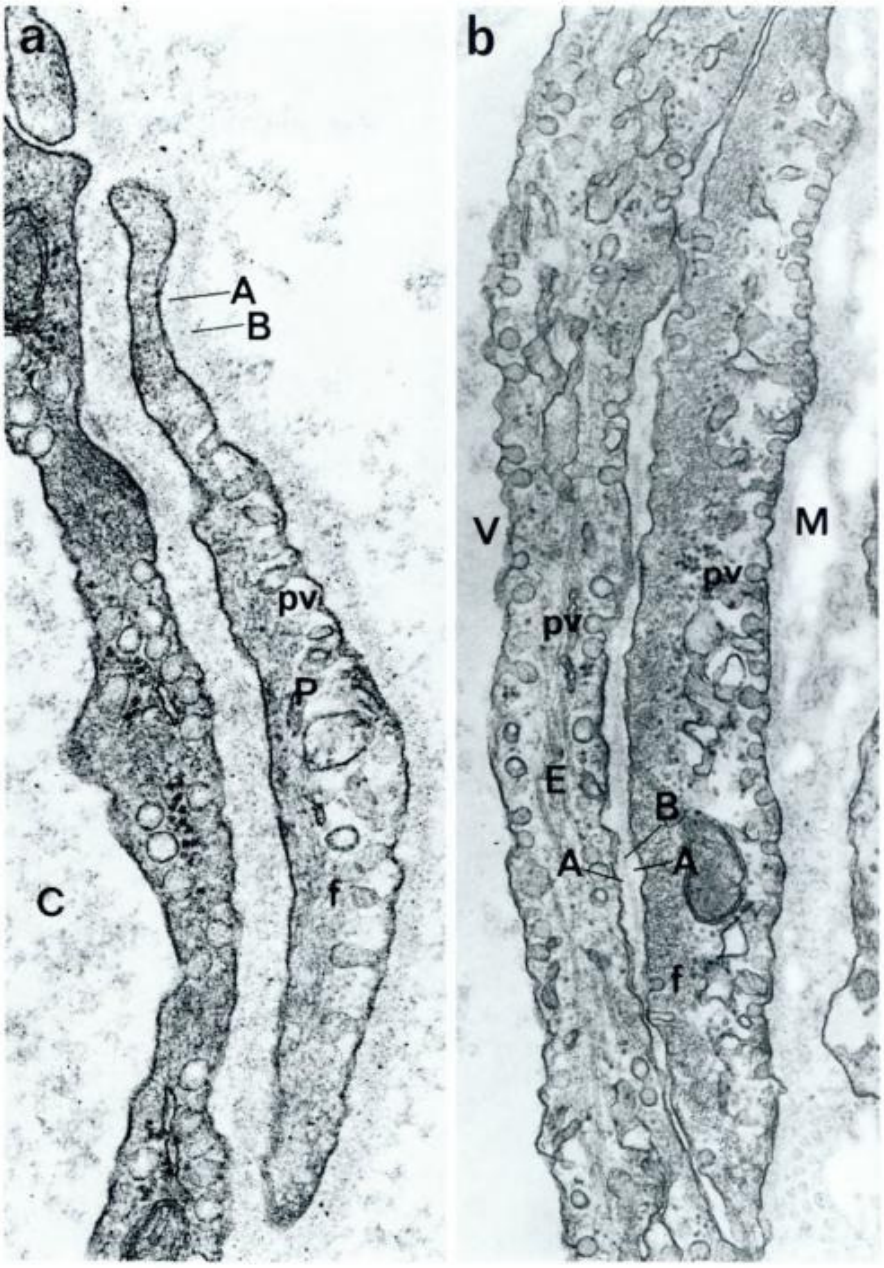

Fig. XII: 29. (*a*) Pericyte process (P), enframed in Fig. XII: 28, shows a web of cytoplasmic filaments (f) and pinocytotic vesicles (pv). Capillary (C). Material of basement membrane (B) surrounds the pericyte process but is separated from its surface by a zone of low electron density (A). Magnification 52 670×. (*b*) Smooth muscle cell (M) on venule (V) shows filaments (f) and vesicles (pv) located predominantly under its right-hand surface. Vesicles in the endothelial cell (E) are more randomly dispersed. Both sides of the basement membrane (B) located between the venule and the muscle cell show zones of low electron density (A). Magnification 38 300×.

48). It has been suggested that the basement membrane constitutes the major permeability barrier of blood vessels (48).

Why is then the partially amorphous, partially structured basement membrane separated from the wall of the endothelial cells? Is it possible that the material of the basement membrane represents a product of nearby "electrode reactions" at the endothelial membrane facing the interstitium? An electron microscopic observation of Low and Weibel (39, 78) now becomes of interest: a zone of low electron density corresponds to the exoendothelial space. Moreover this zone also can be recognized along the surface of pericytes, including their processes. Fig XII: 27 shows a pericyte (P) and one of its processes in contact with the endothelium of a capillary (C) of rat cardiac muscle. The basement membrane (B) is seen not only against the endothelium but also around the body of the pericyte. Beneath the basement membrane is also seen the zone of low electron density (A). Fig. XII: 28 shows this zone between the basement membrane and the periphery of the endothelium (A_p). However, it should also be noted that *a similar but broader zone of low electron density is present between the material inside the capillary and the inner endothelial wall* (A_i). Finally, Fig. XII: 29*a* shows higher magnification of the pericyte process (P) from the enframed section of Fig. XII: 28. The pericyte process is located within the

basement membrane. A zone of low electron density (A) is apparent. Fig. XII: 29 *b* shows endothelium (E) and a smooth muscle cell (M) on venule (V). Between them is the basement membrane material (B), concentrated in the middle between two zones of low electron density to each side (A). The basement membrane can further be seen as a collection of "fibrous" material of varying thickness.

The origin of basement membranes now become of interest as possible products of the endothelial cells. If the redox sites for electron transfer are located, e.g., to the endothelial cell membranes, then the basement membranes may have developed from products of deposition at an electrode equivalent surface, as such depositions develop at any electrode surface of a closed circuit. Fibrous membranes of different composition can also be produced experimentally adjacent to electrodes as an effect of electrophoresis in vivo and in tissue samples (see Chapter XVI).

A logical consequence of such a view is apparent. The endothelial cell should not very likely appear as an interpositioned barrier, carrying anticipated redox mediators e.g. enzyme particles only at the "outer" (interstitial) membrane of the endothelial cell. An explanation is also required for the development of the endothelial fibrin film, described by Copley (13). This film may also develop from products of deposition at an electrode equivalent "inner" surface of the endothelial membrane facing the blood stream. If, indeed the basement membrane develops from material of deposition at the outer (interstitial) electrode equivalent surface of the endothelial cell, the exoendothelial space (13), which seems to be identical with the zone of low electron density, according to Low and Weibel (39, 78), can also get an explanation. Collected "electrode material" adjacent to a surface should physically behave like the basement membrane under the influence of its internal concentration forces. We have encountered this situation earlier (see Figs. XII: 1 and 4) in the creation of "A" and "B" zone effects by products of deposition in tissue adjacent to a metal in in vivo corrosion. A corresponding zone of low density of electrons is also seen in Fig. XII: 28 between the contents of the capillary and the inner surface of the capillary wall. This zone is probably a result of postmortem contraction of material in the lumen of the capillary (see also effects of concentration forces, Fig. XII: 7). The endothelial fibrin film is a structure, continuously exposed to forced convection and should therefore appear differently as compared to the basement membrane and the material inside the capillary, as seen in Fig. XII: 28.

Up to this point we have tried to localize the necessary redox sites in the VICC by looking for electrode equivalent products of deposition as membrane-like structures. In this view, the basement membrane on

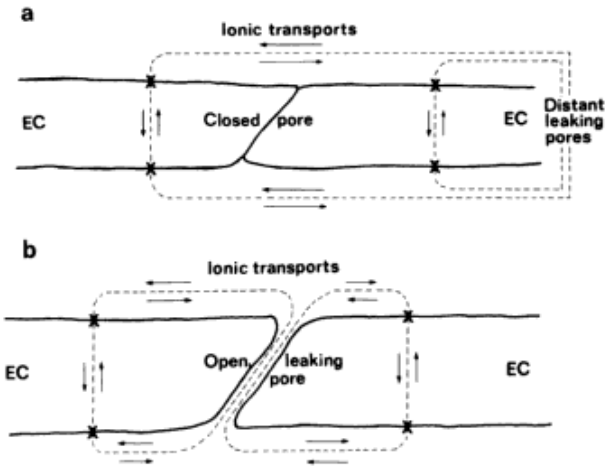

Fig. XII: 30. Suggested mechanism of electric transfer between vascular and interstitial branches of VICC. The surfaces of endothelial cells (EC) possess electrode equivalent sites (X) for reversible redox reactions. Ionic transports through the endothelial cell connect relatively anodic and cathodic "internal" electrode surfaces. "External" electrode surfaces against blood stream and interstitial tissue are connected electrically over blood plasma, leaking pores (stomata) and interstitial tissue fluid. (*a*) When arterial stomata are selectively closed by contraction, conditions for long distance selective transports are created, e.g., over leaking dilated venules and venous capillaries. (*b*) When arterial stomata are open, short-distance transports take place through adjacent arterial stomata.

the outer surface of the endothelial tube and the endothelial fibrous film on its inner surface may indicate the positions of such sites. Fig. XII: 30 *a, b* illustrates how electrode equivalent sites may be located at the surfaces of the capillary endothelium. A long distance electron transfer between the "electrodes" is evidently not very likely because this should require an electron conducting pathway through the endothelial cell. More likely this connection is covered by ionic transports as indicated in Fig. XII: 30. One particular component of transport in the presented view of capillary VICC-functions, the vesicle of Palade, will next be considered.

7. Search for redox sites: the vesicles

The knowledge of the morphologic appearance of vesicles is based on electron micrographs (47, 78, 80). For example, multiple vesicles are seen in the capillary membranes, in a pericyte process and in a smooth muscle cell in Fig. XII: 29. The possibility of transport of proteins through the endothelial cells by means of vesicles has been discussed intensively during the last two decades (53). Vesicles are further thought to transport water through the endothelial cell, a process named pinocytosis. Very little is still known about

their origin and functional role and, e.g., what makes vesiculation start or stop (29). Vesicles are described to move randomly in the cytoplasm (47, 48), in a manner which is compared with Brownian motions (9, 66). A different explanation will soon be presented of their sometimes random appearance (as in the venule V, Fig. XII: 29 *b*) and of their sometimes regular appearance (to the right in the smooth muscle cell M, Fig. XII: 29 *b*). This explanation will suggest an electrogenic mechanism of the development and mode of transport of vesicles.

The presence of vesicles is well known from other biological fields and particularly from the transmission of nervous impulses. The study of neurophysiology tells us that electrical impulses do not directly activate an organ. Instead, the electrical impulses over axons release transmitter substances, which are carried by vesicles (31, 46). In experimental studies it will be shown (Fig. XIV: 8) that *a weak electric current, flowing between two platinum electrodes in blood produces bud-like bubbles of gaseous material extending in dendritic formations from the electrode surfaces*. When electrolysis of water is performed *in the presence of a matrix*, small bubbles of anodic O_2 and cathodic H_2 are virtually pumped far out into the matrix, where these bubbles are retained. There they can be energetically recovered over an experimental fuel cell arrangement. These experiments (Chapter XIII) represent initial attempts to simulate the principle of development, transport and behaviour of vesicles, as well as to simulate some of the actual events connected with the transcapillary transfer of energy in the VICC.

Some of the most important energetic compounds in tissue metabolism are nonionic, e.g., oxygen and glucose. A selective and enhanced closed circuit exchange of compounds between blood and a metabolizing region of tissue must not necessarily be limited to an exchange of ions. Possibilities also exist for electrogenic transport of nonionic materials in the presence of suitable matrices. One of the most important nonionic compounds, water, can be transported in a closed electric circut in a matrix lined with fixed charges. The mechanism of transport we can particularly refer to is evidently in the first hand represented by Type I (anomalous) electroosmosis (Chapter IX). Dielectrics other than water may evidently also move in an electric field. This possibility will be demonstrated experimentally in Chapter XIII.

It is now suggested that the presence of vesicles in the endothelial cells indicates a mechanism of interelectrodic transfer of energy which is in addition to the mechanism of ionic transfer already proposed in Fig. XII: 30. Fig. XII: 31 *a* shows the membranes of an endothelial cell and outlines the suggested principle, that redox reactions lead to the development of basement membrane and fibrin film as "external" pro-

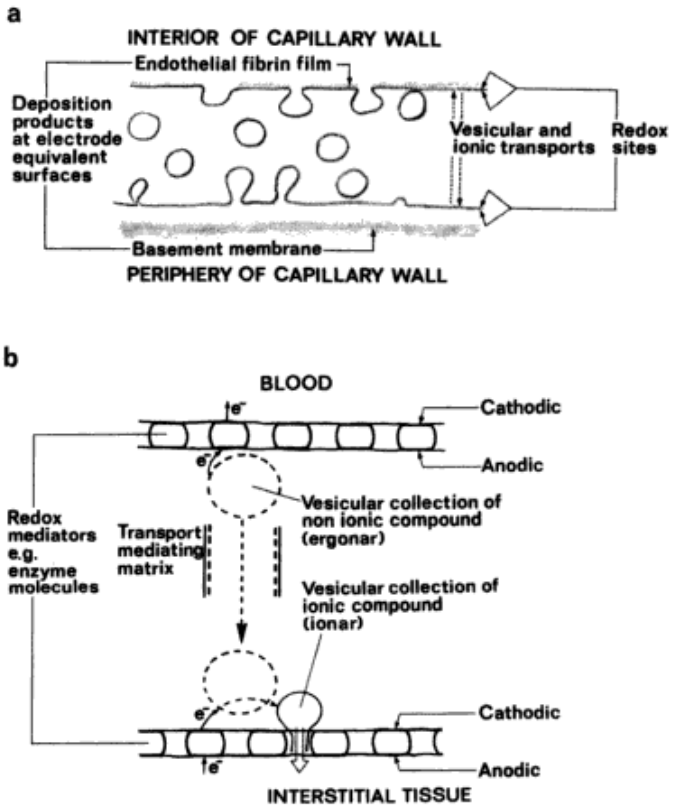

Fig. XII: 31. (*a*) Suggested mechanism of energy transfer over capillary walls in addition to ionic transports illustrated in Fig. XII: 30. Endothelial cells are provided with electrode equivalent sites for reversible redox reactions at the outer and inner surfaces of the endothelial cell membranes. As in any electrophoretic system, reaction products will develop at the electrode surfaces. It is suggested that the basement membrane and the endothelial fibrin film have developed from reactions at the "exterior" electrode surfaces. Vesicles are explained as nonionic collections of products of electrode reactions, transported between the inner electrode surfaces, comparable to electrogenic transport of water in electroosmosis. (*b*) A vesicle produced at the inner surface of an endothelial cell is transported as an ergonar (see Chapter XIII) through the cytoplasm, provided with matrix properties which permit interelectrode transport of dielectrics. On arrival at the opposite electrode, the nonionic compound may ionize by a second electrode reaction. This pinocytotic "pure" transport of water may be combined with hydration of, e.g., cationic compounds leading to enhanced transport of a variety of vesicular contents.

ducts and vesicles as morphologically visible "internal" products in the VICC system. Electrode equivalent redox sites at the endothelial cell membranes are anticipated to be *reversible* and therefore capable of allowing bidirectional ionic and vesicular (nonionic) transports across the endothelial cell. This mechanism also offers an alternative to the previously suggested Brownian type of vesicular motion. A particular pattern of distribution of vesicles adjacent to the inner walls of a cell (M, Fig. XII: 29 *b*) can be regarded as representative of one phase of a unidirectional flow of current. One of the inner "electrode surfaces" should be anodic and the other cathodic. At a later stage when polarity and flow of current are reversed, a mixture will develop of vesicles. We have here assumed, for the sake of simplicity, that the vesicles are transported as water in a closed electric circuit from anode to cathode. A possibility might therefore be that vesicles in pinocytosis are represented by matrix supported transport of micro-clusters of water molecules. Structural elements in the cytoplasm, such as filaments, makes it at least justified to suggest that matrix elements exist to support the electrogenic transport of nonionic material. In this way a principle explaining vesicular transports now appears possible. Redox sites must be located on each side of endothelial membranes, according to this theory for development of basement membrane, endothelial fibrin film and vesicular transport. These sites must each represent one "exterior" and one "interior" reversible electrode equivalent surface (four redox sites). Such an arrangement should allow bidirectional transports of cations and anions as well as bidirectional transport of vesicles. The direction of transport of a dielectric pack of energy (*ergonar*, see Chapter XIII) will be determined by the polarity of the surplus of fixed electric charges of the assumed matrix in the endothelial cytoplasm and the direction of the transcellular electric gradient. The principle of the development and unidirectional transport of a vesicle is presented in Fig. XII: 31 *b*. Several of the participating functions are still unknown. The redox sites are assumed to consist of mediators such as enzyme molecules with the capacity to transfer electrons. Such models of electron conducting enzymes have also been described in the endothelial cytoplasm. The matrix properties of the cytoplasm are, however, still unknown in terms of electrogenic transcellular transports. Related problems associated with transports of dielectric material should in principle be similar to the prerequisites for electrogenic transport of water (see Chapter IX). It should be evident that this model of vesicular transport also includes the mechanism represented by Type III electroosmosis. Any cationic compound can be hydrated and transported in clusters as *electropositive ergionars* (see Chapter XIII).

8. Long and short distance selective transports in tissue over VICC systems

To conclude this presentation, a survey of integrated events is presented in Fig. XII: 32.

Metabolic processes or a *local injury to a tissue* will result in an electric (physicochemical) potential difference in relation to the blood in surrounding vessels (Fig. XII: 32 *a*). The tissues then present their "demand potential" for compensation of their internal metabolic imbalance. The electric potential difference delivers the driving electromotive force for closed circuit transports. This electromotive force consists of metabolic diffusion potentials (or diffusion potentials of catabolic reaction products from injured tissue) and redox potentials between blood and, e.g., hypoxic tissue. Under the influence of the electric field, arterioles and arterial capillaries will contract in certain regions and possibly by means of the pericytes. Contraction of arterial capillaries may then lead to regional closure of leaking arterial stomata at the same time as corresponding veins are wide and continue to keep their stomata open. In Fig. XII: 32 *b* such selective arteriolar and arterio-capillary contractions are seen in dog mesentery while venules and venous capillaries are wide and contain many leukocytes (Fig. XII: 32 *c*, mesentery electropositive, aorta electronegative, 0.1 volt potential difference, 0.03 coulomb, haematoxylin-eosin stain).

A steep transcapillary gradient of an endogenous demand potential of a tissue in relation to blood should develop when the front of diffusion approaches the exterior of the capillary wall. Such a gradient is already present between the thrombus and blood (Fig. XII: 32 *a*). When the minimum potential difference across the capillary wall for the start of redox reactions is exceeded, electrode reactions will take place at the "electrodes" of the capillary walls. Each side of the endothelial membranes should have one anodic and one cathodic surface. Ion exchange will then start through the endothelial cell and over the vascular interstitial channels of the VICC via leaking venules and venous capillaries. Packages (vesicles) of nonionic products (ergonars) from the endothelial electrode surfaces should be transported through the cytoplasm like water in electroosmosis (compare also pinocytosis) and eventually become ionized (= activated) at the opposite electrode.

This preliminary theory for *long distance closed circuit transport* between blood and tissue represents only one of several possibilities. Evidently selective contraction of venules can take place also, although contractions in venules have been observed only rarely in these experiments. Selective closure of venules and venous capillaries would probably also create rather extraordinary conditions, e.g., increase in capillary fil-

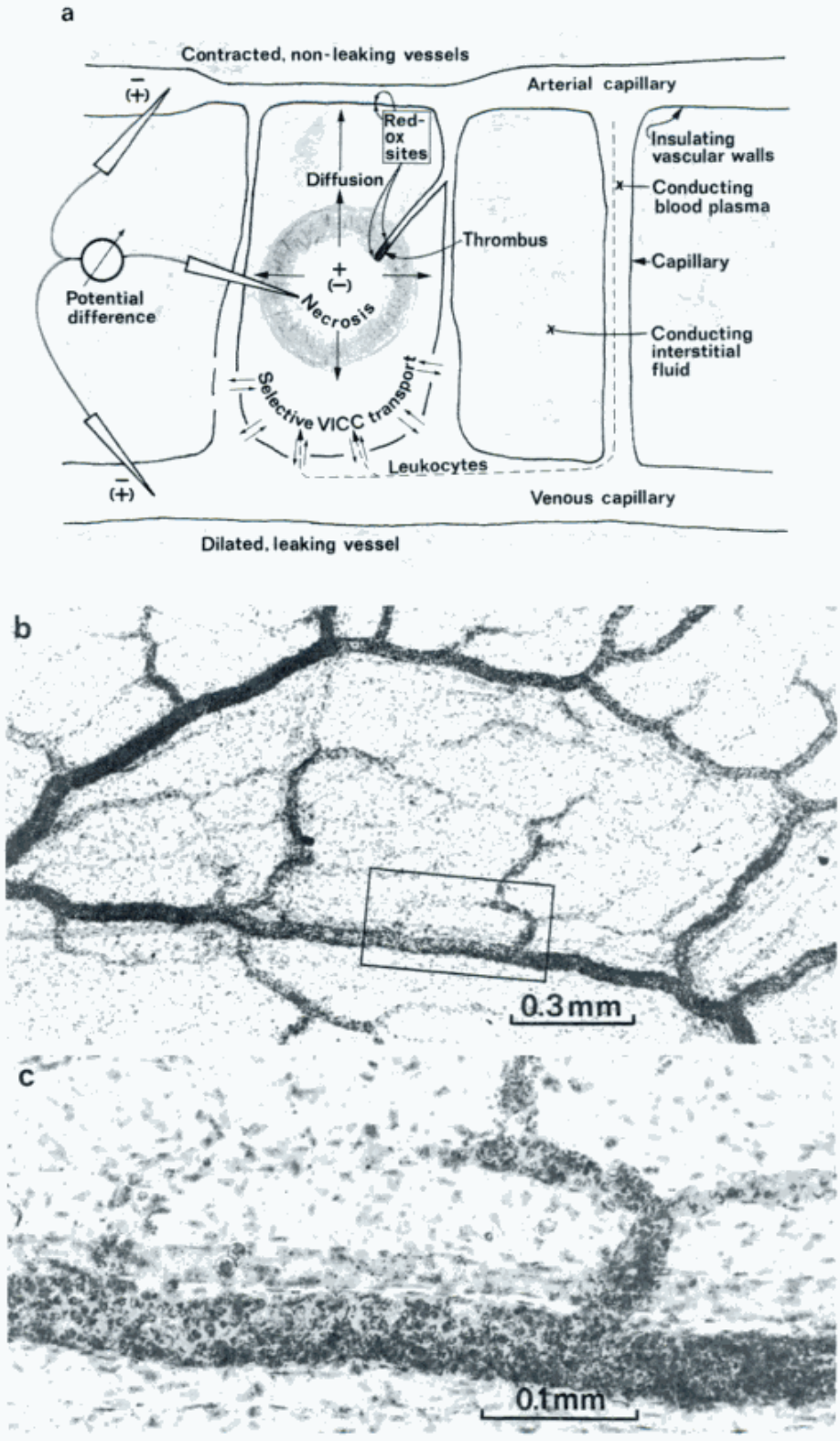

Fig. XII:32. (*a*) Schematic illustration of VICC in "micro-injury" of tissue. Degrading products of an injured tissue produce diffusion potentials. The electric redox potential difference in relation to blood adds to the development of a field-induced regional contraction of adjacent arterial capillaries. The pores of arterial capillaries are then anticipated to close. Redox reactions will start at the outer and inner electrode-equivalent surfaces of the endothelial cell membranes. Two layers of reversible redox sites are necessary at each cell membrane. Transport of ions will start as long-distance transports over blood plasma through open venous capillary pores, through interstitial fluid and as transports through the endothelial cytoplasm. Surfaces of thrombi may also serve as sites for redox reactions. (*b*) Simulation of the "injury potential" difference in *a*, but without producing injury. One platinum electrode was gently positioned against the mesentery of a dog and the other placed in a catheter in the aorta. 0.03 coulomb at 100 mV were passed between mesentery (+) and aorta (−). Field-induced contraction of arterial capillaries makes corresponding venules and venous capillaries fill by collateral circulation of blood. The granulocytes (*c*, dark material in the wide venous branches) are electronegatively charged. They are attracted electrophoretically in the VICC to the anode. Haematoxylin-eosin.

tration pressure and perhaps extensive diapedetic bleedings.

The earlier suggestion that leaking, noncontracted capillaries should only allow minute closed circuits adjacent to the capillary membranes now can be reconsidered and described as a mechanism for *short-distance closed circuit transport* across the capillary walls.

These two systems of electrogenic transports appear to differ in principle by the mechanism of field-induced arteriolar and arterial-capillary contractions. Should this function be found in the future to be related to the presence of pericytes, the short-distance closed circuit transports should logically be localized preferably in regions where capillaries appear with only sparse numbers of pericytes (e.g., in the lungs).

The present experiments have also revealed a discrepancy between morphologic descriptions and function of capillaries. Traditionally we distinguish anatomically between arterioles, capillaries and venules. From the functional point of view it seems more logical to speak about leaking or contracting arterioles and arterial capillaries ("arteriocapillaries"). These capillaries are accompanied by predominantly leaking venous capillaires ("venocapillaries") and venules.

Is there any further direct or indirect evidence that these anticipated functions of the capillaries exist? One argument might be that the clinical, radiologic and experimental observations reported in this book point to the existence of a VICC system. It seems difficult to find an alternative mechanism capable of explaining the multiplicity of biological events which can be explained by the VICC system. Moreover, *one may question if tissue function can "afford" not to take advantage of the exceedingly efficient system for selective transports which closed electric circuits offer*. We will therefore continue in Chapter XIII with a presentation of how such circuits may be activated, which is closely related to the problem of transfer of energy.

F. Conclusions

Evidence has been presented that biologically closed electric circuits (BCEC) exist. These circuits appear to represent an additional, previously overlooked, circulatory system. One important specific circuit is called the VICC (vascular-interstitial closed circuit), which is particularly considered in this study. This circuit is coupled to the mechanisms of bulk transport (diffusion and mechanical circulation) as a system of selective transport. Beyond this capacity for selective transport, BCEC systems are evidently able to influence "local" chemical processes in the circuits, taking place also at "long" distances from the sources of the main driving forces. Thereby BCEC systems can be recognized to contribute to homeostasis. In later chapters other important functions of the interacting transport systems will be demonstrated, with particular emphasis on structural development of tissue and healing processes.

As an introduction to the description of the vascular-interstitial closed circuit (VICC), two mechanisms have been distinguished for corrosion of metal implants in bone. The most common and well known mechanism of corrosion depends on locally different anodic and cathodic parts of the implant, causing what is here called uncomplicated corrosion. The second mechanism is called complicated corrosion, in which relatively cathodic and anodic parts characterize tissues of different local electrochemical potentials adjacent to the metal. Levelling of these differences requires a closed electric circuit, which the metal partly creates. A closed circuit can, however, also be distinguished in tissue without the presence of metal.

This leads us to the concept of biologically closed electric circuits (BCEC). Several kinds of BCEC may yet be distinguished in the future, based on different structural arrangements of tissue components and of body fluids with different conductive properties. This chapter focuses on vascular-interstitial closed electric circuits (VICC). This type of BCEC has two conducting main branches and an intersected regulating mechanism in the capillary walls.

One branch is formed by the electrically insulating walls of "large" vessels surrounding their conductive component, the blood plasma. The other branch is formed by the conducting interstitial fluid and the insulating tissue matrix of cell membranes. The red blood cell membranes also possess a resistive function in the blood. These cell membranes therefore represent a movable part of the matrix of the VICC, variable with the haematocrit.

Electrical junctions between plasma and interstitial fluid are evidently present over the membranes of capillaries.

An analysis of the capillaries with regard to their function in the VICC is of particular interest. The model for transfer of electrons between two redox sites of an enzyme molecule, suggested by Cope (10, 11), has been tentatively accepted to explain the need for necessary electrode-equivalent redox sites of the VICC. *The appearances of the basement membrane around the capillary and the endothelial fibrin film, facing the blood stream, suggests that these structures derive from endogenously developed products at outer "electrode" surfaces of redox sites located in the endothelial membranes*. The material of the basement membrane leaves an exoendothelial space open toward the endothelium. This space seems to correspond to

the space ("A" zone) around a material under contraction by its own concentration forces. The underlying mechanisms are described previously in this chapter in connection with the analyses of in vivo corrosion in the presence of a tissue-matrix. The endothelial fibrin film on the other hand appears different from the basement membrane, presumably partly due to the modifying effect of the streaming blood. These "external" products of electrode reactions should have their corresponding "internal", intracellular products of reaction at the internal redox sites. The vesicles of the endothelial cells are suggested to contain such material. Ions tend to migrate separated in electrophoretic transports. It is suggested that the vesicles, visible in electron micrographs, consist of mainly nonionic collections of electrode products. An electrogenic, closed circuit transport, even of pure nonionic material, is nevertheless possible when the transport is supported by a charged, intracellular "capillary" matrix. Structural intracellular elements as filaments possibly inherit such functions. Intracellular transport of nonionic compounds (e.g., pinocytotic transport of water) may take place in a way analogous to the mechanism of Type I electroosmosis (p. 81). Such a mechanism should then represent an electrogenic, intracellular transport of energetic compounds in addition to ionic transports. Experimental support for the development and transport of vesicles in a matrix is also based on experimental analogues in Chapters IX, XIII and XIV. Another model of vesicular transport is also suggested based on the formation of clusters of hydrated cations.

The capillaries also seem to contain an interesting mechanism for switching between "short-distance" and "long-distance" VICC transport.

When endothelial clefts (stomata) are open in the arterial capillaries, short-distance selective, ionic transports are possible over these leaking pores. Adjacent to their openings, the "outer electrodes" should provide electrode reactions and electron transfer to the "inner electrodes" of the membranous redox sites and start ionic and vesicular transports through the cytoplasm. By exposing mesentery of dogs to electric fields it was found that arterioles and arterial capillaries ("arteriocapillaries") contract and appear empty of blood cells in scattered vascular regions. Simultaneously, corresponding venules and venous capillaries ("venocapillaries") fill with blood, evidently from collateral circulation from adjacent vascular areas without arteriocapillary contractions. The venocapillaries fill selectively with large numbers of granulocytes in dog mesentery near the mesenteric electrode, e.g., at 1–2 V potential difference. Granulocytes also pass by diapedesis through evidently open venocapillary pores to the interstitial tissue. These observations point to the creation of long-distance selective VICC transports of material when tissue is exposed to electric fields. It is suggested that the pericytes may be involved in the mechanism of regional closure of the pores between the endothelial cells.

The electronegative granulocytes or an anionic compound, e.g., Evans blue dye, are electrophoretically attracted to the electropositive region of the tissue. Around an electronegative region in a closed circuit electronegative cells and compounds are repelled. In those veins which have their flow directed toward an electronegative focus, the repelling of granulocytes and anions in the blood stream causes them to accumulate in these veins. These observations contribute to the presentation of an alternative explanation of so-called chemotaxis, which will be further treated in Chapters XIV and XVI. The behaviour of granulocytes in experimental activation of VICC channels illustrates the capacity of selective transports in tissue of this particular BCEC system.

Ionization is a characteristic feature in tissue injury. For example, intravascular thrombosis is a type of injury which appears not to interrupt the conducting pathway. Indeed, intravascular conductivity is increased. The physicochemical potential of tissue injury represents a driving force, which over VICC channels leads to electrophoretic and electroosmotic transports and eventually to healing of the injury. Even small gradients of force in biologic material may be expected to produce significant changes if the "gates" are available, open and the time sufficiently long.

Metabolic reactions not only form new products in tissue but also new electrochemical gradients in BCEC (VICC) channels. The products diffuse and migrate. They become dislocated in an electrochemically activated closed circuit and then easily adsorbed at structural interfaces of tissue matrices in the circuit. In this way structures such as membranes may develop. The principle of this mechanism has been outlined for the development of intraabdominal organ capsules. The mechanisms of development of many other membrane structures, including basement membranes, are little known but might be similarly explained. In future searches for analogues to electrodes in tissue, it seems likely that one of the places where they can be expected to be found is adjacent to (fibrous) membranes.

Biologically closed electric circuits (BCEC) is here used as a general term for structures with the capacity to channelize the exchange of energy in a selective way over long as well as short distances. In addition to the vascular-interstitial closed circuit (VICC) outlined in this study, other circuits can also be anticipated to exist, e.g., in conducting electrolytes in glandular ducts, cerebrospinal fluid, pleural and peritoneal fluid (with or without connections to vascular or interstitial conducting branches). The VICC system may be regarded as a circulation for selective transport in tissue

closely integrated with the nonselective bulk transports by diffusion and mechanical movement in the circulatory system. As a group of systems of selective transport, BCEC systems may be recognized as one of the prerequisites for structural development and function of tissue.

References

1. Aschheim, E.: Traffic of metabolites between blood and tissue. Microvascular Res. 8: 64, 1974.
2. Ballard, K., Malmfors, T., and Rosell, S.: Adrenergic innervation and vascular patterns in canine adipose tissue. Microvascular Res. 8: 164, 1974.
3. Bangham, A., and Pethica, B. A.: The adhesiveness of cells and the nature of the chemical groups at their surfaces. Proc. Roy. Phys. Soc. Edinburgh 28: 43, 1960.
4. Bockris, J. O'M: A basic biological step? Nature 224: 775, 1969.
5. Bockris, J. O'M., and Dražić, D. M.: Electro-chemical science. London, Taylor & Francis Ltd., 1972.
6. Border, W. A., Lehman, D. H., Egan, J. D., Sass, H. J., Glode, J. E., and Wilson, C. G.: Antitubular basement-membrane antibodies in methicillin-associated interstitial nephritis. New Engl. J. Med. 291: 381, 1974.
7. Bruns, R. R., and Palade, G. E.: Studies on blood capillaries. II. Transport of ferritin molecules across the wall of muscle capillaries. J. Cell Biol. 37: 277, 1968.
8. Burger, H. C., and van Milaan, J. B.: Measurements of specific resistance of the human body to direct current. Acta Med. Scand. 114: 584, 1943.
9. Casley-Smith, J. R.: Pinocytotic vesicles: an explanation of some of the problems associated with the passage of particles into and through cells via these bodies. Med. Res. Council Memor. 1: 58, 1963.
10. Cope, F. W.: A theory of enzyme kinetics based on electron conduction through the enzymatic particles, with applications to cytochrome oxidases and to free radical decay in melanin. Arch. Biochem. Biophys. 103: 325, 1963.
11. Cope, F. W.: A kinetic theory of electron and ion transport in particulate and membranous systems, with applications to the cytochrome oxidase, melanin free radical, and pyruvate carboxylase reactions, and to control of enzymes by hormones and radiation. In: King, T. E., Mason, H. S., and Morrison, M. (eds.): Oxidases and related redox systems. New York, Wiley and Sons, 1965, p. 51.
12. Cope, F. W.: A review of the applications of solid state physics. Concepts to biological systems. J. Biol. Phys. 3: 1, 1975.
13. Copley, A. L.: Hemorheological aspects of the endothelium-plasma interface. Microvasc. Res. 8: 192, 1974.
14. Crile, G. W., Hosmer, H. R., and Rowland, A. F.: The electrical conductivity of animal tissues under normal and pathological conditions. Am. J. Physiol. 60: 59, 1922.
15. Curtis, A. S. G.: The cell surface: its molecular role in morphogenesis. London, Academic Press, 1967.
16. Ferguson, A. B., Laing, P. G., and Hodge, E. S.: The ionization of metal implants in living tissue. J. Bone and Joint Surg. 42A: 1, 1960.
17. Folkow, B., and Mellander, S.: Aspects of the nervous control of the precapillary sphincters with regard to capillary exchange. Acta Physiol. Scand. 50 (Suppl. 175): 52, 1960.
18. Frank, E., and Zitter, M.: Metallische Implantate in der Knochen-Chirurgie. Wien, New York, Springer, 1971.
19. Fricke, H.: The conductivity and capacity of disperse systems. Physics 1: 106, 1931.
20. Fricke, H., and Morse, S.: The electric resistance and capacity of blood for frequencies between 800 and 4.5 million cycles. J. Gen. Physiol. 9: 153, 1926.
21. Galleotti, G.: Über die electrische Leitfähigkeit der tierischen Gewebe. Z. Biol. 43: 289, 1902.
22. Geddes, L. A., and Baker, L. E.: The specific resistance of biological material—A compendium of data for the biomedical engineer and physiologist. Med. and Biol. Engng. 5: 271, 1967.
23. Green, D. E., Wharton, D. C., Tzagoloff, A., Rieske, J. S., and Brierley, G. P.: The mitochondrial electron-transfer chain. In: King, T. E., Mason, H. S., and Morrison, M. (eds.): Oxidases and related redox systems. New York, Wiley and Sons, 1965, vol. 2, p. 1032.
24. Guyton, A. C.: A concept of negative interstitial pressure based on pressures in implanted perforated capsules. Circ. Res. 12: 399, 1963.
25. Guyton, A. C., Taylor, A. E., and Granger, H. J.: Circulatory physiology II: Dynamics and control of the body fluids. Philadelphia-London-Toronto, W. B. Saunders Co., 1975.
26. Haydon, D. A.: The electrical double layer and electrokinetic phenomena. In: Danielli, J. F., Pankhurst, K. G. A., and Riddiford, A. C.: Recent progress in surface science. New York, Academic Press, 1964, vol. 1, chapter 3, p. 94.
27. Helmholtz, H.: Studien über elektrische Grenzschichten. Ann. Phys. Chem. 7: 337, 1879.
28. Hemingway, A., and McLendon, J. F.: The high frequency resistance of human tissue. Am. J. Physiol. 102: 56, 1932.
29. Holter, H.: Problems of pinocytosis, with special regard to amoebae. Ann. N. Y. Acad. Sci. 78: 525, 1959.
30. Jordan, J.: In: Pilla, A. A. (ed.): Proceedings of a workshop in bioelectrochemistry, Princeton, New Jersey, October 10–14, 1971, p. 103. National Science Foundation, Washington, D. C., and ESB Inc. Technology Center, Yardley, Pa.
31. Katz, B.: The release of neural transmitter substances. The Sherrington lectures X. Liverpool, Univ. Press, 1969.
32. Kaufman, W., and Johnston, F. D.: The electrical conductivity of the tissues near the heart and its bearing on the distribution of the cardiac action currents. Am. Heart J. 26: 42, 1943.
33. Kefalides, N. A.: Chemical properties of basement membranes. Int. Rev. Exp. Path. 10: 1, 1971.
34. Kinnen, E., Kubicek, W., Hill, P., and Turton, G.: Thoracic cage impedance measurements. (Tissue resistivity in vivo and transthoracic impedance at 100 kc/s). Tech. Doc. Rep. SAM-TDR 64-5, 1964. School of Aerospace Medicine, Brooks AFB, Texas.
35. Kopsch, F.: Lehrbuch und Atlas der Anatomie des Menschen. Band II: 362, 1939.
36. Krogh, A.: Anatomie und Physiologie der Capillaren. Berlin, Springer, 1923.
37. van Lancker, J.: Molecular and cellular mechanisms in disease. Berlin, Heidelberg, New York, Springer Verlag, 1976, pp. 861, 931.
38. Lehninger, A. L.: Biochemistry. 2nd ed. New York, Worth Publ. Inc., 1977.
39. Low, F.: Extracellular compartment of the pulmonary alveolar wall. Arch. Int. Med. 127: 847, 1971.
40. Manjo, G.: Ultrastructure of the vascular membrane. In: Handbook of Physiology. Am. Physical Soc., Washington, D. C. Circulation III: 2293, 1964.
41. Molnar, G. W., Nyboer, J., and Levine, R. L.: The effect of temperature and flow on the specific resistance of human venous blood. U. S. Army Med. Res. Lab. Rep., Fort Knox, Ky. 127, 1953. Project 6-64-12-028.
42. Nordenström, B.: Temporary unilateral occlusion of the pulmonary artery. Acta Radiol. Diagn. Suppl. 108, 1954.
43. Nordenström, B.: Selective catheterization and angiography of bronchial arteries in dog. Acta Radiol. Diagn. 4: 513, 1966.
44. Nordenström, B.: Selective catheterization and angiography of bronchial and mediastinal arteries in man. Acta Radiol. Diagn. 6: 13, 1967.
45. Osswald, K.: Messung der Leitfähigkeit und Dielektrizitätkonstante biologischer Gewebe und Flüssigkeiten bei kurzen Wellen. Hochfreq. Tech. Electroakust. 49: 40, 1937.
46. Ottoson, D., and Shepherd, G. M.: Transducer properties and integrative mechanism in the frog's muscle spindle I. In: Loevenstein, W. R. (ed.): Handbook of Sensory Physiology, Vol. I. Biophysics of receptor action. Berlin, Springer Verlag, 1970.
47. Palade, G. E.: Transport in quanta across the endothelium of blood capillaries. Anat. Rec. 136: 254, 1960.
48. Palade, G. E.: Blood capillaries of the heart and other organs. Circulation 24: 368, 387, 1961.

49. Philipson, M.: Sur la résistance électrique des cellules et des tissus. C. r. Hebd. Séanc. Mem. de la Soc. de Biol. 83: 1399, 1920.
50. Poisenille, J. L. M.: Recherches sur les causes du mouvement du sang dans les vaisseaux capillaires. C. R. Acad. Sci. 1: 554, 1835.
51. Rauch, J. B., and Le Merit, S. L.: The specific impedance of the dorsal columns of cat; an anisotropic medium. Exp. Neurol. 11: 451, 1965.
52. Renkin, E. M., and Rosell, S.: Independent sympathetic vasoconstrictor innervation of arterioles and precapillary sphincters. Acta Physiol. Scand. 54: 381, 1962.
53. Rippe, B.: Permeabilitet genom tunna membraner. (In Swedish). Läkartidningen 78: 674, 1981.
54. Rosenberg, B.: Some problems in the electrical conductivity of proteins. In: King, T. E., Mason, H. S., and Morrison, M. (eds.): Oxidases and related redox systems. New York, Wiley and Sons, 1965, p. 72.
55. Rosendal, T.: The conducting properties of the human organism to alternating current. Copenhagen, Munksgaard, 1940.
56. Rosenthal, R. L., and Tobias, C. W.: Electrical resistance of human blood. J. Lab. and Clin. Med. 33: 1110, 1948.
57. Rouget, C.: Mémoire sur développement, la structure et les propriétés physiologiques des capillaires sanguins et lymphatiques. Arch. Physiol. Norm. Pathol. 5: 603, 1873.
58. Rush, S., Abildskov, J. A., and McFee, R.: Resistivity of body tissues at low frequencies. Circulation Res. 12: 40, 1963.
59. Sawyer, P. N., Pate, J. W., and Weldon, C. S.: Bioelectric phenomena as an etiologic factor in intravascular thrombosis. J. Physiol. 175: 108, 1953.
60. Sawyer, P. N., Burrowes, C., Ogoniak, J. C., Smith, A. O., and Wesolowski, S. A.: Ionic architecture at the vascular wall interface. Trans. Am. Soc. Artificial Internal Organs 10: 316, 1964.
61. Sawyer, P. N., Stanczewski, B., Ramsey, Jr., W. S., Ramasamy, N., and Srinivasan, S.: Electrochemical interactions at the endothelial surface. J. Supramol. Structure. New York, Alan R. Liss Inc., 1973.
62. Schwan, H. P.: Electrical properties of body tissues and impedance plethysmography. J. R. E. Trans. on Med. Electronics PGME 3: 32, 1955.
63. Schwan, H. P., and Kay, C. F.: The conductivity of living tissues. Ann. N. Y. Acad. Sci. 65: 1007, 1956–57.
64. Schwan, H. P., and Kay, C. F.: Specific resistance of body tissues. Circulation Res. 4: 664, 1956.
65. Seel, F.: Grundlagen der Analytischen Chemie. Weinheim, Verlag Chemie, 1960, p. 162.
66. Shea, S. M., and Karnowsky, M. J.: Brownian motion: a theoretical explanation for the movement of vesicles across the endothelium. Nature (London) 212: 353, 1966.
67. Sigman, E., Kolin, A., Katz, L. N., and Jochim, K.: Effect of motion on the electrical conductivity of the blood. Am. J. Physiol. 118: 708, 1937.
68. Srinivasan, S., Cahen, Jr., G. L., and Stoner, G. E.: Electrochemistry in the biomedical sciences. In: Bloom, H., and Gutman, F. (eds.): Electrochemistry, the past thirty and the next thirty years. New York, Plenum Press, 1977, p. 57.
69. Straub, K. D.: Semiconduction in certain proteins. Thesis, Biochem. Dept., Duke University, Durham, North Carolina, 1967.
70. Stricker, S.: Untersuchungen über die Contractilität der Capillaren. Sitzungsber. d. Akad. Wien. Math-Naturwet. Kasse III, Abt. 74, 1886.
71. Szent-Györgyi, A.: Towards a new biochemistry. Science 93: 609, 1941.
72. Tafel, J.: Cited by Bockris, J. O'M., and Dražić, D. M.: Electro-chemical science. London, Taylor & Francis Ltd., 1972, p. 5.
73. Tedner, B. T.: Automatic recording of biological impedances. J. Med. Engin. and Tech. 2: 70, 1978.
74. Thomasset, M. A.: Propriétés bio-électrique des tissus. Lyon Médicale 209: 1325, 1963.
75. Trukhan, E. M.: Determination of the mobility of charge free carriers in biological combinations. Biofizika 11: 412, 1966.
76. Vimtrup, B. J.: Beiträge zur Anatomie der Kapillaren. I. Über kontraktile Elemente in der Gefässwand der Blutkapillaren. Z. Gesamte Anat. 65: 150, 1922.
77. Vimtrup, B. J.: Beiträge zur Anatomie der Kapillaren. II. Weitere Untersuchungen über kontraktile Elemente in der Gefässwand der Blutkapillaren. Z. Anat. Entwicklungsgesch. 68: 469, 1923.
78. Weibel, E. R.: On pericytes, particularly their existence on lung capillaries. Microvasc. Res. 8: 218, 1974.
79. Weiss, L., and Zeigel, R.: Cell surface negativity and the binding of positively charged particles. J. Cell Physiol. 77: 1979, 1971.
80. Whittaker, V. P., and Gray, E. G.: The synapse: biology and morphology. Brit. Med. Bull. 18: 223, 1962.
81. Wilson, D. F., Dutton, P. L., and Wagner, M.: Energy transducing components in mitochondrial respiration. In: Sanadi, D. R., and Packer, L. (eds.): Current topics in bioenergetics. New York, Academic Press, vol. 5, 1973.
82. Wissig, S. L., and Williams, M. C.: Permeability of muscle capillaries to microperoxidase. J. Cell Biol. 76: 341, 1978.
83. Zimmermann, K. W.: Der feinere Bau der Blutcapillaren. Z. Anat. Entwicklungsgesch. 68: 3, 1923.
84. Zweifach, B. W.: The character and distribution of the blood capillaries. Anat. Rec. 73: 475, 1939.

XIII.
Energetics of BCEC systems, ionars and ergonars

A. Components of BCEC systems

Chemical reactions in vivo differ from chemical reactions in vitro by usually being isothermic. Biologic reactions are often modulated in many ways which are energetically economical and functionally highly differentiated. Acceptance of the principle of BCEC means that a variety of closed circuit functions, commonplace in contemporary electronic technology, should also have their correspondence in biology. This correspondence includes not only the functions which drive the circuits but also the influences of "local" reactions along electrochemical gradients over BCEC branches, either in series or in parallel. As will be seen, ionic and nonionic compounds each interact in a way that makes selective distribution and modulation of energy possible over short and long distances. BCEC therefore represent, in the author's view, an important circulatory system in addition to the mechanically driven circulation of blood. Components of this circulatory system are listed in Table XIII: 1.

Selective distributions of compounds thereby become possible, even against existing pressure gradients, and may contribute, for example, to homeostasis.

As far as can be seen now, the mechanical transport system and the electrochemical BCEC systems are closely integrated both morphologically and functionally. Future evaluations of the function of the combination of the two systems will, however, require a

Table XIII: 1. *Components of the circulatory system of BCEC*

I. Matrices	*Structured groups of channelizing components:* Vessels, ducts, interstitial channels, fibrous membranes. Some of these components are contractile and change electrical resistance.
	Components not organized as channels: Erythrocytes and other circultaing cells, cellular components and molecules. Ground substance, fibrous material, nutrients, metabolites, metabolic wastes. Movable "matrices" add variable resistance and capacitance to the circuits.
II. Solvent	*Water*
III.	*Electrode-equivalent interfaces for redox reactions*
IV. Ions	*Ionars:* Collections of ions operating BCEC
V. Ergons	*Ergonars:* Collections of electrically balanced energetic molecules operating BCEC

considerably more differentiated knowledge of the BCEC systems than is presently available. The following presentation will focus on the important problem of how BCEC systems can be activated and utilized in the transfer of energy in tissues. We will start with a general presentation of the author's view on the energy available for such functions. This introductory presentation is intended only as a preliminary approach toward understanding the associated complicated problems. These problems are indeed a consequence of the recognition of the concept of BCEC.

The energy which can drive a BCEC needs first to be identified and defined. One group of energetic compounds is primarily ionic and supplies electric (or more precisely, physicochemical) energy to the system. The other group consists of primarily nonionic energetic compounds. In order to facilitate handling of the actual problems it is now necessary to introduce new, if tentative, terminology (Table XIII: 2).

The term ergon (Greek, ergon = work) is used here to mean a nonionic compound possessing *potential* electric energy, as distinguished from an ionic compound possessing immediately *available* electric energy, in a BCEC system. These two types of energy compounds are integrated in the energy conversion of BCEC systems as ionic and ergonic collections called ionars and ergonars, respectively. Together these collections are termed ergionars. The need for a distinction between ionic and ergonic energies is a consequence of the important differences of their energetic behaviour in a BCEC. Similarly, their appearance as ionars and ergonars has a particular meaning in closed circuit energy exchange. Examples of ergonars include oxygen, glucose, neutral fat, ATP, $NADPH_2$ and nonpolar amino acids, e.g., leucine, valine, methionine and phenylalanine. Water may also be included in this group although it can be regarded in many respects as a special type of matrix material.

BCEC systems require electric energy, supplied directly by ions or indirectly by ergons (after their activation). The electric potentials for redox half-reactions of ions and ergons can be defined by standard reduction potentials. In Table XIII: 3 some known redox potentials are presented (3, 20).

Reduction or oxidation of ergons creates ions, which in turn by oxidation or reduction may create ergonic compounds. In this way we may regard ergonars as precursors of ionars and vice versa. Table XIII: 3 does not tell us when, where and under what biologic circumstances these reactions take place. The answers to these questions require further discussion of the concepts of ionars, ergonars and BCEC.

Ionars and ergonars represent two types of biologic bulk energy. Ergonars are electrically noncharged packages of energy. Their arrivals at places which are suitable for release of this energy depend mainly on

Table XIII: 2. *Energy in BCEC systems: terminology*

Unit	Symbol	Energy collections	
Ion (electrically charged molecule)	△	Ergion	Ionar n× △
Ergon (nonionic energy carrier)	⁎△		Ergonar n×⁎△
			Ergionar

diffusion and mechanical transport from the places of production. Glucose, for example, after liberation from glycogen in the liver, does not "waste" its energy during transport in the blood stream. On arriving at a suitable site of reaction, e.g., a working muscle, it contributes to the need of energy of the local tissue. During transport in bodily fluids, ions will create electromagnetic fields in surrounding tissue. Ergons do not. Selective electrophoretic transport of material according to electric gradients is the case with ionars. Such transport is not possible for ergonars. Nevertheless, ergonars may undergo electrogenic transport, mediated by a suitable matrix. Differences of this kind appear to be important for differentiated transport of energetic compounds in tissue. An electrochemical gradient caused by ionars, e.g., from local metabolic activities in a tissue, should induce compensatory, selective migrations of ionic material in a BCEC. If levelling of physicochemical gradients were to take place exclusively by mechanical transports (forced convection), only an indiscriminate mixing should occur. Diffusion contributes to selective distribution. The tendency for selective distribution of ions in a BCEC also depends on the morphologic distribution of the electrically inactive ergonars. The presence of ergonars adds a resistance and a capacitance in parallel in the circuits. The varying concentrations and locations of ergonars thereby modify the electric activities of the ionars. This mode of action is illustrated in Fig. XIII: 1, where a part of a liquid-containing branch of a closed circuit (*a*) is conductive because of its contents of cations and anions and water molecules (ergons). Water, furthermore, is a "nonionic" compound, which acts as a unique kind of movable matrix. At the same time it contains all the characteristics of an ergonar of a complex nature. The capacity of water to form clusters of molecules of an energy content lower than the summation of energy of "individual" water molecules, emphasizes the importance of recognizing ergonars in energy conversion. The degree of breaking of clusters is influenced by many factors, e.g., the concentrations of ions, temperature and electric fields. The appearance of an ergonar other than the water, e.g., (*b*) a bolus of glucose, may markedly impair conductivity, while (*c*) the same quantity of ergonar in

Table XIII: 3. *Standard reduction potentials of some oxidation-reduction half-reactions*

Reaction	Half-reaction (written as a reduction)	E_0 at pH 7.0[a] (volts)	Reaction	Half-reaction (written as a reduction)	E_0' at pH 7.0[a] (volts)
1.	$\frac{1}{2}O_2+2H^++2e^- \rightarrow H_2O$	0.816	22.	Oxalacetate$+2H^++2e^- \rightarrow$ malate	−0.175
2.	$Fe^{3+}+1e^- \rightarrow Fe^{2+}$	0.771	23.	$FAD+2H^++2e^- \rightarrow FADH_2$	−0.18[b]
3.	$2I^-+2e^- \rightarrow I_2$	0.536	24.	Pyruvate$+2H^++2e^- \rightarrow$ lactate	−0.190
4.	Cytochrome-a_3-$Fe^{3+}+1e^- \rightarrow$ cytochrome-a_3-Fe^{2+}	0.55	25.	Riboflavin$+2H^++2e^- \rightarrow$ riboflavin-H_2	−0.200
5.	$SO_4^{2-}+2H^++2e^- \rightarrow SO_3^{2-}+H_2O$	0.48	26.	Cystine$+2H^++2e^- \rightarrow 2$ cysteine	−0.22
6.	$NO_3^-+2H^++2e^- \rightarrow NO_2^-+H_2O$	0.42	27.	$GSSG+2H^++2e^- \rightarrow 2$ GSH	−0.23
7.	$\frac{1}{2}O_2+H_2O+2e^- \rightarrow H_2O_2$	0.30	28.	$S^0+2H^++2e^- \rightarrow H_2S$	−0.23
8.	Cytochrome-a-$Fe^{3+}+1e^- \rightarrow$ cytochrome-a-Fe^{2+}	0.29	29.	1,3-diphosphoglyceric acid$+2H^++2e^- \rightarrow$ GAP$+P_i$	−0.29
9.	Cytochrome-c-$Fe^{3+}+1e^- \rightarrow$ cytochrome-c-Fe^{2+}	0.25	30.	Acetoacetate$+2H^++2e^- \rightarrow$ β-hydroxybutyrate	−0.290
10.	2,6-Dichlorophenolindophenol$_{(ox)}+2H^++2e^- \rightarrow$2,6-DCPP$_{(red)}$	0.22	31.	Lipoate$_{(ox)}+2H^++2e^- \rightarrow$ lipoate$_{(red)}$	−0.29
11.	Crotonyl-S-CoA$+2H^++2e^- \rightarrow$ butyryl-S-CoA	0.19	32 a.	$NAD^++2H^++2e^- \rightarrow NADH+H^+$	−0.320
12.	$Cu^{2+}+1e^- \rightarrow Cu^+$	0.15	32 b.	$NADP^++2H^++2e^- \rightarrow NADPH+H^+$	−0.320
13.	Methemoglobin-$Fe^{3+}+1e^- \rightarrow$ hemoglobin-Fe^{2+}	0.139	33.	Pyruvate$+CO_2+2H^++2e^- \rightarrow$ malate	−0.33
14.	Ubiquinone$+2H^++2e^- \rightarrow$ ubiquinone-H_2	0.10	34.	Uric acid$+2H^++2e^- \rightarrow$ xanthine	−0.36
15.	Dehydroascorbate$+2H^++2e^- \rightarrow$ ascorbate	0.06	35.	Acetyl-S-CoA$+2H^++2e^- \rightarrow$ acetaldehyde$+$CoA	−0.41
16.	Metmyoglobin-$Fe^{3+}+1e^- \rightarrow$ myoglobin-Fe^{2+}	0.046	36.	$CO_2+2H^++2e^- \rightarrow$ formate	−0.420
17.	Fumarate$+2H^++2e^- \rightarrow$ succinate	0.030	37.	$H^++1e^- \rightarrow \frac{1}{2}H_2$	−0.420
18.	Methylene blue$_{(ox)}+2H^++2e^- \rightarrow$ methylene blue$_{(red)}$	0.011	38.	Ferredoxin$-Fe^{3+}+1e^- \rightarrow$ ferredoxin-Fe^{2+}	−0.432
19.	Pyruvate$+NH_3+2H^++2e^- \rightarrow$ alanine	−0.13	39.	Gluconate$+2H^++2e^- \rightarrow$ glucose$+H_2O$	−0.45
20.	α-Ketoglutarate$+NH_3+2H^++2e^- \rightarrow$ glutamate$+H_2O$	−0.14	40.	3-Phosphoglycerate$+2H^++2e^- \rightarrow$ glyceraldehyde-3-phosphate$+H_2O$	−0.55
21.	Acetaldehyde$+2H^++2e^- \rightarrow$ ethanol	−0.163	41.	Methylviologen$_{(ox)}+2H^++2e^- \rightarrow$ methylviologen$_{(red)}$	−0.55
			42.	Acetate$+2H^++2e^- \rightarrow$ acetaldehyde	−0.60
			43.	Succinate$+CO_2+2H^++2e^- \rightarrow$ α-ketoglutarate$+H_2O$	−0.67
			44.	Acetate$+CO_2+2H^++2e^- \rightarrow$pyruvate	−0.70

Source: I. H. Segel, Biochemical Calculations, 2d ed. (New York: Wiley, 1975), pp. 414–415.

[a] Standard conditions: Unit activity of all components except H^+, which is maintained at 10^{-7}M. Gases are at 1 atm pressure.

[b] The value given is for free FAD/$FADH_2$. The E_0 of the protein-bound coenzyme varies.

an incompletely obstructing location will impair conductivity less. Conductivity also is affected (*d*) by variations of morphology of the conducting vessels. In general, then, the functions of ionars and ergonars are variable, depending on their sizes and distributions in relation to the actual morphology of the BCEC branches. The intensity of closed circuit ionar interactions now may be recognized to be modulated both by ergonars and by variations of the supporting nonconducting walls around the conducting fluid. A purposeful deceleration or acceleration of reactions over BCEC branches may be obtained in this way. (See also Fig. X: 6, as an experimental analogue of induced delay of spontaneous equilibrium). Furthermore, any local narrowing of a conducting branch of a BCEC should lead to local enhancement of current density, a change which may be expected to be accompanied by functional effects. A levelling of electric gradients over closed circuits between different regions of tissue should evidently also contribute to homeostasis.

One way to determine the average balance between ionars and ergonars would be to determine their ratio of concentration (ergionar ratio) in the conducting medium. A more direct and simple way would be to determine the electric resistivity of the conducting medium. Complete analysis of ionar-ergonar interaction in vivo would be extremely difficult to determine, partly for reasons mentioned above, i.e., functional variations of lumina of conducting branches as well as local convection factors. Moreover, one would need to know the morphology of associated, but different BCEC branches and systems as well as the varying sites, magnitudes and times of occurrence of their energies of activation.

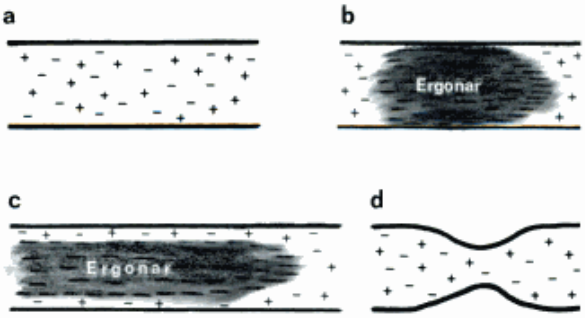

Fig. XIII: 1. Interdependence of components of BCEC systems. (*a*) Electrically conducting branch of a closed circuit, containing water and electrolytes. The vessel wall is electrically insulating. (*b*) Conductivity in this branch is markedly impaired by an ergonar (nonionic collection, e.g., a bolus of glucose) which locally fills the lumen. (*c*) Conductivity is less impaired than in *b* because the same ergonar is more elongated and not occupying the entire cross section of the branch. (*d*) Impairment of conductivity by compression or contraction of conducting closed circuit branch.

What are the mechanisms responsible for the differences of electric reactability of ergonars and ionars? This question can presently be answered only indirectly by pointing toward some mechanisms which are likely to be involved.

The magnitudes of ionic dissociation of different compounds and the buffering capacity of tissue fluids are evidently of importance for the electrical closed circuit events in a BCEC system.

Depending on their different orbits of electrons, the elements differ in their ability to accept or donate electrons. Noble gases, which do not possess valence electrons, are therefore inert and unable to accept or donate electrons. Certain so-called noble metals, e.g., platinum, behave as inert materials by their property to form stable, electron-conducting surface films (PtO). Platinum is therefore often suitable as electrode material. The tendency for an element or molecule to deliver or to accept electrons in relation to another element or molecule is determined by what is called its electronegativity (17). The electronegativity of an element is further characterized, according to Mulliken (12), by the difference between its ionizing energy and its electron affinity. These concepts are evidently of considerable interest with regard to the release of electric energy of ions and ergons.

Ions carry an excess of electric charge immediately available for short and long distance reactions. Ergons do not "waste" their electric energy immediately and anywhere, e.g., during their transport. But at suitable sites of reaction they are able to release their energy when needed. Ergonars even cooperate along this line. Thus, glucose releases eighteen times as much energy in the presence of oxygen than in its absence (22). But oxygen, as an ergon, must protect its capacity for necessary redox reactions during transport in the blood. This protection is possible partly as a function of the microenvironment, which supports one of the ergonic characteristics (the saving of electric energy) of oxygen during its transport. The basic information which allows us to recognize this important mechanism behind the enhanced ergonar function of oxygen is a result of extensive studies on the binding of oxygen to haemoglobin and myoglobin. A brief review of the relevant literature follows.

The structures of myoglobin and haemoglobin have been elucidated by Kendrew (8, 9) and Perntz (18). The capacity of myoglobin and haemoglobin to bind oxygen depends principally on a nonpolypeptide unit, the haem group. The haem is a prosthetic group of myo- and haemoglobin. It contains an organic protoporphyrin part and an iron atom, which can appear in ferrous (Fe^{++}) or ferric (Fe^{+++}) states of oxidation. Only ferrohaemoglobin can bind oxygen (29). Ferrihaemoglobin is also called methaemoglobin. Corresponding functions also apply to myoglobin (9). The prosthetic haem group in both myoglobin and haemoglobin is surrounded by the apoprotein, which inside consists almost entirely of nonpolar amino acids (27). Glutamine, asparagine, lysine and arginine, without side chains, are present in the interior of the molecule (18). Residues that have both a polar and nonpolar part, such as threonine, tyrosine and tryptophan, are oriented so that their nonpolar portions point inward. Only two polar residues, each a molecule of histidine, are present inside the myoglobin and haemoglobin molecule. Each of these histidines is very close to the iron in the haem group. The iron atom is directly bonded to one of the histidines (histidine F8, called the proximal histidine). The oxygen binding site of the iron is opposite the histidine F8, while the second histidine (E7, called the distal histidine) is nearby (22). In ferrimyoglobin the oxygen binding site is occupied by water, in deoxymyoglobin it is empty, in oxymyoglobin it is occupied by O_2 (26). When O_2 occupies the binding site, it does not oxidize Fe^{++} to Fe^{+++}. How is this possible? The oxygen binding site of the iron atom is remarkably small in relation to the volume of the whole myoglobin molecule. This relationship gives a hint of the function of the polypeptide portion of the molecule surrounding the haem (25). The haem can be isolated. In a water solution it is able to bind oxygen for a short time when its Fe^{++} is oxidized to Fe^{+++}. Fe^{+++}, however, can not bind oxygen. In some way the polypeptide portion of haemo- and myoglobin stabilizes Fe^{++}.

An answer to this problem of binding oxygen has been given by Jai Wang (25) in an experimental model. When the haem group is imbedded in a polystyrene matrix containing a derivative of imidazole, it can

undergo reversible oxygenation. The matrix preparation mimics that of polypeptides. Wang proposes that imidazole has a role similar to that of the proximal F8 histidine, while the polystyrene provides the haem group with a nonpolar hydrophobic environment. It is more difficult for electrons to leave ferrous iron in a nonpolar milieu than in water. The nonpolar haem-binding site in myo- and haemoglobin therefore protects ferrous iron from oxidation by exclusion of water (22).

Myoglobin and haemoglobin are structurally similar, but they are functionally different in their properties as oxygen carrying molecules. For example, the affinity of haemoglobin for oxygen depends on pH, while that of myoglobin is independent of pH. In haemoglobin the oxygen binding is also affected by the affinity of haemoglobin for CO_2. Haemoglobin has a lower affinity for oxygen than myoglobin, an essential property from the point of view of transfer of oxygen from blood to muscle. When temperature or the concentration of H^+ or CO_2 increases, then oxygen is released from haemoglobin (Bohr effect), while these factors do not affect the capacity of myoglobin to bind oxygen (19). Several other factors are also involved in the mechanisms of binding and release of oxygen and CO_2 to haemoglobin.

The point of this review may now be evident. The microenvironment of the haemoglobin molecule acts selectively to protect the ergonar oxygen from being ionized during its transport in the blood stream. Upon contact with myoglobin, the oxygen is transferred from haemoglobin and accumulated in the myoglobin, still in a protected, ergonic state until its oxidizing properties are needed.

After this introductory presentation of components of BCEC systems, it is now appropriate to consider the energy of ions and ergons.

B. Ionic energy

Current concepts of energy exchange in chemical reactions will now be surveyed briefly, as a necessary prelude to considering biochemical reactions in the presence of biologically closed electric circuits. This survey is mainly based on the authoritative presentations of Lehninger (10), Nobel (14), Bockris and Dražić (1), Morowitz (11) and Newman (13).

The total energy μ of an ionic species j in a tissue is conventionally expressed as a sum involving its chemical activity, volume and pressure conditions, electrical potential and gravity (14):

$$\mu_j = \mu_j^0 + RT\ln a_j + \bar{V}_j P + z_j FE + m_j gh \qquad \text{(Eq. XIII: 1).}$$

The potential energy μ_j of the particular species j is here related to a standard reference level by the factor μ_j^0.

The next term represents chemical activity. R is the gas constant and T is temperature. The "effective concentration" is denoted as a_j of a species j, which will be experimentally examplified in several sections of this book. a_j is a product of the activity coefficient γ_j and the concentration c_j. The chemical activity term $RT\ln a_j$ is conventionally expressed in units of energy per mole.

The effect of pressure-volume is expressed by the term $\bar{V}_j P$, where $\bar{V}_j$ represents the differential increase in partial molar volume after a differential amount of j is added.

The effect of electrical potential is expressed by $z_j FE$, where z_j represents the charge number of j, F is Faraday's constant and E the actual electrical potential.

The last term $m_j gh$ includes an expression for gravity, where g is the gravitational acceleration factor and h the height of a mass m in relation to a reference level.

In calculations and descriptions of biologic energetics, Gibbs' free energy (G) expresses the maximum sum of different energy qualities which are available for work. Gibbs' free energy of a system therefore consists of many components, which with regard to ionic energy in a tissue may be expressed as:

$$G = \sum_j n_j \mu_j \qquad \text{(Eq. XIII: 2).}$$

n_j represents here the number of moles of species j in the system and μ_j the physicochemical potential of species j. These components of stored energy may be released either by individual chemical reactions between two reactants or by a series of reactions. In simplest form, A and B may react, producing C and D:

$$aA + bB \rightleftarrows cC + dD$$

where a, b, c, d represent participatory moles of A, B, C, D.

The bulk energy change of the reaction expressed by ΔG is then expressed:

$$\Delta G = -a\mu_A - b\mu_B + c\mu_C + d\mu_D \qquad \text{(Eq. XIII: 3).}$$

The signs of this equation are determined by a decrease (negative) of reactants and an increase (positive) of the products. ΔG represents in Eq. 3 the bulk change of free energy, which, by considering the individual energy factors of Eq. 1 can be expressed

$$\begin{aligned}\Delta G = &-a\mu_A^0 - b\mu_B^0 + c\mu_C^0 + d\mu_C^0 \\ &+ RT(-a\ln a_A - b\ln a_B + c\ln a_C + d\ln a_D) \\ &+ P(-a\bar{V}_A - b\bar{V}_B + c\bar{V}_C + d\bar{V}_D) \\ &+ FE(-az_A - bz_B + cz_C + dz_D) \\ &+ gh(-am_A - bm_B + cm_C + dm_D) \qquad \text{(Eq. XIII: 4).}\end{aligned}$$

Eq. 4 is somewhat troublesome to handle in practice. Simplified versions are therefore sometimes accepted. Most chemical tissue reactions, for example, take place at constant temperature and often at constant pressure. If the volume of the reactants $(a\bar{V}_A+b\bar{V}_B)$ is the same as the volume of the products $(c\bar{V}_A+d\bar{V}_D)$ the pressure-volume expression in Eq. XIII: 4 is zero. Moreover, the sum of the terms in the second to last parenthesis in Eq. XIII: 4 equals zero because no charge is created or destroyed, i.e., the term (az_A+bz_B) equals the term (cz_C+dz_D). The last partial reaction in Eq. XIII: 4 also is zero because no mass is created or destroyed by the reaction. The constant terms of Eq. XIII: 4 $(-a\mu_A^0-b\mu_B^0+c\mu_C^0+d\mu_D^0)$ can be replaced by ΔG^0. Eq. XIII: 4 can now be simplified to:

$$\Delta G=\Delta G^\circ+RT\ln\frac{(a_C)^c\,(a_D)^d}{(a_A)^a\,(a_B)^b} \qquad \text{(Eq. XIII: 5).}$$

When local chemical reactions are of the type presented in Eq. XIII: 5, their electrical energy is converted between the reactants at short distances of contact. In an electrolyte solution separated ions of opposite charge balance each other electrically. In spite of the absence of net electric charge the ionic separation is one of the prerequisites for new ionic recombinations. For local chemical reactions, the electrochemical potential is often expressed in the simplified version of Eq. XIII: 1 as follows:

$$\mu_j=\mu_j^0+RT\ln a_j+zFE \qquad \text{(Eq. XIII: 6).}$$

Formulas for calculation of electrochemical energy in the transfer of ions include oxidation–reduction reactions, where the redox potential E_j may be written:

$$E_j=E_j^0-\frac{RT}{zF}\ln\frac{(\text{reduced}\,j)}{(\text{oxidized}\,j)} \qquad \text{(Eq. XIII: 7).}$$

C. Interdependence of energies, including gravity

The abbreviations leading to Eq. XIII: 5–7, useful for chemical in vitro reactions, may be regarded from a slightly different point of view in in vivo situations.

It is easy to recognize that all four partial energy factors of μ_j (Eq. XIII: 1) are interdependent. For instance, a local change in concentration of ions will influence local volume-pressure conditions, and vice versa. The piezoelectric properties of dry and living bone tissue probably reflect such connections. Examples from physiologic studies of membranes are similar. Such considerations led Teorell (23, 24) to describe the integrated functions of chemical energy, volume-pressure and electric energy of a system he called the membrane oscillator. This concept represents an excitable system which is able to convert electrochemical energy into mechanical work. As interdependence of all four energy factors, and particularly of gravity, is not immediately obvious, the factor of gravity will now be the subject for some consideration.

It may seem unconventional to include a gravitational term in Eq. XIII: 1. Gravity is, however, an important and often overlooked factor. Small but constant forces are known empirically to produce considerable effects in vivo when they are allowed to act over long periods of time. Thus, the relative distribution of air and blood in lungs depends, for example, to a large extent on gravity. Gravity is known to affect the ratio between ventilation and perfusion in upper and lower parts of the lungs (28). Even the ratio between systemic and pulmonary arterial flow can be anticipated to vary in different parts of the lungs as a function of gravity. Gravitational forces are relatively less influential on blood in the high pressure bronchial arteries than in the low pressure pulmonary arteries. Weight of the blood and, to some extent, of the lungs themselves makes the peripheral air spaces larger at the apices of human lungs than at the bases. Gravity-induced relative effects on ventilation and on the pulmonary and bronchial circulations in different parts of the lungs can therefore be expected to trigger biological mechanisms which are of importance for the physiologic and pathophysiologic distribution of blood flow and ventilation. For example, well-ventilated portions of lung trigger their divisions of the pulmonary arteries to dilate and preferentially distribute blood to them (5). A shunting of systemic arterial blood, as from the bronchial arteries, to precapillary pulmonary vessels, will, however, constrict local pulmonary vessels.

Gravity has long been known to influence the localization of pulmonary tuberculosis. Thus, pulmonary tuberculosis in man is found most commonly in the apices of the lungs, while in the bat, which hangs upside down during hibernation, the disease tends to occur in lung near the diaphragm. In the cow, pulmonary tuberculosis is preferentially dorsal.

When the left side of the heart fails to pump adequately, the resultant oedema distributes preferentially to dependent parts of the lung (and other dependent parts of the body), a well known reaction related to gravity. Orthostatic reactions, balance and orientation are other simple and familiar examples of gravitational forces in animals.

Deep diving animals such as whales are exposed to very high external pressure when they dive as deep as 70 m under the surface of the sea. The external water pressure then compresses peripheral capillaries, promoting central diversion of blood. To prevent overload

on the heart and lungs, these animals possess valves which regulate the amount of venous blood that is allowed to flow into the thorax and reach the heart. It is in fact easy to find many morphological and functional adjustments to the force of gravity in animals as well as in plants. Furthermore, the force of gravity can be utilized in angiography to modify flow in vessels and to direct contrast material into predetermined vascular regions (15, 16). The author is aware that most gravitational effects of the type described above may be considered as "systemic", meaning that the mass of any individual molecule is so small that the gravitational force is apparent only on large, concentrated collections of molecules of different masses. However, this view could then also be applied to the chemical potential whose activity coefficient is dependent on concentration. For example, the gravitational effect of external sea water on distribution of blood in a whale, 70 m deep in the sea, should not be regarded as simply an effect of the weight of water. It is the gradient between reactants that counts in any concept of potential.

The main message of this discussion on gravity is that this factor must not be neglected in considering the truely "systemic" BCEC reactions. *VICC, e.g., represents an additional electrogenic circulatory system integrated with the mechanical bulk transport system of blood and lymph circulation.* Ionars and ergonars may present small but important volume-pressure and gravitational forces. The effects of even small gradients in vivo are particularly influenced by the factor of time. The "electrochemical" simplified Equation XIII: 6 is practical and useful in most in vitro reactions. In biology, when reactions in vivo take place in highly specialized matrices and over long time periods, all four energy components of the total physicochemical potential must be considered. The term "electrochemical" is, however, often used in the broad sense of "physicochemical" when electric and chemical energies are dominating.

D. Ergonic energy

The principle of BCEC makes it necessary also to consider the interactions of noncharged species as an integrated factor in closed circuit functions. These interactions lead us to the following considerations:

Whereas an ion is electrically charged, the electrical state of an ergon is internally balanced but electrically unstable. Ergons, like ions, are carriers of physicochemical energy. The total energy of an ergonic species e might then be expressed:

$$\mu_e = \mu_e^0 + RT \ln a_e + [z_e FE]^* + \bar{V}_e P + m_e gh \quad \text{(Eq. XIII: 8)}.$$

The total ergonic energy has the electric component $= [z_e FE]^*$. The asterisk means that this energy is utilized only under certain conditions. One may expect this utilization as a result either of redox reactions or of an externally induced imbalance of the electronic state of the ergon by mechanisms involved in the creation of electronegativity.

Eq. XIII: 1, 8, being nonstoichiometric, do not clearly express the internal relations between the partial energy factors of an ion or an ergon. Temperature, for example, is formed incorporated only in the expression for chemical potential. At the same time it is evident that temperature also affects pressure-volume and electrical potential. Pressure-volume, moreover, is closely related to gravity and to chemical and electrical potentials.

In a visual attempt to bridge these inadequacies, the physicochemical potential is presented graphically in Fig. XIII: 2 as tetrahedrons of ionic and ergonic energies. The energy components of μ_j are present in BCEC systems as ionars $(n \cdot \mu_j)$ and ergonars $(n \cdot \mu_e)$.

The interdependence of energy factors (1–4) of ions and the respective energy factors (1–4*) of ergons is demonstrated. The total amount of energy is represented by the volume of the tetrahedron. The relative magnitudes of the different energy components are represented by its shape. Each of these energies may vary in a positive or negative direction, as indicated by negative and positive vectors of force (arrows). A value for each of the energy components is necessary, as a tetrahedron must always have volume. The factor $[z_e FE]^*$ of an ergon is to be regarded as potentially available energy, despite balancing internal electrical forces. This formulation is appropriate because of the inherent tendency of an ergon to transform into an electrochemical reactant in a suitable surrounding. The tendency of an ergon to carry excess balanced charge is indicated by dashed arrows. Because a change of any one of the four energies will affect the shape of the tetrahedron, the model illustrates the interdependence of all the energetic components.

E. Conversion of ionic and ergonic energy

The energy of ions and ergons is utilized in the activation of BCEC systems (Fig. XIII: 2). These energy carriers then appear in collections as ionars and ergonars. They are further dependent on each other and on the structural and functional characteristics of BCEC channels. Ionars and ergonars change their shapes and densities (concentration–dilution) in relation to the channels of reaction. These channels include interstitial spaces, blood and lymph vessels, ductal canals and body cavities. Of great importance also are their dimensions, and abilities to vary their calibre.

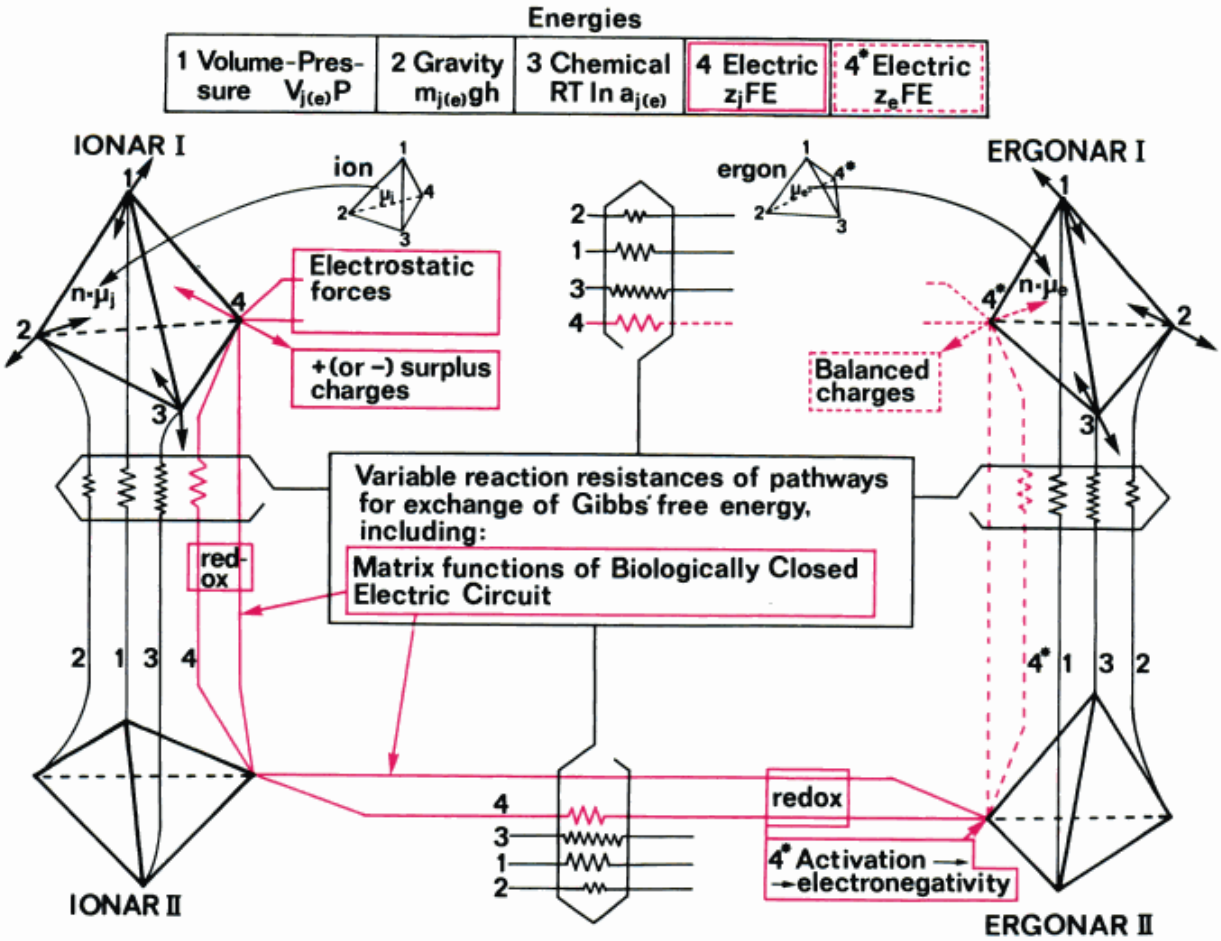

Fig. XIII: 2. Principle of exchange of energy over BCEC systems. The quadripartite energy of ergonars and ionars is depicted graphically as tetrahedrons. The electrical system of BCEC circuits is depicted in red. Ions and ergons carry four energy factors (1–4). Ions carry a + or − surplus of immediately available electric energy (4) while an ergon carries balancing + and − charges (4*). These ergonic charges may be brought into imbalance, leading to a varying degree of electronegativity. Collections of *n* ions or *n* ergons are represented by ionars and ergonars I and II. Factor 4* permits ergonars (e.g., oxygen or glucose) to "save" their energy from reactions during transport until suitable conditions for energy exchange are available. Activation of factor 4* is necessary for redox reactions of ergonars. The electromotive force of BCEC systems is directly dependent on factor 4 of ionars and indirectly on factor 4* of ergonars.

For further explanation, see text.

Ionars and ergonars thus change by diffusion, convection, local chemical and physical reactions in surrounding media and by changes of the channels of reaction. Ionars, in contrast to ergonars, will also change their concentration by electrophoretic transports over BCEC channels. These circumstances make it understandable that a defined number of ions or ergons does not always mean the same from the point of view of distribution of energetic compounds. The logarithmic expression for chemical activity does include the activity and concentration coefficient $a_{j(e)} = \gamma_{j(e)} c_{j(e)}$ for both an ion and an ergon, but does not include the matrix dependence which affects all four energy components. Vesicular transport, e.g., is suggested (Chapter XII) to represent a matrix mediated BCEC transport of ergonars. A complete definition of an activated, functioning BCEC is obtained by including all the variables of the channels of reaction, the ionic and ergonic potentials, the conductivity of the supporting electrolytes and the variable spatial locations of the reactants.

Ionar and ergonar energy can be further considered with regard to various specific partial mechanisms, e.g., diffusion, short and long distance chemical reactions, capillary flow, gravity and influences of fixed charges.

We will, however, now turn to mechanisms associated with ergionic transports and possible influences on physicochemical reactions in a BCEC system. Fig. XIII: 2 represents an attempt to show the interactions of the available Gibbs' free energy of ionars and ergonars. Thus, the paired ionars I and II and the paired

Table XIII: 4. *Energy-converting mediators*

Channelizing media	Membranes, tissue matrices, vessels, ducts, etc.
Transport media	Blood, gas, tissue and cell fluid, secretory products, etc.
Redox systems	
Chemical catalytic systems	
Transport systems	Mechanical systems for bulk transport Osmosis and convection of fluids, diffusion BCEC systems for selective transports

Table XIII: 6. *Some physicochemical effects supported by BCEC systems*

Selective transports
Structural development and functional effects
Healing of injured tissue
Promotion of homeostasis
Modulation of "local" chemical reactions
Generation of physicochemical potentials
Electric and magnetic effects by currents in BCEC channels
Effects of currents induced in BCEC circuits by external electromagnetic fields

ionar II and ergonar II are exchanging free energy. Each pair of reactants may exchange the energy of any one of the four partial energy components (1-4, 1-4*). The rates of these exchanges are determined by the ΔG^0 free energy of the reactants. The electrical factor of an ergon is then brought into a state of activation associated with a change of balance of its electrical charge. The BCEC channels then constitute pathways for selective ionic transports in ionar-ionar, ionar-ergonar and ergonar-ergonar reactions. As in any electrical closed circuit system, BCEC systems should also lead to a number of interesting effects, i.e., on "local" reactions even far away from the sources of the flow of current created by physiological or pathological polarization of tissue. Future acceptance of the principle of BCEC logically must also mean that local magnetic fields are induced by the flow of current. The exposure of a BCEC system to moving external magnetic fields, whether manmade or natural, will also induce a flow of current in the circuits. In this sense *BCEC systems must be considered not only as an additional circulatory system for selective transports and influences on local metabolic events, but also as receptors for influences by external magnetic and electric fields, in addition to their own ability to produce electromagnetic fields.*

Metabolic and catabolic processes can be described to exchange energy among different regions of tissue by energy-converting mediators. Table XIII: 4 lists examples. They are components both of systems for mechanical bulk transport (e.g., the gastrointestinal tract, blood and lymph circulation) and of BCEC systems for selective electrical transports.

The mechanical and electrical transport channels may be identical, e.g., vascular-interstitial communicating channels. This identity should lead to integrated mechanical and physicochemical events, as listed in Table XIII: 5.

Table XIII: 6 lists some anticipated general physicochemical effects of BCEC systems.

Table XIII: 5. *Integrated factors in energy exchange of BCEC systems*

Electrical	Polarization
	Electron transfer
	Migration
	Formation and recombination of ions, ergons
	Electroosmosis, fixed charges
	Ionar-ergonar ratio, resistance and capacitance of circuit
	Autoinduction of electric and magnetic fields
	Induction of current by external electromagnetic fields
Mechanical	Forced convection, pressure-volume forces
	Interferences by matrices
Chemical	Diffusion, concentration forces
Gravitation	Separation

F. Development of ionars

Diffusion may be regarded as caused by forces which are relatively integrating (dispersing) or disintegrating (concentrating). When diffusion takes place as a spread of a species (A) into the surroundings (B), the process is one of dispersion forces integrating (A) and (B). The reverse takes place when the process is dominated by an internal approach or disintegration of components of (A) respectively (B) by concentration forces.

The well known concept of a *liquid junction potential* or diffusion boundary potential must now be considered. This potential develops at the interphase between liquids of different concentration. Whenever, for instance, a small amount of a concentrated solution of HCl comes in contact with a weaker solution of HCl, differences in ionic mobility permit the protons to diffuse more rapidly than the chloride ions. The separation of ions is then counteracted by the liquid junction potential. Some values of ionic mobility are compiled in Table XIII: 7.

Table XIII: 7. *Ionic mobility* u_j ($cm^2 V^{-1} s^{-1}$) 25°C

	H^+	Li^+	Na^+	K^+	OH^-	Cl^-	NO_3^-
$u_j \cdot 10^4$	36.2	4.0	5.2	7.6	20.7	7.9	7.4

Ionic diffusion takes place according to Fick's first law $-Q = D(\delta c/\delta x)$ in which Q (in mol $m^{-2} s^{-1}$) is the quantity of ions traversing a unit area of solvent per unit time. The factor D is the diffusion coefficient, which expresses (in $m^{-2} s^{-1}$) the proportional ability of an ion to diffuse a distance dx in a solvent at a concentration difference dc. In a nonsteady state this concept can often be expressed as x = constant $\sqrt{Dt}$, where D = diffusion constant ($m^{-2} s^{-1}$) and t = time (sec). It is evident that liquid junction potentials will, starting from zero in a closed container, develop a maximum potential difference and then return to zero.

Considering a nonstationary condition, the amount of material Q passing a unit area A per second over a distance dx will lead to the following equation

$$QA - \left(Q + \frac{\delta Q}{\delta x} dx\right) A = \frac{\delta c}{\delta t} A dx, \qquad \text{(Eq. XIII: 9)},$$

which in words tells us that the inflow of material Q through the area A, minus the rate of Q through the area A over the distance dx, equals the concentration change per unit time through the distance dx through the same area A. This equation can then be simplified to the well known continuity equation $-\delta Q/\delta x = \delta c/\delta t$. By substituting Fick's first law into the continuity equation we obtain Fick's second law $\delta c/\delta x = D(\delta^2 c/\delta x^2)$, which in a three-dimensional distribution, gives $\delta c/\delta t = D(\delta^2 c/\delta x^2 + \delta^2 c/\delta y^2 + \delta^2 c/\delta z^2)$. This equation describes one function of local administration of a drug during *application of direct current in tissue* (Chapter XIV). In many instances, a more general expression for diffusability of material is used than the one for ionic mobility:

$$\text{Diffusion coeff} = D_j = u_j \cdot \frac{RT}{z_j F} \qquad \text{(Eq. XIII: 10)}.$$

Values of charge number, equivalent conductances and diffusion coefficients of some selected ions at infinite dilution in water at 25°C are compiled in Table XIII: 8 (13).

Table XIII: 8 shows that most ionic diffusion coefficients are about 1 or 2×10^{-5} cm^2 sec^{-1}, except for hydrogen ions and hydroxyl ions, for which D_i is 9.3 and 5.3×10^{-5} cm^2 sec^{-1}, respectively.

The equivalent conductance Λ of salt is obtained by summation of the values of each ion pair

$$\Lambda = \lambda_+ + \lambda_- \qquad \text{(Eq. XIII: 11)}.$$

Table XIII: 8. *Values of equivalent conductances and diffusion coefficients of selected ions at infinite dilution in water at 25°C*

ion	z_i	λ_i^0 $\frac{mho-cm^2}{equiv}$	$D_i \times 10^5$ cm^2/sec
H^+	1	349.8	9.312
Li^+	1	38.69	1.030
Na^+	1	50.11	1.334
K^+	1	73.52	1.957
NH_4^+	1	73.4	1.954
Ag^+	1	61.92	1.648
Tl^+	1	74.7	1.989
Mg^{++}	2	53.06	0.7063
Ca^{++}	2	59.50	0.7920
Sr^{++}	2	59.46	0.7914
Ba^{++}	2	63.64	0.8471
Cu^{++}	2	54	0.72
Zn^{++}	2	53	0.71
La^{+++}	3	69.5	0.617
$Co(NH_3)_6^{+++}$	3	102.3	0.908
OH^-	−1	197.6	5.260
Cl^-	−1	76.34	2.032
Br^-	−1	78.3	2.084
I^-	−1	76.8	2.044
NO_3^-	−1	71.44	1.902
HCO_3^-	−1	41.5	1.105
HCO_2^-	−1	54.6	1.454
$CH_3CO_2^-$	−1	40.9	1.089
SO_4^-	−2	80	1.065
$Fe(CN)_6^{3-}$	−3	101	0.896
$Fe(CN)_6^{4-}$	−4	111	0.739
IO_4^-	−1	54.38	1.448
ClO_4^-	−1	67.32	1.792
BrO_3^-	−1	55.78	1.485
HSO_4^-	−1	50	1.33

The actual conductivity of a tissue then depends on the sum of different $\Lambda_{i\pm}$ and their concentrations in relation to "nonconducting" substances. Among the "nonconductors", bone, fibrous tissue, dielectric components in cell membranes, sucrose, neutral fat, gas and water are the most important. Biologic tissues can therefore be regarded as electric conductors possessing different intersected ohmic and capacitative resistances. This property also makes it possible theoretically to predict the existence of preferential pathways for electric current in tissues.

Fig. XIII: 3 shows how an ionic separation may take place by diffusion at the interface between a droplet of a strong HCl solution in a weak HCl solution. The ionic separation leads to one electropositive and one electronegative phase.

The individual proton and chloride ions represent here the smallest components of an ion pair. The symbol ⚠ indicates that each ion carries four physico-

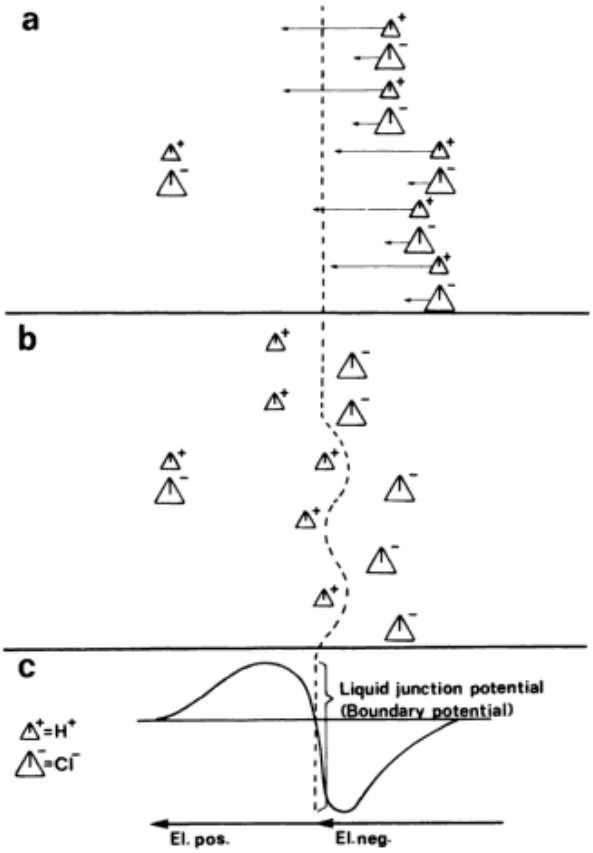

Fig. XIII: 3. Liquid junction potential arising from the development of two ionars (spatially separated collections of ions). (*a*) Droplet of concentrated HCl solution to the right, in diluted HCl solution. The dotted line indicates only an interface and is not a membrane. Each ion carries a physicochemical charge of four interdependent energy components (visualized as a tetrahedron symbol △). (*b*) Because protons diffuse more rapidly than other ions, a relative excess of protons collects temporarily to the left and an excess of chloride ions to the right, giving rise to a transient electric potential difference. (*c*) The potential profile through these phases shows two collections of ions (ionars), one electropositively and one electronegatively charged. The shapes and charges of their cross sectional charge profiles are different, although their total charge is equal.

For further explanation, see text.

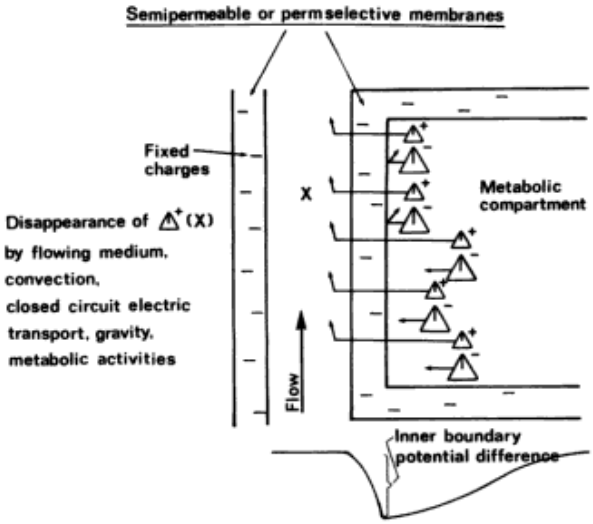

Fig. XIII: 4. Development of an ionar: modifying factors. Diffusion or different speeds of recombination of ions may enhance ionic separation during metabolic activity. The presence of a semipermeable or permselective membrane will contribute to the development of ionic separation. Resorption and flow of metabolic products can be expected to remove externally diffused ions. The electric potential of such a metabolic ionar versus the different electric potential of another tissue region may lead to the development of a self-driving system within the channels of a BCEC.

For explanation of symbols, see Figs. XIII: 2, 3.

chemical energies (Eq. XIII: 1, Fig. XIII: 2). Due to diffusion of the ions, an electric junction potential will develop. Before diffusion, electroneutrality was present inside and outside the droplet. The chemical dispersion forces are, however, stronger than the concentration forces, which leads to some degree of separation. The resulting electric liquid junction potential is therefore an example of the internal dependence of chemical and electrical forces leading to spatially new energy constellations of transient, diffusing ionars. Also in this connection, volume-pressure and gravitational energy components must not be neglected. Fig. XIII: 3, it should also be noted, shows that one of the energy components, the liquid junction potential, presents different profiles of positive and negative electric charge for each ionar.

The creation of ionic separation can be shown as follows (Fig. XIII: 4). Assume metabolic activities have started in an organ surrounded by a semipermeable or permselective membrane. Some of the ionic metabolites will diffuse through the membrane. Other ions are relatively retarded and concentrate within the metabolic compartment. Various factors outside the membrane, such as mechanical or electric transports or ionic recombinations, lead to removal of ions which have passed the membrane barrier. These changes may result in a transmembranous difference of physicochemical potential. The compartment therefore carries an ionar. This step is important: it leads logically to a search for the mechanisms which are involved in the spontaneous levelling of the actual potential differences. The evident importance of modern electric technology based on closed circuits may here have its biological counterpart. This counterpart, however, appears to be even more complicated than contemporary electronic machinery. To begin, simultaneous interferences must take place among all four ionic energy factors. And, indeed, they behave differently in relation to each other and to surrounding media. The presence, for example, of a mechanical flow on one

side of a membrane may change the transmembranous potential gradients. A change of turgor pressure by impaired circulation may interfere with transmembranous ion and water transports and favour gravitational influences. Selective ionic transports may take place without any mechanical gradient of flow in a BCEC. Reactions may be modified differently by catalysts and intersected redox reactions. Available free ionic energy among ionars is, in other words, selectively available. The availability of this energy also depends on the functions of different energy-converting mediators.

The principal difference between the physicochemical energy of ionars and ergonars is the electrical factor. An ion presents either a reduced or oxidized state of charge while an ergon presents the possibility of being reduced or oxidized from an unstable but balanced state. Nevertheless, just as with ions, the four potential energy components of ergons are interdependent. For the time being, any attempts to prove such a statement must rely on logical theory. Ions as ergons are particles which participate in redox reactions. The oxidation or reduction of ergons leads to the creation of ions. An oxidation or reduction of ions may also lead to the creation of ergons. The close relationship between these two types of energy carriers is evident. Nevertheless, they function differently in many respects during energy conversion. The development of ionars and ergonars and their behaviour in a closed electric circuit will now be considered experimentally. We will study electrolysis first of water and then of a salt solution, to illustrate the basic principle of creation and interaction of ionars and ergonars in a matrix over a closed electric circuit.

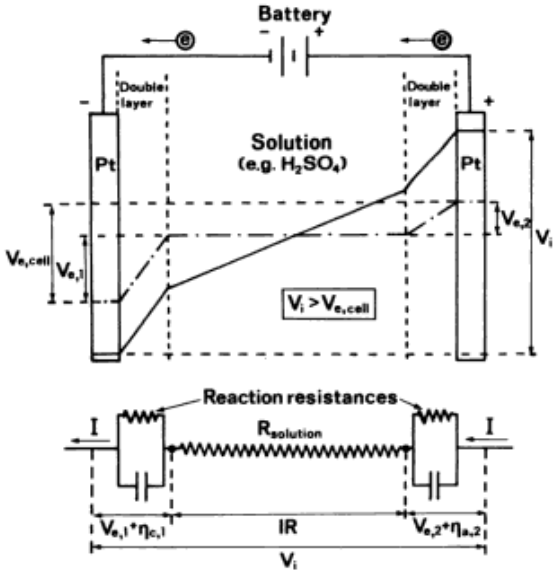

Fig. XIII: 5. A driven electric cell. When there is no net current, the cell has an equilibrium voltage, $V_{e,\text{cell}}$ (broken line). When the current is increased, the cell voltage V_i is larger by the sum of the overpotentials (η) developed, plus the IR drop (full line). Below, simplified equivalent circuit (From Bockris and Dražić).

G. Ionars and ergonars in experimental electrolysis of water

Certain partial functions of BCEC systems are more conveniently demonstrated in in vitro than in in vivo studies. Such is the case with production and interaction of ionars and ergonars in closed circuit reactions over a matrix.

We will carry out two electrolytic experiments: first, water is treated in a closed circuit *driven system* by an external source of electric power, which leads to the creation of ionars and ergonars. Later, it will be shown how these energetic compounds can release their energy as a *self-driving system* in a closed circuit. The ergonars participating in the reactions are $n \cdot H_2O$, $n \cdot O_2$ and $n \cdot H_2$ while the ionars are $n \cdot H^+$ and $n \cdot (OH)^-$. Polymers of these compounds will not be considered in this experiment, which is intended to deal only with some basic principles.

Consider a whole electrochemical cell in vitro, as described by Bockris and Dražić (1). Two platinum electrodes (Fig. XIII: 5) are immersed in an electrolyte solution and connected with each other via cables and an electric battery. The electric double layer at the electrode surfaces is shown to represent a capacitance and resistance in parallel. When there is no net current, the cell has an equilibrium voltage, $V_{e,\text{cell}}$ (broken line). When current is flowing, the cell voltage V_i is greater than $V_{e,\text{cell}}$ by the sum of the overpotentials[1] plus the IR drop in the solution. The voltage drop IR is linear and is a function of the current passing and the resistance of the solution.

Fig. XIII: 6 shows the situation when the cell functions as a battery which is discharged over the outer circuit. In this case the overpotentials are subtracted from the total equilibrium cell voltage. The electric double layers (2, 6, 7) extend away from the electrode surfaces usually only a few (to perhaps 50) Å. We will now take a look at corresponding events in the presence of a matrix.

Unlike the conditions in a nonstabilized electrolyte solution, the conversion of energy in closed circuit electric transports, e.g., in a vascular-interstitial closed

[1] Overpotential represents the electric potential in excess of the equilibrium potential in electrode reactions. At equilibrium potential, electrode reactions proceed, but without any net flow of current between the electrodes.

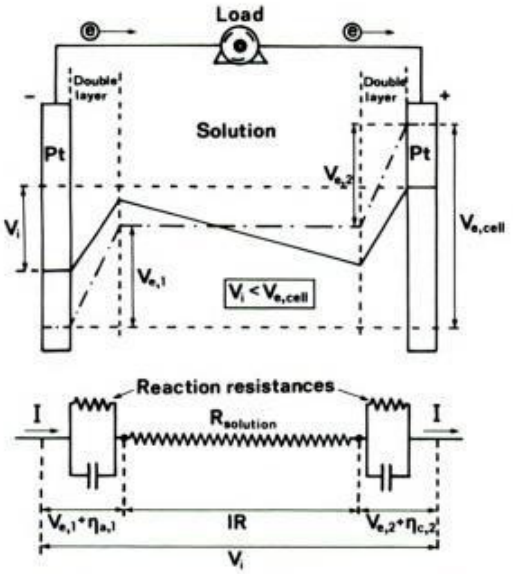

Fig. XIII: 6. A self-driving electric cell. The direction of flow of current is opposite to that of the current in the driven cell, and the overpotentials (η) have opposite signs. The cell voltage V_i is less than $V_{e,cell}$ by the sum of all overpotentials plus IR drop (from Bockris and Dražić).

circuit (VICC), presents modifications of energy exchange. The interstitial branches of VICC channels possess important matrix functions, e.g., by their "capillarity" and the existence of fixed surface charges, at the same time as they create conducting channels for the biologically closed electric circuit. As an aid toward insight into the actual problems, an in vitro analogue, as simplified as possible, is presented.

Platinum string electrodes were placed against a matrix of T-shaped filter paper, impregnated with litmus and soaked in water on a perspex plate (Fig. XIII: 7 *a*). Either four or ten volts were applied over the electrodes, starting electrolysis. Hydroxyl ions, colouring litmus blue, and hydrogen molecules are then produced at the cathode. Protons, colouring litmus red, and oxygen gas are produced at the anode. The induced changes of potential between the two platinum electrodes were measured with Ag–AgCl electrodes in 2 M KCl agar bridges, 5 mm in length, in glass capillaries with an internal tip diameter of 1 mm. A grounded reference electrode of equal construction was positioned at the end of the "stem" of the T-shaped filter paper. The perspex plate holding the water-soaked filter paper and the reference electrode was moved by a driving mechanism (Grass chart writer). The "recording" electrode was fixed at one of the pen-holders of the instrument. It was found that the presence of litmus in the filter paper had no observable influence on the tracings of potential.

Recordings are illustrated (with litmus in the filter paper and during application of four volts over the electrodes), first from the cathode to the anode (Fig. XIII: 7 *b*, left half) and then in the opposite direction (Fig. XIII: 7 *b*, right half). These tracings show roughly the same profile of potential, indicating that no apparent leak of current has taken place through the recording circuit. Each tracing between the electrodes shows an S-shaped profile of potential, with the cathodic field electronegative in relation to the anodic

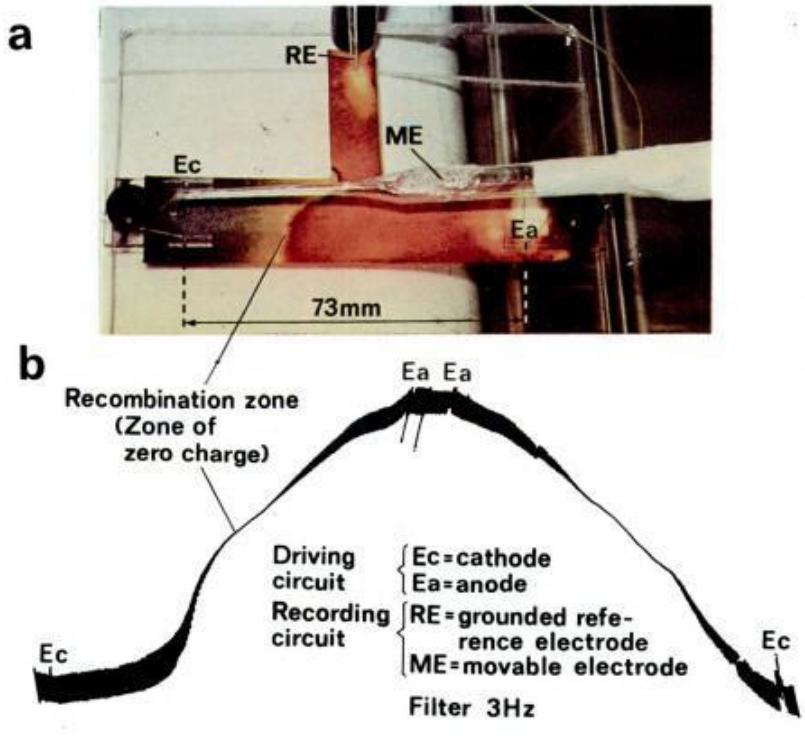

Fig. XIII: 7. Experimental production of ionars and ergonars by electrolysis of water in filter paper impregnated with litmus. Four volts cell voltage. (*a*) Cathode to the left shows blue OH^- reaction and anode to the right red H^+ reaction. These two ionars, $n(OH)^-$ and nH^+, diffuse and migrate until they meet, where water (an ergonar) is produced by ionic recombination. (*b*) Electric potential difference, traced over the filter paper from left to right, then from right to left, shows electronegative cathodic and electropositive anodic potentials in relation to the grounded reference electrode (RE). Superimposed oscillations (2–3 per second) attenuate in the direction of the zone of zero charge, where water was produced. These oscillations are produced mainly by disturbances in conductivity caused by bubbles of nH_2 and nO_2 (ergonars) trapped in the matrix.

For further explanation, see text.

field (or the same polarity as the power source). Oscillations of the tracings are also seen, of greatest amplitude close to the cathode. They diminish successively in the direction away from the cathode. The amplitude of the oscillations increases again toward and at the anode. The frequency of these oscillations averaged around 2–3 per second, depending on the speed of movement over the matrix. As the filter paper dried, the irregularity of these oscillations increased while their frequency decreased. "Jumps" in the tracings were usually produced when the "recording electrode" passed over the platinum string electrode. The impedance of the recording circuit was in this experiment only one megohm. A frequency filter of 3 Hz was used.

The electrochemical events in this part of the experiment can be explained as follows. The water itself, being a nonionic compound (ergonar), is a precursor for the development of an attenuating collection of OH^- ions (ionar) in the cathodic area and a corresponding collection of H^+ ions (ionar) in the anodic area. These ionars move by diffusion and migration in the electric field (as demonstrated in Fig. XIII: 7 *a* by the colouring of the filter paper, which had been prepared with litmus before water was added and current was applied). The two coloured fronts in Fig. XIII: 7 *a* meet according to the relative speed of diffusion and migration of the hydroxyl and hydrogen ionars and recombine to form water (in a recombination zone). The movements of these ionars were found to be very sensitive to gravitational influences in the experiments. In the example illustrated, the filter paper and its support had to be properly adjusted in the horizontal plane with a water-level.

In the alkaline environment of the cathodic surface the reaction proceeds:

$$2H_2O+2e^- \rightarrow H_2+2OH^-$$

and in the acid environment of the anodic surface:

$$H_2O-2e^- \rightarrow \tfrac{1}{2}O_2+2H^+.$$

A flow of current between the electrodes has been explained to proceed in the following way (4, 17). Both H^+ and OH^- are strongly hydrated in water as H_3O^+ (oxonium) or even larger complexes, e.g., $H_9O_4^+$. These ions are short lived. They can dissociate rapidly, recombine and allow protons to jump along hydrogen bonds. These changes correspond to a rapid transfer of charge:

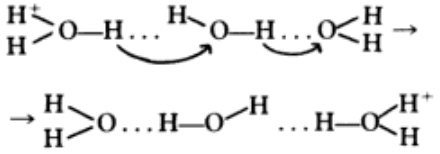

Similarly one proton of a water molecule can jump along a hydrogen bond to combine with an OH^- ion:

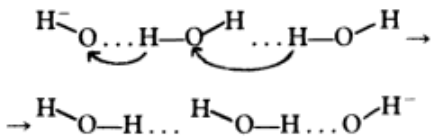

Both processes should lead to a flow of current, corresponding to the equivalent flow of electrons in the electrical cables between the power source and the electrodes.

The interesting function of the matrix now entering the picture is its capacity to reduce the effects of convection and also to adsorb and trap reaction products. Without a matrix, the distinct zones of alkalinity, acidity and recombination ("zone of zero charge", Fig. XIII: 7 *a*) could hardly develop. Moreover, hydrogen and oxygen gas should readily disappear from the system except for adsorption against the electrodes as gas bubbles. The bubbles prevent water diffusing to the electrodes, thereby counteracting the process of electronation and deelectronation. The electrolytic process may then even cease, sometimes rapidly. If we now turn to the reaction in Fig. XIII: 8, we will find that the bulk water in the matrix represents an ergonar (= an ionar precursor). Electrolysis gives rise to local accumulations of one cathodic, $n(OH^-)$, and one anodic, $n(H^+)$ ionar and two new ergonars, the cathodic-adsorbed hydrogen gas, nH_2, and the anodic-adsorbed oxygen gas, nO_2.

Let us now try to identify these energy collections of ionars and ergonars (Figs. XIII: 8–11).

By using the same arrangement as shown in Fig. XIII: 7 *a*, electrolysis of water was first produced in a matrix of filter paper impregnated with litmus. Electrolysis was allowed to proceed until the litmus reactions showed that the alkaline and acidic zones touched each other. This process took as long as 24 hours (the electrolysis had to be performed in a humid chamber to prevent drying of the matrix). Fig. XIII: 8 *a* shows the actual matrix with litmus reactions, platinum electrodes (Ec, Ea) and position of the reference electrode (RE) of the recording circuit. The Ag–AgCl electrodes of the recording circuit are not shown.

Tracings of the electric potential between the (Ec, Ea) electrodes were first performed from the cathode to the anode and then back, during application of 4 volts externally applied voltage over the electrodes (Fig. XIII: 8 *b*). Irregular oscillations are seen corresponding to the alkaline, relatively electronegative zone but only minor oscillations corresponding to the acidic, electropositive zone.

What is the origin of the oscillations? One explanation may be that the recording electrode passes trapped gas bubbles adherent to the matrix. Larger

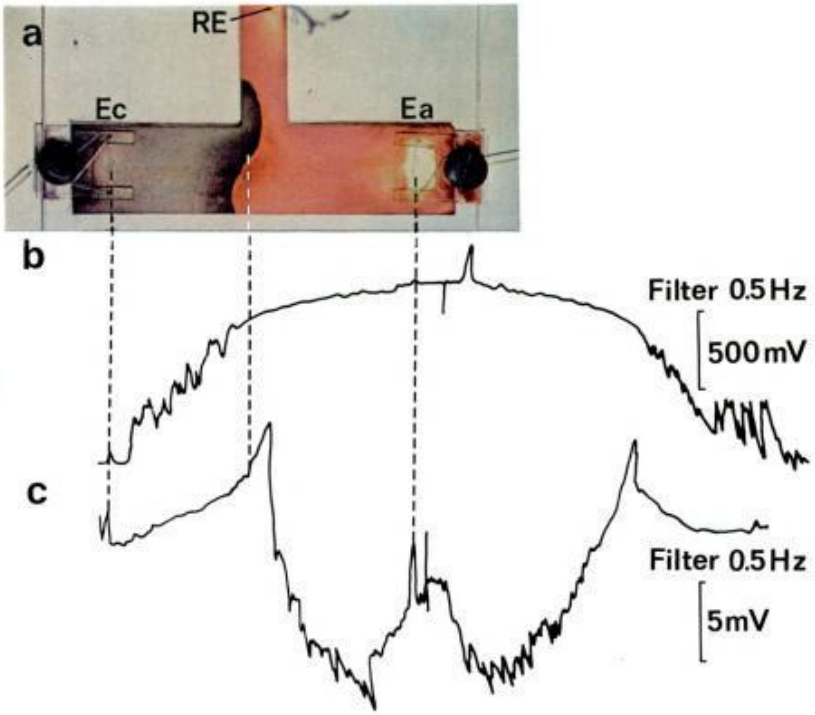

Fig. XIII:8. Electrolysis of water in filter paper matrix impregnated with litmus and exposed to open air. (*a*) Hydroxyl ions produced at cathodic electrode (*Ec*). Protons are produced around anode (*Ea*). (*b*) Measurement of potential over the matrix during application of four volts cell voltage. When the external power source is disconnected (*c*), a minimal leak of current through the recording circuit indicates a self-driving system. Unexpectedly, the cathodic potential is electropositive and the anodic potential partly electropositive. This finding indicates the presence of a disturbing reaction (CO_2 from surrounding air, see further text).

oscillations are therefore seen in the cathodic area than in the anodic, perhaps because twice as much hydrogen gas is evolved as is oxygen gas. Differences in dissipation from the matrix are also a possible additional factor. Still another possibility must not be overlooked. The Ag–AgCl electrodes are provided with 3 M KCl-agar bridges. On contact with the water-soaked matrix, the salt will diffuse from the bridge and start to migrate in the applied electric field, $n\mathrm{K}^+$ toward the cathode and $n\mathrm{Cl}^-$ toward the anode. These migrating ionars will increase conductivity between the gas bubbles and modify local electric potentials.

A prerequisite for recording of voltage differences with the actual instrument (Grass Polygraph Model 7B) is a minimal flow of current through it. The effect of changing the impedance of the recording circuit from 10 megohms to 1 megohm is shown in Fig. XIII:9. The matrix was now soaked in a 2 M KCl solution and 4 volts applied between the platinum electrodes for about one hour. A tracing of the potential from left to right and then back, compared to the grounded reference electrode, shows a nearly symmetrical profile of potential (Fig. XIII:9*a*), when the impedence of the recording circuit was 10 megohms. When the impedance is lowered to 1 megohm, the symmetry became distorted considerably (Fig. XIII:9*b*), caused by a leak of current, now apparent, through the recording instrument. In this case we will, however, make use of a minimal leak of current through the recording circuit in attempts to activate the energy of the $n\mathrm{H}_2$ and $n\mathrm{O}_2$ ergonars anticipated to be trapped in the matrix. In fact, we are intending to start hydrogen and oxygen fuel cell reactions over the recording circuit. We will proceed stepwise and next disconnect the external power source, which was done

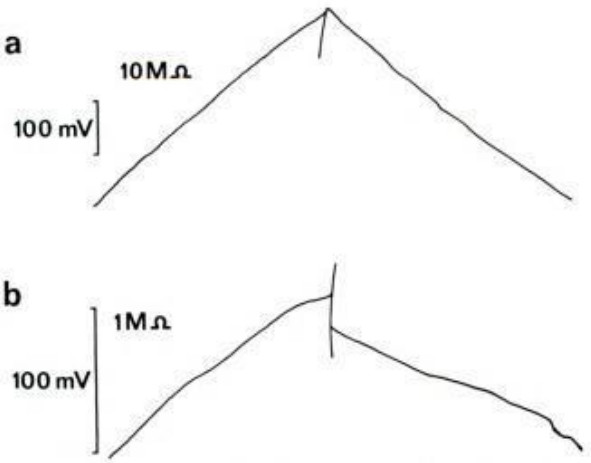

Fig. XIII:9. Electrolysis of 2 M KCl solution (in filter paper matrix, 4 volts between platinum electrodes). (*a*) 10 megohms impedance of the recording circuit. Tracings of potential from left to right and then back over the matrix show only slight asymmetry. (*b*) When impedance of the recording circuit is lowered to 1 megohm, the increased leak of current through the instrument distorts considerably the two branches of the tracing of potential. Filtering excludes superimposed oscillations.

before the tracing of potential shown in Fig. XIII: 8*c* was obtained. Immediately upon disconnecting these cables the voltage is lowered by the applied 4 volts, including the IR drop over the matrix.

The system is now characterized electrically by the sum of the metal potentials and the remaining diffusion potentials. One might expect a profile of potential remaining across the matrix to be determined by hydroxyl ions to the left and protons to the right. However, as seen in Fig. XIII: 8*c*, the left part of the matrix is electropositive in relation to the right part. Fresh litmus paper, soaked in water and placed on the matrix, showed persistent alkalinity (pH 10-11) to the left and acidity (pH 2-3) to the right.

Is it perhaps possible that the nH_2 and nO_2 ergonars have started "fuel cell" reactions over the recording circuit? Such reactions are, however, not possible. First, the KCl-agar bridge prevents effective contact between gas in the matrix and the "recording" electrode surface. Secondly, the half-cell potential of an Ag–AgCl electrode at 25°C is +210 mV, relative to a NHE, while the H_2 potential at pH 10 is −590 mV. Consequently, even on contact with the electrode, a H_2 reaction could result only in a lowering of this potential component. Furthermore, this possibility is only hypothetical as the actual electrode can only trace the diffusion potential. Similar arguments may be raised against an action of trapped oxygen in the acidic part of the matrix as an explanation for its relatively lowered potential. Because the potential of O_2 at pH 3 is +1 050 mV, the potential on the right acidic part of the matrix should be elevated. Instead, the experimental conditions presented prevent action of the hydrogen and oxygen ergonars, which under other conditions could be very powerful. Such a restriction of function is a characteristic property of ergonars, which may be recognized as extremely important for transport and conversion of energy in biology. Unlike ionars, ergonars can "save" their stored electrical energy until they arrive at a reaction site suitable for release of energy. We will return to this problem soon and show how we can activate the nH_2 and nO_2 ergonars in the actual experiment. First, however, the potential profile of the self-driving system (Fig. XIII: 8*c*) needs explanation.

The diffusion and migration of ions over the KCl bridge as described above may contribute to some extent to changing the potential in the matrix.

Another factor to consider is the possibility of contamination from CO_2 in surrounding air, because CO_2 is easily dissolved in water,

$$CO_2 + H_2O \rightarrow H^+ + HCO_3^-$$

On the alkaline left side this reaction will lead to:

$$OH^- + HCO_3^- \rightarrow CO_3^{2-} + H_2O$$

which means a diminished electronegative potential, while on the acidic right side:

$$H^+ + HCO_3^- \rightarrow H_2CO_3 \rightarrow H_2O + CO_2$$

which means a diminished electropositive potential.

The resulting potential profile in Fig. XIII: 8*c* apparently also depends on several other factors in addition to the matrix reactants and reaction products described above. For example, variations in concentration should appear by matrix adsorption of locally formed water as well as by migration of HCO_3^-, protons and hydroxyl ions. For these reasons the studies were continued in attempts to exclude possible sources of error.

The possibility of contamination of the distilled water by foreign material was first checked in terms of its conductivity ($\varkappa$), which revealed:

$$\varkappa(24°C) = 0.3 \times 10^{-5} \text{ ohm}^{-1} \text{ cm}^{-1} \text{ (pH 6.4)}$$

as compared with theoretically "clean" water:

$$\varkappa(24°C) = 0.4 \times 10^{-7} \text{ ohm}^{-1} \text{ cm}^{-1} \text{ (pH 7.0)}$$

An acidic contamination by easily soluble atmospheric CO_2 was therefore highly suspected. The water was therefore "washed" with flowing argon gas for 24 hours before testing. Next, the electrolyses and measurements of potential were performed in a chamber which allowed the whole experiment to be performed under continuously flowing argon gas. To prevent drying of the matrix, the argon gas was wetted with water (free of CO_2) before it was led through the electrolysis chamber.

Testing of the potential recording system also showed that loss of potential at 1 megohm impedance of the recording instrument was too high when redox reactions were started over the recording circuit. A digital voltmeter with 20 megohm impedance was, however, found suitable for the purpose. Moreover, to avoid mechanical stirring effects by the electrode moving over the matrix, measurements of potential were made at regularly intermittent distances along the matrix (2.5, 5 or 10 mm apart). Employing these modifications, new experiments were then undertaken.

In Fig. XIII: 10 the litmus-filter paper shows an alkaline reaction to the left and an acidic reaction to the right (one hour after application of 10 volts between the platinum electrodes (Ec, Ea), positioned 7.5 cm apart on the matrix, previously soaked in argon-treated distilled water). The electrolysis and subsequent steps of the experiment were performed under protection of flowing argon gas in the electrolysis chamber. During electrolysis (*A*) the potential was measured between the nonpolarizable Ag–AgCl reference (Ag I) and "recording" (Ag II) electrodes. The potential difference recorded over the matrix between these electrodes was 6.71 volts after one hour. The

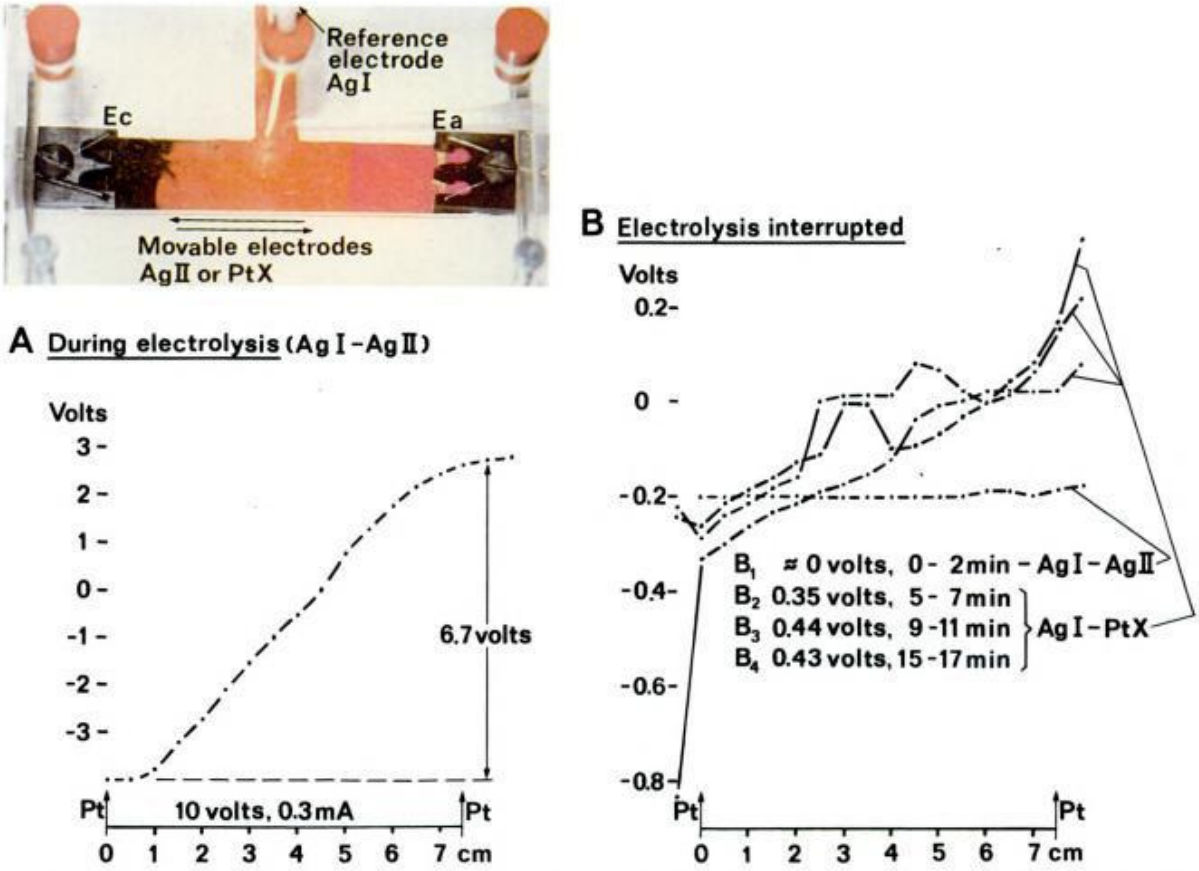

Fig. XIII: 10. Electrolysis of distilled water on litmus-filter paper, protected from atmospheric CO_2 by continuous washing with argon gas. Stationary reference (Ag I) and movable (Ag II) are Ag–AgCl electrodes (2 M KCl-agar bridges). PtX is a movable platinum electrode. (A) During electrolysis with 10 volts, the electric potential measured over the matrix at regular intervals (instrument impedance 20 M-ohm) revealed a difference of 6.71 volts. (B) During interrupted electrolysis, one measurement B_1 was performed with nonpolarizable Ag I and Ag II electrodes. Accumulated OH^- and H^+ ions appear not to affect the potential difference over the matrix, which is likely to depend on compensatory effects by migration of potassium and chloride ions from the KCl bridge of the Ag II electrode. B_2–B_4 represent three measurements of potential over the matrix (Ag I and PtX electrodes). These measurements revealed electric gradients of 0.35–0.44 volts. The disturbing effect from atmospheric CO_2 is now excluded. See also discussion (Section H) in text.

electrolysis was then interrupted (*B*) and one measurement (B_1) of potential was made over the matrix between the two nonpolarizable electrodes (Ag I and Ag II), which revealed no appreciable potential difference. Three further measurements of potential were then made between the Ag I reference electrode and a "recording" *platinum electrode* (*PtX*). These tracings showed B_2=0.35, B_3=0.44 and B_4=0.43 volts difference over the matrix between the cathode and anode.

The magnitude of these potential differences may be explained as produced by the platinum, whose potential should be determined by the Pt–PtO electrode in relation to existing alkaline and acidic surroundings. However, the participation of nH_2 and nO_2 ergonars in redox reactions in the matrix cannot be excluded. In order to explore further this possibility, an augmentation of associated reactions became necessary. The experiments were therefore continued in the following way:

The production of ergonars was increased by increasing the time of electrolysis and the amount of current. Instead of only water in the matrix, a 2 M KCl solution was now used. The concentration of KCl was made identical with the concentration of KCl in the salt bridge of the nonpolarizable Ag–AgCl electrodes, thereby excluding any possible error from diffusion potential at these electrodes.

The experiment (Fig. XIII: 11) was carried out as in the previous experiment but with 4.1 volts between the electrodes for 12 hours. After this time the alkaline and acidic fronts had met and formed a recombination zone about 27 mm from the cathode and 48 mm from the anode. Around the anode chlorine bleached the litmus to about 5 mm from the electrode. Close to the recombination zone on the acidic side a dark red zone, four mm broad, in the litmus also accumulated. After 12 hours of electrolysis, a potential difference of 0.4 volts was measured over the matrix (Fig. XIII: 11 A).

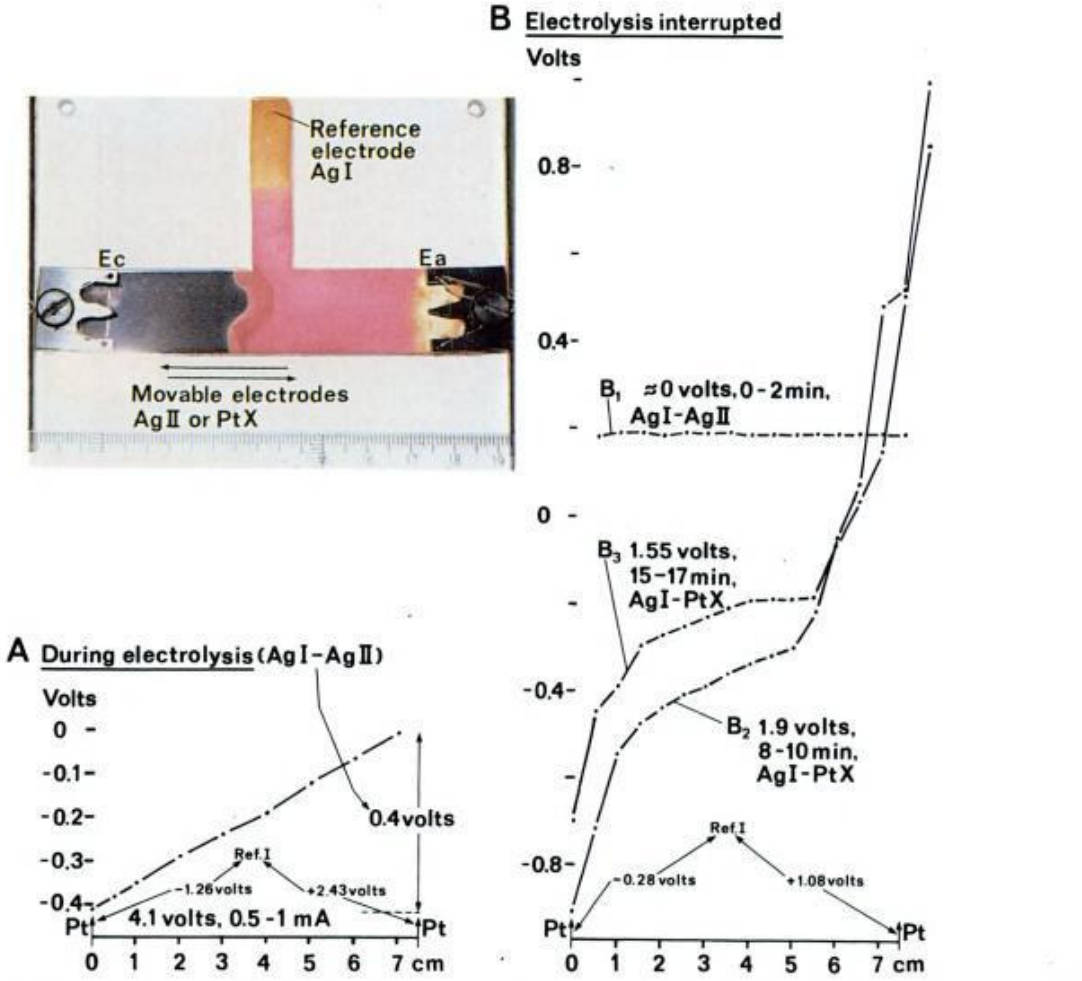

Fig. XIII: 11. Production of ionars and ergonars by electrolysis: creation of conditions which release electric energies from ergonars. Enhancement of electrolysis by supply of a supporting salt and by prolongation of time of treatment to 12 hours (2 M KCl solution, litmus-filter paper under protection of argon gas). Reference (Ag I) and movable (Ag II) are Ag–AgCl electrodes with 2 M KCl-agar bridges. PtX is the movable platinum electrode. (A) During electrolysis at 4.1 volts cell voltage, a 0.4 volt potential difference is measured over the matrix. In this case the compensatory effect on the alkaline and acidic products is caused by migration of the counterions of the supporting electrolyte, K^+ and Cl^-. (B) Electrolysis is interrupted. (B_1) The diffusion potential is measured with Ag I and Ag II electrodes. The matrix shows electric equilibrium. (B_2, B_3) When the Ag II electrode is replaced by the platinum (PtX) electrode, redox reactions are started at the metal surface by $n H_2$, $n O_2$ (and $n Cl_2$) ergonars, trapped in the matrix. A minimal amount of current leaks through the recording circuit, a requirement for the electrode reactions. The potential differences of 1.55 and 1.9 volts over the matrix have a magnitude that can not be explained by the pH dependence of the potential of the platinum metal. See also discussion (Section H) in text.

Measurement of the potential of the platinum electrodes (Ec, Ea) in relation to the reference Ag I electrode showed +2.43 volts (anode) and −1.26 volts (cathode) potential.

The electrolysis was then interrupted (*B*) and the potential was again measured over the matrix using nonpolarizable Ag–AgCl electrodes. The potential measurements (B_1) revealed no appreciable voltage difference over the matrix. The "recording" Ag–AgCl electrode (Ag II) was then replaced by a platinum electrode (PtX). The first tracing over the matrix (B_2) now showed a potential difference of 1.9 volts. Five minutes later a new potential measurement (B_3) showed a potential difference of 1.55 volts. Measurements were then made of the Pt electrodes in relation to the Ag I reference electrode which revealed +1.08 volts (anode) and −0.28 volts (cathode). All the experiments in this section were performed with the same nonpolarizable Ag–AgCl electrodes and platinum electrodes.

H. Discussion of experimental results

The experiments in this section illustrate how an ergonar (water), by electrolysis in a matrix, gives rise to ionars ($n(OH)^-$ and nH^+) and ergonars (nH_2 and nO_2). The ionars diffuse and migrate in the closed electric circuit and recombine eventually into water. The cathodic nH_2 and anodic nO_2 ergonars appear as gas bubbles, trapped in the matrix, far away from the places of their production. They "save" their electrochemical energy until conditions are created which allow them to start redox reactions. In the experiments, such a condition was created when a polarizable electrode (platinum) was brought into contact with these ergonars. This result was possible to demonstrate by means of combined "measuring and reaction circuits".

Differences of electric potential are then created of a magnitude which can only be explained by redox reactions at the ergonar-platinum interface. When the movable electrode was passed from the cathode toward the recombination zone, oscillations of potential were observed. The amplitudes of oscillation decreased during this passage. When the movable electrode then continued toward the anode, the amplitudes of oscillation increased. These findings can be explained by variations of the spatial distribution and concentrations of ergonars (gas bubbles) in the matrix. It is remarkable that these ergonars are apparently "pumped" several centimetres out into the matrix and do not localize only adjacent to the surfaces of the electrodes.

The first part of the experiments on electrolysis of water yielded unexpected results when the driven system was turned into a self-driving system. The potential difference did not remain electronegative in the cathodic area or electropositive in the anodic area, as was expected. The diffusion potential appeared reversed and distorted, but in a constant way. Because CO_2 is easily soluble in water, contamination of the water by CO_2 from the surrounding air could possibly explain these discrepancies. The water was therefore washed with argon gas in order to avoid interference of CO_2 in the experiments.

New experiments included such precautions. After one hour of electrolysis of CO_2-free distilled water, the potential differences were measured over the matrix with a digital voltmeter (impedance = 20 megohm). Intermittent measurements over the matrix revealed a difference of 6.71 volts during application of 10.0 volts cell voltage (Fig. XIII: 10A). After disconnection of the external power source, the diffusion potential over the matrix did not show any appreciable voltage difference (Fig. XIII: 10B_1). This finding was interpreted as an effect of diffusion of KCl from the 2 M KCl agar bridge of the "recording" electrode and the matrix. When the recording Ag–AgCl electrode was replaced by a platinum electrode a potential difference of 0.35–0.44 volt was obtained over the matrix (Fig. XIII: 10B_2–B_4). These measurements of potential are now in accord with expected findings when the disturbing effect of CO_2 contamination is excluded. Yet the potential differences B_2–B_4 are of a magnitude which does not exclude that they might be produced by the PtX electrode at different pH levels in the matrix. To check such a possible explanation, new experiments were performed under conditions of increased production of ergonars in the matrix.

Electrolysis in these experiments was enhanced when performed with 2 M KCl solution in the matrix (Fig. XIII: 11). In this way also a diffusion potential between the salt bridge and the matrix could be excluded. The supporting electrolyte now allowed a larger flow of current between the driving (Ec, Ea) electrodes than previously, leading to an augmentation of nH_2 and nO_2 ergonars (and to the additional development of an nCl_2 ergonar). The resulting IR drop over the matrix, after a prolongation of the electrolysis to 12 hours, was now 0.4 volts at 4.1 volts cell voltage (Fig. XIII: 11A). After the external power source was disconnected, no appreciable difference of diffusion potential was measured over the matrix (Fig. XIII: 11B_1), a result in this case also interpreted as caused by compensatory migration of potassium and chloride ions. Measurements of the potential over the matrix using the same platinum electrode and Ag–AgCl reference electrode as in the previous experiment now gave potential differences as large as 1.9 and 1.55 volts (Fig. XIII: 11B_2, B_3). The development of potential differences of this magnitude cannot be explained as caused by the Pt–PtO electrode potential. The pH dependence of platinum electrodes does not lead to variations of this magnitude. A starting of cathodic and anodic fuel cell reactions by matrix-adsorbed nH_2, nO_2 and nCl_2 ergonars does, however, explain fully the large potential differences as a result of redox reactions taking place on the platinum electrode.

I. Summary and conclusions

This chapter analyzes theoretically and experimentally the integrated mechanisms of BCEC systems with special respect to their activation.

The conducting structure of one specific BCEC system, the vascular-interstitial closed circuit (VICC, see Chapter XII), consists of plasma and interstitial fluid. The walls of the blood vessels act as electric insulators except at the capillary membranes, where electric con-

nection is made with the conducting interstitial fluid. Function of a unit of the circuit requires it to contain in principle a minimum of four interfaces (two electrode equivalents) for redox reactions in the capillary walls (Chapter XII). Besides the channelizing organized "large" vessel walls of the circuit, the VICC also contains a "movable matrix" of blood cells, which add a variable factor of circuit capacitance and resistance, due to the dielectric properties of the cell membranes. Changing haematocrit as well as functional and morphologic variations of cross-sectional areas of the circuit will evidently also influence flow of current.

The energy for activation of BCEC systems is delivered by ionic and nonionic compounds. Collections of these appear as energy "packages", tentatively called ionars and ergonars. A major argument for the introduction of this concept is the need for convenient definition of the locations and characteristics of the sources of energy for selective transports in tissue over BCEC channels. Ionars and ergonars are integrated parts in the resistive components of BCEC systems. Resistive effects of ionars and ergonars are influenced by their concentrations as well as by their spatial distributions in BCEC channels.

Ergonars are precursors of ionars. Ionars are precursors of ergonars. They each contain four qualitatively interdependent types of energy (chemical, volume-pressure, electrical and gravitational). Consequently, a variety of pathways exists for the exchange of energy. BCEC channels and their driving forces therefore may constitute important mechanisms for selective transports of energy.

The electrical factor of ionars is immediately available for reactions, while the electrical factor in the energy of ergonars needs to be activated before it becomes available. Ergons thereby save their electric energy until conditions are favourable for its release. An example is also given, illustrating how this important characteristic ergonic behaviour of a molecule is enhanced by its microenvironment. Thus, the ergon O_2 is carried in red blood cells, protected by haemoglobin from possible reactions with its surroundings during transport.

On activation, an ergonar turns into an ionar. In this way ionars are directly, ergonars indirectly, capable of interacting over BCEC channels to level or augment their physicochemical potentials via their electrical factors. Reactions, not only over short distances but also over long distances are possible between ionar and egonar couples over BCEC channels. A change of differences of physicochemical potential then becomes possible, e.g., by selective electrophoretic transports of simple and complex ions. A selective transport of water also takes place as electroosmosis.

Such transports in closed circuit vascular-interstitial channels justify considering BCEC as a circulatory system complementary to the circuits of mechanical transport and diffusion. The pumping of blood represents an indiscriminate bulk transport of material, while BCEC systems add selective transports in tissue. Influences are also possible on "local" chemical reactions far away from the driving forces of a BCEC. An acceptance of the principle of BCEC systems must therefore lead to a revised concept of the progress of local biochemical reactions. Reactants and reaction products are indeed under the influence of superimposed forces, which by their transporting capacity can be anticipated also to contribute to homeostasis. In this context it is too early to discuss the quantitative transfer of individual ions or ionars in a BCEC system. This may be evident, e.g., because of the complex ionic and ergonic compositions and concentrations in the conducting pathways. In experimental studies of certain multicomponent solutions, the moving-boundary method can, as an example, not be used for transport studies of ions. In theoretical models, however, ionic transference numbers, obtained by the less accurate method of Hittorf may be used (13). Finally, it will become necessary in future analyses also to consider the transports on the basis of modern concepts of irreversible nonequilibrium thermodynamics.

The movements of collections of ions (ionars) in a closed circuit will of necessity induce magnetic fields in surrounding tissue. Conversely, motion of an external magnetic field in relation to BCEC channels will induce electric transports in these channels. BCEC systems can be expected therefore also to act as receptors for surrounding manmade as well as natural electromagnetic fields.

Ionars and ergonars, e.g., as developed by anabolic and catabolic processes, are subject to modifications by diffusion, free and forced convection, pressure-volume and gravitational forces, chemical reactions and closed circuit electric transports. The principle of the ionar-ergonar concept is illustrated in their experimental production in in vitro experiments with electrolysis of water contaminated by CO_2, clean water and water with an added electrolyte, KCl. These experiments also demonstrate how different conditions must be created for the release of ionic and ergonic energy. Both ionic and ergonic carriers of energy as well as the matrix functions of BCEC are necessary for a functionally complete BCEC system.

The mechanism of electrogenic production, transport, and retrieval of energy of ergonars, outlined in these experiments, may give a clue about the origin and function of the vesicles discussed in Chapter XII. It is suggested that vesicles within endothelial cells, as well as the vesicles which, e.g., develop at nerve endings, may partly represent collections of nonionic material (ergonars) as a result of biologic electrode reactions. The ergonic materials produced then represent

precursors for subsequent retrieval of energy or liberation of transmitter substances as a result of secondary electrode reactions. An additional mode of development and transport of vesicles is also proposed, based on the principle of Type III electroosmosis (p. 82). Any cationic compound can become hydrated and thereby appear in clusters. With this view *vesicles may represent microclusters or more specifically "pure" ergonars as water in pinocytes or electropositively charged ergionars*, which are electrically transported toward an electronegative receptor site within an activated BCEC. The time of transport of vesicles across a capillary membrane is estimated to be about one second (21). The electrogenic development and transport of vesicles, containing ergonic or ergionic material, may therefore permit the modulation of time of transport and the rate of production of the precursors. As in electroosmosis the suggested partial mechanisms of electrogenic transport of vesicles may very well be integrated. This theory suggests many components and consequences yet to explore. Thus, the origin and function of vesicles in nerve transmission, along these lines, requires the identification of an additional BCEC system. This system should consist of an axon branch, nerve-endplate "electrodes" for activation of ergonars, and an "external" branch, all electrically connecting the "internal" axon branch.

We will now return to biological tissues in further attempts to identify BCEC systems in vivo.

References

1. Bockris, O'M, J., and Dražić, D.: Electro-chemical science. London, Taylor & Francis Ltd., 1972.
2. Chapman, D. L.: A contribution to the theory of electrocapillarity. Philosophical Magazine 25: 475, 1913.
3. Diem, K., and Lentner, C. (eds.): Scientific tables. 7th ed. Basle, Switzerland, Ciba-Geigy, 1971.
4. Eigen, M., and De Maeyer, L. In: Hamer, W. J. (ed.): The structure of electrolyte solutions. New York, Wiley, 1959.
5. von Euler, U., and Liljestrand, G.: Observation on pulmonary arterial blood pressure in the cat. Acta Physiol. Scand. 12: 301, 1946.
6. Gouy, M.: Électricité. Sur la constitution de la charge électrique à la surface d'un électrolyte. Compt. rend. hebd. des sèances de l'Acad. d. sci. 149: 654, 1909.
7. Helmholtz, H.: Studien über elektrische Grenzschichten. Ann. Phys. Chem. 7: 337, 1879.
8. Kendrew, J. C.: The three-dimensional structure of a protein molecule. Sci. Amer. 205: 96, 1961.
9. Kendrew, J. C.: Myoglobin and the structure of proteins. Science 139: 1259, 1964.
10. Lehninger, A. L.: Biochemistry. 2nd ed. New York, Worth Publ. Inc., 1977.
11. Morowitz, H. J.: Entropy for biologists—an introduction to thermodynamics. New York, Academic Press, 1970.
12. Mulliken, R. S.: Cited by Hägg, G. (ed.): Allmän och oorganisk kemi. Stockholm, Almqvist & Wiksell, 1973.
13. Newman, J.: Electrochemical systems. Englewood Cliffs, N.J., Prentice-Hall Inc, 1973.
14. Nobel, P. S.: Introduction to biophysical plant physiology. San Francisco. W. H. Freeman & Co., 1974, p. 92.
15. Nordenström, B.: Temporary unilateral occlusion of the pulmonary artery. Acta Radiol. Suppl. 108, 1954.
16. Nordenström, B.: Contrast examination of the cardiovascular system during increased intrabronchial pressure. Acta Radiol. Suppl. 200, 1960.
17. Pauling, L.: The nature of the chemical bond and the structure of molecules and crystals. Ithaca, New York, Cornell University Press, 1948.
18. Perntz, M. F.: The hemoglobin molecule. Proc. Roy. Soc. 173: 113, 1969.
19. Roughton, F. J. W.: Transport of oxygen and carbon dioxide. In: Handbook of physiology. Section 3, Respiration. 1: 767, 1964.
20. Segel, I. H.: Biochemical calculations. 2nd ed. New York, Wiley, 1975, p. 414.
21. Shea, S. M. and Karnowsky, M. J.: Brownian motion: a theoretical explanation for the movement of vesicles across the endothelium. Nature (London) 212: 353, 1966.
22. Stryer, L.: Biochemistry. San Francisco, W. H. Freeman & Co., 1974.
23. Teorell, T.: Oscillatory electrophoresis in ion exchange membranes. Arkiv för kemi 18: 401, 1961.
24. Teorell, T.: Non-linear transports and oscillations in fixed charge membranes. Some possible biological implications. In: Sélégny, M. (ed.): Charged gels and membranes II. Dordrecht, Holland, Reidel Publ., 1976, p. 205.
25. Wang, J. H.: Synthetic biochemical models. Accounts Chem. Res. 3: 90, 1970.
26. Watson, H. C., and Nobbs, C. L.: The structure of oxygenated and deoxygenated myoglobin. Colloq. Ges. Biol. Chem. Mosbach-Baden, Springer, 1968. p. 37.
27. Watson, H. C.: The stereochemistry of the protein myoglobin. Progr. Stereochem. 4: 299, 1969.
28. West, J. B. (ed.): Regional differences in the lung. New York, Academic Press, 1977.
29. Wittenberg, J. B.: Myoglobin-facilitated oxygen diffusion: role of myoglobin in oxygen entry into muscle. Physiol. Rev. 50: 559, 1970.

XIV.
Experimental activation of vascular-interstitial closed circuits (VICC)

Electrolysis of tissue was introduced to neurophysiology in 1895, when Golsinger (16) devised a direct current technique of producing lesions in the brain. The lesions, pinhead sized, were produced in animals by 20 mA between a needle and an abdominal plate electrode.

In 1908 Brande, Home and Davy (9) made experiments on electrolysis of blood and serum. They found that "strong currents" always yielded coagulation at the cathode, while "weak currents" did not. Both currents produced slight coagulation at the anode.

Horsley and Clarke (20) showed in 1908 that ions migrate during electrolysis of tissue, leading to separation of different ions. Small molecules were found to move farther in their migrations than large molecules. These investigators observed a blue litmus reaction around the cathode but a bleaching of litmus around the anode, a finding which they ascribed to the production of chlorine from NaCl. Moreover, they identified a ring of acid reaction outside the area of bleaching.

Further contributions to this field of research are appropriate for later discussion in Chapter XVII, on therapeutic attempts to utilize the principles of closed circuit electric transports in tissue. We will concentrate in this chapter on some of the changes which we can produce experimentally and expect to find when electric current flows over BCEC channels in living tissue.

It has earlier been stressed in this book that even very low potential gradients can be expected to produce significant changes in biologic material when the "gates" are opened, as in a closed circuit, and when a small amount of current is allowed to flow for a long time. An example of this effect is, for instance, encountered in in vivo corrosion of so-called inert metal implants (Chapter XII).

As time extends over days, months and even years, the discreteness of changes per unit of tissue may be difficult to show in spontaneous, in vivo closed circuit reactions. The use of artificial electric polarization of tissue during relatively short periods of time is therefore not necessarily comparable with what we can expect to encounter in many biologic situations. Nevertheless, relatively brief application of direct current of high density may be helpful as a guide for understanding structural and functional mechanisms of tissues.

When a DC potential is applied between two platinum electrodes in a living tissue, several effects can be noticed. The quantity of charge transported between the electrodes can be determined as the product of

current and time, expressed in coulombs (amp-sec). Thus, a current of one mA over 24 hours gives 86 coulombs and is equivalent with 10 mA over 2.4 hours. Current per unit time can be increased by increasing the voltage between the electrodes. If the total quantity of current transported is held constant, differences of electrode potential may lead to differences in quality of material in the tissue. Such effects can be explained by the fact that different materials possess different specific energy levels of ionization. Moreover, different materials possess different molecular and ionic adsorption characteristics, which each vary with electrode potential, actual concentrations and the properties of the tissue matrix. The covering of an electrode by adsorbed molecules is characteristic for all materials and solutes. In this way different electrode potentials can be expected to affect the competitive adsorptions of different molecules and therefore the qualitative composition on the electrode surfaces and in the supporting media between the electrodes.

Increasing voltage will increase the speed of ionization of tissue (see also Chapter XVII) and enhance the effects of polarization. Gas formation, for instance, will be more extensive and produce more pressure effects when electrode potentials are large rather than small, under conditions of equivalent total charge transport. Experimental demonstration of these effects is described in Chapter IX in the studies of pressure changes and electrical induction of transport of water in cotton wool and lung tissue.

Gas formed at the electrodes may interfere with conductivity. Heat may also be liberated at relatively high voltages, leading to evaporation of water and coagulation of protein. Furthermore, the catalyzing action of the material of an electrode will vary with varying electrolyte composition.

A number of different factors in tissue influence the effects of different electrode voltages at equal total amounts of transported charge. Blood circulation, convection, diffusion, regional changes in conductivity, matrix effects, buffering by fluids, etc., will each affect ionic transports. These influences may be evident already from the fact that the circulation of blood and lymph will in varying degree supply and remove material in the electric field. The total effect of these factors per unit time relates also to the current density in the electric field. In this way a variable biologic influence of qualitative and quantitative changes can be established between the electrodes.

When anodic and cathodic reactions develop in a tissue, secondary effects can also be expected. For example, ionization products in the electric field should interfere indirectly with zeta potentials of cells and modify the transmembranous ionic transports of individual cells. Experimental support for these assumptions will also be presented in terms of the behaviour of blood and fat cells (Chapter XVI).

Our immediate interest now will turn to some gross morphologic expressions of the functions of the postulated biologically closed electric circuit, as simulated by leading electric current between electrodes in tissues.

A. Materials and methods

Initial experiments could not be performed easily in the lung because of the technical difficulties connected with direct visual inspection of this organ in vivo. Because the actual problems appear to be of a general biologic character, the easily accessible mesentery and omentum of dogs were used in a series of 20 experiments. In this way it was hoped that some additional direct evidence might be obtained for the existence of the proposed VICC. In these studies platinum electrodes were used.

Control experiments were also performed in kidneys and lungs of dogs. In these experiments as well as in the experiments on mesenteric tissue, Evans blue dye or a radiographic intravascular contrast medium (Urografin®, 50%) was injected intravenously or intraarterially at the same time as direct current was applied between the electrodes.

Dogs were anaesthetized with intravenous sodium pentobarbital.

A radiopaque plastic catheter (internal diameter, 1.5 mm) was introduced via a femoral artery or vein and placed in the aorta or inferior vena cava with its tip at the approximate level of the diaphragm. A platinum string was introduced through the catheter and used as one electrode at the tip.

A midline incision was made in the abdomen and a piece of mesentery or omentum carefully pulled out through the incision and placed on a glass plate for support. Another platinum electrode was then placed against the mesentery. In other experiments both electrodes were placed against the mesentery.

A DC potential difference was then applied between the platinum electrodes. The potential was obtained by means of a voltage generator in series with a milliampere meter of high accuracy.

Voltage differences between 100 mV and 10 V were tested. When morphologically visible changes were produced, the experiments could be checked or modified repeatedly in the same animal with a fresh piece of mesentery.

The vessels and other tissues of the mesentery were inspected at different magnifications with an operating microscope. Photographs were taken of the mesenteric electrode and surrounding tissues. The mesentery under and around the electrode was excised at the end of

the experiments and fixed in formalin on a glass slide before fixation. Staining was usually performed with haematoxylin and eosin before microscopy.

B. Charging and discharging of tissue

When 100 mV DC voltage was applied between one electrode resting against the mesentery and one electrode in the aorta or vena cava, one to several microamperes could be observed to pass between the electrodes. The current increased continuously, first slowly and then more rapidly. After a while the flow of current decreased or became interrupted, usually from gas produced at the electrodes.

In this way the tissue became electrically charged, as shown in Chapter VI (Fig. VI: 13). When the external power source was then disconnected and the two terminals short-circuited over a microampere meter, such a charged "biologic battery" was found to discharge. Similar discharge from a carcinoma and granuloma, spontaneously polarized, is shown in the patients in Figs. VI: 11 and 12.

C. Diapedetic bleedings

Diapedetic extravasation of red blood cells is one of the early visible changes around the electropositive electrode. This extravasation can be seen in Fig. XIV: 1 as many sites of bleeding along small arterial branches after the application of DC current in small quantity (1.0 μA, 30 min, 1.0 V). This voltage represents the potential difference actually measured between the electrodes. Focal arterial contractions and associated intraarterial thromboses also interrupt the blood stream in many places. Sometimes these blood clots were seen washing away, resulting in temporary restoration of circulation through the artery. Diapedetic bleedings were also observed, but to a much lesser extent, around the electronegative mesenteric electrode.

The normal transcapillary openings between blood and extravascular spaces, which contain water and electrolytes, may be considered as leaking junctions. When an electric potential is applied across capillaries some of them appear to open further, as shown by the transcapillary passage of red blood cells.

After a while the diapedetic blood as well as the thrombosed blood in the vessels becomes brown. White foam (Fig. XIV: 2) produced by gas then develops around the electropositive electrode against the mesentery. The surrounding brown dots represent diapedetic blood.

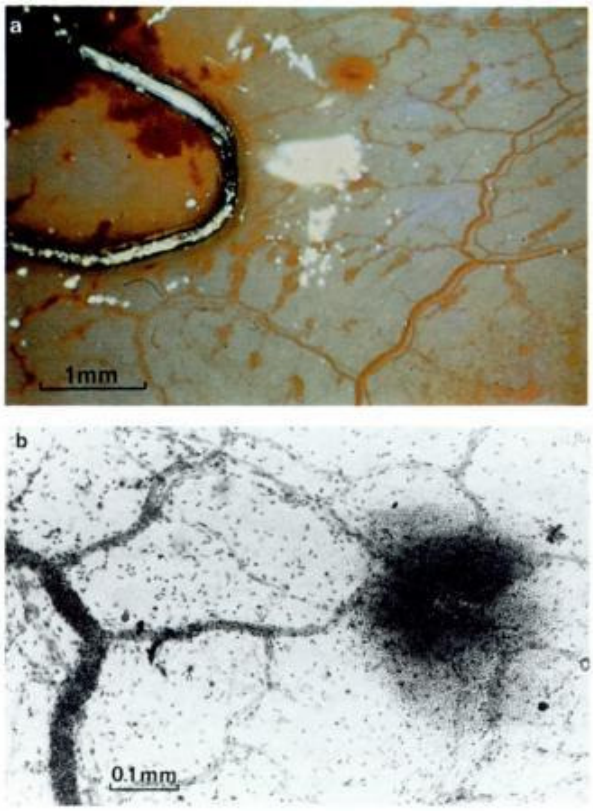

Fig. XIV: 1. Effects of electric current in small quantity (1.0 μA, 30 min, 1.0 V), passed between aorta (cathode) and mesentery (anode) of an anaesthetized dog. (*a*) In vivo photomicrograph shows diapedetic bleedings as irregular dots around the platinum anode. (*b*) Local diapedetic bleeding. Narrow empty arteriocapillaries, wide venocapillaries with granulocytes. Haematoxylin-eosin stain.

Fig. XIV: 2. Foam of oxygen and chlorine gas develops at the electropositive electrode against dog mesentery. Diapedetic blood appears as brown dots in the mesentery near the electrode. Electrode size 4×4 mm. Cathode in the aorta.

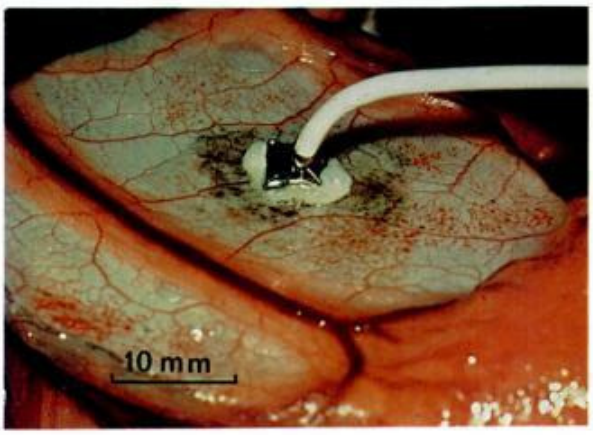

D. Vascular pockets, ischaemic dystrophy and perifocal enhancement of radiographic contrast

An in vivo photograph (Fig. XIV: 3) shows narrowing and discolouration of vessels in the lower part of the figure, close to the electropositive electrode. Blood at this moment was not flowing through the discoloured vessels but was flowing freely in the artery and vein seen in the upper part of the figure.

The open branches, still red, of these vessels produce in this way *vascular pockets* around the electrode. Circulation is completely suspended around these pockets. Similar vascular changes of irregular narrowing and thrombosis of vessels around spontaneously polarizing lesions have already been described (Chapter III, G). The absence of pulsations sometimes observed in the vessels around carcinomas, reported by Marchal and Marchal (26), and the frequent presence of extensive thrombosis in vessels around carcinomas (11) may therefore possibly be determined by bioelectric events.

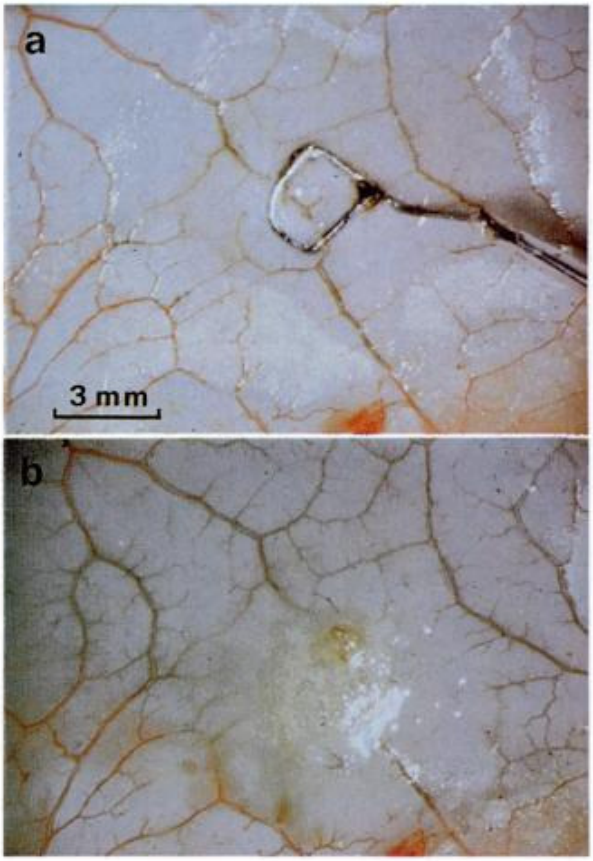

Fig. XIV: 4. Demonstration of dystrophy in tissue around site of DC electrode. (*a*) Platinum anode against dog mesentery. Cathode in the aorta. Extensive thromboses, discolouration and desiccation developed around the anode after a total of 0.20 coulombs (5 V overpotential). (*b*) After a change of polarity and passage of another 0.06 coulombs, tissue water entered the newly cathodic region, which previously had become dry when anodic. An "avascular" region is seen at the former site of the electrode. Vessels are blocked by thrombosis and probably also compressed by inflowing tissue water. Such vascular changes around a polarizing tissue may subsequently lead to local dystrophy and circular displacement of tissue (creation of an "A" zone effect = radiographic halo formation, Fig. XI: 9). These mechanisms of interference with circulation of blood create conditions whereby a tumour may regress, either spontaneously or by artificially induced polarization (see Chapter XVII on tumour therapy).

Fig. XIV: 3. Impairment of circulation induced after 25 minutes at 5 V electrode potential around an anode (out of sight below the figure) against the mesentery of an anaesthetized dog. Some vessels are narrowed. Brown discoloured vessels are blocked by thromboses. Thromboses contribute to the development of dystrophy of tissue adjacent to the electrode ("A" zone effect). Red blood continues to flow in larger arteries and veins (upper part of figure), which connect with open sections of the blocked vascular branches. After injection, radiographic contrast medium flowing in the large vessels was found to escape through the partly open vascular pockets. Some contrast medium was found to remain for a prolonged time in the pockets while some contrast leaked through capillary membranes into the interstitial tissue, producing "radiographic contrast enhancement".

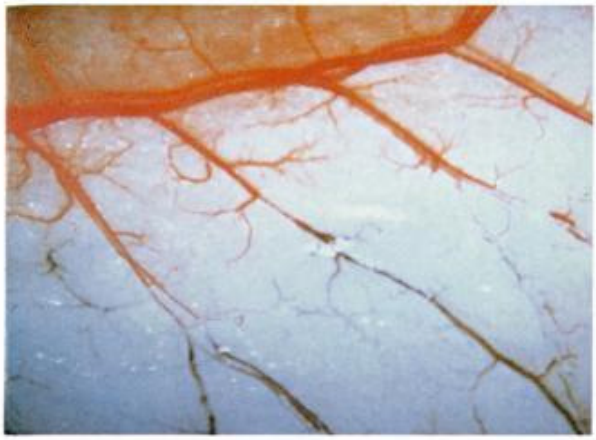

We will now focus our interest on a possible role of *field-induced vascular effects within a VICC, leading to tissue dystrophy*. A positively charged body in tissue may be surrounded by extensive thrombotic changes which impair local circulation of blood. Such a mechanism should then produce a radiolucent, dystrophic "A" zone around a tumour. *This mechanism may also be one of several explanations for the occasional observation of spontaneous regression of malignant tumours. This aspect is particulary important because it may represent one of Nature's own ways to combat a malignant tumour, and*

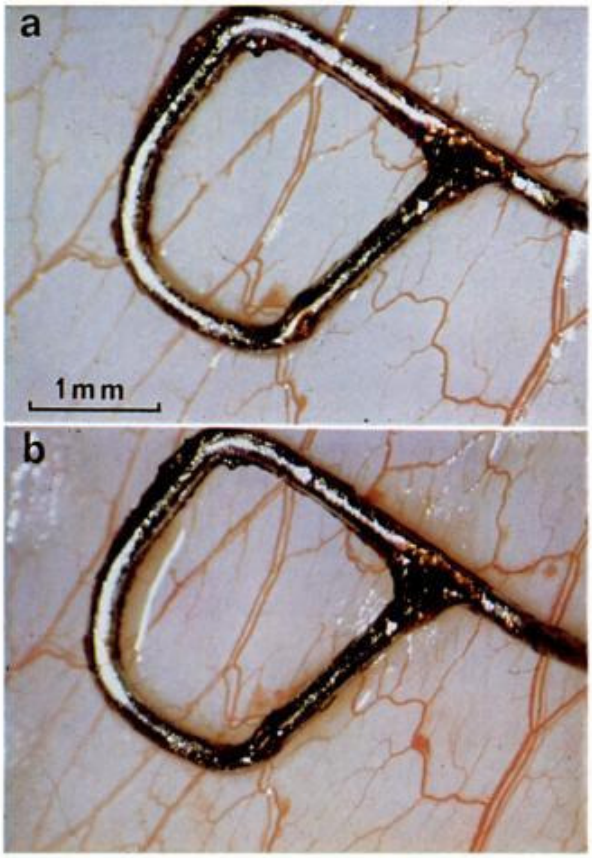

Fig. XIV: 5. Transport of fluid to region of mesenteric cathode. Anode in aorta. (*a*) Vessels are seen before application of 4.2 V overpotential. (*b*) After 1.01 coulombs, fluid is seen to accumulate against the electrode. Vessels are preserved. Circulation of blood continued both inside and outside the electrode loop.

also be a process which can be simulated artificially in tissue by supply of electric energy over implanted electrodes (Chapter XVII).

Early effects of direct current on vessels around the anode are illustrated in Fig. XIV: 4 *a*. Five volts were applied between the electropositive mesenteric electrode and the electronegative aortic electrode. Discolouration began in many small vessels after 0.05 coulombs. Rather extensive discolouration and thrombosis could be seen in the vessels around the anodic electrode after 0.20 coulombs. Tissue in this region became desiccated. Polarity was then reversed and 0.06 coulombs were passed between the electrodes. Tissue fluid reentered the region around the mesenteric electrode. An "avascular" zone developed around the electrode (Fig. XIV: 4 *b*). After extensive inflow of water, one can imagine that circular displacement of tissue structures may occur. Such displacement of tissue may later be enhanced by dystrophic changes due to nutritional disturbances.

Fig. XIV: 5 *a* shows a platinum electrode against the mesentery. 4.2 V were then applied between this electrode and the electropositive platinum electrode in the aorta. After 0.01 coulombs, fluid is seen to accumulate against the cathode (Fig. XIV: 5 *b*), but the vessels are unchanged. No vessels narrowed, blood did not discolour, no thrombi are seen.

When the current is increased between the electrodes, vessels narrow around the electronegative electrode and local circulation slows markedly. Diapedetic blood is destroyed and becomes brown. This material will then disappear and the cathodic area looks empty (see also Fig. XIV: 9 *a*). The arterial branches are then empty and collapsed. Some veins contain morphologically changed, pale red blood cells, which do not stain with haematoxylin and eosin. In this way ischaemia is produced around the cathode as well as around the anode. When longstanding, such effects must inevitably lead to ischaemic dystrophy of the affected tissues.

The formation of vascular pockets, as seen in Fig. XIV: 3, may also explain the development of so-called perifocal contrast enhancement in angiography. Contrast medium distributed in functioning vessels around a tumour will escape, e.g., by the force of gravity, into the blindly ending pockets formed by partly thrombosed or contracted vessels. Because capillary permeability is increased, some molecules of the contrast medium will also probably leak through the capillary walls into the peritumoural interstitial tissue.

E. Ionization and ionic recombinations

When a few volts are applied between two electrodes placed against mesentery, gas is produced at the electrode surfaces. The gas can be seen as foam, more developed around the cathode than around the anode. Oxygen and chlorine are produced at the anode, hydrogen at the cathode (20). Around the electronegative electrode the tissue becomes alkaline, around the electropositive electrode it becomes acid.

Acid-base effects were shown by placing wet strips of litmus paper on the mesentery after the passage of 0.9 coulomb at one volt between the electrodes (Fig. XIV: 6). The red coloured part around the anode corresponds to pH 1, the blue-black around the cathode corresponds to pH 12. A thin uncoloured zone is also seen between the red and blue areas. The development of alkaline and acid regions in electrolysis of water within a matrix has been discussed earlier in connection with electric transport of water (Chapter IX). The experiment in Fig. XIV: 6 shows how this process can present in a living tissue. It is apparent that a recombination of hydroxyl and hydrogen ions must take

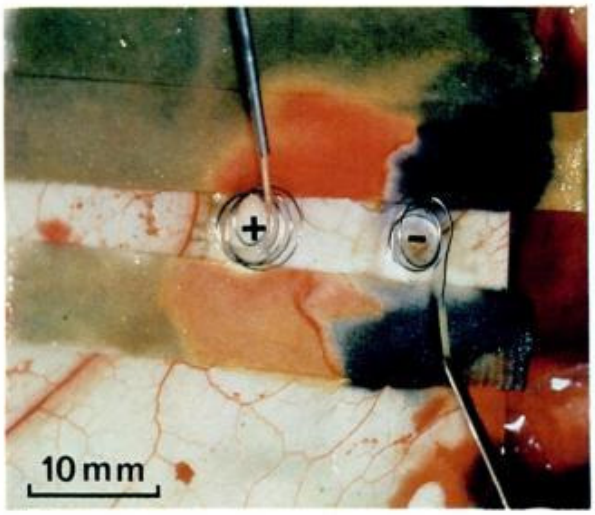

Fig. XIV: 6. Acid-base effects of electricity in mesentery between electrodes. After 1 V and 0.9 coulomb, strips of wet litmus paper were placed on the tissue beside the electrodes, showing a pH of about 12 around the cathode and about 1 around the anode.

place between the blue and red areas. The change of the yellow colour of the litmus paper of pH 7 into white indicates that other mechanisms are also involved. Thus, bleaching of the litmus might very well depend on local accumulation of chlorine, which is also liberated at the anode (20).

For the distribution of material in an electric field the ionic mobility u_i ($cm^2\ V^{-1}s^{-1}$) is of fundamental importance. Ionic mobility for simple ions at strong dilution and 25°C (12) is shown in Table XIV: 1.

Migrating and diffusing ions produced at the electrode surfaces tend to recombine when they meet. For the most rapid ions, the hydroxyl ions and the protons, such recombinations should take place according to their respective mobilities, about ⅓ of the distance from the cathode to the anode. In the same way other recombinations can be expected to take place at different distances between the electrodes, depending on the relative speeds of transport of the reactants.

The diffusion and migration of protons and hydroxyl ions produced at the electrode-tissue interfaces is always greater than the diffusion of produced oxygen, chlorine and hydrogen gas, as shown in Chapter XIII. This fact means that a primary destructive effect on tissue around the electrodes is produced by cathodic alkalinity and anodic acidity. The chlorine gas, which diffuses relatively slowly, will secondarily bleach some of the already acidic, devitalized tissue around the anode. These effects are most easily demonstrated when the electrodes are positioned at large distances from each other. For example, when the anode is placed in the lung parenchyma and the cathode only a few cm distant in the pulmonary artery of a dog (see Figs. XIV: 20, 21), a recombination zone of protons and hydroxyl ions is not established because of tissue circulation, convection and buffering by tissue fluids. Consequently, central bleaching of tissue is produced by chlorine diffusing slowly in the dark tissue already destroyed by acidity.

At a short electrode distance, the propagation of protons and hydroxyl ions may stop at the creation of a recombination zone. In a tissue matrix, local accumulations of acidic and basic material can also be seen against the recombination zone (Fig. XIV: 6). The rapidly diffusing and migrating protons and hydroxyl ions prevent each other from further movement because they recombine as water. In this case the slowly diffusing chlorine gets its chance to reach the recombination zone and bleach the material in this region. It is important to realize that the diffusion and migration of protons around the anode produce the devitalization of tissue both at "long" and "short" distances between the electrodes. These distinctions about electrochemical destruction of tissue around the anode warrant emphasis because some incorrect interpretations have appeared in recent literature (37), claiming that chlorine produced around the anode causes the primary destruction of tissue.

The ionization and transport of material after application of an external source of energy means that energy is transferred to the tissue and tissue entropy is decreased. Such changes can be observed directly in several ways. The possibility of discharging the tissue as mentioned in Section B is one, some mechanical effects are other examples.

Table XIV: 1. *Ionic mobilities (u_i) for some simple ions, expressed in $cm^2\ V^{-1}\ s^{-1}$ 25°C*

	H^+	Li^+	Na^+	K^+	OH^-	Cl^-	NO_3^-
$u_i \cdot 10^4$	36.2	4.0	5.2	7.6	20.7	7.9	7.4

F. Transport and mechanical effects

Particle size and structural properties of the tissue matrix are important mechanical factors in tissue electrophoresis. As always, temperature, pressure-volume and gravity factors will also influence the combined effects of electric field forces and chemical forces.

The exchange of fluid in tissue by electroosmosis, osmosis, convection and circulation of blood and

lymph is also of fundamental importance for ionic transports, possible recombinations of ions and distribution of movable dielectric material in the tissue. The existence of narrow spaces lined with fixed charges is, for example, a prerequisite for the development of "true" (anomalous) electroosmosis (see Chapter IX). An electrophoretic transport of water by recombination of protons and hydroxyl ions will also need a "capillary" matrix to counteract hydrostatic recirculation.

Mesenteric water transport can easily be seen as accumulation of water around the cathode and a dehydration of the tissue around the anode. In Fig. XIV: 7 a dry zone in the mesentery shows a white spot at the former site of the anodic electrode. Such electroosmotic dehydration gives an uneven distribution of water, seen as local oedema around the electronegative electrode. In the case of a distant cathode, a hydropic zone is also seen peripheral to the anodic hydropenic zone, due to the outflow of water from the anode. Accumulation of water around both the dry anodic zone and the cathode produces mechanical effects by local increases in turgor pressure.

Similar uneven distribution of material in the electric field is caused by ionic dissociation, but takes place also as a transport of dielectrics. By dipole induction, such particles will move to the anode as well as to the cathode, whenever they are located close to the electrodes and where the electric field gradient is steep. The gradual disappearance of brown material from intravascular blood cells and from diapedetic interstitial blood also appears to be an expression of electrophoretic transports.

Gas, produced locally at the electrodes, increases pressure in the tissues. At the surface of the anode, O_2 and Cl_2 are produced, while H_2 is produced at the surface of the cathode. Around the cathode, the volume of H_2 is twice as great as the volume of O_2 around the anode (20). Chlorine gas adds its volume to the volume of oxygen around the anode. Living tissue, however, resorbs gas. An equilibrium will therefore become created around the electrodes between the rates of production and elimination of gas. When a 10 V potential is applied to electrodes implanted in vivo in various tissues, e.g., liver, lung or fat, the gas produces within about an hour a radiographically visible cavity in the tissue around each electrode. The cavity around the cathode is always larger than that around the anode. The relative differences of gas production are in themselves a result of a complex series of events. Variations in anodic current density, e.g., by physical factors such as dehydration and electrode depositions, will to some extent lead to changes in the relative content of hydrogen, chlorine and oxygen in the tissue.

A direct microscopic study of the gas produced at the electrodes is shown in Fig. XIV: 8. Two platinum strings each 0.2 mm thick were fixed on a glass slide. The space between the electrodes was filled with some drops of human blood. A 6 volt direct current poten-

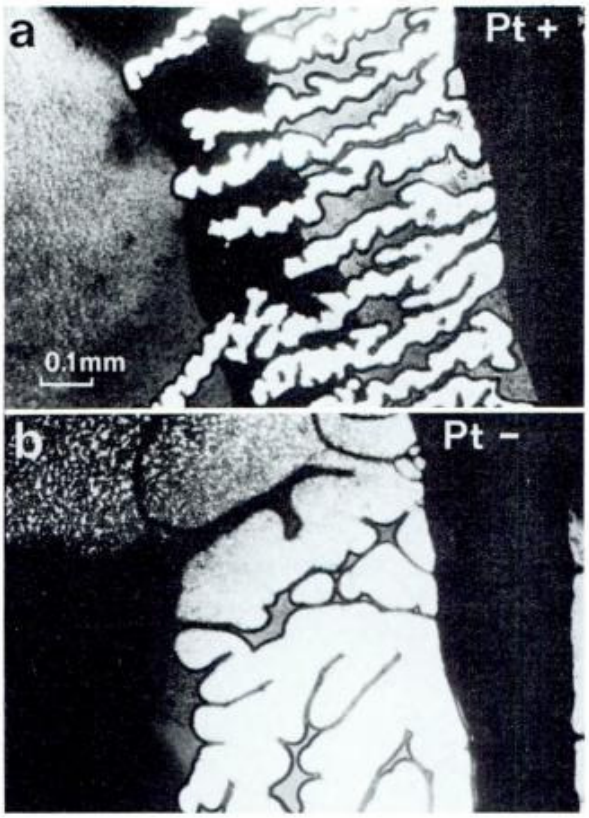

Fig. XIV: 8. Streams of gas arising from the surface of platinum electrodes in human blood (direct microscopy). (*a*) Oxygen and chlorine at the anode after 0.138 coulomb, 6 V. (*b*) Hydrogen at the cathode after 0.142 coulomb, 6 V. The oxygen-chlorine gas shows thinner "dendrites" than the hydrogen gas.

Fig. XIV: 7. A white, dry site of destroyed tissue and blood. Oxygen and chlorine gas denotes the former site of a mesenteric anode.

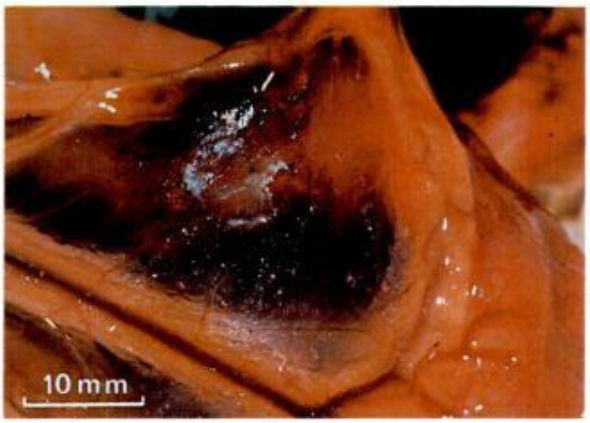

tial was applied between the electrodes. Dendritic bubbles of gas arise from the anode (oxygen-chlorine, Fig. XIV: 8 *a*) after 0.138 coulombs and from the cathode (hydrogen, Fig. XIV: 8 *b*) after 0.142 coulombs. The oxygen-chlorine gas produces more delicately protruding gas bubbles than does the hydrogen gas. In a suitable matrix it was shown (Chapter XIII) that gas bubbles are liberated and transported away from the electrodes. This mechanism of electrogenic ergonar production and transport might be considered in future research on vesicular development and function.

G. Conductivity changes

The mechanical effects of gas production, which is most pronounced around the cathode, will influence conductivity within the circuit. The spontaneous increase in the amount of current in the early stages of tissue electrolysis can be ascribed to the continuous increase in the amount of ionization of the tissue. As the process goes on, polarization at the electrode surfaces will counteract the process of ionization. Thus, gas produced at the electrodes may even completely interrupt the flow of current through the circuit. Dehydration around the anode has also been found capable of interrupting the circuit in experiments with mesentery and lung tissue.

The influence of gas produced at the electrodes in a tissue can be diminished by applying a relatively low current over a correspondingly longer time. The rate of gas resorption is then relatively more prominent than the rate of gas production.

The application of low rates of current flow through the circuit still cannot entirely abolish the effects of gas production and dehydration of the tissue. These effects depend on several factors. The adhesion of polarized material against the electrode surfaces and gas adsorption cannot be avoided. Gas in a tissue will become trapped in the matrix. Secondary changes in morphology will also take place, e.g., within the vessels. Thrombosis around the anode will interfere with the resorption of gas and other polarization products and with the supply of water to the dehydrated tissue.

H. Effects on red blood cells and their distribution

We will first summarize briefly some aspects of chemical transformation of haemoglobin. According to Lemberg and Legge (23), the prosthetic group (iron protoporphyrin) called haem is rather unstable and easily oxidizable. Haemoglobin is split into globin and a cationic haemin in acid solution and into globin and an anionic haemin in basic solution. If haemin is dissolved in excess alkali and titrated with acid, electroneutral haematin will precipitate.

From these data one may already anticipate that certain changes will take place in in vivo electrophoresis. Acid haemin should develop around the anode (which easily reaches a pH of 2, while pH at the cathode reaches beyond 12). Base haemin should therefore be found around the cathode. On the migration of cells containing acid and base haemin in the electric field, these haemins should attract each other. Cells with haemin of equal polarity should repulse each other. As pH changes, charged haemin compounds develop readily, while proteins are less changed. If a solution of haemoglobin is shifted as far as pH 12 (which may occur in applied in vivo electrophoresis), denatured globin haemochrome is formed (23). When this compound is allowed to autooxidize, or when dilute sodium hydroxide is added to haemoglobin or to oxyhaemoglobin and the solution is partly neutralized, a denatured globin haemichrome is formed, which is called cathaemoglobin. Solutions of cathaemoglobin in weakly alkaline solution are brownish and have a characteristic haemichrome spectrum, a weak band at 558 μm and a stronger one at 530 μm (23).

In in vivo electrophoresis the material around the cathode may be characterized macroscopically by evolution of hydrogen, alkaline reaction, oedema, and a brownish material, which should contain cathaemoglobin.

When the pH of a solution of haemoglobin is made more acid than 3–4 (which is the case around the anode in tissue electrophoresis), the linkage of the prosthetic group with the protein is ruptured, while the protein is denatured. The purple colour of the haemoglobin then changes to reddish-brown and shows a rather indistinct, two-banded spectrum in the green of haem, protected by protein from flocculation (23). In the presence of oxygen the ferrous iron in the haem is oxidized to ferric iron. Acid haematin is then formed, which has a band in the red at 660 μm and a feeble band in the green. When oxyhaemoglobin is acidified, oxidation of the protein in addition to the iron atom takes place (23).

As a preliminary survey of the morphologic distribution and general appearance of field-induced changes in in vivo electrophoresis, acute experiments were performed first on dog mesentery and lung and also, after four weeks observation time, on dog lungs.

Cathodic mesentery of a dog is shown in Fig. XIV: 9 *a* (haematoxylin-eosin). One coulomb of current at 5 volts has passed between two mesenteric

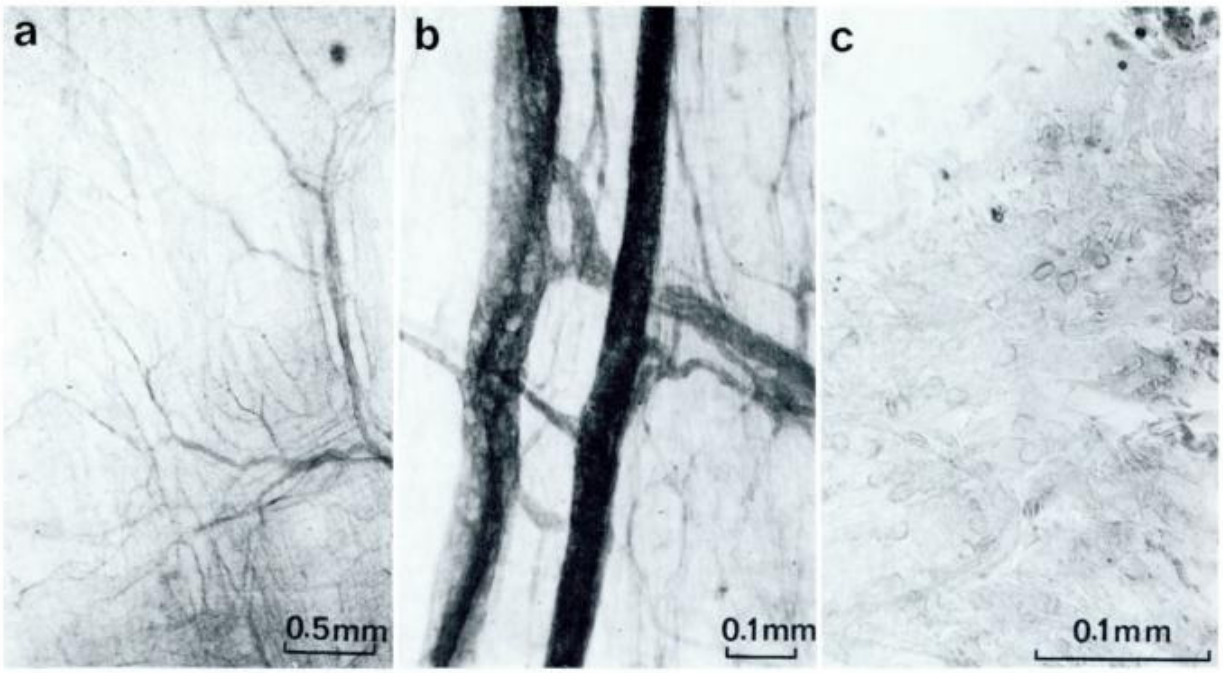

Fig. XIV: 9. Effects of in vivo electrophoresis on red blood cells in dog mesentery. Anode and cathode, 3 cm apart, rest against the mesentery (5 V, 1 coulomb). Cathodic field, stained with haematoxylin and eosin after fixation in formaldehyde. (*a*) The tissue appears empty of cells. Vessels appear dark and depleted of normal blood cells. (*b*) The central dark narrow vessel is an artery containing decomposed blood. The larger vessel is a vein with dark material and round or oval bodies, which are likely to be red blood cells depleted of pigment. (*c*) Some extravascular cells, presumably erythrocytes, show cell membranes darker than the pale interiors. This change of the red blood cells has been interpreted as an effect of the cathodic field depleting the cells of pigment.

electrodes, placed about 3 cm from each other. The tissue looks "empty", as if no normal blood cell elements were present in the field. Higher magnification (Fig. XIV: 9 *b*) shows an artery and a vein containing dark material but no normal cell elements. A vein, the larger vessel, contains numerous, clearly visible, round and oval bodies. Their nonstructured, transparent content is seen surrounded by dark material, which is also nonstructured. The light material does not stain with haematoxylin and eosin.

Some interstitial cells in an adjacent part of the cathodic field appear as ring-structures, as seen in Fig. XIV: 9 *c*. These cells have been interpreted as diapedetic red blood cells which have lost most of their pigment, making their membranes visible. Dark material, like that seen in the vessel in Fig. XIV: 9 *b*, was found in the interstitial tissue and was also interpreted as modified blood pigment.

Red blood cells in the anodic field revealed varying degrees of central accumulation of dark material, which presumably consists of transformed blood pigment. These observations were therefore extended by studying human CPD-adenin® (Terumo, Japan) blood on glass slides. Direct current was applied between platinum electrodes at 6, 12 and 18 volts, with current densities of 1–5 mA over 5 to 10 minutes. Material treated in this way was sampled from different parts of the anodic and cathodic areas, smeared on glass slides, dried and stained (haematoxylin and eosin, polychrome methylene blue, van Gieson or May-Grünewald-Giemsa). In these studies remarkable transformations could be seen in red blood cells.

Cathodic erythrocytes contained multiple particles of birefringent material, located inside and often close to the cell membranes (Fig. XIV: 10 *a*). In other areas particles were seen at the outer surface of cells or, even in in vivo experiments, in the surrounding medium (Fig. XIV: 14 *a*). Other cathodic red blood cells were pale, as if they contained a reduced amount of haemoglobin. They also showed crenations (Fig. XIV: 10 *b*).

Blood material from the area close to the anode also showed considerable morphologic changes. Many cells showed a concentration of centrally located, birefringent material connected with the interior cell walls with thin radiating structures, like spokes in a wheel (Fig. XIV: 10 *c*). The cytoplasm of many anodic cells also contained round inclusions interpreted as vacuoles of varying sizes (Fig. XIV: 10 *d*). These structures seem to develop as small light areas in the cytoplasm, which appears granulated. Some of the vacuoles grow and take up more and more of the intracellular space.

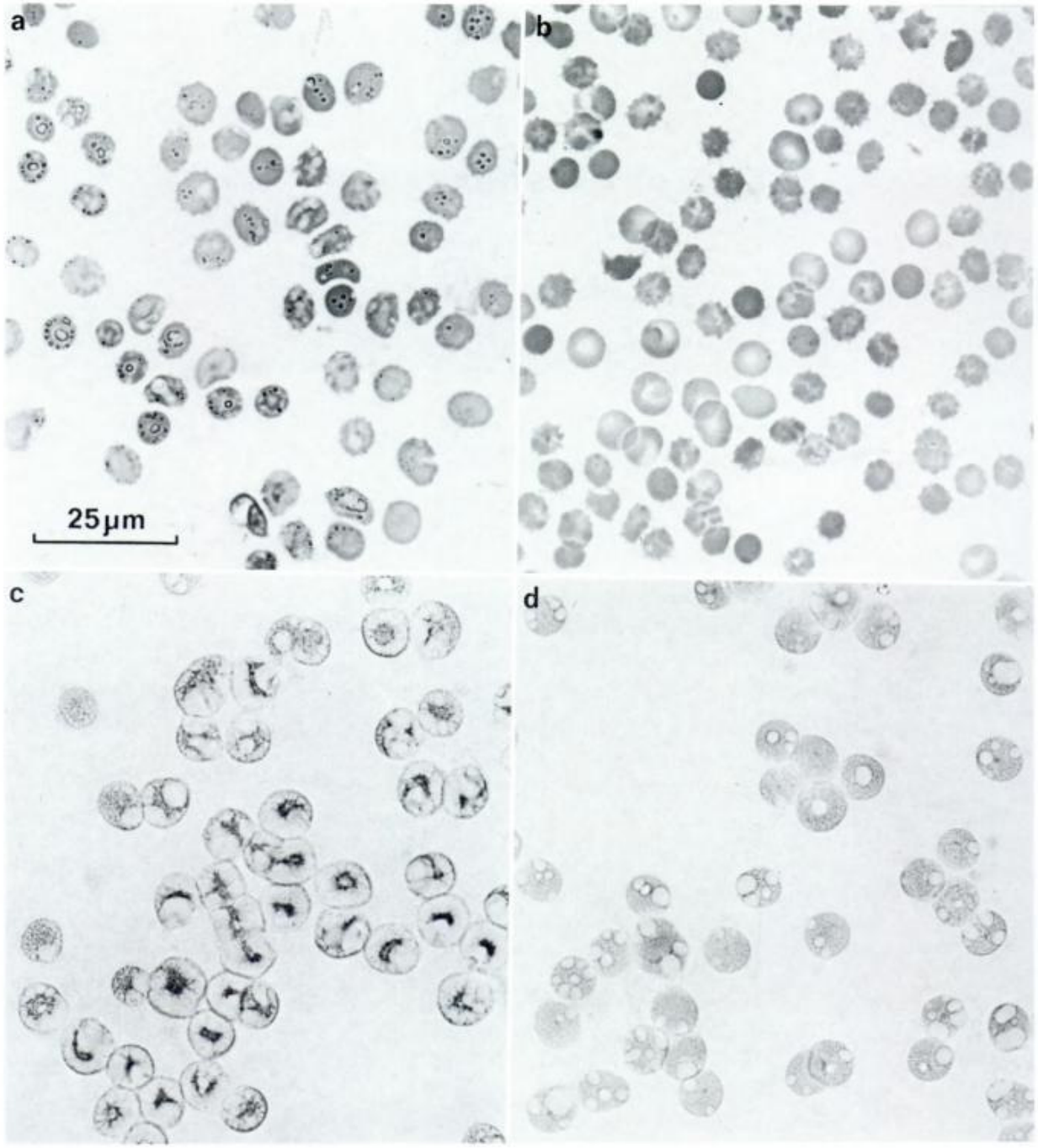

Fig. XIV: 10. Erythrocytes after exposure to direct electric current (6 V, 0.5 coulomb). (*a*) Blood near cathode. Birefringent particles, probably alkaline haematin, are seen in cells. These particles can sometimes also appear outside cells in the surrounding medium. (*b*) Other cathodic erythrocytes are either dark or pale. Some show crenations. (*c*) Anodic blood. Haematin, probably acidic, accumulates centrally and is connected with the interior cell walls by thin radiating structures, like spokes in a wheel. (*d*) Anodic blood. Large vacuole-like changes are seen in the cytoplasm, possibly preceding the changes seen in *c*.

The "spokes" seem to develop at the contact surfaces of the vacuoles. At the same time the granulated material seems to condense in the centre of the cells.

Only a preliminary explanation of the field-induced structural changes in the blood can be given so far. Strong alkalinity is present in the vicinity of the cathode. As reported earlier, it is known that weakly acidic and alkaline solutions split haemoglobin into its globin and prosthetic parts. Alkaline (electronegative) haem may then represent the particles of birefringent blood

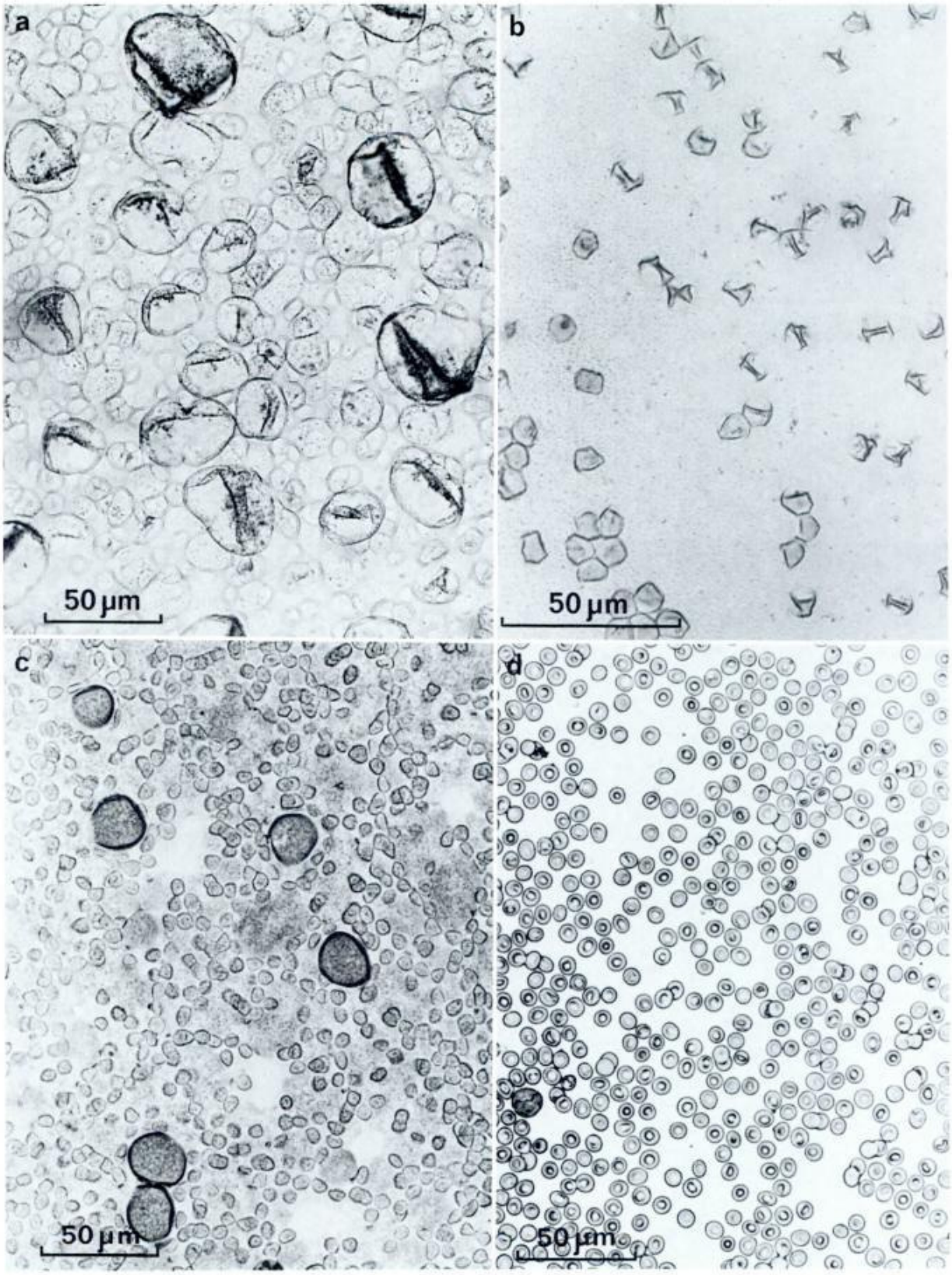

Fig. XIV: 11. "Giant erythrocytes" after exposure of blood to direct current. (*a*) Erythrocytes from the cathodic area seem to fuse into "giant cells" with characteristic arrangements of blood pigment. In normal-sized erythrocytes the haemoglobin is granulated or (*b*) arranged like Roman numerals II and V. (*c*) The anodic area contains different "giant cells" appearing as round structures which contain a fairly homogeneous, granulated material surrounded by a membrane-like structure. Other blood cells appear smaller than normal. (*d*) Control. The same normal blood, untreated.

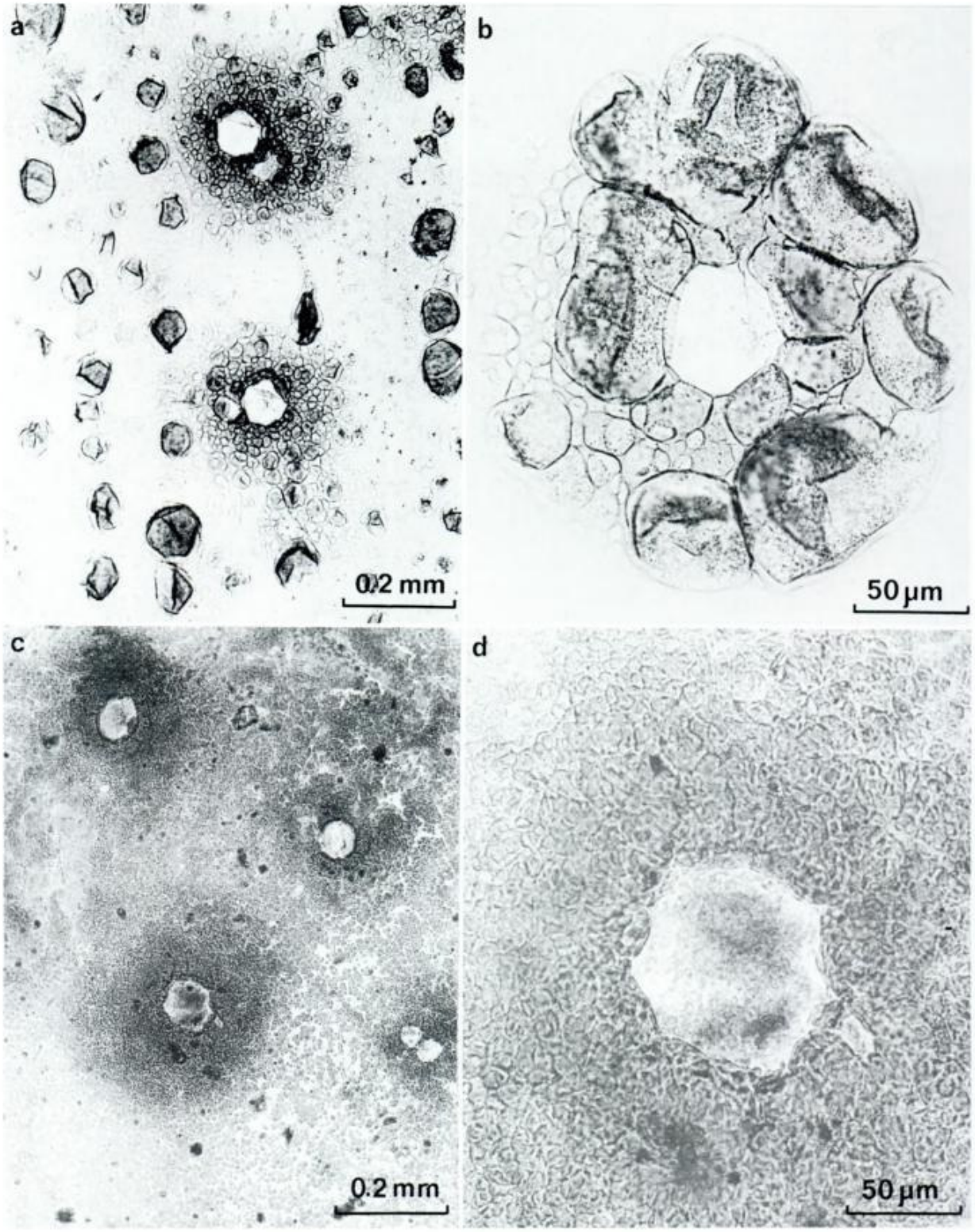

Fig. XIV: 12. Transformation of blood by direct current. (*a*) "Giant cells" near the cathode are arranged in clusters. The "cells" in each cluster are presumed to adhere to a centrally located, undefined material. (*b*) Detail view of a cluster. The pigment in the "giant cells" is arranged more or less in a circle. (*c*) Similarly structured conglomerates of blood material in the anodic region. (*d*) Detail view of an anodic conglomerate. A membrane-like, thin structure forms an interface between this "intercellular space", which contains a faintly stainable material, and the surrounding anodic cells.

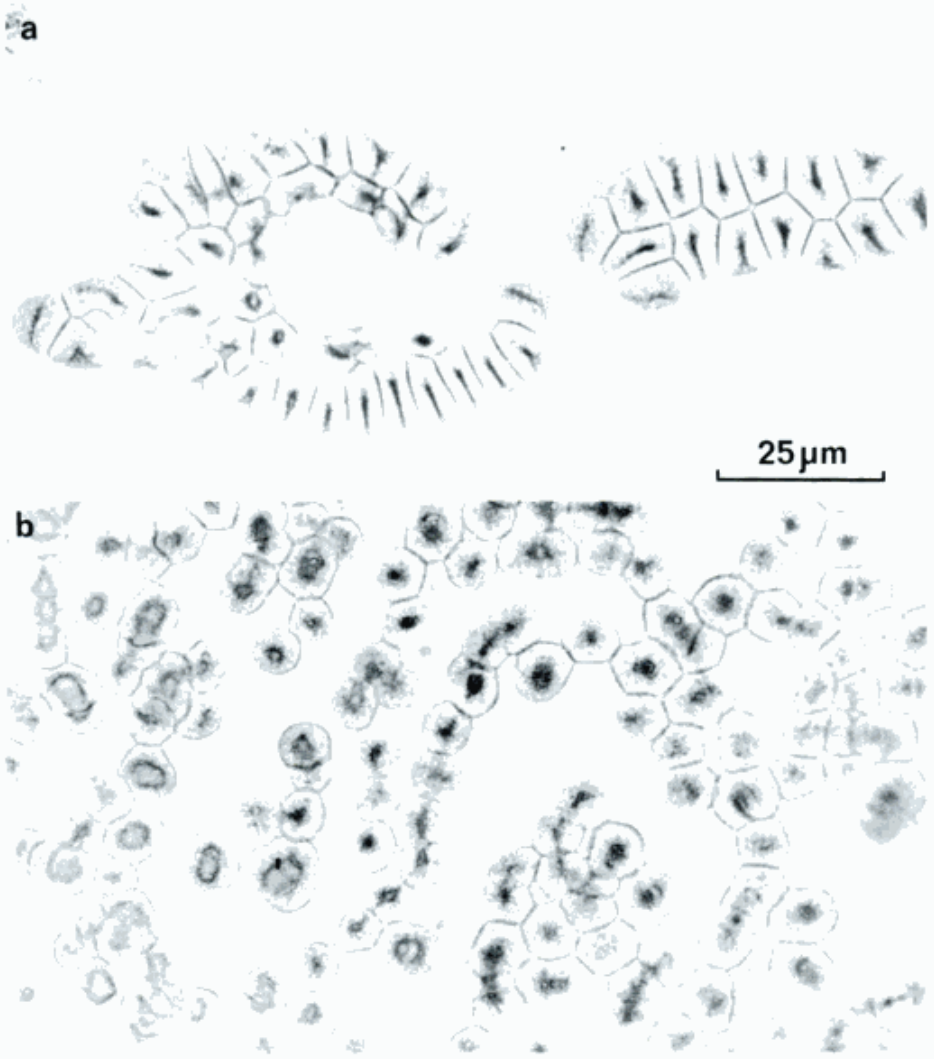

Fig. XIV: 13. Behaviour of pigment in red blood cells after electrophoresis. Cathodic alkalinity and anodic acidity produce electronegative and electropositive blood pigment, respectively. Competitive concentration forces among cells and electrostatic forces of haemin of equal polarity are interpreted to produce mutual *repelling* of pigment in adjacent cells, as seen in *a* (which represents cathodic blood). Same arrangement of pigment was also observed in anodic blood. (*b*) Cathodic blood showing rows of erythrocytes with internal *attraction* of their blood pigment. This finding was also observed in anodic blood, (see Fig. XIV: 10*c*). Such attraction of pigment should take place when adjoining cells contain blood pigment of opposite polarity.

pigment, which move toward the cell periphery after the cells have moved electrophoretically from the electronegative into the electropositive electric field. The particles even leave the cells and are seen attached to the outer cell surface. Before these cells have left the electronegative field, however, the alkaline haem may concentrate inside the cells. In the anodic field acidic haem should be produced. This pigment should then also behave differently when the blood cells appear in the electropositive field and after an electrophoretic transport into the electronegative field. Associated mechanisms are complex and do not at present allow any definitive analysis. The varied behaviour of blood pigment in these studies clearly shows, however, that chemical and structural modifications do take place inside as well as outside cells in the electric field.

Cathodic cell populations in the in vitro electrophoresis of blood appeared partially fused, in some way, resulting in enormously large "cells" (Fig. XIV: 11*a*). These "cells" appeared in varying sizes ranging from the normal size of red blood cells to well beyond ten times this diameter. These "giant cells" appear enclosed in a structure which looks like a cell membrane and contains partly structured dark material. This material may often be seen as linear, parallel or angulated linear structures (like Roman numerals II or V). The dark material appears not only in the "giant cells" but also in cathodic cells of lesser size (Fig. XIV: 11*b*) (see also the presumed early stages of linear formation of haemoglobin in Fig. XIV: 13*a*, *b*).

The anodic area contained blood cells (Fig. XIV: 11*c*) which were smaller than untreated blood cells (Fig. XIV: 11*d*). These small anodic cells showed granulated cytoplasm. Another kind of "giant cells" also appeared in the anodic area (Fig. XIV: 11*c*). These "cells" contained an evenly distributed granular substance surrounded by a dense membrane-like structure.

Structural arrangement of cathodic "giant cells" was also observed in smears from cathodic blood (Fig. XIV: 12*a*, *b*). In smears from anodic blood, local accumulation of structured material could also be seen

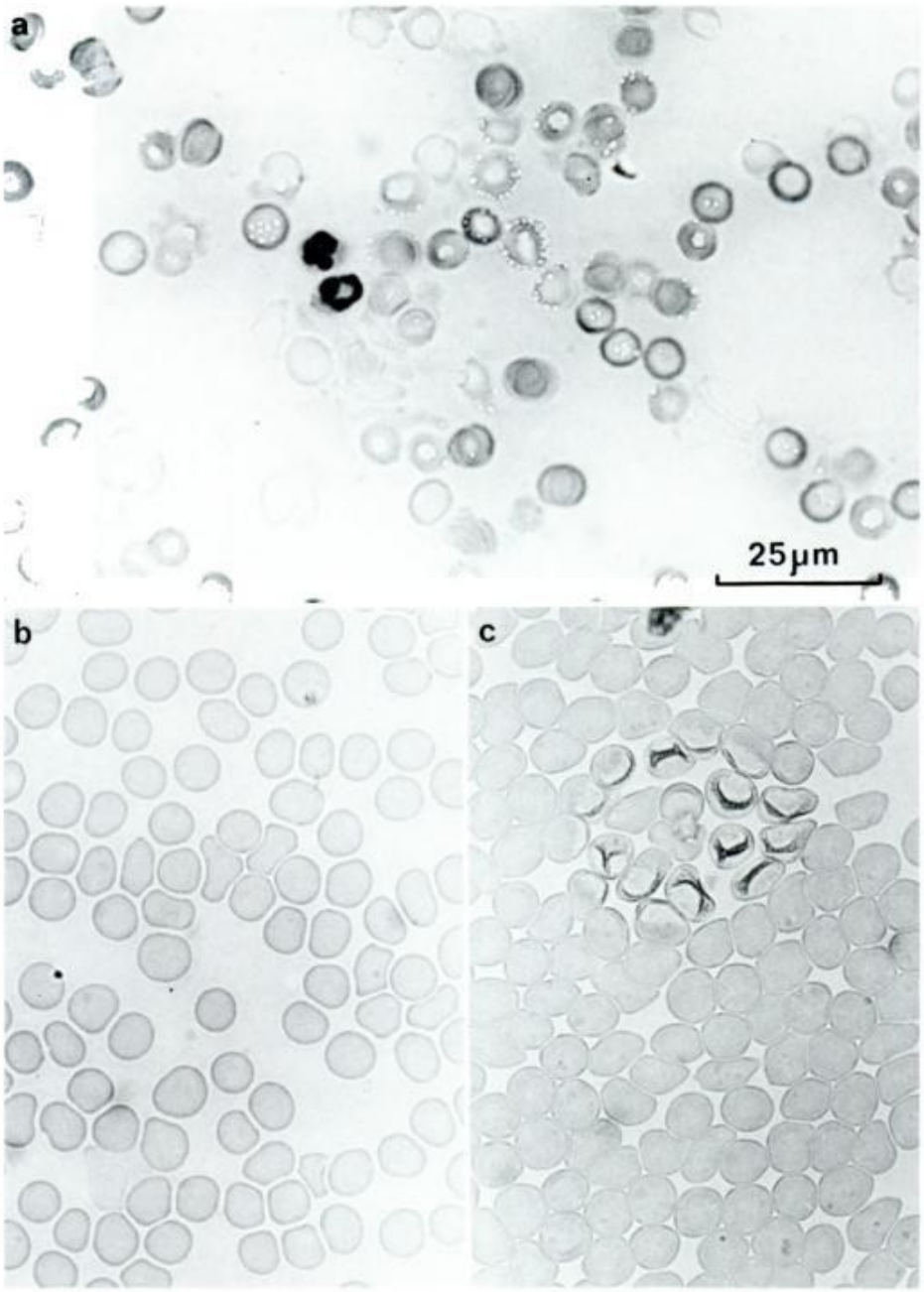

Fig. XIV: 14. Effects of direct current on dog blood. 1 700 coulombs at 10 volts were applied in vivo between the aorta (cathode) and neck muscles (anode). A sample of venous blood from the animal was heparinized and centrifuged. Blood smears were made from (*a*) top layer, which showed birefringent particles inside and just outside the periphery of red blood cells (compare Fig. XIV: 10 *a*), and (*b*) bottom layer, which showed mainly normal erythrocytes, and (*c*) minor changes similar to those produced in vitro (compare Fig. XIV: 11 *b*) were found in a few regions.

around some lighter amorphous material, surrounded by a polycyclic, thin or membrane-like structure (Fig. XIV: 12 *c*, *d*).

Curious differences in local arrangements of haemoglobin were observed in the anodic and cathodic fields. Thus, haemoglobin became concentrated in cells near the cathode (Fig. XIV: 13 *a*) or appeared as if mutually repelling haemoglobin in adjoining cells. To a lesser extent, haemoglobin also appeared as if it were attracting when cells were close together (Fig. XIV: 13 *b*).

Haemoglobin in cells from near the anode (Fig. XIV: 10 *c*) showed similar differences in distribution ("attracting and repelling haemoglobin"). Concentration of haemoglobin in separate cells or "repelling haemoglobin" in adjoining cells was common in both anodic and cathodic fields.

Changes in erythrocytes could also be produced in in vivo experiments with direct current in dogs. Thus, blood is shown from a dog in Fig. XIV: 14 after it had received 1 700 coulombs at 10 volts between the aorta (cathode) and the neck musculature (anode). Blood was taken from a vein and heparin added. After centrifugation, blood from the top and bottom layers was

smeared on slides. Erythrocytes from the top layer (Fig. XIV: 14 *a*) showed birefringent haemoglobin particles inside and just outside cells, very much like the cathodic cell material which was shown in Fig. XIV: 10 *a*. Blood from the bottom layer (Fig. XIV: 14 *b*) showed cells which have been interpreted as appearing normal, although they seemed possibly less stainable than control blood. Some changes were, however, found in this blood (Fig. XIV: 14 *c*), which resembled cathodically transformed erythrocytes.

The morphologic changes observed in blood from the anodic and cathodic fields varied considerably with the distance from the electrodes. Erythrocytes at the anodic electrode surface were completely destroyed. At a sufficient distance from the electrodes, normal cells were seen in both the anodic and cathodic fields.

Thus far we may conclude that considerable morphologic changes can be observed in red blood cells in both the anodic and cathodic fields. As will be shown in Chapter XVI, fat and water in adipose tissue can be induced electrophoretically to move over cellular membranes. It is therefore likely that similar mechanisms are also involved in the development of the morphologic changes just described for red blood cells. The experimental conditions in vivo and in vitro are certainly not comparable in many respects with spontaneous in vivo conditions. Nevertheless, an augmented experimental activation of anticipated BCEC channels may give us a hint about the capability of this biokinetic mechanism to modify the structure of cells and tissues. With this possibility in mind we will now consider the in vivo behaviour of leukocytes in a VICC activated experimentally in mesentery.

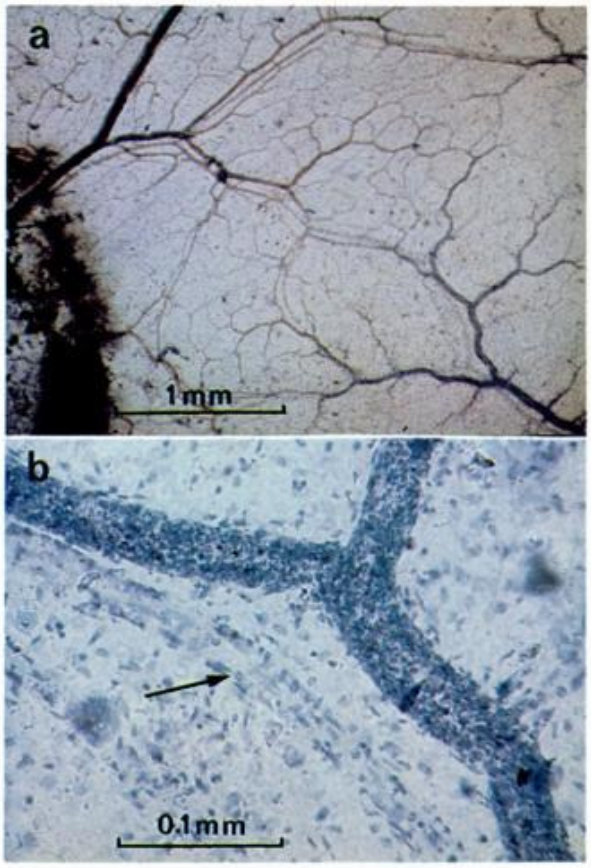

Fig. XIV: 15. Accumulation of granulocytes around the anode after application of direct current to dog mesentery. (*a*) 0.002 coulombs were delivered at 1 V overpotential between an anodic mesenteric electrode and an aortic cathodic electrode. Mesentery then was fixed in formaldehyde and stained with haematoxylin and eosin. Brown material accumulated at the site of the anode (left). The blue vessel to the right is a vein. It is entirely filled with granulocytes. Brown material in the large vessel to the left consists mainly of decomposed granulocytes. (*b*) Detail view shows white blood cells in vein. Adjacent artery (arrow) is collapsed and empty.

I. Accumulation of granulocytes

One of the dramatic morphologic changes in the electric field is marked accumulation of granulocytes around the anode at "low" voltages.

One volt, which must still be regarded biologically as a relatively high voltage difference, was applied between the electropositive platinum electrode placed against the mesentery of a dog and the electronegative platinum electrode in the aorta (Fig. XIV: 15). After 0.002 coulombs (60 minutes, 0.6 μA), the current was interrupted and a piece of the mesenteric tissue excised around the site of the anode. The tissue was then placed on a glass slide, fixed in formalin and stained with haematoxylin and eosin. Dark brown material was found to have accumulated near the edge of the electropositive electrode (Fig. XIV: 15 *a*). The large dark vessel in the figure is a vein, which anastomosed with a blue vein in the right-hand side of the figure. This blue material consists of granulocytes (Fig. XIV: 15 *b*) completely filling the vein. No red cells could be seen in these vessels. Adjacent arteries are narrow and empty of blood cells. By following the blue vessel branches to the black ones it can be seen that the black material consists of granulocytes, increasingly decomposing from right to left.

Fig. XIV: 16 *a* shows a vein leaking granulocytes about one cm from the cathode. Anode and cathode in this experiment were each placed on dog mesentery (2 volts, 2.80 coulombs).

Granulocytes are attracted to the walls of veins before they pass into interstitial tissue. This attraction is seen in Fig. XIV: 16 *b* as "margination of leukocytes"

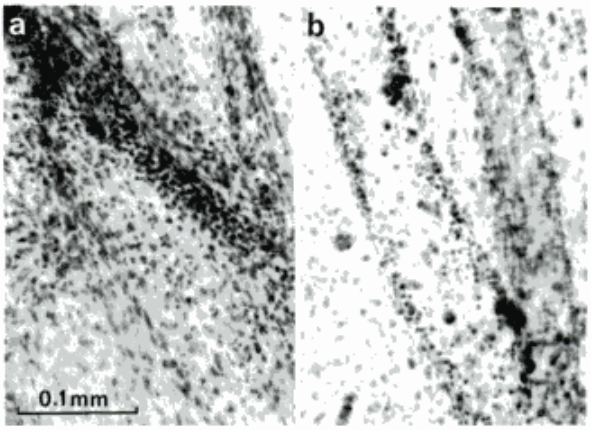

Fig. XIV: 16. Accumulation of granulocytes around electrodes in dog mesentery. (*a*) Granulocytes leaking through veins into the interstitium (2 V, 2.8 coulombs) one cm from the cathode. (*b*) White blood cells marginating to the walls of a vein (large vessel, left) near the anode. Right vessel is an almost empty artery.

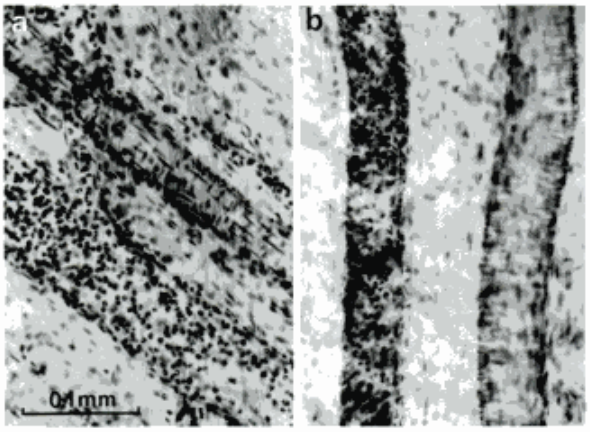

Fig. XIV: 17. Accumulation of granulocytes and altered vascular calibre induced by direct current in dog mesentery. (*a*) Mesentery cathodic and inferior vena cava anodic: a vein, containing granulocytes, is wide. An adjacent artery, empty of cells, is narrow. (*b*) Mesentery anodic and vena cava cathodic: a vein, packed with granulocytes, is narrow. The adjacent artery, empty of cells, is wide.

in a vein containing a moderate increase in quantity of these cells. Mesenteric electrode was anodic, aortic cathodic (2 volts, 1.2 coulombs). The same collection of leukocytes in veins occurred when the polarity was reversed.

While granulocytes were accumulating selectively in veins, adjacent arteries have been empty of blood cells. Leukocytes accumulated in veins also when the cathode was on the mesentery and the anode placed in the inferior vena cava, or when the polarity of these electrodes was reversed. This finding is illustrated in Fig. XIV: 17, which also shows that in both instances the adjacent arteries were empty. (See also regional "arteriocapillary" contractions and "venocapillary" accumulation of granulocytes in Chapter XII.)

The distribution of individual cells may be taken as support for the theory that BCEC systems represent an additional circulatory system capable of selective transports. It may be possible that BCEC systems can transport selectively not only electrolytes but also charged particles as large as blood cells.

The mechanism of electrophoretic transport of charged particles very likely depends on many factors. Thus, it is known that granulocytes make their way

Table XIV: 2. *Surface-charge characteristics and nature of chemical groups contributing to surface charge per cell surface area for platelets, lymphocytes, and erythrocytes*

					Negatively charged groups				
						Phosphate susceptible to[b]			
Cell type	Anodic electrophoretic mobility (μm/sec/V/cm)	Apparent electron charges ($\times 10^6$)	Corrected electron charges ($\times 10^6$)	Amino groups (+) ($\times 10^5$)	NANA α-carboxyl (pK_a 2.6)[a] ($\times 10^5$)	RNase[c] ($\times 10^5$)	Alk. phos.[d] ($\times 10^5$)	Weak acidic (pK~4) ($\times 10^5$)	$-$SH groups ($\times 10^6$)
Platelets[c]	0.85±0.04	1.8	2.04	2.42	8.9	–	5.0	6.5	0.28
Lymphocytes[d]	1.09±0.08	9.34	10.29	9.5	29.0	8.7[f]		55.5	1.98
Erythrocytes[e]	1.08±0.03	10.29	10.29	Not detected	62.0	–	–	40.9	Not detected

[a] Surface areas of cells: 28.27 μm^2; 113 μm^2; 163 μm^2. Electrokinetic data obtained in physiological saline (0.145 M NaCl; pH 7.2 at 25°C).
[b] May be present but $<5\times10^5$ per cell.
[c] *Thromb. Diath. Haemorrh. Suppl. 26:* 53 (1967); *26:* 370 (1971).
[d] *Int. Arch. Allergy 42:* 69 (1972).
[e] *Arch. Biochem. Biophys. 135:* 356 (1969).
[f] *Exp. Cell Res. 50:* 441 (1968).

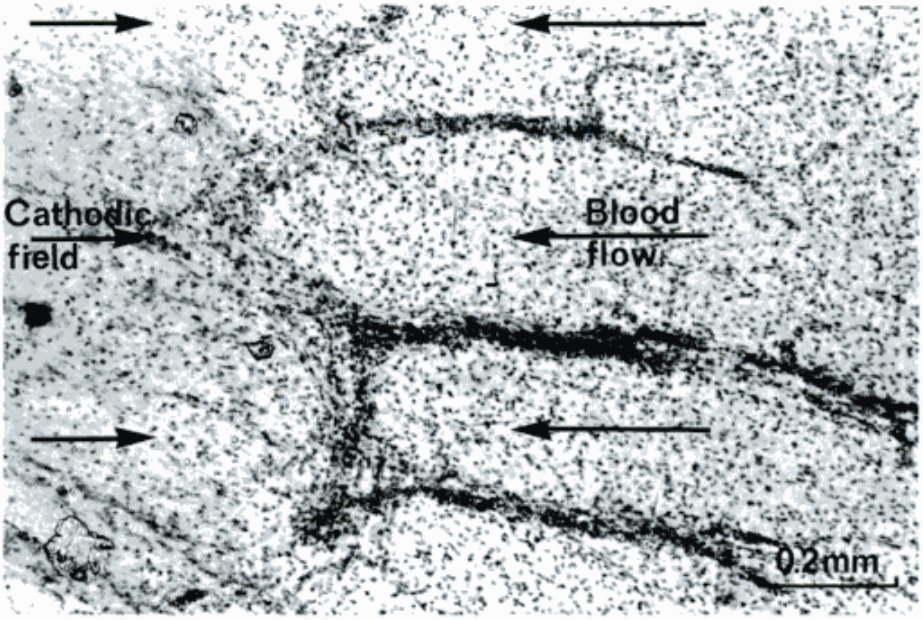

Fig. XIV: 18. Illustration of interaction between blood flow and cathodic field leading to accumulation of granulocytes. The flow of blood in veins is directed toward the cathode. The electronegative electric field will selectively counteract the flow of electronegatively charged granulocytes which leads to an increasing accumulation of granulocytes in these vessels. See also accumulation of an electronegative chemical compound (Fig. XIV:19).

through pores in the capillary membranes by means of pseudopods. Also various matrix factors in tissue may influence electrophoretic transport of different cells. The relation between their surface charges and the strength of the superimposed electric field might be important elements in the mechanism of selective transport of cells in tissue. In this connection, surface characteristics of blood platelets, lymphocytes and red blood cells are of particular interest. A compilation of actual data from the literature (30) is presented in Table XIV: 2.

A surplus of fixed electronegative charges also characterizes granulocytes. In a closed electric circuit any cell with a surplus of electronegative charges will tend to move toward the anode and be repelled by the cathode. This fact does, however, not necessarily mean that all electronegative cells will migrate to the same extent. Differences in excess of charge and steric position of charges in relation to the matrix should influence the transports, as well as factors such as surface friction, size and pliability of the cell. The repellent force of a cathode or an electronegative phase of a degrading tissue was also found to influence the distribution of blood cells. Thus, the area immediately around a cathode was always free of granulocytes and red blood cells when granulocytes were attracted to the anode. Distal to the zone free of granulocytes, collections of granulocytes could, however, be seen in vessels and interstitial tissue. This finding might be explained as a *selective repellent force* on these cells flowing in blood toward the electrode, resulting in a relative increase in their local concentrations. Fig. XIV: 18 illustrates the effect of such a *flow and field interaction* leading to the accumulation of granulocytes. Two 4×4 mm large platinum electrodes were gently placed on the mesentery of a dog. After 100 mV, 10 μA, 30 minutes, veins directed toward the cathode filled with granulocytes up to a certain distance from the cathodic surface. During the flow of blood in these veins, the electronegative field of the cathode must evidently selectively retard the electronegatively charged granulocytes, which thereby will accumulate (see also Section K on selective flow and field accumulation of an electronegative dye around the cathode).

J. A revised view of so-called "chemotactic" accumulation of granulocytes in inflammation

Van Lancker (22), in an excellent monograph on molecular and cellular mechanisms, states: "The nature of the mechanism that directs the movement of the leucocyte against a concentration gradient of a chemotactic substance is completely obscure. ... There seems to be no obvious common denominator in all agents capable of eliciting chemotactism. ... Little is known of the machinery which brings the cell to respond to the cell of the chemotactic agent."

A survey of the field of chemotaxis has been made by Harris (17, 18). His conclusion was almost a damnation of the biological meaning of chemotaxis. In his

view, chemotaxis is an in vitro phenomenon which probably has no relevance in vivo.

In an authoritative survey in 1978 on leukocytic locomotion, Stossel (43) refers to several partial mechanisms but remarks that "whether any of the above "explanations" for the components of locomotion and for the locomotion per se turns out to be correct, remains to be seen."

Wilkinson and Allan also stated in 1978 (52, 53) that a number of researchers have found "the loose use of the word chemotaxis to describe migration of cells in the presence of an attractant is increasingly unsatisfactory and confusing". They therefore propose a definition of chemotaxis as "a reaction by which the direction of locomotion of cells is determined by substances in their environment".

Most remarkable about the concept of chemotaxis is the fact that this commonly used term is not related to any defined biokinetic mechanism. As long as the concept of chemotaxis varies from describing a specific effect to a whole biokinetic process including anticipated but unknown chemical and humoural factors, confusion will persist.

The reader may already have a presentiment of an alternate explanation for the attraction of leukocytes in inflammation: granulocytes are well known to carry a surplus of fixed electronegative charges on their surfaces (1, 2, 5, 50). Granulocytes should therefore be attracted to the anode within a closed electric circuit, as shown in the experiments earlier presented. Corresponding in vivo to experimental circuitry powered by an external battery, is the VICC system, powered by physico(-electro-)chemical gradients between the injured and surrounding normal tissues. We will discuss this alternate mechanism in more detail after reviewing some essential information from the literature on chemotaxis and inflammation. Some of the relevant literature on chemotaxis is also presented in Chapter XVI, Section U, where a corresponding discussion is made on the background of spontaneous accumulation of lymphocytes in breast carcinomas.

Leukocytes are considered to respond to a variety of chemoattractants "most likely" by way of specific receptors on their surface (21, 46, 47). In this theory it is assumed that chemical substances released at the endothelial surfaces possess the capacity to "glue" leukocytes to the vessel walls, producing marginations (8). Alternatively, leukocytes in some way may be bound electrostatically to the endothelial cells, as described for thrombocytes (38–42). The essential drawback in these prevailing theories on margination is that no "glue" has yet been identified. Moreover, electrostatic attraction of charged leukocytes to charged endothelial sites should interfere with diapedetic migration through the vessel walls (27).

It can be concluded that the inflammatory accumulation of leukocytes in blood vessels and, particularly, the adhesion of leukocytes to endothelial walls have not yet been explained satisfactorily.

The local accumulation of polymorphonuclear leukocytes in inflammation appears first in the vessels. Some of these vessels are widened (24, 54). The leukocytes either adhere to the vessel walls, a process called leukocytic margination (14), or fill the lumens of the small vessels. The leukocytes next migrate through the vessel walls via "diapedetic transport" (17) into the interstitial tissue. In the interstitium the leukocytes are thought to be attracted in some way to the cause of inflammation, e.g., bacteria. The mechanism of vasodilatation in inflammation is only known to a certain extent (24). Focal liberation of serotonin, histamine and histamine-like substances (15, 35, 44, 45) are involved, e.g., as a result of stimulation of sympathetic nerves through axon reflexes (29). A direct effect by the injurious agent on the capillaries is often discussed. Various peptides and proteins, isolated in inflammatory tissue (4, 6, 10, 31), have been thought to produce an increase in capillary permeability. This group of substances includes leukotaxine, exudime, bradykinin, substance P, kallidine and plasmin (13, 32, 33, 49). The prostaglandins (7) induce local signs of inflammation, e.g., erythema and oedema, and have also been suggested to function as mediators of inflammation (28).

A large number of substances have been studied with regard to their chemotactic properties. Rivkin and Becker (36) have shown that cyclic AMP, histamine, epinephrine, isoproterenol and prostaglandin E inhibit chemotaxis of polymorphonuclear leukocytes in rabbits. Cyclic nucleotides, e.g., 3′, 5′ guanosine monophosphate, strongly attract polymorphonuclear cells (19, 36). N-formyl-methionyl-methionyl-methionine, N-formyl-methionyl-leucylphenyl-alanine and other peptides, as well as different suspensions of bacterial cultures, are often used as chemoattractants in experimental chemotaxis (46).

The diapedetic process has been studied by light and electron microscopy. These studies have revealed only that white blood cells either appear to be pushed somehow through the endothelial cells or that they actively pass between endothelial cells by means of pseudopods (25, 34). In this case the spaces between endothelial cells are enlarged or thought to be widened by some action of the leukocytes.

The interstitial accumulation of leukocytes is generally believed to be caused by "chemical signals" from the injured tissue to the leukocytes. Bacteria are believed to attract leukocytes, as judged from in vitro experiments. Menkin (33) extracted from inflammatory tissue an unidentified polypeptide he called leucotaxine with "chemotaxic properties".

The attraction of leukocytes in inflammation and

their engulfment of bacteria and necrotic tissue material are still to a large extent not well understood.

The present studies focus our interest on the fact that one essential part of inflammation, the accumulation of granulocytes, can be produced experimentally in abundance by in vivo electrophoresis without the use of bacteria, "chemotactic compounds" or by inducing primary tissue injury (the platinum electrodes were placed gently on the mesentery), inoculating microorganisms or using chemical agents. The present studies also include other components of inflammatory responses: thrombosis, capillary leaking, diapedesis, transport of water, producing oedema, and, as we will also see in late phases of healing, the formation of scar tissue.

In this view, *the accumulation of granulocytes in inflammation may be regarded as a special case of an electrochemical field reaction within a biologically closed electric circuit (the vascular-interstitial closed circuit, VICC), combined with electrophoretic transport of granulocytes.*

To summarize, a damaged tissue presents a fluctuating electrochemical potential in relation to surrounding normal tissue. This potential difference will produce a driving force in a vascular-interstitial closed circuit (VICC), attracting the electronegative granulocytes to the initially electropositive injured tissue. During this phase arteriocapillaries contract in certain regions while venocapillaries permit diapedetic passage of the electronegatively charged granulocytes. An electrophoretic transport with accumulation of electronegatively charged cells, i.e., red blood cells, thrombocytes and leukocytes should then take place. It is still not clear if the magnitude of the driving potential difference of the circuit, the specific surface charges of the cells or other mechanisms are responsible for the preferential attraction of a certain type of cells. Massive attraction of granulocytes to the anode, for instance, was observed preferably at "relatively low" voltages (in the tested region of 1 to 3 volts). In the region of 10 volts a minor increase in quantity of identifiable granulocytes was present around the anode. This finding has been interpreted as an effect of a too violent interference of the electric field with forces which in spontaneous inflammation probably interact very delicately.

Several other factors may also influence the electrophoretically accumulated cells. When, for instance, the polarity of an injured tissue changes from anodic into cathodic, one must assume that the granulocytes attracted during the anodic phase will in the new cathodic surrounding become trapped and electrochemically changed. Electronegatively charged blood cells flowing in vessels toward a cathodic tissue region should selectively become retarded in the blood stream and consequently increase in concentration. Certain extracts or chemicals added locally to a tissue should also be able to produce positive or negative "chemotaxis", depending on their polarity. It is therefore possible to include different partial factors connected with "chemotaxis" under one common mechanism: *electrophoretic, selective transport of electronegatively charged granulocytes in a biologically closed, activated electric circuit.* Acceptance of such a mechanism for charged blood cells to enter a tissue suggests that therapeutic accumulation of granulocytes might be induced by an external electric DC power source over electrodes. Another aspect may be to look for "leukotaxic agents" with regard to their properties to polarize a tissue. It should be evident that VICC mechanisms may also be capable of influencing the distribution of other cell elements in blood, i.e., lymphocytes, platelets and red blood cells.

K. Local accumulation in tissue of a charged chemical compound

The principle of the proposed mechanism for accumulation of granulocytes in an injured tissue should also apply for charged chemical compounds. To confirm this hypothesis, Evans blue dye, which is electronegative, was selected for investigation.

An overpotential of 4.2 volts was applied between two platinum electrodes against a piece of mesentery of an anaesthetized dog. After one coulomb had passed through the tissue, the usual vascular changes were seen in the tissue in an area about 15 mm in diameter around each electrode. A few grains of Evans blue dye were dissolved in 20 ml of saline. This solution was then injected into the aorta via a catheter while current was applied to the mesenteric electrodes. After a few minutes a ring of blue stain could be seen against the brown-yellow zone around the *electronegative* electrode (Fig. XIV: 19). A very small amount of blue stain could also be seen around the electropositive electrode. Electrophoretic tests of the dye in vitro showed that it moves in water solution to the *electropositive* electrode. Nevertheless, upon repeated tests of injecting the dye into the dog aorta, the dye always accumulated in tissue around the electronegative electrode. These tests also included the *simultaneous* application of current and injection.

It is evidently possible to attract a charged compound to a polarized part of a tissue. In the experiment described, the electronegative Evans blue dye possibly combined in the blood stream with some other compound or compounds provided with a surplus of elec-

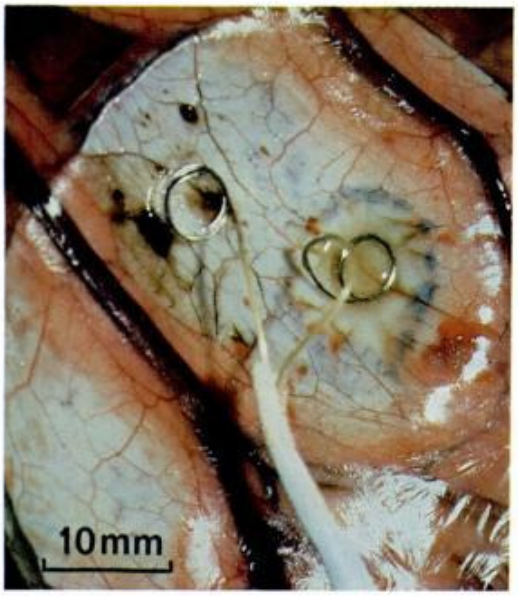

Fig. XIV: 19. Electrophoretic attraction of a charged compound, injected intravascularly. After 1 coulomb at 4.2 V overpotential was passed between two mesenteric electrodes, dilute electronegative Evans blue dye was injected into the aorta. It accumulated as a blue ring around the cathode. This accumulation is explained as an interaction between blood flow toward the cathode and the repellant force of the cathodic field.

tropositive charges compared to the magnitude of negative charges on the molecules of the dye. In this way the resulting combination might be attracted to the electronegative and not to the electropositive electrode. A more likely explanation is the one illustrated in Fig. XIV: 18 for accumulation of granulocytes in veins directed toward a cathode. According to this mechanism the electronegative dye, flowing in arteries or veins in the direction of the cathode should accumulate in these vessels by the opposing electric field force of the cathode.

This experiment demonstrates that artificial electric polarization can cause a chemical compound to accumulate locally in a tissue. It also shows that the polarities of the electric field and of the charge of the compound are not the only factors which determine where the compound will accumulate in an in vivo experiment.

L. Direct current studies in the dog's lung

The directly observable tissue changes by direct current in mesenteric tissue were also studied in the lungs of dogs.

Platinum strings, 0.25 mm thick, were coated with Teflon. The coat was removed for a length of 0.5–2.5 cm at each end of each string. One end was then inserted for a distance of 0.5–1.0 cm into the tip of an ordinary biopsy needle, 1 mm thick and 16 mm long. Bending the string at the tip of the needle formed a hook. The string-containing needle was then inserted percutaneously under fluoroscopic control into the lung of an anaesthetized dog. The needle was removed, leaving the string electrode in place. The hook served the purpose of keeping the electrode in place.

Two platinum electrodes were inserted into the lung of a dog at a distance between them of about 5 cm. Alternatively, one platinum electrode was inserted in lung and the other electrode, a stainless steel guide wire, was inserted through an intravascular catheter into the pulmonary artery or aorta. The introduction of one electrode through a transvenous catheter into the pulmonary artery makes it possible to use the branching pulmonary arterial tree as the conducting pathway between the electrodes. When an electrode is in the aorta, bronchial arteries serve as the conducting pathway.

The electrically induced changes in tissue around a small, 5 mm long, intrapulmonary electrode as anode, with the cathode positioned in a supplying vessel 3 cm or more distant, were found to be almost spherical. The longer string electrodes gave a more elliptical shape to the changes in tissue.

Experiments were performed in ten dogs, first as chronic studies over four weeks and then acutely in each animal. Current was first applied between two electrodes in one lung. Four weeks later, current was applied between electrodes in the contralateral lung. Each animal was then sacrificed immediately by intravenous injection of a large dose of sodium pentothal.

The acute effects of an applied current between an intravascular electrode and a percutaneously inserted string electrode in pulmonary parenchyma may be seen in a representative example in Fig. XIV: 20. The anodic platinum string electrode was inserted percutaneously into the parenchyma of the left lower lobe and the cathodic catheter and its guide wire of stainless steel into the left pulmonary artery (Fig. XIV: 20 *a* and *b*). Before current was applied, an arteriogram of the dog's left lower lobe was made with 20 ml of 60% Urografin. This study was normal, as seen in lateral projection (Fig. XIV: 20 *c*).

An electric potential of 20 volts DC was then applied between the catheter guide wire and the platinum electrode, which was made electropositive. The initial current of about 15 milliamperes increased spontaneously and gradually to about 55 milliamperes, at which level it remained. A total of 180 coulombs was given.

Arteriography was then performed. Urografin (60

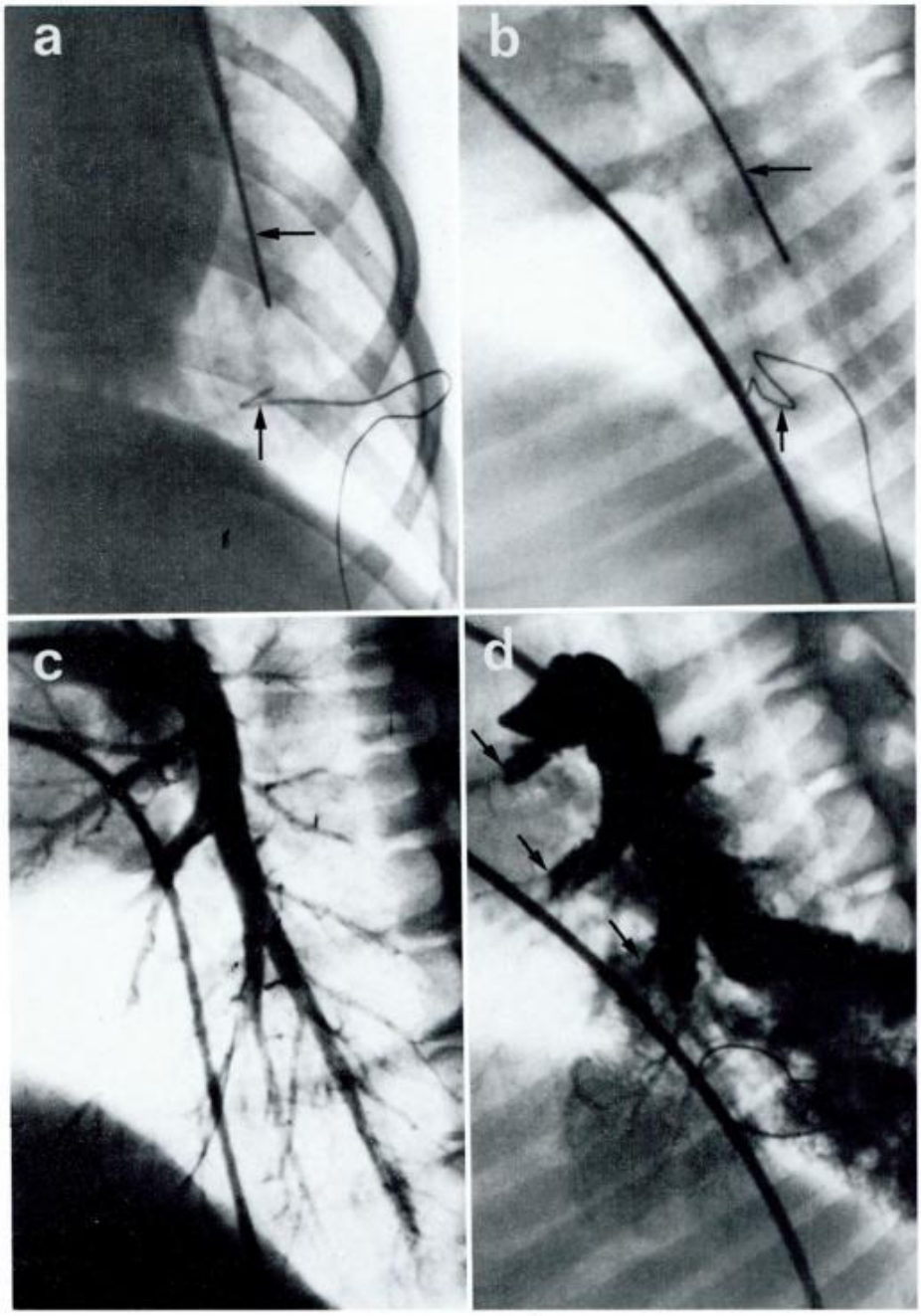

Fig. XIV: 20. Acute effects of direct current between a pulmonary artery and parenchyma of a dog's lung: radiographs in vivo. (*a*) Anteroposterior and (*b*) lateral radiographs before application of current. Transvenous catheter in left pulmonary artery. Guidewire in lower lobe pulmonary artery serves as cathode (←). Platinum electrode percutaneously inserted in lower lobe serves as anode (↑). (*c*) Control arteriogram, lateral projection, shows normal left lower lobe pulmonary arteries. After 180 coulombs at 20 V had passed between the electrodes, repeat arteriogram (*d*) shows blocking of pulmonary arterial branches (↘) near the cathode and leakage of contrast medium into the interstitial tissue near the anode (diffuse opacities in lower right part of figure).

percent, 20 ml) was again injected through the catheter in the pulmonary artery. A cone-shaped constriction and nearly complete blocking of proximal pulmonary arterial branches were found adjacent to the electronegative electrode (upper contrast-filled vessels in Fig. XIV: 20 *d*). Nearer the electropositive electrode the contrast medium extravasated into the interstitial tissue, as seen in the lower part of Fig. XIV: 20 *d*.

At autopsy the left lower lobe was found to be bright red (Fig. XIV: 21). Under the intact pleura a dark region was seen, which on palpation corresponded to a firm tumour-like mass at the site of the anode. When the lung was incised, this mass was firm, like a granuloma. Its centre was white, completely dry, and measured 8×8×15 mm. The periphery of the mass was also dry but black. The total size of the white and black "granuloma" was 3.2×2.0×2.0 cm. The surrounding lung tissue contained an increased amount of blood.

The site of the intravascular cathode revealed no gross thrombi either on the electrode or in the vessels. Perivascular tissue, however, was rather dark and ex-

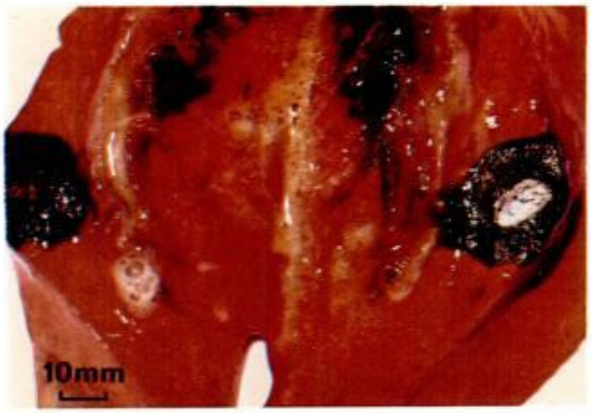

Fig. XIV: 21. Acute effects of direct current between a pulmonary artery and parenchyma of a dog's lung: autopsy specimen (same dog as in Fig. XIV: 20). Section through lower lobe reveals a 3.2×2.0×2.0 cm black dry mass around the anode. The cathodic region in the mid upper part is oedematous and dark from blood pigment. Vessels in the cathodic region were not blocked by thrombosis. The vascular blocking shown near the cathode in Fig. XIV: 20 appeared to be produced by compression from interstitial oedema. The anodic lesion showed a small central gas cavity surrounded by white-gray, chlorine-bleached material. Surrounding black area is caused by HCl-destroyed blood (proton diffusion and migration from anodic surface).

ceedingly oedematous. Liquid flowed freely from the freshly incised tissue in this region.

Histologic sections of the mass around the anode showed "inflammatory" changes of moderate infiltrations of leukocytes and marginal accumulations of leukocytes in vessels. Oedema dominated in the tissue around the cathode. No thrombotic blockings were seen in the vessels around the anode. The blocking of the passage of the contrast medium in this region was interpreted as produced by pressure of interstitial oedema. All dogs showed similar findings.

When two electrodes were implanted directly in the lung of a dog, the acute and chronic effects of direct current (10 volts, 200 coulombs) were as follows:

1. Acute anodic

Chlorine and oxygen gas produced a gas pocket close to the electrode. A bleached, gray-white, dry zone was found around the gas pocket. This zone was surrounded by a larger, dry, gangrene-like, black zone. This black zone was sharply demarcated against the surrounding, nondestroyed lung parenchyma and had an increased density. On palpation it felt like a granuloma or tumour. The surrounding lung tissue was dry close to the destroyed black zone, but peripheral to this zone the tissue was oedematous. The black and white zones showed an acidic reaction. Microscopically they represented completely destroyed tissue. An increased number of granulocytes was usually seen in the veins and in the interstitium. Thromboses were found in many small vessels and capillaries. Small arteries were often narrow and empty of red blood cells.

2. Acute cathodic

Hydrogen gas produced a larger gas pocket around the cathodic tissue electrode than chlorine and oxygen gas produced around the anodic tissue electrode. The tissue around the cathodic gas pocket was diffusely darkly coloured and oedematous. The tissue fluid was pinkish and alkaline. The large amount of oedema fluid probably partially compressed the vessels, but active contraction of vessels, as was seen in the mesentery, is possibly also produced in the cathodic field.

Histologically, arteries and veins usually did not contain blood cells close to the electrode. The dark material was probably alkaline haem, laked from red blood cells. Conglomerates (probably blood protein) appeared as round or oval bodies in vessels. The empty blood cells could be recognized in the interstitium by their membranes, which showed increased contrast between the interior of each cell and the surrounding tissue.

3. Four weeks anodic

The appearance of this tissue was similar to that of dry black gangrene. Volume of the tissue was decreased, as an effect of dehydration and shrinkage of tissue by scarring. Extensive thromboses blocked vessels. Lymphocytes were now found in the interstitial tissue, which was also fibrotic. The adjacent pleura was fibrotically thickened.

Fig. XIV: 22 *a*, surveys the anodic zone after four weeks. The dark part was dominated by infiltration of lymphocytes. Scarring was also seen at higher magnification (Fig. XIV: 22 *b*).

4. Four weeks cathodic

Tissue remained somewhat distended by oedema fluid. Hyaline degeneration and phagocytosis of cells were found alongside pulmonary fibrosis. The pleura was thick close to the electrode.

Fig. XIV: 22 *c* surveys the cathodic zone. The pleura is locally thickened. Some fibrous septa partly cross the lung tissue. Lymphocytes are seen in Fig. XIV: 22 *d* at higher magnification.

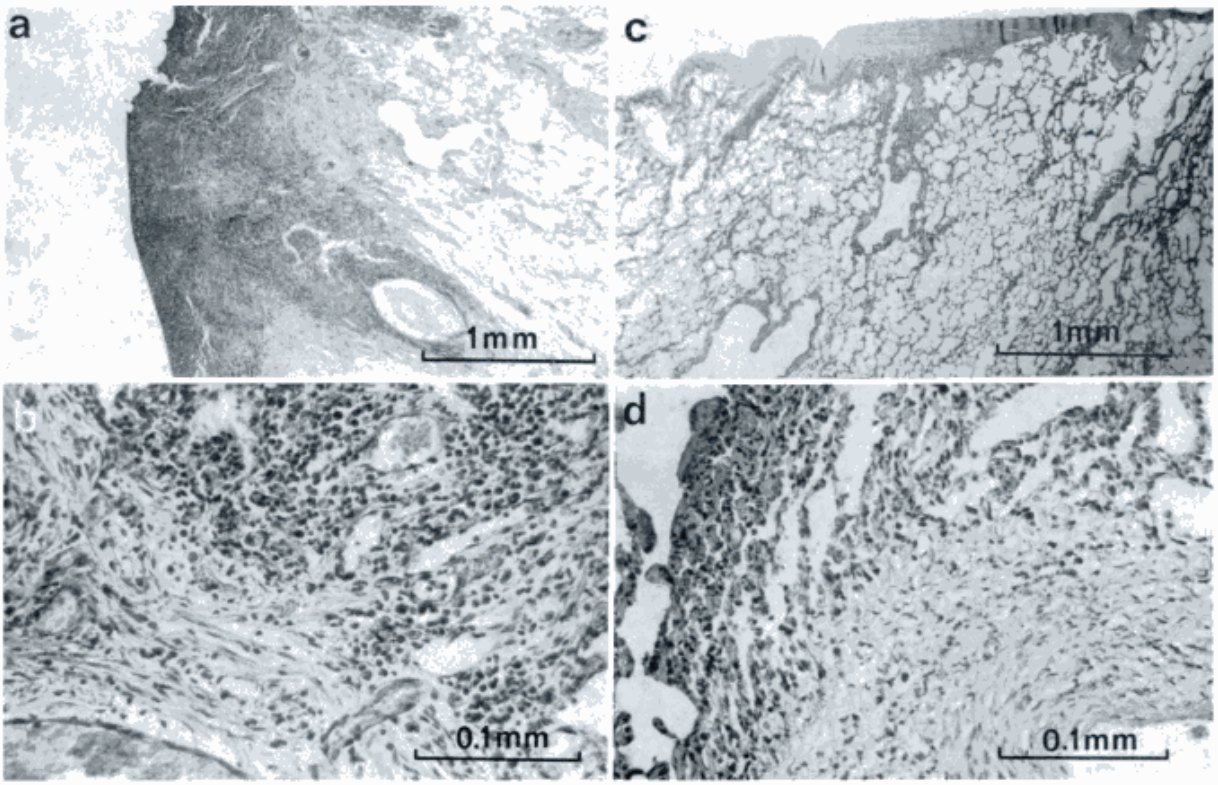

Fig. XIV: 22. Chronic effects of direct current between intrapulmonary electrodes in a dog's lung. Four weeks after exposure to 200 coulombs at 10 V. (*a* and *b*) In the anodic area, tissue is more dense than normal and extensively infiltrated with lymphocytes (dark regions of *a*) and contains some fibrosis. (*c* and *d*) In the cathodic area, the pleura is locally thickened. The lung tissue is slightly more dense than normal but less dense than the anodic tissue. Some fibrosis, lymphocytes and hyaline degeneration are present.

M. Discussion

This chapter surveys some tissue and cellular changes induced by activation of a closed electric circuit in tissue. By the use of an external direct current source and electrodes, it is anticipated that we activate one or several physiologic VICC branches. Functional and developmental effects of activated VICC components can in this way be driven beyond the limits of their physiologic tolerance. Structural changes provoked in this way should facilitate our recognition of those functional and structural effects in which BCEC systems are involved.

In studies of this kind one should not forget that the amount of current per unit time flowing through a physiologic BCEC system is by engineering standards very low, probably often in the range of micromicroamperes. The current may, however, flow continuously and with changing direction and magnitude among complex systems of ionars (Chapter XIII), which polarize against each other.

The experimental use of unphysiologically high voltage differences between electrodes can be expected to produce unforeseen effects in a living tissue. The obvious risks of leading current between electrodes over a vital organ such as the heart need no further discussion in this connection. What must be pointed out, however, is that preferential pathways for current in a living tissue vary with voltage difference and current density. This property is easily recognized if we consider the functions of one conducting BCEC branch, the blood vessels. Because more blood is present in the peripheral branches than in the stem of a blood vessel, the resistance to current flow must be lower in the periphery than in the stem of the vessel. Consequently, the insulating properties of the vessel walls must be larger in the stem (thicker wall) than in the peripheral vessels. This balance should correspond to actual physiologic current densities and voltage levels. If we overload the system either with too high current densities or by too high energy levels, the system goes out of order. Current will break through at unexpected sites of least resistance.

To direct the reader's attention to one specific fundamental physiologic function of the BCEC, granulocytes were studied as they were selectively attracted to

an anodic electrode, gently placed against tissue, with the cathode in a supplying vessel. Further, a mechanism of flow and field interaction has been described for selective accumulation of granulocytes around an electronegative electrode. It has been proposed that these experiments simulate the endogenous spontaneous mechanism of focal accumulation of granulocytes in tissue. Heretofore, an explanation for this characteristic function of granulocytes has been lacking. This explanation is also of practical interest because electrophoretic transport of granulocytes within a BCEC can easily be arranged with electrodes and an external power source for possible therapeutic purposes. These experiments have also been used as a starting point toward future revision of the unfortunate concept of "chemotaxis". For too long this concept has served as a loose term concealing lack of knowledge concerning the true character of important biologic mechanisms. It would not be surprising if several separate biologic mechanisms are included within "chemotaxis". The acceptance of the basic concept of BCEC makes it possible to define at least one such mechanism as an electrophoretic closed circuit transport of charged cells and chemical compounds among polarizing regions of tissue.

The acute and chronic in vivo experiments with large doses of current were made to study secondary healing processes in the anodic and cathodic sites of tissue. In these sites partial reactions have been encountered, characteristic of spontaneous healing of tissue. It has therefore been proposed that the energy-liberating, catabolic process in spontaneous tissue healing might be supported by an artificial activation of the involved circuits over implanted electrodes from an external source of direct current power. Research to be conducted along these lines will require considerably more information than is now available concerning induction of healing processes by direct current. We will therefore proceed with studies of partial healing phenomena in a different kind of tissue, the female breast (Chapter XVI), to broaden our base for further discussions on therapy in Chapter XVII. Chapter XV will now conclude the discussion of our initial problem: the corona structures around pulmonary masses.

References

1. Abramson, H. A., Moyer, L. S., and Gorin, M. H.: Electrophoresis of proteins and the chemistry of cell surfaces. New York, Rheinhold Publ. Co., 1942.
2. Abramson, H. W.: Electrophoresis of cells and proteins. New York, Hafner Publ. Co., 1968.
3. Adler, J.: Chemotaxis in bacteria. Science 153: 708, 1966.
4. Aldrete, J. S., Sheps, S. S., Bernatz, P. E., and Didier, E. P.: Vasoactive polypeptides of surgical significance. Mayo Clin. Proc. 41: 399, 1966.
5. Bangham, A. D., Pethica, B. A., and Seaman, G. V. F.: The charged groups at the interface of some blood cells. Biochem. J. 69: 12, 1958.
6. Bayliss, W. M.: On the origin from the spinal cord of the vasodilator fibres of the hind-limb and on the nature of these fibres. J. Physiol. (Lond.) 26: 173, 1901.
7. Bergström, B., and Samuelsson, B.: The prostaglandins. Endeavour 27: 109, 1968.
8. Boyden, S.: Cellular recognition of foreign matter. Int. Rev. Exp. Path. 2: 311, 1963.
9. Brande, W., Home, E., and Davy, H.: Cited by Horsley, V., and Clarke, R. H.: The structure and functions of the cerebellum examined by a new method. Brain 31: 84, 1908.
10. Bruce, A. N.: Vasodilator axon-reflexes. Quart. J. Exp. Physiol. 6: 339, 1913.
11. Dahlgren, S., and Nordenström, B.: Transthoracic needle biopsy. Stockholm, Almqvist & Wiksell, 1966.
12. Diem, K., and Lentner, C.: Scientific tables. 7th ed. Basle, Ciba-Geigy, 1971.
13. Elliott, D. F.: Bradykinin and its mode of release. Ann. N.Y. Acad. Sci. 104: 5, 1963.
14. Grant, L.: The sticking and emigration of white blood cells in inflammation. In: Zweifach, B. W., Grant, L., and McCluskey, R. T. (eds.): The inflammatory process. New York, Academic Press, 1965, p. 197.
15. Green, J. P.: Uptake, storage and release of histamine. Uptake and binding of histamine. Fed. Proc. 26: 211, 1967.
16. Golsinger: Cited by Horsley, V., and Clarke, R. H.: The structure and functions of the cerebellum examined by a new method. Brain 31: 84, 1908.
17. Harris, H.: Role of chemotaxis in inflammation. Physiol. Rev. 34: 529, 1954.
18. Harris, H.: Mobilization of defensive cells in inflammatory tissue. Bact. Rev. 24: 3, 1960.
19. Hill, H. R.: Cyclic nucleotides as modulators of leucocyte chemotaxis. In: Gallin, J. I., and Quie, P. G.: Leucocyte chemotaxis. New York, Raven Press, 1978, p. 179.
20. Horsley, V., and Clarke, R. H.: The structure and functions of the cerebellum examined by a new method. Brain 31: 84, 1908.
21. Keller, H. U., and Sorkin, E.: Studies on chemotaxis. V. On the chemotactic effect of bacteria. Int. Arch. Allergy 31: 505, 1967.
22. van Lancker, J. L.: Molecular and cellular mechanisms in disease. Vol. 2. Berlin-Heidelberg-New York, Springer-Verlag, 1976, p. 778.
23. Lemberg, K., and Legge, J. W.: Hematin compounds and bile pigments. New York, Interscience Inc., 1949.
24. Lewis, T.: Blood vessels of the human skin and their responses. London, Shaw and Sons, 1927.
25. Luft, J. H.: The ultrastructural basis of capillary permeability. In: Zweifach, B. W., Grant, L., and McCluskey, R. T. (eds.): The inflammatory process. New York, Raven Press, 1965, p. 121.
26. Marchal, M. M., and Marchal, M. T.: Nouvelle méthode de ciné-densigraphie étalonnée permettant de diagnostic différentiel du cancer du poumon. Compt. rendus des séances de l'Académie des Sciences 23: 458, 1951.
27. Marchesi, V. T.: The site of leucocyte emigration during inflammation. Quart. J. Exp. Physiol. 46: 115, 1961.
28. Marx, L., and Jean, L.: Prostaglandins: mediators of inflammation? Science 177: 780, 1972.
29. Massart, J., and Bordet, C.: Recherches sur l'irritabilité des leucocytes et sur l'intervention de cette irritabilité dans la nutrition des cellules et dans l'inflammation. J. Med. Chir. Pharmacol. (Brussels) 90: 169, 1890.
30. Mehrishi, J. N.: Positively charged amino-groups on the surface of normal and cancer cells. Europ. J. Cancer 6: 127, 1970.
31. Menkin, V.: Biology of inflammation. Chemical mediators and cellular injury. Science 123: 527, 1956.
32. Menkin, V.: Biochemical mechanisms in inflammation. 2nd ed. Springfield, Ill., Charles C. Thomas Publ., 1956.
33. Menkin, V.: Chemical mediators in relation to cytologic constituents in inflammation. Amer. J. Path. 34: 921, 941, 1958.
34. Movat, H. Z., and Fernando, N. V. P.: Acute inflammation.

The earliest fine structural changes at the blood-tissue barrier. Lab. Invest. 12: 895, 1963.
35. Riley, J. F.: Functional significance of histamine and heparin in tissue mast cells. Ann. N.Y. Acad. Sci. 103: 151, 1963.
36. Rivkin, I., and Becker, E. L.: Effect of exogenous cyclic AMP and other adenine nucleotides on neutrophil chemotaxis and motility. Int. Arch. Allergy Appl. Immunol. 50: 95, 1976.
37. Samuelsson, L.: Electrolytic destruction of tissue. Doctoral dissertation. University of Lund, Sweden, 1980.
38. Sawyer, P. H., and Pate, J. W.: Bio-electric phenomena as an etiologic factor in intravascular thrombosis. Amer. J. Physiol. 175: 103, 1953.
39. Sawyer, P. N., Ziskind, H. S., and Harshaw, D. W.: In: Wesolowski, S. A., and Dennis, C. (eds.): Ion metabolism of the blood vessel wall. Fundamentals of vascular grafting. New York, McGraw-Hill Publ., 1963.
40. Sawyer, P. N., Stanczewski, B., Ramsey, Jr., W. S., Ramasamy, N., and Srinivasan, S.: Electrochemical interactions at the endothelial surface. J. Supramol. Struct. 1: 417, 1973.
41. Seaman, G. V. F., and Vassar, P. S.: Changes in the electrokinetic properties of platelets during their aggregation. Arch. Biochem. Biophys. 117: 10, 1966.
42. Spector, W. G., and Willoughby, D. A.: Chemical mediators. In: Zweifach, E. W., Grant, L., and McCluskey, R. T. (eds.): The inflammatory process. New York, Raven Press, 1965, p. 427.
43. Stossel, T. P.: The mechanism of leucocyte locomotion. In: Gallin, J. I., and Quie, P. G. (eds.): Leucocyte chemotaxis. New York, Raven Press, 1978, p. 143.
44. Uvnäs, B.: Mode of binding and release of histamine in mast cell granules from the rat. Fed. Proc. 26: 219, 1967.
45. Uvnäs, B.: Histamine storage and release. Fed. Proc. 33: 2172, 1974.
46. Ward, P. A., Lepow, J. H., and Newman, L. J.:Bacterial factors chemotactic for polymorphonuclear leucocytes. Am. J. Path. 52: 725, 1968.
47. Ward, P. A.: Leucotaxis and leucotactic disorders. Am. J. Path. 77: 520, 1974.
48. Weber, C. L.: Über absolute Geschwindigkeit der Jonen. Z. physik. Chemie 4: 182, 1889.
49. Webster, M. E., and Pierce, J. V.: The nature of the kallidins released from human plasma by kallikreins and other enzymes. Ann. N.Y. Acad. Sci. 104: 91, 1963.
50. Weiss, L., and Zeigel, R.: Cell surface negativity and the binding of positively charged particles. J. Cell Physiol. 77: 179, 1971.
51. Wilkinson, P. C.: Chemotaxis and inflammation. Edinburgh and London, Churchill and Livingstone, 1974.
52. Wilkinson, P. C., and Allan, R. B.: Assay systems for measuring leukocyte locomotion: an overview. In: Gallin, J. I., Quie, P. G. (eds.): Leukocyte chemotaxis. New York, Raven Press, 1978, p. 1.
53. Wilkinson, P. C., and Allan, R. B.: Binding of protein chemotactic factors to the surfaces of neutrophil leukocytes and its modification with lipid-specific bacterial toxins. Mol. Cell. Biochem. 20: 25, 1978.
54. Zweifach, B. W.: Microvascular aspects of tissue injury. In: Zweifach, B. W., Grant, L., and McCluskey, R. T. (eds.): The inflammation process. New York, Academic Press, 1965, p. 161.

XV.
Corona structures around pulmonary masses: vascular-interstitial closed circuit effects

The structural modifications which have here been named the corona structures are not always present around tumours and granulomas of the lung. When present, corona structures show a wide range of radiographic appearances. All of their structural components are therefore not easily demonstrable in any single case, which is probably the major reason why these structures have long been overlooked. Also it is always difficult to recognize structures before their developmental mechanisms and pathophysiological significance are apparent.

To demonstrate the wide range of appearances of corona structures, attempts have here been made to present both "easy" and "difficult" cases. Trained radiologists will recognize that to present data for frequency of appearance of these structures is difficult, similar to the situation in radiologic assessment of peripheral pulmonary vascular changes, as in pulmonary emphysema.

It is now obvious that the corona structures have nothing to do with malignancy per se of a lesion, as was once suspected. The corona structures appear not infrequently around malignant tumours, but occasionally also around granulomas and benign tumours. The structures seem to depend on a *common biokinetic mechanism, which includes a local liberation of energy after spontaneous necrosis, bleeding or infection and the channelizing of this energy over biologically closed electric circuits (BCEC).*

The polarization of local tissue has been demonstrated by measuring the *electric injury potential* between tumours or granulomas of the lung and surrounding tissue. The channelizing of the energy takes place over vascular-interstitial conducting channels. In this system the walls of "large" vessels electrically insulate the plasma, which is the conducting medium. The existence of vasa vasorum of large vessels may therefore be regarded as an expression of the normally poor exchange of water, electrolytes and nutrients across the walls of these vessels. *The large vessels function as cables which are insulated and electrically conducting. The plasma is electrically connected to the interstitial fluid over the walls of the capillaries,* which, of course, are permeable to water and electrolytes. *It is also suggested that electrode-equivalent sites in the circuit are localized to the endothelial cell membranes of the capillaries, which also possess a mechanism of variable "short"- and "long"-distance selective electrogenic transports. This BCEC is here named the vascular-interstitial closed circuit (VICC).*

The morphology and function of this circuit are seemingly very simple. On closer inspection, its complexity and importance for biochemical reactions and morphology will soon become apparent. At this juncture, we will only summarize and discuss implications

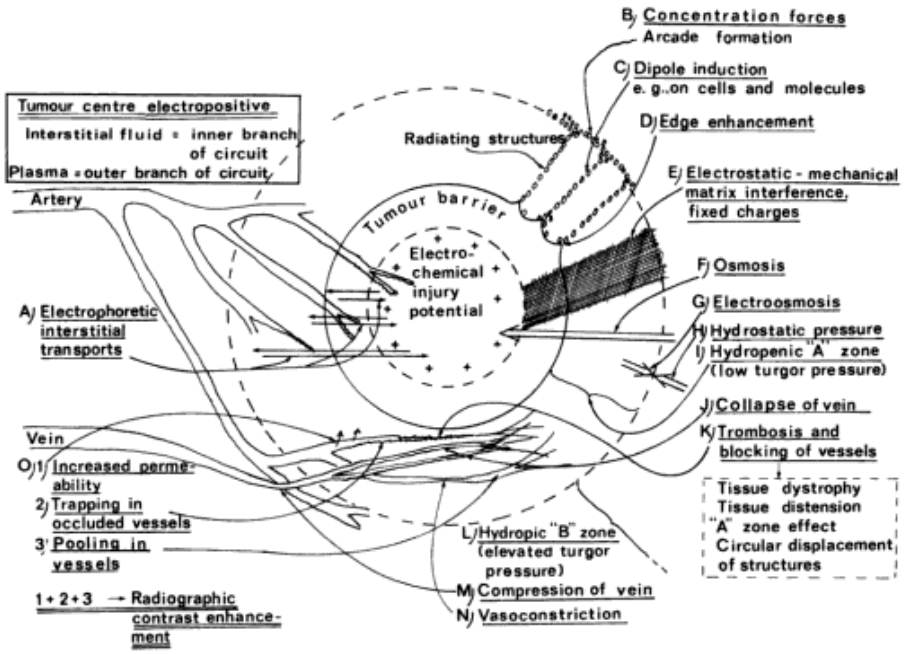

Fig. XV: 1 a. Degradation and polarization of a tumour in an electropositive phase, compared to the surrounding tissue: physiologic and structural effects. Closed circuit transports of ions and water are induced over a vascular-interstitial closed circuit. Dielectric material undergoes dipole induction. The resulting effects are modified by chemical concentration forces, volume-pressure changes in the matrix and circulatory changes. The driving electrical force of the degrading, energy-liberating, catabolic process of injury will fluctuate from anodic (*a*) into cathodic (*b*) phases, attenuating toward a state of equilibrium ("healing"), as is the case with all spontaneous reactions. The tumour barrier represents the outer permeable sieve of the tumour.

of the VICC as a mechanism for developing corona structures in the lung. In turn, appreciation of this mechanism will facilitate understanding in other chapters the *research based on the principle of BCEC systems*. To avoid repetition, several concepts treated in preceding chapters will be mentioned only in passing: the levelling of a *fluctuating ionic energy potential* between polarizing tissue regions *over BCEC channels*, and the necessity of *intersected redox steps* in the circuits.

Fig. XV: 1 is designed to illustrate the relation of the actual biokinetic events and the structural modifications they cause during (*a*) a phase of anodic polarization of a lung tumour and (*b*) during a phase of cathodic polarization.

The electropositive, degrading centre of the tumour (Fig. XV: 1 *a*) will induce *electroosmotic outward drift* of water, which will be modified by *inward osmotic transport of water*, entering the tumour. In the relatively electronegative surroundings of the tumour, outward electroosmotic transport of water will produce a radiolucent zone, the *hydropenic "A" zone*. The outward *displacement of water against a hydrostatic gradient* will then lead beyond the "A" zone to a radiodense, *hydropic "B" zone*.

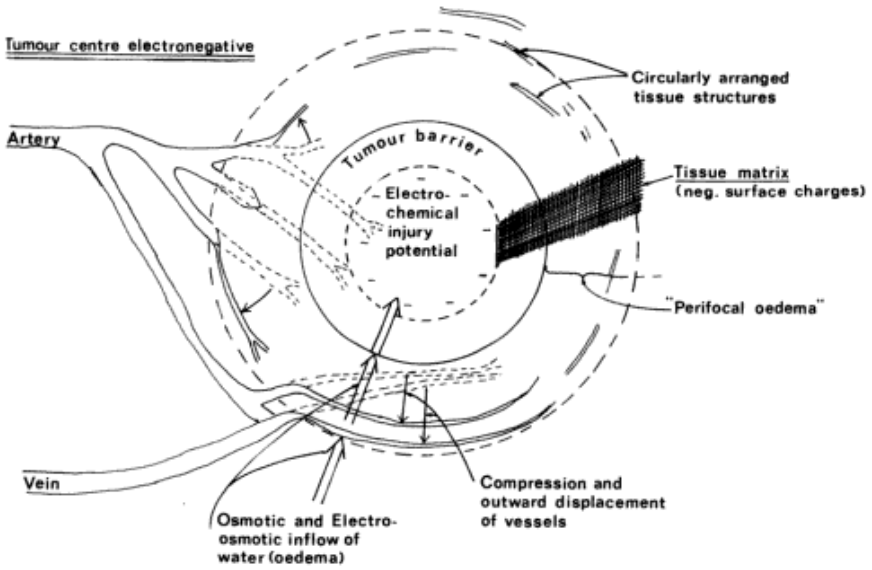

Fig. XV: 1 b. The tumour of Fig. XV: 1 *a*, but its polarity in relation to surrounding tissue has become reversed. For simplicity, only some effects on water transport have been indicated. Note that osmosis and electroosmosis now tend to move water toward the electronegative tumour, causing perifocal oedema, and local compression and outward displacement of structures in the peritumoural tissue such as vessels.

In the subsequent phase (Fig. XV: 1 *b*), when the injured tissue in the centre of the tumour becomes cathodic in relation to the surrounding normal tissue, water will disappear from the oedematous "B" zone tissue and move instead to the previously dry anodic tissue. Compression and peripheral dislocation of vessels around the tumour will result from this new movement of water. Osmotic inflow of water entering the degrading tissue will also be enhanced by electroosmotic inflow. The phase of liquefaction of the necrotic tissue now ensues.

Under the influence of an electric field, the permeability of capillaries also changes. Combined with changes in hydrostatic pressure, the electric field effects will modify local content of water in the various parts of the electric field. The *regional distribution of water* is therefore one factor which is *demonstrable by radiographically observable changes of radiopacity in pulmonary tissue*.

Simultaneously, radiographic differences of opacity are produced also by media other than water. *Dehydration around a lung tumour will increase compensatorily the amount of air* around the tumour, radiographically enhancing the radiolucency of this water-depleted zone.

Changes of radiographic opacity further may be produced by *electrophoretic transport of materials*, e.g., cellular debris and macromolecules, which may possess varying attenuation coefficients for x-rays.

Field-induced increase of capillary permeability can also explain the finding in angiography of the so-called *contrast enhancement effects* (page 176) around neoplasms, abscesses and haematomas (6, 9, 12). Contrast enhancement may also be increased by capillary thromboses, causing blindly ending vascular pockets, which in turn may lead to redistribution of blood flow.

Spontaneously occurring dystrophy of peritumoural tissue may follow thromboses in capillaries and other small vessels near a lesion in the lung during spontaneously or artificially polarized electropositive phases of the tissue. These electric effects may also enhance other structural changes in the peritumoural tissues, e.g., *circular displacement* of structures, and the development of "A" and "B" zones. During the electronegative phase these alterations are also enhanced by the development of perifocal oedema, local *destruction of red blood cells* and their laking of blood pigment (page 180).

Vascular narrowings and thromboses around a polarizing lung lesion can be demonstrated by densitometry. In 1946 Marchal (7) reported that *vascular pulsations are often decreased* on roentgen densitometry *around carcinomas of the lung*. He described this finding as a sign of malignancy. Now it appears likely that vascular narrowings and thromboses caused the decrease in observed pulsations, which in the present study have been found to develop spontaneously around polarizing tumours. These electric field effects on vessels are absent around nonpolarizing malignant tumours. They can, however, also be found around polarizing granulomas or benign tumours. It is the author's opinion, therefore, that the decreased pulsations around a tumour are not a valid radiologic sign of malignancy.

A VICC-system will also permit *electrophoretic transports of anions and cations* in interstitial spaces (Fig. XV: 1 *a*). Some of these charged units are nonpermeable, e.g., cells and macromolecules. These nonpermeable ions accumulate in the inner and outer parts of the "tumour barrier", leading to a charge separation not unlike a *Donnan distribution* of ions at a semipermeable membrane. This analogue includes also a net accumulation of charge, a "slipping plane" (see Fig. X: 8) outside a polarizing lesion. An excess of counterions is then trapped in the outer boundary of the tumour barrier and in adjacent surrounding tissue, partly as an effect of electrophoretic transports within the VICC. The "slipping plane" of an outwardly decreasing concentration of cations will even present an amount of charge which may exceed the charge of the central degrading process. This is in turn an effect of concentration (adsorption) forces. The resulting excess of charge of the periphery of such a centrally polarizing lesion does not represent thermodynamically available energy, except during the time of development of the "slipping plane".

The surface topography of a polarizing body influences structural development by modifying the induced electrical forces (page 95). This effect is explained as follows: when the surface of a charged body has protruding edges, so-called edge enhancement will develop in the electric field. The induced electric field will become stronger along imaginary "field lines" starting at the protrusions. These "lines" proceed straight in the tissue and may alter the configurations of existing structures. Movable dielectric compounds, e.g., cells, debris, macromolecules, etc., tend to orient themselves along the field lines. In this way, radiating structures will start to develop around any polarizing degrading tumour or granuloma provided with small protrusions on its surface. In vivo, such radiating structures may extend several cm into the tissue. This observation indicates that the electric field is produced within a closed electric circuit. Corresponding electrostatic fields can only influence material close to the charged body.

Experiments with electrically charged bodies and nonionic corpuscular grains (Chapter X) showed, on grounding the terminals, that the grains spontaneously produced several *free zones*, each several millimetres in diameter, *close to the terminals*. These zones were ascribed to the effects of concentration forces among the grains. After a potential difference was applied be-

tween the terminals, the grains formed *radiating structures by dipole induction* in the dielectric material. *Arches and arcades* were also produced as a consequence of interactions among concentration forces, edge enhancements and the applied electric field forces. *The modulation of edge enhancement by supporting matrices* could also be simulated (Fig. X: 4).

Thus far, we have based our discussion mainly on in vitro experiments of the effects of induced closed electric circuits on dielectrics, matrices and concentration forces. The corona structures in vivo are, however, also partly explained by closed circuit effects on transport of ions.

The closed circuit structural changes produced in vitro were also produced in vivo in dogs (Chapter XI) and demonstrated radiographically in vivo around tumours in patients (Chapters III, IV). The structural changes are not specific to the biologic type of tissue. As we will see shortly (Chapter XVI), closed circuit electric forces are also capable of inducing changes in the quality of the different components in a tissue. Such mechanisms, for example, are involved in qualitative differentiation of *radiating fibrous tissue structures*.

The radiating structures which are radiographically visible around lung tumours can be seen histologically to consist mainly of fibrotic material (3). This material contains both retractible hygroscopic fibres and collagen fibres, which are nonhygroscopic. Like ordinary scar tissue, radiating structures around a lung lesion may contract. The contraction explains the development of changes here described as *lamellae* and *retraction pockets* filled with pleural fluid (Chapter III). Local dehydration of tissue in the hydropenic zone has been interpreted as leading to the contraction of fibrotic radiating structures.

Electrochemical polarization within a BCEC will produce boundary phenomena at the inner and outer barriers of a centrally necrotizing tumour. Varying profiles of potential appear in and around a tumour, depending on the directions of potential gradients in the tissues and the amount and quality of transportable permeable and nonpermeable ions. In this way it can be understood that an autolytic electronegative phase is able to attract permeable cations, i.e., calcium and magnesium. Combination of these two ions with phosphate and carbonic ions in the autolytic tissue should eventually lead to the intratumoural *precipitation of calcium and magnesium phosphate and carbonate*, which are the main constituents in calcified, previously injured tissue. Healed granulomas of infectious origin in the lung commonly contain calcification, radiographically demonstrable in vivo. Pulmonary neoplasms occasionally contain foci of microcalcification, practically always invisible to clinical radiography but demonstrable histologically.

The presence of "A" and "B" zones, radiating structures, circular displacements of tissue structures, arches and arcades, lamellae and retraction pockets (Chapter III) consequently do not indicate that the underlying pathologic process is malignant or benign. Nonspecific processes of degradation, however, such as bleeding, necrosis, or infection, are very common in malignant tumours. These degrading processes may induce any one or several of the above-listed eight structural changes, which should always raise clinical suspicion of possible malignancy. As will be shown in the next chapter, the same reasoning also applies to the occurrence of pathological ductal and vascular structures.

The spontaneous accumulation of granulocytes in injured tissue and around the anode in experimental electrophoretic polarization of tissue has also been described (Chapter XIV). Because granulocytes are electronegative, in an electric field they must move to the anode. The proposed *vascular-interstitial closed circuit (VICC) can then explain the attraction of granulocytes as an electrophoretic process in a locally polarizing tissue*. This process is a further example of biological effects which can be produced in tissue under the influence of an activated BCEC. Already at relatively low levels of applied potential, e.g., 1–2 V, granulocytes are attracted extensively around the anode. When potential differences are relatively high, e.g., 5–10 V, the attracted granulocytes are to a large extent destroyed.

So-called chemotactic movement of white blood cells toward bacteria and necrotic cell material has traditionally been described as induced by "chemical signals" (1, 2, 5). Neither such signals nor the actual forces which stimulate the white cells to move have been adequately defined so far. It is here suggested that *the accumulation of granulocytes in acute tissue injury may be explained as electrophoretic transport of these electronegative cells to the region of an electropositive field in a BCEC*. Once the white blood cells have crossed the capillary membranes and entered the interstitial tissue spaces, the cells can hardly be anticipated to take the same way back to the blood stream after the polarity of the pathologic process is eventually reversed. This process is again an example of the influence of a matrix in the transformation of tissue. *In addition, a mechanism of interaction between blood flow and electric fields has been described, which is capable of accumulating granulocytes around an electronegative focus of a VICC*.

Whatever the further background mechanisms may be behind the local attraction of white blood cells out of the blood stream, it appears possible now to *utilize for therapy the proposed electrophoretic mechanisms of attraction*. Under fluoroscopic control, tiny platinum electrodes can easily be inserted percutaneously into

tissue. Electric potential differences of suitable magnitude, duration and polarity can then be applied between the electrodes to attract large numbers of white blood cells into the diseased region. Correspondingly, electrophoretic transport and destruction of microorganisms can be obtained against the anode (bacteria are reported to carry a surplus of electronegative charges, except *Spirochaeta pallida*, which is electropositive). Four weeks after artificial electrophoretic treatment of lung tissue in a dog (Chapter XIV), scars were found at the previous sites of the anode and cathode. "Inflammatory" reactions were evident in the surrounding tissue. Granulocytes at this time were not present; lymphocytes were seen at the previous sites of electropositive electrodes. Cavitation was also noted around the electrodes, residual from the mechanical effects of gas produced electrochemically from transformed tissue around the electrodes.

Because different chemical agents can carry a net surplus of electric charges, they may potentially be attracted to locally diseased tissue in order to affect beneficially a pathologic process. This proposed principle was initially tested experimentally with Evans blue (Chapter XIV). This compound accumulated, well visible, in vivo in the tissue around the cathode. The therapeutic possibilities of electrochemical attraction appear to warrant further study.

Morphologic changes have also been observed in *individual red blood cells* (page 180). In the electric field the transport of material over the cell membranes is evidently altered in different ways around the anode and cathode. The mechanisms of these changes seem to offer possibilities for studies of the function of cell membranes themselves.

The existence of a *BCEC allows ionic transports among adjacent polarizing tissue regions or organs. The BCEC may be involved in embryonic development of structures, including membranes and organ capsules.* How membrane structures develop is still poorly understood and has been a subject of intense discussions in the past (4, 8, 10, 11). Structures developing as polarization products over a BCEC offer a proposed mechanism which can easily be simulated in vivo.

These first 15 chapters have presented lines of discovery arising from the original radiologic observation of *corona structures around pulmonary tumours*. It is now apparent that most of these structures can be explained as *products of physicochemical polarization over a BCEC*. In fact, we seem here to have encountered a basic biokinetic mechanism of healing, structuring and function of tissue. The next chapter extends these lines of investigation by considering another organ which commonly contains tumours, the female breast.

References

1. Athens, J. W.: Blood: leucocytes. Ann. Rev. Physiol. 25: 195, 1963.
2. Boyden, S.: Cellular recognition of foreign matter. Int. Rev. Exp. Path. 2: 311, 1963.
3. Dahlgren, S., and Nordenström, B.: Transthoracic needle biopsy. Stockholm, Almqvist & Wiksell, 1966.
4. Edds, M. V., Jr., and Sweeny, P. R.: Chemical and morphological differentiation of the basement lamella. In: Rudnick, D. (ed.): Synthesis of molecular and cellular structure. Society for the Study of Development and Growth, Symposium 19. New York, Ronald Press, 1960, p. 111.
5. Harris, H.: Mobilization of defensive cells in inflammatory tissue. Bact. Rev. 24: 3, 1960.
6. Hatam, A., Bergvall, U., Levander, R., Larsson, S., and Lind, M.: Contrast medium enhancement with time in computer tomography. Differential diagnosis of intracranial lesions. Acta Radiol. Suppl. 346, 1975.
7. Marchal, M. M.: De l'enregistrement des pulsations invisibles du parenchyme pulmonaire ainsi que des pulsations cardiovasculaires par la cinédensigraphie. Arch. Mal. du Coeur 39: 345, 1946.
8. Nadol, J. B., Jr., Gibbins, J. R., and Porter, K. R.: A reinterpretation of the structure and development of the basement lamella: an ordered array of collagen in fish skin. Dev. Biol. 20: 304, 1969.
9. Nordenström, B., Ovenfors, C.-O., and Törnell, G.: Coronary angiography in 100 cases of ischemic heart disease. Radiology 78: 714, 1962.
10. Pierce, G. B., Jr., Beals, T. F., Ram, J. S., and Midgley, A. R., Jr.: Basement membranes. IV. Epithelial origin and immunologic cross reactions. Am. J. Pathol. 45: 929, 1964.
11. Porter, K. R.: Morphogenesis of connective tissue. In: Stephens, C. A. L., Jr., and Stanfield, A. B. (eds.): Cellular concepts in rheumatoid arthritis. Springfield, Ill., C. C. Thomas, 1966, p. 6.
12. Steinkoff, H., and Aviles, C. H.: Contrast enhancement response of intracranial neoplasms. Its validity for the differential diagnosis of tumours in CT. In: Lauksch, W., and Kazner, E. (eds.): Cranial computerized tomography. Berlin, Springer, 1976.

XVI.
Tissue transformations over BCEC in cancer of the breast

Radiographic demonstration in the lung of corona structures raises the important question of their possible demonstration in other organs. The variety of pathological conditions in which pulmonary corona structures appear indicates that these structural changes are not specific to particular pulmonary diseases. Nevertheless, the structural changes are sufficiently characteristic to suggest a specific type of reaction in tissue.

The lungs happen to be a favourable organ for radiologic examinations because air provides excellent contrast with intrapulmonary structures of radiographic water density. The female breast is a similarly favoured organ, except that fat is the component providing contrast with the structures of radiographic water density.

Our mammographic collection was therefore reviewed to see if tissue changes in the female breast, similar to those in lung, could be found. Even a brief review of a series of routine mammograms of breast carcinomas showed structural changes easily recognizable as similar to corona structures around lung lesions.

A number of structural changes around carcinomas of the breast have been well described, i.e., radiating structures, "skin thickening", skin retraction and microcalcifications (2, 6, 14, 19, 21, 30, 31, 38, 41, 42, 48, 49, 55, 60, 66, 67, 82). The presence of these particular structural alterations, however, lacks as yet a fully acceptable explanation. In part they are even interpreted incorrectly. Moreover, this chapter identifies additional radiographically visible structures around breast cancers, similar to those around lung cancers. These changes have, to the author's knowledge, not been described previously and consist of the *radiolucent "A" zone*, the *formation of arches and arcades* and the presence of *circularly arranged structures* in the tissue surrounding certain cancers. Also corresponding to the corona complex in the lung are *radiating fibrous structures*, *skin thickening* and *skin retraction*. We will therefore start to make an introductory identification of structural components of the *corona complex of the breast*. Their development and significance will be the subject of further analysis later in this chapter.

The mammographic images shown in this chapter are all made with compression technique, except for the xeroradiographs, which do not require compression.

Some of the radiographically demonstrable changes in tissue around a breast cancer are shown in Fig. XVI: 1. *Thin radiating structures* extend perpendicularly to the surface of the tumour, a "*radiolucent*" *zone* is

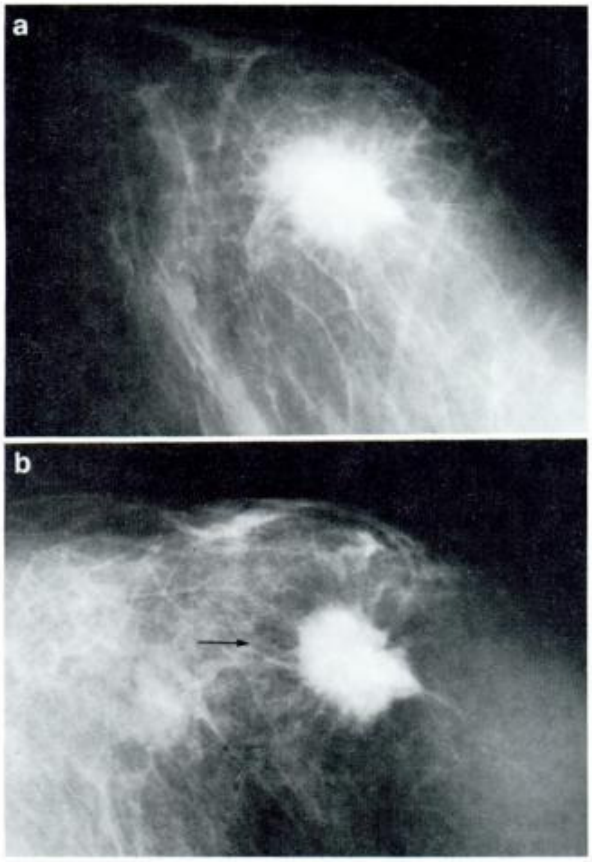

Fig. XVI: 1. Corona structures around a ductal breast carcinoma (62-year-old woman). (*a*) Thin radiating structures emerge from the surface of the tumour. (*b*) The same tumour (different exposure and projection) shows calcification, a peritumoural radiolucent "A" zone (dark "halo" around the tumour), so-called skin thickening (corresponding to a hydropic "B" zone), skin retraction and circularly arranged structures (arrow) at the periphery of the radiolucent "A" zone.

adjacent to the tumour and *calcification* is in the tumour. In many other cases scattered *microcalcifications* are present. These morphologic changes in cases of breast cancer are often accompanied by what is called *thickening and local retraction of the skin* (Fig. XVI: 1 *b*), which represents a special case of a "B" zone.

Some of the radiographically demonstrable coronal changes in breast cancer are also shown in the xeroradiograph in Fig. XVI: 2. A radiolucent zone 2–3 mm broad surrounds the carcinoma. Many thin radiating structures extend from the surface of the tumour into the surrounding breast tissue. The skin adjacent to the tumour also appears thickened and retracted toward the cancer. Some microcalcifications were also found histologically in this tumour after mastectomy.

As in the lung, corona structures in the breast accompany a wide variety of pathologic conditions. Different morphologic observations have been the subject of many fruitless attempts in the past to obtain "reliable" diagnostic or radiologic signs of malignancy, especially in lesions of the breast and lung. Radiographic demonstration of mammary microcalcifications, when present in groups of more than 10 particles, has been considered specific for malignancy (52). "Malignant microcalcifications" are, however, not specific for malignancy (14, 55). Microcalcifications remain useful in the mammographic analysis of possible carcinoma of the breast but their demonstration can no longer be regarded as pathognomonic of cancer.

Similar statements can in the author's opinion be made about many other diagnostic signs in current use, e.g., radiating fibrous structures, "skin thickening" and retraction, increased calibre of mammary vessels and local increase of temperature in the breast.

As long as the pathogenesis of these different changes in tissue remains unclear, attempts to evaluate their diagnostic and biologic significance will continue as gropings in the dark.

Final proofs of all possible correlations between the observed structural changes around tumours and their underlying pathophysiology are an impossibility to present at this time. Nevertheless, the author hopes that the evidence from breast lesions, just as from lung lesions, will focus the reader's attention on the ability of the concept of activated, biologically closed electric circuits (BCEC) to explain structural development in tissue injury and particularly around cancers.

Like lung cancers, cancers of the breast vary in their radiographic appearance. One or several of the radiographic signs shown in Figs. XVI: 1 and 2 may be absent. It is understandable that variations in the appearance of the tissue around breast tumours have for a long time been thought to depend on such factors as the structural or cellular type of the tumour.

Evidence to be presented in this chapter suggests that locally polarizing injuries inside a breast carcinoma act through a BCEC to induce morphologic changes both inside and outside the cancer. Such injuries are commonly encountered in tissue as nonspecific degrading processes, including inside malignant tumours. Degradation of tissue can be looked on as nonspecific, but it still must be regarded as a highly specific part of a biologic cycle. It represents the final phase of living cellular structures. Often it also represents the beginning of integration of material and energy into new structures.

BCEC systems enable morphology to be regarded as a manifestation of ongoing physiologic events. As long as morphology is regarded statically, our possibilities to understand morphologic variability will be stunted.

Electric polarization in breast tumours will now be described. Correlations will be shown to be possible between certain morphological changes of breast lesions and their electric properties.

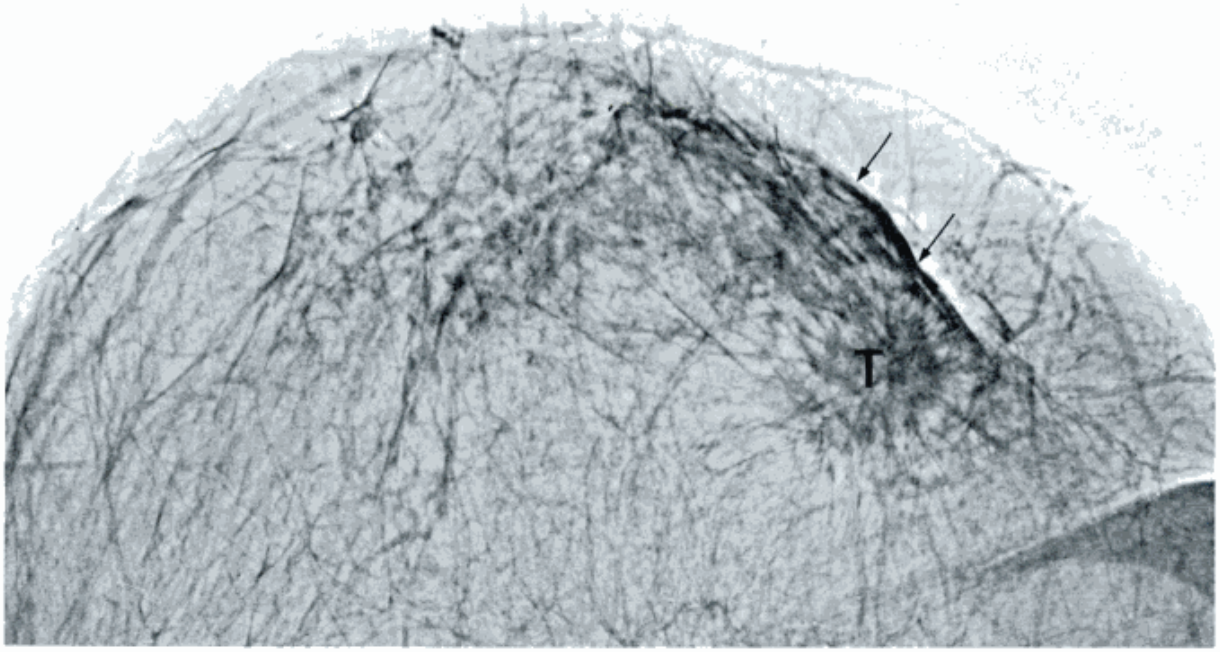

Fig. XVI: 2. Corona structures around a breast carcinoma (68-year-old woman, xeroradiograph exposed without compression of the breast). Radiating structures extend perpendicular to the surface of the tumour (*T*). A thin radiolucent "A" zone outlines the periphery of the tumour. Overlying skin is "thickened" and retracted (arrows).

A. Electric polarization in breast cancer

In the breast, as well as in the lung or any other tissue, any local injury, e.g., focal bleeding or necrosis, creates a source of liberation of energy. The developing physicochemical energy potential can easily be recognized by its electric potential (*"electric injury potential"*). By means of a second prerequisite, the proposed *biologically closed electric circuit* (*BCEC*), available energy will be released efficiently, permitting electrophoretic and electroosmotic transports between the injured and surrounding noninjured tissues.

Assuming these two important components, the development and appearance of many of the characteristic morphologic changes in and around breast tumours, like those of lung tumours, can be explained.

Breast tissue becomes injured in a variety of ways, e.g., trauma, focal necrosis from nutritional disturbances within a lesion, haemorrhage and infection.

Our first task will therefore be to explore the electric properties of tumours in the breast.

1. Case material and methods

Measurements of tissue profile of electric potential were made in mammary tumours of 16 consenting patients. These studies were performed in association with diagnostic biopsy and implantation of metal indicators immediately before surgical treatment. The aim was to search for possible spontaneous electric polarization in breast tumours similar to the findings in pulmonary tumours.

The same type of nonpolarizable, silver-silver chloride electrodes with potassium chloride bridges was used as in the final series of measurements of potential in lung tumours. The DC potential was measured between a grounded electrode in the subcutis of the ipsilateral shoulder and the "exploring" electrode, which was moved through the tumour and the adjacent tissue. Retraction of the exploring electrode was obtained by means of the driving mechanism of the recording instrument, the Grass chart writer (Model 7B, Polygraph, Grass Instrument Company, 101 Old Colony Avenue, Quincy, Mass. 02169, USA), in order to assure as good a correlation as possible between electrode position and tracing.

Localization of the tumours and introduction of the electrodes were made with a stereotaxic instrument previously developed by our group (16, 76) for biopsy of nonpalpable breast lesions (Fig. XVI: 3) (Manufactured by TRC AB, P.O. Box 50100, S-104 05 Stockholm, Sweden). This instrument allows the insertion of biopsy cannulas (75) to a predetermined place in the breast with a precision of ± 0.5 mm. After the x, y and z coordinates in the system were calculated, the elec-

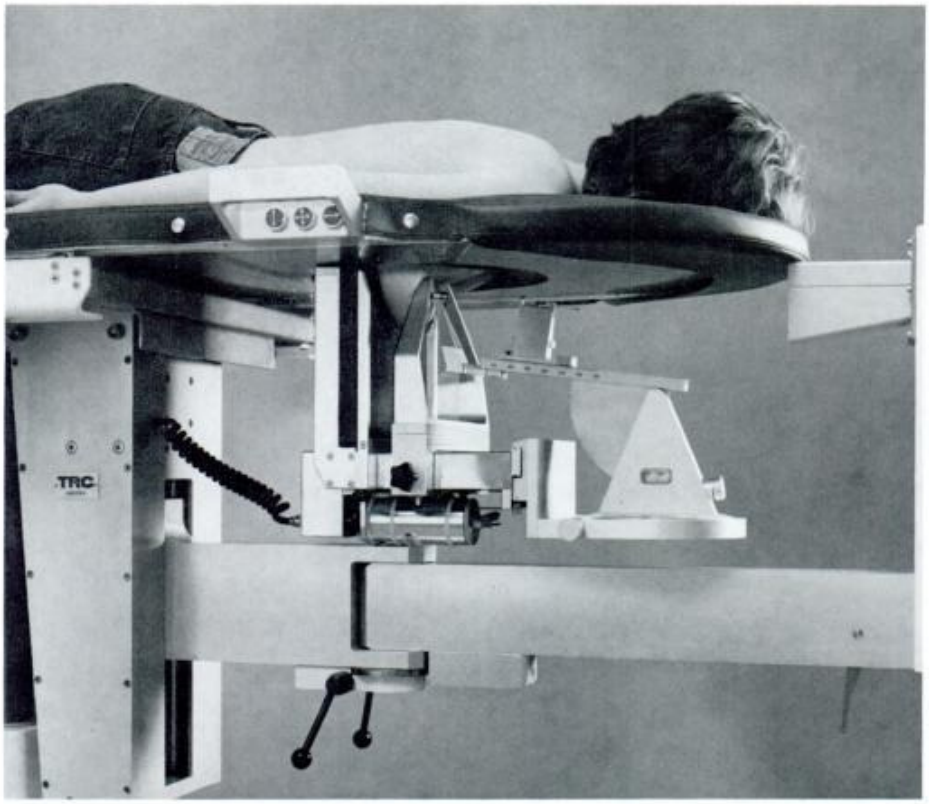

Fig. XVI:3. Stereotaxic radiographic unit developed for exact localization and percutaneous needle biopsy of nonpalpable breast lesions. The instrument was used in this study for the insertion of nonpolarizable electrodes to measure electric potentials of breast tumours and their surroundings in relation to a grounded reference electrode in the subcutis.

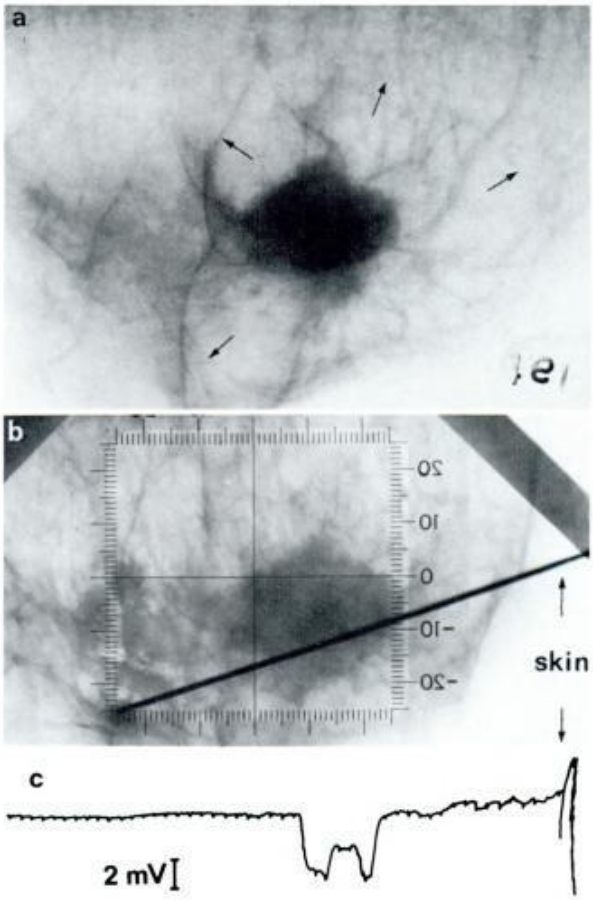

trode was inserted perpendicularly to the x-ray beam in the plane of the calculated z-coordinate. It was then possible stereoradiographically to document the position of the electrode in relation to the surfaces of a tumour and the skin.

2. Results

Electric potential measurements in 16 mammary carcinomas and surrounding tissues revealed characteristic patterns. Fig. XVI:4*a* shows the radiograph of a breast cancer. Small radiating structures extend more or less perpendicular to the surface of the tumour. In

Fig. XVI:4. Electric potential of a breast carcinoma. Mammography (*a*) shows an undifferentiated fibrous breast cancer, appearing as a lobulated tumour (64-year-old woman). Some radiating and thin "circular" structures (arrows) are evident at a distance from the cancer. (*b*) Position of the inserted electrode. (*c*) Potential tracing obtained as the electrode was evenly retracted. The cancer contains a W-shaped negative potential in relation to surrounding tissue. An ecg is superimposed on the tracing. Correlations between the measured potentials and specific anatomic sites were obtained by using the chart driving device to retract the electrode. Grounded reference electrode in the subcutis of the shoulder.

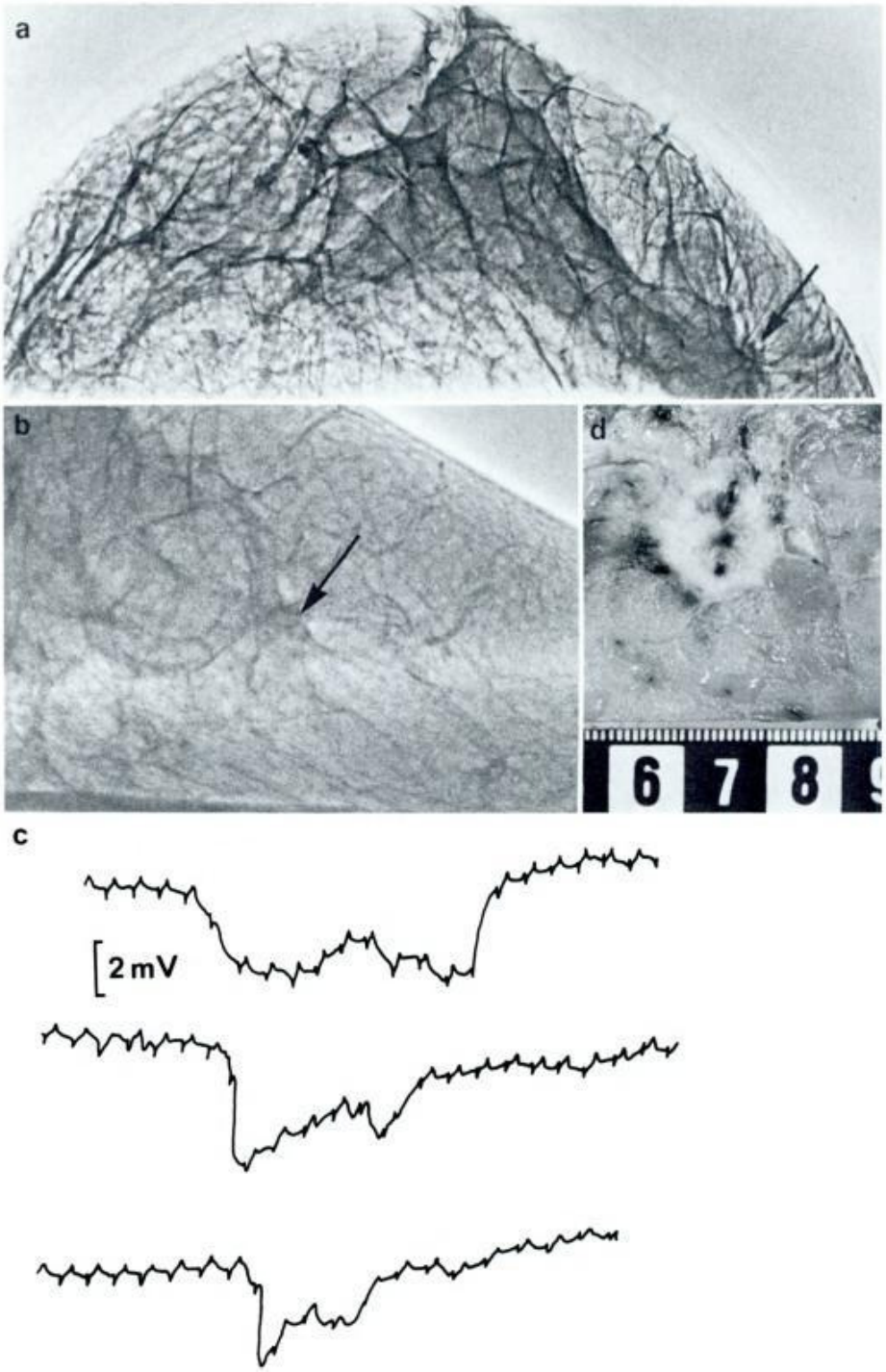

Fig. XVI: 5. Electric potential of a well differentiated ductal breast carcinoma (arrows) in a 57-year-old woman. (*a*) Craniocaudal, (*b*) lateral xeroradiographs. (*c*) Three tracings of potential through the tumour are shown. (*d*) The postoperative specimen contains three bleeding tracks, representing the three paths of the electrode. W-shaped potential inside the tumour is negative relative to surrounding tissue. Ecg is superimposed in the tracings. Grounded reference electrode in the subcutis of the shoulder.

the breast tissue around the tumour some thin structures (arrows) may also be seen in a circular arrangement. Such thin structural alterations are common around breast carcinomas, but to the knowledge of the author, have not been described previously (see also Figs. XVI: 1, 6, 14 *b*, 22 and 23).

The exploring electrode is shown in Fig. XVI: 4 *b* in the breast before it was slowly and evenly pulled out. Fig. XVI: 4 *c* shows the tracing of the tissue profile of electric potential as the needle was pulled out. The regular fine changes represent a superimposed ecg. Inside the tumour the tissue potential was 5 mV negative compared with the tissue surrounding the tumour. In the central part of the tumour the negative potential was elevated 2.5 mV, making the profile of potential look like a W.

The tracings usually vary depending on the course of the electrode passing through the tumour. For example, Fig. XVI: 5 (craniocaudal (*a*) and lateral (*b*) xeroradiographs) shows a carcinoma in the medial and

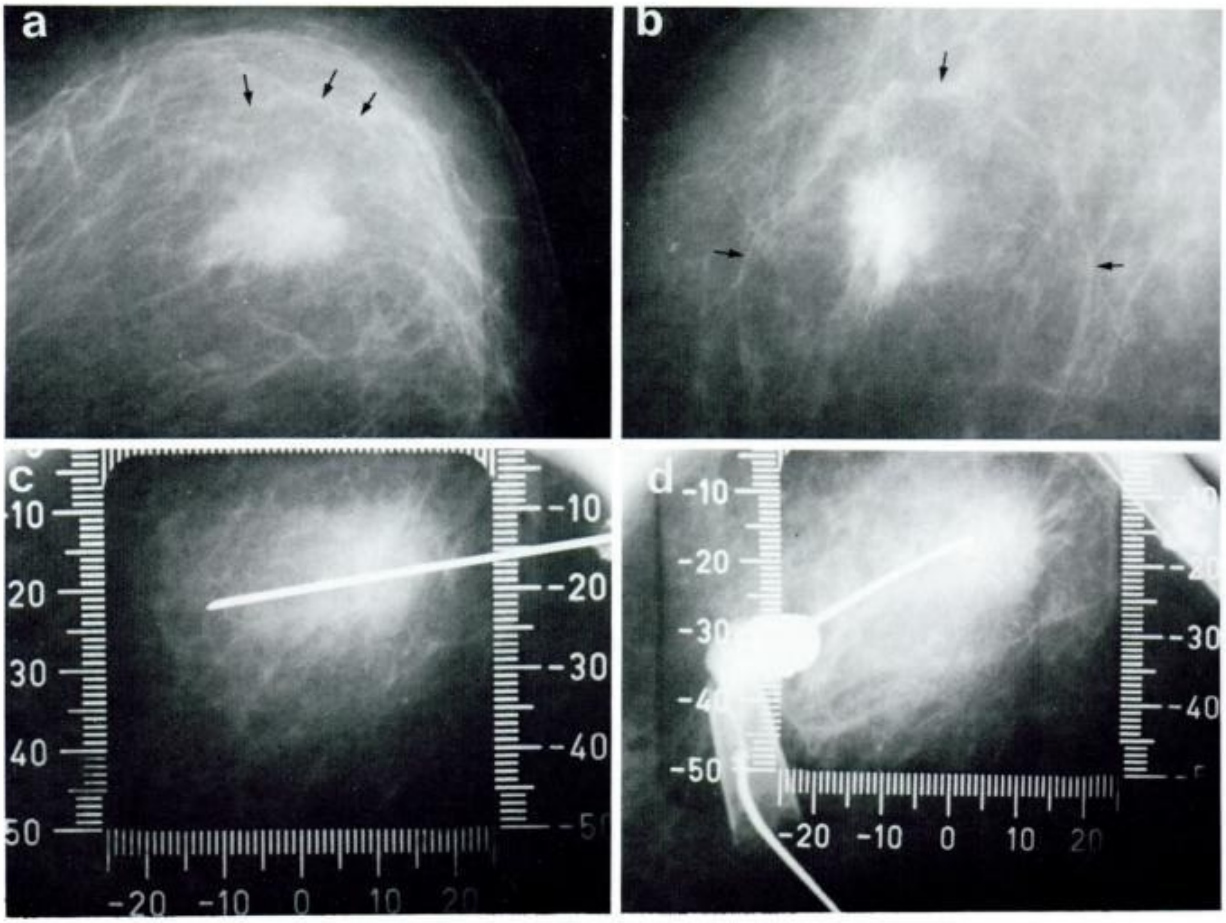

Fig. XVI: 6. Mammograms of ductal breast carcinoma (80-year-old woman, G. P.) before measurement of electric potential (see Fig. XVI: 7). (*a*) The tumour is surrounded by radiating structures. Arches are suggested (arrows). (*b*) Firm compression stretches these arches, which now form a circular structure (arrow). This result is possible because of the existence of peritumoural "B" zone oedema (see Table XVI: 2 for analysis of tissue water). (*c*) Lateral and (*d*) frontal views of electrode in relation to the cancer before one of the measurements of potential.

superior part of the left breast. No radiolucent zone is seen, but the cancer does show some irregular radiating structures. The postoperative specimen (*d*) demonstrates in the tumour some small haemorrhages, produced during the preoperative needle biopsy and insertion of the needle electrode. The three electric potential recordings in Fig. XVI: 5 *c* show negative W-shaped deflections as the electrode passed through the tumour. The amplitude of the superimposed ecg remained unchanged.

An explanation for the slightly different appearances of the three tracings in Fig. XVI: 5 *c* may be that a spontaneous redistribution of material has taken place inside the degrading tissue and between it and surrounding tissue. Small differences in the site of passage of the electrode will result in different profiles of potential, as illustrated in one patient with seven tracings of potential from slightly different parts of the tumour (Figs. XVI: 6 and 7). Two radiographs of this tumour (Fig. XVI: 6 *a*, *b*) reveal very thin radiating structures at its surface. Fig. XVI: 6 *a* shows some arches in the peritumoural tissue (arrows). On firmer compression of the breast a circular structure can be seen (Fig. XVI: 6 *b*, arrows), which is partly composed of stretched arches (left) and partly of a vessel (right). This effect is explained by the compression augmenting the local turgor pressure of peritumoural oedema. The oedema was verified after mastectomy (see Table XVI: 2).

Electric potential in this tumour (Fig. XVI: 7) was negative in relation to its surroundings. The first five tracings illustrate a W-shaped pattern, while the two bottom tracings show only a V-shaped pattern. This finding has been interpreted as follows: the interior of the tumour contained material with a surplus of negative charges. The centre of the tumour contained a smaller surplus of negative charges than the periphery. When the electrode traversed the central part, the

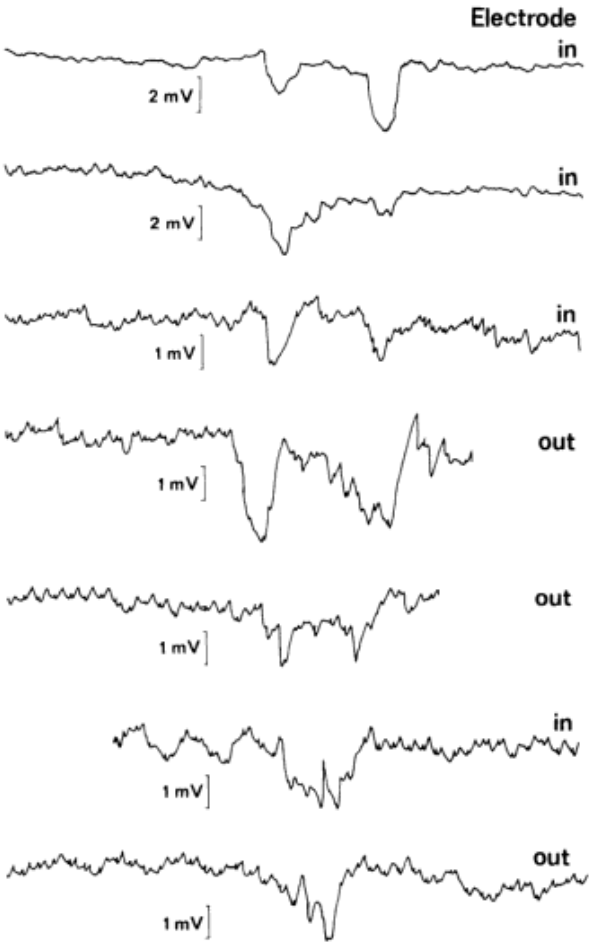

Fig. XVI:7. Seven tracings of electric potential through different parts of a breast carcinoma (same patient as in Fig. XVI:6, before mastectomy). Tracings of potential were obtained by inserting (in) or retracting (out) the exploring electrode. The upper five tracings show a W-shaped tissue profile of potential and the lowest two a V-shaped profile. These findings are interpreted as caused by an electronegative interior of the tumour but a less electronegative tumour centre (W-shape). When the electrode passed excentrically through the tumour only one negative deflection (V-shape) was obtained. Grounded reference electrode in the subcutis of the shoulder.

profile of potential was W-shaped, as seen in the five top tracings. When the electrode traversed only the periphery of the tumour, outside the less electronegative central region, only one negative deflection occurred. Its profile was V-shaped, as seen in the two bottom tracings.

To the right of the tracings of potential (Fig. XVI:7) is indicated whether the tracing was obtained on introducing (in) or retracting (out) the electrode. This distinction is important because slight changes of pressure in the agar–KCl bridge may produce artefacts. As is evident, the tracings were not influenced by this mechanical factor.

A *broad radiolucent zone* was seen around the mammary carcinoma shown in Fig. XVI:8. The tumour, which contains microcalcifications, is also surrounded by radiating structures. The irregular radiolucent zone is identified by its low x-ray attenuation, indicated by the less blackened areas. Below this zone, a less radiolucent zone is seen, which ordinarily might be described as "skin thickening". These zones resemble the previously described hydropenic "A" zone and hydropic "B" zone in the lung.

The exploring electrode is seen in Fig. XVI:8*b* after its introduction through the centre of the tumour. The tip of the electrode is now positioned in the "A" zone to the left of the tumour. Upon slow, even withdrawal of the electrode, a *positive potential complex* corresponded to the site of the tumour, as seen in Fig. XVI:8*c*.

The carcinoma shown in Fig. XVI:1 is also surrounded by a clearly visible radiolucent zone, approximately one cm wide. A positive potential was obtained in this tumour in relation to surrounding tissue, as seen in Fig. XVI:9.

The poorly differentiated ductal carcinoma seen in Fig. XVI:10*a* also showed a positive deflection of potential in relation to surrounding tissue (Fig. XVI:10*b*). This tumour is seen surrounded by a relatively broad, radiolucent "A" zone and a radiodense "B" zone. No radiating structures or circularly running structures are seen in the tissue surrounding this tumour. In these respects its radiographic appearance is rather similar to that of a pulmonary hamartoma.

The electronegative potentials of the breast cancers illustrated are representative of the findings for twelve of the patients. Three carcinomas and one fibroadenoma were electropositive in relation to surrounding tissue. The potential profiles can for most carcinomas be described as W- or M-shaped. The electric potential differences between maximum deflection in the tumour and surrounding tissue have varied by ±15 mV among different tumours. These studies of electric potential were performed on only one occasion in each patient before mastectomy. As in the lung, each of the breast tumours showed a characteristic and reproducible profile of potential, but, as also was found in lung tumours, no correlation was found with the histologic type of neoplasm.

3. Discussion and conclusions

Collecting a series of patients for studies of electric potential presents many difficulties. The material is therefore not randomized and is limited to 117 pulmonary lesions, mostly carcinomas (Chapter VI), and 16 mammary tumours, including 15 carcinomas. Trac-

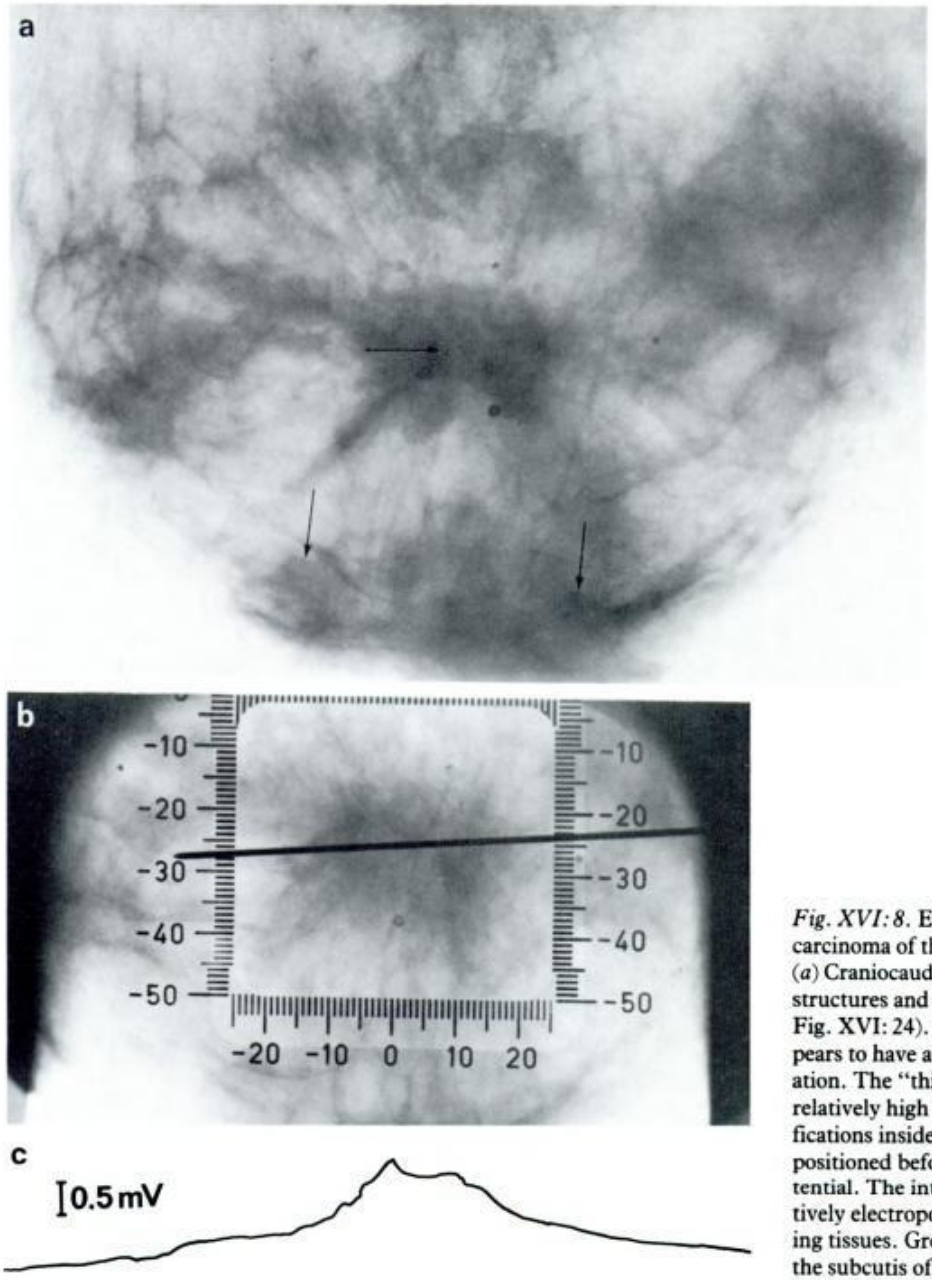

Fig. XVI: 8. Electropositive potential in a carcinoma of the breast (29-year-old woman). (*a*) Craniocaudal mammogram. Radiating structures and peritumoural arches (compare Fig. XVI: 24). Tissue around the tumour appears to have a relatively low x-ray attenuation. The "thickened" skin (↓ ↓) shows relatively high x-ray attenuation. Microcalcifications inside tumour (→). (*b*) Electrode positioned before retraction. (*c*) Profile of potential. The interior of the tumour was relatively electropositive in relation to surrounding tissues. Grounded reference electrode in the subcutis of the shoulder.

Fig. XVI: 9. Tracing of electric potential from a breast cancer in a 62-year-old woman (mammograms already shown in Fig. XVI: 1). Two positive deflections suggest an M-shape of potential profile through the tumour. Grounded reference electrode in the subcutis of the shoulder.

ings of tissue profile of electric potential of bronchogenic carcinomas sometimes showed a positive potential in relation to surrounding lung tissue (Chapter VI). Inside these tumours, the potential was often lower than at the surface of the tumour. The potential profile then resembled an M. In other cancers of the same histologic type a deep negative potential could be observed, sometimes with a W-shaped potential profile. In other cases no significant deflection of potential was found in relation to the surronding lung tissue. It is now apparent that electric potentials of mammary neoplasms in relation to their surrounding normal tissue are similar to those of pulmonary tumours. The

same types of M- and W-shaped profiles of potential have been encountered in breast as in lung.

Different tissues grow at different rates. A difference of electric potential should then arise as a "developmental potential" for abnormal tissue in relation to the "functional demand potential" of the surrounding normal tissue. If this reasoning is correct, then one might expect that a rapidly growing tumour should present a correspondingly large potential difference in relation to its surroundings. No such correlation has yet been observed. On the contrary, at least in the lung, any histologic or cytologic type of tumour may possess an electropositive, electronegative or zero potential. Potential measurements therefore can not be used for differential diagnosis. This finding has led to the hypothesis that a common denominator explaining the varying polarity and amplitude of tumour potentials in relation to surrounding tissue may be the degenerative phenomena often encountered in tumours.

A degrading process such as spontaneous necrosis or bleeding in lung tumours was earlier proposed to produce a nonspecific physicochemical potential of tissue injury. The degrading of tissue in this view represents a dynamic process. Depending on the phase of the degradation, electric polarization may be either positive or negative. Regardless of polarity, BCEC channels will aid in levelling of the potential difference. We do not know how intensely the potential difference is being generated or how efficiently the levelling of the potential gradient takes place. The magnitude of measured potential difference is therefore of little importance. We can only conclude that potential differences can be recognized between tissue regions, a prerequisite for electrogenic transport of material between the two tissue regions. The total amount of transported material does depend, however, on the factor of time. Transports of considerable amounts of material are therefore possible at relatively low gradients if the transports take place over long periods of time.

Three of the breast carcinomas (Figs. XVI: 8, 9, 10) showed positive potentials in relation to the grounded subcutaneous electrode. Two of these cancers also contained calcium deposits, which makes it likely that they (at least for some time) contained regions which were relatively electronegative, thereby attracting cations such as calcium over a closed electric circuit.

Next we will study the morphologic appearances of altered tissue around and inside breast tumours. These alterations will then be compared with the appearances and biokinetic background of similar structures around pulmonary carcinomas. Finally we will show also that many of the structural changes in the breast, like those in the lung, can be produced by experimental polarization of tissues over closed electric circuits.

Fig. XVI: 10. Electropositive potential in a poorly differentiated ductal breast carcinoma (55-year-old woman). (*a*) Mammogram. The tumour is surrounded by an irregularly radiolucent "A" zone (dark halo) which in turn is surrounded by a radiodense "B" zone (white halo). No calcifications, radiating structures or circularly displaced structures are seen in this case. (*b*) Tracing of potential through the tumour, which had a relatively electropositive centre. Ecg is superimposed on tracing. Grounded reference electrode in the subcutis of the shoulder.

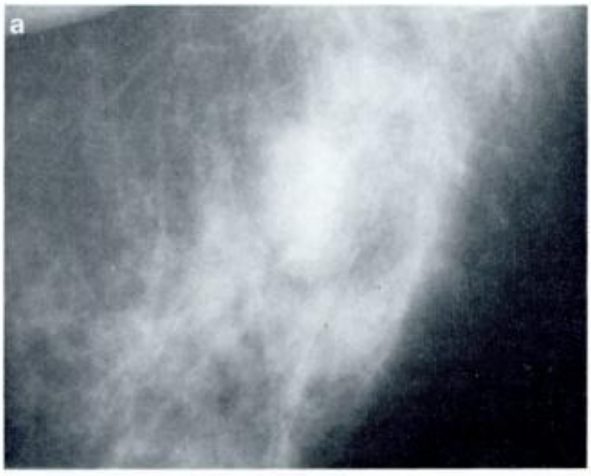

B. Radiating structures

Infiltrating duct cell carcinomas accompanied by fibrosis represent the most common type of breast cancer. The fibrosis commonly appears in a stellate radiating pattern about these tumours. Although these so-called scirrhous carcinomas represent 70 per cent of all mammary carcinomas (55), variably pronounced perifocal fibrosis is also seen around other types of breast carcinomas, i.e., around medullary and lobular carcinomas. On the other hand, any kind of breast cancer, including infiltrating duct cell carcinoma, may appear without fibrosis.

Fibrosis in breast, moreover, is also observed around nodular mammary tuberculosis (65). Sclerosing adenosis, fibroadenomas, chronic mastitis and healed fat necrosis are other benign conditions presenting "productive" fibrosis (55).

Fibrosis around mammary carcinomas is, therefore, a common but nonspecific feature of the disease. The validity of the term "scirrhous carcinoma" as a characteristic feature of a specific type of carcinoma is therefore questionable.

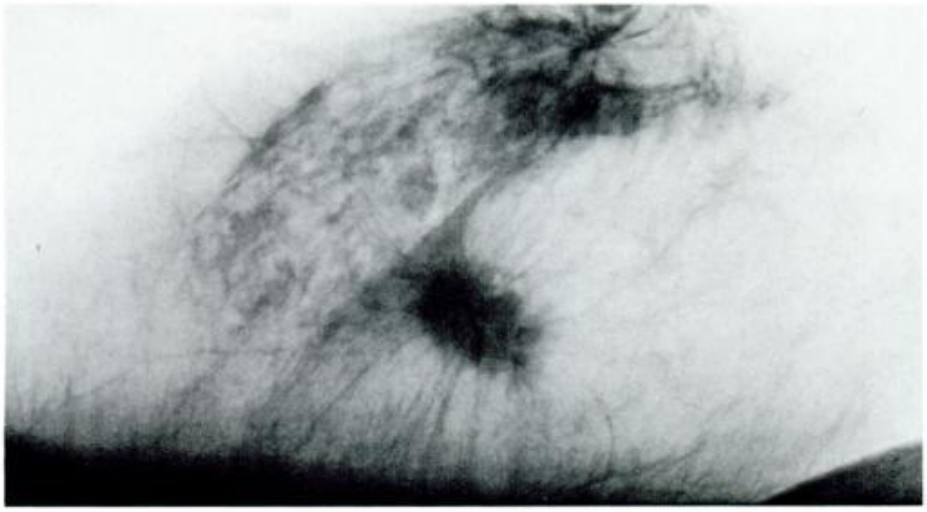

Fig. XVI: 11. Variable straightness of radiating structures. Mammograms of ductal breast carcinoma (66-year-old woman). Thin radiating structures extend several cm into the tissue surrounding the tumour. The curved shapes of some of these structures appear "relaxed".

The literature on breast cancer calls radiating structures by many names: spicules, cicatricial changes, sunburst changes, stellate strands, productive fibrosis, scirrhous changes, spiculae, spiculations, perifocal striate fibrosis, striae, productive fibrosis or hyalinosis, long radiating fibrous tentacles, "Krebsfüsse", dendritic margins and shaggy margins.

Histochemically, radiating structures are characterized by fibrotic material containing elastin, collagen and hyaline components (7, 20, 49). Near the tumour the radiating structures may contain blood vessels, extravascular white blood corpuscles and also carcinomatous cells, often arranged in rows. Sometimes cancer cells are found isolated, forming discontinuous streaks or islands within the fibrotic tissue. Distant from the tumour the peripheral parts of radiating structures usually contain only fibrotic material without other cell or tissue components. For simplicity and accuracy of description, then, the nonspecific term *radiating structures* is here introduced as a term suitable for radiographic descriptions.

Radiating structures are believed by some examiners to represent a reaction of tissue in the surroundings of a tumour and are therefore not to be regarded as produced directly by tumour growth (20, 55, 68). The opinion has also been put forward that radiating scar tissue (and adenosis) is involved as a primary factor in the growth of breast cancer (6, 12, 34, 48, 67, 86) but this has been doubted by McDivitt, et al. (27), Haagensen (47), Fenoglio and Lattes (33), Tremblay (90) and Azzopardi (9).

An antigen-antibody reaction is also considered to take place around tumours (15, 25), leading to the formation of fibrin and hyaline as well as an amyloid-like substance (89).

Radiating structures do not develop from the tumour itself, according to von Albertini (3), but more likely arise from the surrounding tissue. Gullino and Grantham (46), Underwood (91), Douglas and Shivas (28), on the other hand, all consider the fibrotic reaction to be an expression of the biologic characteristics of the tumour tissue.

The radiating structures around mammary carcinomas also contain a considerable amount of elastic tissue, compared with normal breast (28).

In an excellent monograph on mammography, Hoeffken and Lanyi (55) state: "The stellate fibrous extensions are called cancer feet. This is not actual tumor tissue but rather a fibrotic reaction of adjoining breast tissue to the carcinoma. With extensive spread, however, even these fibrotic hyalinized bonds of connective tissue may be invaded by tumor cells. So far there is no satisfactory explanation why such a desmoplastic response is elicited by scirrhous carcinoma or what may be the histochemical or immunologic cause for this response."

The topography of the radiating structures around mammary carcinomas is of considerable interest. The structures are usually arranged in approximately straight lines perpendicular to the tumour surface. They may proceed far out into the surrounding breast tissue regardless of its basic structural arrangement. In this respect the radiating structures around certain breast tumours behave the same as the radiating structures around certain lung lesions.

Thin radiating structures of variable straightness in two examples (Figs. XVI: 11, 12) can be seen extending several cm into the tissue around a breast carcinoma. The radiating structures in Fig. XVI: 11 are not quite straight and therefore appear "relaxed". In other cases the radiating structures appear straight, as if they were contracted. The carcinoma in Fig. XVI: 12 shows an abundance of radiating structures which are moderately straight. Peripherally they are thin. Close to the

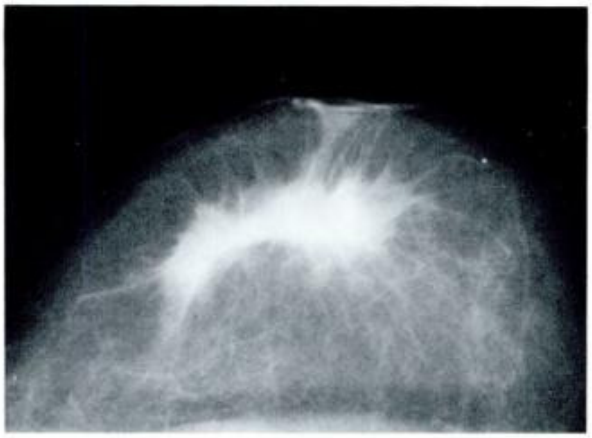

Fig. XVI: 12. Variable thickness of radiating structures. Mammogram of a breast carcinoma (68-year-old woman). Many radiating structures are moderately straight. Some, however, look as if they retract the nipple and adjacent "thickened" skin. They are thicker at the tumour than in their peripheral parts.

tumour they are broad. Some of them appear to be retracting a locally "thickened" part of the skin.

Discussion

Radiating structures around mammary and pulmonary lesions appear similar. They develop more or less perpendicular to the surface of the lesions, regardless of the topography of the underlying normal structures.

The presence of positive or negative polarization in relation to the tissue surrounding a breast tumour should, as in the lung, be able to produce radiating structures over the proposed biologically closed electric circuits. Electrophoretic and electroosmotic transports over a BCEC should build up the radiating structures from different available interstitial ions, nonorganized cells, debris and macromolecules, all of which then should be oriented under the influence of the electric field. In this connection it should be pointed out that ionic material will not be the only material to move in the field. Nonpolar molecules which are not organized may be transported, where the field gradient is steep, as a result of dipole induction. Furthermore, we may also anticipate that stored energy of ionars and ergonars (Chapter XIII) in a closed electric circuit may convert their energy and interact with surrounding material. Thus, radiating structures should develop under the influence of positive as well as negative polarization of a lesion. It is possible or even likely that the physicochemical potential of a degrading tissue must change its polarity to develop "complete" radiating structures. These structures represent, in the author's opinion, a special type of scar tissue induced by tumoural degradation and liberation of energy over a BCEC. This hypothesis also explains why radiating structures sometimes include islands of electrophoretically "displaced" tumour cells close to the tumour surface but not in the distal parts of the radiating structures. The "ebb and flow" of moving anions and cations over a BCEC is probably a necessity for the development of all kinds of scar tissue. Proofs for the validity of this theory will be presented later in this chapter. They conform with the biokinetic explanation offered for corresponding structural changes in the lung.

C. Peritumoural changes of radiopacity

In the breast, as in the lung, a radiolucent "A" zone (a decrease in x-ray absorption around a lesion) can sometimes be seen, sometimes not. Peripheral to the "A" zone, a "B" zone can also sometimes be seen as a region of increased x-ray absorption. The "B" zone in

Fig. XVI: 13. Skin thickening near a moderately well differentiated adenocarcinoma of the breast (65-year-old woman). Mammography shows two adjoining tumours (*T*), surrounded by radiating structures and an "A" zone. To the left of the nipple, indicated by a small metal ball, are two elongated opacities (*B*). These so-called skin thickenings correspond to hydropic "B" zones in the lung (see page 20) and retraction pockets in the pleura (see page 35). Two thick radiating structures (*L*) extend to the "B" zones. The radiating structures correspond to lamellae in the lung producing pleural retraction pockets.

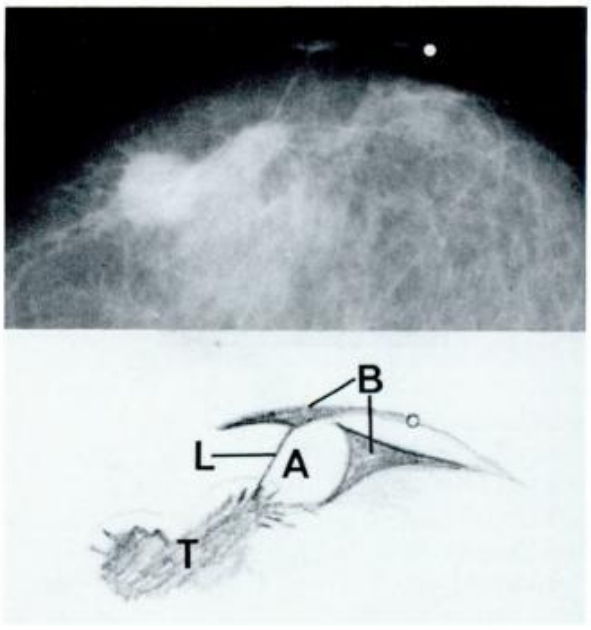

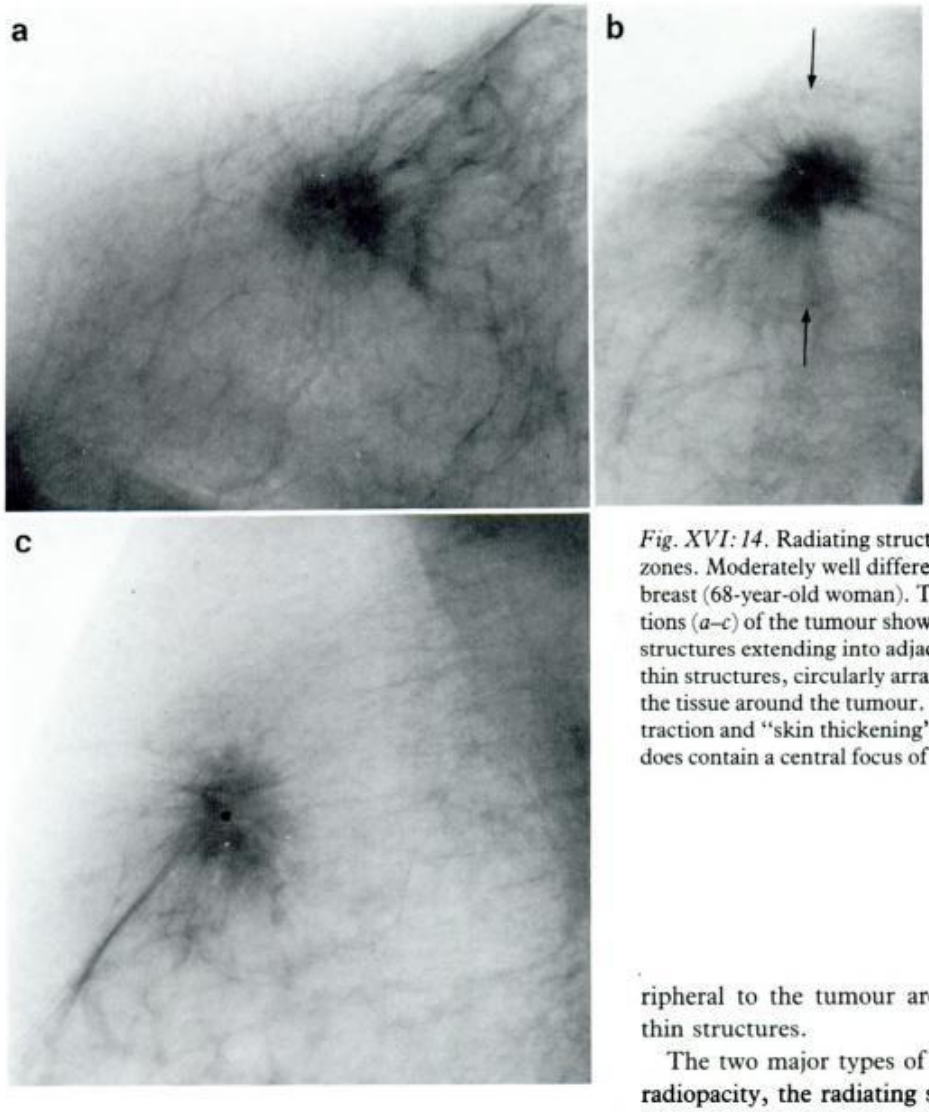

Fig. XVI: 14. Radiating structures without "A" or "B" zones. Moderately well differentiated adenocarcinoma of the breast (68-year-old woman). Three mammographic projections (*a–c*) of the tumour show numerous thin radiating structures extending into adjacent breast tissue. Additional thin structures, circularly arranged (arrows), can be seen in the tissue around the tumour. "A" and "B" zones, skin retraction and "skin thickening" are not present. The tumour does contain a central focus of calcification.

the breast appears most often, as will be seen, as local "skin thickening".

The radiologic appearance of a radiolucent "A" and a radiopaque "B" zone, seen as "skin thickening" near breast carcinomas, has already been illustrated (Figs. XVI: 1, 2, 8, 12). Fibroadenomas may also present with a radiolucent "A" zone surrounded by a radiopaque "B" zone. Fig. XVI: 13 illustrates two adjoining mammary carcinomas surrounded by radiating structures and a radiolucent "A" zone. Two distal opacities, which would usually be called "skin thickening", appear similar to the hydropic "B" zone close to the pleura in the lung. Two thick structures lead to each of the densities. The left one is similar to a lamella (see Fig. III: 27) in the lung.

The carcinoma in Fig. XVI: 14 *a–c* is quite different. Although the radiating structures appear numerous and similar, "A" and "B" zones are not evident. "Skin thickening" and skin retraction are absent. Peripheral to the tumour are some circularly arranged thin structures.

The two major types of peritumoural alterations of radiopacity, the radiating structures on one hand and "A" and "B" zones on the other, have been brought together in this section in order to discuss possible causes of the presence of an "A" and "B" zone around some tumours and their absence around others, seemingly without regard to the presence or absence of radiating structures.

Discussion

Previous chapters on the "A" zones in the lung consider the possibility of local electroosmotic displacement of water. Air in alveoli should replace some of the tissue water in the "A" zone. Such a redistribution of water and air will appear radiographically as a local "halo" or "emphysema", although no "real" tissue is necessarily lost.

The radiolucent "A" zone and radiopaque "B" zone around mammary carcinomas are from this radiologic point of view very similar in appearance to the changes around certain lung lesions.

The question is now: What is the background for

the development of a perifocal, radiolucent zone around a breast cancer? Oedema around the edge of a breast lesion produces increased absorption of x-rays. The only possible material in the breast which can produce a decrease in x-ray absorption is fat. The appearance of a mammographic "A" zone might then be explained as in the lung except on the basis of fat as the low contrast medium.

A general increase of fluid in the breast tissue is known to produce enlargement and hardening of the breast, e.g., in the premenstrual phase, or when regional lymph nodes are blocked, or when cardiac pump failure increases venous and lymphatic pressures in the breast. The nipple stiffens, enlarges and increases in prominence. The skin appears thickened (55).

The possibility of relative outward movement of water from a positively charged surface has been treated in Chapter IX.

In the periphery of the lung, a tumour produces stasis by blocking the flow of pleural and interstitial fluid from the periphery to the hilar lymph nodes. In the breast, lymph flows mainly from the areola and deep glandular tissues to the axilla and along perforating intercostal vessels to the anterior intercostal and retrosternal lymph nodes.

The lymphatics of the breast intercommunicate extensively, so local stasis of lymph does not usually characterize mammary tumours. Nevertheless, local stasis may be found occasionally, especially in the vicinity of the areola. The hydropenic adipose tissue around the tumour may then appear radiolucent because fat attenuates x-rays rather poorly. The development of a hydropic "B" zone (cutaneous oedema) beyond the hydropenic "A" zone, on the other hand, requires balancing hydrostatic counterpressure. This counterpressure appears to develop most easily in the region close to the skin and the areola. In addition, the local forces causing cutaneous retraction over a breast tumour will contribute to the localization of the "B" zone water (see also Section J).

Electric closed circuit interstitial transport of material other than water should also be possible between a tumour and surrounding tissue. A corpuscular "B" zone may develop in this way either in the skin as another type of "skin thickening" or anywhere else in the tissues surrounding the tumour as a radiopaque structure oriented parallel to the tumour surface. Special cases of such corpuscular "B" zones will be described in Sections F–I and T.

As in the lung, a radiolucent "A" zone around a breast tumour may also result from extensive capillary thromboses. The electric field induces thromboses near the tumour during its electropositive polarization. The thromboses can then be anticipated to produce dystrophic changes of peritumoural tissues near the tumour, yielding a structurally depleted region ("halo" or "A" zone) around the tumour. Circular arrangement of vessels and development of septa in the surrounding tissue are part of the process and will be further treated in Section H. Interphase phenomena between "A" and "B" zones will be discussed in Section I.

In the next two sections it will be shown that electric polarization can partially separate fat and water in an experimental analogue to a BCEC system. In this way we may find an experimental explanation of the perifocal density changes seen as a radiolucent "A" zone and a radiopaque "B" zone. We will then see how a negative or positive polarization of a lesion will influence the perifocal density changes in different but predictable ways (Section F).

D. Fat-water distribution: closed circuit effects and radiographic appearance in vitro

The influence of an electrically closed and activated circuit on a mixture of fat and water was next investigated. The development of differences of radiographic attenuation and changes in electric conductivity in a fat-water medium is illustrated in the following in vitro experiment.

An aluminium ball was fixed with glue to the centre of the bottom of a glass jar (Fig. XVI: 15). The inside of the periphery of the jar was covered with thin aluminium foil. Both the central ball and the peripheral foil were connected with a cable to the electrical charging device previously described for demonstrating the orientation of corpuscular elements in an electrostatic field (page 94). A layer 2 cm deep of a mixture of 25 % lanolin and water was poured into the jar. Initially, both terminals were grounded. A radiograph taken of the jar with mammographic technique (Fig. XVI: 15 *a*) reveals the fluid is fairly homogeneous.

Some hours after the application of a 500 V positive potential on the central ball against the grounded periphery, a new radiograph was exposed (Fig. XVI: 15 *b*). One broad radiolucent zone, about 10 mm wide (*x*), surrounds the ball while another zone, even more radiolucent and about 2 mm thick (*y*), is seen at the surface of the ball. When the contents of the jar were poured out, a thick solid layer of white fat stuck to the ball (Fig. XVI: 15 *c*). This layer constituted most of the broad radiolucent zone. An inner layer, 2 mm thick, corresponded to the inner radiolucent zone.

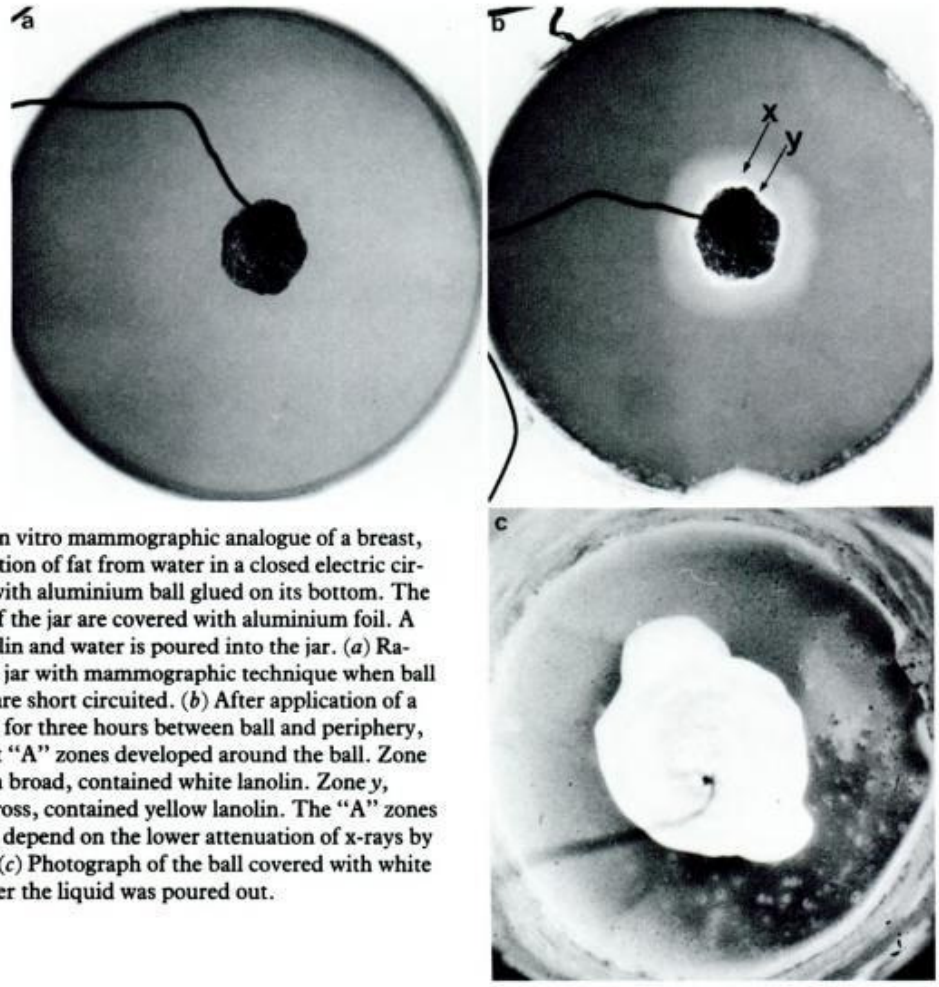

Fig. XVI: 15. In vitro mammographic analogue of a breast, showing separation of fat from water in a closed electric circuit. Glass jar with aluminium ball glued on its bottom. The internal walls of the jar are covered with aluminium foil. A mixture of lanolin and water is poured into the jar. (*a*) Radiograph of the jar with mammographic technique when ball and periphery are short circuited. (*b*) After application of a 500 V potential for three hours between ball and periphery, two radiolucent "A" zones developed around the ball. Zone *x*, about 10 mm broad, contained white lanolin. Zone *y*, about 2 mm across, contained yellow lanolin. The "A" zones in this example depend on the lower attenuation of x-rays by fat than water. (*c*) Photograph of the ball covered with white firm lanolin after the liquid was poured out.

Discussion

The use of a 500 volt potential across the liquid is certainly not very close to physiological conditions. Appreciable separation of fat and water could, however, also be accomplished after a couple of days with a 2 volt potential between the electrodes. Electrophoretic movements will of course take place also at low voltages and current densities. The time for the development of structures secondary to polarization of a tumour can therefore not be neglected. It is known that the development of a tumour takes months or even several years.

For the lungs, radiologic recognition of structure depends to a large extent on the differences between air and lung tissue in the absorption of x-rays. Lung tissue behaves radiographically like water. For the breast, the radiographic role of fat corresponds to that of air in the lungs. Most of the fat in the breast is already structured and would therefore not be expected to move like air in the lungs. Nevertheless, the development of an "A" zone around a breast tumour should be possible by the movement of water in relation to immovable fat. Lipid, moreover, is not immovable, as will be shown in Sections F and J, which show lipid of fat cells mobilized, transported and accumulated within a closed circuit applied both in vitro and in vivo.

First, however, we will illustrate, in a simplified way, the principle for conductivity changes which have been encountered in vivo in the lung (Fig. VI: 21) and in the breast on passing an exploring electrode through "A" and "B" zones.

E. Local alteration of conductivity in a fat-water mixture

When an exploring electrode passed from the "A" zone into the "B" zone (see Fig. VI: 21) in the tracings of electric potential in lung, occasionally the superim-

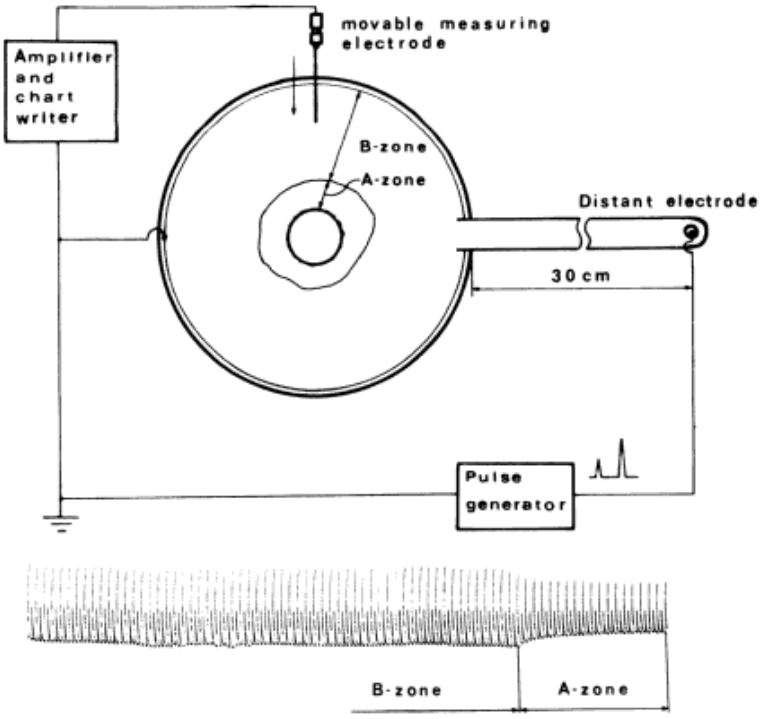

Fig. XVI: 16. In vitro electric analogue of a breast: "electrocardiographic" amplitude differed in the "A" and "B" zones. Same experimental arrangement as shown in Fig. XVI: 15 for separation of lanolin and water. A pulse generator produced small and large pulses, simulating an "ecg". Electric potential was traced at different positions between the periphery of the jar and a movable electrode. When the electrode entered the "A" zone, the amplitude of the pulses decreased suddenly. Electrophoretically produced changes of conductivity can explain this decrease. Compare also ecg changes in the "A" zone in the lung (Fig. XVI: 21) in an example of increased "A" zone conductivity.

posed ecg signal suddenly changed its amplitude. The subcutaneous reference electrode was grounded in these studies.

An explanation for this phenomenon may be that local electrical conductivity has changed due to redistribution of water, ions and molecules surrounding the lesion. The electrophoretic study of water and lanolin lends itself to ready illustration of this possibility. The experiment was arranged as seen in the upper part of Fig. XVI: 16.

A "halo" or "A" zone was electrophoretically produced around the central aluminium ball in the glass jar containing 25% lanolin and water (see Fig. XVI: 15). A measuring electrode was fixed to a mechanical holder on a motor driven bar, which allowed the electrode to be moved evenly in the lanolin-water mixture as the tip moved from the periphery toward the surface of the ball. An ecg-simulating double signal was produced by a pulse generator at the distant electrode in the water-lanolin solution. This signal was received by the exploring electrode, relative to the grounded periphery of the jar, as seen charted in the lower part of Fig. XVI: 16. When the electrode was moved evenly from the periphery to the ball, the amplitude of the induced signal suddenly decreased, as expected, when the "A" zone was entered.

Similarly in the human lung, when an electrode explores through the radiologically observed "A" and "B" zones, sudden change of amplitude of the ecg at the zonal interface can therefore be explained as indicating that the water-ion composition and concentration differ in the two zones (page 64).

In the experiment with water-lanolin, the amplitude decreased in the "A" zone, where concentration of fat was high.

In patients with mammary carcinomas, amplitude of a superimposed ecg should be expected to decrease when the exploring electrode passes through an "A" zone around the tumour. In the present small series of breast cancers this finding has, however, not yet been verified. Electrode sites were not selected with the intention of obtaining a superimposed, disturbing ecg signal.

"A" zone conductivity in the lung is not like that predicted for the breast. The pulmonary hydropenic "A" zone showed a higher ecg amplitude than the hydropic "B" zone, a result indicating in the lung higher conductivity in the "A" than in the "B" zone.

Discussion

These experiments show in vitro radiographic and electrophysiologic correlations with the relative separation of fat and water in a closed electric circuit. These results also form indirect evidence for the existence of biologically closed electric circuits.

The fat phase in the experiment with lanolin and water has a lower conductivity than the water phase. The water phase obviously carries a higher ionic con-

centration. Tissue structures of the "A" zone in the lung, on the other hand, present relatively higher conductivity than those of the "B" zone. This seeming paradox is possible despite the fact that the amount of poorly conducting air must be increased in the "A" zone, as judged by its low attenuation of x-rays. If the "A" zone is produced mainly by electroosmotic outflow of water to the "B" zone, ionic concentration in the "A" zone nevertheless may be relatively higher in the conducting channels of the "A" zone than in the "B" zone.

The influence of an activated closed electric circuit on distribution of water and fat in dog and human fat tissue is presented in quantitative and histologic experiments in the next section.

F. Closed circuit transports of fat and water in mammary fat tissue

Material for these in vitro and in vivo experiments was mammary fat tissue from four dogs and recent mastectomy specimens from two women.

1. Method

The cylindrical mid-part of a 10 ml plastic syringe was used as an electrophoretic chamber. This chamber was filled to a length of about 2.5 cm with an excised piece of mammary fat tissue. The flat ends of two plungers were each covered with platinum foil connected to a platinum cable and then inserted into the cylinder. As the plungers were pushed toward each other, air was allowed to escape through small perforations in each plunger. In this way most of the air could be removed from the specimen of tissue.

The cables were then connected to an electric DC-power unit and a milliampere meter. Photographs and soft tissue radiographs were taken of the specimen before and after different time periods of electrophoretic treatment. The sample was later frozen in the cylinder, which was divided lengthwise in two. One of these parts was saved for histological sections. The other part was subdivided crosswise in two approximately equal parts, one from the electropositive and one from the electronegative field. Water and fat content was determined from each of these parts as follows:

After careful weighing, the samples were placed in 110°C temperature for 16 hours, by which time all water had evaporated. Dry weight was then determined. Chloroform was used to dissolve the fat material. By filtering the solution, nonsoluble material was then removed. This step was repeated three times. The fat content was finally determined by weighing after evaporation of the chloroform.

In vivo electrophoresis was also performed in four dogs under general anaesthesia with sodium pentobarbital. A needle was used to place two platinum string electrodes through the skin into subcutaneous mammary fat tissue. After DC voltage was applied between the strings, photographs of the experimental area were taken at intervals. Blocks of tissue were later excised around the electrodes for histologic sections and determinations of fat and water content.

2. Results

Human breast fat (Fig. XVI: 17) is seen in an electrophoretic chamber photographed during application of 40 volts between the electrodes and after 3, 28 and 31 coulombs (*a–c*, respectively). A zone of fat-like material, semitransparent to light and of yellow to yellow-red colour, developed near the anode to the right and moved to the left, increasing in thickness. This "liquid fat" is seen in the radiograph (Fig. XVI: 17 *e*) as a zone of decreased x-ray attenuation. In addition to the broad "liquid fat" zone, some thin light zones also developed in the specimen. The latter became bright yellow to brown in the cathodic region. Fig. XVI: 17 *d* illustrates histologic sections (haematoxylin-eosin) through a "liquid fat" zone. Empty "fat pools" with membrane-like delineation of some dark material have developed across the specimen. The pools, surrounded on both sides by small and partly flat cells of fat, contained "liquid fat", which partly flowed from the specimen when it was removed from the electrophoretic chamber. The fat zone never crossed the mid-part of the chamber in its move from the anode toward the cathode, even though electrophoresis was continued for 20 and 40 days in two of the experiments. The experiments showed little current after the first day, mainly because of anodic dehydration and gas production at the surfaces of the electrodes.

In vivo electrophoresis in a dog under sodium pentobarbital anaesthesia is shown in Fig. XVI: 18 *a*. Two platinum string electrodes were inserted percutaneously in the breast fat so that they were 20 mm apart. At 10 volts, a mean current of 32 μA crossed the tissue for two hours, corresponding to 0.23 coulombs. By this time the tissue around the cathode was red and swollen. Tissue around the anode was seen to be grey and shrunken. A clear fluid came out on the skin around the cathode. This fluid could be sucked up with a syringe through a thin cannula. When the content was blown out on a water surface, some of the material floated in droplets as liquid fat.

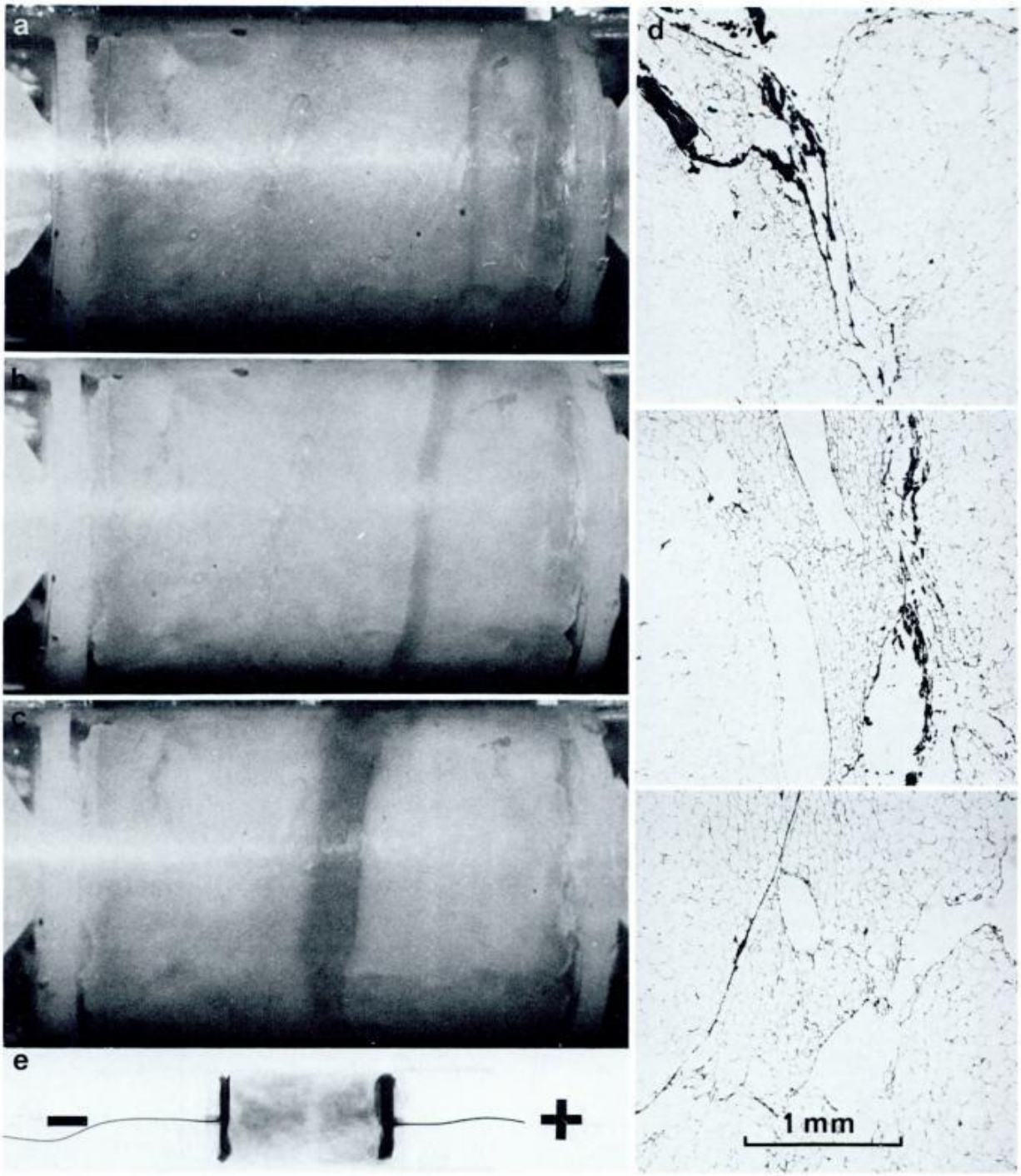

Fig. XVI: 17. Movement of human breast fat in an electrophoretic chamber between two platinum electrodes. Cathode to the left, anode to the right. 40 V electrode potential difference. (*a*) 3 coulombs, 2 min. (*b*) 28 coulombs, 14 min. (*c*) 31 coulombs, 205 min. The relative increase in time depends on electroosmotic, anodic dehydration. A fat zone moves from right to left, increasing in thickness (photographs *a–c*). Soft tissue radiograph *e* shows the low x-ray attenuation of fat as a white band, which corresponds to the fat zone in *c*. (*d*) A composite of three photomicrographs of the fat zone shows empty pools surrounded by small fat cells and dark material. Electronegative breast fat moves initially from cathode to anode, but reverses its transport under the influence of the strong acidity in the anodic field, which makes the fat in the anodic field electropositive. An equilibrium is then obtained between electronegative and electropositive fat in the midpart of the electrophoretic chamber.

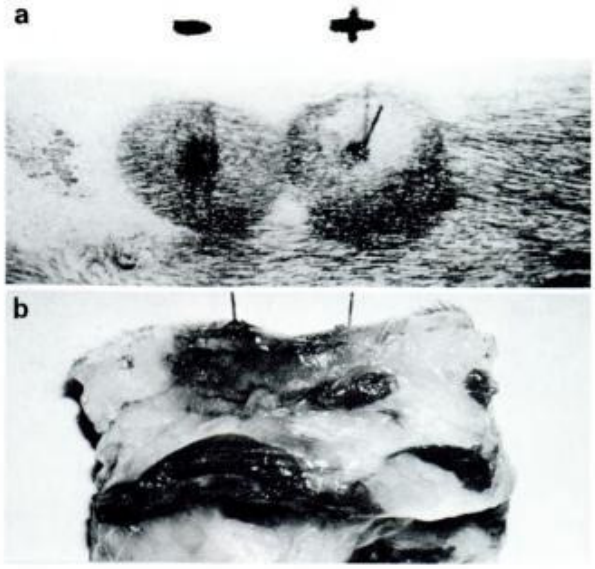

Fig. XVI: 18. In vivo movement of mammary fat and water under the influence of direct electric current. (*a*) Platinum string electrodes were introduced percutaneously into the subcutaneous breast fat tissue of an anaesthetized dog. After 23 coulombs at 10 V the tissue was swollen with leaking liquid fat around the cathode (−) and shrunken around the anode (+). (*b*) A section through the tissue between the electrodes shows red-brown, swollen tissue around the cathode and grey-white, shrunken tissue around the anode. In vivo, fat moves as shown in vitro (Fig. XVI: 17). An undisturbed supply of tissue fluid makes the cathodic tissue swell due to electroosmotic transport of water.

After incision with a knife, the tissue around the cathode appeared brown-red and flabby, while around the anode the tissues were grey and dry (Fig. XVI: 18 *b*).

The distribution of water and fat in the cathodic and anodic halves of each specimen was analyzed (Table XVI: 1).

The table includes electrophoretic results from in vitro and in vivo experiments on dog breast fat tissue and from in vitro results on human breast fat tissue. The figures in Table XVI: 1 show the per cent of water and fat based on weight in relation to the total fresh weight of the cathodic and anodic halves of each specimen.

Water was more concentrated in the cathodic piece of tissue and fat more concentrated in the anodic piece. This tendency was the same in in vitro specimens of dog and human breast fat, and also in in vivo dog skin and dog breast fat.

Control determinations of fat not subjected to elec-

Table XVI: 1. *Electroosmosis and fat electrophoresis: per cent of water and fat in the cathodic and anodic halves of experimental specimens*

Specimen		Cathodic half	Anodic half	Untreated controls		Voltage, time, amount of current
Breast fat (dog)	H_2O	7.9	6.1			10 V, 48 hours
in vitro	Fat	73.5	79.1			= 173 coulombs
	H_2O+fat	81.4	85.2			
	Residual	18.6	14.8			
Breast fat (dog)	H_2O	26.4	21.7			10 V, 2 hours
in vivo	Fat	49.8	58.1			= 23 coulombs
	H_2O+fat	76.2	79.8			
	Residual	23.8	20.2			
Breast skin (dog)	H_2O	49.1	41.4			10 V, 2 hours
in vivo	Fat	16.7	32.7			= 23 coulombs
	H_2O+fat	65.8	74.1			
	Residual	34.2	25.9			
Breast fat (dog)	H_2O			9.3	8.8	No current
in vitro	Fat			63.2	63.6	
	H_2O+fat			72.5	72.5	
	Residual			27.5	27.5	
Breast fat (human)	H_2O	13.4	11.5			10 V, 48 hours
in vitro	Fat	79.4	82.6			= 180 coulombs
	H_2O+fat	92.8	94.1			
	Residual	7.2	5.9			
Breast fat (human)	H_2O			6.2		No current
in vitro	Fat			83.8		
	H_2O+fat			90.0		
	Residual			10.0		

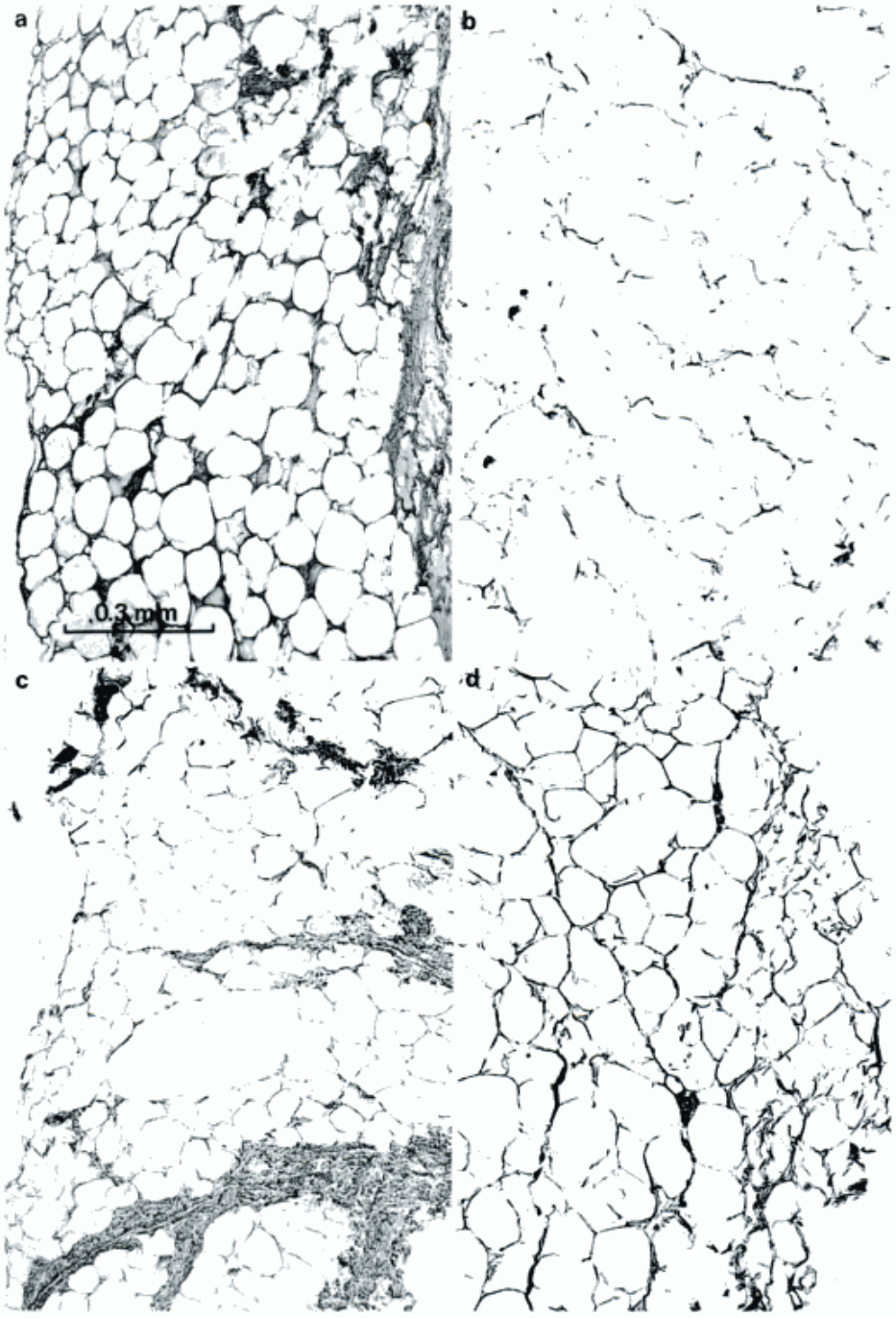

Fig. XVI: 19. Histologic appearance of dog mammary fat tissue after influence of direct current and formalin fixation, which dehydrates the tissue. (*a*) In vivo and (*c*) in vitro cathodic tissues after electrophoresis show shrunken and small fat cells and occasional interstitial fat droplets. (*b*) In vivo and (*d*) in vitro anodic tissues from the same experiments show large, distended or ruptured fat cells. In addition, Fig. *d* shows small fat cells to the right where the tissue has been in direct contact with the anode. Irregular, granulated material with a forked appearance in *c* represents early stages of formation of cathodic fibrous tissue (see Sections K–M).

tric current showed only slight differences of fat and water content in two dog mammary fat specimens of equal weight. The sum of fat and water in the control specimens was 72.5% of the total weight, meaning that the residual "matrix" in the dog fat tissue was 27.5% of the total fresh weight.

The sum of fat plus water in the electrophoretic experiments revealed larger "matrix residual" in the tissues of the specimens of the cathodic fields than of the anode. These relations of fat, water and residual "matrix" material become particularly interesting when the morphologic structures are studied histologically.

Histologic sections (after formalin fixation) are shown from in vivo (*a* and *b*) and in vitro (*c* and *d*) electrophoresis of dog breast fat tissue in Fig. XVI: 19. Figs. *a* and *c* show fat cells from cathodic parts, *b* and *d* from anodic parts of the specimens. Cathodic cells appeared small and shrunken, especially near the cathode. Stainable fat droplets could also be seen in the

cathodic interstitial tissue outside cells. Fat cells around the anode (*b*, *d*) appeared large and distended, except for the material immediately adjacent to the anode, where the cells were small (*d*). It also looks as if many cells or cell groups ruptured in the main part of the anodic tissue to an extent which is not observed in fat tissue from the cathodic tissue.

Appearing like forked dendrites in Fig. XVI: 19*c* is some irregularly structured, granular material. Some similar material parallel to the cathodic surface of the specimen is also seen in Fig. XVI: 19*a*. These materials are interpreted to be early stages of transformation of blood.

3. Discussion and conclusions

The electrophoretic transport of water and fat in these experiments is complex and not easily explained. The conditions are also not exactly the same in the in vivo and in vitro experiments. We will first consider the in vitro studies:

It is evident that fat leaves cells in the cathodic region through cell membranes which look intact to light microscopic examination. The exit of fat from cells leaves them appearing small and shrunken. Cathodic fat droplets appear in the interstitium and later disappear from this region, which becomes pale and yellow. This fat moves toward the anode, shown by the analytic results, indicating that a bulk portion of original fat material should be electronegative. Interstitially migrating electronegative fat then seems to enter disrupted anodic fat cells, explaining their distension and the many sites of what appear to be broken cell membranes. The fat-water ratio in the cathodic region is now lowered due to loss of fat and some increase in electroosmotic accumulation of water, according to the analyses. The ratio is correspondingly elevated in the anodic region due to inflow of electronegative fat and electroosmotic loss of water.

What happens, then? How can the liquid fat zone in vitro be explained? It starts to develop close to the anode and moves, increasing in thickness, toward the mid-part of the electrophoretic chamber.

Anodic fat in vitro and in vivo very close to the anode must leave the fat cells, because these cells appear small. Electronegative fat may partly be electrophoretically pulled out and become mixed with cathodic fat, which is moving toward the anode. This explanation may account for the presence of freely floating fat at the surface of the anode both in in vivo and in vitro experiments. Fat disappears from the anode probably because the anodic acidity, by proton liberation, should change the polarity of fat from electronegative to electropositive. Some of this fat can be expected to move in the direction of the cathode. As the electrophoresis continues, electropositive fat will be produced and follow the migration and diffusion of protons. This transport will leave anodic, small cells behind and produce a zone of increasing distension of fat cells where cathodic electronegative and anodic electropositive fat meet. The increasing thickness of this zone, the distinct anodic and cathodic interphases, and tendency to reach the mid-part of the electric field can be explained in this way. When the turgor pressure is high enough, fat cells will rupture and develop fat pools surrounded by small cathodic and small anodic fat cells. This explanation of fat movement in the electrophoretic chamber is in agreement with the well known fact that a compound can change its polarity according to surrounding acidity or alkalinity.

Water can easily disappear in vivo by electroosmosis from the anodic region, which therefore shrinks. Water will accumulate in the cathodic region, which therefore swells. These phenomena are influenced by the local circulatory conditions in vivo, which are eliminated in vitro. Otherwise, the same explanation holds for movements of fat and water in vivo as for the movements in vitro.

Both the in vitro and in vivo specimens had to be fixed in formalin for the preparation of the histologic examination. During the process of fixation, formalin dehydrates tissue specimens. This dehydration is the reason for the seemingly contradictory appearance of swollen cathodic tissue in vivo and shrunken cathodic fat cells without distended spaces in the histologic preparations.

G. Peritumoural water and fat, including atrophy of fat adjacent to electronegative mammary carcinomas

Considerable difficulties arise on attempting to determine the regional amount of tissue water in the lung. Opening the pleural space, for instance, alters distension of tissue and vascular perfusion, thereby radically changing the local distribution of tissue water.

In the breast, a subcutaneous and therefore relatively accessible organ, the conditions are more favourable than in the lung for such determinations. Attempts were therefore made to determine the relative amounts of water and fat in the breast tissue around different breast tumours as soon as possible after mastectomy.

Sites for excision of pieces of tissue around breast tumours were selected by means of pre- and postoperative mammography. Pieces of reference tissue were also excised from regions of breast tissue appearing

grossly normal. The different samples were weighed and dried at a temperature of 110°C for 16 hours. The per cent loss in weight was then determined as an expression of the relative water content. The relative fat content was then determined by dissolving the material in chloroform, and filtering and drying the fat-chloroform solution, as previously described (Section F).

Specimens from two patients will be illustrated. The mammary carcinoma of an 80-year-old patient (G. P., Fig. XVI: 6) presented with thin radiating structures and also circular tissue structures about 2–4 cm from the surface of the tumour. The radiographic density of the tissue inside compared to outside the circular structures did not show any definite differences. The electric potential of the tumour was also measured (Fig. XVI: 7).

Fig. XVI: 20 *a* shows a radiograph of a breast carcinoma of a 60-year-old woman (B. S.). Some radiating structures are evident at the tumour surface. As in the previous case, the surrounding tissue shows circularly arranged structures but no radiographically clear change in density, such as an "A" zone. The profile of electric potential of this tumour showed intratumoural negative deflections (Fig. XVI: 20 *b*) similar to the previous case. The potential in the centre of the tumour was relatively elevated and even slightly positive in relation to the surrounding breast tissue.

After operative removal of these two carcinomas, their relative content of fat and water was determined both close to the tumour and in distant parts of the same breast, which presumably were not affected by the tumour (Table XVI: 2).

Each of the two subjects shows the same findings: relatively higher water content and lower fat content close to the electronegative tumour compared to distant normal fat tissue of the breast. The fat-water ratio close to the two electronegative tumours is similar to the ratios produced in vitro in human mammary fat tissue and in vitro and in vivo in dog mammary fat tissue adjacent to the electronegative electrode (Section F).

Table XVI: 2. *Fat–water content of breast tissue around two electronegative mammary carcinomas: per cent of total weight*

Patient		Close to tumour surface	Peripheral tissue
G. P.	H_2O	14.1	7.2
(Figs.			7.6
XVI: 6, 7)	Fat	77.2	86.9
			86.4
B. S.	H_2O	8.8	5.2
(Fig.		11.8	5.4
XVI: 20)	Fat	71.2	78.2
		72.8	78.6

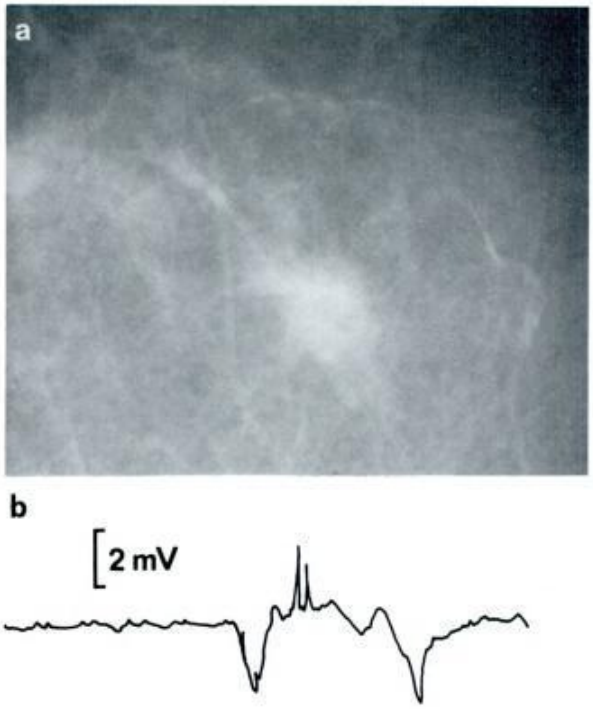

Fig. XVI: 20. Breast carcinoma analysed for fat and water content of surrounding mammary tissue. (*a*) Mammogram, 60-year-old woman (B. S.). Radiating and circular structures are evident without clearly visible changes of density such as an "A" zone. (*b*) Profile of electric potential through the tumour shows negative potential in the periphery of the tumour and slight elevation of potential in the centre, compared to surrounding noncancerous breast tissue. Ecg is superimposed on the tracing. Table XVI: 2 shows analysis of fat and water from this breast (B. S.).

These two cases may therefore represent the appearance of *true perifocal oedema* around electronegative tumours.

As was shown in the studies of electric potential, a mammary tumour may also present an elevated electric potential in relation to surrounding tissue. In these cases a clear radiolucent "A" zone could be seen. Fat–water analyses of the tissues around such tumours should presumably show a relatively lower content of water and higher content of fat. As of this writing, however, no such specimens have yet been analyzed.

Discussion and conclusions

Water moves in an electric field from the electropositive to the electronegative side, while fat moves in the opposite direction, according to the analysis of in vitro

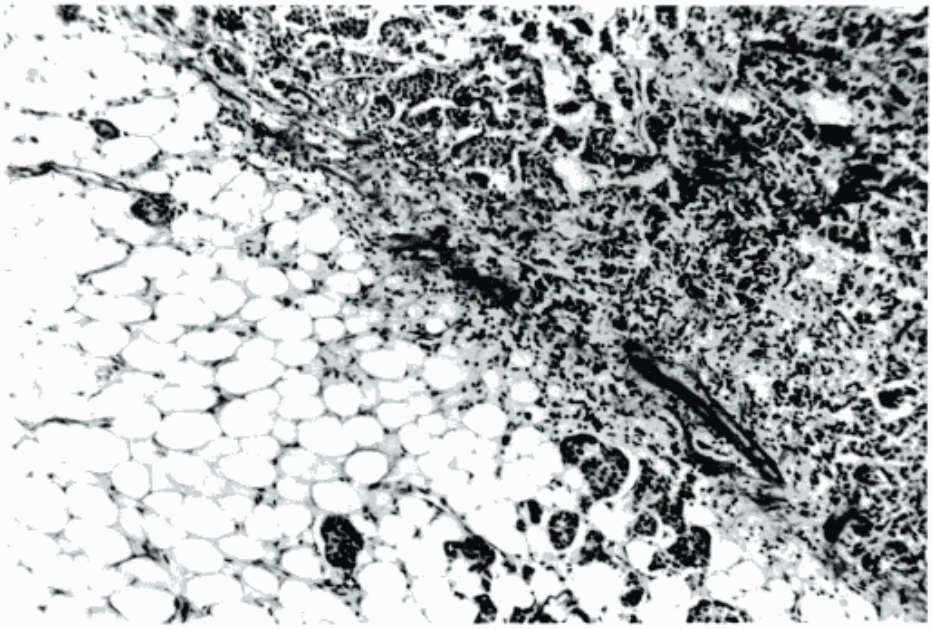

Fig. XVI: 21. "Atrophic" fat cells adjacent to a human breast carcinoma, histologic section. Also observe large numbers of white blood cells in the tumour and in adjacent fat tissue. (Photograph courtesy of Dr I. Sümegi, Karolinska Hospital, Stockholm.)

and in vivo electrophoresis of breast fat tissue in Section F.

Studies of human fat tissue adjacent to two electronegative carcinomas of the breast, compared to distant fat in the same breast, have shown that the relative amount of fat and water in these regions corresponded to what was found in the electrophoretic experiments. This result is consistent with and may therefore indirectly point to the possibility of spontaneous electrophoresis and electroosmosis in vivo over a BCEC.

Of equal interest is the observed experimental shrinking of fat cells adjacent to the cathode and the "atrophic" appearance of fat cells around the anode.

It is now relevant to review a well-known but as yet unexplained structural phenomenon, which develops adjacent to tumours in fat tissue. Carcinomas in the breast, in the subcutis or in other sites of adipose tissue often show what pathologists call "atrophic" fat cells adjacent to the surface of the tumour (89).

Such a case is shown in Fig. XVI: 21. This histologic section through a breast cancer shows small, "atrophic" fat cells close to the tumour tissue. In the upper right-hand part of the figure the fat cells are larger and almost normal in size. Presently an explanation for the atrophy of peritumoural cells is lacking. In the author's opinion, a spontaneous polarization of a tumour in relation to its surroundings should be capable of producing peritumoural fat atrophy as a consequence of fat mobilization and transport over a BCEC. The spontaneously atrophic, peritumoural fat cells are characteristically small. Their walls are even. In these respects the peritumoural fat cells are most similar to the "atrophic" fat cells adjacent to the anode in an electrophoretic experiment.

H. Circular displacement of tissue structures around breast tumours

Circular displacement and narrowing of vessels have been previously described around lung tumours (Chapter III). Similar radiographically visible structures have also been observed and demonstrated (Figs. XVI: 1, 4, 6, 20) around certain breast tumours. The basic morphologic differences between the two organs are of considerable importance in the evaluation of these structures.

As has been pointed out earlier, compression is often applied against the breast in mammography, which may displace structures considerably.

In xeroradiography, a mammogram can be obtained without compression technique. Such a xeroradiogram is seen in Fig. XVI: 22, where a small carcinoma resides close to the chest wall. A preoperative stereotaxic needle biopsy and electric potential study revealed an electronegative mammary carcinoma. The small tumour is surrounded by radiating structures and concentric arrangements of curved linear structures, which all seem to have their centre in the tumour.

Concentric arrangement of structures can also be recognized frequently in ordinary mammograms (e.g., Figs. XVI: 1, 4*a*, 6*a*, *b* and 14*b*).

To explain the development of circular structures around a breast tumour, once the effect of external compression can be excluded, an activated BCEC should be considered. This mechanism is capable of

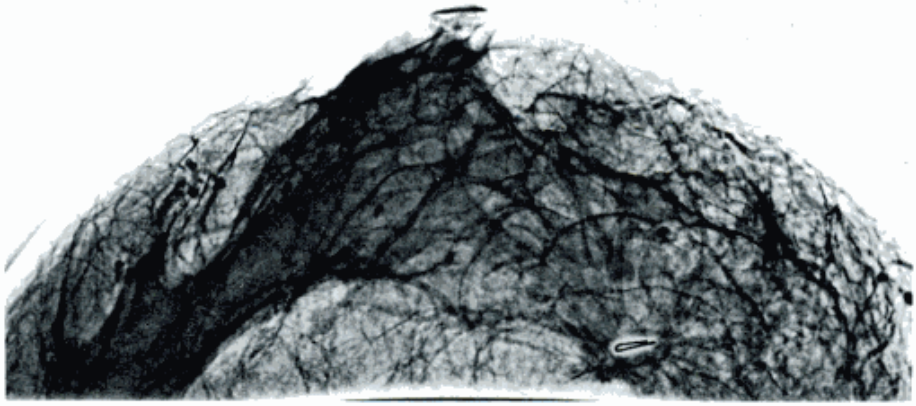

Fig. XVI: 22. Xeroradiograph of a small carcinoma of a breast without the use of external compression technique. Concentrically surrounding the tumour are many radiating and circular structures. After stereotaxic needle biopsy for cytologic diagnosis of this nonpalpable tumour, a metal clip was placed in its centre as a guide to the surgical excision.

producing anionic, cationic and water transports between a tumour and its surroundings. Moreover, it is easy to recognize that secondary biologic effects will also take place within a BCEC, contributing to the development of circularly arranged structures. Thus, thrombosis of capillaries will take place in the surroundings of a polarizing tumour over a VICC (Chapter XIV). Such thromboses, developing during an electropositive phase of the tumour, should produce local dystrophic changes in the poorly nourished tissue, which will yield due to retractive forces in the well nourished surrounding tissue. This mechanism should contribute to circular displacement of tissue, as has also been observed in the lung (Figs. III: 30 *b*, 34 *b*).

During an electronegative phase of a polarizing tumour, a net inflow of water toward it will increase local water pressure and thereby further contribute to the circular displacement of structures (Figs. XVI: 6, 20, 22).

Broad, circularly running structures of a different origin may be identified around a tumour as a result of electroosmotic transport of water. Such a collection of water then represents what has previously been defined as a hydropic "B" zone. Such structures were shown to disappear in the lung when air entering the pleura changes the flow conditions in the lung (Chapter III, Section D). Fig. XVI: 23 shows a corresponding situation in the breast. This patient's xeroradiograph (Fig. XVI: 23 *a*), obtained without compression technique, shows broad circular segments in the tissue surrounding the carcinoma. These circular structures could not be demonstrated on radiography of the surgically removed breast (Fig. XVI: 23 *b*). This result is in accord with the disappearance of a hydropic "B" zone in the lung when the pleura is opened. The local accumulation of electroosmotically transported fluid producing such a "B" zone (a special case of a circularly arranged "structure") requires, of course, an exact balance of interacting forces, which differ in vivo and in a surgical specimen.

Peripheral displacement of tissue structures during an electropositive phase of the tumour should be considerably enhanced during a phase of electronegative polarization. An electroosmotic inflow of water toward the tumour, causing perifocal oedema, could then simply move tissue structures outward as a consequence of locally increased turgor pressure. Thus, in cases of true perifocal oedema, as in the patients shown in Table XVI: 2 (Figs. XVI: 6 and 20), very well developed circular structures can be seen radiographically. They can also be influenced and change their appearance by external compression.

Conclusions

It seems altogether plausible that the development of circular tissue structures around certain breast and lung tumours involve similar mechanisms. Polarization of tissue over a BCEC as the common mechanism explains the transporting of materials and secondary biologic tissue changes which can satisfy most of the requirements for the production of circularly arranged structures in both breast and lung.

We will now take a closer look at some other structural details in the breast encountered in patients with breast cancers. We will start with a short description of the appearance and development of arches, which, when appearing in a row, form an arcade.

I. Arches and arcades

A large carcinoma in the breast with many radiating structures and small calcifications is shown in Fig. XVI: 24. A broad structure extends from the tumour to the areola, which is somewhat retracted toward the tumour. The skin also shows increased radiopacity around the areola. A 6 mm broad, diffuse, semicircu-

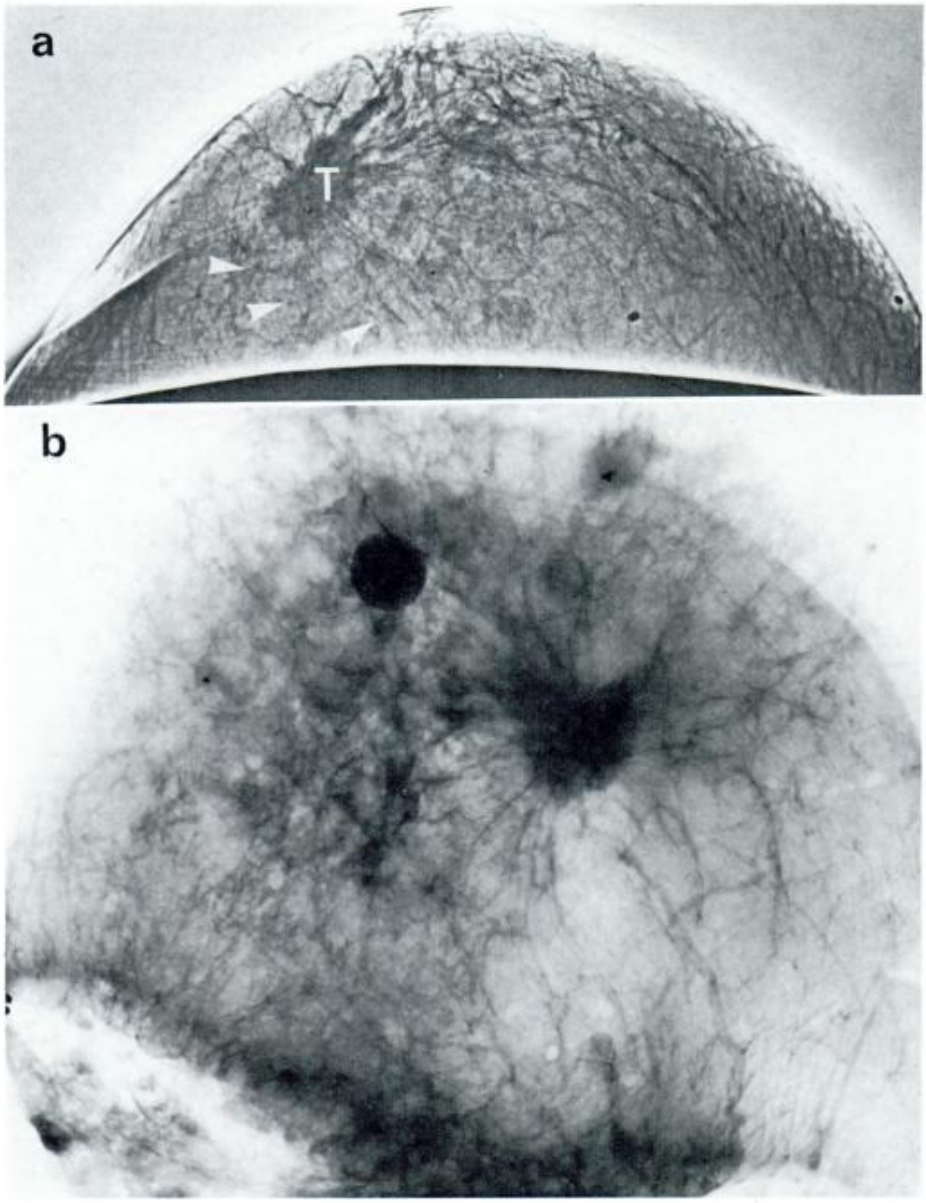

Fig. XVI:23. Hydropic "B" zones producing "false circular structures" around a carcinoma of the breast. (*a*) Xeroradiograph. A breast cancer (*T*) is surrounded by arcs of "B" zones, which appear as broad circular opacities (arrowheads) near the tumour. These opacities are interpreted as local oedema (hydropic "B" zones), disappearing (*b*) after mastectomy.

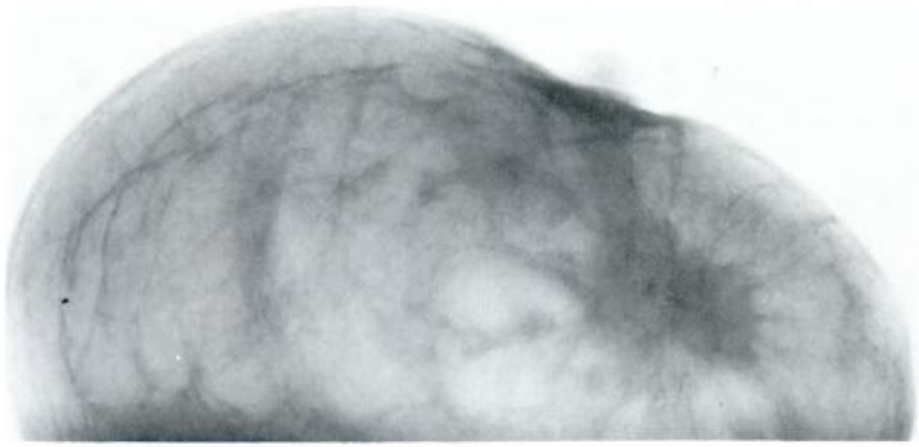

Fig. XVI:24. Mammogram showing arches around a carcinoma of the breast in a 52-year-old woman. Radiating structures join into large arches, giving the tumour and surrounding tissue an appearance like the cut surface of a citrus fruit. Retraction of the nipple, microcalcifications and a radiolucent "A" zone are all evident. The band-shaped density to the left is believed to be a skin fold due to compression of the breast. (Mammogram courtesy of Prof. D. Tevčev and Prof. M. Grunevski, University of Skopje, Yugoslavia.)

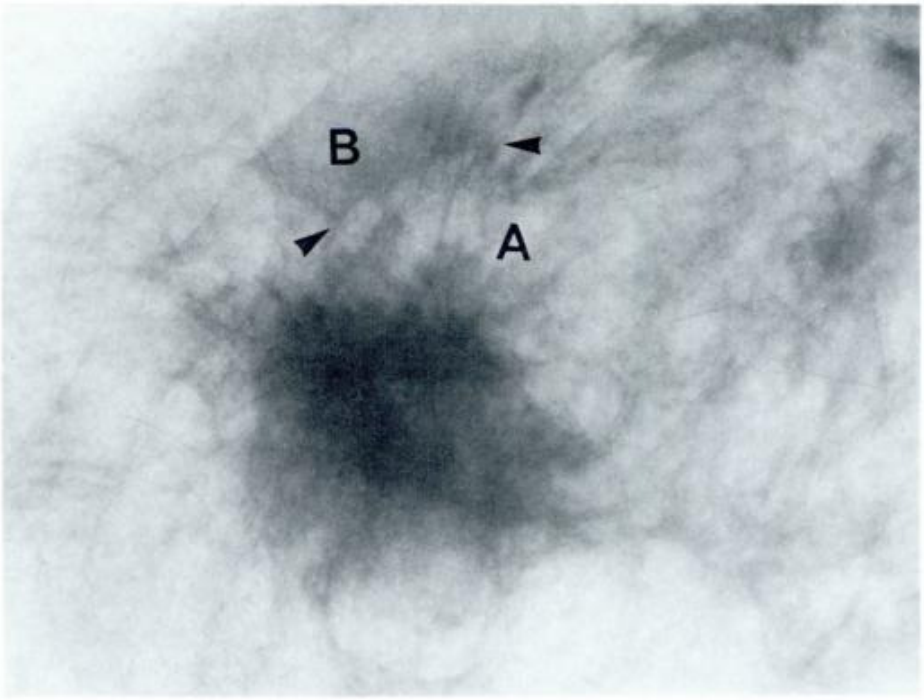

Fig. XVI: 25. Many radiating structures appear associated with relatively small arches. Mammogram, undifferentiated carcinoma, 74-year-old woman. At the interface between an "A" zone and a local "B" zone, a row of small arches forms an arcade (arrowheads), through which some radiating structures pass.

lar density in the left side of the breast is probably a skin fold produced by the compression of the breast during radiography.

A radiolucent "A" zone is particularly prominent below and to the left of the tumour. Radiating structures diverge from the tumour but arc back to rejoin so as to produce arches, corresponding to what has been described around lung tumours (Chapter III). These arches combine to form together an arcade in the tissue 2 to 2.5 cm from the surface of this tumour. The tumour and the surrounding tissue appear rather like the cut surface of a divided citrus fruit. The number and size of the arches correspond roughly to the number and distances between radiating structures. To the immediate left of the illustrated tumour, adjacent arches can be seen to share one radiating structure.

When a tumour has a large number of radiating structures, the arches appear correspondingly smaller (Fig. XVI: 25). In this patient with breast cancer a radiolucent "A" zone is seen above the tumour. The "A" zone ends at a sharp borderline with some small arches forming an arcade against the peripheral, local opacity of a "B" zone. Some thin radiating structures also pass through the "A" and "B" zones.

Arches and arcades as illustrated in Figs. XVI: 24 and 25 appear in principle the same as the arches and arcades around lung tumours. They also appear the same as the arches and arcades which can be produced experimentally in vitro and in vivo in dog lungs (Chapter XI).

Discussion

Arches forming an arcade peripheral to a tumour in the lung have already been explained (Chapter X). They are produced as interphase phenomena between an "A" and a "B" zone under the influences of physicochemical forces of nonorganized materials as well as of electric field forces over a polarizing BCEC. It is likely that adsorption between adjacent fluid-matrix phases plays an important role in these processes. However, linear structures at an interface should not be confused with circular displacements of preformed structures, such as vessels and septa of fat tissue. As has been pointed out earlier, such structural displacements may have several causes: perifocal tissue atrophy due to nutritional disturbances within an "A" zone, retraction forces of surrounding nonatrophic tissue, and perifocal oedema during an electronegative phase of the tumour.

Peritumoural fibrosis may shrink tissue, as suggested in Fig. XVI: 24, in which some radiating structures appear to have coalesced and retracted the nipple. Such shrinkage could contribute to the formation of arches in the tissue between pairs of radiating structures. In such an explanation, the broad radiating structures between the tumour and the nipple should be regarded as an equivalent to the lamella (Fig. XVI: 13) described around lung tumours (Chapter III, Section F).

This parallel leads us to a short analysis of two well

known structural components in breast cancer: so-called skin thickening and retraction. The parallel between breast and lung is opportune, because, in the opinion of the author, nearly identical mechanisms underlie peritumoural changes in the lung and in the breast. The mammographic changes are demonstrable as arches and arcades, retraction of the nipple, retraction of the skin and thickening of the skin.

J. "Skin thickening" and retraction: a result of altered distribution of tissue water

Local thickening and retraction of the skin of the breast is a well known clinical sign of an underlying pathological process, whether caused by trauma, infection, or as is usual, a carcinoma. The retraction of the skin is associated with juxtatumoural scar tissue, which for primary breast neoplasia is usually part of the mass of a so-called scirrhous carcinoma.

Scirrhous carcinoma, which is the most frequent type of breast cancer, is characterized by the development of peritumoural "fibrous strands" (radiating structures) and hyalinization of peritumoural connective tissue. Scirrhous carcinomas may develop in the stomach, breast or other organs. They usually grow slowly. They are reported to consist of either anaplastic cells or varying degrees of differentiation of adenoid structures (55). In the author's opinion, such cancers do not represent a specific type of cancer. A scirrhous cancer may instead be regarded as a particular transformation of tissue induced by electrochemical polarization of the tumour. The most common source of energy for such reactions is, in the author's opinion, the occurrence of degradation of tumour tissue. Such processes may in turn be more or less common in different kinds of tumours. Although scirrhous carcinomas are generally slowly growing, the biologic behaviour of their cells is not necessarily "benign". Even rapid, multifocal degradations coupled to injury-induced healing and fibrous induration may keep the total amount of viable tumour tissue low for a relatively long time. *So-called productive fibrosis and peritumoural scar tissue of malignant tumours may in this way be regarded as an expression of spontaneous, incomplete healing of the tumour.* The prerequisites for such reactions are energy-liberating processes, e.g., spontaneous necrosis, bleedings or infection, and the existence of a BCEC. The common observation of fibrosis forming around the intracardiac electrode and around subcutaneous pacemaker devices is in the author's opinion an in vivo "experiment" demonstrating this principle.

The fibrous radiating structures, often long and straight, around a scirrhous cancer of the breast contain different kinds of fibrous materials. Nonhygroscopic collagenous fibres can be seen in histological sections as birefringent files. Hygroscopic fibrous material between these files is known to be an important constituent in scar tissue, according to Asthbury (7).

Islands of cancer cells may be imbedded in fibrous material close to the surface of a tumour. The fibrous tissue of the radiating structures around a scirrhous breast cancer shows a striking similarity to other fibrous tissues, e.g., the scars of wound healing.

Post-traumatic scar tissue retracts during certain phases of its evolution. Similar retraction can often be observed at the surface of lung peripheral to a lung tumour or to a pneumonia healing with "productive fibrosis". Fibrous tissue around a lung tumour may then produce "lamellae" and "retraction pockets" in the pleura, according to the mechanism described in Chapter III, Section H. Given this parallel background, skin thickening and retraction superficial to a pathologic process in the breast may be explained as follows:

Local degeneration in a breast tumour leads to local polarization. The polarization directs over the BCEC the growth of fibrous radiating strands. These strands contain partly collagenous fibrous elements, which are both nonhygroscopic and hygroscopic. Depending on the degree of water content, the hygroscopic material will stretch or shrink. When the tumour is electropositively polarized, a hydropenic "A" zone and a hydropic "B" zone will be produced. In the hydropenic zone close to the tumour surface, the hygroscopic fibrous elements will shrink. When these elements extend to the subcutaneous tissue, retraction of the skin ensues. At the same time, water in the hydropic "B" zone will tend to collect in the retracted skin, partly as a result of the retraction forces on this tissue by the fibrous strands. The usually sharp border between the "thickened skin" and the underlying tissue is then explained as a balancing effect between the local hydrostatic water pressure in the skin and electroosmotic forces tending to displace water outward within the BCEC. The increased water content in so-called skin thickening can in this way be described as partly a result of electroosmotic water transport and partly as "retraction oedema" (Fig. XVI: 26). This skin "thickening" then corresponds to the pleural fluid which collects locally in the "retraction pocket" outside a fibrosing lung lesion. Whenever fibrous material is collected into a thick radiating structure (see Fig. XVI: 13), a lamella (Chapter III, Section F) is formed, which may pull the subcutaneous hydropic tissue so that this

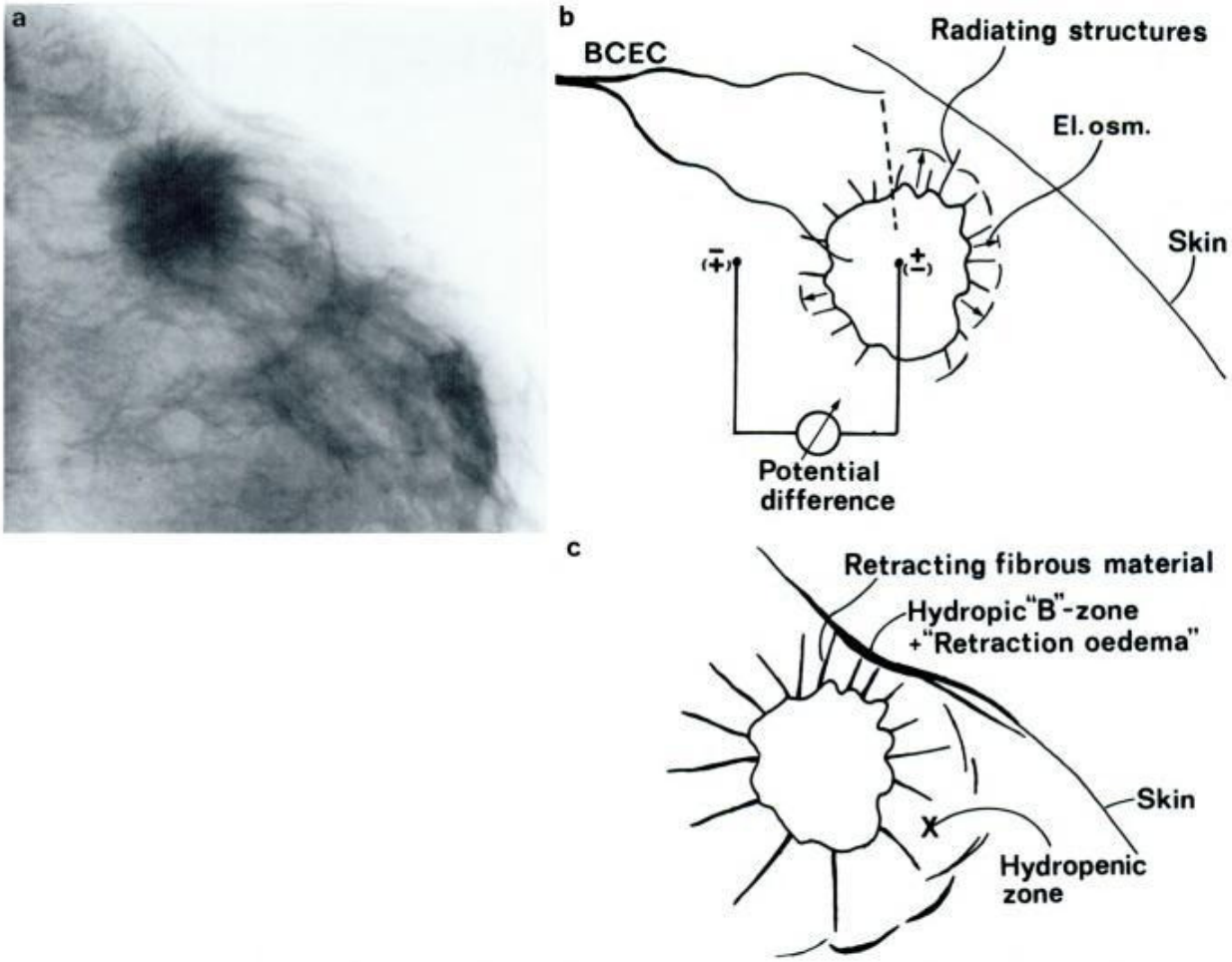

Fig. XVI: 26. Skin "thickening" and retraction near a carcinoma of the breast. (*a*) Mammogram, 80-year-old woman. Skin is retracted and "thickened". A radiolucent "A" zone is suggested, surrounding the tumour. Numerous radiating structures are evident. A "circular" structure is seen to the right of the tumour. (*b*) As the tumour polarizes, water will flow outward by electroosmosis over the BCEC (electropositive phase of tumour). This leads to development of a hydropenic "A" zone and retraction of hygroscopic components of the fibrous material of the radiating structures. (*c*) Radiating structures extending to the cutis will retract the skin and enhance the accumulation of electroosmotically transported water in the skin. The "circular" structure (lower right) corresponds internally to the external "skin thickening". Retraction forces of the radiating structures in this region are counterbalanced by retraction forces of the normal tissue distal to the "circular" structure. The thickness of the "circular" structure is the same as that of the "skin thickening", further suggesting their common pathogenesis as hydropic "B" zones.

tissue appears as half an arch on each side of the lamella. Two adjacent lamellae (or thick radiating structures) will then produce an arcade. It may now be apparent that radiating structures and lamellae, arches and arcades, nipple and skin retraction and skin thickening are to a large extent the result of identical biokinetic mechanisms, which appear differently in different surroundings.

We will now consider the validity of the proposed explanations, first in terms of the retracting function of fibrous tissue.

Histologic sections of breast tissue around scirrhous carcinomas show the birefringent collagenous fibres as sometimes undulating (Fig. XVI: 27 *a*) and sometimes straight (Fig. XVI: 27 *b*). One's first impression may be that the underlying fibres represent artefacts of preparation. This explanation, however, is highly unlikely because identical appearances of undulating structures are seen irrespective of the direction of cutting the specimen. This observation was experimentally checked as follows:

Tissue surrounding a scirrhous breast cancer was excised and divided into four pieces. Two pieces ($a+b$) were placed in saline solution and frozen. The remaining two pieces ($c+d$) were kept in a dry place in a refrigerator overnight in order to become slightly dehydrated. Frozen sections were then prepared of the four pieces. Pieces $a+c$ were cut as closely as possible

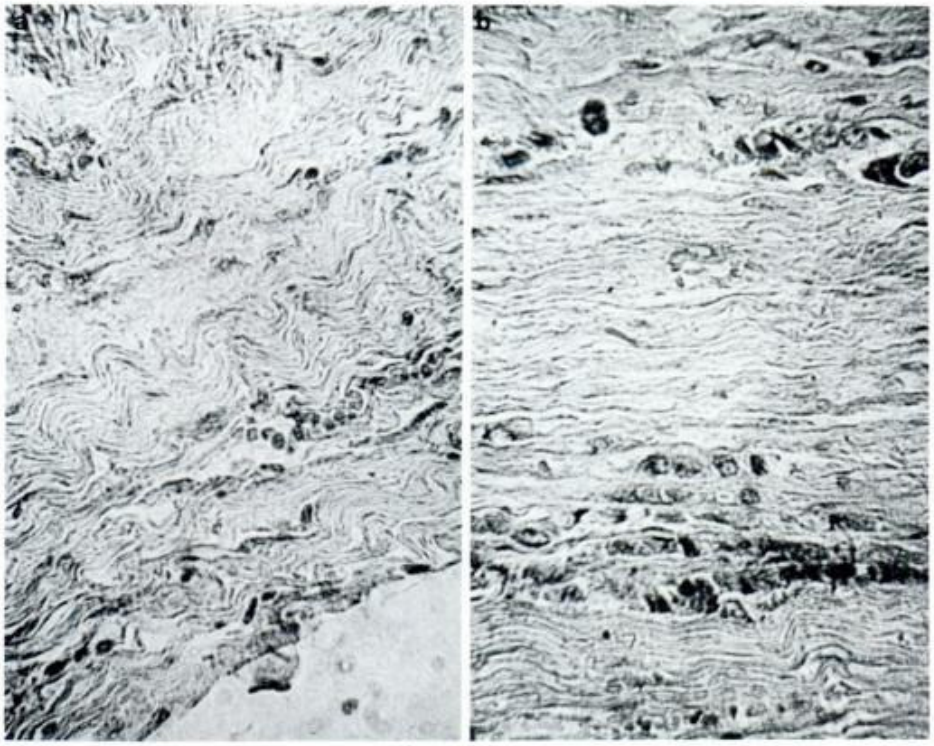

Fig. XVI: 27. Variable appearances of fibrous strands radiating from a scirrhous carcinoma of the breast (histologic sections, haematoxylin-eosin). (*a*) Undulating course of partly birefringent fibres. (*b*) Straight course of fibres in another part of the same specimen. The undulating fibrous structures are not necessarily artefacts of preparation. Identical appearances can be obtained regardless of the direction of cutting the specimen (see further Fig. XVI: 28).

Fig. XVI: 28. Dehydration shrinks hydrophilic components of fibrotic tissue between nonhydrophilic, birefringent collagen fibres. Histologic frozen sections (haematoxylin-eosin, *a–d*, same magnification). Arrows indicate directions of cutting. (*a, b*) Two specimens of fibrous tissue from a breast cancer after soaking in saline solution overnight. The collagen fibres are straight, regardless of the direction of cutting. (*c, d*) Corresponding fibrous tissue after overnight dehydration of the material. The collagen fibres undulate, regardless of the direction of cutting.

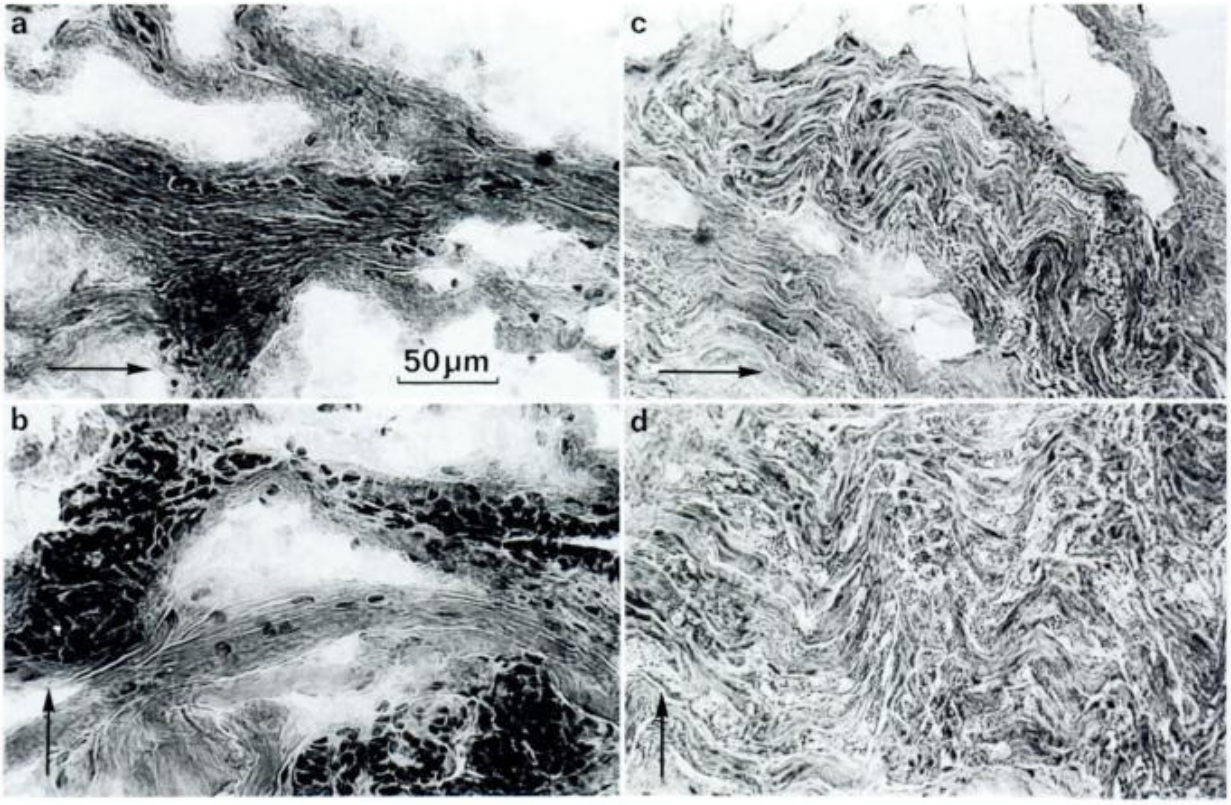

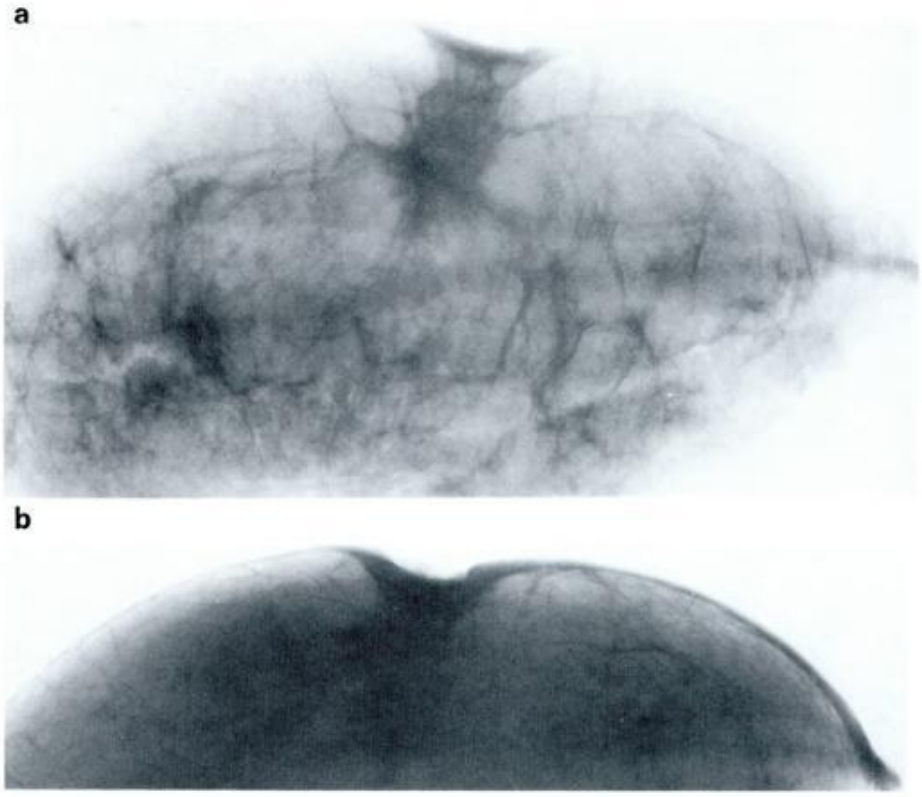

Fig. XVI: 29. "Skin thickening" near a mammary carcinoma (40-year-old woman, I. J. in Table XVI: 3). Mammogram, mastectomy specimen. (*a*) The tumour is surrounded by fibrous radiating structures and possibly an "A" zone with some circular structures. (*b*) The same specimen. Radiograph of the skin, which is thickened to the right and below the retracted nipple but is of normal thickness to the left.

along the extensions of the fibrous radiating material, pieces *b*+*d* perpendicular to the extensions. The sections were mounted and stained. Fig. XVI: 28 *a* and *b* shows the material which had been kept in saline solution. All the birefringent collagenous material in these two specimens appeared rather straight and nowhere undulated. This finding was interpreted as an indication that the hygroscopic fibrous material between the collagenous fibres was hydrated and contributed to the straight appearance. The dehydrated material (Fig. XVI: 28 *c* and *d*), on the other hand, showed a characteristic undulating course of birefringent nonhygroscopic collagen fibres, which was interpreted as produced by shrinkage of the adjacent hygroscopic fibrous material. In none of the sections was there any correlation between the direction of cutting and the appearance of the fibrous material.

It seems likely that undulating courses of fibrous tissue around a breast cancer may be caused by local dehydration of hygroscopic components of fibrous tissue. Local dehydration may in turn result from electroosmotic outflow of water, leading to shrinking of the hygroscopic material of the fibrous tissue strands and retraction of the skin. In such areas the "skin thickening" should be called a local oedema of the skin, which in certain parts could also be called retraction oedema. We may now recognize the equivalence of these structural changes around a breast cancer and the previously described pleural retraction pocket near a peripheral lung cancer (Chapter III, Fig. III: 35).

Fat and water content were also analyzed quantitatively for the so-called "skin thickening" over two breast carcinomas and for skin from parts of the breast specimens which appeared radiologically normal. Fig. XVI: 29 *a* shows the mammogram of one of them, patient I. J. This carcinoma is surrounded by numerous thin radiating structures and possibly a radiolucent "A" zone. Fig. XVI: 29 *b* shows "skin thickening" both to the right and under the retracted nipple. Table XVI: 3 presents the analytical values for the two patients.

Table XVI: 3. *Fat–water content of "skin thickening" over breast cancers and normal skin*

Patient		"Skin thickening"	Normal skin I	Normal skin II
I. J.	H_2O	77.5	62.6	63.5
	Fat	0.2	3.9	3.9
	Residual	21.0	32.9	31.7
	Lost	1.3	0.6	0.9
A. C.	H_2O	79.5	72.3	–
	Residual	18.0	25.6	–
	Lost	2.5	2.1	–

The results indicate that so-called "skin thickening" correlates with a relative increase of water content (local oedema), explaining the local increases in x-ray attenuation seen in the mammogram.

K. Closed circuit production of fibrous radiating structures: cathodic and anodic types of fibrosis

Fibrous radiating structures often develop around carcinomas in the lung as well as in the breast. This observation has here been interpreted as a consequence of two phenomena: physicochemical polarization of the lesions and the existence of biologically closed electric circuits. Radiating structures were previously also produced experimentally in vitro and in vivo (Chapters X, XI). A closed electric circuit is a necessity for their experimental production. This section will show experimentally that radiating structures can be produced very efficiently over closed circuits even in "dead" tissue and also that material in these structures looks like and may possibly be identical with the fibrous material around tumours.

One prerequisite for the development of radiating structures is the presence of so-called electric edge enhancement (Chapter X). To utilize this phenomenon, circular electrode plates of platinum were therefore perforated at multiple sites with a needle. Small protrusions of the metal were produced in this way on the side of the electrode plate facing the tissue specimen.

A piece of human breast fat in a plastic 10 ml syringe between two plungers, each provided with a platinum electrode, is shown in the soft tissue radiographs of Fig. XVI: 30. Platinum strings were connected to the electrode plates and to a generator of direct current. Fig. XVI: 30*a* shows the specimen before any current was applied. Some already existent fibrous structures can be seen in the fat, which is essentially free from such material close to the electrodes. Fig. XVI: 30*b* shows the specimen after 10 days (25 coulombs) and Fig. XVI: 30*c* after 17 days (30 coulombs), during application of 10 volts over the material. During the first hour a current of a few mA flowed with increasing intensity through the specimen. The current then usually decreased to very low values (a few μA). As days passed, radiopaque structures developed in the fat. In the cathodic part of the chamber, clear linear structures were seen after 10 days. More cathodic and anodic material is seen after 17 days than after 10 days. After 17 days the anodic

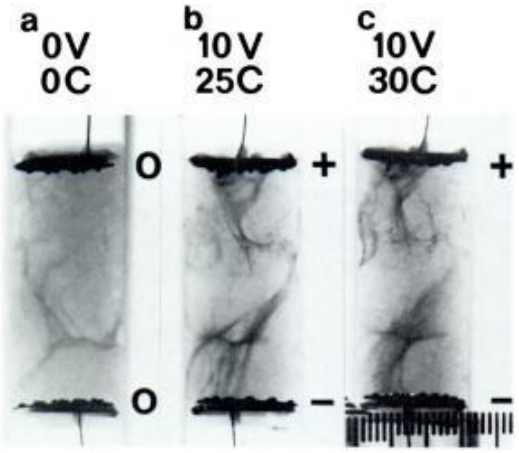

Fig. XVI: 30. Direct current treatment of human breast fat in a plastic chamber between two platinum electrodes with protruding edges. Soft tissue radiographs. (*a*) Before electrophoresis, practically no fibrous tissue in parts of the specimen immediately adjacent to the electrodes. (*b*) After 10 days, 25 coulombs at 10 V. (*c*) Slightly different projection, after 17 days, 30 coulombs at 10 V. Fibrous tissue is produced as "radiating structures" due to field enhancement at some of the electrode protrusions. These structures are not straight, which is explained by preferential pathways for current in the tissue. Note macroscopic differences of cathodic (−) and anodic (+) fibrous tissue as well as many small "dots" in the anodic part of the specimen.

part of the specimen (+) showed some very small dark dots and more delicate irregular structures than the cathodic portion (−).

The newly formed linear structures in the cathodic and anodic regions close to the electrodes were easy to identify in histological sections because no or only

Fig. XVI: 31. Histopathologic appearances of radiating structures experimentally induced in cathodic and anodic regions of breast fat (*a–f*), compared with fibrotic tissues arising in vivo around a breast cancer (*g–j*). (*a–c*) Cathodic, (*d–f*) anodic newly formed radiating structures. Same specimen as in Fig. XVI: 30. *Cathodic fibrosis* looks like a stretched mesh of fibres (*a, b*) which never shows any fibroblasts. During development some groups of fat cells diminish in size (*c*) and form a central "nucleus" before they disappear (see further on development of cathodic fibrosis, Figs. XVI: 33, 36). *Anodic fibrosis* shows dense, irregular fibrous material with fibroblast-like cells (*d, e*) and scattered groups of cells of an epithelial type (*e, f*). (*g, h*) Some fibrous tissue from the surroundings of a breast cancer appears as a mesh, similar to experimentally produced cathodic fibrous tissue. It contains cellular structures of variable appearance. Some are flat and of a fibroblast type. Others appear with rounded cellular nuclei (arrows). (*i–j*) Tissue from another part of the tissues surrounding the same tumour. This fibrous tissue is particularly irregular and dense. It contains a large number of fibroblasts and looks like experimentally produced anodic fibrous tissue (*a, b, d, e* van Gieson, *c, f–j* haematoxylin-eosin stain).

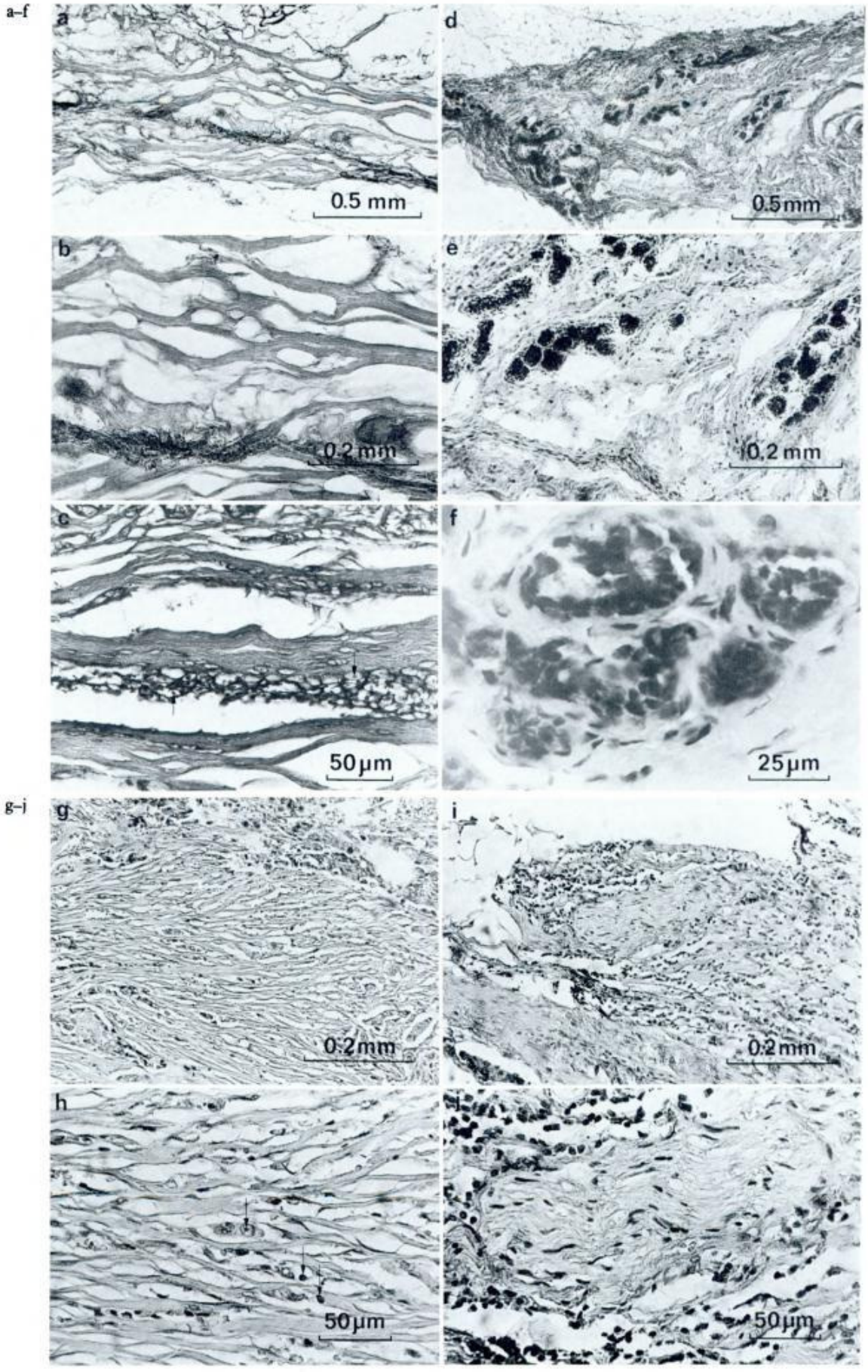

minimal amounts of fibrous tissue were there before the application of current. Histologic sections of the newly formed radiating structures are shown in Fig. XVI: 31 from close to the cathodic electrode (*a*, *b*, *c*) and the anodic electrode (*d*, *e*, *f*). The cathodic and anodic structures resemble elements of spontaneously developed fibrous tissue material. They also show distinct internal structural differences. Both materials contain birefringent and nonbirefringent components. The cathodic material shows a net-like loose mesh mainly oriented in the direction between the electrodes. The anodic material is more compact and irregular in appearance and shows islands of what will later be shown as epithelial-like cells and many spool-shaped small structures which look like fibroblasts. No fibroblast-like structures were seen in cathodic fibrous material.

Both "cathodic" and "anodic" types of fibrosis now can be recognized in the radiating scar tissue around a breast carcinoma, as shown in Fig. XVI: 31 *g–j*. The experimentally produced cathodic, mesh-like fibrous tissue (Fig. XVI: 31 *a*, *b*, *c*) may be compared with the endogenously developed fibrous mesh-like tissue of Fig. XVI: 31 *g*, *h*. This endogenous tissue, however, does contain some fibroblast-like cells, unlike the experimental cathodic fibrous tissue.

The experimentally produced anodic, dense fibrous tissue contains large amounts of fibroblast-like cells (Fig. XVI: 31 *d*, *e*, *f*). The endogenous anodic type of fibrous tissue also contains large amounts of fibroblasts (Fig. XVI: 31 *i*, *j*). The groups of epithelial cells seen in Fig. XVI: 31 *d*, *e*, *f* will be discussed later. A mixture of anodic and cathodic types of endogenously developed fibrosis around a tumour is in agreement with the conception of fluctuating changes of polarity of a degrading tissue, and hence the direction of flow of current. Production of fibrosis is, in this view, a result of the flow of current over BCEC channels. This far-reaching statement will, however, shortly be further supported by other observations.

Recently the opinion has been expressed that fibrosis in breast cancer might be a primary carcinogenic factor (67). In the author's opinion this conclusion is not very plausible. Formation of scar tissue is a common reaction in various tissues to different kinds of injury. Degenerative changes or traumatic injuries are frequently encountered in normal breast tissue. Very often, spontaneous necrosis and haemorrhage occur in breast cancers. In the following it will be seen that many of the structural modifications of cells and tissue which can be seen inside and around breast cancers can be induced by direct current. Even the possibility of *carcinogenic effects* by endogenous or induced currents in tissue might be considered in future research.

The closed circuit treatment of tissue samples shows that it is possible to produce newly structured material in both the cathodic and the anodic fields even in a "dead", excised piece of tissue. Radiating "fibrous" tissue structures can be produced in tissue samples of mammary fat by direct current when the electrodes are provided with small protrusions causing local spots of high current density. The sites where the fibrous tissue structures develop depend not only on the locations of the protrusions on the electrodes. At some protrusions no structures will develop. This phenomenon has been interpreted as an effect of inhomogeneity with regard to conducting properties of the tissues. Preferential pathways of current in tissue, even if it looks histologically homogeneous, can fully explain such a phenomenon.

The experimentally produced fibrous material very much resembles scar tissue, although it is apparently different in the cathodic and anodic fields. This result is not surprising as long as a unidirectional mode of current has been applied. Evidence has been presented, both experimentally and theoretically, that a spontaneous tissue injury will produce a fluctuating potential over BCEC, thus allowing anions as well as cations to contribute to the healing process and consequently also to the formation of complete or "mixed" fibrous tissue.

Experiments were therefore also arranged to fluctuate the electric potential over samples of fat tissue. Before these experiments are described, we will, however, extend the present experiments of producing radiating structures into attempts to produce membranes with unidirectional current.

L. Closed circuit production of fibrous membranes

A tentative explanation for the production of fibrous organ capsules was given in Chapter XII. It was assumed, for example, that the liver and its surrounding organs will produce asynchronous, physiologic fluctuations of potential, which should lead to "ebb and flow" movements of anions and cations to the organs' surfaces. A deposition of material should then lead to the production of fibrous capsules as long as the driving force over the BCEC is strong enough to induce the ionic movements. The thickness of an organ's capsule should then correspond exactly to the physiologic driving force over the BCEC. The capsules of organs may consequently be regarded as analogues to the products of polarization at electrode surfaces.

This section contains experiments showing how fibrous membranes can be produced by the use of this principle, but in a simplified way.

We will again make use of the electrophoretic cham-

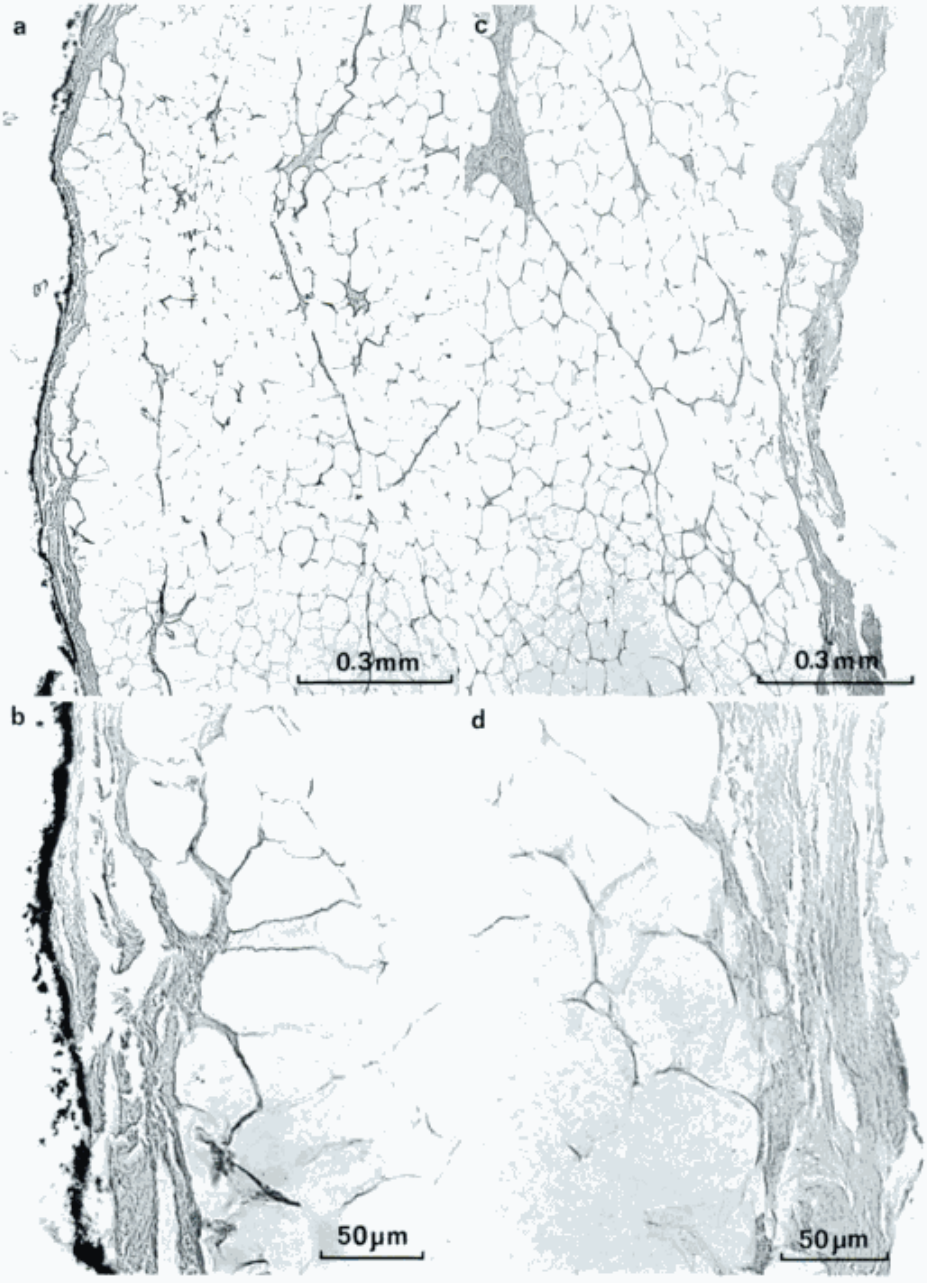

Fig. XVI:32. Production by direct current in vitro of (*a*, *b*) cathodic and (*c*, *d*) anodic membranes using flat platinum electrodes against human fat tissue. Photomicrographs show the cathodic membrane to be thin and covered with a thin layer of a brown-black material. The anodic membrane is thicker and more irregular (haematoxylin-eosin).

ber. This time we will use flat electrodes without protrusions on their surfaces. As always, deposition of material will take place on electrode surfaces when they are immersed in an electrolyte and current flows through the circuit. Such material on an electrode surface is difficult to retrieve undestroyed for histologic studies. We will, however, make use of a tissue matrix as a supporting medium between the electrodes to take care of this problem. At sufficiently high densities of current, gas produced at the metal surfaces will "lift off" nongaseous deposited material. Such material will adhere to the matrix by interface adsorption and thus become available for histologic studies.

Thus, histologic sections of cathodic and anodic membranes produced on breast fat are seen in Fig. XVI: 32. These membranes consist of birefringent material structured differently from the material of radiating structures in the cathodic and anodic fields, as shown in the previous section. The cathodic membrane is thinner and smoother than the anodic. On its surface lies a deposition of some dark material, which is absent on the anodic side. In the cathodic and anodic fields there were also several membranous structures in the fat tissue, parallel with the electrode surface.

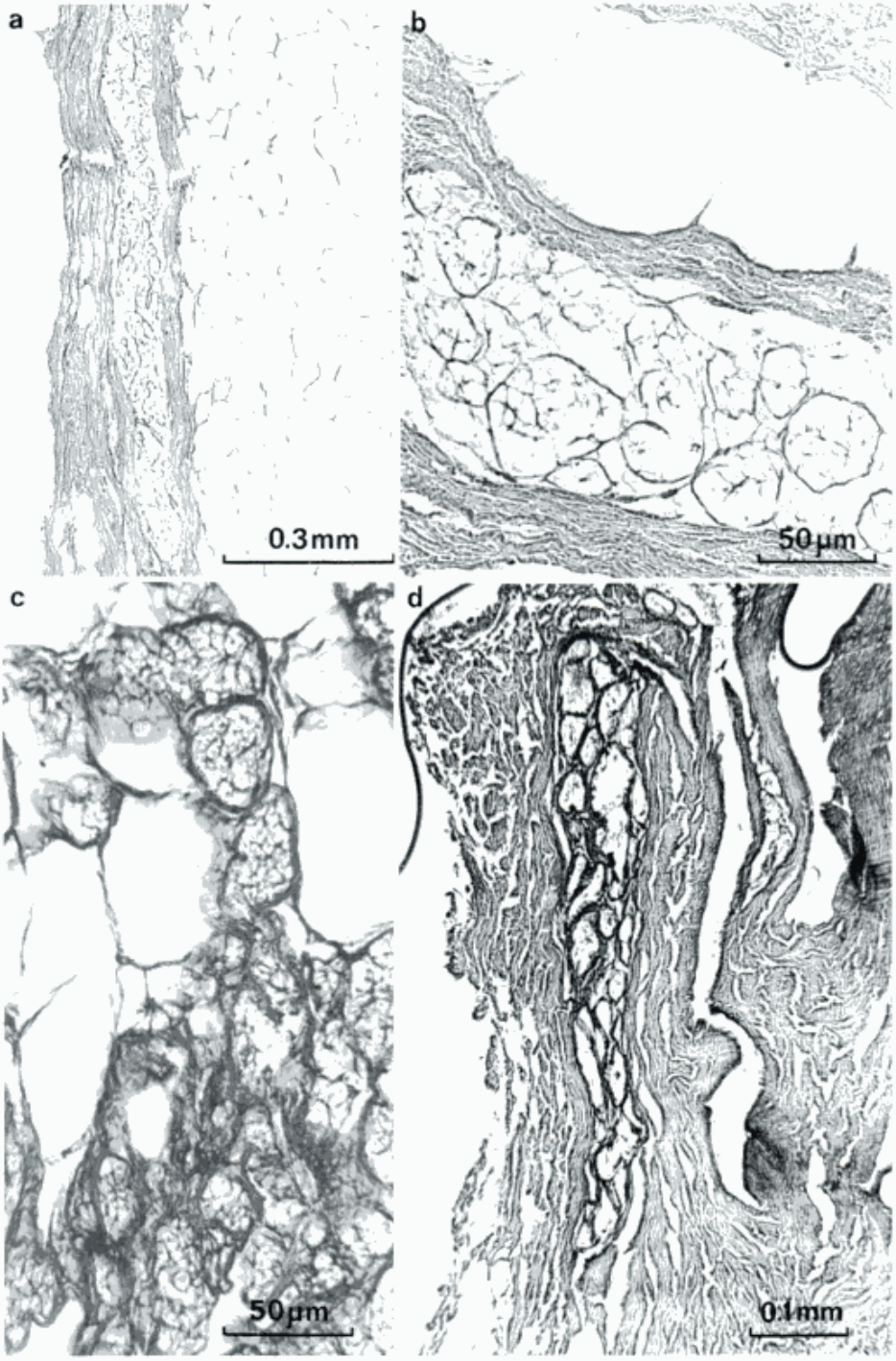

Fig. XVI: 33. Development of cathodic fibrous tissue. (*a*) The cathodic membrane adjacent to fat tissue contains islands of "atrophic" and modified fat cells. (*b*) Modified fat cells of various sizes show formation of a reticulum. (*c*) A region of gradual transformation of atrophic fat cells, which otherwise appear normal, shows reticulum structures and thickened cell membranes. (*d*) A row of fat cells with reticulum shows from top to bottom gradual disappearance of cell content and thickening of cell membranes, leading to mesh-like cathodic fibrosis without fibroblasts (*a*, *b*, von Kossa, *c*, *d*, haematoxylin-eosin stains).

M. Closed circuit production of cathodic and anodic fibrous tissue

Detailed analysis of the background biokinetics of the development of radiating structures and membranes is beyond the scope of the present study. Nevertheless, the reader may be interested in some preliminary observations of the transformation of fat material close to the electrodes, as affected by current applied unidirectionally.

An overview (Fig. XVI: 33*a*, von Kossa stain) of a piece of a fibrous cathodic membrane reveals a number of small fat cells, appearing relatively normal. Many cells inside the membrane structure have been interpreted as fat cells undergoing transformation. These

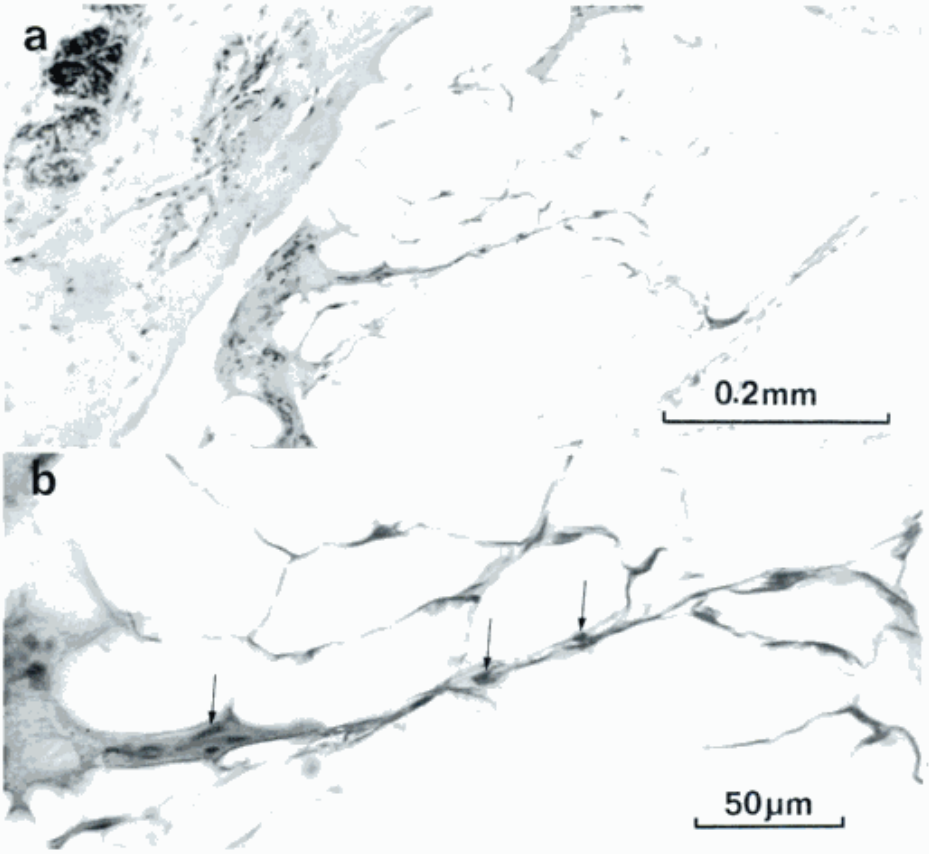

Fig. XVI: 34. Development of anodic fibrosis. (*a*) Overview of dense, anodic fibrosis containing numerous fibroblast-like cell elements. Some of these elements form circular groups, while a few are positioned at the edge of the fibrotic tissue and in a thickened intercellular space. (*b*) Magnified view of *a*. A thin, fibrotic, intercellular structure contains "fibroblasts" (arrows) adjacent to some fat cells. The membranes of the fat cells are of normal thickness. Such findings suggest that anodic fibrosis with "fibroblasts" develops interstitially (haematoxylin-eosin).

cells, seen under higher magnification in Fig. XVI: 33 *b*, are of varying size and contain a delicate reticulum. Such cells under the same magnification but stained with haematoxylin-eosin are shown in Fig. XVI: 33 *c*. The upper part of this figure contains small normal fat cells, cells which partly contain reticular structures and some cells which are filled with reticular structures. The latter have thick cellular walls. Fig. XVI: 33 *d* shows a row of thick-walled fat cells with some reticular structures (upper part of figure). The lower part of Fig. XVI: 33 *d* shows that the cells are elongated and have lost their reticular content. The elongated and thickened fat cell membranes seem to fuse and produce a fibrous tissue which looks like a stretched mesh, as was also shown in Fig. XVI: 31 *a*, *b* in the description of cathodic radiating fibrous structures.

Anodic fibrous tissue contains fibroblast-like cell elements, which do not appear in the cathodic fibrous tissue. The anodic fibrous tissue seems to develop between fat cells in the interstitial tissue. When a thin fibrous tissue strand is seen at the edge of a large anodic fibrous complex, a chain of "fibroblasts" can be seen together with some fibrous tissue in the interstitial space (Fig. XVI: 34). Because fibrous tissue can be produced in "dead" fat tissue under the influence of direct current, it seems likely that the fibrous strand, containing fibroblast-like cell elements (Fig. XVI: 34 *b*, arrows) represents a preferential pathway of current between the electrodes. Fibrous tissue is a poor electric conductor. A flow of current in interstitial spaces, producing interstitial fibrosis, can nevertheless be possible if the current is flowing in the space between cells and the surface of the developing interstitial fibrous strand. The following observations may serve as a support for this hypothesis:

When a supporting matrix is used in the membrane experiments, as is the case with specimens of fat tissue, membrane structures are produced not only at the electrode surfaces. Fibrous membranes also develop parallel to the electrodes at several sites in each fat specimen (Fig. XVI: 35 *a*, van Gieson, *b*, Alizarin stain, with anodic sides to the right). Because fibrous tissue is a relatively insulating electric material, it can be expected to be a barrier to the flow of current. Current might then flow along the surface of the barrier in the interstitial conducting medium. When it reaches the edge of the fibrous barrier, the current should tend to take new pathways in the specimen. The edge of the fibrous tissue and its surrounding conducting medium then represent a region of modified conductivity. Hence the pattern of flow of current should be modified. An anticipated resulting modification of tissue structure by such a mechanism is shown

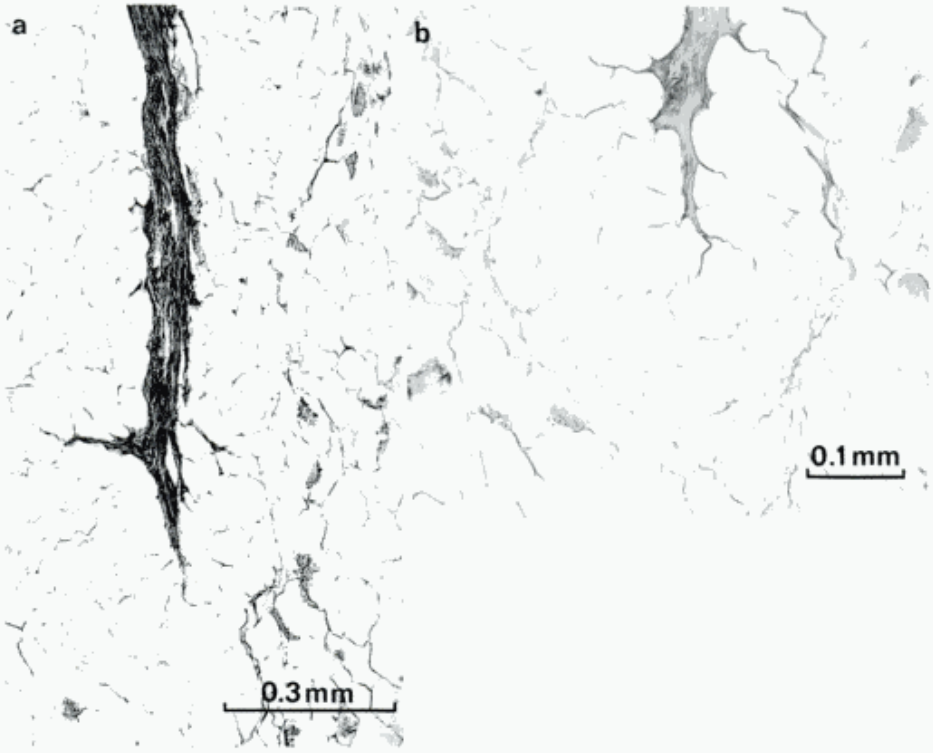

Fig. XVI: 35. Membranous fibrous structure produced by direct current in a fat specimen. Cathodic side to the left and anodic side to the right. (*a*) This membrane has a direction more or less perpendicular to the main direction of current between the electrodes. Because fibrous tissue is a poor conductor, current should flow along its surface. At the edge of the membrane, a region of modified conductivity is entered. (*b*) At the edge of a fibrous membrane, fat cells are small and possess tortuous membranes. Observe also small bush-like structures to the right of the fibrous tissue in *a* and around the edge of the fibrous tissue in *b*. (*a*) van Gieson stain, (*b*) Alizarin stain.

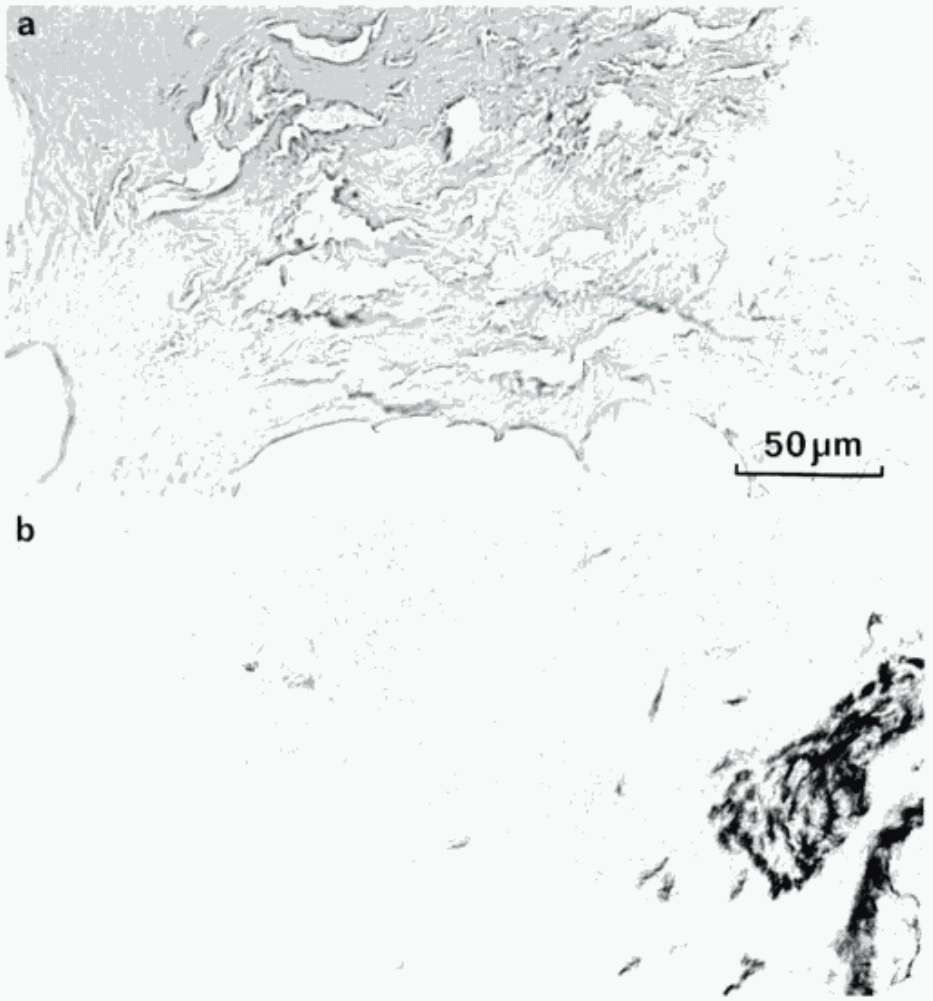

Fig. XVI: 36. (*a*) Experimentally produced, fully developed *cathodic fibrous tissue* from human breast fat. The mesh-like fibrous tissue is now dense but contains crevices with irregular, birefringent borderlines. No fibroblasts or other cells are present. (*b*) Fully developed *anodic fibrous tissue* from same preparations as *a*. This fibrous tissue is homogeneous and dense, with irregularly arranged, thin, partly birefringent fibres. Large areas do not contain fibroblasts. Other areas contain fibroblasts, either scattered or in dense collections. The lack of fibroblasts in cathodic fibrosis and the lack of correlation between the amount of anodic fibrous tissue and the numbers and locations of fibroblasts is striking (haematoxylin-eosin).

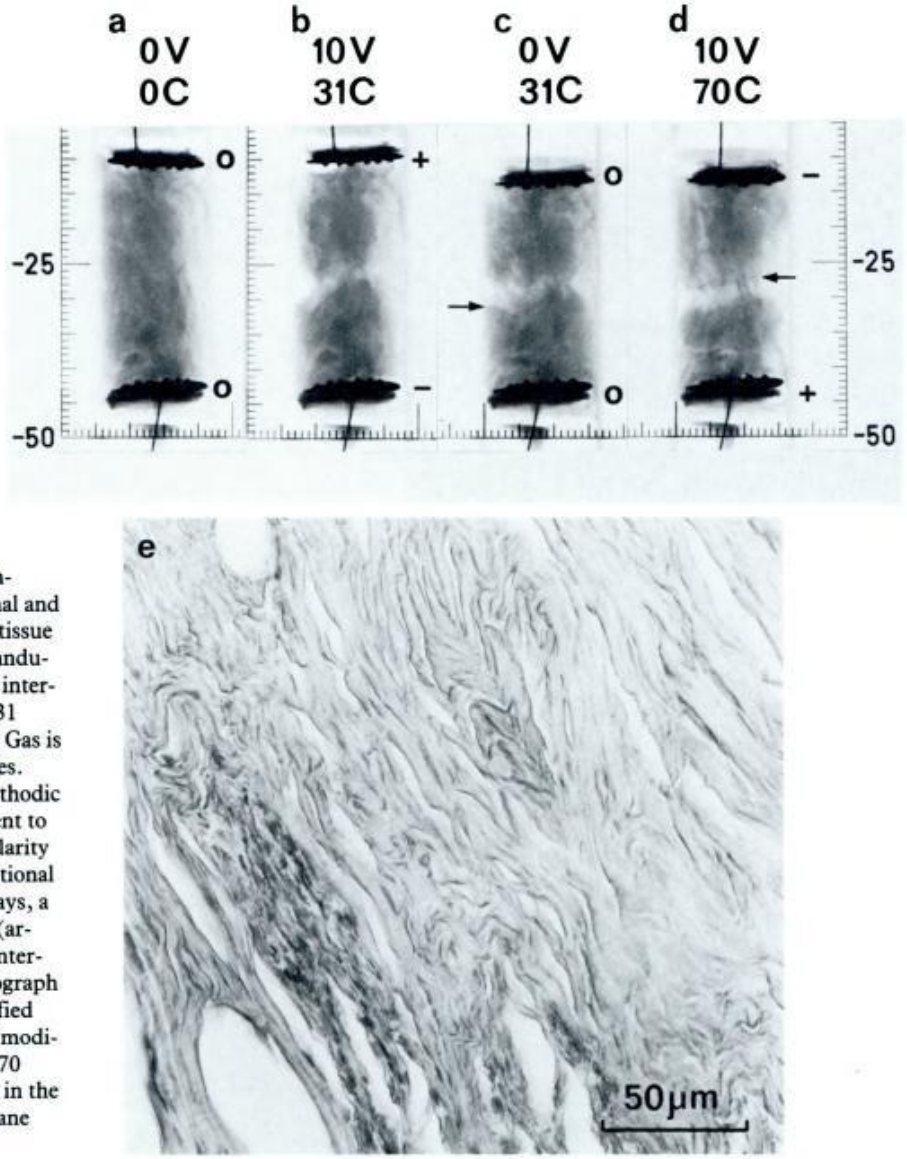

Fig. XVI: 37. Intermediate membranes produced by unidirectional and reversed direct current. (*a*) Soft tissue radiograph of original fat and glandular breast tissue material. (*b*) An intermediate fat zone appeared after 31 coulombs at 10 V for three days. Gas is produced at the electrode surfaces. (*c*) After removal of gas a thin cathodic membrane (arrow) is seen adjacent to the intermediate fat zone. (*d*) Polarity was then reversed. After 39 additional coulombs over a total of seven days, a new cathodic membrane is seen (arrow) at the opposite side of the intermediate fat zone. (*e*) Photomicrograph shows to the right dense, "modified cathodic" and to the left dense "modified anodic" fibrous tissue after 70 coulombs. Note fibroblasts only in the left "anodic" part of the membrane (van Gieson stain).

around the edge of the fibrous membrane in Fig. XVI: 35 *b*. The fat cells are small and somewhat shrunken around the edge of the membrane. Another detail of interest in Fig. XVI: 35 *a*, *b* is a presence of some small intracellular "bushes" situated in the tissue at a certain distance (0.2–0.3 mm) from the fibrous membrane along its anodic side in (*a*) and around its edge in (*b*). The small "bushes" contain birefringent material but do not stain for calcium ions with Alizarin (*b*). We will return to this problem in Section S, which deals with experimental production of microcalcifications.

In *fully developed cathodic fibrous tissue* from breast fat, the mesh-like structures are thickened and present crevices with irregular, birefringent borderlines. Such fibrous tissue never shows fibroblasts (Fig. XVI: 36 *a*).

Fully developed anodic fibrous tissue from breast fat shows a compact, homogeneous tissue of irregular, delicate, birefringent fibres. Fibroblasts may be completely absent in large parts of the tissue or are present in local conglomerations or are sparsely scattered in the tissue (Fig. XVI: 36 *b*, same slide preparation as Fig. XVI: 36 *a*).

The effect of reversal of polarity on membrane formation is shown in Fig. XVI: 37. Human breast fat with some glandular tissue was used. Its radiographic appearance before application of current is shown in Fig. XVI: 37 *a*. Ten volt electrode potential was applied. After 31 coulombs an intermediate fat zone is seen and some gas formation at the electrode surfaces (Fig. XVI: 37 *b*). The electrodes were then moved closer together for removal of the gas pockets and to improve electrode contact (Fig. XVI: 37 *c*). A thin membrane-like structure is also seen at the previously

cathodic side of the fat zone (arrow). Ten volts were then applied with reversed polarity. After an addition of 39 coulombs, a new membrane-like structure can be seen at the new cathodic side of the fat zone (Fig. XVI: 37 *d*). One membrane structure was therefore obtained on each side of the fat zone of the specimen. Each of these membranes appeared as mixed anodic and cathodic types of fibrous tissue, as seen in Fig. XVI: 37 *e* (from the upper membrane of Fig. XVI: 37 *d*). This membrane shows to the right, cathodic fibrous tissue with irregular crevices and no cellular elements. To the left, anodic fibrous tissue shows a group of fibroblasts and small, atrophic fat cells, without cytoplasmic reticulum.

Knowledge about development of fibrous tissues remains in many respects incomplete. Even the origin of fibroblasts is not known with certainty. They are thought to derive from proliferation of local connective tissue, metaplasia of "wandering cells" or even from metaplasia of endothelial cells of the capillaries. Ross and Benditt (81) have claimed that fibroblasts may develop from a multipotential cell of haematogenous origin. Little is known of the factors which induce and stimulate fibroblast production in wound healing. It is claimed that substances liberated at the development of necrosis may possibly induce fibroblast proliferation.

From the present experiments it is already evident that the flow of current over a "dead" piece of tissue may lead to new structural formations as fibrous tissue. Ordinarily, we look upon such developments as reactions of a living tissue. It is further remarkable that two different kinds of fibrous tissue develop from the same material and that "fibroblasts" appear in the anodic but not in the cathodic fibrous tissue. Furthermore, the "fibroblasts" in the anodic, fibrous tissue may be completely absent in large parts of this tissue. In other parts they are densely packed or sparsely scattered.

These observations must raise the possibility that fibroblasts may not be necessary for the production of fibrous tissue. A search of the literature has yielded no conclusive proof that fibrous tissue is produced only by fibroblasts. Fibroblasts are thought to produce *polypeptide precursors of collagen* in their cytoplasm in association with membrane-bound ribosomes (81). Confusion still remains regarding the cytological steps between the intracellular synthesis of collagen precursors and the appearance of extracellular collagen fibrils. This question becomes even more timely in attempts to explain the experimental results here presented. Mechanisms associated with production of fibrous tissue have long been known to be complex. We will therefore offer only a preliminary view toward explaining the experimental results.

It seems highly improbable that fibroblast-like cells present only in the vicinity of the anode should have the capacity to produce large amounts of "cathodic fibrous tissue" far away (about 2–3 cm) from their location in an isolated specimen of fat tissue. The quantity of cathodic fibrous tissue also increased toward the cathodic electrode. The quantity of "anodic fibrous tissue" increased toward the anodic electrode. The fibroblast-like cells also appeared in groups with relatively small amounts of anodic fibrous tissue between the cells in certain regions. In other anodic regions large amounts of anodic fibrous tissue between the cells in certain regions. In other anodic regions large amounts of anodic fibrous tissue were present without any fibroblast-like cells.

It is possible to explain the experimental results if we assume that an intracellular and extracellular precursor for cathodic and anodic fibrous tissue were already present when the electrophoretic process was started. Under the influence of direct current the precursor of fibrous tissue then transformed into cathodic and anodic fibrosis. The formation of specific cathodic and anodic fibrous tissues is preliminarily explained as a result of cathodic alkalinity and anodic acidity during the electrically induced transformation of the precursor material. The experimental results lead in this view to the logical conclusion that the precursor(s) for cathodic and anodic fibrous tissues must have been already produced by normal cells. A similar process also appears to occur adjacent to endothelial cells, which in their basement lamina contain fibrous structures.

The exposure of cells to direct current can lead to considerable cellular transformations (Chapter XIV). The development of fibroblasts may therefore be explained as a result of such electrogenic transformation of cells. The experimental results suggest further that the presence of fibroblasts in fibrous tissue does not necessarily prove that these cells are the only cellular element to which can be attributed the ability to produce precursor material of fibrous tissue. The experiments also indicate that *fibrous tissue develops from intracellular and extracellular precursor material under the influence of direct current.*

The production of scar tissue in healing processes is still poorly understood. For increased understanding of these processes in the future, it will be necessary to consider the role of spontaneous, endogenous direct currents in tissue over BCEC channels.

N. Closed circuit production of anodic tissue channels

Anodic and cathodic channels can also be produced in fat tissue by passing electric current over a tissue

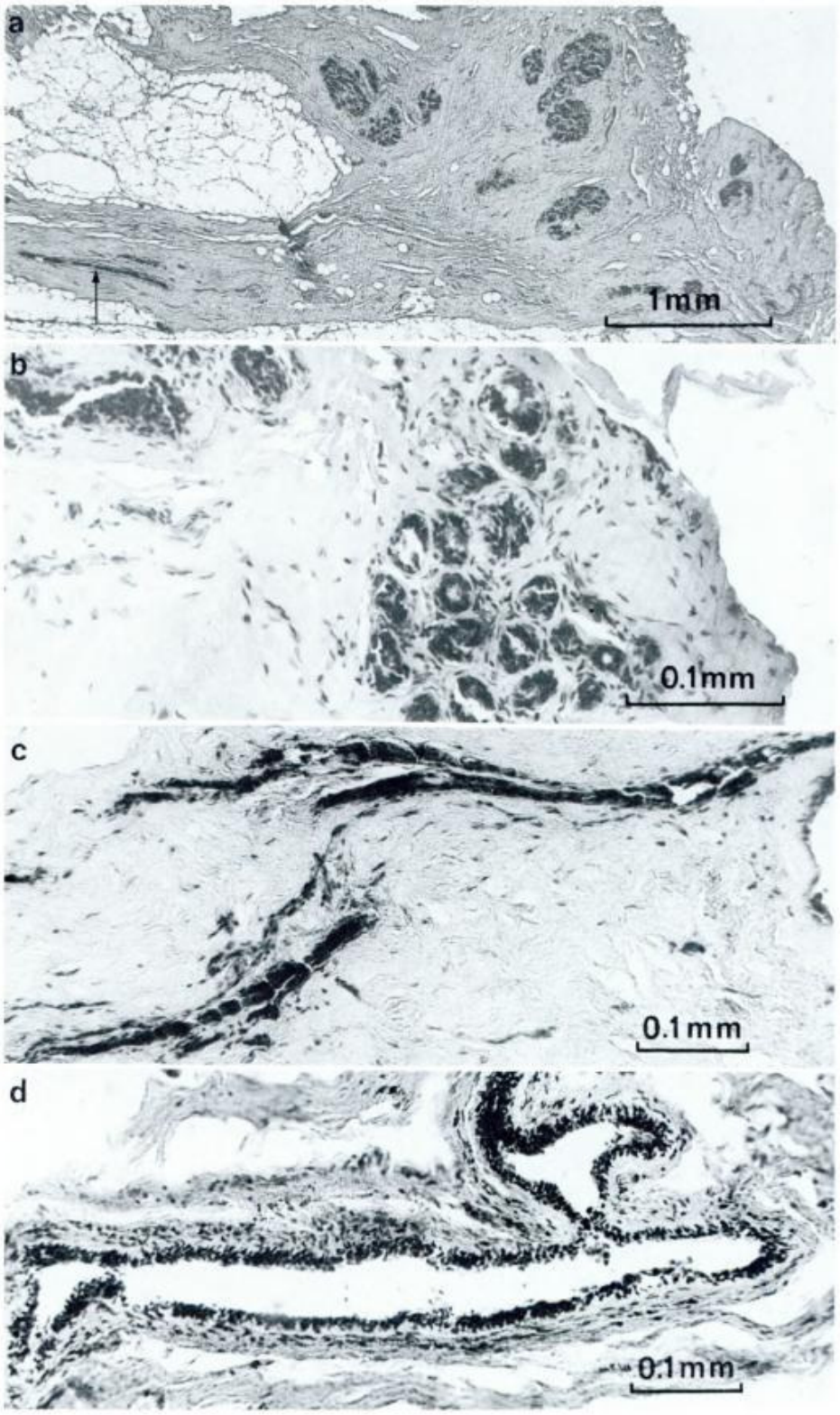

Fig. XVI: 38. In vitro production of anodic channels in human breast fat (10 V, 30 coulombs, 17 days). (*a*) Overview of newly developed anodic fibrous strand. Same experiment as shown in Fig. XVI: 30. Anode to the right. In the fibrous tissue, "islands" of cells are seen (right part of Fig.) as well as dark "rods" (arrow). (*b*) Magnified view of groups of cells, some of which form a central lumen. The "islands" of cells are surrounded by circular fibres and fibroblasts. (*c*) Lenthwise section of a rodlike collection of cells partly forming a primitive lumen. (*d*) Fully developed channel, lined with epithelial cells in the same specimen (see further Figs. XVI: 39, 40 and text). (*a–c*) Haematoxylin-eosin, (*d*) van Gieson stain.

sample. The possibility of producing anodic channels is presented in this section and cathodic channels in Section O. A discussion on possibilities of producing vascular channels follows in Section P.

The photomicrographs of Fig. XVI: 38 *a* show experimentally produced anodic fibrous tissue in breast fat (10 V, 30 coulombs). The anode had been positioned to the right (same specimen as shown in Fig. XVI: 30 *c*). In the right part of the specimen (close to the anode) some dark structures are seen as rounded

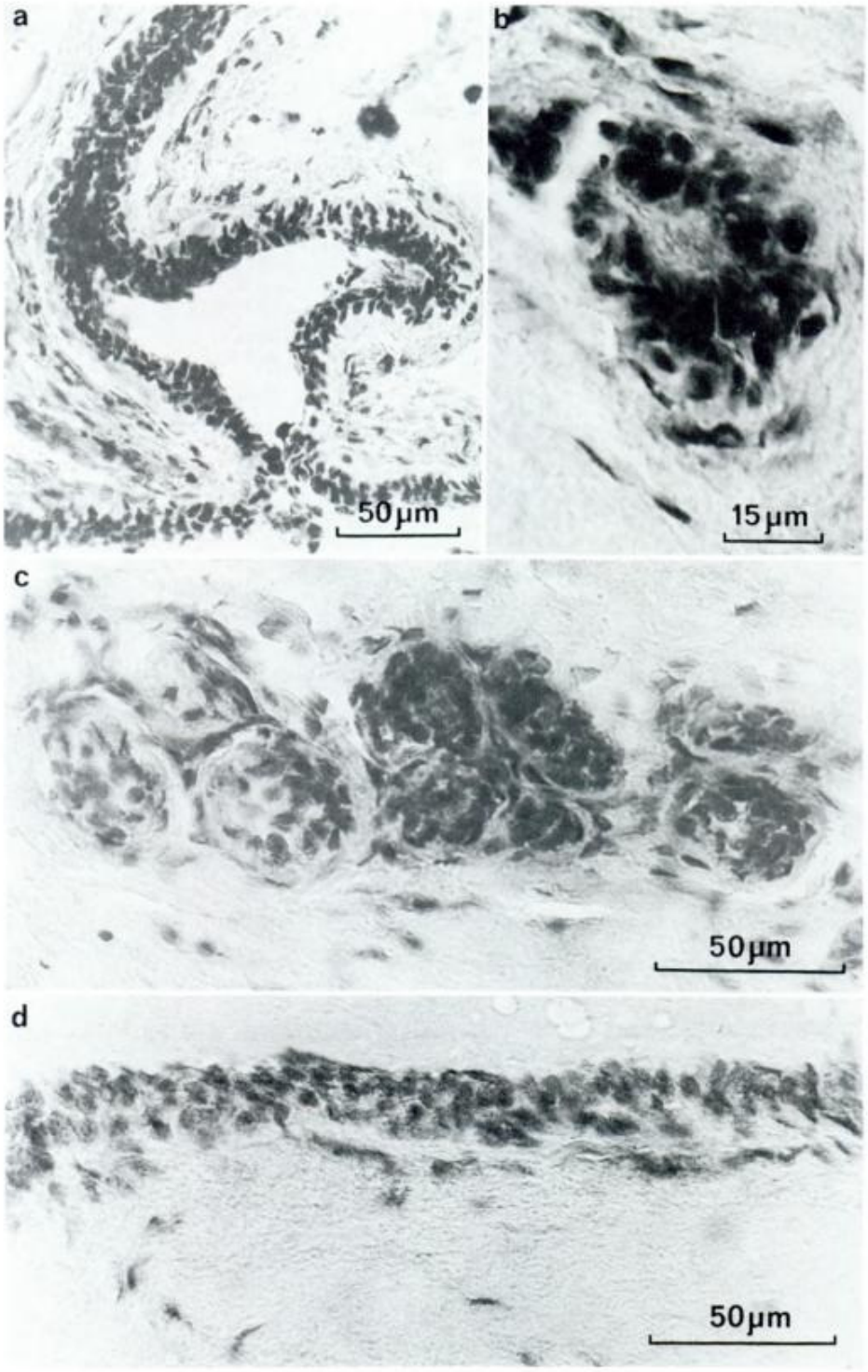

Fig. XVI:39. In vitro production of anodic channels in human breast fat (10 V, 30 coulombs, 17 days). (*a*) Structural arrangements of cells of the ductal channel shown in Fig. XVI: 38 *d*. (*b*) Cells of epithelial type form ring-like structures tending to form a lumen. (*c*) Several "islands" of epithelial cells, interpreted as anodic "rods" surrounded by circularly arranged fibrous tissue. (*d*) Lengthwise section of "rod" of epithelial type of cells (see further Fig. XVI: 40).

"islands" or groups of material. To the left are rod-like dark structures (arrow). Further analyses of the "islands" (Fig. XVI: 38 *b*) show collections of cells, some of which form a ring with a light centre. They are surrounded by circularly arranged fibrous tissue containing "fibroblasts". The dense groupings of cells represent cross-sections of "rods" and the ring-shaped groups of cells cross-sections of primitive channels. A lengthwise sectioned, tortuous, partly open "rod" is shown in Fig. XVI: 38 *c*. A channel structure with a well-developed lumen is shown in Fig. XVI: 38 *d*. Some details of these structures are further illustrated in Fig. XVI: 39. Thus, the arrangement of the epithelial cells of the partly well-developed channel is shown

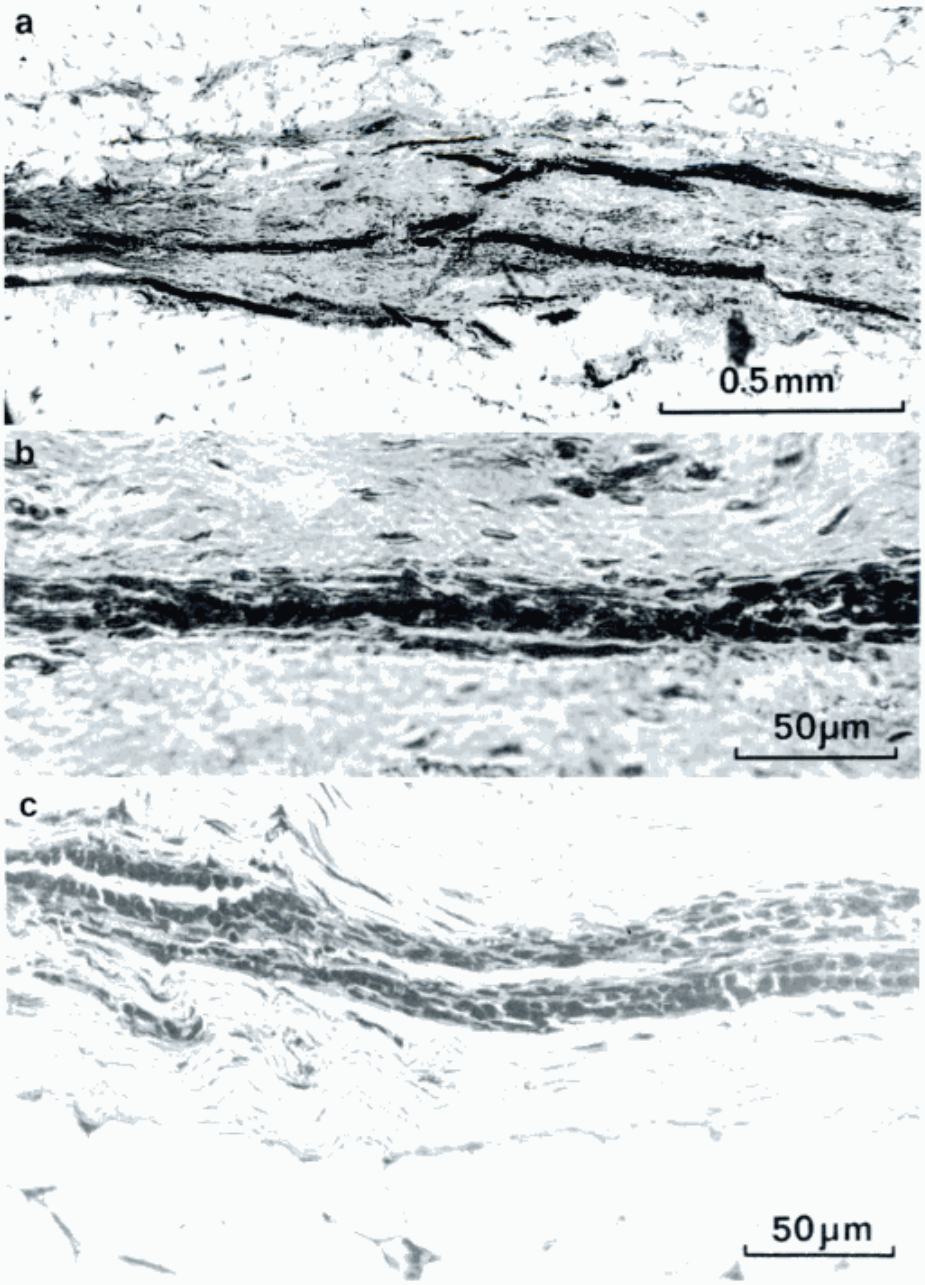

Fig. XVI: 40. In vitro production of anodic channels in human fat tissue (10 V, 30 coulombs, 17 days). (*a*) "Rods" develop in the same direction as the fibrous structures. (*b*) They are solid and consist of cells of the same type as shown in Fig. XVI: 39 *c*, *d*. They are surrounded by fibrous tissue containing "fibroblasts". (*c*) Certain parts of such "rods" appear as if they are forming a lumen (van Gieson stain).

in Fig. XVI: 39 *a*. Circular arrangement of epithelial cells forming a lumen is shown in Fig. XVI: 39 *b*, while circular arrangement of fibrous material around collections of cells is shown in Fig. XVI: 39 *c*. A detail of a lengthwise sectioned "rod" is shown in Fig. XVI: 39 *d*. It contains an epithelial type of cells.

We are now approaching an important problem: were the groups of cells in the fibrous tissue already present before the electrophoretic treatments, or do they represent newly formed structures? More observations are evidently necessary before we can discuss this question.

A fibrous anodic strand with several well-developed, dark rod-like structures is shown in Fig. XVI: 40 *a*. The "rods" are oriented in the same direction as the fibrotic strand. They are only encountered in anodic, never in cathodic fibrosis. As seen in Fig. XVI: 40 *b*, these "rods" consist of cellular elements. In the centre they are rounded like the cells shown in Fig. XVI: 39 *c*, *d*. Some "cells" have the appearance of fibroblasts and are preferably located outside the rounded "cells". Certain portions of such "rods" show initial development of lumina of channels (Fig. XVI: 40 *c*). Figs. XVI: 38–40 were all obtained from the anodic part, close to the electrode, of the specimen shown in Fig. XVI: 30. This sequence illustrates the development of

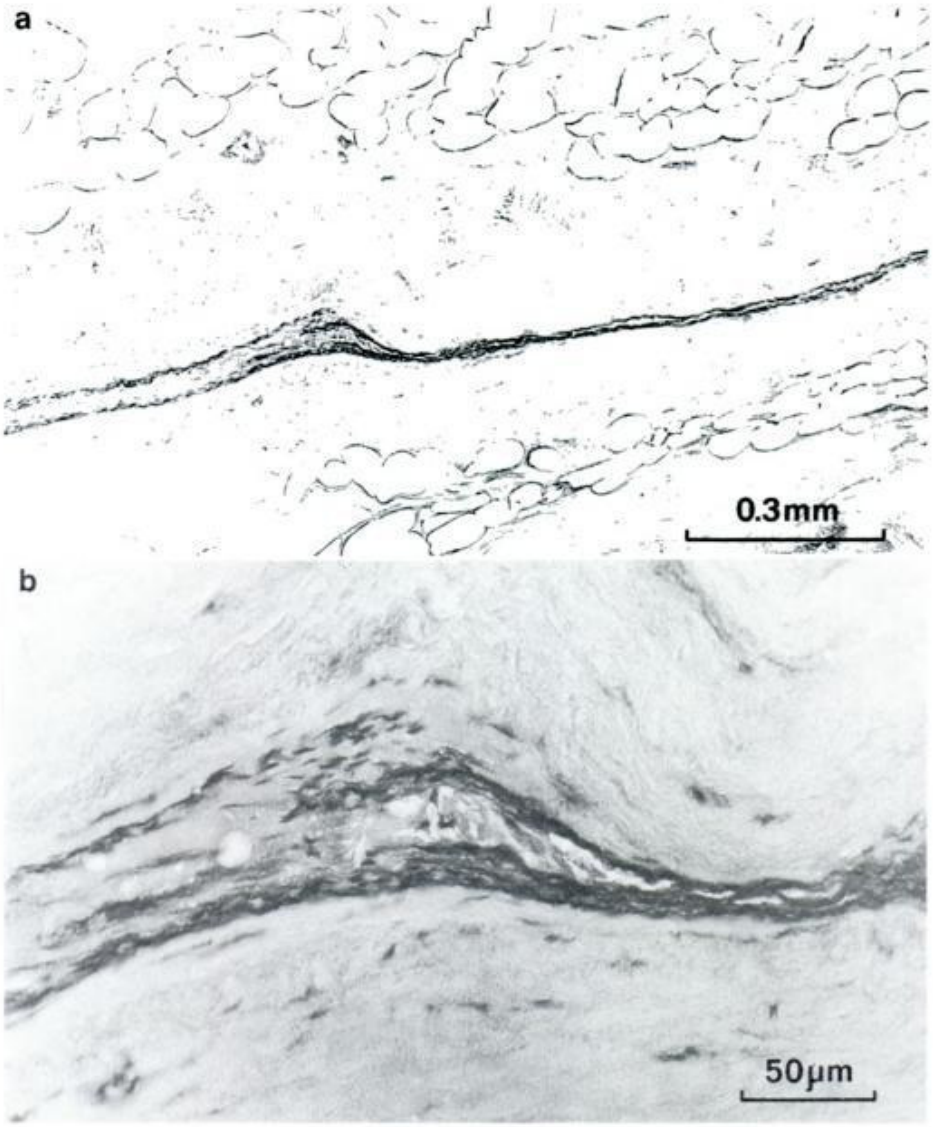

Fig. XVI:41. In vitro production of anodic channels in human breast fat by reversal of flow of current. Initial dose: 20 V, 30 coulombs during 3 days. Thereafter the current was reversed: 20 V, 8 coulombs, 7 days. (*a*) Overview of a primitive channel in fibrous tissue in the newly anodic side of the specimen. Cellular elements tend to arrange forming a tube. (*b*) This structure contains cells which look like fibroblasts. No cells of epithelial type are present (haematoxylin-eosin stain).

channels which look very much like adenotic formation of primitive galactophores in breast tissue. We will soon return to these problems. It is, however, necessary first to describe some other anodic structures which were produced with a slightly modified technique.

Human fat tissue was first treated with 20 V, 30 coulombs for 3 days. The current was then reversed (20 V, 8 coulombs, 7 days). In the now anodic side of the specimen (Fig. XVI: 41) structures were obtained consisting of delicately arranged rows of fibroblast-like cells, surrounded by dense anodic fibrous tissue. Fig. XVI: 41 *a* shows an overview of such a structure, which evidently tends to form a channel. The magnified view of Fig. XVI: 41 *b* shows no rounded, epithelial type of cells, as in the previously described anodic channel. Cross-sections of well-developed structures forming lumina and containing fibroblast-like cells in their walls are shown in Fig. XVI: 42 *a, b*. The dense anodic type of newly formed anodic fibrous tissue surrounds these structures. These new channels appear to be clearly different from the channels which look like primitive galactophores. Perhaps these thin-walled channels with fibroblast-like cells represent early stages of vascular channels.

In order to establish whether similar anodic structures can be produced by direct current in fat of a tissue other than breast, *fresh abdominal subcutaneous fat* was obtained during surgery on three otherwise normal patients with inguinal hernias. These tissues were treated like the samples of breast fat tissue. Ten volts were applied between the platinum electrodes to the specimens (2–3 cm long) of abdominal fat tissue for two to five weeks. As in the breast fat studies, the initial current of a few mA decreased rapidly to a few microamperes during the following hours. Still,

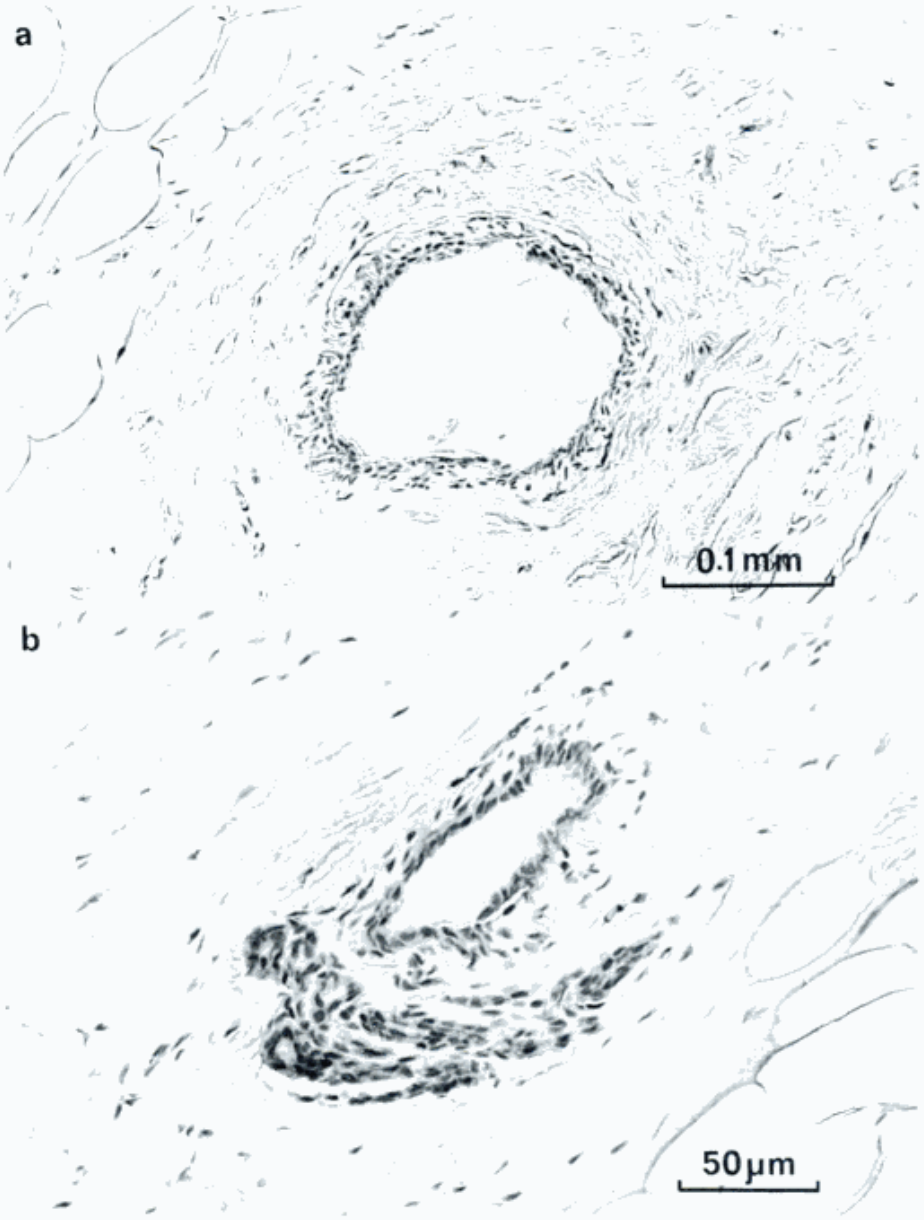

Fig. XVI: 42. In vitro production of anodic channels. (*a*, *b*) Cross-sectioned channels, interpreted to contain the same type of cells in their walls as the tubular structures of Fig. XVI: 41. Tubular channels of this type could possibly represent the anodic phase of early development of vessels (haematoxylin-eosin stain).

changes in the radiographic appearance could be seen during the following weeks. It might be mentioned in this connection that fat tissue undergoing electrophoretic treatment even for weeks shows no signs of bacterial decomposition, which otherwise takes place after a few days in untreated specimens.

Developed anodic fibrous tissue strands of abdominal fat were found to contain scattered fibroblast-like cells (Fig. XVI: 43 *a*) or centrally located groups of cells in the fibrous tissue (Fig. XVI: 43 *b*, *c*). Rod-like structures could also be identified but of another appearance than in breast fat. Thus, in Fig. XVI: 44 *a* a small structure is seen to the left, showing a central dark, irregular line (arrows). To the right in Fig. *a*, a "channel" is seen with an open lumen (*X*) and fibroblast-like cells in the wall, which in turn is surrounded by some fibrous material. Fig. XVI: 44 *b* shows another "channel" without fibroblasts, surrounded by thick bluish-stained fibrous material (haematoxylin-eosin). This channel was found in the mid-part of the specimen. A "channel" structure from the cathodic part of the same specimen is seen in Fig. XVI: 44 *c*. This channel shows only a wall of fibrous tissue without any cellular elements or differently stainable layers.

We are now almost ready to discuss the possibility that the structures described are induced by the current applied to the tissue specimens. For the moment, some of the indications pointing toward this possibility will be summarized. The objection that the structures

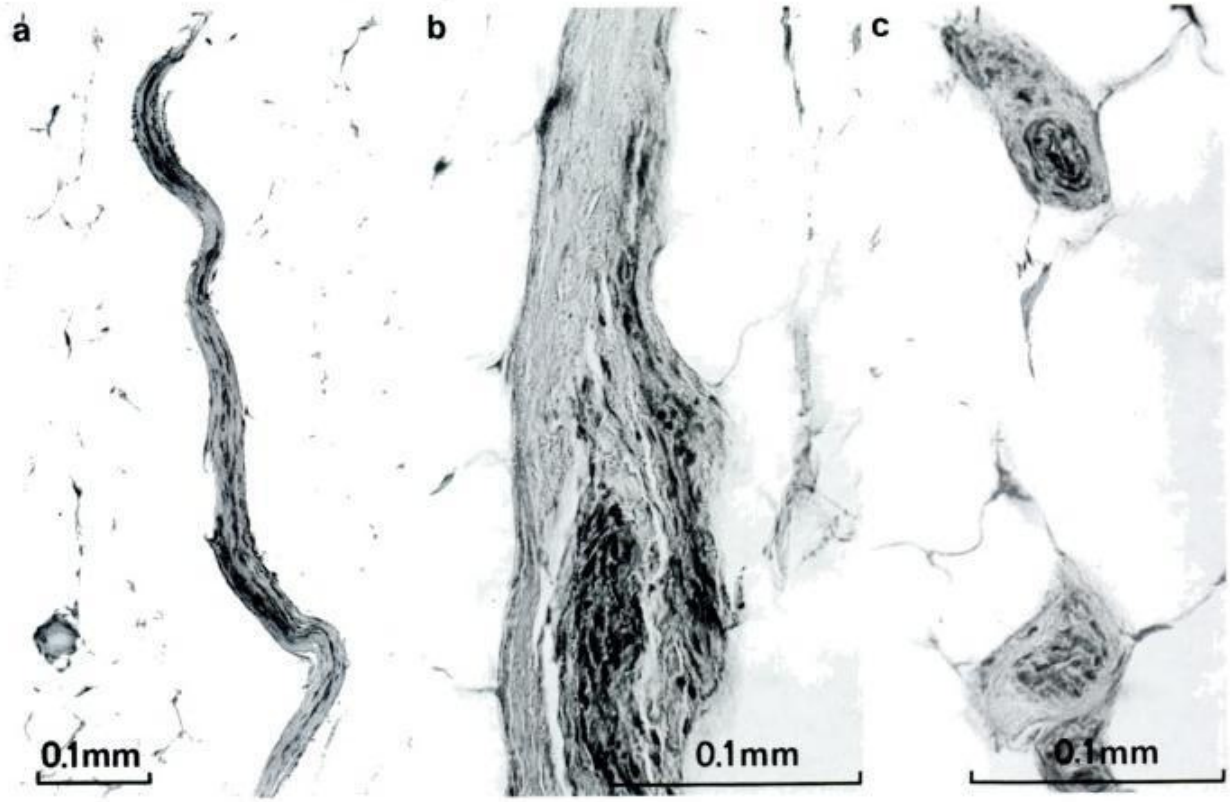

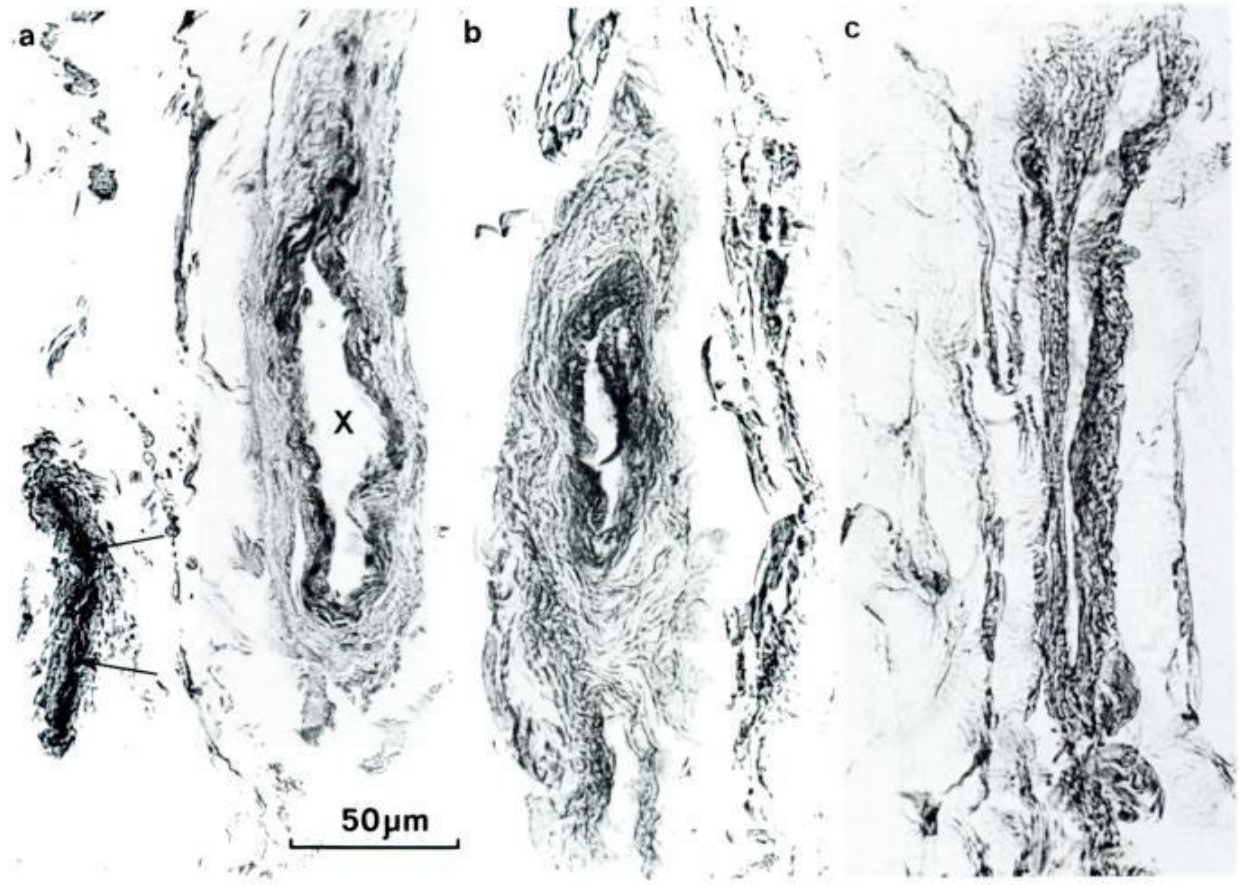

Fig. XVI: 43. In vitro production of anodic fibrosis in human abdominal fat tissue. 10 V, 1–2 microamperes for 30 days produced anodic fibrous tissue strands with (*a*) scattered fibroblasts, (*b*) collections of fibroblasts along a new fibre, (*c*) fibroblasts located centrally in the fibrous tissue (haematoxylin-eosin stain). See also Fig. XVI: 44.

described after treatment of fat tissue samples might have been present before the treatments is evidently not valid for the development of anodic and cathodic fibrosis. The anodic and cathodic fibrous tissues are histologically of distincly different appearances. These tissues are furthermore radiographically different and developed clearly during the electrophoretic treatments, as seen in serial radiographs. The rod-like, tubular and suggested vascular structures in the fibrotic material, on the other hand, have a spatial distribution and size which make it difficult or impossible to detect them by radiographic techniques. Different evidence indicates, however, that the structures described may be newly formed. (*a*) The rod-like and tubular structures, lined by cells, were not found in no specimens of untreated fat from the same breast tissue. (*b*) The tubular structures with an appearance similar to that of primitive galactophores have been found only in the treated samples in connection with newly developed fibrous material and (*c*) have been found only in anodic fibrous tissue. (*d*) When they are seen in lengthwise sections, they are oriented in the same way as the fibrous strands. (*e*) "Channels" of only fibrous material, containing fibroblast-like cells, have been encountered only in anodic parts of electrophoretically treated breast fat and abdominal fat. (*f*) "Epithelial cells" of primitive "galactophores" are encountered only in anodic fibrous tissue.

The possibility that direct current may induce modifications of tissues and cells can not be excluded, on the basis of the data thus far. If this possibility is correct and if we were also able to follow a preferential pathway for current through the tissue from the anodic to the cathodic side of the specimen, then we should be able to observe a gradual change in the modifications of the tissue. This observation will shortly be undertaken, but first we must try to identify cathodic structures which may correspond to the anodic structures described.

Fig. XVI: 44. In vitro production of "channels" by electrophoretic treatment of human abdominal fat tissue. Same tissue sample as in Fig. XVI: 43. (*a*) Rod-like structure (arrows) in anodic fibrous tissue adjacent to a structure interpreted as a cross-sectioned channel with a well developed lumen (X). The "channel" has cells in its wall and is surrounded by circularly arranged fibres. (*b*) "Channels" from the mid-part of the same specimen show no fibroblasts in the dark (bluish) stained wall, which is surrounded by a thick layer of fibrous tissue. (*c*) "Channel" from the cathodic part of the same specimen. No fibroblasts or particularly stainable layers are seen in the wall (haematoxylin-eosin stain).

O. Closed circuit production of cathodic tissue channels

In the cathodic field in electrophoresis of breast fat tissue, many of the cellular elements successively disappear. Instead, fibrous tissue develops which does not contain fibroblasts. Other structural transformations can, however, also be recognized. In order to demonstrate the relative differences between anodic and cathodic transformation of fat tissue, the cathodic changes will, as far as possible, be demonstrated in the same material as was used for demonstration of the anodic changes.

The gradual development of cathodic atrophy of fat cells, reticular structuring of their cytoplasm and formation of cathodic fibrosis were described in Section M (Fig. XVI: 33). Many cells in the anodic fibrous tissue were also described to form groups surrounded by fibrous enclosures (Figs. XVI: 38, 39). These anodic grups can be compared with strange-appearing groupings of "cells" in cathodic tissue (Fig. XVI: 45). The survey in Fig. XVI: 45 *a* shows multiple cross-sectioned and one lengthwise sectioned grouping of "cells" in cathodic fibrosis. The enlarged view in Fig. XVI: 45 *b* shows small circularly arranged fat "cells" inside a fibrotic enclosure around each group of "cells". The individual "cells", which represent new structural elements, each show a central, condensed material like a cellular nucleus. Each group of "cells" contains in its centre an "extracellular" collection of material, which looks like a local accumulation of fibrous tissue (*X*) and which extends as radiating structures between the "cells" to the circular fibrous sheet surrounding each group of "cells". Between the groups of "cells" (Fig. XVI: 45 *b*) are also seen large "cells", some of which look empty. Some have the appearance of the grouped "cells" and contain a "nucleus". An enlarged view of a lengthwise sectioned "core" is shown in Fig. XVI: 45 *c*. The groups of "cells" of this type may disappear gradually (Fig. XVI: 46 *a*). Another line of transformation of small "cells" contains blue staining of their cytoplasm with haematoxylin-eosin (Fig. XVI: 46 *b*).

The development of cathodic channels by disap-

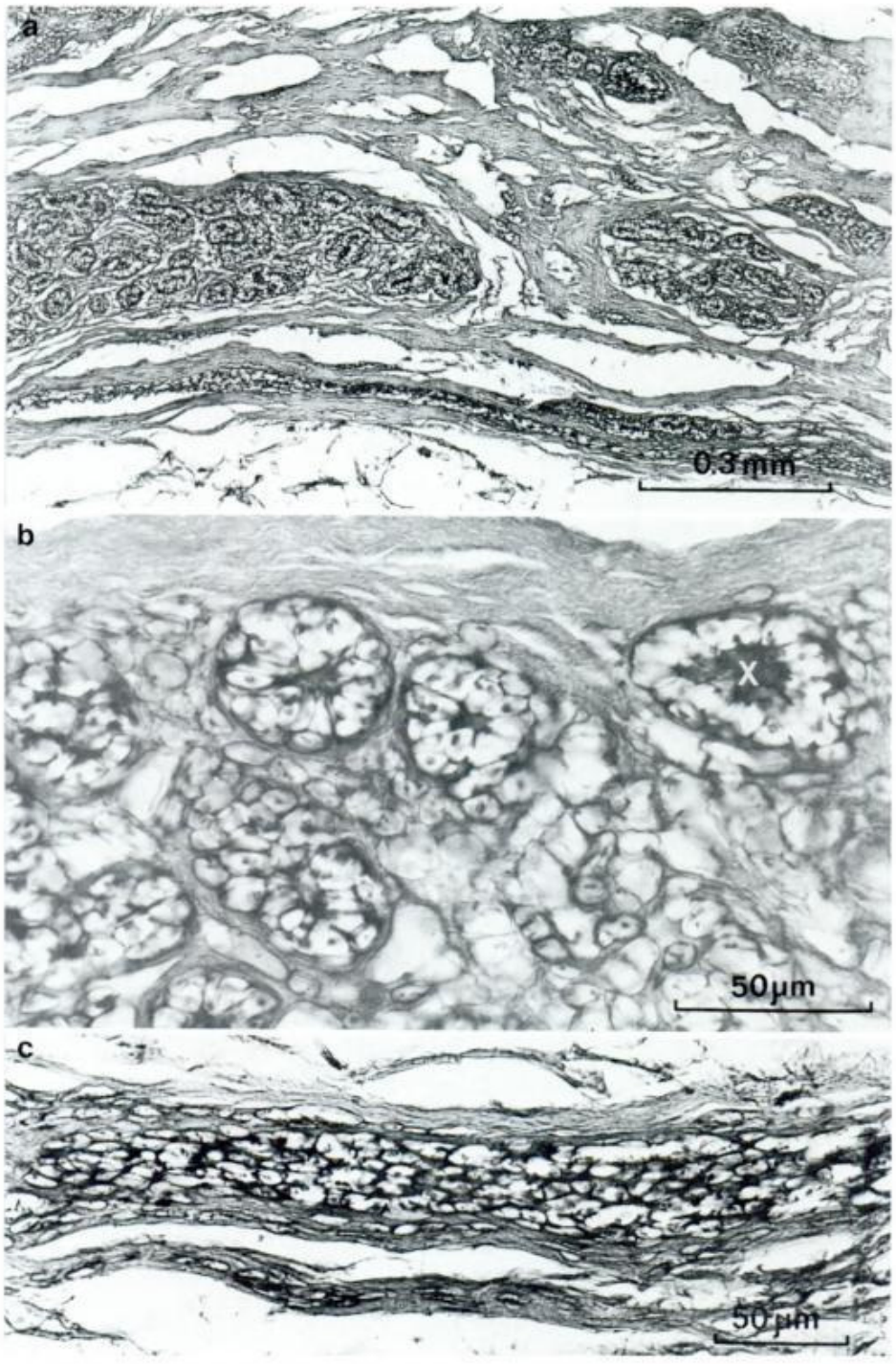

Fig. XVI: 45. In vitro production of cathodic channels in human breast fat (10 V, 30 coulombs, 17 days). (*a*) Overview of newly formed cathodic fibrosis, containing collections of transforming fat cells. (*b*) "Cells" of neoplastic appearance are arranged in groups inside a fibrous enclosure. The "cells" contain dark material in the centre. The middle of each group contains a possibly fibrous material (X) with radiating structures which extend to the fibrous enclosure. The groups are assumed to represent cross-sectioned "cores" of transforming fat cells. (*c*) Lengthwise section of a "core" of fat cells (haematoxylin-eosin stain).

pearance of transformed fat "cells" is illustrated in Fig. XVI: 47. The central location of a "core" of small transforming fat cells in a new-formed, cathodic fibrous strand is seen in Fig. XVI: 47 *a*. Its right part shows the formation of a primitive lumen. Fig. XVI: 47 *b* shows the small cells containing "nuclei"

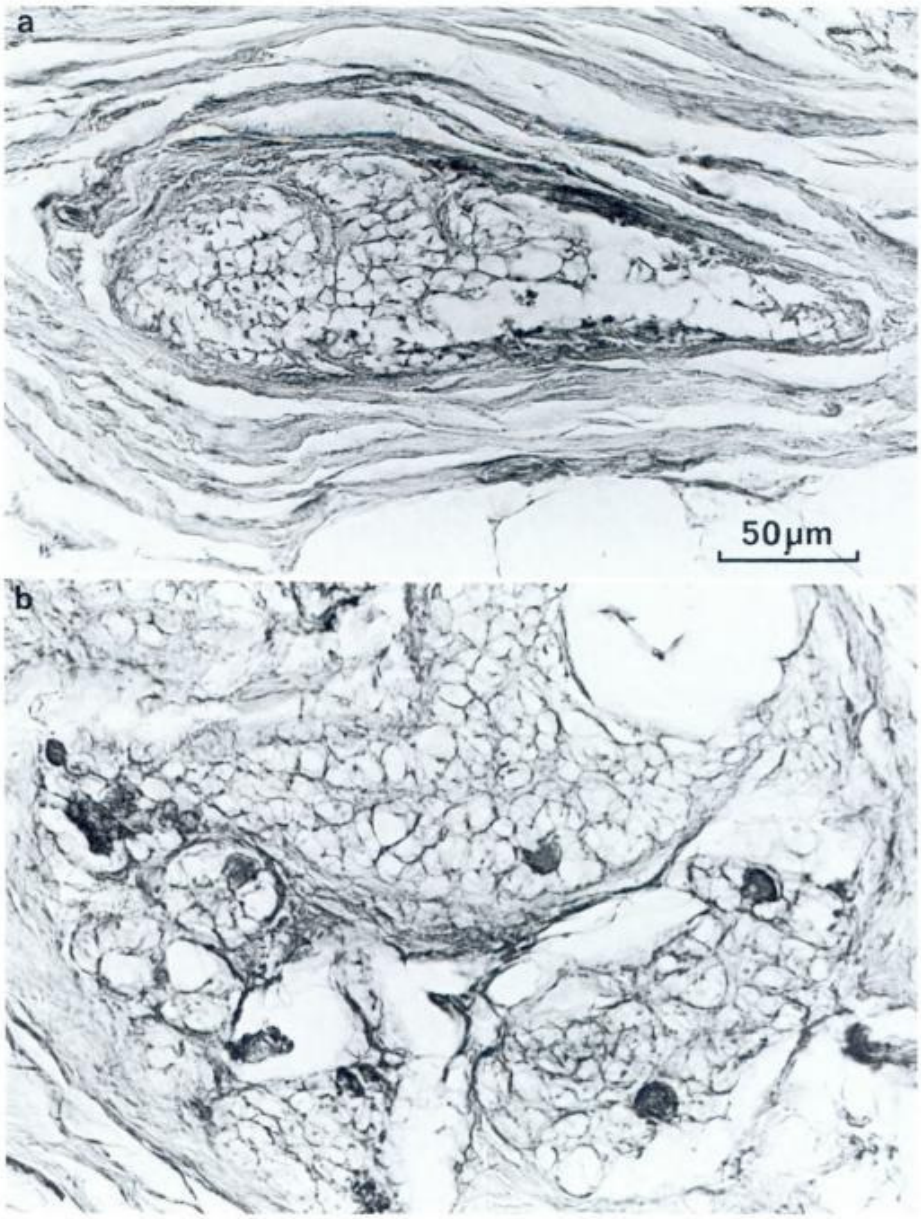

Fig. XVI: 46. Two lines of development of transformed cathodic fat "cells". (*a*) The small cells with a central dark "nucleus" may gradually dissolve, leaving a lumen surrounded by a fibrous wall without fibroblasts. (*b*) Some of the small "cells" forming groups contain bluish (dark) cytoplasm (haematoxylin-eosin stain).

and disappearing cellular walls. A newly formed cathodic channel is seen in Fig. XVI: 47 *c, d*. This channel does not contain any cells in its "walls" or in the surrounding fibrous tissue. The wall of the channel takes relatively more blue stain with haematoxylin-eosin than does the surrounding fibrous tissue. The inner surface of the channel is lined with a birefringent sheet (arrows, Fig. XVI: 47 *d*).

Other structural developments leading to channels in the cathodic fat tissue have also been observed. These will be described in connection with a discussion on the possible role of flow of current over BCEC pathways in angiogenesis, Section Q. We will now continue to analyse the critical question of whether the structural modifications in the anodic and cathodic fields have developed under the influence of the applied current or if they were present in the fat tissue specimens before treatment.

P. Transformation of tissue and cells across the intermediate zone between anode and cathode

We have now described some structural characteristics of "pure" anodic and cathodic breast fat tissue in Sec-

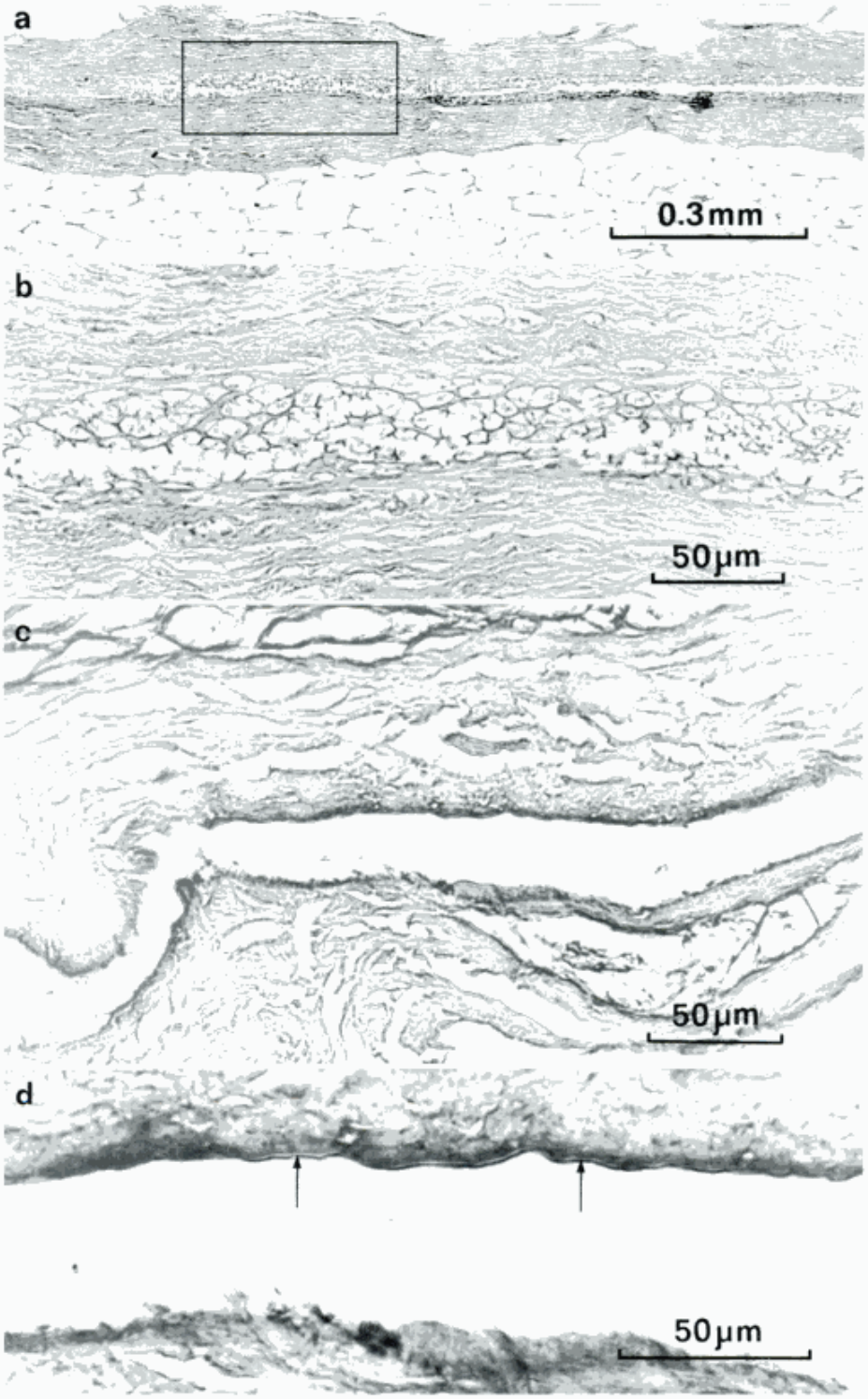

Fig. XVI:47. In vitro production of cathodic channels in human breast (10 V, 30 coulombs, 17 days). (*a*) Overview of fibrous strand with central "core" of atrophying fat cells forming a channel. (*b*) Magnified view shows atrophic fat cells with centrally located dark material. The lysing of the walls of many of these cells is evident. (*c*) Well developed cathodic channel in fibrous tissue. No cells of any kind are present. The walls of the channel are more blue-stained than surrounding fibrous tissue. (*d*) The inner surface of the wall is lined with a birefringent thin structure (arrows) (haematoxylin-eosin stain).

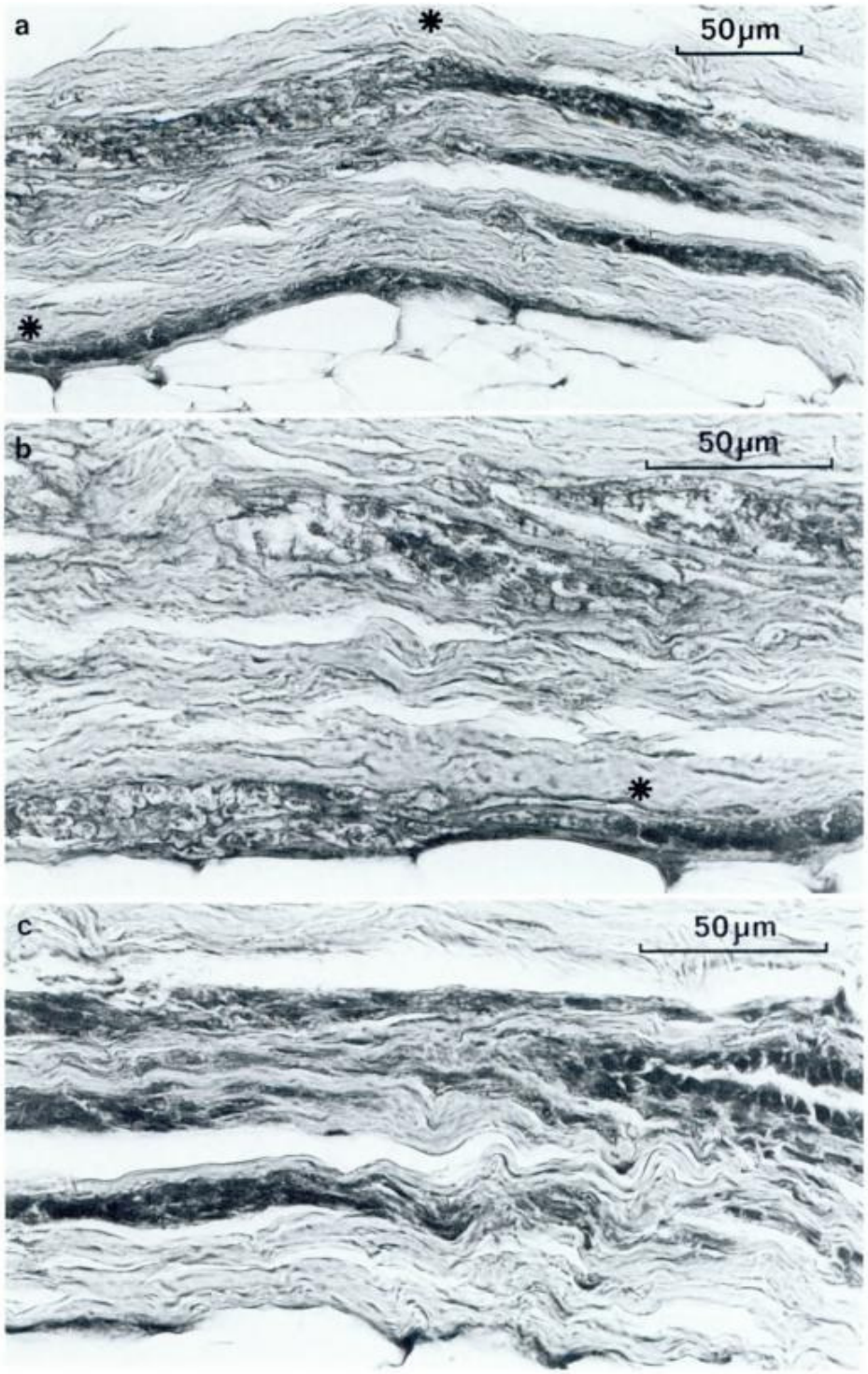

Fig. XVI: 48. The transition between cathodic "cores" (left) and anodic "rods" (right) in the intermediate zone between the cathodic and anodic fields of electrophoretically treated human breast fat (10 V, 30 coulombs, 17 days). (*a*) Overview of the intermediate zone. Two transitions between cores and rods are indicated by asterisks. (*b*) Enlarged extension of the zone in the cathodic direction (left of *a*) (see also Fig. XVI: 45 *a*). (*c*) Enlarged extensin of the zone in the anodic direction (right of *a*) (see also Fig. XVI: 40 *c*). The cathodic core contains light cells with multiple dots (*a*, *b*) and the anodic rod contains dark small cells (*a*, *b*, *c*). These cells develop gradually into larger round or cubical cells of epithelial type outlining a lumen (*c*, to the right) (haematoxylin-eosin stain).

tions N and O. The appearances of these structures differ considerably from each other. If they are the result of the current applied over each specimen, a continuous transition between the structural changes should be present in an intermediate zone between "pure" anodic and cathodic transformations. Anodic "rods" and cathodic "cores" extend along newly formed anodic and cathodic fibrous strands. "Rods" and "cores" should then have some connections in the fibrous tissue. A serach of serial sections was therefore undertaken to find the transition between "rods" and "cores" in an intermediate zone between anodic and cathodic tissue. This task proved not easy. A look at the direction of newly formed fibrous tissue (e.g., Fig. XVI: 30) shows that it develops as curved or crooked extensions, which should correspond to preferential pathways for current between the electrodes. Therefore the intermediate zone for a specific pathway of current can not be found positioned in a predictable plane through the specimen. Different lengths of preferential pathways for current through the specimen and variations of conductivity should lead to different gradients of flow of current. Hence intermediate zones of transition between cathodic "cores" and anodic "rods" should appear in different sites in the tissues.

An overview of an intermediate zone between cathodic "cores" and anodic "rods" is shown in Fig. XVI: 48 *a*. After staining with haematoxylin-eosin, the anodic fibres showed dominating birefringence and the cathodic fibres a bluish colour under polarized light and a red filter. This difference facilitated recognition of the intermediate zone, which appeared to be irregularly extended. Already from Fig. XVI: 48, which represents a microphotograph taken under ordinary light, it may be evident that a cathodic "core" to the left continues into an anodic "rod" to the right (upper part of Fig. *a*). The left part of Fig. *a* is seen as an enlarged cathodic extension in Fig. *b*, and the right part of Fig. *a* as an enlarged anodic extension in Fig. *c*. In the upper part of Fig. *b*, transforming cathodic fat "cells" are seen. In the lower part of Fig. *b* another transition is seen between a cathodic "core" and an anodic rod. More in the cathodic direction the cathodic "cells" appeared as shown in Fig. XVI: 45 *a*. Finally, in Fig. XVI: 48 *c*, a gradual change of the anodic "rods" is seen as rather clearly visible cells of epithelial type which start to outline a lumen to the right. The continuation of this channel in the anodic direction was earlier shown in Fig. XVI: 40 *c*. The appearance of cathodic and anodic "cells" in the intermediate zone gives the impression of a gradual change of their appearance. The cathodic "cells" in this zone show multiple small dots in their "cytoplasm". Deeper in the cathodic field the "cells" contain one single structure which looks like a cellular nucleus (to the left in Fig. XVI: 46 *a*). The "cells" also appear in structured groups. The anodic "cells" in the intermediate zone appear spindle-shaped and stain dark-blue with haematoxylin-eosin. Deeper in the anodic field they become rounded or cubical, they increase in size and develop an epithelial appearance before they form tubular ducts (Figs. XVI: 38 *c*, 40).

At this point we may conclude that the easily detectable new formations of cathodic and anodic fibrosis are not the only structural changes which take place in a fat specimen under the influence of applied direct current. Very easily recognizable modifications of structures and cells are also obtained, which look like cellular and structural differentiation. The most complex structural components are also obtained relatively close to the two electrodes as cathodic and anodic groupings of newly formed complex structures. It is rather remarkable that these can be produced even in a piece of "dead" tissue. *Electric induction of structural modifications of cells and tissue is therefore possible. Corresponding spontaneous transformations in tissue should evidently also be possible over activated BCEC systems.* Given this background, we will next discuss the possibility of formation of new vessels over activated BCEC systems.

Q. Discussion on closed circuit development of vessels

The presentation of the material in Sections N, O and P indicates that different channels may develop in a tissue when exposed to weak direct current over a relatively long time, i.e., 2–5 weeks. Some of these channels were interpreted tentatively as possible early stages in the development of vessels in breast fat tissue (Figs. XVI: 41, 42) and in normal subcutaneous abdominal fat (Figs. XVI: 43, 44). These assumptions were made merely because blood and lymph vessels are the only remaining channels we would expect to develop in these tissues. A tentative explanation for early development of galactophores in breast fat was presented in the previous Sections N, O and P. A different approach will now be illustrated to identify, if possible, newly formed vessels after electrophoretic treatment of abdominal and breast fat tissue.

Newly formed vessels are common in granulation tissue and often around malignant tumours. In Figs. XVI: 49 and 52, comparisons will be made between endogenously developed pathological vessels and vessel-like structures from electrophoretically treated abdominal and mammary fat tissue. Thus, a thick-walled cathodic channel of multiple round cells and a central, narrow lumen is shown in Fig. XVI: 49 *a*, *b*. This

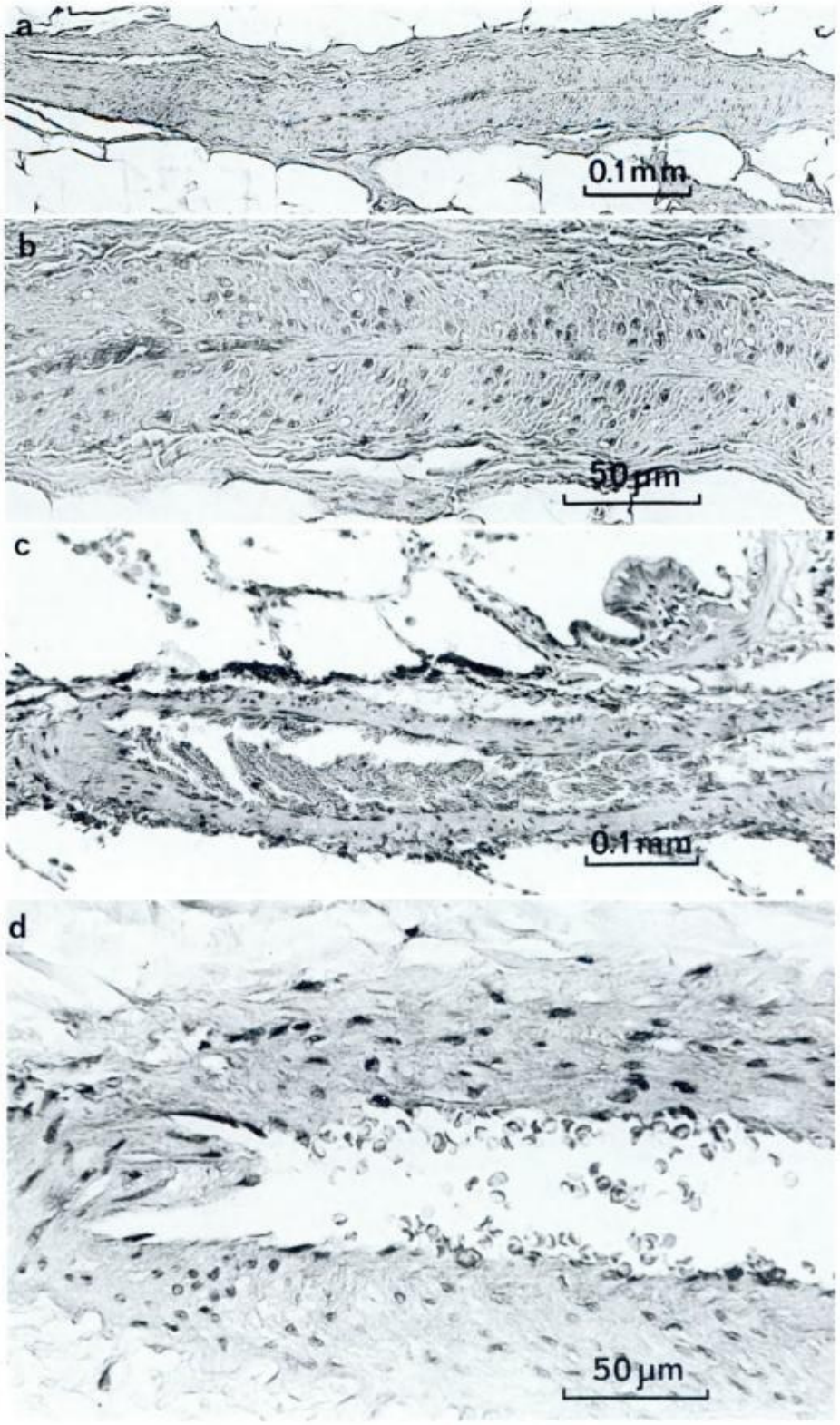

Fig. XVI:49. Comparison between electrophoretic, in vitro production of cathodic tissue channel in human abdominal fat and spontaneously developed pathological vessel around a carcinoma of the lung. (*a*) Overview of cathodic fibrous strand in human abdominal fat containing a partly open, centrally located, narrow channel. (*b*) The channel is lined with birefringent fibres and a thick layer of organized cells. (*c*) Overview of pathological vessel in the lung adjacent to a carcinoma. (*d*) The cellular components in the wall of the vessel appear similar to the newly formed structure seen in Figs. *a*, *b* (haematoxylin-eosin stain).

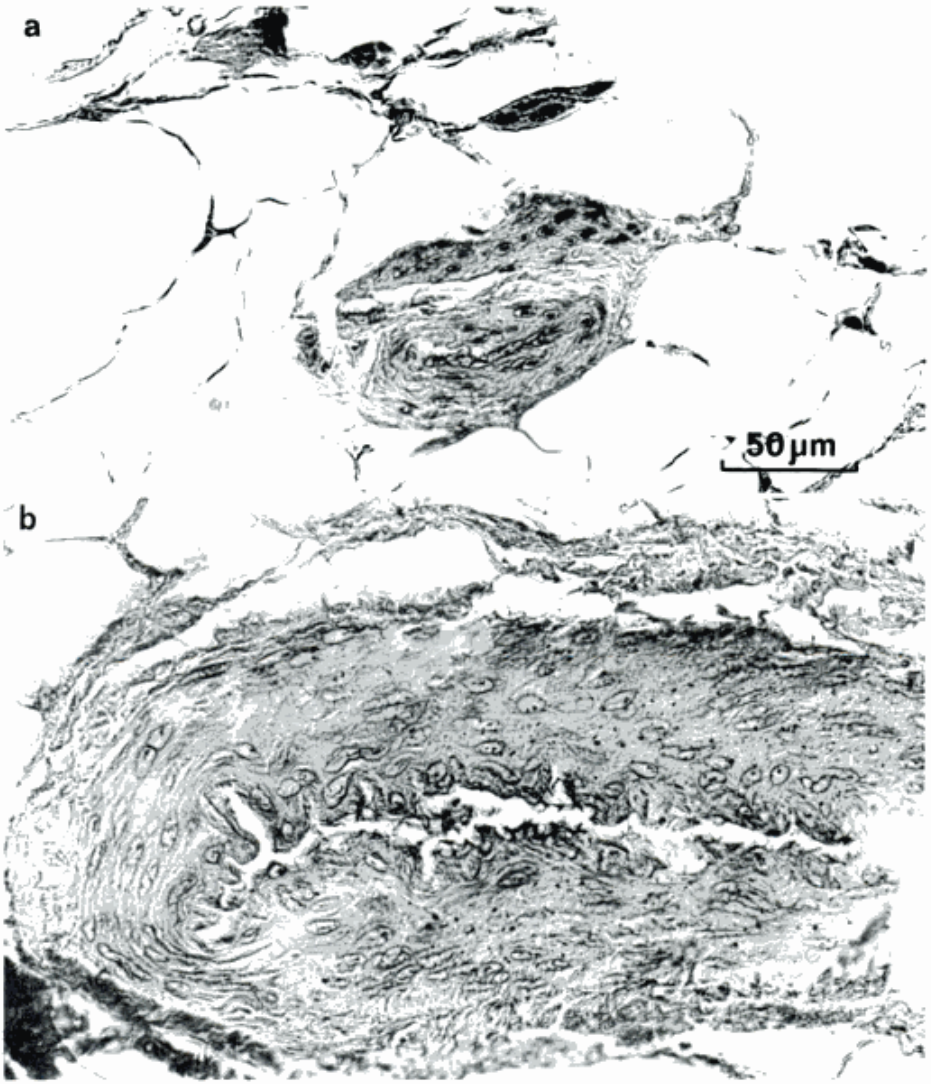

Fig. XVI: 50. Development of cathodic "channels" by electrophoretic treatment of normal human subcutaneous abdominal fat tissue. (*a*) Suggested "early" stages of development of the type of structure which is shown in Fig. XVI: 49 *a*, *b*. (*b*) Channel-like structure with well developed lumen. Light cellular structures in the thick wall of the "channel" contain dark, point-like "nuclei", like those which develop in cathodic fat (see Fig. XVI: 48 *a*, *b*). Same slide preparation as Fig. XVI: 49 *a*, *b* (haematoxylin-eosin stain).

structure was obtained after electrophoretic treatment of normal subcutaneous abdominal human fat (10 V, about 20 coulombs, 4 weeks). In Fig. XVI: 49 *c*, *d*, microphotographs are shown from a spontaneously developed pathological vessel adjacent to a pulmonary carcinoma. This vessel also has a thick wall but a well developed lumen. The magnified view shows cellular elements which have an appearance similar to the cellular elements of the newly formed structure in the abdominal fat specimen. The variability of newly formed structures from normal abdominal fat treated electrophoretically is, however, rather wide. Thus, the structures shown in Fig. XVI: 50 *a* are interpreted as early stages of development of the structures shown in Fig. XVI: 49 *a*, *b*. The structures shown in Fig. XVI: 50 *b* represents, on the other hand, a presumably later phase of development. These examples (Figs. XVI: 49 *a*, *b* and 50 *a*, *b*) were all obtained from the cathodic field and the same slide preparation (haematoxylin-eosin).

Structures similar to those shown in Figs. XVI: 49, 50 also developed after treatment of breast fat. Thus, Fig. XVI: 51 *a*, *b*, *c* illustrates structures obtained from the cathodic field of an electrophoretically treated specimen from human breast fat. In the overview (*a*) one small and one large circular structure are seen. Both contain fibrous elements and "cells" in their walls similar to the appearance shown in newly developed structures in cathodic abdominal fat (Figs. XVI: 49 *a*, *b* and 50 *a*, *b*). The enlarged view (Fig. XVI: 51 *b*) shows that the large channel contains fibres of different directions, indicating a tendency toward structural differentiation. Fig. XVI: 51 *c* shows that the small structure does not have a fully developed lumen.

One line of possible development of vascular channels was suggested in the description of atrophy of breast fat cells (Fig. XVI: 47) and in abdominal fat (Fig. XVI: 44). The complete lack of cellular elements in these channels indicate that they represent only one

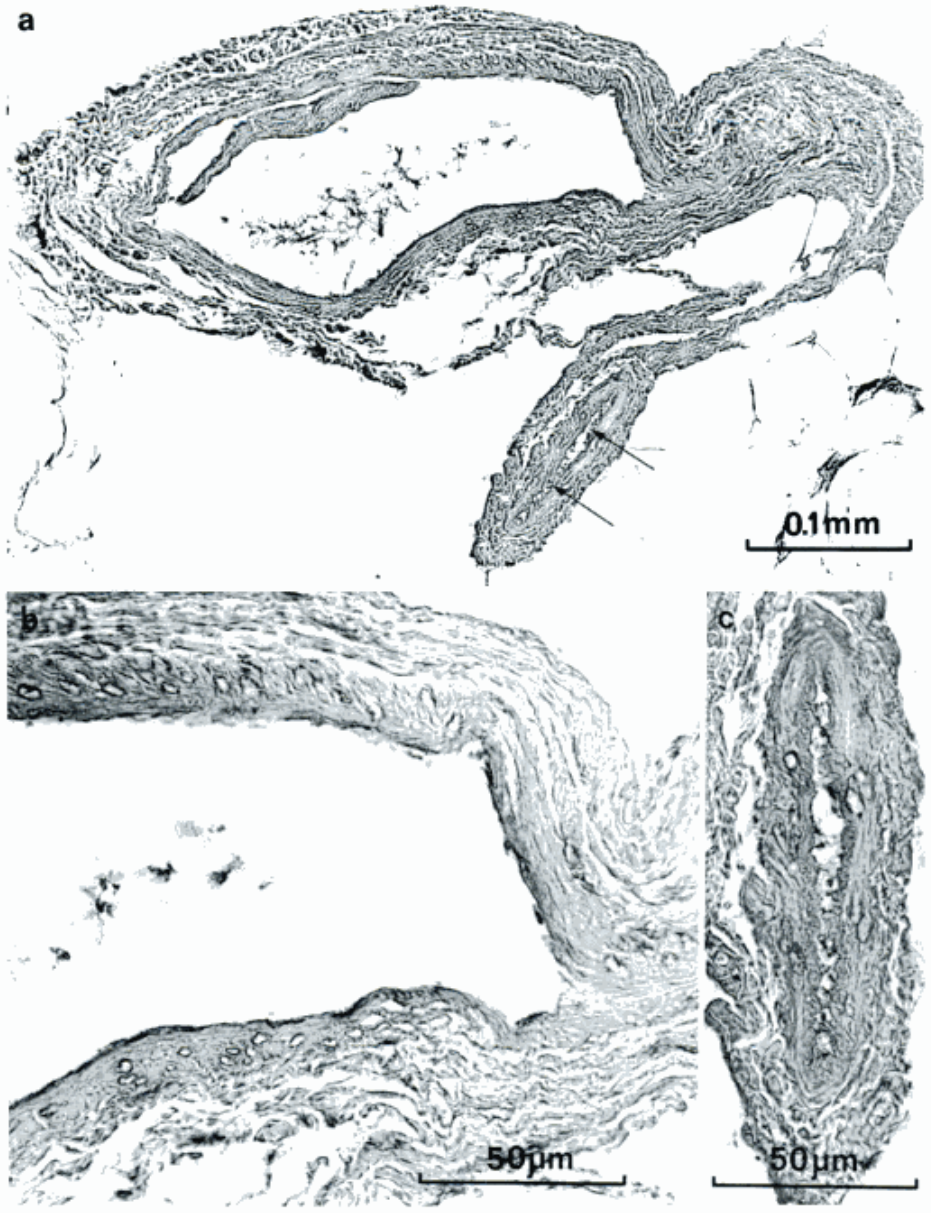

Fig. XVI: 51. Development of cathodic "channels" by electrophoretic treatment of human breast fat tissue (10 V, approximately 26 coulombs, 7 days). (*a*) Overview of two circular structures interpreted as cross-sectioned "channels". The lumen of the smaller channel has not yet fully opened (arrows). (*b*, *c*) The walls of both structures show fibres in different directions and small cells with light "cytoplasm". The appearance of the walls of the large structure gives an impression of an ongoing differentiation of layers (haematoxylin-eosin stain).

stage in the development of channels. Some channels formed by atrophy of fat cells do have, however, an appearance which is rather similar to that of pathological vessels around breast carcinomas. In Fig. XVI: 52 *a*, a cathodic channel is seen in breast fat after electrophoretic treatment (10 V, appr. 26 coulombs, 7 days). Fig. XVI: 52 *b* shows a pathological vessel in a fibrotic strand adjacent to a mammary carcinoma. Each specimen shows cathodic transformation in the fat cells, some of which also showed reticulation in their cytoplasm.

The material presented in this section is intended only as a stepping stone for a preliminary discussion of the possibility that BCEC mechanisms might be involved in the development of vascular channels.

Recent work on tumour angiogenesis has been concentrated on the assumed production of what has been called a tumour-angiogenetic factor (TAF), mitogenic to capillary endothelium and thought to stimulate the formation of vessels (35, 36, 37, 58). Thus, new tumour capillaries have been elicited after a tumour is enclosed in a Millipore filter chamber (45) and the chamber implanted in a cheek pouch of a hamster. Such studies have led to the assumption that the induction of capillary growth was caused by a diffusable substance named the tumour-angiogenetic factor. This anticipated factor has not been characterized chemically. It has been extracted from tumours and placental tissue (37). That the development of vessels is essential for growth of solid neoplasms has long been known. Vascularization of tumours takes place only by capillary proliferation. Neoplastic vessels of a tumour are

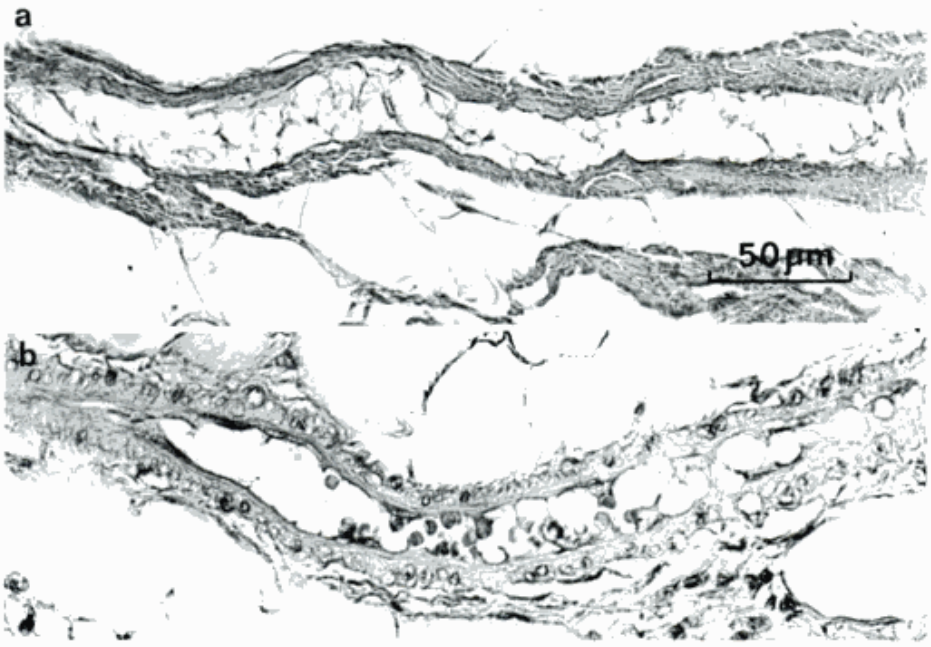

Fig. XVI: 52. Comparison between electrophoretic in vitro production of a cathodic tissue channel in human breast fat and a spontaneously developed pathological vessel around a mammary carcinoma. (*a*) Cathodic fibrous strand in breast fat contains fat cells, which seem to disappear, leaving a lumen. (*b*) Pathological vessel in a fibrous strand around a breast carcinoma. Both channels (*a* and *b*) seem to develop by atrophy of fat cells, leaving a fibrous channel (haematoxylin-eosin stain).

thought to be unique in that the neoplasms usually do not contain "veins" and "arteries" but a rich network of capillaries bounded only by an endothelial epithelium. This type of capillary growth is, however, not unique to neoplasms; it also occurs in granulation tissue (45). The mechanism that induces the growth of tumour vessels and granulation vessels is, however, considered as unknown (45).

Many factors and mechanisms seem likely to be involved in these events. The existence or nonexistence of a TAF need not necessarily exclude the possible existence of an electrogenic component, which has been simulated in the present experiments by leading direct current over "dead" tissue in an electrophoretic chamber. The metabolism or degrading processes of a tumour may produce electric polarization of the tumour against its surroundings and hence induce an electric current over a BCEC. More specifically, such circuits may be represented by VICC (vascular-interstitial closed circuits) for development of vessels. A spontaneous current over such connections should be able to induce an outgrowth of new vessels.

When a primitive vessel is subjected to spontaneous fluctuations of polarity of the driving electromotive force caused by, e.g., a necrotizing process in the tumour, the vessel may eventually develop further into a mixed anodic and cathodic vessel, as a result of bidirectional flow of current. The development of a complete vessel should further require, e.g., the modifying influence of blood and the mechanics of circulation. New primitive channels can be expected to grow at sites of preferential conductivity through capillary membranes and in preferential pathways for current in the interstitial tissue. In future attempts to improve vascularity in tissue, it may prove useful to consider this new view of angiogenesis. From this discussion it also appears evident that a mechanism for outgrowth of ductal channels and induction of neoplasia can be derived as a BCEC effect over ductal-interstitial closed circuits.

R. Microcalcifications: historical review

Microcalcifications in carcinoma of the breast were first described by Salomon in 1913 (83). Their importance for the recognition and early diagnosis of breast cancer was pointed out by Leborgne (65). Unfortunately, "malignant" and "benign" as characterizing terms for these calcifications are in many ways misleading and have been used rather frequently in many publications in the last few years.

Citoler and coworkers (22, 23) found only 15 of 113 breast carcinomas to contain so-called microcalcifications. Attempts to define what is typical for microcalcifications in malignant breast tumours have been made by Gershon-Cohen (42), Egan (31), Baclesse and Willemin (10), Hoeffken and Lanyi (55), Lamarque (60), Barth (14) and others. In a recent survey, Lanyi (63) found that size, number, dispersion, opacity and contour of breast calcifications were not characteristic as signs of malignancy. Nevertheless, it is well known that mammographic microcalcifications very often call the attention of the examiner to the region where a carcinoma is growing.

Gerlach and Thiemann (40) as well as Pape and Stegner (78) have performed electron microscopic studies of breast carcinomas. Because the female breast has the capacity to excrete calcium during lactation, the suggestion has been put forward that the breast also may have the capacity to accumulate calcium particles intracellularly in cancer cells as a result of metabolic cell activities.

Ahmed (2) supports the theory of active secretion of calcium because mammary epithelium is capable of concentrating calcium ions (87). In ultrastructural studies, Price, Hanrahan and Florida (79) reported that both electron diffraction and electron probe analysis showed that the crystalline material is hydroxyapatite ($Ca_5PO_4)_3OH$. Chemical analyses of some microcalcifications have been made by Moros, Pinter and Molnar (71), who found the following composition: calcium 25.4%, magnesium 2.6%, carbonate 5.8% and carbon 13.8%. Spectrophotometric examinations showed that the calcium and magnesium are predominantly bound to phosphate. Under certain assumptions, the following molecular composition has been suggested (cit. by Hoeffken and Lanyi) (55):

$Ca_3(PO_4)_2$	55.0%
$CaCO_3$	9.7%
$Mg_3(PO_4)_2 \cdot H_2O$	13.3%
Albumin	22.0%

For an understanding of the different aspects of degenerative changes of tissue, the mechanisms of autolysis are of fundamental importance. An excellent survey of the relevant literature has been made by van Lancker (62). A short recapitulation of selected aspects of autolysis follows:

The destruction of cellular components, e.g., by hypoxia, is caused mainly by hydrolytic enzymes released from lysosomes (29, 92). Phosphate ions will be available from hydrolysis of ATP when living tissue is exposed to hypoxia (4, 56, 74), which further leads to autolytic changes (8, 26, 77). A decrease in oxygen supply to the tissue further leads to elevated concentrations of hydrogen ions, lactic acid, CO_2 and other metabolic products. The acids promote an increase of proteolytic activities. The release of hydrolytic enzymes also alters membrane permeability, which in some way is coupled with a cellular inflow of Ca^{++}, Na^+ and water.

In studying cellular death, Judah and Spector (58), McLean and coworkers (64) have found that the coupling of oxidation to phosphorylation is completely blocked within 30 minutes after the onset of autolysis. Another early manifestation of injury was found to be a loss of ATP. Simultaneously, the degrading tissue becomes acid. Under these circumstances it is difficult to understand how calcium, which is known to precipitate in alkaline environments, can precipitate in acidic tissue. As we are here dealing with pathological precipitation of calcium, the only explanation is to assume somehow that local factors trigger the precipitation of the salt. Exactly what precipitates calcium is not known. One proposal is that changes in the matrix lead to crystallization of the calcium salts because the altered matrix may act as a seed for the precipitation of hydroxyapatite. Irving, reviewing the mechanism of mineralization in cartilage and bone (57), believes that collagen is a focus for calcification. No calcification, however, was seen in collagen in breast carcinomas in the studies of Ahmed (2). Anderson (5) has described extracellular vesicles as foci for calcification in bone mineralization. Acidic phospholipids have also been considered as targets for mineralization of bone (88). Phospholipids and phosphoproteins, such as casein, are the most likely foci for calcifications in breast cancer, according to Ahmed (2). It may also be mentioned that acidic phospholipids are probable target substances for calcifications of aortic valves (59). In all calcifications it therefore seems necessary to begin with some kind of matrix, which under certain circumstances serves as a target for mineralization.

Recently Hoeffken and coworkers (55) have stated, "The pathogenesis of calcium deposition in the various forms of fibrocystic disease and breast carcinoma is still an enigma in spite of intensive investigations using electron microscopy, ordinary microscopy as well as chemical and radiological methods."

S. Closed circuit production of microcalcifications

Possibilities of locally precipitating calcium in tissue will be explored in this section by means of fluctuating physicochemical potentials over a closed circuit. These experiments, like the previous experiments in this chapter, were conducted as driven systems and must therefore be compared with corresponding reactions of endogenous self-driving systems in vivo over BCEC. A recapitulation of some aspects of tissue injury will facilitate understanding the experiments to follow.

The experiments on autolysis of blood (Chapter VII) revealed that early in autolysis protons are produced. Later in autolysis protons are lost. The tissue then changes from being a proton donor into a proton acceptor. Fluctuation of pH was found to be about one pH unit or approximately 60 millivolts. These changes are logical consequences, because ATP is not produced over the Krebs cycle when oxygen is lacking. Phosphate ions will then accumulate, because their recombination or dissipation (e.g., by diffusion) is slower than corresponding proton reactions. A contri-

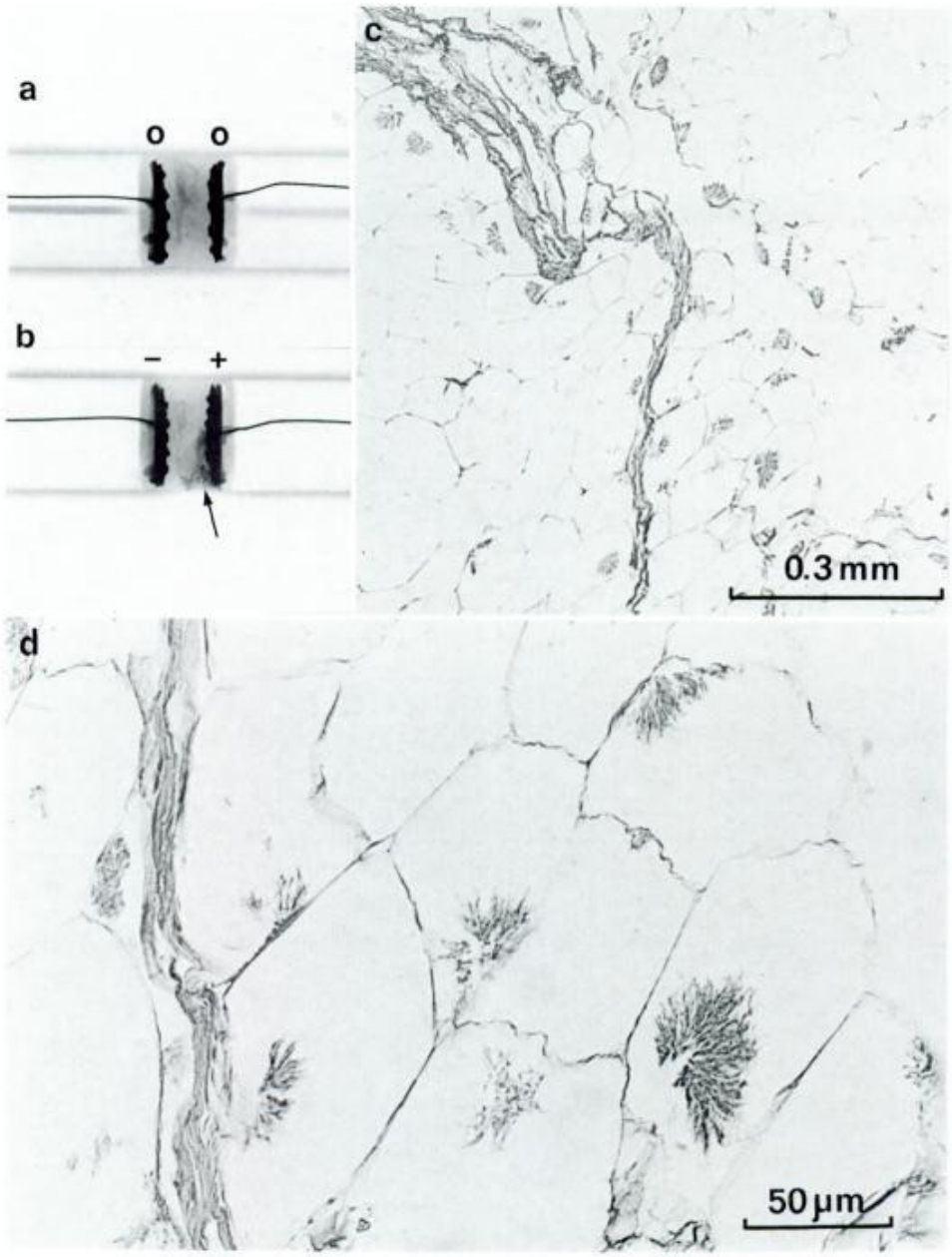

Fig. XVI: 53. In vitro production of anodic matrices, which subsequently are utilized for creation of microcalcifications in breast fat. (*a*) Soft tissue radiograph prior to application of direct current. (*b*) After 25 coulombs at 10 V (26 days), small "dots" are seen at natural size in the lower part of the anodic field (arrow). (*c*) Photomicrograph (haematoxylin-eosin) of anodic membrane with many "dots" in the anodic fat. (*d*) Detail photomicrograph. These "dots" are bush-like structures which develop at the inner membrane surface of fat cells. The "dots" contain birefringent material. No calcium was shown with von Kossa or Alizarin stains. See further Fig. XVI: 54.

bution of phosphate to the development of an electronegative reaction of the autolyzing tissue is now of obvious interest. A drive toward electrochemical equilibrium between the electronegative necrotic tissue and the surrounding tissue can now take place in the form of an inflow of cations and an outflow of anions. The normal surrounding tissue can supply cations. Electrostatic attraction and repulsion of ions in such events are not likely quantitatively to be very efficient, because the transports have to take place over relatively large distances. The transports can, on the other hand, take place with considerable efficiency over a BCEC, e.g., the VICC (vascular-interstitial closed circuit).

Among the available inflowing cations, calcium and magnesium can be expected to combine with accumu-

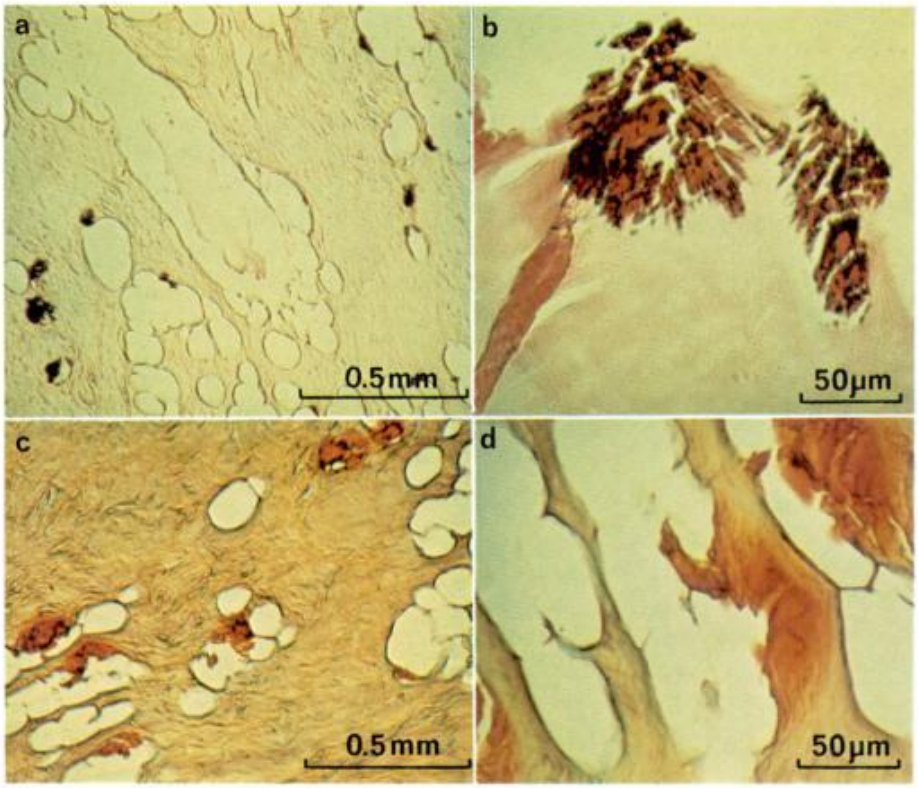

Fig. XVI: 54. Microcalcifications produced in vitro in breast fat by means of reversed flow of direct current. Unidirectional electrophoresis of breast fat first led to "dot"-like structures in the anodic fat (as shown in Fig. XVI: 53). The current was then reversed (10 V, 8 coulombs, 7 days). The previously acid anodic tissue then became alkaline, leading to precipitation of calcium in the "dots", which serve as matrices for the precipitation. (*a*) Overview of calcified matrices. (*b*) Larger magnification (haematoxylin-eosin). (*c–d*) Specific staining of the calcium ions is positive with Alizarin.

lated phosphate ions in the necrotic tissue, resulting in precipitation of hydroxyapatite when the isoelectric region for this complex compound is reached. The accumulation of increasing amounts of calcium and magnesium phosphate will diminish the anionic resources of the autolytic process, thereby leading to a tendency of the tissue to turn into an electropositive reaction. Thus, the total reaction attenuates and fluctuates as it moves toward equilibrium.

It is obvious that the stepwise description of these events must in reality represent a continuous process. For example, a local "accumulation" of protons or phosphate ions must be regarded as an expression of their time-related statistical representation. The summation of the events of all reactants will in time produce a fluctuating electrochemical potential which inexorably moves toward equilibrium of the total reaction (note further possible cascade reactions, page 118).

If these assumptions are correct, it should be possible to produce calcifications in tissue by means of a fluctuating electric potential over a closed circuit which includes a section of tissue.

In the hypothetical model, calcium and magnesium phosphate have been anticipated to precipitate during an electronegative phase of the injured tissue. What happens during the initial, preceding electropositive phase? Perhaps the answer is found in the development of a suitable matrix for the precipitations, according to what has been assumed to be a necessary prerequisite in bone formation.

In the electrophoretic experiments with 10 volts and "unidirectional" current over human or dog fat tissue, no calcium precipitation was ever observed in histological sections of the material (prepared with von Kossa or Alizarin stains, which are suitable for its detection). Fig. XVI: 53*a* shows a specimen of fat before and Fig. XVI: 53*b* after delivery of 25 coulombs at 10 V. The arrow points to small "dots" of increased x-ray attenuation in the lower part of the anodic area. Fig. XVI: 53*c* shows a fibrous membrane and "dots" in a histologic section of the anodic region. These dots consist of partially birefringent material arranged as "radiating structures" or "bushes" in fat cells. These "bushes" are intracellularly attached to the cell membranes and do not stain for calcium (Fig. XVI: 53*d*). Because the "bushes" were produced in the acidic, anodic field it was thought that they could possibly represent local matrices and constitute focal sites for later precipitation of calcium.

The experiments were therefore continued with subsequent polarity of the electrodes reversed in experiments where "dots" had been identified radiographically in the anodic field. In such experiments, focal precipitations of calcium were produced (Fig. XVI: 54). Fig. XVI: 54*a*, *b* shows blue haematoxylin-eosin staining of experimentally produced microcalcifications, while *c* and *d* show specific staining of the

calcium ion with Alizarin. The experimental calcifications show arrangements of the crystals similar to the matrix of the anodic "bushes". The microcalcifications also show some birefringence, which might be caused by the matrix. In these experiments the calcium precipitation in the bush-like matrices could not be demonstrated with von Kossa stain. Alizarin specifically stains the calcium ion, von Kossa the phosphate ion. The calcium precipitate is therefore possibly present in the specimen as carbonate or oxalate but not as phosphate.

Discussion

The experimental, direct current production of microcalcifications in breast fat now raises the question of the mechanism of their development at certain sites rather than diffusely in the tissue. This finding may depend on differing susceptibilities for injury of individual cells and cell groups. The number of matrices in the anodic phase and the number of calcium-precipitations in the cathodic phase have been found to be greater close to the electrode than in the centre of the specimens. The general viability of breast cancer cells, moreover, can be expected to be less than that of normal cells. When exposed to spontaneous local nutritional disturbances, as by compression or impaired blood supply, focal sites of necrosis can be expected to develop. The local injury should then produce a spontaneously fluctuating potential, leading to the production of microcalcifications according to the mechanism which is outlined in principle above.

These studies support the assumption that microcalcifications per se are not pathognomonic for malignancy. Focal cellular necrosis, however, is more likely in a carcinoma than in normal tissue. Therefore, microcalcifications are often found in a neoplasm, but are diagnostically specific only as an indication of a preceding injury to tissue and not as an indication of cancer. As a matter of fact, all calcifications after injuries of tissue, e.g., calcium in the soft tissues of the shoulder, in cartilage, discs, tendons, local haematomas, and lymph nodes, are known to consist of hydroxyapatite.

Accordingly, deposition of calcium in a previously injured tissue should not be considered as a disease per se but as part of the healing process, as is the development of scar tissue. *Calcinosis reparativa* would therefore be a proper name for the development of such "pathological" calcifications.

T. The yellowish zone around breast carcinomas

Pathologists have for years noticed that carcinomas of the breast often show a yellowish zone adjacent to the tumour (11, 32, 80, 89).

Such a yellowish zone is seen around the breast carcinoma in Fig. XVI: 55 *a*. The adipose tissue within a distance of 10 to 15 mm from the edge of the tumour has a more orange colour than fat in the periphery of the specimen. Fig. XVI: 55 *b* shows a radiograph of the tumour. A photomicrograph (Fig. XVI: 55 *d*) of a histologic section demonstrates moderately extensive atrophy of fat cells at the edge of the tumour. Infiltrating round cells are also present.

Bahrmann (11) found the yellow zone in 80 % of 200 breast cancers, but never around a fibroadenoma. In occasional cases a yellow zone was also seen in the breast around tuberculous, luetic and actinomycotic foci.

Macroscopically the yellow zone is seen most easily in daylight. In artificial light the zone may show only a slightly different colour from that of ordinary fat. Metastatic carcinomas in fat tissue, whether from the breast or other primary sites, may also show a yellow zone. Examples of this phenomenon have been shown in the subcutis and adjacent to the stomach and colon (89, 32).

According to Falk and Pfeifer (32), the yellow zone and peritumoural atrophy of fat cells are caused by some kind of reaction of the stroma. As the fat cells get smaller, the more apparent is the yellowish zone. No satisfactory explanation of the development of so-called atrophic fat cells and the yellowish zone has yet been presented.

The experiments with in vitro electrophoresis of lanolin (Fig. XVI: 15) revealed that this material contains bright yellow fat with low attenuation and white fat with higher attenuation for x-rays. These fatty compounds separate easily from each other by electrophoresis.

In vivo electrophoresis in an anaesthetized dog with two platinum electrodes inserted into breast fat showed relative movement of water to the electronegative electrode and of fat from this electrode (Table XVI: 1). Small fat droplets were even seen between the "atrophic" fat cells on the electronegative side and distended fat cells on the electropositive side. Simultaneously, the colour of the fat was greyish on the electropositive side and brownish on the electronegative side. From the experiments on mesentery (Chapter XIV) it was found that diapedetic and intravascular thrombosed blood became dark brown after some time. The introduction of electrodes percutaneously into breast fat in vivo in a dog was also associated with

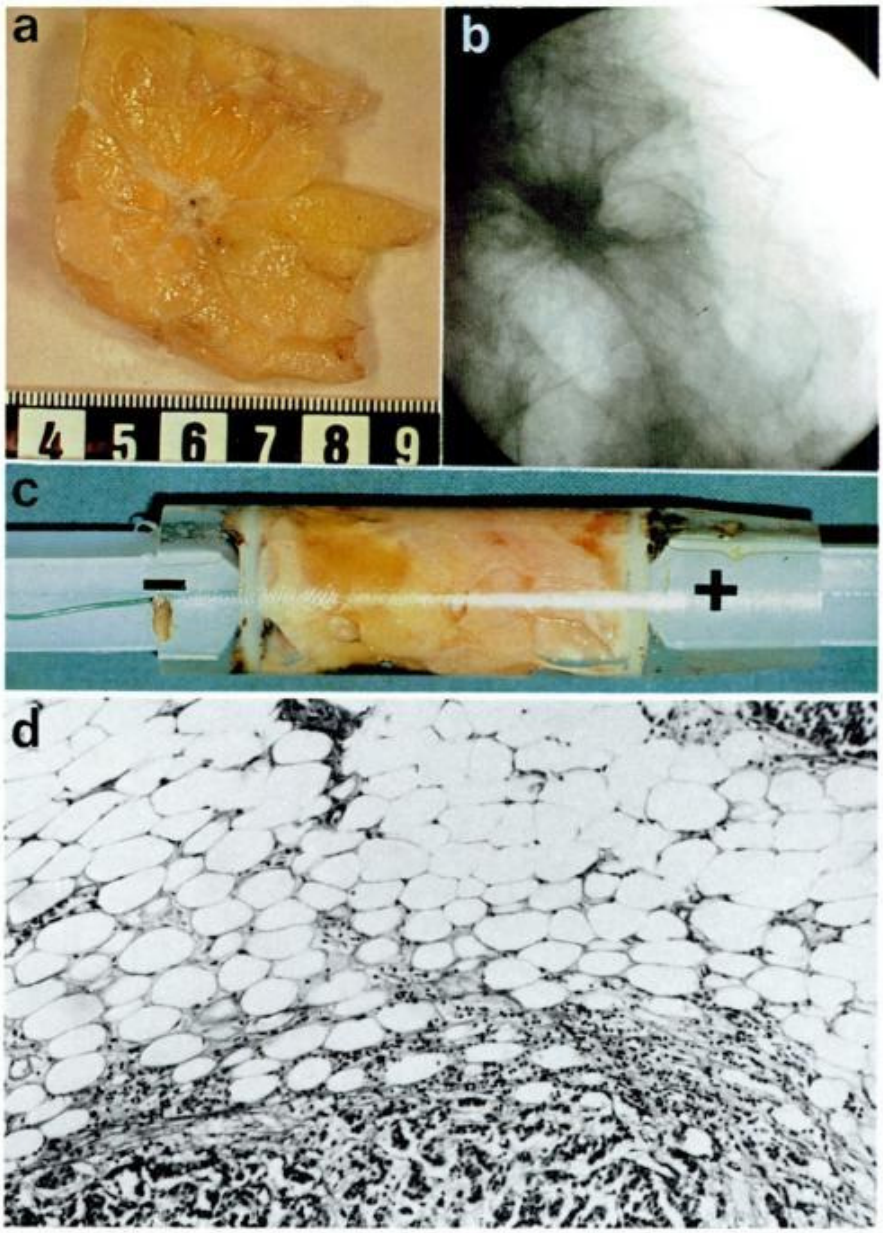

Fig. XVI: 55. The yellowish zone around a breast carcinoma. (*a*) Photograph of surgical specimen (centimetre scale). The yellowish zone is 10 to 15 mm broad and shows dark yellow fat. Preoperative stereotaxic needle biopsy caused two bleeding points inside the tumour and two in the yellow zone. (*b*) Mammogram, preoperative, shows radiating structures around the tumour. (*c*) Electrophoresis of breast fat makes cathodic fat turn successively yellow-orange-brown while the anodic fat increases in whiteness. (*d*) Histological section from edge of the cancer shows "atrophic, small fat cells" adjacent to the tumour, which is known to be accompanied by a yellowish zone.

some small local bleedings, which could explain the brownish discolouration of the fat tissue in these experiments.

In order to avoid any possible effect of local blood derived from injury, experiments were performed with fresh fat tissue obtained from human mastectomies. This fat tissue was treated with electrophoresis as shown in Fig. XVI: 17. The result of the treatment was a red-yellow zone, which can be seen close to the electronegative electrode (Fig. XVI: 55 *c*). This zone initially was light yellow. As the electrophoresis proceeded, the zone became increasingly red-yellow to brown-yellow. In one experiment the fat material was illuminated with fluorescent light. The cathodic fat then showed light yellow fluorescence. The anodic white fat did not fluorescence but appeared white-yellow.

The development of small, atrophic fat cells adjacent to a carcinoma of the breast, as seen in Fig. XVI: 55 *d*, is usually associated with development of yellow-red discolouration of adjacent fat. As was discussed in connection with the experiment shown in Fig. XVI: 17, some fat is also mobilized adjacent to the anode and is very likely influenced by anodic acidity. This fat meets the electronegative fat from the cathodic field close to the anode. It now appears understandable that the atrophic fat cells typical of the anodic type are surrounded by a yellow zone of cathodic fat.

Bahrmann (11, 12) made the observation that the more atrophic the fat cells appear at the edge of the tumour, then the more dark yellow appears the yellow zone. He also observed that the yellow zone can best be seen in daylight or photographed with a blue filter.

Sümegi[1] (89) found that the yellow zone fluoresces yellow in fluorescing light. A light green-blue chlorophyll-alcohol solution gives the zone a red fluorescence in blue fluorescent light.

It is evident that the present tests of the yellowish material must be extended for conclusive identification. At this point in our understanding, the yellowish zone around a breast carcinoma appears to be a result of electrophoretic transports of fat material within a BCEC.

U. Electrophoretic accumulation of lymphocytes around and inside breast carcinomas

Lymphocytes are often found inside a breast carcinoma and in the tissues surrounding the tumour (Fig. XVI: 56). Around the tumour they are usually increasingly concentrated toward its surface. The presence of lymphocytes in cancers has been thought to be part of an immunologic reaction (24). Sometimes, fewer lymphocytes are present in the tumour than adjacent to its surface. It has been assumed that in such cases more lymphocytes are destroyed inside than outside the tumour due to a particularly strong immunologic reaction inside the tumour.

The mechanism responsible for the accumulation of white blood cells around tumours, different kinds of infectious tissue lesions and in immunologic reactions is still unknown (62). The usual explanations are often restricted to discussions based on the concept of "chemotaxis", which was treated in Chapter XIV, Sections J and K, in connection with anodic accumulation of granulocytes. Because chemotaxis is regularly included in discussions of lymphocytic accumulations, this mechanism will also be considered in this connection.

Chemotaxis is assumed to be a result of a variety of not very well defined chemicals present in bacteria and in inflammatory exudates (17, 50, 51). In acute inflammation, polymorphonuclear cells accumulate. In chronic inflammation such as tuberculosis, monocytes are common. Positive and negative chemotaxis are thought to exist. In practice, only attraction has been observed.

"Positive chemotaxis" is induced by many bacteria, including *Streptococcus pyogenes, Micrococcus pyogenes, Diplococcus pneumoniae, Escherichia coli, Bacillus antracis, Salmonella typhi* and *Corynebacterium diphtheriae*. Leukocytic migration, on the other hand, is inhibited by certain toxins, e.g., from *Clostridium tetani*.

Using exudates from inflamed tissue, Menkin (70) claimed to have prepared a compound he called leucotaxine which could attract leukocytes. On the basis of photographic studies of migrating leukocytes, Harris (50) concluded that no product prepared from inflammatory exudates exhibited such properties. Harris (50) suggested instead that polymorphonuclear migrations result from the random distribution of polymorphonuclear cells passing by diapedesis through the walls of the capillaries into the interstitial spaces.

This explanation of Harris may, in the author's opinion, be partly but not entirely accepted. The local accumulation of leukocytes in inflammation is often intense. A random distribution by local diapedesis should not selectively affect the accumulation of white blood cells in the diseased area in relation to other blood cells, e.g., erythrocytes. Additional mechanisms are probably also responsible for the selective accumulation (43). Boyden (17) assumes that leukocytes possess the ability to "recognize" certain foreign materials.

The studies of "humoural leukotaxic factors" have largely been carried out with bacteria, viruses and inflammatory exudates (1, 69). Nevertheless, leukocytes migrate also in aseptic necrosis (61). This observation indicates that neither an infectious agent nor its toxic products are necessary for accumulation of leukocytes (18).

Table XVI:4

Chemotactic substances	Chemotactic inhibitors
"Leucotaxine" from exudate, probably a polypeptide	Toxins from bacteria
Calcium	A serum β-globulin
Complement factor in serum	An α-globulin
An γ-globulin factor of unknown nature	
Polysaccharide from Diplococcus pneumoniae	
Necrotic tissue	
Colloidin particles	
Cellulose particles incubated with serum	
Precursors of chemotactic agents in plasma with activators in liver, heart muscle	
Kallikrein	

[1] The author is greatly obliged to Prof. I. Sümegi, who supervised these tests and supplied the author with valuable information from his research on pathologic tissue components around tumours in fat tissue.

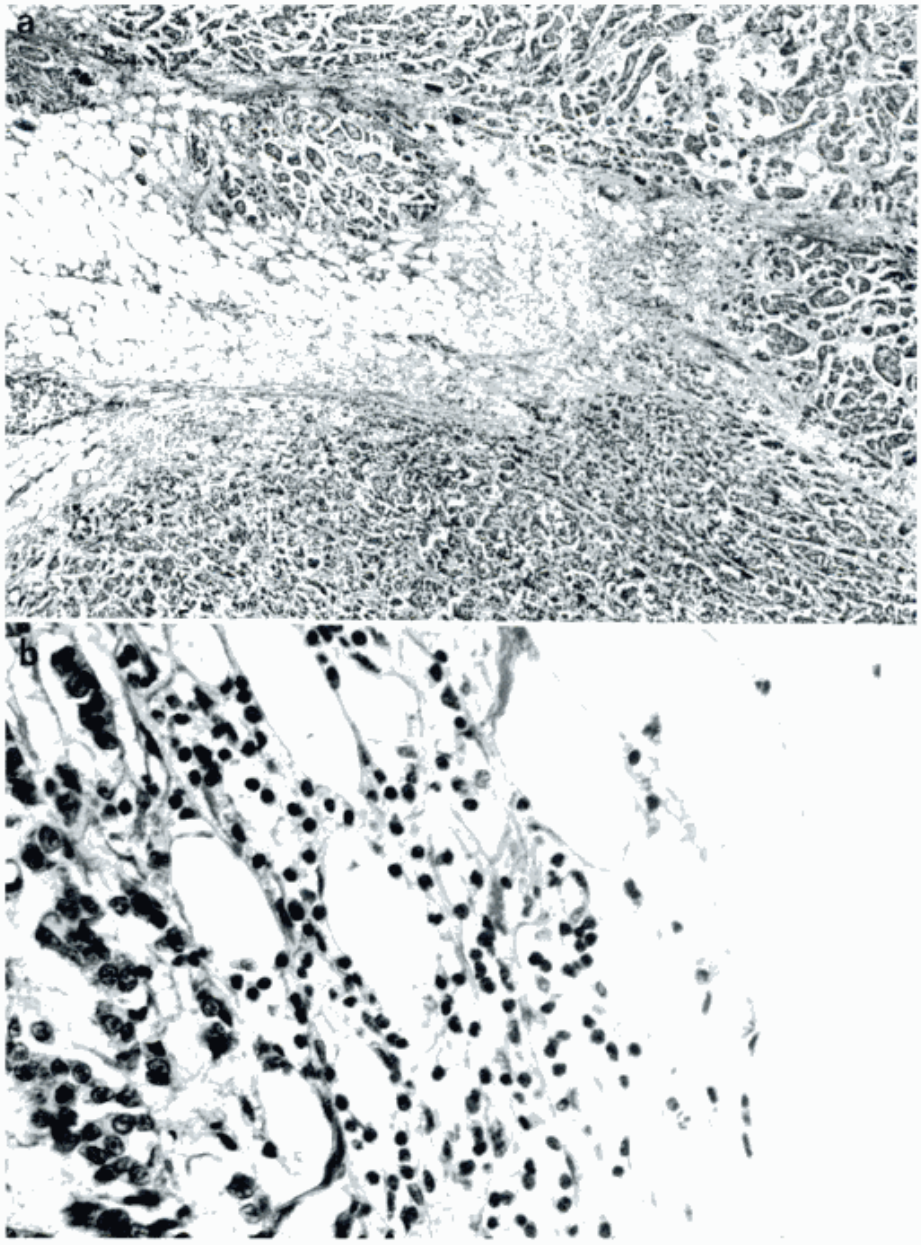

Fig. XVI: 56. Histologic sections through the edge of a mammary carcinoma. (*a*) Overview, atrophic fat cells (middle left of Fig. *a*) are adjacent to the carcinoma. Many lymphocytes are infiltrating the tumour tissue. (*b*) Lymphocytes are also found in the fat tissue surrounding the tumour.

Active participation of leukocytes in diapedetic extravasation must also be discussed (44). The sizes of leukocytes are variable. In phagocytosis they change their shape by producing pseudopods. The shapes of the leukocytes also vary when they migrate through narrow spaces in capillary walls.

The testing of chemotactic effects of different materials from bacteria and exudates (17) has led to the description of a wide range of chemotactic compounds, some of which are collected from van Lancker (62) in Table XVI: 4. As can be seen from this table, no common or specific chemical factor is evident among these substances.

Polymorphonuclear cells are in general assumed to be attracted in acute conditions by bacteria, viruses and their exudates, different serum compounds and tissue factors. No specific factor is known to accumulate the white blood cells. Theories have also proposed that the chemotactic substances are released by the leukocytes themselves. Selective chemical agents or variations of tissue pH have also been thought to produce the accumulation of different types of white blood cells (72).

Harris (51) believes that the polymorphonuclear cells and monocytes leave the blood stream by diapedesis at the same time. Due to the longer survival time of monocytes, the relative number of monocytes increases in time. This analysis could then explain the

relative increase in number of monocytes in chronic inflammation. It is also known that cells other than leukocytes show "chemotaxis". For example, bacteria are attracted or repelled by a variety of organic and inorganic compounds.

On the whole, chemotaxis is a confusing and far from clearly defined concept.

In the present work, different aspects and examples have been presented of electrophoresis and electroosmotic transports around different tissue lesions. Nonspecific injury of tissue and the existence of the proposed VICC must therefore be considered in attempting to explain local accumulation of white blood cells inside and around an injured tissue. A local injury will create an electrochemical potential in relation to the surrounding tissues. This potential difference will constitute an energy source for transports regardless of the source of the injury, e.g., bacteria, viruses, aseptic necrosis, local bleeding in a tumour or any other cause of degradation of tissue.

In the studies here reported of in vivo electrophoresis (Chapter XIV) it was found that diapedesis is induced in capillaries on the electropositive side of an electric field and that polymorphonuclear cells accumulate massively in the vessels and in the interstitial tissue around the electropositive electrode.

When a breast carcinoma develops a local injury, i.e., from necrosis or bleeding, electronegative white blood cells should be attracted to the tumour during its phase of electropositive polarization as an electrophoretic process within the VICC. This explanation of the acute accumulation of leukocytes is based on several known or assumed prerequisites:

1) It is known that certain parts of cells carry positively and negatively charged groups. Lymphocytes as well as granulocytes carry a surplus of electronegative fixed charges on their surfaces (13, 39, 53, 54, 73, 84, 85, 93, 94, 95). Their negative zeta potentials have a magnitude of 15 to 20 mV at physiological pH and in 0.145 molar NaCl solution. Lymphocytes and platelets are charged mainly by phosphatides of the cephalin type, polymorphonuclear leukocytes mainly by carboxyl groups. The electronegative surface charge of erythrocytes is determined by phosphate groups.

2) Charged particles, e.g., leukocytes, will move in a closed electric circuit to a region of polarity opposite to their charge. Leukocytes therefore move to the anode in an electrophoretic chamber.

3) In spite of their relatively large size (diameter 6–20 μm), leukocytes are capable of passing by diapedesis through capillary membranes.

4) In vivo analogues to the circuitry of an electrophoretic chamber are here assumed to exist as vascular-interstitial closed circuits (VICC) (Chapter XII).

5) After any kind of injury to a tissue, an electrophysico-chemical potential develops in relation to surrounding normal tissue. The electric component of the physicochemical potential then delivers the driving energy for transports over BCEC channels.

Intravascular and interstitial accumulation of leukocytes was produced in an in vivo experimental model of spontaneous accumulation of leukocytes over a BCEC (Fig. XIV: 15). In such experiments, electrodes leaned very gently against normal mesentery of a living dog. One to five volts were applied between the anodic mesentery electrode and the reference electrode in the aorta or inferior vena cava. The electrode potential varied between 1–5 volts, giving rise to a current of a few microamperes. Massive accumulation of granulocytes could be obtained in vessels already at 0.002 coulombs of current. So-called margination of leukocytes was observed in vessels. Leukocytes then accumulated in great quantity around the anode. These experiments indicate that previous tissue injury is not obligatory for the anodic accumulation of leukocytes. The behaviour of leukocytes in such experiments is most easily explained as a result of electrophoretic transport over a closed circuit, driven by an external source of electrical power.

6) Previous discussions in the literature of chemotactic attraction of leukocytes have overlooked the possibility of electrochemical injury potentials, whether spontaneously or externally created. As far as the author can ascertain, each of the factors for which a chemotactic effect has been reported is capable of polarizing tissue. If this view is accepted, then *any agent which is capable of driving electropositive polarization within a BCEC may electrophoretically attract leukocytes. A driving electronegative polarization may, however, also cause electronegative leukocytes to became accumulated according to the mechanism of flow and field interference already described in Chapter XIV.* Many other factors are, however, also likely to be involved in the selective, electrophoretic accumulation of charged cells or compounds. Thus, the sizes and shapes of cells as well as the steric locations and magnitudes of surface charges should influence the transports. Furthermore, different matrix factors as well as steepness and magnitude of the superimposed electric field are evidently of importance in the presented explanation of selective electric accumulation of cells in tissue. Certain partial mechanisms in the transport of cells may even be explained as, e.g., the formation of pseudopods of the granulocytes. These pseudopods make it possible for the white blood cells to "flow" through narrow pores in the capillary membranes. The mechanism we then have in mind has its correspondence in electroosmosis Type I (Chapter IX). The principle of electrophoretic transport is capable of explaining the accumulation of leukocytes in different kinds of tissue injury. A corresponding mechanism may also explain the accumulation in tissue of lymphocytes, because lymphocytes

also carry a surplus of electronegative charges on their surfaces.

How is the presence of lymphocytes explained in chronic inflammation and granulocytes in acute inflammation?

Once leukocytes have entered the interstitial tissue by diapedesis through capillaries, they are trapped and unable to find the same way back to the blood stream when the electric polarity of the lesion is subsequently reversed. Some of them may, however, reenter the blood stream over interstitial lymphatic channels. A gradual decrease of the granulocyte/lymphocyte ratio may nevertheless preliminarily be explained by the mechanism proposed by Harris: the granulocytes disappear more rapidly than lymphocytes (i.e., by different life span), which therefore gradually leads to local lymphocytosis. It was also shown experimentally in Chapter XIV, when dog lung tissue was electrically polarized in vivo by an external power source between two platinum electrodes, that three weeks after the treatment lymphocytes and not granulocytes were accumulated around the electrodes. The common histologic finding of lymphocytes inside and outside resected breast tumours should be interpreted only to mean that these tumours are usually resected in a "late" phase rather than in an acute phase of a degrading process of the tumour.

V. Conclusions

The structural modifications of tissue around focal lung lesions, which are called the *corona structures*, can also be identified around breast cancers. The corona structures in the breast include the radiolucent "A" zone, the radiopaque "B" zone, which may appear as a local skin thickening, the small arches forming an arcade, the circularly arranged structures and the radiating structures, extending from the tumour surface far out into surrounding breast tissue.

The biokinetic mechanisms behind the development of these structures, as well as the development of fat atrophy, microcalcifications, the yellow fat zone around certain cancers in fat tissue and the accumulation of leukocytes can be traced back to a common process of spontaneous "healing". This tendency of "healing" is evidently insufficient for the development of a "true healing" of a carcinoma. In previous chapters of this book, the mechanism for the actual, insufficient process of "healing" has been identified. This is based on a BCEC system (which contains biologically closed electric circuits). It represents a previously undescribed mechanism for selective transport of material in tissue, closely integrated with the mechanical, nonselective systems of transport, e.g., the circulation of blood. The specific BCEC of particular interest in this connection is the vascular-interstitial closed electric circuit (VICC). This consists of vessels, which were found to act as electrically insulated, conducting "cables" as the vessel walls have a high electric resistivity around the conducting blood plasma. The plasma has an electric connection over the capillary membranes with the interstitial fluid, which, like plasma is a good conducting medium. These two "electrical branches" form a closed circuit which is driven by the electromotive force between a local injury (i.e., necrosis or bleeding in a tumour) and the surrounding noninjured tissue around the tumour. The injury is a catabolic energy-liberating process, which presents a fluctuating electric injury potential. This potential leads to ebb and flow of transports in the circuit, resulting in modifications of tissue which we can identify radiographically as the corona structures and histologically as several modifications in the tissues and cells.

As in the lung, it was also found that breast tumours sometimes present an electric gradient of potential in relation to surrounding tissue. This occurs when the tumours contain regions of degradation. The magnitude of electric potential varies with time because it represents a spontaneous process which, like all such processes, proceeds in a fluctuating, attenuating fashion toward equilibrium. The duration of such fluctuations over days, weeks or months makes transports possible of considerable amounts of material, even with small gradients of potential.

None of the actual structural modifications in breast cancer is pathognomonic for malignancy. However, the coincidence of necrosis and malignancy is high. Therefore the structural modifications do often develop in breast cancer.

The general biokinetic mechanisms in the development of corona structures in lung cancer are described in preceding chapters and applied to the particular conditions of breast cancer in this chapter. To deepen understanding of the actual problems, the reader is advised also to study the content of the preceding chapters. Thereby insights will be obtained, e.g., in the construction and mechanism of activation of actual BCEC systems, and the mechanisms of transport of water in the circuit which produce the characteristic perifocal differences of attenuation for x-rays.

So-called skin thickening is explained as a local electroosmotic transport of water to the retracted skin. The retraction, on the other hand, is produced by electroosmotic local dehydration of hygroscopic elements in fibrous, radiating structures.

Besides water, fat is also transported in the activated BCEC system, producing both atrophy of fat cells adjacent to breast cancer and also the well-known red-yellow fat zone which is often seen around malignancies developing in fat tissue.

By electrophoretic transports, an interphase is

formed between a hydropenic and a hydropic zone, which leads to the development of arches and arcades and circularly arranged structures around breast cancers.

Fibrous structures such as membranes can be produced by the influence of direct current. The endogenous development of fibrous, radiating structures can be simulated experimentally by electrodes, provided with small protrusions, which cause electrical edge enhancement. In this way cathodic fibrous tissue was produced without the presence of fibroblasts. In the anodic fibrous tissue "fibroblasts" were present. Their distribution in the fibrous tissue raises the question that they may not be necessary for the production of fibrous tissue.

In anodic fibrous tissue, channels also develop with an appearance of primitive galactophores and "blood vessels". In cathodic fibrous tissue, channels develop, lined with a birefringent membrane. These channels may also lead to the development of pathological vessels. The transformation of tissue structures and cells is distinctly different in the cathodic and anodic fields. Such transformation was produced by leading a weak current of a few microamperes over the tissue over a period of two to five weeks. In different ways evidence has been presented that the development of primitive galactophores can be induced in "dead" pieces of breast fat tissue by direct current within the anodic field. Electrophoresis of fat samples is possible prolonged over weeks without bacterial decomposition of the tissue specimens.

Breast fat tissue subjected to direct current develops small "bushes" of birefringent material in the anodic field. By simulating the endogenous *fluctuating* potential, histologically typical microcalcifications can be produced.

An important factor in the histological appearance of breast cancer is the accumulation of lymphocytes inside and around the tumours. In Chapter XIV (pp. 189–191), current views on accumulation of granulocytes as a result of "chemotaxis" are discussed. In the view of the author, the anodic phase of a lesion causes granulocytes to be attracted electrophoretically to it over the vascular-interstitial closed circuit (VICC). This is possible because leukocytes are provided with a net surplus of electronegative charge on their surfaces. Certain components in such a mechanism, e.g., magnitude and steric arrangement of charges as well as field strengths and matrix characteristics, have to be considered for futher understanding of this theory of accumulation of granulocytes. By applying this basic principle, an explanation for accumulation of lymphocytes in breast cancer is also proposed.

References

1. Adler, J.: Chemotaxis in bacteria. Science 153: 708, 1966.
2. Ahmed, A.: Calcifications in human breast carcinomas: Ultrastructural observations. J. Path. 117: 247, 1975.
3. von Albertini, A.: Histologische Geschwulstdiagnostik. 2 Aufl. Stuttgart, Thieme Publ., 1974, p. 287.
4. Alberty, R. A.: Effect of pH and metal ion concentration on the equilibrium hydrolysis of adenosine triphosphatase to adenosine diphosphatase. J. Biol. Chem. 243: 1337, 1968.
5. Anderson, A. C.: Calcium accumulating vesicles in the intercellular matrix of bone. In: Hard tissue growth, repair and remineralizations. Ciba Foundation Symposium 11: 213, 1973.
6. Andersson, I.: Mammographic screening for breast carcinoma. Malmö, Sweden, Dissertation, 1980, p. 26.
7. Asthbury, W. T.: In: Mercer, E. M. (ed.): Keratin and keratinization. New York, Pergamon Press, 1961, p. 255.
8. Azzone, G. F., and Massari, S.: Thermodynamic and kinetic aspects of the interconversion of chemical and osmotic energies in mitochondria. European J. Biochem. 19: 97, 1971.
9. Azzopardi, J. G., and Laurini, R. N.: Elastosis in breast cancer. Cancer 33: 174, 1974.
10. Baclesse, F., and Willemin, A.: Atlas of Mammography. Libraire des Facultés, Paris, 1967.
11. Bahrmann, E.: Über eine sammartig dunkelgelbe Verfärbung des Fettgewebes im Bereiche von Karzinomen, besonders der Mamma. Langenbecks Arch. u. dtsch. Z. Chir. 279: 109, 1954.
12. Bahrmann, E.: Die Mastopathie als Vorläufer des Mamma-Karzinoms. Dtsch. Gesund.-Wis. 17: 1762, 1962.
13. Bangham, A. D., and Pethica, B. A.: The adhesiveness of cells and the nature of the chemical groups at their surfaces. Proc. Roy. Phys. Soc. Edinburgh 28: 43, 1960.
14. Barth, V.: Atlas der Brustdrüsenerkrankungen. Stuttgart, Ferd. Enke Verlag, 1977.
15. Berndt, H., and Landmann, R.: Zwei epidemiologische Typen des Mammarkarzinoms. Arch. Geschwulstforsch. 33: 157, 1969.
16. Bolmgren, J., Jacobson, B., and Nordenström, B.: Stereotaxic instrument for needle biopsy of the mamma. Am. J. Roentgenol. 129: 21, 1977.
17. Boyden, S.: Cellular recognition of foreign matter. Int. Rev. Exp. Path. 2: 311, 1963.
18. Bradly, H. C.: Autolysis and atrophy. Physiol. Rev. 18: 173, 1938.
19. Buchwald, W. R., and Hülse, R.: Vermeidbare und nicht vermeidbare Fehlinterpretationen bei der Mammographie. Arch. Gynaek. 211: 42, 1971.
20. Busch, W., and Merker, H. J.: Elektronenmikroskopische Untersuchungen an mennschlichen Mammarkarzinomen. Virchows Arch. Path. Anat. Abt. A. 344: 356, 1968.
21. Castano-Almendral, A., Glätzner, H., and Siedentopf, H. G.: Vergleichende mammographische und histologische Befunde. Arch. Gynaek. 211: 43, 1971.
22. Citoler, P., Lanyi, M., Schmitz, H. K., Tissmer, R., and Zippel, H. H.: Die Verkalkungen der Mamma. Korrelation zwischen mammographischem und histologischem Befund. Dt. Krebskongress, München, 1974.
23. Citoler, P., and Derbolowski, S.: Stellt das lobuläre Carcinoma in Situ der Mamma eine Rarität dar? Vortrag auf der Sitzung der Nordrhein-Westfälischen Pathologen am 4.12. 1971 in Düsseldorf. Cited by Hoeffken and coworkers, 1977.
24. Craddock, C. G., Longmire, R., and McMillan, R.: Lymphocytes and the immune response. Part I. New Engl. J. Med. 285: 324, 1971.
25. Cutler, S. J., Zippin, C., and Asire, A. J.: The prognostic significance of palpable lymph nodes in cancer of the breast. Cancer (Phila.) 23: 243, 1969.
26. van Dam, K., and Meyer, A. J.: Oxidation and energy conservation by mitochondria. Ann. Rev. Biochem. 40: 115, 1971.
27. McDivitt, R. W., Stewart, F. W., and Berg, J. W.: Tumors of the breast. In: Atlas of pathology. Fasc. 2. Washington, AFIP, 1968.
28. Douglas, J. G., and Shivas, A. A.: The origins of elastica in

breast carcinoma. J. Coll. Surg. Edinburgh 19: 89, 1974.
29. De Duve, C.: General properties of lysosomes, the lysosome concept. In: De Renek, A. V. S., and Cameron, M. P. (eds.): Lysosomes. Ciba Foundation Symposium. Boston, Little, Brown and Co., 1963.
30. Egan, R. L.: Mammography: Report on 2000 studies. Surgery 53: 291, 1963.
31. Egan, R. L.: Fundamentals of mammographic diagnoses of benign and malignant diseases. Oncology 23: 126, 1969.
32. Falk, H., and Pfeifer, K.: Praktische Sektionsdiagnostik mit Schnellmethoden für Gerichtsmediziner and Pathologen. Leipzig, Thieme, 1964, p. 205.
33. Fenoglio, C., and Lattes, R.: Sclerosing papillary proliferations in the female breast. Cancer 33: 691, 1974.
34. Fisher, E. R., Palekar, A. S., Kotwal, N., and Lipana, N.: A nonencapsulated sclerosing lesion of the breast. Am. J. Clin. Path. 71: 240, 1979.
35. Folkman, J.: Tumor angiogenesis: Therapeutic implications. New Engl. J. Med. 285: 1182, 1971.
36. Folkman, J.: Anti-angiogenesis: New concepts for therapy of solid tumours. Ann. Surg. 175: 409, 1972.
37. Folkman, J.: Tumour angiogenesis. Cancer J. for Clinicians 22: 226, 1972.
38. Gallager, H., and Martin, J. E.: The study of mammary carcinoma by mammography and whole organ sectioning. Cancer (Phila.) 23: 855, 1969.
39. Gasic, G. J., Berwick, L., and Sorrentino, M.: Positive and negative colloidal iron as cell surface electron stains. Lab. Invest. 18: 63, 1968.
40. Gerlach, M., and Thiemann, H.: Elektronenmikroskopische Untersuchung der metastatischen Kalzifizierung. Klin. Wschr. 43: 1262, 1965.
41. Gershon-Cohen, J.: Breast roentgenology. Historical review. Am. J. Roentgenol. 86: 879, 1961.
42. Gershon-Cohen, J.: Atlas of mammography. Berlin, Springer, 1970.
43. Gesner, B. M., and Ginsburg, V.: Effect of glycosidases on the fate of transfused lymphocytes. Proc. N. Acad. Sci. U. S. 52: 750, 1964.
44. Grant, L.: The sticking and emigration of white blood cells in inflammation. In: Zweifach, B. W., Grant, L., and McCluskey, R. T. (eds.): The inflammatory process. New York, Academic Press, 1965, p. 197.
45. Greenblatt, M., Warren, B. A., and Konnineni, V. R.: Tumour angiogenesis: Ultrastructure of endothelial cells in mitosis. Brit. J. Exp. Path. 53: 216, 1972.
46. Gullino, P. M., and Grantham, F. H.: The influence of the host and the neoplastic cell population on the collagen-content of a tumour mass. Cancer Res. 23: 648, 1963.
47. Haagensen, C. D.: Diseases of the breast. Sec. ed. Philadelphia, Saunders, 1971.
48. Hamperl, H.: Zur Frage der pathologisch-anatomischen Grundlagen der Mammographie. Geburtsh. u. Frauenheilk. 28: 901, 1968.
49. Hamperl, H.: Strahlige Narben und obliterierende Mastopathie. Virch. Arch. A. 369: 55, 1975.
50. Harris, H.: Role of chemotaxis in inflammation. Physiol. Rev. 34: 529, 1954.
51. Harris, H.: Mobilization of defensive cells in inflammatory tissue. Bact. Rev. 24: 3, 1960.
52. Hassler, O.: Microradiographic investigations of calcifications of the female breast. Cancer (Phila.) 23: 1103, 1969.
53. Haydon, D. A.: The surface charge of cells and some other small particles as indicated by electrophoresis. I. Zeta potential surface charge relationships. Biochim. Biophys. Acta 50: 450, 1961.
54. Heard, D. H., and Seaman, G. V. F.: The influence of pH and ionic strength on the electrokinetic stability of the human erythrocyte membrane. J. Gen. Physiol. 43: 635, 1960.
55. Hoeffken, W., Lanyi, M., Gajewski, H., and Lennartz, K.-J.: Mammography. Stuttgart, Thieme Publ., 1977.
56. MacInnes, D. A.: The principles of electrochemistry. New York, Dover, 1961.
57. Irving, J. T.: Theories of mineralization of bone. Clin. Orthop. 97: 225, 1971.
58. Judah, D., and Spector, W. G.: Reaction of enzymes to injury. Br. Med. Bull. 10: 10, 1954.
59. Kim, K. M., and Huang, S.: Ultrastructural study of calcification of human aortic valve. Lab. Invest. 25: 357, 1971.
60. Lamarque, J.-L.: Le sein. Radiodiagnostic clinique. Paris, MEDSI Médecine et Sciences Internationales, 1981.
61. Van Lancker, J. L., and Holtzer, R. L.: The release of acid phosphatase and beta-glucuronidase from cytoplasmic granules in the early course of autolysis. Am. J. Path. 35: 563, 1959.
62. Van Lancker, J. L.: Molecular and cellular mechanisms in disease. Berlin, Springer, 1976.
63. Lanyi, M.: Differentialdiagnose der Microverkalkungen. Radiologe 17: 213, 1977.
64. McLean, A. E. M., McLean, E., and Judah, J. D.: Cellular necrosis in the liver induced and modified by drugs. Int. Rev. Exp. Path. 4: 127, 1965.
65. Leborgne, R.: Diagnosis of tumors of the breast by simple roentgenography. Calcifications in carcinomas. Am. J. Roentgenol. 65: 1, 1951.
66. Levitan, L. H., Witten, D. M., and Harrison, E. G.: Calcifications in breast disease. Mammographic-pathologic correlation. Am. J. Roentgenol. 92: 29, 1964.
67. Linell, F., Ljungberg, O., and Andersson, I.: Breast carcinoma. Aspects of early stages, progression and related problems. Acta Path. Microbiol. Scand. Section A, Suppl. 227, 1980.
68. Lundmark, D.: Breast cancer and elastosis. Cancer (Phila.) 30: 1195, 1972.
69. Marchesi, V. T.: The site of leucocyte emigration during inflammation. Quart. J. Exp. Physiol. 46: 115, 1961.
70. Menkin, V.: Biochemical mechanisms in inflammation. 2nd ed. Springfield, Ill., Thomas Publ., 1956.
71. Moros, L., Pinter, M., and Molnar, J.: Composition of microcalcifications. In: Hoeffken, W., Lanyi, M., Gajewski, H., and Lennartz, K.-J. (eds.): Mammography. Stuttgart, Thieme Publ., 1977, p. 163.
72. Moscona, A.: In: Brennan, M. J., and Simpson, W. L. (eds.): Biological interactions in normal and neoplastic growth. Boston, Little, Brown and Co., 1962.
73. Moscona, A. A.: Studies on cell aggregation: Demonstration of materials and selective cell-binding activity. Proc. Nat. Acad. Sci. 40: 742, 1963.
74. Nobel, P. S.: Free energy: The currency of life. In: Calcer, N. (ed.): Nature in the round. London, Weidenfeld and Nicolson, 1973, p. 194.
75. Nordenström, B.: Stereotaxic screw needle biopsy of nonpalpable breast lesions. In: Westinghouse-Logan, W. (ed.): Breast carcinoma: The radiologist's expanded role. New York, John Wiley & Sons, Inc., 1977, pp. 313–318.
76. Nordenström, B., Rydén, H., and Svane, G.: Breast. In: Zornoza, J. (ed.): Percutaneous needle biopsy. Baltimore/London, Williams & Wilkins, 1980, Chapter 5, p. 43.
77. Palmer, J. M., and Hall, D. O.: The mitochondrial membrane system. Progr. Biophys. Molec. Biol. 24: 125, 1972.
78. Pape, C., and Stegner, H.-E.: Vortrag Dtsch. Ges. für Elektronenmikroskopie, Karlsruhe, 1971. Cited by Hoeffken and coworkers, 1977.
79. Price, H. M., Hanrahan, J. B., and Florida, R. G.: Morphogenesis of calcium laden cytoplasmic bodies in malakoplakia of the skin. Human Pathol. 4: 381, 1973.
80. Reuterwall, O.: Om läkningsföreteelser i strålbehandlade cancer mammae. Nord. Med. 12: 3429, 1941.
81. Ross, R., and Benditt, E. P.: Wound healing and collagen formation. I. Sequential changes in components of guinea pig skin wounds observed in the electron microscope. J. Biophys. Biochem. Cytol. 11: 677, 1961.
82. Rubin, P. (ed.): Updated breast cancer. New York, American Cancer Society, Inc. Reprinted by the American Cancer Society, Inc., with permission from the International Journal of Radiation Oncology, Biology, and Physics. © 1977, 1978, Pergamon Press, Inc.
83. Salomon, A.: Beiträge zur Pathologie und Klinik der Mammakarzinome. Arch. klin. Chir. 103: 573, 1913.
84. Seaman, G. V. F., and Heard, D. H.: The surface of the washed human erythrocyte as a polyanion. J. Gen. Physiol. 44: 251, 1960.

85. Seaman, G. V. F.: Surface potential and platelet aggregation. Thrombos. Diathes. Haemorrh. (Stuttg.) Suppl. 26: 53, 1967.
86. Semb, C.: Fibroadenomatosis cystica mammae. Acta Chir. Scand. Suppl. 10: 1, 1928.
87. Simkiss, K.: Calcium in reproductive physiology. A comparative study of vertebrates. London, 1967, p. 112.
88. Shapiro, I. M.: The association of phospholipids with anorganic bone. Calcif. Tissue Res. 5: 13, 1970.
89. Sümegi, I., and Rajka, G.: Amyloid-like substance surrounding mammary cancer and basal cell carcinoma. Acta path. microbiol. scand. Sect. A. 80: 185, 1972.
90. Tremblay, G.: Elastosis in tubular carcinoma of the breast. Arch. Path. 98: 302, 1974.
91. Underwood, J. C.: A morphometric analysis of human breast carcinoma. Brit. J. Cancer 26: 234, 1972.
92. Wainio, W. W.: The mammalian mitochondrial respiratory chain. New York, Academic Press, 1970.
93. Weiss, L.: Studies on cellular adhesion in tissue culture. Exp. Cell Res. 53: 603, 1968.
94. Weiss, L., Bello, J., and Cudney, L.: Positively charged groups at cell surfaces. Int. J. Cancer 3: 795, 1968.
95. Weiss, L., and Levinson, C.: Cell electrophoretic mobility and cationic flux. J. Cell Physiol. 73: 31, 1969.

XVII.
Application of the principle of BCEC for treatment of cancer

In preceding chapters the reader's attention has been focused on the existence of biologically closed electric circuits (BCEC), and the importance of such systems for tissue function, structural development and healing processes. Spontaneous polarization within different BCEC systems over vascular, interstitial, ductal or other conducting pathways are involved in these reactions. In this chapter we will manipulate the systems in attempts to improve healing. This is possible because the circuits can be activated in many ways, e.g., by local supply of chemical agents, heat, pressure or electric energy. These studies will be performed in two ways. In one series local tissue injury will be produced in tumours by diathermia in order to induce spontaneous healing. In a second series electric energy will be delivered to the tumour and its surroundings as direct current over electrodes. Before the theoretical background and actual treatments are described, previous attempts to use electric current for treatment of tissue will be briefly surveyed.

In 1895 the electrophysiologist Golsinger (24) placed "unipolar" electrodes in the brains of dogs and produced focal injuries of tissue. A large "indifferent" electrode was placed on the abdomen of the animal, and 20 to 40 mA current were used. Eight coulombs gave a lesion the size of a pinhead and 36 coulombs a lesion as "large as a cherry".

Similar experiments were performed shortly thereafter by Sellier and Verger (60, 61). Using bipolar electrodes, they applied 8, 10 and 12 mA for 7 to 10 minutes and produced spherical lesions "the size of a pea".

Horsley and Clarke in 1908 (31) studied the tissue effects of direct current in the brain, using bipolar electrodes. They stated that "for a unit of time, e.g., 1 minute, there will be about a 1 mm breadth of destruction for each unit of current employed".

Hetherington and Ranson (30) produced lesions of about 1 mm diameter in the brain with 2 mA during 20 seconds and Krieg (35) 1.5 mm lesions in the brain with 2 mA for 15 seconds. Carpenter, Whittier and Mettler (13) used "unipolar" anodic electrodes and produced 1 mm lesions in the brain with 5 mA for 15 seconds. Hendley and Hodes (29) produced 2 mm lesions with 3 mA for 20 seconds in the brain. Anand, Dua and Schoenberg (2) made lesions of 1 to 1.5 mm diameter with 3 mA during 30 seconds in cat and monkey brains.

Platinum electrodes, which resist electrolytic destruction, were found by Louchs, et al. (38), to be superior to other metal electrodes in experiments of this kind.

Iontophoresis is another use of direct current in biology. An ionic compound is applied, often through

a micropipette, against neurons or other drug-sensitive tissues, by means of a pulse of direct current. It has already been shown (pp. 191–192) that it is not always possible in iontophoresis in vivo to predict where an ionic compound will be deposited simply on the basis of its polarity and the polarity of the electric field. Electrode reactions may also destroy or modify the iontophoretic agent. Nevertheless, ionic compounds can in principle be directed electrically to a tissue for therapeutic purposes. Remarkably enough, this therapeutic possibility has been neglected in practical medicine. Tissue and cells may also be considerably changed by an electric field or by the flow of electric current, as has been illustrated with blood and fat tissue (Chapters XIV and XVI).

In 1920 Ingvar (33) briefly described reactions of cells to galvanic current in tissue cultures. He applied a current of 2–4 billionths of an ampere and observed a directing influence of the applied electric forces on cells.

Induction of a callus by means of an electret has been reported by Fukada, Takamatsu and Yasuda (22). Phillips (48) has made use of alternating and direct currents to obtain vascular thrombosis for control of gastrointestinal haemorrhage and for the possibility of closing arteriovenous shunts. Yoneda, Matsuda and Shimizu (81) have produced electrothrombosis of arteriovenous malformations.

After the discovery of the piezoelectric polarization of bone subjected to load (5, 10, 21, 89, 99), many experimental and clinical attempts have been made to enhance healing of injured bone by the use of alternating (73, 74) and direct current (3, 6, 14, 25, 32, 37, 80). Formation of bone around the cathode and destruction of bone around the anode were described after 10 to 50 microamperes between two electrodes in experiments by Andrews and Friedenberger (3) and by Göhre (25). Clinical experiments to improve bone healing have yielded both encouraging and less beneficial results (37).

A conference on electrically mediated mechanisms of growth in living systems, published in the Annals of the New York Academy of Sciences (37), included recent experimental and clinical work focused particularly on the enhancement of bone healing by electric stimulation. From these studies it is evident that electric currents can support bone healing. Various results have been reported with the use of both alternating and direct currents and different positions of the electrodes. According to the way many of these experiments have been arranged, it seems possible that a beneficial effect may have been obtained in some cases simply as a reaction to a new injury. Traditional surgical management of a poorly healing fracture is to revise the injury in order to let the healing process start anew. A true enhancement of a healing process should be adapted as closely as possible to physiological healing. Unfortunately, we still do not have sufficient basic knowledge about these processes.

Some of the most urgent information to be collected should, in the author's view, include careful mapping in vivo of the *spontaneous fluctuations of the electric potential* in physiological healing. The normal fluctuations toward the "intermediate equilibrium" which we call healing could then possibly be used, with a suitably modulated current-time integral, to decrease the time of healing. Such a tailored driving force over electrodes between a site of injury and, for instance, a supplying vessel should then, of course, be applied with the site of injury initially electropositive. A suitable fluctuation of polarity of the external electric power source should then follow. In this view, a sufficient supply of suitable materials of varying kinds, at varying phases of the treatment, also must be considered before healing can be enhanced as a simulation of physiological events.

The effect of direct current on Jensen sarcomas in rats was studied by Reis and Henninger (51) already in 1953. A platinum anode was placed in the tumour and the cathode on the leg of the animal. 18–20 mA at 60–70 V were delivered over 15–20 minutes. After 8–10 treatments the tumours showed regression. The beneficial effects were ascribed to a deelectronation by anodic oxidation (50). This technique was also used in one patient with vulvar cancer (51).

Local heating of pulmonary metastases with diathermia was used in 50 patients, reported previously by the present author (39, 40), who later also reported on the first treatments of lung tumours with direct current (41).

Gardner, et al. (23), studied tumour cells injected into rats during application of a DC potential between two electrodes in the liver. They found that tumour cells were attracted around the anode. No tumour cells were observed around the cathode.

Bellamy, Hinsull, Watson and Blanche (7) inoculated rats with carcinoma cells (Walker 256) in a platinum loop connected to a platinum disc by a length of silicon rubber. Tumour growth was inhibited, a result interpreted as indicating the implant changed the microenvironment. The presence of a charged foreign body such as metal, which has its own electric potential, obviously can change the distribution of charges close to the metal surface. The potential differences in these experiments were only a few mV. Similar experiments of small quantities of direct current inhibiting tumour growth have also been performed by Schanble, Mutaz and Gallick (59). The possibility of controlling malignant tumour growth by direct current has also been mentioned by Srinivasan, et al. (66).

In patients, direct current has also been used to coagulate blood in vessels leading to a tumour. This

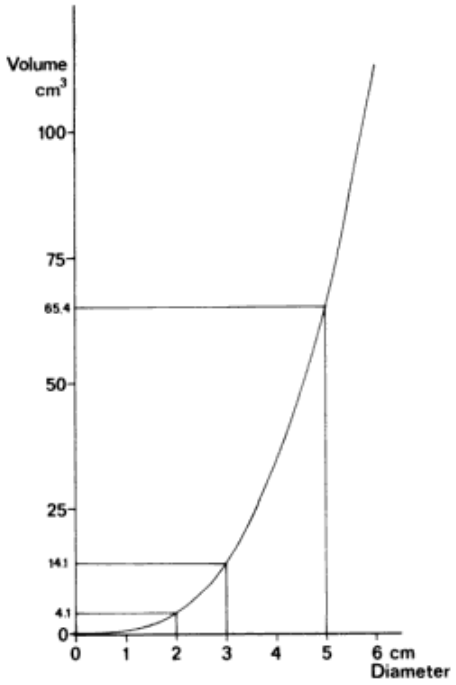

Fig. XVII: 1. Volume of spherical tumour increases exponentially with the diameter. This relationship must be considered in determining dose of treatment.

technique is based on the observation of Sawyer and Pate (58) that the intima of vessels is electronegative in relation to the outer wall. When the vessel wall is locally injured, the intimal polarity is locally reversed, inducing an electrostatic apposition of electronegative thrombocytes, which leads to formation of intraluminal thrombosis.

Recently Samuelsson, Olin, Berg and Jönsson (53–57) have reported experimental electrolytic destruction of tissue in pig, rabbit and rat with direct current.

In the author's opinion, any percutaneous technique which is intended for local destruction of a cancer can be applied only to relatively small tumours, i.e., less than about 3–4 cm in diameter. The reason is that a volume of tissue considerably larger than the radiographically apparent size of the tumour must be treated. Strands of radiographically invisible tumour cells often grow into the tissue surrounding the main tumour mass. The diameter of a spherical tumour vs. its volume is plotted in Fig. XVII: 1. For example, a tumour 2 cm in diameter has a volume of 4.1 cm^3. Radiographically invisible, centrifugal growth of the tumour by only 5 mm means a sphere of 3 cm diameter must be treated, i.e., 14.1 cm^3 of tissue. When locally destroying lung tumours with diathermia in the 1960's (39), the author achieved permanent destruction of lung metastases when they were about 1 cm in diameter. After technical improvements, which will be reported below, tumours of 2 cm diameter can now be successfully treated with diathermia as a primary destruction of the tumour tissue. Larger tumours in the periphery of the lung and of diameter up to 4 cm can, however, be treated successfully by means of direct current, as will be shown in these studies.

Before the initial mode of tumour therapy with direct current is described, *Section (A)* will discuss the occasional reports of spontaneous regression of proven malignant tumours. This clinical mystery is important because it is possible that spontaneous regression of tumours may be explained as an effect of spontaneous polarization within a BCEC. The possibility of spontaneous regression of tumours will be tested in two ways.

Section B presents a modified technique of *diathermia for producing nonspecific injury polarization of tumours.* The intention has been to destroy tumour tissue primarily by heat, thereby producing local electrochemical polarization, similar to that which occurs by spontaneous degradation in tumours. In this way the proposed mechanism of spontaneous healing over a polarizing BCEC was intended to become activated for the healing of the injured tissue and any remaining viable tumour tissue. This procedure represents therefore an *artificially induced self-driving system.*

Direct current treatment of tumours is described under *Sections C* and *D*. Two main effects are utilized. One is to obtain, if possible, a complete destruction of the tumour tissue by the liberation of protons at the surface of the anode, which is placed in the tumour. The other effect involves the induction of different biological and electrochemical reactions in the tissues surrounding the tumour. In this way, some of the spontaneously occurring processes of healing in tissue injury are intended to be induced. This procedure also represents the use of a *driven system* during the treatment, leading to an injury-induced *self-driving system* after the applied current is discontinued.

As shown by the experimental and clinical studies in the previous chapters, a large variety of tissue reactions can be induced. In general, application of direct current between a tumour and its surroundings will induce two kinds of transports: ions of the supporting electrolytes and electrolytic products from the surfaces of the electrodes. These transports thereby modify the conditions for survival of neoplastic cells. The transports also lead to the development of recombination products and the appearance of true "biological reactions", such as anodic accumulation of leukocytes, formation of capillary thromboses and scar tissue, water transport and changes of individual cells. In this way possibilities may exist for local treatment of regions of tissue larger than the tumour tissue primarily destroyed around the anode. To date many possibilities remain for optimizing the conditions of treatment,

e.g., with regard to electrode technique, suitable voltage, fluctuation of voltage, current-density and duration of treatment.

When direct current of "low" energy is used, the local destructive effects are low. Nevertheless, considerable effects on surrounding tissue can be expected when the current is allowed to flow over a long period of time, e.g., several hours. When direct current of "high" energy is used, local destruction close to the electrodes becomes pronounced. A large number of variables as yet undefined will influence these effects in individual tissues in vivo. Only extensive experimental and empirical testing will tell us how the treatment technique can be optimized. Alternatives to presently available clinical techniques of treating cancer are desirable. This need applies particularly for treating primary neoplasms in the most surgically inaccessible locations, e.g., brain, pancreas, liver, spine and prostate. Electrochemical treatments should offer promising results in these organs as well as for metastatic disease in various parts of the body.

A. Spontaneous and induced healing of cancers

The spontaneous disappearance of verified cancers is very rare, but well documented (20, 28, 63). Everson (18) and Everson and Cole (19) reviewed the subject extensively. Initially they considered 600 cases of reported spontaneous regressions but finally accepted only 47 as sufficiently documented by microscopic findings to justify inclusion in their series. Later they extended the study to include 120 authenticated cases. The authors admit that many of the discarded cases may also have been true expressions of spontaneous regression. Dunphy (16), Shimkin (62), Stewart (67) and others have also emphasized both the existence of spontaneous healing of cancers and the importance of recognizing such occurrences as a means of adding to our knowledge of environmental variations in the relationship of tumour and host.

The mechanism of spontaneous healing of a malignant tumour is still obscure. Presumably immunologic or hormonal, the mechanism has been thought to be a change in the environment of the tumour. For example, Smithers (64) noted that after three of his patients with breast cancer experienced a natural menopause, their tumours regressed for as long as seventeen years. In most cases, however, the process of spontaneous regression remains obscure.

Seen in the light of BCEC mechanisms, the therapeutic problem now is how best to support spontaneous tendencies toward healing of a growing tumour, when its foci of internal injury release energy only intermittently and often weakly. The energy released in spontaneous injury may be sufficient to induce ionic exchange by diffusion and migration over a BCEC, e.g., in healing ordinary wounds and fractures. Such conditions should perhaps be called *nonprogressive injuries*. Conversions of energy in biology usually take place with remarkably little loss of energy. The possibility is worth serious consideration that most of the energy necessary for ionic transports in healing a nonprogressive injury may be provided by the injury itself. In this view, infectious injuries or locally degrading injuries in cancers may be called *progressive injuries*. The critical point is that the healing induced in progressive injuries either temporarily or permanently lags behind the advancing primary pathologic process. Logically, extensive local destruction might release enough energy for the healing also of progressive injuries. Obviously enough, this solution is possible only in selected instances, usually most "elegantly" by surgical removal of the diseased tissue (and sometimes unfortunately also a large quantity of normal tissue). The ideal solution would be selectively to depress the disease by supporting physiologic healing mechanisms while preserving normal tissue. How electric current can be suitably used toward these goals is, of course, not easily answered. It will, however, be seen that direct current can offer beneficial effects on malignant tumours regarded as unsuitable for more traditional types of therapy.

B. Diathermic production of local tissue injury in lung tumours

1. Dry electrodes

A technique for local electrocoagulation of small solitary tumours in the lung has previously been described by the author, based on an experience of 30 patients (39, 40).

As much as possible of the centre of each of these solitary and relatively small tumours was electrocoagulated with an ordinary surgical electrocoagulation apparatus. The neutral large electrode was applied to the patient's skin. The active electrode consisted of a thin, Teflon-coated, stainless steel string, electrically insulated except at its tip.

This electrode, 0.5 mm in diameter was introduced percutaneously under biplane fluoroscopic control. A thermoelectric detector needle (0.9 mm in diameter)

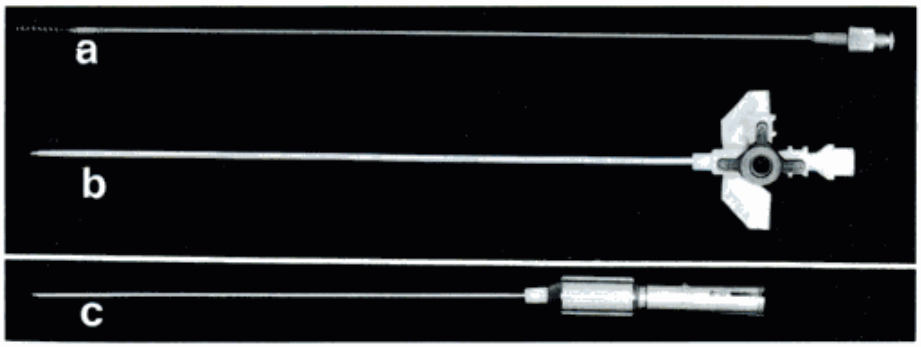

Fig. XVII: 2. Electrodes for "wet" diathermic electrocoagulation of pulmonary tumours. (*a*) Spiral screw soldered to a cannula. The exterior of the cannula is insulated with Teflon. This electrode is inserted through a Teflon tube (*b*) and anchored in the tumour tissue by the spiral part, which is screwed into the tumour. High frequency current applied between the tumour electrode and an indifferent, large, skin electrode produces heat in the tumour. Saline solution infused through the electrode maintains moisture and increases the quantity of sodium chloride in the tumour, enhancing conductivity. The transmitted heat is measured by an electrothermometer (*c*), which is placed at the edge of the tumour.

(Fig. XVII: 2 *c*) for recording of the generated temperatures was then similarly introduced and positioned at the edge of the lesion. Injured bronchial arteries inside the tumour sometimes bled, appearing fluoroscopically as a local blurring of the surroundings of the tumour. The bleedings stopped spontaneously. No serious complications occurred in any of these patients. This technique proved to be successful in causing necrosis of small neoplasms, usually small metastases less than 1 cm in diameter.

A drawback of this technique has been that much heat is generated in the tumour near the electrode. Nearby tissues desiccate easily, interrupting the electric current. Tumours larger than 1 cm in diameter were therefore usually unsuitable for this type of treatment.

In order to overcome these difficulties, a Teflon tube (1.5 mm in diameter, of the type shown in Fig. XVII: 2 *b*) was first inserted into the tumour. A 1.2 mm diameter needle served as stylet. After removal of the stylet, a Teflon-coated needle electrode, 1.0 mm in diameter (Fig. XVII: 2 *a*), was inserted through the Teflon tube. This modification made it possible to remove the electrode for occasional cleaning, which improved the efficiency of the electrocoagulation procedure.

2. Electrodes perfused with liquid

This technique presents certain advantages compared with the dry electrode technique.

The active electrode consists of a stainless steel cannula, 1 mm thick and insulated by Teflon. A spiral screw, 1 cm long, is soldered to the tip of the cannula (Fig. XVII: 2 *a*). The hub of the cannula is connected both to a surgical diathermia apparatus and via a Teflon tube (50 cm long and 2 mm wide) to a lymphography syringe. This syringe is filled with saline solution, which is slowly and evenly injected through the electrode during treatment. A large metal plate attached to the patient's arm is used as an indifferent electrode. In order to avoid a large pneumothorax, which might easily displace an electrode, it was found useful to place percutaneously an ordinary pleural drainage tube in the pleural space two days before implantation of the electrode.

Twenty minutes before the procedure the patient is administered a tranquilizer, such as Valium®, intramuscularly. Under local anaesthesia and biplane fluoroscopic control, the thin Teflon tube (Fig. XVII: 2 *b*) is inserted percutaneously into the tumour. Material for cytologic study is obtained via the cannula by means of a small screw needle instrument (44, 45). The material is stained immediately and examined microscopically. In the meantime the electrode is inserted through the Teflon tube, screwed into the tumour tissue and connected to the electrocoagulation apparatus and the lymphographic syringe. A forceful aspiration with the syringe must precede these manoeuvres in order to make sure that the tip of the Teflon tube is not positioned in a pulmonary vein, which might possibly introduce spontaneous inflow of air into the left side of the heart. The tip of the electrothermometer needle (Fig. XVII: 2 *c*) is placed in the tumour close to the surface.

Accuracy is required for implanting the electrodes. This requirement led to cooperative work with representatives of the x-ray industry, resulting in the development of the so-called BINO and SINO[1] units (42).

[1] Manufactured by Siemens-Elema, Stockholm, under the trade name of Angioscope.

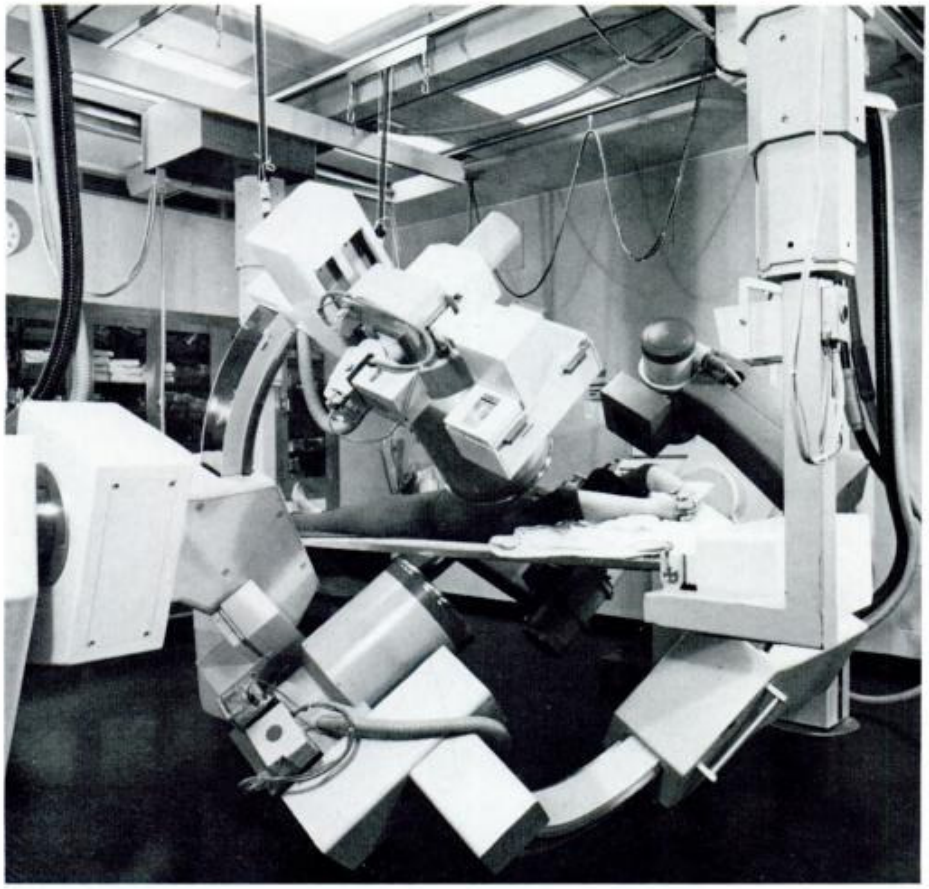

Fig. XVII: 3. Biplane fluoroscopic unit, designed for separate positioning of two arch-suspended x-ray tubes and image intensifiers in any direction in relation to the subject. The patient table, suspended in a coordinate system from the ceiling, allows positioning of the patient independent of the arch construction. Elevation of the table top, rotation of the patient and movements of the arches are controlled by servo motors from a control panel.

Fig. XVII: 4. Piece of meat (moosesteak) after local diathermic production of heat over an electrode perfused with saline solution. The cut surface through the boiled tissue is approximately 2.5×1.5 cm and grey-white. Diathermia over a dry electrode produces a small, black region of dry tissue, which easily breaks conductivity of the circuit.

This biplane equipment (Fig. XVII: 3) allows individual placements of two arch-suspended radiographic tubes and image intensifiers. The patient is examined on a roll sheet table suspended from the ceiling by telescopic stands, which are movable in a coordinate system. Nearly all the movements of the arches and of the patient table are performed remotely via servo motors from a control panel.

About 2–3 drops of saline solution per second are injected during the electrocoagulation. In this way the tissue close to the electrode tip is kept wet, securing a continued complete circuit over a prolonged time compared with the use of dry electrodes. Evaporated water escapes as steam between the wall of the cannula and the inner wall of the Teflon tube. At the same time the amount of salt increases in the tumour tissue, enhancing conductivity.

Usually the recorded temperature at the edge of the tumour was elevated to about 60°C for 4 to 5 minutes during each of these treatments. This level of heat means that the tissue is "boiled" rather than "fried", as with the dry electrode technique. The result of such a boiling of a piece of moosesteak is shown in Fig. XVII: 4. The tissue is opaque only in the coagulated

area. The effect in a lung tumour in vivo is difficult to predict, because it depends to a large extent on circulation of blood and ventilation, cooling the tissues.

3. Results

Twelve pulmonary metastases in eight patients as well as primary carcinoma of the breast in two patients have been treated by electrodes perfused with liquid. Table XVII: 1 surveys relevant clinical data of these ten patients.

Seven of the patients were women and three men. Ages varied between nineteen and sixty-four years. The size of each tumour at the time of treatment varied between 6 and 37 (mean 18) mm in diameter.

Eight of the tumours regressed after treatment, five showed progression and one was indeterminate. The two largest tumours showing regression had initial diameters of 29 to 30 mm. Longest observation time with persistent regression has been four years and eight months in one patient. No serious complications have occurred. In four patients small to moderate asymptomatic pneumothoraces developed. Before electrocoagulation was performed, ten of the tumours had continued to grow in spite of cytostatic therapy.

The courses of two patients with lung metastases and the two with breast tumours will now be described and illustrated in detail.

Case 1. A fibroliposarcoma of the uterus was excised from a 19-year-old woman. One year after operation a tumour 2 cm in diameter was found in the right lung (Fig. XVII: 5 *a*). The diagnosis of metastasis from the primary tumour was confirmed (Fig. XVII: 5 *b*) by a screw needle biopsy (44, 45) obtained under local anaesthesia. The Teflon tube (Fig. XVII: 2 *b*) was then

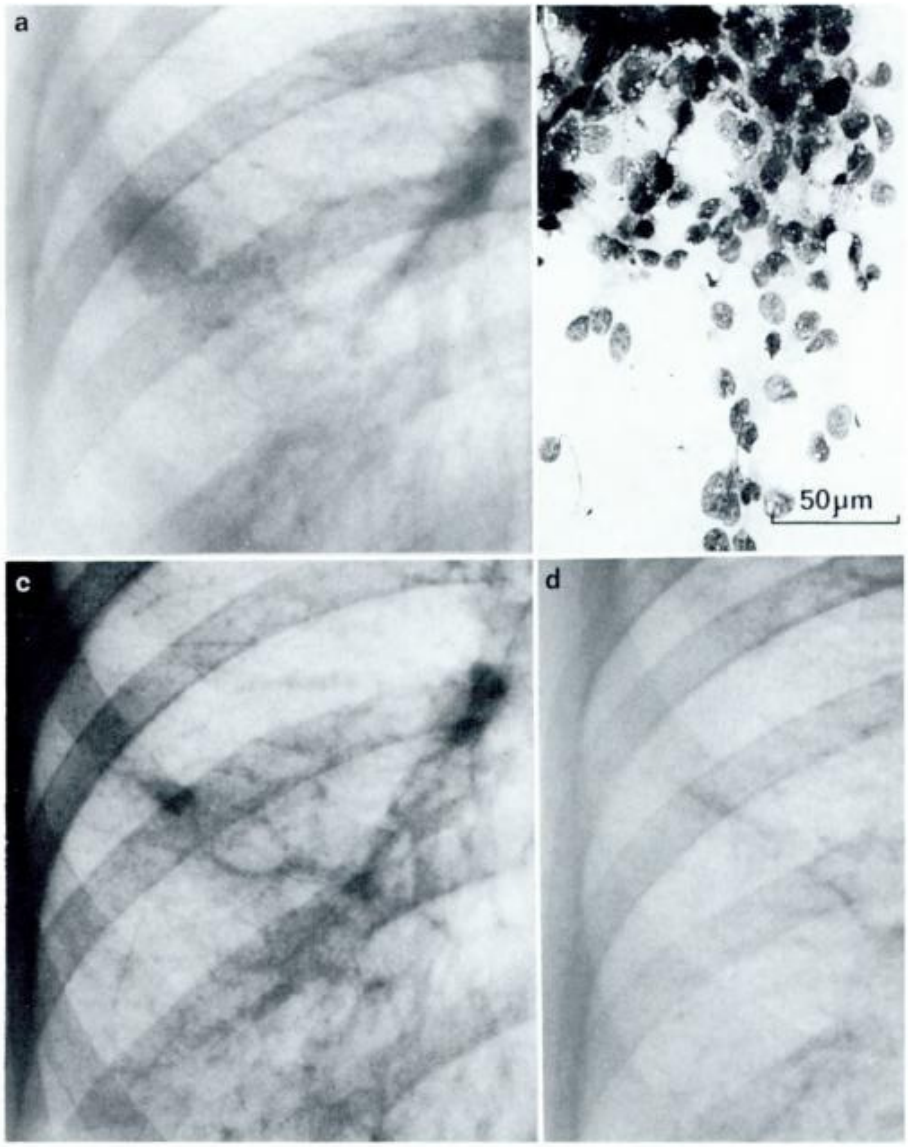

Fig. XVII: 5. Electrocoagulation followed by decrease in size of a metastatic fibroliposarcoma in the right lung. (*a*) Before treatment. (*c*) After 485 days. (*d*) After 1490 days. (*b*) Cytologic specimen obtained by percutaneous needle biopsy of the tumour before treatment. May-Grünewald-Giemsa stain.

Table XVII: 1. *Results of treatment by electrocoagulation (liquid-perfused electrodes) of metastatic cancer in the lungs in eight patients (no. 1–8) and primary carcinoma of the breast in two patients (no. 9, 10)*

No.	Patient Age	Primary tumour	Date of electrocoagulation Size of tumour (mm)	Observation time (days) Size of tumour (mm)	Effect on treated tumour	Comments
1.	B.K. ♀ 19	Fibroliposarcoma of uterus Resection 1977	I 9/2 1978 19×19×19	1 490 7×5×2	Regression	Continuous growth of four pulmonary metastases during cytostatic therapy before electrocoagulation of one, and later electrochemical treatment of three of the metastases (see Table XVII: 2).
2.	G.B. ♀ 32	Malignant melanoma of skin Resection 1976	I 27/4 1977 29×29×30	240 23×20×22	Regression	Previous cytostatic therapy, followed by tumour growth until electrocoagulation. Death from haemorrhage in one of several cerebral metastases. Small pneumothorax during electrocoagulation.
3.	A.T. ♀ 59	Carcinoma of uterus Resection 1974	Ia 31/5 1977 26×27×31	134 34×34×37	Progression	Tumours I and II initially of approximatively the same size. After two treatments, growth of tumour I accelerated compared to growth of the untreated tumour II.
			Ib 12/10 1977 34×34×37	583 68×68×73	Progression	
			II 31/5 1977 29×35×38 (untreated)	134 36×43×43	Progression	
				583 62×58×65	Progression	
4.	G.P. ♀ 52	Carcinoma of breast Resection 1969	I 18/11 1976 21×19×19	1 480 14×12×14	Regression	Previous cytostatic and antioestrogen therapy followed by growth of multiple pulmonary metastases. After electrocoagulation, regression of the two heated tumours. Small pneumothorax and small haemoptysis during electrocoagulation. Progression of untreated metastases in lung and skeleton.
			II 8/12 1977 16×14×12	1 080 2×2×2	Regression	
5.	J.D. ♂ 52	Hypernephroma Resection 1974	I 8/10 1976 13×10×12	1 145 9×11×9	Regression	Multiple pulmonary metastases increased in size after previous cytostatic treatment. Small pneumothorax each time of electrocoagulation. Noncoagulated tumours progressed rapidly. Death of widespread metastases.
			II 26/10 1976 16×13×15	630 8×8×8	Initial regression	
				1 127 49×52×60	Progression	
			III 9/11 1976 16×15×15	315 23×22×23	Progression	
				830 56×105×67	Progression	
			IV 17/2 1977 9×10×9	1 010 30×42×40	Progression	
6.	U.L. ♀ 37	"Malignant adenoma" of parathyroid Resection 1972	I 3/11 1976 6×15×7	60 16×10×10 (cavity)		Cytostatic therapy failed. Twelve months after electrocoagulation, death of widespread metastases.
				455 10×6×6 (scar)	Regression	
7.	B.R. ♂ 50	Carcinoma of thyroid Resection 1967	I 15/2 1977 30×30×30	415 45×42×47	Progression	Fourteen months after electrocoagulation, death of widespread, rapidly growing metastases.
8.	L.V. ♂ 42	Hypernephroma Resection 1977	I 14/12 1977 18×18×18	200 17×15×15	Regression	Cytostatic therapy failed. Seven months after electrocoagulation, death of widespread metastases. Small pneumothorax.
9.	M.Ö. ♀ 58	Adenocarcinoma of breast	I 2/11 1976 13×13×10	850	Progression	Failed cytostatic and hormone treatments. Distant metastases at the time of electrocoagulation. Death of widespread metastases.
10.	M.B. ♀ 64	Adenocarcinoma of breast	I 12/10 1977 29×26×26	550 19×8×13	Regression	Failed cytostatic and hormone treatments. Distant metastases at the time of electrocoagulation. Death of widespread metastases.

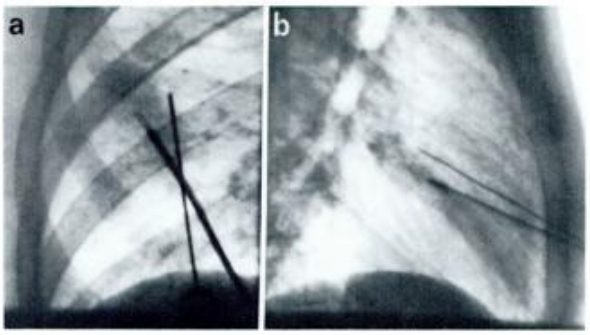

Fig. XVII: 6. Screw-cannula-electrode at the edge of the tumour shown in Fig. XVII: 5 *a*, just before the screw was placed in the tumour. Thermoelectric electrode positioned at the anteromedial aspect of the surface of the tumour. (*a*) Anteroposterior view. (*b*) Lateral view.

introduced into the tumour and the needle was removed. The electrode, with a metal spiral at the tip, was then passed through the Teflon tube and screwed into the tissue of the tumour, and thereby secured in a fixed position. Fig. XVII: 6 *a* and *b* illustrate posteroanterior and lateral projections of the electrothermometer needle at the surface of the tumour and the tumour electrode just before placement into the tissue of the tumour.

The indifferent electrode was then applied to the patient's right arm and saline solution infused slowly under diathermy. The temperature at the tumour surface was maintained at about 60°C for 5 minutes, as seen in Fig. XVII: 7.

No pain, bleeding or other complications occurred but the patient experienced "a sensation of heat somewhere inside" during the treatment.

When a treatment is successful by this method, the tumour regresses slowly but apparently continuously. The diminished size of the residual tumour in this patient can be seen after one year, four months in Fig. XVII: 5 *c*. Four years and one month after treatment only a minimal scar remained (Fig. XVII: 5 *d*).

Case 2. This 32-year-old woman, who six years earlier had had a malignant melanoma excised from the skin of a breast, had another malignant melanoma excised from her right leg. Shortly thereafter, a large metastasis (40×30×30 mm) was excised from the right frontal lobe of the brain. One month later a tumour, 2 cm in diameter and of very low radiographic opacity, was found in the lower lobe of the left lung (Fig. XVII: 8 *a*). This tumour grew during two months of treatment with different cytostatic agents (Dacarbazinum, DTIC, Vincristinum, and Oncovin).

This solitary pulmonary metastasis was then treated with electrocoagulation. The screw electrode cannula was secured to the tumour, as in the previous case. Diathermy was applied and temperature at the surface of the tumour was monitored (Fig. XVII: 8 *d*) during the continuous infusion of saline solution. A small pneumothorax was found after the treatment but no bleeding occurred.

After 2 months, the regressing tumour (Fig. XVII: 8 *b*) is clearly more radiopaque than before electrocoagulation. The increase in density is most likely caused by intratumoural accumulation of calcium. The size of the tumour decreased further, as shown 8 months after the treatment (Fig. XVII: 8 *c*).

Six weeks later, cerebral symptoms recurred as metastatic disease reappeared in the brain. She died shortly thereafter.

In the two patients with breast carcinoma and distant

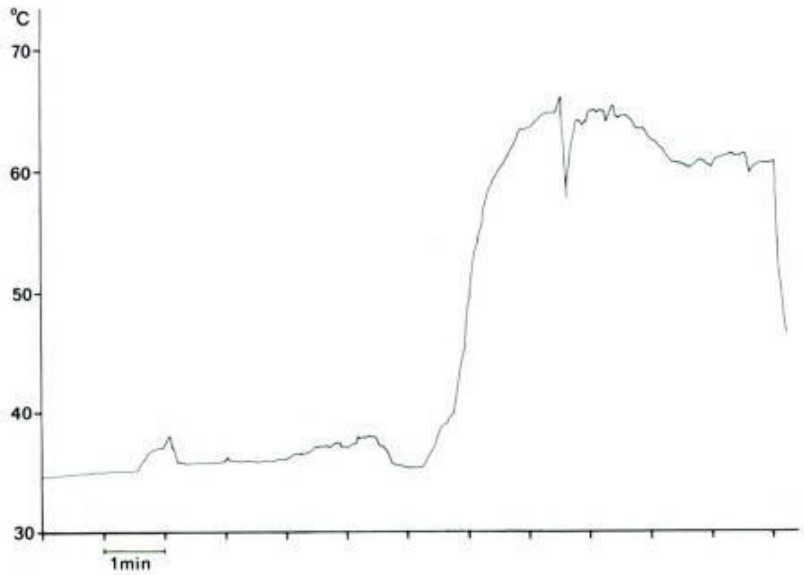

Fig. XVII: 7. Temperature of about 60°C for 5 minutes at the edge of the tumour shown in Fig. XVII: 5 *a*. Tracing obtained from electrothermometer placed at the surface of the tumour.

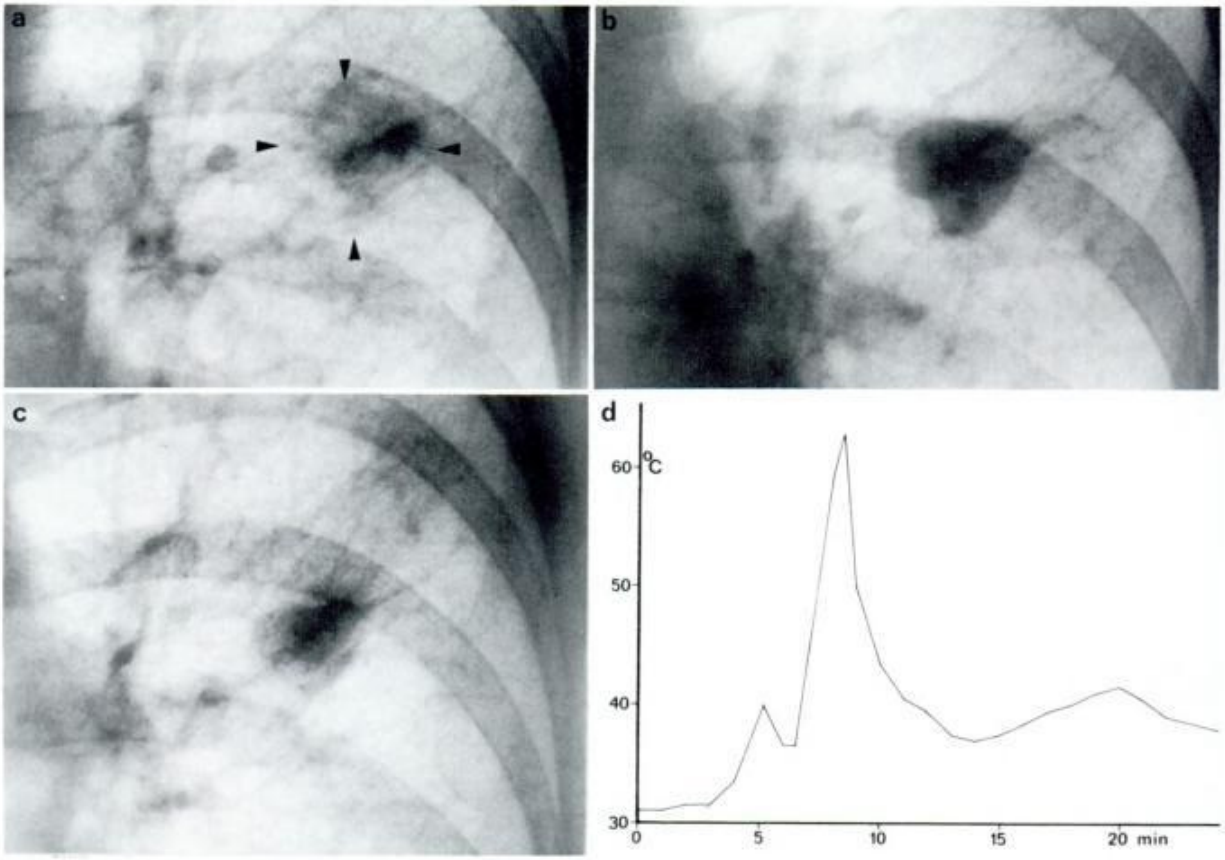

Fig. XVII: 8. Electrocoagulation (liquid-perfused electrode) of metastatic melanoma of low radiopacity (*a*) is followed by a considerable increase in opacity of the tumour 60 days later (*b*). 180 days later (*c*), the tumour has clearly decreased in size. The increased radiopacity probably represents an inflow of calcium into the injured tumour tissue. (*d*) Temperature measured at the surface of the tumour during electrocoagulation.

metastases (Cases 9 and 10 in Table XVII: 1), the breast tumours were treated with local electrocoagulation. The diagnosis of each cancer was made by screw needle biopsy.

The cell sampling for cytologic diagnosis and the placement of the active electrode and temperature probe in the mammary tumours were performed by means of the stereotaxic instrument previously described (9, 43). The biopsies and treatment were each performed under local anaesthesia. The indifferent electrode was placed on the arm of the patient. The treatments, each of which lasted about 30 minutes, were well tolerated.

Fig. XVII: 9*a* shows one of the breast cancers (case 9) before treatment, when it measured 13×13×10 mm. Fig. XVII: 9*b* shows the liquid electrode in the centre of the tumour and the thermometer at its edge. During the treatment, vapour escaped through the Teflon tube as well as through the electrode cannula. No bleeding or general reactions were produced by the treatment. The tumour is seen immediately after treatment in Fig. XVII: 9*c*, and 11 months later in Fig. XVII: 9*d*. The cancer appeared to have increased in size but showed internal accumulation of calcium and some radiating, fibrous structures in the surrounding breast. Fig. XVII: 9*e* shows the tumour enlarged and differently shaped 2 years, 4 months after the treatment.

The second patient with breast cancer (case 10) is shown before treatment in Fig. XVII: 10*c*. Numerous radiating, fibrous structures surround the tumour. Fig. XVII: 10*a*, *b* shows stereoradiographs (±15°) of the position of the electrode perfused with liquid and of the electrothermometer in relation to the tumour. The temperature was elevated at the tumour edge to 60°C for six minutes. This carcinoma appeared to stop growing after treatment. It is shown 1 year, 6 months after treatment in Fig. XVII: 10*d*, shortly before the patient died from widespread metastases, which were already established before the treatment.

In both of the two patients with breast cancer treated in this way, the clinical course and initial radiographic appearances were almost identical. They both suffered from many distant skeletal metastases, which

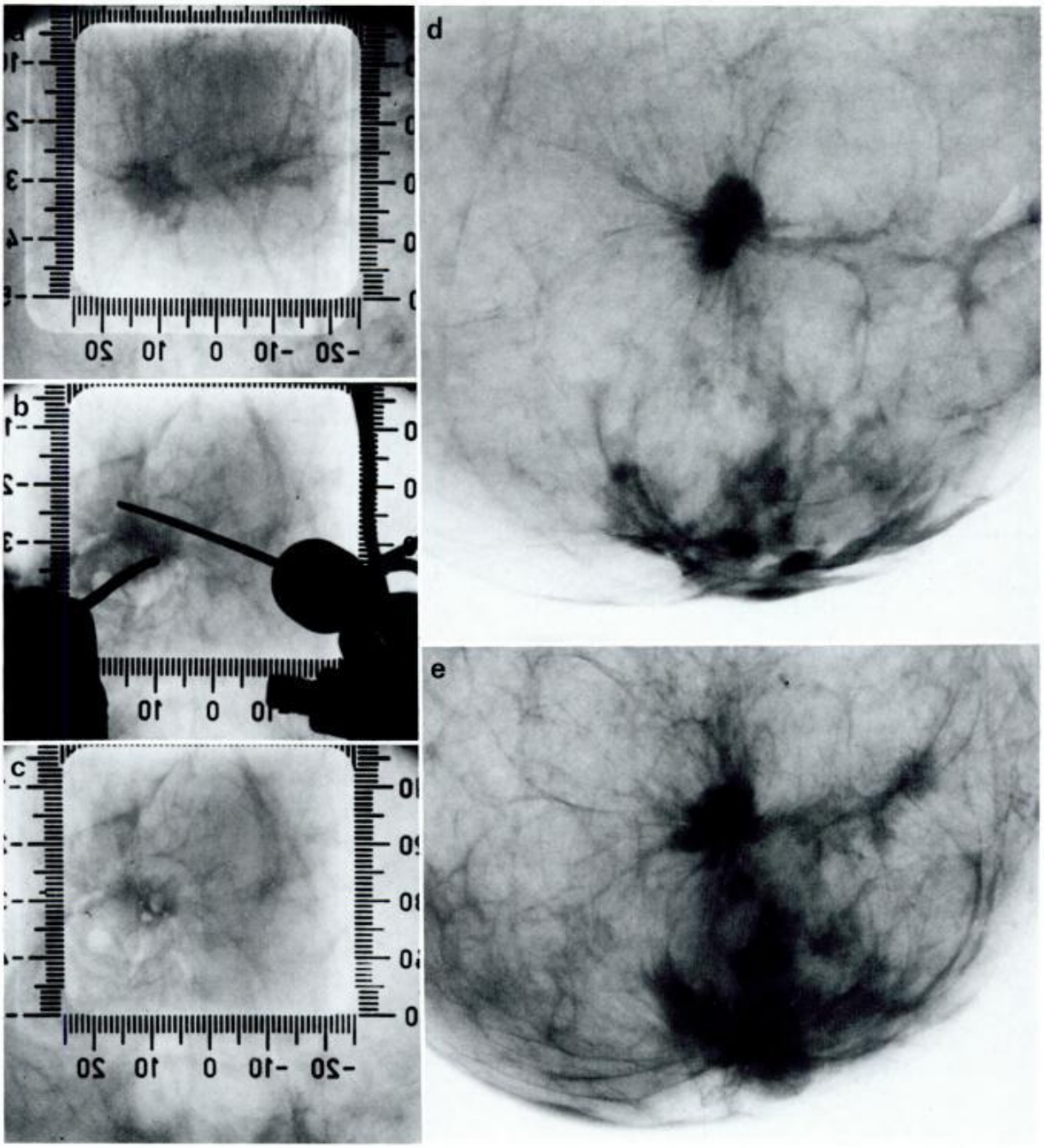

Fig. XVII: 9. Electrocoagulation of a breast carcinoma. The diagnosis was established in this 59-year-old woman by stereotaxic screw needle biopsy. Many distant metastases precluded local surgical excision. Local electrocoagulation, 1976, (*a*) immediately before, (*b*) during, (*c*) immediately after electrocoagulation (stereotaxic equipment, liquid-perfused electrode). (*d*) Radiograph 330 days later shows numerous, thin, radiating, fibrous structures emanating from the enlarged tumour. (*e*) 850 days after treatment and shortly before the patient died. The treated tumour has enlarged and changed its shape the last 520 days. Radiating fibrous structures have increased in number. Subareolar radiopacities and retraction of the nipple have increased. New infiltrations lateral to the treated tumour are seen.

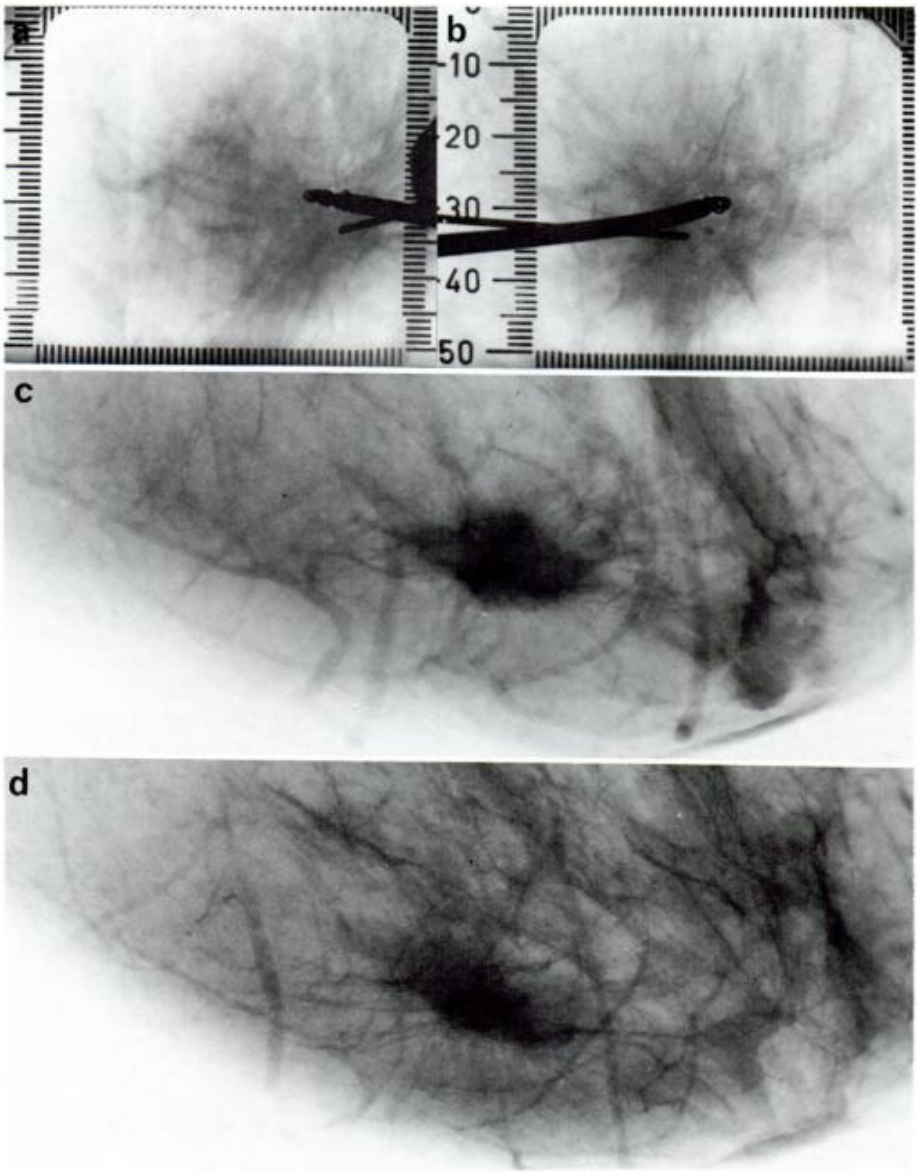

Fig. XVII: 10. Electrocoagulation of breast cancer by liquid-perfused electrode. The tumour is surrounded by radiating, fibrous structures before treatment (*c*). Stereoradiographs (*a, b*) of the tumour and electrodes inserted by means of stereotaxic instrument. (*d*) 550 days after treatment, shortly before the patient died. The tumour is slightly smaller than before treatment.

made it impossible to obtain follow-up biopsies after the treatments. One tumour progressed, one regressed. Unfortunately, necropsies were not obtained for these two patients.

In summary, the small number of patients and short observation time allow little conclusion about the long term effects of electrocoagulation of lung and breast cancers, except to observe that the procedure is feasible and may be beneficial in certain patients. The treatments are relatively easy to perform and are not very distressing to the patients.

4. Complications

Complications have been limited to the occasional development of a small pneumothorax in the pulmonary cases, which is easily managed by a pleural suction drain. No serious bleedings or cardiac arrhythmias have been encountered. On two occasions the spiral part of the electrode was lost in the tumour tissue after the electric current corroded the stainless material. It should therefore be made of a more corrosion-resistant metal, which still must allow the electrode to be secured in some way in the tumour tissue. Occasionally during treatment the patients reported a sensation of pain, coinciding with too little saline solution perfused, which can result in sudden disconnections and reconnections of the electric circuit. Pain is also easily produced when the electrode is located close to the pleura, which in such cases should be anaesthetized. The treatment can be repeated. Histologically, the distance after electrocoagulation between completely destroyed, necrotic tissue and normal tissue is only 2–3 mm.

5. Discussion

Considerable evidence (47, 52, 76) indicates that malignant cells are more sensitive to heat than are most normal cells. Electrocoagulation with large external electrodes has also been practiced in the treatment of neoplasms of skin and mucous membranes, e.g., carcinoma of the vulva (8).

For deeply situated tumours, technical control during treatment is considerably more complicated, but not at all impossible (39). Introducing irrigation of the active electrode has been an improvement in such cases. Compared to electrocoagulation with dry electrodes, the volume of destroyed tissue can be increased. The risks of cutting a vessel or depositing material on the electrode, leading to interruption of the current, are also almost completely excluded.

The drawback of the technique is the uncertainty about the transmission of heat to different parts of the tumour. Local variations in vascularity may interfere uncontrollably with the transmission of heat.

In retrospect, it now seems evident (see Table XVII: 1) that the electrocoagulations of the tumours of patient no. 5 (perhaps excepting tumour I) were not performed with sufficient transmission of the generated heat to devitalize all malignant cells of tumours II, III and IV. Only part of the tissue of these tumours was destroyed. These electrocoagulations were performed at an early stage in the development of the technique. A minimum of 60°C measured at the edge of a tumour for at least five minutes has therefore been introduced as the standard "dose" in these treatments. The treatments appear to have been effective only in tumours smaller than 2 cm in diameter.

The mechanism of healing of tissue injured by heat, as described in this section, must be considered in comparison with previously described results. Several of the phenomena of healing described in this section can be recognized as requiring the mechanism of a fluctuating potential over a BCEC. The decrease in size of these tumours can in a traditional way be explained as a result of resorption of destroyed material. Certain details in the transformations of the tissues are, however, not easily explained in a traditional way. Increase in radiographic density in a coagulated metastasis (Fig. XVII: 8 *b*), the development of an "A" zone around a tumour, and late signs of fibrous tissue production (Fig. XVII: 9 *d*, *e*) suggest that the proposed mechanism of healing of injury over BCEC channels has been activated in these transformations.

C. Induction of healing reactions in tumours by direct current

1. Introduction

Once the background of results was available from the in vitro and in vivo studies of the effects of direct current on tissues (Chapters XIV and XVI), a technique was developed for applying direct current to treatment of tumours. The technique proved acceptable. A brief first report on electrochemical treatments in five patients with otherwise untreatable pulmonary metastases was given in 1978 (41).

Complete primary destruction of a malignant tumour in lung was not attempted for cancers which are large and positioned centrally, i.e., close to large vessels. The evident reason is the risk of producing serious vascular injury.

The present method is based on the assumption that the primary destruction of tissue around the anode is supplemented by the ability of direct current to induce specific biological healing reactions in surrounding tissues. Some of the mechanisms of healing, as discussed in previous chapters, can now be induced and enhanced by a method which appears to support tendencies toward spontaneous healing. Some general aspects of the mechanism of tumour healing after ionization of tissue will now be considered.

Direct current ionizes tissue, as does ionizing radiation. In radiotherapy, selective destruction is produced in malignant tumours (15, 17, 34). Several factors, e.g., the degree of oxygenation of the tissue, influence the destructive effects. Ionizing radiation is known to be far more destructive to intracellular nuclei than to cytoplasm (11). It is also believed that the biochemical constituent most sensitive to the effects of ionizing radiation is DNA (49). When quanta of radiation bombard DNA in a solution, free radicals are generated from the DNA and the medium. The free radicals then react with the DNA. A few protons administered to the chromosomes produce considerable damage, such as chromosomal ruptures, while more than 1 000 protons do not affect the cytoplasm (71).

Effects similar to the damage by ionizing radiation in tumour therapy can also be anticipated to occur when direct current ionizes tissue. Certain observations in this study indicate that ionization of tissue via electrodes appears to affect normal and malignant tissues differently. At the same time, considerable differences exist between these two ways to ionize tissue. In electrochemical treatment, electric energy can be selectively applied to obtain ionization. New materials

develop at the electrode surfaces. These materials and those of the supporting medium migrate and diffuse in the electric field. Furthermore, direct current induces in tissue many structural modifications which appear indistinguishable from those of ordinary wound healing.

Resistivity and capacitance vary in different biologic tissues. An electric current in tissue therefore encounters local barriers which will change its directions. Air, bone, fat, matrices of cellular membranes and walls of vessels present relatively higher resistivity than blood plasma and interstitial fluid. Patterns of different preferential pathways for current in tissue can therefore be expected, as can different intensities of transport and electrochemical reactions. Varyingly differentiated flow patterns can be expected to develop as functions of energies (potential differences) and densities of current (amount of current per cross-sectional area of the path of flow).

It has long been known that elevation of electrode overpotential increases current logarithmically (69). Moreover, one can also predict that the patterns of current flow must be modified by local variations in electric capacitance and resistivity of tissues at different overpotentials. These local variations indicate that an equal amount of current which has passed between electrodes at different voltage differences should mean a different spatial distribution of current in the tissues and hence different regional biologic effects.

It is apparent that the amount of energy delivered to tissue by direct current can not be expressed in the same terms as are used for radiotherapy. Radiation treatment of deeply situated cancers is limited to the use of high energy photons. Therefore in radiotherapy the factor of minimum ionizing energy is indiscriminate for different kinds of matter. Ionization by direct current, on the other hand, can be produced over a large range of "low" to "high" energy levels. Low energy levels appear feasible, because they can be used to build up the therapeutic dose of energy from the inside of a tumour. In this way the use of direct current may theoretically induce a large range of different biological ionizing effects.

At "low" electrode voltages, only outer electrons with low binding energies are likely to be affected, which may suffice for interference with important biologic tissue and cell functions. When current densities are kept low, the extent of destruction of tissue by heat is also kept low.

At "very high" electrode voltages, electrons of lower kinetic energy will also be removed, resulting in different qualitative changes of the ionized tissue compared with the changes induced by low voltage ionization. Increased destruction around the electrodes will then become evident and the preferential pathways for current in different tissues will become less differentiated (see also Fig. XVII: 14). Increasing heat will evaporate water, resulting in elevation of pressure in the tissues. Thermic and electrically induced precipitation of protein will become prominent.

Direct current will also produce different biologic effects in the anodic and cathodic fields.

Since the beginning of the century, it has been well known (31) that the destructive effect around the anode is caused by diffusion and migration of protons, which make the tissue black. The cellular components of blood also turn black around the anode. Erythrocytes are known to produce electropositive haemin in the acidic surroundings of the anode, while electronegative haemin is produced in the basic surroundings of the cathode (36). Haematin is the electroneutral component (36). The central part of the brown-black material around the anode will be grey-white, due to bleaching by liberated chlorine gas (see Fig. XIV: 21). This focal discolouration of the black tissue has no effect whatsoever on the devitalization of the anodic tissues. The anodic tissues have already been destroyed by an abundance of easily diffusing and electrophoretically migrating protons. This point needs stress because the production of chlorine gas has recently and erroneously been suggested (53–57) as responsible for the destruction of tissue around the anode. The destructive effect around the cathode is caused by production of hydroxyl ions.

In addition to the migration and diffusion of ionized products at the electrode surfaces, other charged compounds will move throughout the electric field. Leukocytes, which are negatively charged, will at proper electrode voltages accumulate massively in the anodic tissue. Microthromboses also will be induced. They are probably mediated by electrophoretic accumulation of thrombocytes. Complex ions of proteins, fat and carbohydrates will be transported. Their charges will become modified under the influence of the actual acidic or alkaline surroundings in the electrical field. The water pressure of tissue will decrease around the anode (Chapter IX). This drying of tissue around the anode looks like dry gangrene. Around the cathode the interstitial oedema will to a large extent compress the vessels.

Extremely complex modifications of tissue components, cells and cellular contents are still further modified by matrix interference in the electric field, including tissue and blood circulation and convection factors. The size, shape and location of electrodes in relation to the structures of affected tissues will influence the shape and size of the anodic and cathodic fields. Of particular importance also is the fact that tissue cells, including cancer cells, carry a surplus of fixed negative charges. An anode in a tumour will therefore tend to keep the malignant cells together. Consequently an electrode should not, at least as a first

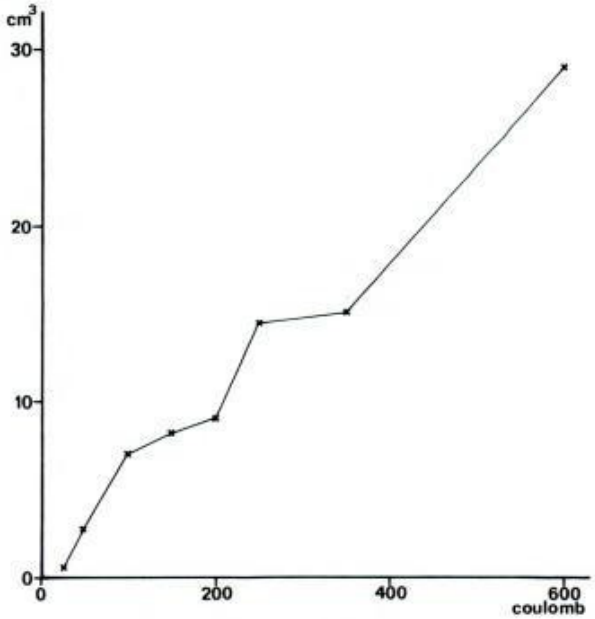

Fig. XVII: 11. Volume of necrotic shoulder muscle in a dog as a function of quantity of direct current passed between the anode, percutaneously inserted in the muscle, and the cathode in the thoracic aorta (10 volts potential). Destruction of muscle was defined as both white and black necrosis.

step in a treatment procedure, be placed in a tumour and be made cathodic. An intratumoural cathode can be expected to repel tumour cells and therefore increase the risks of producing distant metastases.

All these factors, and probably still unknown ones, make it desirable to define the conditions of treatment as carefully as possible, e.g., applied voltage, total amount of current, ionized tissue volumes and "electrode technique". This last factor includes definition of size, shape, material, polarity and position of electrodes. It is, however, apparent that a fully meaningful definition of electrode "position" is often difficult to obtain. In a strict sense it should require detailed knowledge of topography, resistivity and circulatory conditions of all components of the tissues.

Fig. XVII: 12. Section through perianodic tissue in the shoulder of a dog subjected to 150 coulombs direct current in vivo. Cathode in the aorta (10 volts).

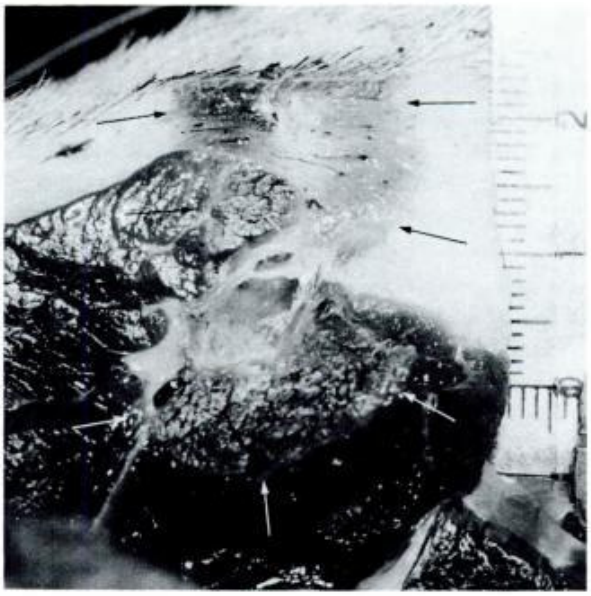

2. Preliminary technique

In dog experiments a technique was developed after initial testing of different voltages and amounts of current on lung, skin, fat, liver and muscle tissue. The intention was to use the reaction to anodic injury as a preliminary indication of the effect of treatment. A platinum string 0.2 mm thick and 20 mm long was used as the anode in each of eight dogs. The active surface of the anode was 12.6 mm^2. The strings were introduced percutaneously into the skin, subcutis or muscle tissue of the side of the neck. The cathode was a stainless steel arteriographic guide wire in the thoracic aorta. The active surface of the cathode was 190 mm^2. Ten volts of DC current were then applied between the electrodes.

Initial levels of current were about 10 mA, which increased gradually to about 30 mA during one hour. As the amount of current at 10 volts increased, the volume of the black, destroyed tissue increased (Fig. XVII: 11). Fig. XVII:12 shows a section through a lesion produced with 150 coulombs. The volume of destroyed tissue around the anode was in this case about 8 cm^3.

A cavity will be produced around the anode as gas is produced and the tissue dehydrates.

When the anode is placed in subcutaneous fat tissue, the tissue shrinks and becomes dehydrated and greyish. In muscle (or lung tissue) the destroyed area consists of amorphous material without visible cells. Fig. XVII: 13 illustrates (*a*) a completely destroyed, (*b*) an intermediate and (*c*) a normal zone in muscle around the anode. The width of the intermediate zone is approximately 0.3 mm. The tissue (*c*) adjacent to such lesions contains cells characterized by various degrees of cloudy swelling. Extensive capillary thromboses are also present in "normal" tissue around the lesions. In vivo such thromboses should eventually lead to circulatory disturbances peripheral to the tissue which has been primarily destroyed. A massive accumulation of leukocytes can also be induced in the vessels and tissue around the destroyed zone. The destroyed and intermediate zones also are dehydrated, due to electroosmosis. These extensive changes are

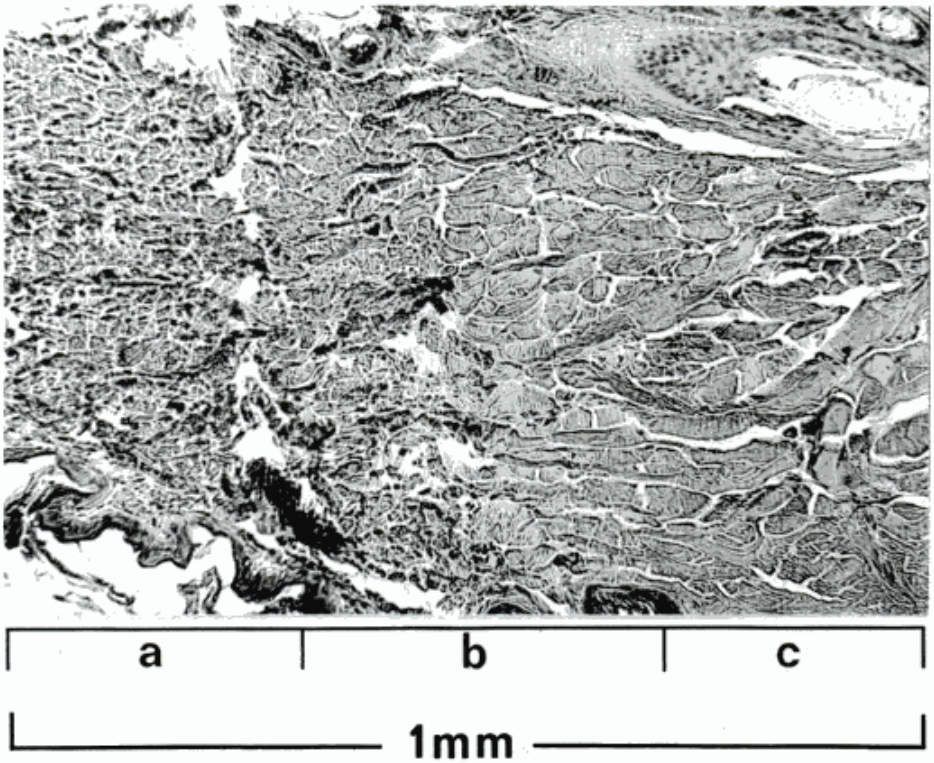

Fig. XVII: 13. Perianodic necrosis of muscle after 10 volts, 150 coulombs, direct current in a dog. Histologic section from edge of necrotic zone shows (*a*) complete coagulation necrosis, (*b*) a transition zone to (*c*) normal-appearing tissue. Haematoxylin-eosin stain.

easily observable field effects, clearly indicating that possibilities exist for modifying the environment of a lesion outside the region of primary destruction. It is evident that field effects are capable of modifying normal as well as abnormal components of tissue. Only empirical tests of electrochemical treatment with direct current will be able to supply conclusive information about possible selective effects on neoplastic tissue.

Preliminary technical tests have showed that circular or point-shaped electrodes produce circular or spherical primary lesions and that long string electrodes produce cylindrical or ovoid lesions. These results require that the anode and cathode must also be separated by a distance of at least the expected diameter of the primary, proton induced, black anodic lesion at a potential difference between the electrodes of less than 15 volts. Forty volts applied between one subcutaneous electrode (anode) in the left thoracic wall and one (cathode) in the right abdominal wall in a dog produced cylindrical interelectrode damage in the skin, ribs, lung, diaphragm, stomach, liver and the abdominal wall as an effect of an electric short circuit between the electrodes (Fig. XVII: 14). The current through this dog was allowed to cross the tissues for over four hours. Coagulation necrosis appeared in a cylindrical core through the different interpositioned tissues, without any regard to their morphologic boundaries. The diameter of this core was about 4–5 cm and the border with surrounding tissues rather well demarcated.

The application of an electric field over the heart is generally to be avoided (72). It was, however, found that transpulmonary direct current at 20 volts in the dog produced no disturbances of rhythm or any other evidence of cardiac injury. The current was led through an arteriographic guide wire (cathode) in a plastic catheter introduced intravenously through the heart and placed with its tip in a pulmonary artery. The anode was placed in the pulmonary parenchyma.

Cardiac arrhythmias caused by direct current have been previously studied in experiments by Phillips (48). In two experiments in dogs he tried to induce cardiac arrhythmias via a grounded electrode (cathode) over the left upper chest and the anode in the coeliac axis. Current flow as much as 10 mA produced no cardiac irregularities. When the anode was placed in the aortic arch and the grounded plate was placed against the buttocks, no irregular heart beats were observed (current $\leq$10 mA). Even when the anode was placed in the left ventricle, currents below 2–3 mA had no effect on the myocardium. Above this level, however, premature contractions were produced. At 6 mA the cardiac rhythm became very irregular. Fibrillation was induced at levels of 8 mA or higher.

Whenever current is applied, voltage must be increased slowly, e.g., from no current to 10 V in one minute. Whenever a treatment is concluded, voltage

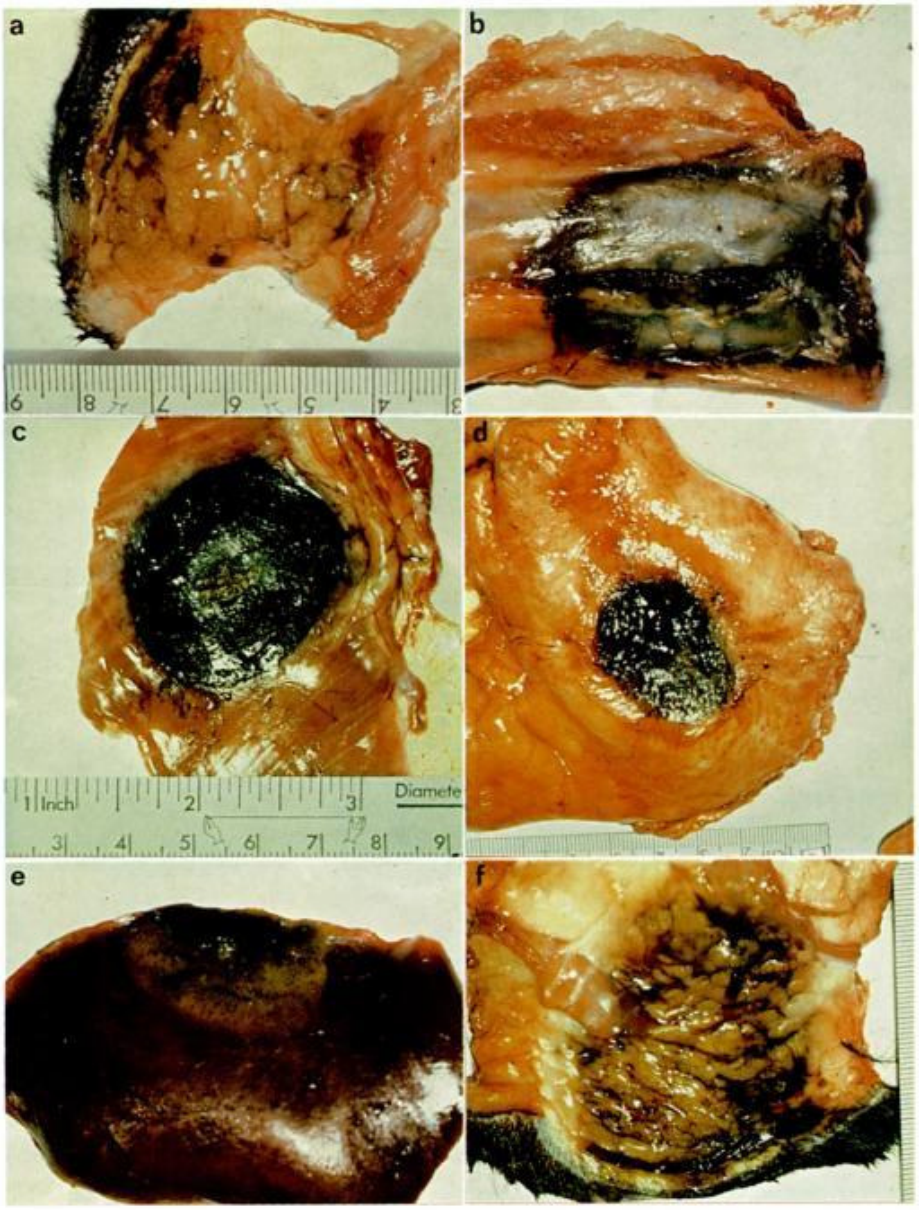

Fig. XVII: 14. Direct current at high voltage (40 volts in this example) short-circuits most physiological, preferential pathways for current in different tissues. An indiscriminate mass of coagulation necrosis is the result. Anodic electrode in the left thoracic wall of a dog, cathodic electrode in the right abdominal wall. (*a*) Chest wall. (*b*) Ribs. (*c*) Diaphragm. (*d*) Stomach. (*e*) Liver edge. (*f*) Abdominal wall.

must be decreased slowly to zero. Otherwise, rapid changes of current produce undesirable effects, e.g., pain or muscle contractions. When electrodes were placed 4–10 cm apart in the lungs, no apparent side effects were observed in dogs given ≈15 coulombs of current per kg bodyweight, either immediately or during an observation time of 3 weeks following each experiment of treatment with direct current.

3. Preliminary conclusions

At the interfaces of electrode and tissue, easily detectable morphologic changes can be seen in animal experiments. At these interfaces a *primary ionization* takes place. A *secondary ionization* is, however, also suggested in living material at electrode-equivalent sites (Chapter XII, XIII, XIV) as a function of *field-induced migration and diffusion of primarily ionized materials* from the regions of the active surfaces of the electrodes. These migrations and diffusions (e.g., of protons from the anode and hydroxyl ions from the cathode) will interfere with the functions of living cells, which thereby become injured and will consequently deliver ionized material. Further cellular and tissue disturbances will ensue from electric field forces, leading to sequences of injury reactions.

The supporting electrolytes and their associated variously charged materials (e.g., thrombocytes, leukocytes, red blood cells, charged metabolites and cell debris) will be transported in the electric field under the influence of the tissue matrix. Dielectric materials

such as water will also be transported in the electric field, a process depending to a large extent on the tissue matrix (Chapter IX). Tissue acidity and alkalinity in the anodic and cathodic fields, respectively, will also influence the chemical composition of transported materials. Distinction should also be made between the influence of a tissue matrix in vitro and in vivo. The living tissue provides a variety of active effects, such as buffering capacity and effects of tissue circulation. Altered physicochemical properties of matrices of tissue, e.g., their surface charges, are also part of the secondary injury of tissue. In order to direct attention to such important, extremely complex discrepancies between electrophoresis in vitro and in vivo, the author deliberately chose a somewhat provocative term for direct current treatment of tumours in the preliminary report, "Electrophoretic ionization in the treatment of malignant tumours" (41). The damage to the tissue by induced "cascades" of injury reactions are, however, only a portion of all the biologic effects, i.e., the many complicated biologic reactions connected with healing of an injured tissue. It seems appropriate to conclude that "*direct current treatment*" or "*electrochemical treatment*" should be more adequate terms. They include all possible technical variations and effects, e.g., electrolysis, electrophoresis, electroosmosis and other known and still unknown interferences with biologic processes in the electric field.

The goal of direct current treatment of malignant tumours is of course to try selectively to suppress neoplastic growth. Presumably, both primary injury and secondary induction of biological processes in the electric field form the basis of the suppression. Moreover, DC treatment may be recognized as enhancing physiologic mechanisms of spontaneous healing, induced by energy supplied over electrodes from an external source of DC power. This initial, artificial phase of "simulated healing" is then anticipated to continue after a treatment is concluded, as a process of spontaneous "true" healing of the injured tissue over BCEC channels. These channels are probably predominantly the vascular-interstitial closed circuits. The initially driven system is turned into a self-driving system over these channels.

We will now consider technical problems of the electrodes and application of direct current in the planning of electric treatment of patients with pulmonary cancers.

4. Electrodes

Different electrodes serve different purposes. Four types of electrodes have been constructed:

Type 1. A 300 mm long, 0.25 mm thick, solid platinum-iridium string is coated with layers of Teflon, except for a length of 1–2 cm ending 0.5–1 cm from the tip. The string is bent 180°. The tip as far as the bend is inserted into the tip of a 172 mm long, 1 mm thick, Rotex biopsy cannula (44, 45). The cannula contains the usual indwelling screw needle for sampling of cellular material. The construction and insertion of this electrode, as well as cell sampling, are shown in Fig. XVII: 15.

The electrode and cannula are introduced under local anaesthesia through a small incision in the skin. Under fluoroscopic television control, the cannula and electrode are passed through the pleura into the tumour in the lung (Fig. XVII: 15 *a*). The electrode is released from the cannula by retracting the cannula to the edge of the tumour (*b*). A cytologic sample is then taken in the usual way with the instrument. The screw needle is in this procedure driven by rotation into the tumour tissue (*c*), whereupon the hub of the cannula is rotated until it is advanced over the screw (*d*). The cannula and screw are then retracted together with cytologic material protected in the grooves of the screw needle. The material is then smeared on a glass slide and examined after suitable staining (44, 45). Cellular material may, of course, be collected as a separate procedure before insertion of the electrode, when doubts exist as to the character of the lesion.

This platinum electrode is suitable as an anode in small tumours (about 2 cm diameter or less). It is also suitable as a tissue cathode. Because mechanical strain rather easily breaks this electrode during treatments of tumours larger than 2 cm (which require about 2 hours of treatment), a second and stronger type of electrode was devised:

Type 2. This electrode (Fig. XVII: 16) may serve as an anode or a cathode in direct current treatment. Two or more platinum strings are twisted together to minimize points of local strain. The electrode is inserted and cell material obtained in the same way as described above for the simple platinum string electrode. The increased thickness of the combined electrode strings makes them suitable for use as a guide wire over which a plastic tube is inserted (Fig. XVII: 16 *b*). The hooked end of each string then helps to anchor the electrode in direct contact with tumour tissue. The plastic tube also allows aspiration of gas produced along the surface of the electrode. The plastic tube is kept in place by slightly stretching the indwelling platinum strings against the plastic tube. The strings are then fixed in place by plugging the hub of the tube with a small stopper.

Type 3. This electrode (Fig. XVII: 17) has been designed to maximize the area of the electrically active surface. The electrode also is suitable for percutaneous insertion and biopsy, in principle as described for Types 1 and 2. In addition, it provides a canal for direct access to the internal part of the active electrode

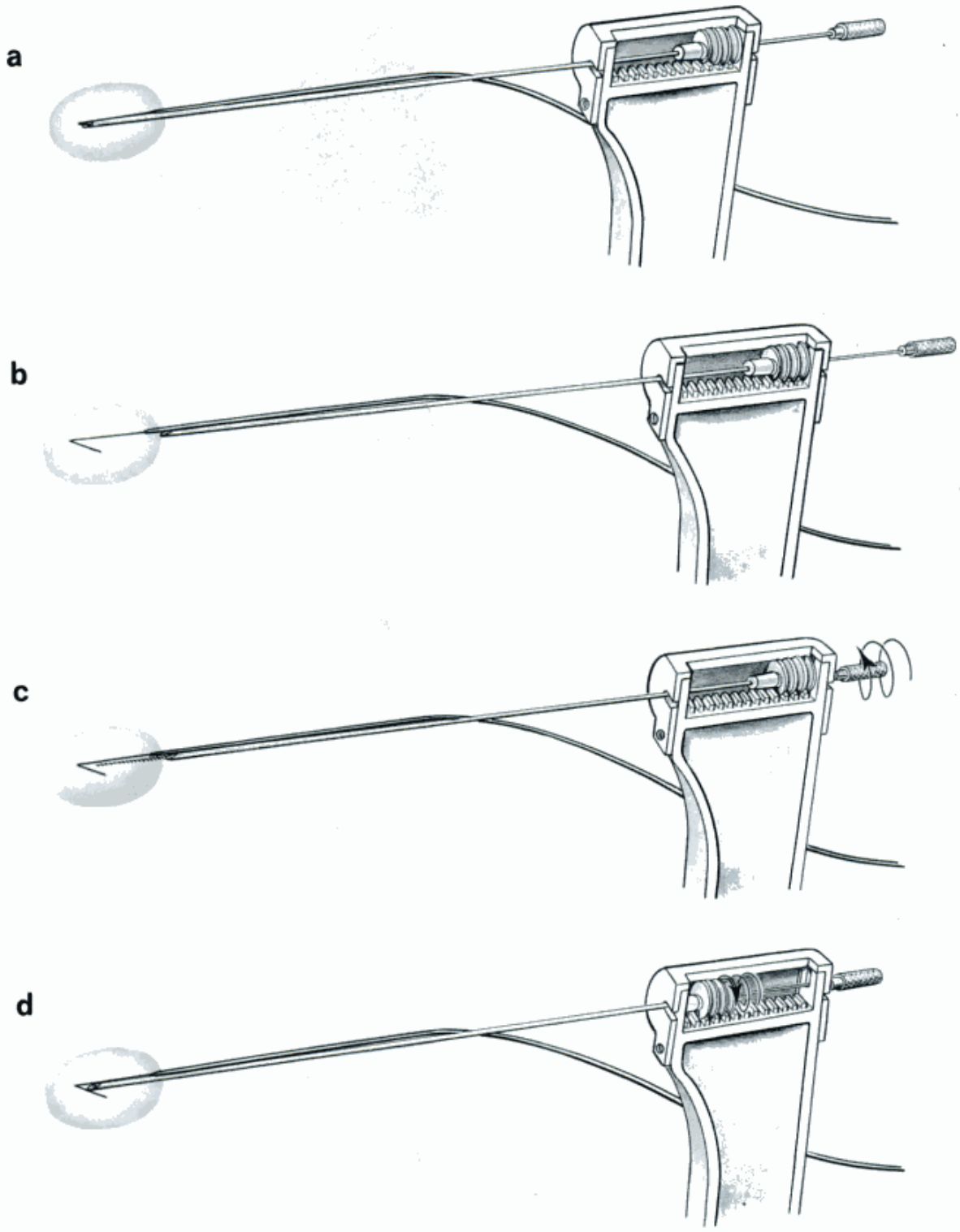

Fig. XVII: 15. Direct current treatment. Insertion of a Type 1 platinum string electrode into a tumour, followed by sampling of tumour cells for cytology. (*a*) The tip of the electrode is bent, inserted into the tip of a 1 mm thick Rotex biopsy cannula, and placed in the tumour. (*b*) The cannula is retracted. The hook helps to anchor the electrode. (*c*) Before the cannula is removed, a biopsy may be obtained, when necessary, by rotation of the indwelling screw needle into the tissue and (*d*) advancement of the cannula over the screw so that cellular material is secured inside the cannula and protected in the grooves of the screw before the instrument is removed.

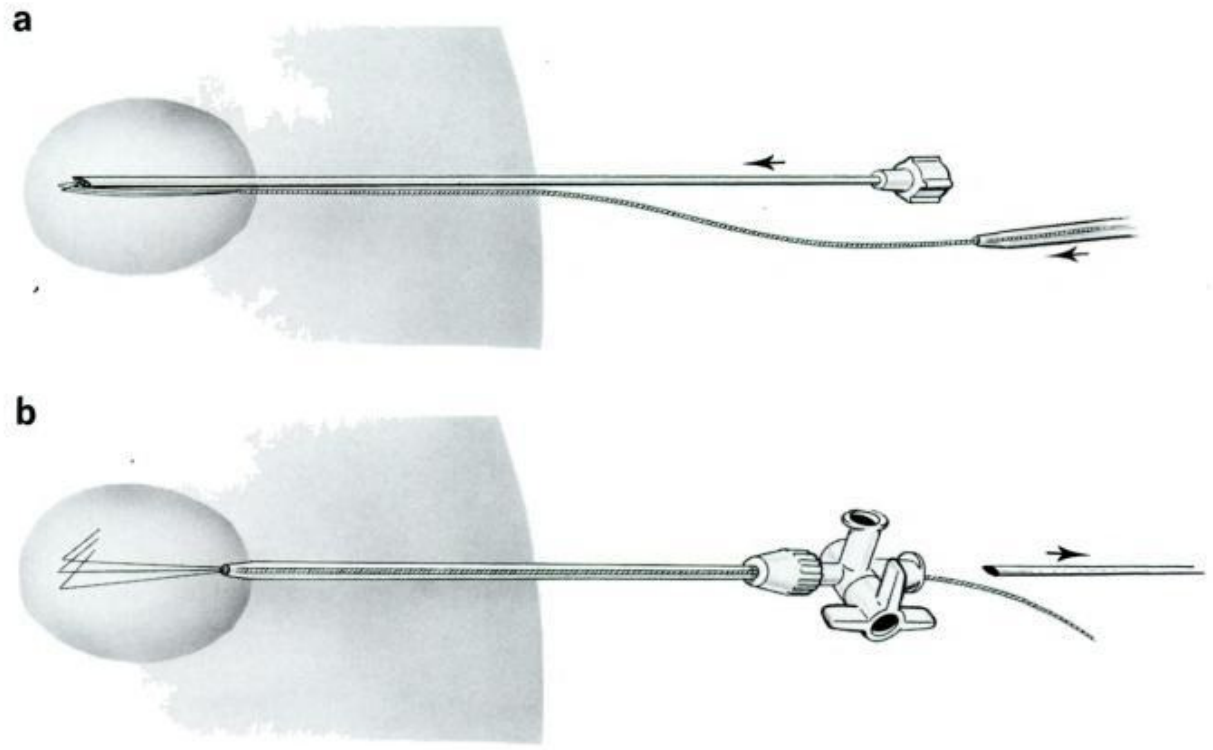

Fig. XVII: 16. Direct current treatment. A Type 2 electrode of twisted platinum strings surrounded by a plastic tube. The hooked ends of the strings (*a*) are inserted as shown in Fig. XVII: 15. (*b*) After the cannula is removed, a Teflon tube with stopcock is passed over the twisted platinum strings to the edge of the tumour. The tube serves both as an insulator of adjustable length and as a channel for removal of gas produced along the electrode during the treatment.

area. This electrode is intended primarily to be used in "large" tumours.

The electrode contains four layers. An inner screw needle resides in a Rotex steel cannula, surrounded by a Teflon tube. Outermost are platinum electrode rings, which can be varied in number or length according to the size of the lesion. As it enters the rings, the Teflon tube tapers and becomes thin-walled. The most distal electrode ring has a tapered tip and is welded to three platinum strings. These strings run outside the thin part of the Teflon tube and are tightly pressed against the other electrode rings so as to make electrical contact with them. Proximal to the electrode rings, the Teflon tube widens, which helps hold the rings in place in situ. The strings run inside the wide part of the Teflon tube and pass outside the tube through a hole at the beginning of the thin part. Proximally the strings emerge from the plastic hub, where they are accessible for connection to the source of direct current.

The active electrode surface can be varied by the number and size of the platinum rings. The length of the thin part of the Teflon tube is adjusted accordingly. Slots in the Teflon tube make it possible to aspirate gas and to inject pharmacological agents or saline solution through the electrode canal. The screw needle is 0.55 mm thick at its base and tapered to the tip over a distance of 16 mm. The steel cannula is 1 mm thick. The external diameter of the electrode rings is 1.9 mm. The purposes of the screw needle are twofold: to obtain cellular material for cytologic examination from the site of the electrode and to control placement of the electrode by stabilizing its position in the tumour. When the cannula and the larger platinum electrode are introduced, the position of the screw needle determines their positions.

Type 4. Some tumours are not solid, but semisolid or cavitary inside. Gas produced at the electrode surfaces causes or enlarges cavitation in the tumour. Therefore, it may be difficult to keep an electrode in place for longer than a few minutes. Gas also jeopardizes contact between electrode and tissue, and can disconnect the current.

The Type 4 "winged" electrode shown in Fig. XVII: 18 is designed to overcome these drawbacks. The platinum electrode is tapered distally and grooved proximally. Three platinum strings are soldered to the most proximal groove. A sling of nylon thread runs through two holes in the electrode and passes proximally the length of the Teflon tube and out the stop-

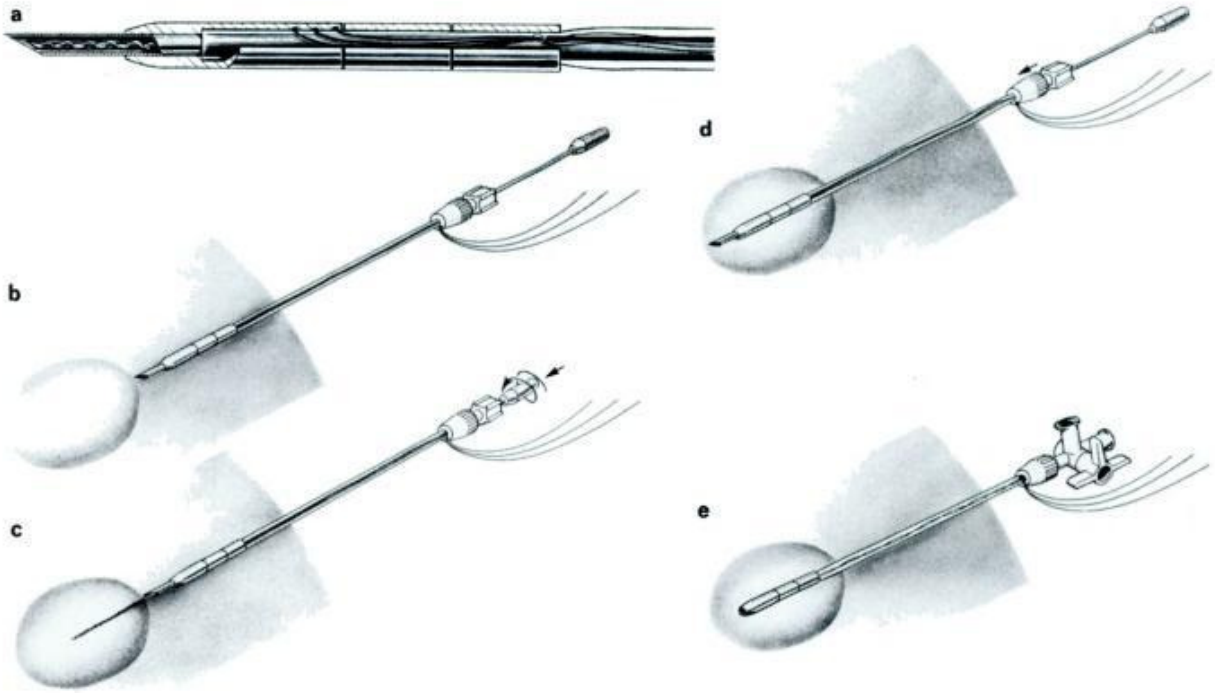

Fig. XVII: 17. Direct current treatment. Construction and insertion of a platinum electrode (Type 3) with a relatively large surface area. (*a*) The active electrode surface consists of one to several segments of platinum tubes, as indicated by diagonal lines in cross section. Three platinum strings are here welded to the distal platinum tube, which has a conical tip. The strings run between the cylindrical platinum tubes and a thin-walled Teflon tube. At the base of the proximal platinum tube, the Teflon tube widens. There the platinum strings pass through a hole into the proximal larger part of the Teflon tube. (*b*) The electrode is advanced to the edge of the tumour by means of a Rotex biopsy instrument. (*c*) The screw needle is introduced to serve as a guide for advancing the cannula and platinum rings. (*d*) The cannula and the platinum tube are introduced into the tumour. The cannula and indwelling screw needle are then removed. The grooves of the screw hold material for cytologic examination. (*e*) The platinum sections can be varied in number and length according to the size of the tumour. The intratumoural part of the Teflon tube is thin and slotted lengthwise. Gas produced at the surface of the electrode can be aspirated from the tube. Saline solution or pharmacologic agents, e.g., cytostatic compounds, can also be infused through the tube.

cock. The platinum strings emerge close to the stopcock connection. The Teflon tube is provided distally with 4 slots, which allow the segments between the slots to fold outward when the nylon string is pulled. The electrode is inserted the same way as is electrode Type 3, above, using a screw needle and cannula. The folded, slotted Teflon section anchors the electrode tip in place, even if gas pressure and dehydration happen to produce an anodic intratumoural cavity. The nylon threads are maintained taut by a small stopper plugged into the stopcock. The opened wings also permit easy communication between the Teflon tube and the inner part of the tumour. In this way, gas can be removed and pharmacological agents or saline solution infused into the tumour. This electrode is intended for use as an anode.

Given the principle that vascular branches of the VICC selectively conduct current, selective positioning of the cathode in a vessel merits consideration. For that purpose, a specifically cathodic electrode has been developed (Fig. XVII: 19). This electrode consists of a plastic radiopaque catheter, curved at the tip and perforated by a row of side holes along the inner curvature. The perforations permit electrochemical contact between blood and the metal. After percutaneous insertion by Seldinger technique, the catheter is placed in the chosen vessel, e.g., a pulmonary artery. A metal electrode is placed inside the catheter. To date, an ordinary stainless steel guide wire has been accepted for this purpose. The guide wire is positioned along the whole length of the catheter but does not protrude beyond the tip of the catheter. The distal part of the catheter is curved, to further minimize the risk of injury to the vessel wall by contact with the metal of the cathode.

To use direct current for treatment of a cancer an important principle must be noted:

Cells of mammals, including cancer cells, carry a net surplus of fixed electronegative charges (1, 4, 26, 27, 70, 75). This surplus means that those cells which are

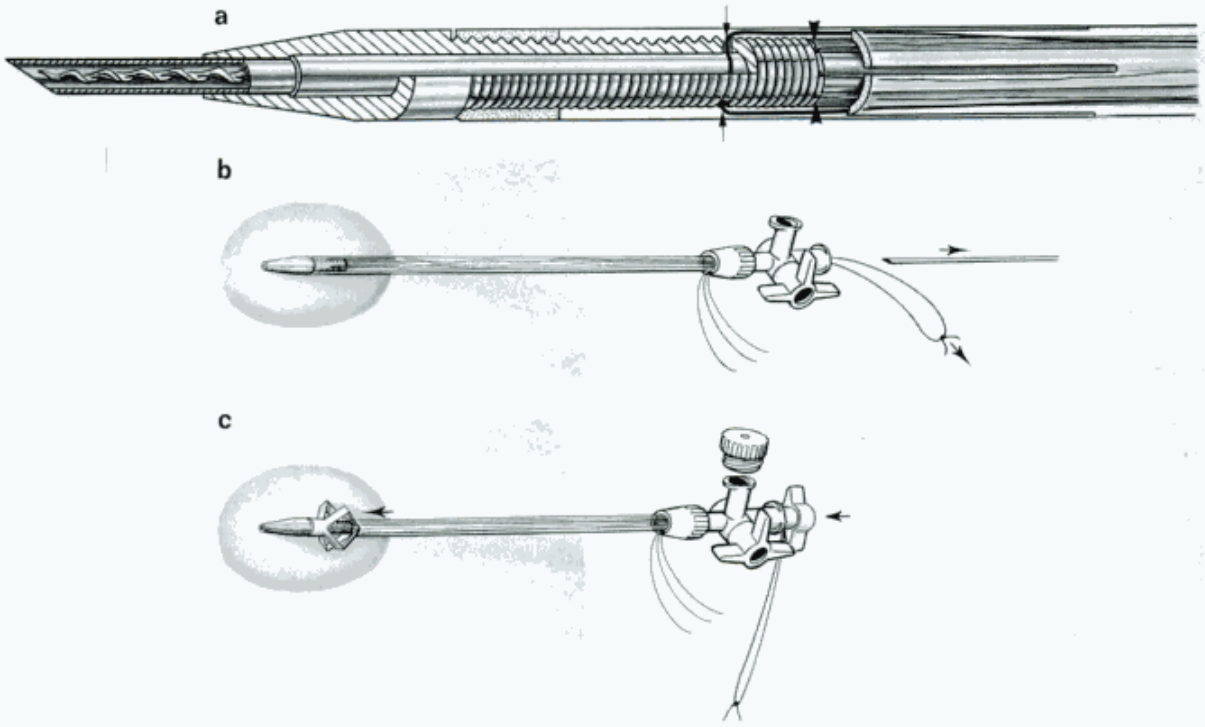

Fig. XVII: 18. Direct current treatment. Electrode of Type 4, designed to remain fixed in a cavitary tumour. (*a*) A tapered platinum tube is screwed proximally into a plastic tube. The distal end of the tube contains four longitudinal slots. A nylon string runs through holes (thin arrows) in the platinum tube and passes through the plastic tube. Three platinum strings are welded on the most proximal groove (arrow-heads). (*b*) By pulling the nylon thread (oblique arrow), retracting the biopsy screw needle (horizontal arrow) and pushing the plastic tube (*c*) into the tumour, four wings fold out, securing the electrode in the cavitary tumour. The tube is also available for removal of gas and infusion of liquid solutions, e.g., saline or cytostatic compounds. This electrode is introduced in the same way as is the electrode shown in Fig. XVII: 17.

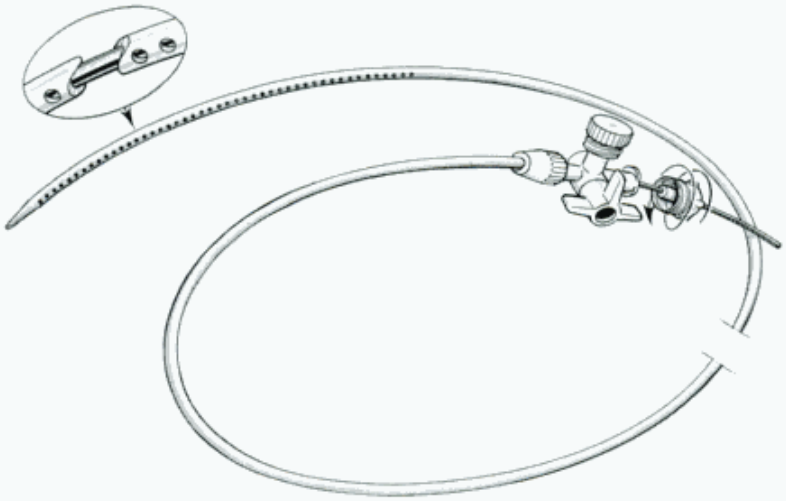

Fig. XVII: 19. Direct current treatment: intravascular cathodic electrode in a catheter. Multiple side holes along the concavity of a plastic catheter prevent the metal in the catheter from directly contacting the wall of a vessel. The metal string of the electrode is provided with a stopper. The three-way stopcock allows intravascular infusion through the holes in the catheter.

easily detached, such as malignant cells, will move in a superimposed electric field from the cathode toward the anode. The electropositive field around the intratumoural anode will, therefore, tend to keep all movable cancer cells in place during the direct current treatment. The application of an electronegative potential in a cancer, on the other hand, can be expected to tend to repel the neoplastic cells away from the tumour and therefore increase the risk of producing metastases.

The tumour electrode must initially be anodic. The cathode must be kept away from malignant cells. Because cancer cells are electronegatively charged, they will be kept together around the anode but be transported away from the cathode. If an intratumoural electrode is cathodic, the subsequent spread of tumour cells is very likely.

5. Application of electrodes

Direct current treatment can easily be performed in a patient treated with a tranquilizer (e.g., morphine-scopolamine, 5–10 mg, i.m.) and local anaesthesia (Xylocaine®) in the skin and pleura. In this way it is possible to communicate with the patient during the treatment.

The insertion of electrodes is performed percutaneously as described above after careful radiologic localization of the lesion with plain films, biplane fluoroscopy, and, if necessary, computerized tomograms.

Computerized tomograms are in many cases indispensable. In biplane televised fluoroscopy, one selected projection may be optimal while the perpendicular view is insufficient to localize a small lesion. In such cases a computerized tomogram makes it possible to determine the exact distance between the planned site of pleural puncture and the margin of the lesion. An electrode can then be introduced to the predetermined position by means of a suitable projection at fluoroscopy. Fig. XVII: 20 illustrates the role of computerized tomography in determining the most suitable direction and depth for percutaneous insertion of electrodes. Parallel white lines indicate planned introduction of the anode into the carcinoma and the cathode into the lung parenchyma between the tumour and the hilum.

The placement of electrodes can in theory be widely varied for DC treatment of pulmonary neoplasms (Fig. XVII: 21). Electrodes can (theoretically) be placed on the skin, or inserted directly through the chest wall. Electrodes can also be inserted via a catheter into the pulmonary artery, a systemic artery, a systemic vein, a bronchus or in the pleural space. The venous routes and the pleural space are of particular interest because they provide pathways for current which include the lymphatics. A large skin cathode is not very suitable for treating pulmonary lesions because of the risk of eddy currents between the skin and the anodic tumour

Fig. XVII: 20. Computerized tomography as an aid to percutaneous insertion of electrodes in direct current treatment of a metastasis in the lungs. Blackness represents air in lung. The patient is supine and viewed as a transverse section seen as if the viewer were looking from the direction of the patient's feet toward the patient's head. The carcinoma, approximately 2 cm in diameter, is situated anterolaterally in the periphery of the right lung. Reconstructions optimize imaging detail of (*a*) margins of the cancer, (*b*) soft tissues of the chest wall. Biplane fluoroscopy best visualized the lesion when one of the planes was as marked by the white lines. In this plane the centre of the lesion was 8.5 cm from the surface of the skin (measured distance of the shorter straight white line). The longer white line marks the anticipated position of the cathodic electrode.

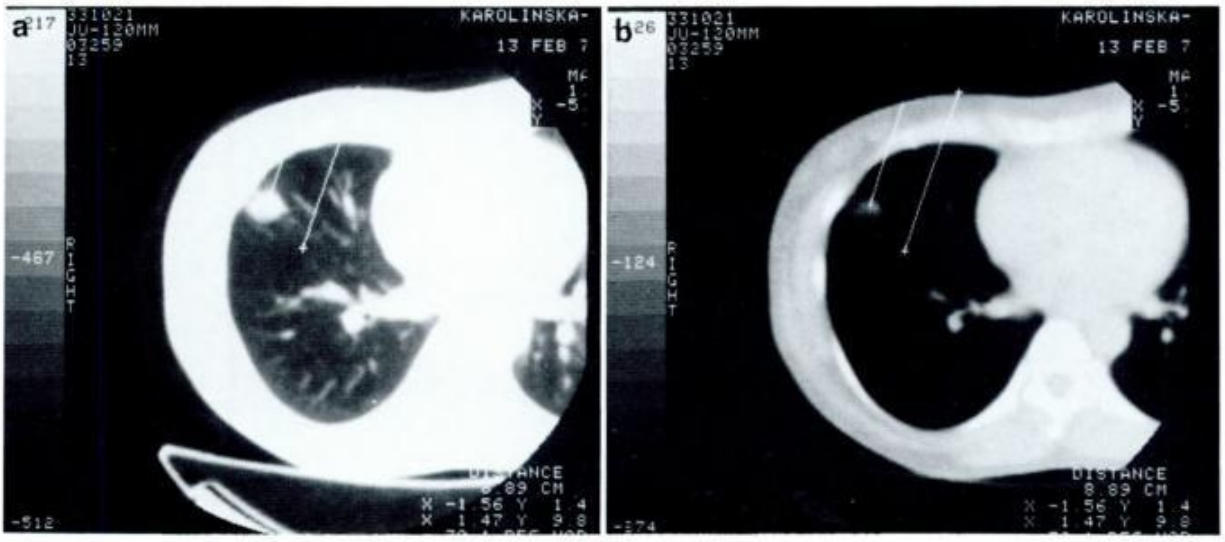

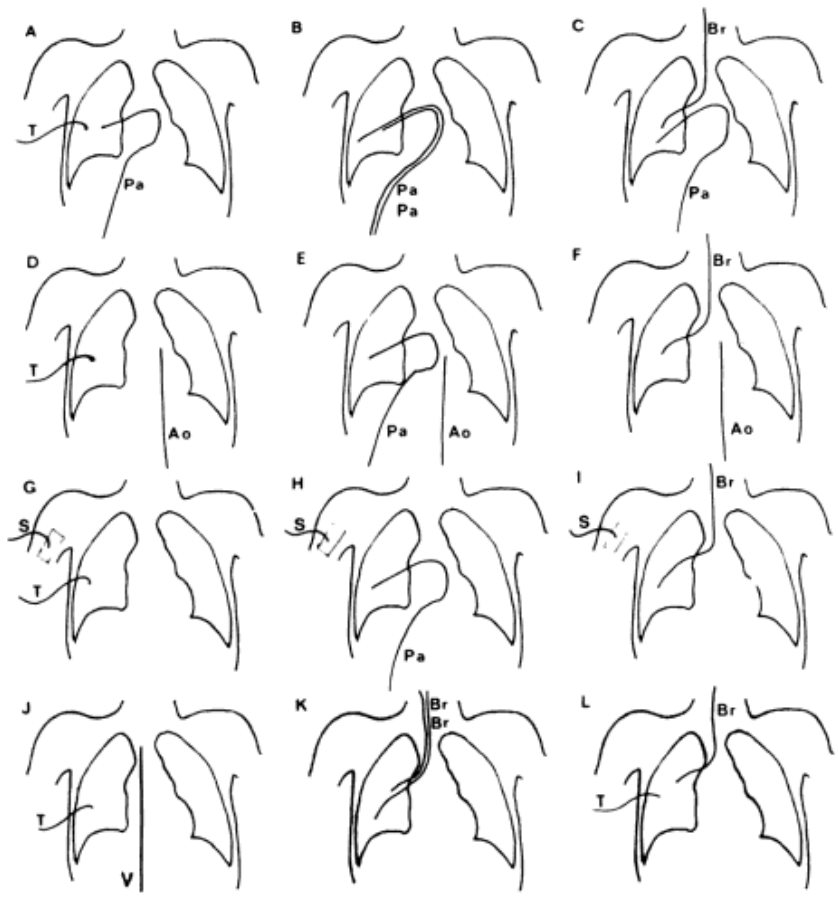

Fig. XVII: 21. Different (theoretical) possibilities for placement of electrodes in D.C. therapy of cancers in the lung. *T* = transthoracic; *Pa* = via a catheter in the pulmonary artery; *Br* = through the tracheobronchial tree; *Ao* = via a catheter in the aorta or bronchial artery; *S* = large electrode on the skin; *V* = via a catheter in a vein.

Fig. XVII: 22. Position of electrodes for direct current treatment of a lung tumour. The tumour electrode should be anodic. (*a*) The cathodic electrode is ideally positioned. It is outside the tumour and proximally placed in the same segment to maximize interelectrode flow of current over the conducting interstitial fluid and intravascular plasma. (*b*) Unsuitable position of the cathode, positioned in an adjacent pulmonary lobe or segment. When interlobar pleura (dashed line) or any other poorly conducting membrane is interposed between the anode (in the tumour) and the cathode, flow of current will take an unpredictable roundabout way, perhaps via the hilum.

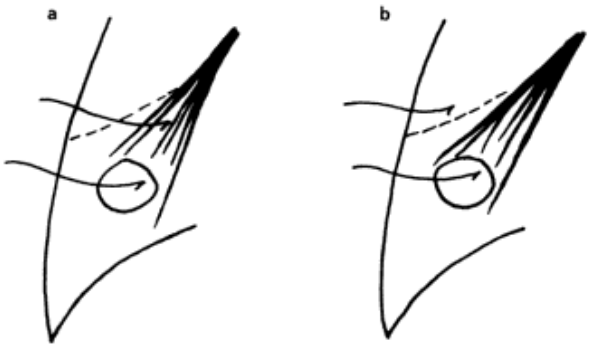

electrode in the lung. This is obviously important for avoiding the leading of current through the myocardium.

The structures of the treated organ also are important in direct current treatment, because they affect the pathways for current. For example, Fig. XVII: 22 *a* illustrates the cathode positioned across the vascular bundle central to a lung tumour and inside the same segment or lobe as the tumour, assuring favourable conductivity and spatial distribution of current. Fig. XVII: 22 *b*, however, shows the cathode positioned beyond the interlobar pleura, which hinders current flow. Any air leak into the pleural space will further enhance the hindrance, so that the current must pass in a wide arc over the hilar tissues. This broad and indirect course is unnecessary. Resistance to flow will be increased and may even theoretically produce unexpected reactions, e.g., from nerves in the hilum.

Pneumothorax is a likely complication of transthoracic insertions of electrodes. In order to control this complication, one should introduce a pleural drainage tube before the electrodes are to be implanted. When the pleural tube is connected to a suitable suction device, collapse of the lung can be prevented. During the treatment, pressure in the pleura must be continu-

ously maintained at subatmospheric levels, so that the lung is maintained expanded. Constant size and position of involved lung are necessary to prevent a pneumothorax from dislocating the electrode from the tumour. Absence of pneumothorax is also obviously necessary for respiratory comfort and safety of the patient. The pleural drainage tube should be kept in place a day or two under constant suction after conclusion of a treatment with direct current.

6. Voltage and current

In experiments on animals, up to 40 volts have been applied between electrodes in the lung.

In patients, usually 10 volts (range, 1.5–15 volts) have been used. Initially, current should be applied by evenly elevating the voltage from 0 to the desired level, which in practice has been performed during one minute. Similarly, the current should be lowered slowly, e.g., over about a minute, on concluding the treatment. Otherwise the patient will experience pain or unpleasant contractions of local muscles by faradic stimulation.

The actual amount of current passing through the circuit increases continuously in the beginning, as a function of continuously increasing ionization of tissue. Electroosmotic, electrolytic and electrophoretic phenomena associated with deposition of material on the surfaces of the electrodes will then diminish the rate of increase in conductivity. The current may even suddenly become interrupted, usually as a consequence of gas forming at the electrode surfaces. As voltage and current increase, the likelihood of newly formed gas blocking the flow of current also increases. Sudden pain will then be felt by the patient. Increase in voltage may then temporarily restore conductivity until a new spontaneous interruption takes place. This method of restoring current should be avoided. Instead, one should either wait until the accumulated gas on the electrodes has spontaneously resorbed, or remove the gas, e.g., by suction and infusion of saline solution. These procedures require electrodes such as those described with a channel available for suctioning and injection.

The total quantity of coulombs passed between the electrodes must be determined, as it offers an expression of the "dose" delivered. Because the current is continuously changing, continuous integration of current and time is necessary to determine the dose in coulombs.

In order to deliver about 200 coulombs at 10 volts to a patient with a lung tumour, 2–3 hours has been found necessary when the distance has been 5 cm between two platinum electrodes, each with a total surface of 20 mm^2. The initial current has usually been 5 to 10 mA, which then increased spontaneously to a maximum of 30 to 40 mA.

Because control of applied voltage and current is critical for the qualitative effects of DC treatment, a DC Treatment Processor[2] (Fig. XVII: 23) has been constructed. This processor automatically adjusts current and voltage not to exceed predetermined values.

[2] Developed in cooperation with Mr Jerker Olsson and Tekniska Röntgencentralen AB (TRC). The instrument is manufactured and sold by Tekniska Röntgencentralen AB, P.O. Box 50100, S-104 05 Stockholm, Sweden.

Fig. XVII: 23. Processor developed for direct current treatments. (*a*) External display of variables in a course of DC treatment. (*b*) Block diagram of the apparatus.

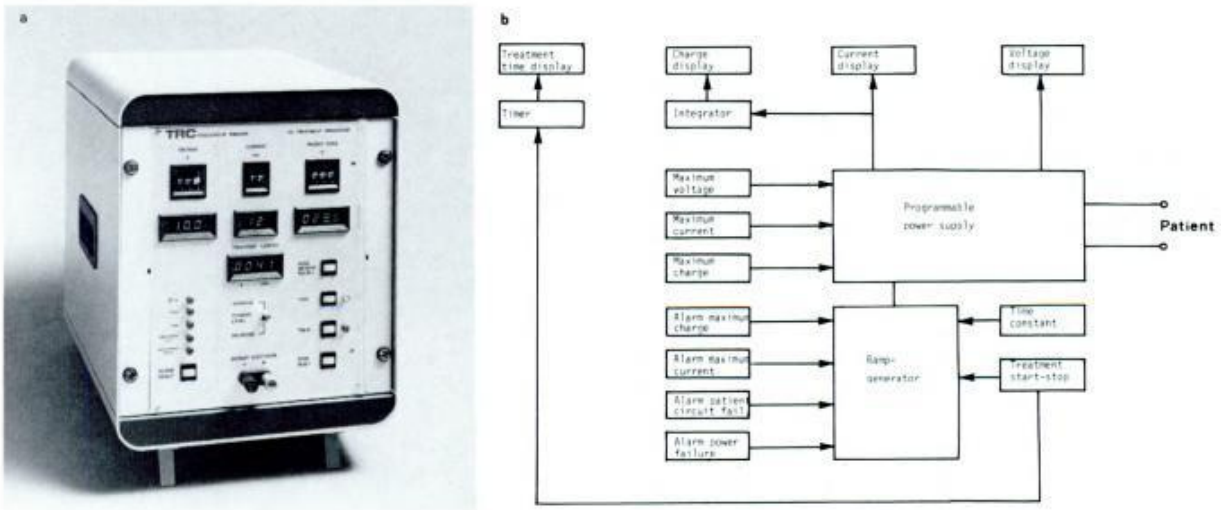

Within chosen limits, the apparatus can keep current and voltage constant. The actual current is measured and integrated over time. Current, voltage and accumulated charge are presented in a digitized form and can be displayed on a chart writer. In the event of undesired changes of currents, alarms are activated. Initial and concluding currents are modulated gradually, to prevent pain and muscle spasms for the patient.

7. Discussion

For definite control of a cancer, the specific quantities of current and voltage needed are still in the process of definition. It does now appear clear that at voltages of 10 volts or less, heat produced around the electrodes is only a minor consideration. At higher voltages, sparks can produce considerable local heat.

Prominent destructive effects are known to take place *around the cathode* at "high" voltages, while very minute but permanent changes are produced at "low" voltages (31). The most destructive effect around the cathode is produced by alkalinity, which may locally reach a value of pH 12. Blood pigment is then transformed into dark alkaline haem. Some of the destructive effects are produced by the pressure of hydrogen evolved at the cathode. Inflowing electroosmotic water around the cathode also elevates the local turgor pressure, which causes compression of vessels.

Around the electrodes interactions also take place between blood flow and electric field forces on charged particles, as described for cathodic accumulation of leukocytes (Chapter XIV).

Around the anode relatively extensive changes in tissue are obtained also at fairly low voltages (below 10 volts). The destructive effect around the anode is produced by an abundance of protons, liberated by electrolysis at the surface of the electrode. After the protons diffuse and migrate in the electric field, a region of dark acid haem is produced (pH≈2). Centrally around the anode the dark material is bleached by liberated chlorine gas. This gas and liberated oxygen increase the pressure around the anode, leading to cavitation. Electroosmotic dehydration of the destroyed, dark anodic area produces a rather well demarcated border against surrounding tissue.

To these cathodic and anodic primary destructions of tissue around the electrodes are added several, easily distinguishable, acute biological reactions (Chapters XII, XIV) around the cathode. Considerable local oedema develops around the cathode. The tissue is soft, partly dark coloured or pinkish and shows a decreased amount of red blood cells and leukocytes. Around the anode the tissue is dry and shows extensive thromboses in capillaries, contractions of capillaries, diapedetic haemorrhages, discolouration of vessels and accumulation of large numbers of leukocytes, which are both intravascular and perivascular. Such accumulations of leukocytes occur preferably at low electrode potentials (e.g., 0.1 V). After intravascular injection, a charged chemical compound may accumulate selectively around one of the electrodes, indicating that this principle also may be utilized for therapy.

The anodic and cathodic reactions described form the basis for the hypothesis that direct current can be used to control tumour growth. The control derives partly from destruction of tumour tissue and partly from field-induced modifications of the environment of the tumour.

There are many difficulties in defining proper dosage for treatment with direct current. The amount of current flowing between the electrodes is not a conclusive way to measure the magnitude of treatment. This effect can be explained as follows:

When anode and cathode are placed very close (e.g., 1 cm,) to each other, large amounts of current may pass through the circuit and yet the spatial extent of biologic and destructive effects will be quite limited. When large distances (e.g., 10 cm) separate the electrodes, local densities of current per unit volume of tissue are lower (with an equivalent flow of current) than when the electrodes are closer. A treatment may nevertheless be produced by some primary destruction of the tumour supplemented by biochemical alterations also in a relatively large volume of tissue. The positioning of the electrodes is in any case an exceedingly important factor to consider in direct current treatment. Moreover, the influence of the electrode technique also correlates directly with the conductivity of tissue, buffering capacity of tissue fluids and influences by tissue circulation. Because direct current in many ways influences and interferes with biological reactions, extensive destruction of tissue by direct current does not necessarily correspond with beneficial biologic influences on surrounding tissue. As an example, many leukocytes can be attracted to the anode at relatively low electrode voltages (2–3 volts) but are massively destroyed in the anodic field at 10 volts (Chapter XIV). Varied reactions of other cells and tissue components have also been observed under the influence of direct current (Chapter XIV). Conducting properties of different tissues may also produce unforeseen pathways for the current.

The interactions of many variable factors can therefore explain why different effects can be obtained in tissues even with essentially comparable amounts of current. Furthermore, it seems likely that DC treatment should be most beneficial when the technique approaches the mechanisms of closed circuit transport in spontaneous healing. This consideration implies the use of energies perhaps in the range of a few volts and a few microamperes over long time periods. It also implies a future introduction of slowly fluctuating,

attenuating potential differences between diseased and healthy tissue. Knowledge about beneficial effects of such approaches can obviously be obtained only from extensive, systematic, experimental and clinical trials.

D. Direct current treatment of malignant tumours in lung: experience in 20 patients

1. Case material

Direct current treatment of cancers in lungs of the first five patients in this series was reported by the author in 1978 (41). This initial trial series proved that DC treatment could lead to regression of cancer in patients who, for various reasons, were unsuitable for operation or other established forms of treatment.

After these initial experiences, the clinical series has been enlarged to 20 patients and a total of 26 treated cancers. A survey of this case material is presented in Table XVII: 2 (pages 310–312).

The ages of the patients varied between 20 and 76 years. Ten were women, 10 men. Fifteen had metastatic cancer in one or both lungs. Five had primary lung cancers. Seven were considered unsuitable for surgery because their general physical condition was poor. Other patients have been unsuitable for radiotherapy or failed to respond to treatment with cytostatic agents. Eight patients have also suffered from other major diseases, including coronary atherosclerosis, hypertension, diabetes, emphysema or respiratory insufficiency (post poliomyelitis). In one instance (patient no. 10) treatment was performed for a solitary pulmonary metastasis from a breast carcinoma. This patient was in excellent condition but she refused surgery, radiotherapy and treatment with cytostatics.

2. Preparation of patients

All patients gave their consent after they were informed that the treatments were part of a preliminary clinical trial. Each patient was examined with cardiorespiratory function tests, blood chemistry tests and radiographic studies appropriate to performance of a thoracotomy. Because pneumothorax commonly complicates needling of a lung, it was found suitable to insert a large pleural drainage tube prophylactically into the pleural space before treatment. All treatments were performed under local anaesthesia at the sites of insertion of the electrodes and after medication of the patient with Valium® and morphine-scopolamine. In this way it has been possible for the patient to report on pain or other reactions during the course of the treatment.

3. Technique of treatment

The platinum electrode (anode) has always been implanted percutaneously in the tumour under biplane, televised, fluoroscopic control. The cathode (same electrode as anode type 1 or 2) has been implanted (see Table XVII: 2) at a distance of at least one diameter of the tumour from the edge of the tumour. The site of the cathode has been either between the tumour and the hilum (18 instances) or it has been inserted through a catheter from a femoral vessel into an ipsilateral branch of the pulmonary artery (5 instances), in the subclavian vein (2 instances) or into the aorta (6 instances). The aortic location of the cathode was chosen with the intention of utilizing the bronchial arteries as a selective pathway for current in primary pulmonary malignancies, which are known to have their main blood supply derive from the bronchial arteries (77).

The DC Treatment Processor contains appropriate safety circuits and has been connected to a Grass direct writing instrument for continuous recording of voltage, current and time during treatment. Facilities for recording of ecg and respiration have been available. Five patients have been treated for more than one tumour. Only a single treatment has been applied to each tumour, except for three tumours. Patient no. 17 (Table XVII: 2) received three treatments of one tumour and two treatments of another. Patient no. 19 received two treatments of one tumour. The first treatments of these patients' tumours were performed at an electrode potential of 10 volts and the last at 1.5–3.5 volts. In spite of the low current densities, 400, 665 and 710 coulombs could be given, during 2–5 days, in the ward. Five, 7 and 15 volts have each been applied in one patient. The amount of current has varied between 65 and 1 330 coulombs.

The diameter of the smallest tumour was 10 mm, the largest 75 mm. Because few indications existed to guide an optimal choice of voltage and amount of electric energy to be given, an arbitrary amount of current of 100 coulombs per cm of tumour diameter (at 10 V potential) was chosen as the preliminary dose. This amount means that in case this dose will be found sufficient to arrest growth of small cancers, a diameter should be encountered above which growth is not arrested, because volume increases exponentially in relation to diameter of a tumour (Fig. XVII: 1). Collecting information about dose requires, of course, a large number of patients. Several factors make it also necessary to modify the treatments. In fact, pain or fatigue in several old or weak patients made it impossi-

ble to follow the preliminary setting of treatment dose. An average of only 80 coulombs at 10 volts potential could be applied per cm diameter of the tumours (Table XVII: 2, see also Fig. XVII: 43).

One of the most difficult factors to evaluate are the local circulatory conditions around a tumour. Good circulation means, for example, efficient buffering, dilution and disappearance of anodic protons and hence a decrease in direct, destructive effects on tumour cells. Technical problems arise when obscuring structures, e.g., thickened pleura, make it difficult to position the tumour electrode in the centre of a tumour. If the electrode is not located centrally, an unnecessarily large treatment dose will be required to obtain reliable treatment. Movements of the patient also can easily dislocate the tumour electrode. This problem is particularly the case in cavitary tumours and cancers with soft consistency, e.g., melanomas and oat cell carcinomas. Many technical factors can be improved. The results in the patient group are therefore far from representative of the full potential of the method.

All treatments except four have been performed in the radiologic laboratory under biplane fluoroscopic control. Duration of these treatments has varied between one to three and a half hours. Three tumours (patients no. 17, 19 and 20) were treated in the ward by delivery of 400, 665, 710 and 1330 coulombs at 1.5–5 volts. These treatments each lasted two to five days.

4. Case analysis of treated patients

Five primary and 21 metastatic cancers have been treated in 20 patients.

a) *Mortality*

None of the patients has died in connection with the direct current treatments. Thirteen patients have died during the observation periods after the treatments. The deaths of nine of these will first be analysed in connection with some comments on the treatments. These patients are numbered as in Table XVII: 2. Causes of deaths of the other four patients (3, 11, 14 and 15) are listed in Table XVII: 2.

Patient no. 4. This patient suffered from hypertension, severe coronary arteriosclerosis, diabetes mellitus and a pelvic sarcoma with multiple metastases in the lungs. Two of these metastases were treated and regressed during observation times of 485 and 444 days, respectively. Multiple other small metastases in the lung parenchyma, distant from the sites of the electrodes, also appeared to regress after treatment of the two larger metastases. These findings are analysed in detail later (see also Fig. XVII: 36). The patient died from local recurrence of her pelvic tumour and metastases to the brain.

Patient no. 6 had been operated for an osteosarcoma of the right leg in 1978. One metastasis (I) of 23 mm diameter in the right upper lobe was treated with 130 coulombs at 10 volts, the cathode in the lung parenchyma. After 50 days of observation the tumour had decreased in size, while the untreated metastasis (II) of about equal size in the left lung had increased in volume about 2.5 times. Because of this rapid growth and the seemingly beneficial effect of the DC treatment of the rightsided tumour, surgical removal of the untreated tumour deserved serious consideration. Unfortunately, the treated rightsided tumour was then surgically removed instead of the left one and the specimen was lost. The patient subsequently died from his disease. No autopsy was performed.

Patient no. 8. Previously a cutaneous malignant melanoma and one brain metastasis had been resected. She appeared with one metastasis in the right lung. During treatment with DC current a pneumothorax developed slowly, causing displacement of the platinum string electrode in the tumour. The patient's condition was not affected by the treatment but she developed various cerebral symptoms 3 weeks later and died. Autopsy revealed many large metastases in the brain, one of which had bled into the ventricular system. The part of the lung tumour where the anode had been positioned showed complete necrosis over a diameter of 10 mm. An intermediate zone of partial cellular destruction was seen in a 2–3 mm broad zone. Beyond this zone, melanoma cells appeared microscopically unchanged.

Patient no. 9. After a right lobectomy for a pulmonary adenocarcinoma, local recurrence was verified by percutaneous needle biopsy. DC treatment was performed but positioning the anode was difficult because thickened pleura partly obscured visualization of the tumour. The tumour continued to grow rapidly after treatment. The patient died from multiple metastases in the right lung. At autopsy local scar tissue was seen anterior to the large metastasis. It was assumed that the anode had not been correctly positioned in tumour tissue.

Patient no. 12. A large metastasis from a testicular teratocarcinoma was present in each lung. Treatment of each metastasis was attempted with direct current. Pleural thickening precluded an implantation of an electrode into the right lesion. The left metastasis was treated and stopped growing during an observation time of 410 days. The patient died from widespread metastases. Autopsy was not performed.

Patient no. 13. The treatment dose for this solitary metastasis became less than originally planned due to the patient's poor general condition. 180 days after

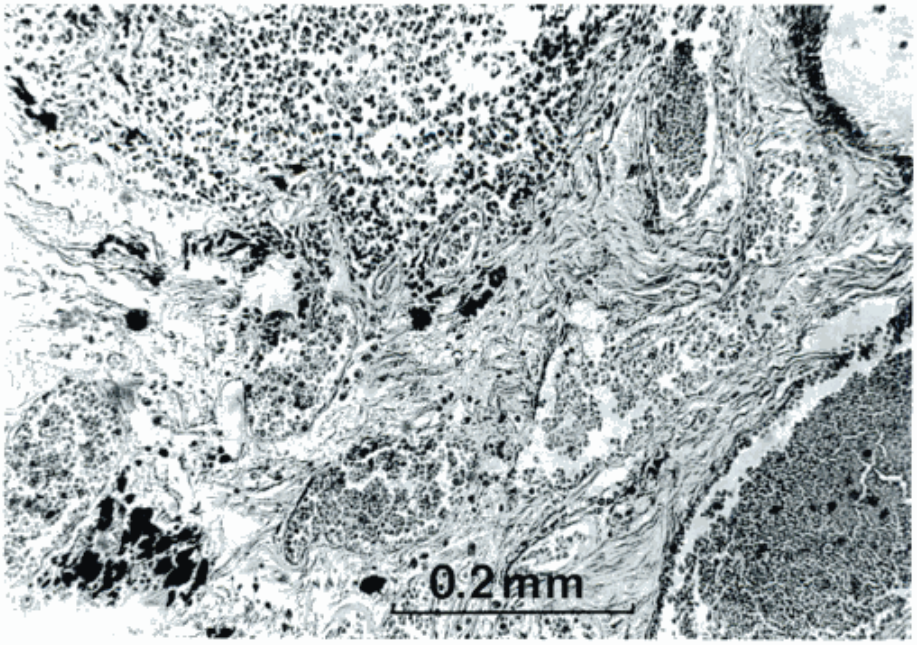

Fig. XVII: 24. Histologic section, edge of large primary carcinoma of lung (patient no. 18), three weeks after treatment when the patient suddenly died from a coronary infarction. Tumour cells appear probably viable. Fibrosis is abundant. Clusters of calcification are also evident.

the treatment, the size of the tumour had increased considerably. The tumour showed a large central cavity. After 345 days the tumour had partially collapsed and decreased in size. The patient died shortly thereafter of cerebral metastases.

Patient no. 16. This 54-year-old patient with poorly differentiated squamous cell carcinoma of lung was not a candidate for surgery because of ventilatory insufficiency after poliomyelitis. During direct current treatment, only 200 coulombs at 10 volts could be given to the 40×45×57 mm large tumour. The patient died of multiple metastases after 1 year, 10 months. At autopsy the primary lung tumour had increased in size to 65×65×65 mm.

Patient no. 17. This 56-year-old woman had an adenocarcinoma of the uterus resected in 1977, followed by radiation treatment. Intrapelvic scar tissue then developed and blocked the ureters bilaterally. Permanent bilateral nephrostomies were established. One large metastasis developed in the lower lobe of the right lung and one in the upper lobe of the left lung. The right metastasis was treated three times with a total of 1 135 coulombs (electrode voltage 3.4–10 V). The left metastasis was treated twice with a total of 560 coulombs (1.5–10 V electrode potential). Despite these considerable efforts to arrest tumour growth, both metastases continued to grow rapidly, the more vigorously treated right one even more rapidly than the left tumour. New metastases appeared and death occurred soon thereafter.

Patient no. 18. Cardiac insufficiency from previous myocardial infarctions was a contraindication to surgery for this patient's primary lung cancer. He tolerated DC treatment (400 coulombs, 10 volts) very well. Three weeks later he died suddenly from a new myocardial infarction. Autopsy revealed widespread regions of necrosis in the treated tumour. Cancer cells, probably viable, were found at the edge of the tumour (Fig. XVII: 24).

b) *Beneficial effects of DC treatment*

Although each of the above nine patients died, DC treatment appears to have been locally effective in patients no. 4, 6 and 12. We will, however, also review some more obvious beneficial effects of DC treatment. Each patient's number corresponds to those in Table XVII: 2.

Patient no. 1. This 66-year-old woman represents one of the longest observation times. A bilateral salpingo-oophorectomy was performed in 1973 for mesonephroid adenocarcinoma of the ovary, stage IA, histologically class IV. 4 000 rads of external radiation were given. Routine chest radiography in February, 1978, revealed a 20×15×15 mm tumour in the lingula. In April, 1978, screw needle biopsy showed polymorphic carcinoma, strongly probably metastatic from the ovarian tumour. In Fig. XVII: 25 cytologic material is shown from the lung tumour (*a*) and histologic material from the ovarian tumour (*b*). Operative removal of the pulmonary metastasis was rejected because of severe cardiac disease.

By June, 1978, the pulmonary tumour measured 25×17×17 mm. After Valium® (10 mg) and morphine-scopolamine (50 mg) were administered intramuscularly, DC treatment was performed under local

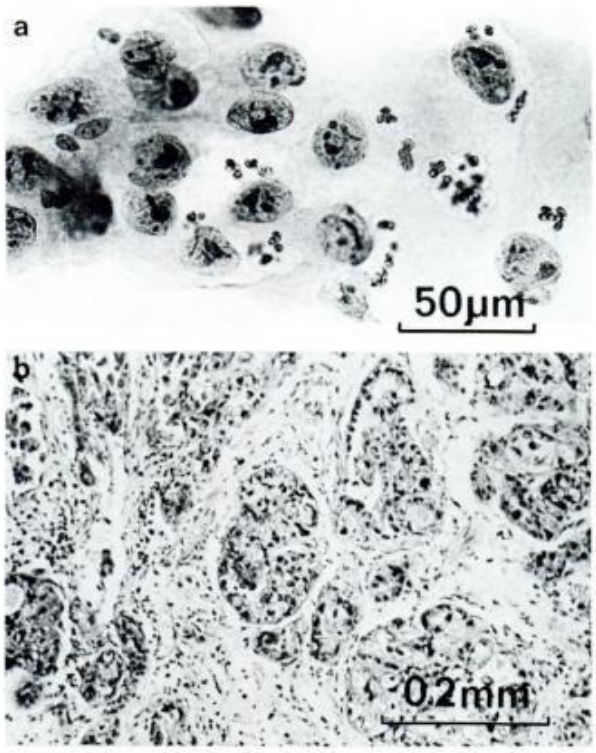

Fig. XVII: 25. Adenocarcinoma of ovary, metastatic to lung (patient no. 1). (*a*) Cytologic preparation, screw needle biopsy, pulmonary metastasis. Papanicolaou stain. (*b*) Histologic section from the primary tumour of the ovary. Haematoxylin-eosin stain.

anaesthesia with Xylocaine®. A cardiac catheter was introduced percutaneously via a femoral vein and passed into the left pulmonary artery. A normal pulmonary angiogram was obtained before the treatment (see Fig. XVII: 28 *a*). Two platinum electrodes, each 0.2 mm in diameter, were introduced percutaneously via a biopsy needle 1.0 mm thick. The noninsulated, distal part of the platinum thread was 25 mm long. Five mm from the tip the thread was bent to form a hook to secure its position. The anode was placed in the tumour, the cathode in adjacent tissue separated from the tumour by a distance of approximately its diameter (Fig. XVII: 26).

DC treatment was started at 10 volts between the electrodes. As seen in Fig. XVII: 27, current initially was 10 mA. Then it increased to about 20 mA. At the first dotted line (*a*), the current was spontaneously interrupted and gas could be seen fluoroscopically around the electrodes. The patient then complained of pain, which disappeared quickly when the current was switched off. Because the cumulative amount of current was considered insufficient, the treatment was then continued at 15 volts between the electrodes. The current started again at about 35 mA and the patient did not notice any pain. It increased to about 55 mA when new gas again interrupted the circuit and the patient reported some pain. After another period of rest (*b*), 15 volts was again applied. Shortly thereafter the patient reported pain again. As the total amount of coloumbs now was 180, the treatment was interrupted and the electrodes were pulled out. Other than pain, the sole complication was a minimal pneumothorax, which resorbed spontaneously within a day. No pain was reported by the patient after the conclusion of the treatment.

A new pulmonary angiogram was performed immediately after the treatment. Compared to the study before treatment, it showed that several vessels appeared narrower and displaced away from the cathode (Fig. XVII: 28 *b*).

Radiography the next day showed diffuse haziness around the site of the electronegative electrode, an appearance suggesting local oedema. Fig. XVII: 29 chronicles the decrease in size of the treated metastasis. Fig. XVII: 29 *a* shows the metastasis before treatment. Fig. XVII: 29 *b* shows an infiltration at the previous site of the cathodic electrode. Around the tumour, the tissue is also infiltrated and surrounded by radiating, probably fibrous, structures. Two months after the treatment (Fig. XVII: 29 *c*) most of the cathodic infiltrate has disappeared and the tumour has

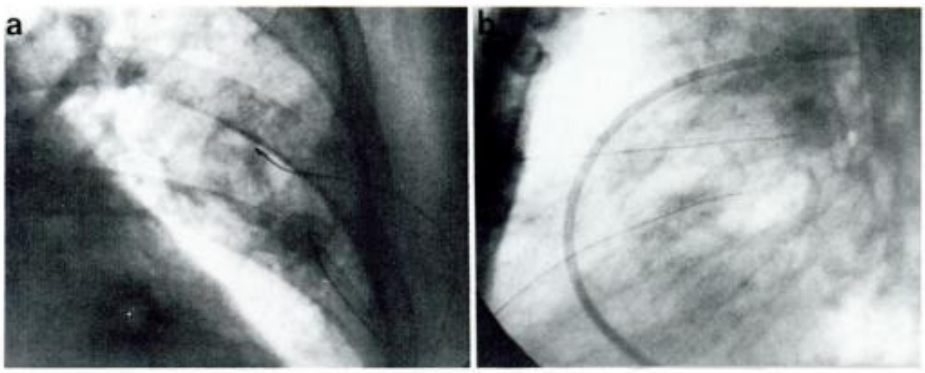

Fig. XVII: 26. Direct current treatment of metastatic ovarian carcinoma in the lingula of a 66-year-old woman (patient no. 1). Largest diameter of the tumour was 2.5 cm. (*a*) Anteroposterior view. (*b*) Lateral view. Percutaneous platinum electrodes: anode in the tumour, cathode in lung tissue 2.5 cm distant from the tumour. A cardiac catheter is positioned in the pulmonary artery for angiography.

slightly decreased in size. It is now surrounded by thicker radiating structures. In Fig. XVII: 29 *d*, *e* progressive decrease in size of the tumour is seen after seven and fifteen months. A small residual of probable scar tissue is indicated by an arrow in Fig. XVII: 29 *f* (after 2 years, 5 months). The patient has to date (after 4 years, 4 months) presented no new pulmonary metastases or metastases elsewhere.

One diameter of the tumour vs. time is plotted in Fig. XVII: 30. The size of the tumour decreased over an interval of greater than 2.5 years. More rapid decrease occurred during the first six months than during the later period of observation.

Patient no. 2. A mesenchymal fibroliposarcoma of the uterus was excised from this 20-year-old woman in 1977. She received chemotherapy (Dactinomycine, Cyclophosphamide and Vincristine) after the operation. Shortly thereafter, two metastatic tumours appeared in each lung (in 1978). One metastasis in the right lung was treated by electrocoagulation (see Fig. XVII: 5), the other three were treated by direct current.

The cellular material shown in Fig. XVII: 31 *a*, *b* was taken from a large tumour (35×37×42 mm) in the right lower lobe. Well differentiated (*a*) and moderately well differentiated (*b*) cells are shown. Fig. XVII: 31 *c*, *d* shows a comparable morphologic appearance of histologic sections from the primary intrapelvic sarcoma.

Fig. XVII: 32 *a* shows the tumour before treatment, (*b*) one year and (*c*) 3 years, 9 months after treatment. The volume of the tumour diminished to less than one fifth of its volume before treatment.

The treatment was performed under medication and local anaesthesia, like the previous case. Fig. XVII: 32 *d* shows the positions of the two platinum electrodes at the beginning of the treatment. Immediately after the treatment (Fig. XVII: 32 *e*), cavities containing gas (white arrows) are seen at the sites of the electrodes in the tumour and pulmonary parenchyma. A circular, diffuse haziness is also seen in the lung around the site of the cathode, representing oedema (hydropic "B" zone). A radiolucent "A" zone also developed around the anodic neoplasm (Fig. XVII: 32 *f*). 250 coulombs were delivered at 10 volts. The flow of current vs. time is shown in Fig. XVII: 33. The patient tolerated the treatment without difficulties. Some fluid, however, was observed in the pleural space during and after the treatment. It resorbed spontaneously within a few days. No pneumothorax or other complications occurred.

Two other metastases in this patient, each in the left lower lobe, were also treated with direct current. Their sizes also decreased (Table XVII: 2). Computerized tomography proved useful in determining the position of these lesions (Fig. XVII: 34 *a*, *b*). Each tumour,

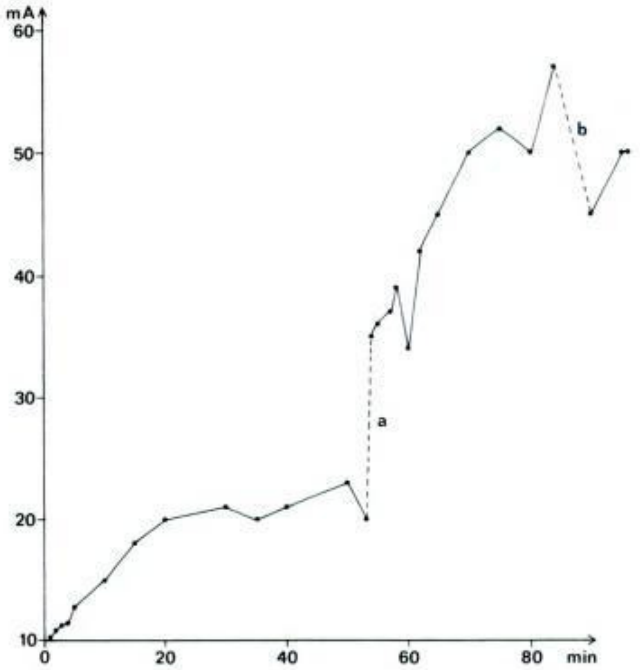

Fig. XVII: 27. Current supplied to the lung tumour of patient no. 1. At 10 volts, current increased from 10 to 20 mA during the first 55 minutes, when gas, accumulating at the electrodes, interrupted the current (*a*). Applied potential was elevated to 15 volts and flow of current resumed, increasing from 35 to 55 mA over 30 minutes, when a new interruption occurred (*b*). After a few minutes of waiting, additional current could be supplied at 15 volts. Total dose was 180 coulombs.

Fig. XVII: 28. Left pulmonary angiogram of patient no. 1. (*a*) Before treatment, the pulmonary arteries show normal size and calibre. (*b*) Immediately after treatment the lingular artery is displaced medially and small vessel branches are less prominent around the cathode.

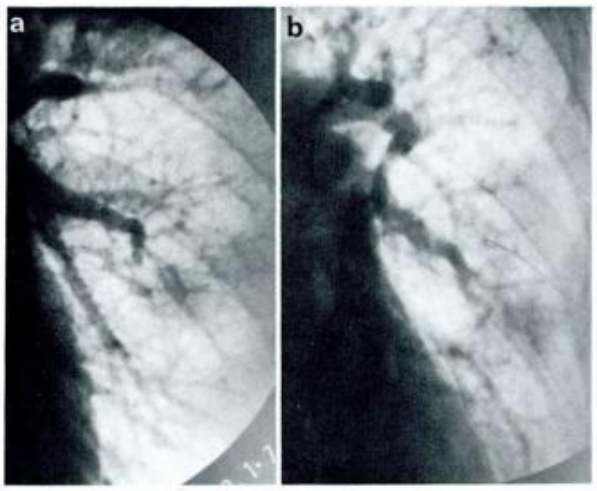

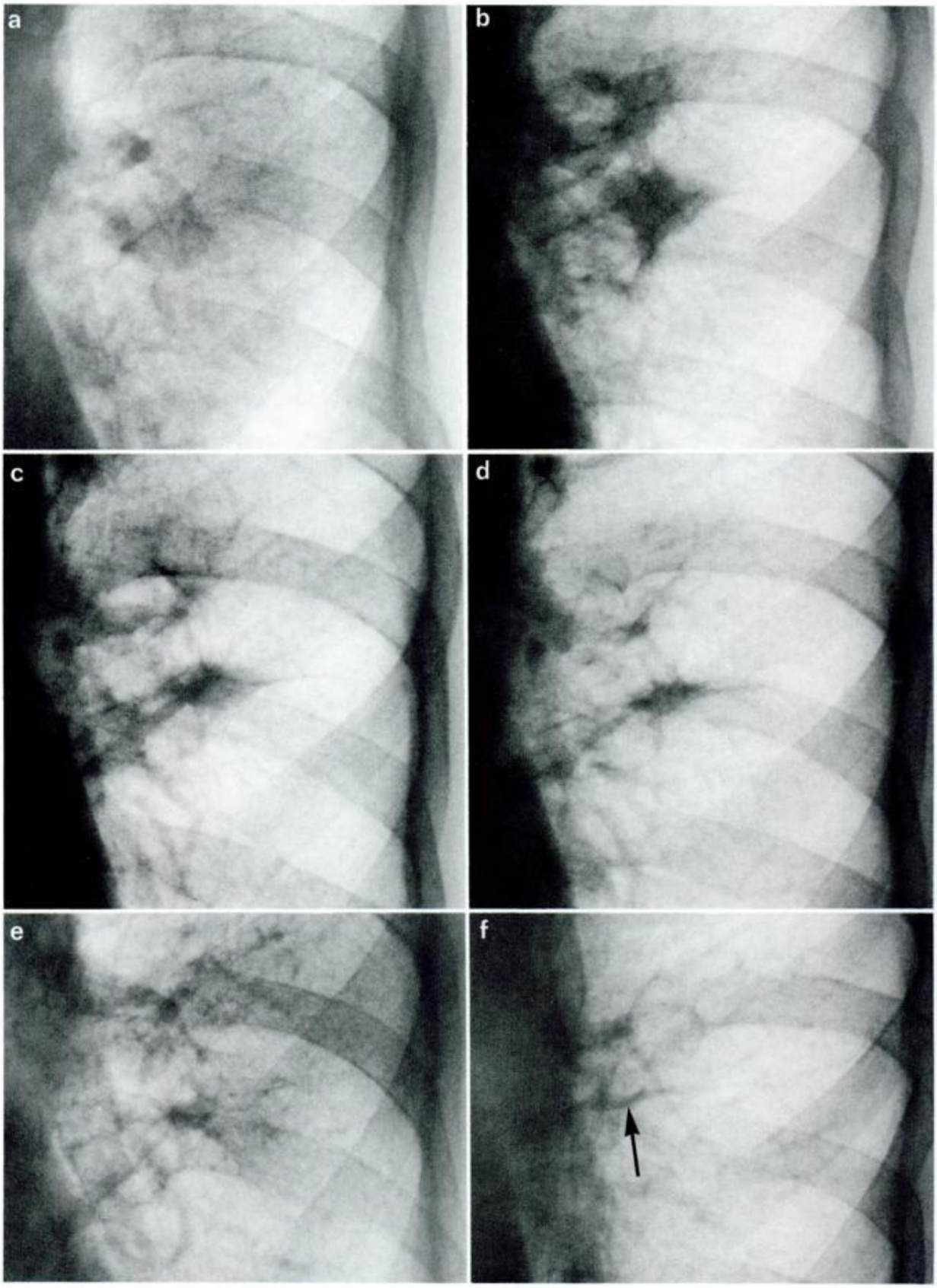

Fig. XVII: 29. Serial radiographs of metastatic ovarian carcinoma in the left lung of patient no. 1, before and after direct current treatment. (*a*) Before treatment. (*b*) 30 days after treatment. The tumour and the tissue at the site of placement of the cathode are surrounded by radiating, probably fibrous, structures. (*c*) 60 days after treatment. Regression is clearly observable. The fibrotic strands appear more prominent. (*d*) After 210 days, (*e*) 450 days and (*f*) 885 days, a very small residual or scar is seen at the site of the tumour (arrow).

Fig. XVII:30. After direct current treatment, decrease in one diameter of the metastatic ovarian carcinoma, patient no. 1, over a span of 2 years, 5 months.

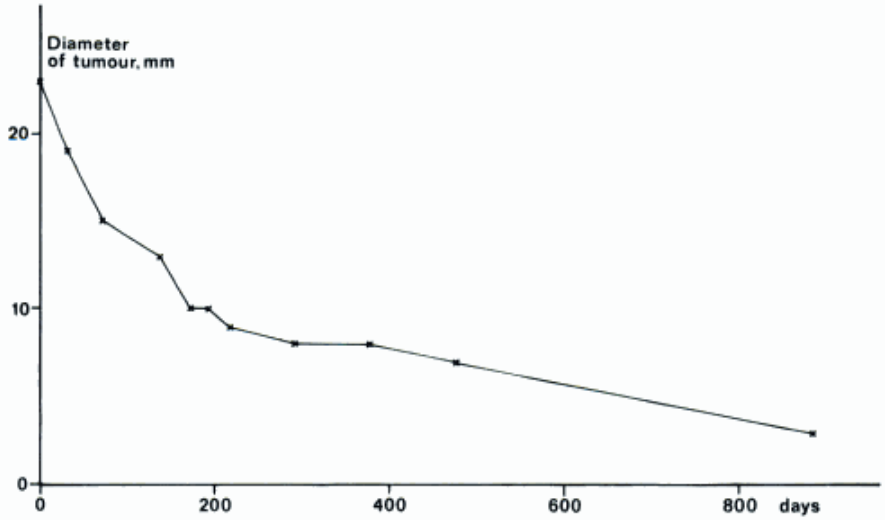

Fig. XVII:31. Patient no. 2. Comparison between cytologic samples obtained by screw needle biopsies from a pulmonary metastasis (*a*, *b*) and histologic sections of primary mesenchymal fibroliposarcoma of the uterus (*c*, *d*). (*a*) Well differentiated sarcomatous cells. (*b*) Moderately well differentiated tumour cells. Observe numerous lipid granulations. Air-dried smear. The cellular morphology in (*c*) corresponds to that in (*a*), that in (*d*) to that in (*b*). May-Grünewald-Giemsa stain (*a*, *b*). Haematoxylin-eosin stain (*c*, *d*).

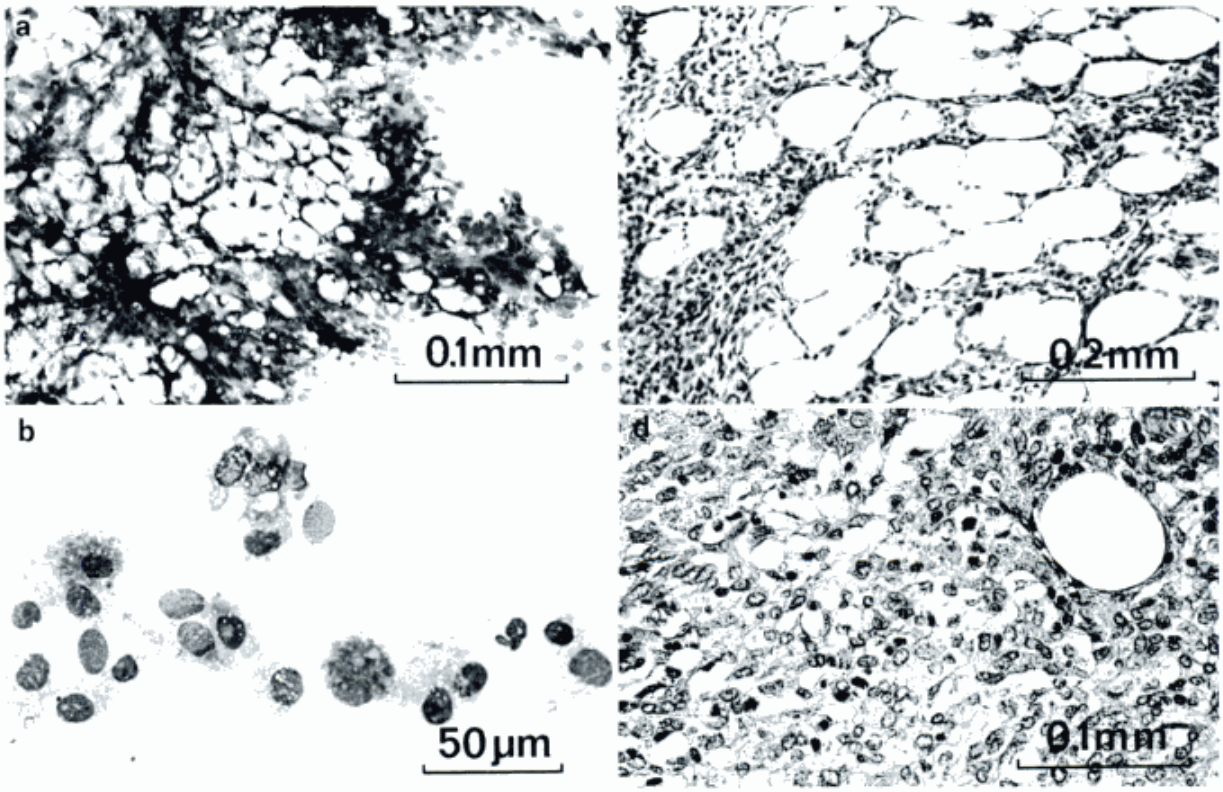

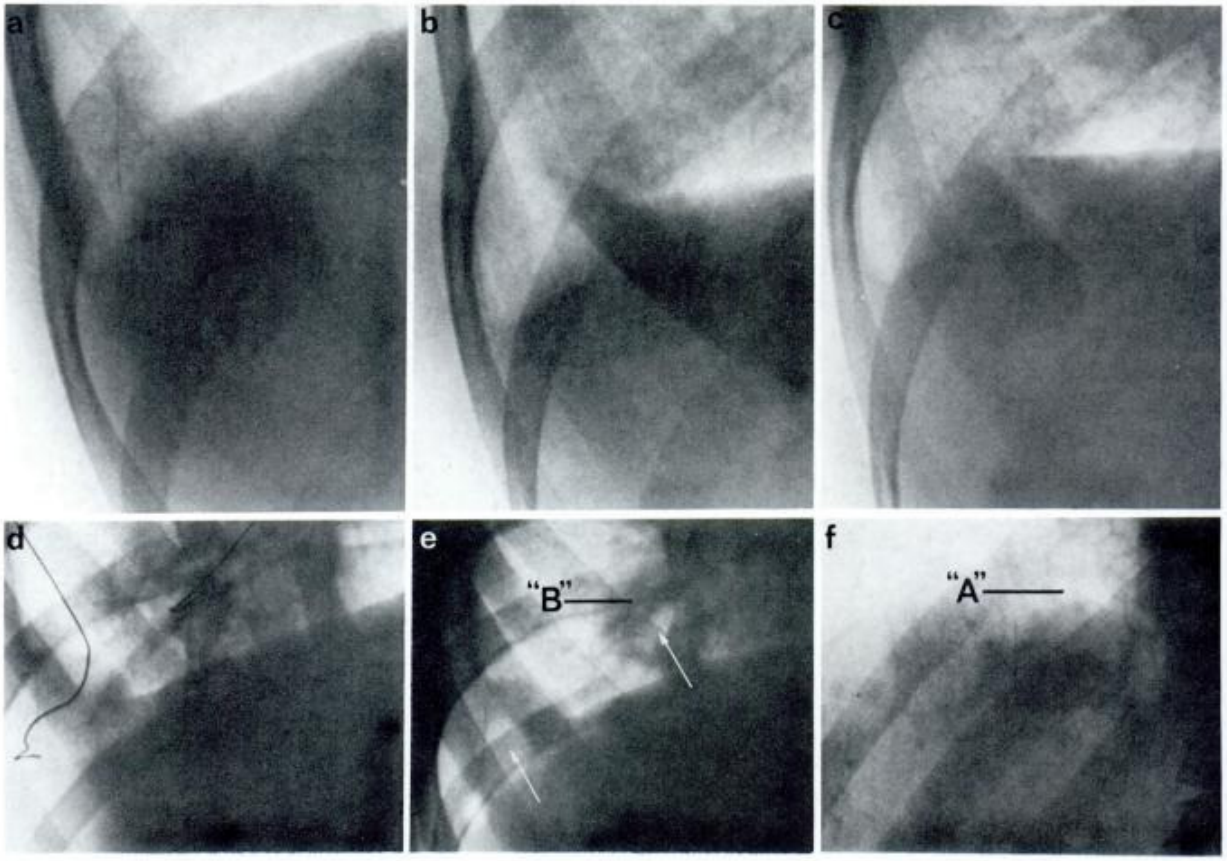

Fig. XVII: 32. Pulmonary metastasis, right lower lobe, patient no. 2. (*a*) Before treatment, (*b*) 380 days after, and (*c*) 1 370 days after treatment. The tumour has diminished to less than one fifth of its previous volume. (*d*) Positions of anodic intratumoural electrode and cathodic parenchymal electrode. (*e*) Immediately after treatment. Gas cavities at sites of electrodes (white arrows). New parenchymal opacity (hydropic "B" zone) in the cathodic region. (*f*) A radiolucent "A" zone around the anodic tumour is also evident immediately after treatment.

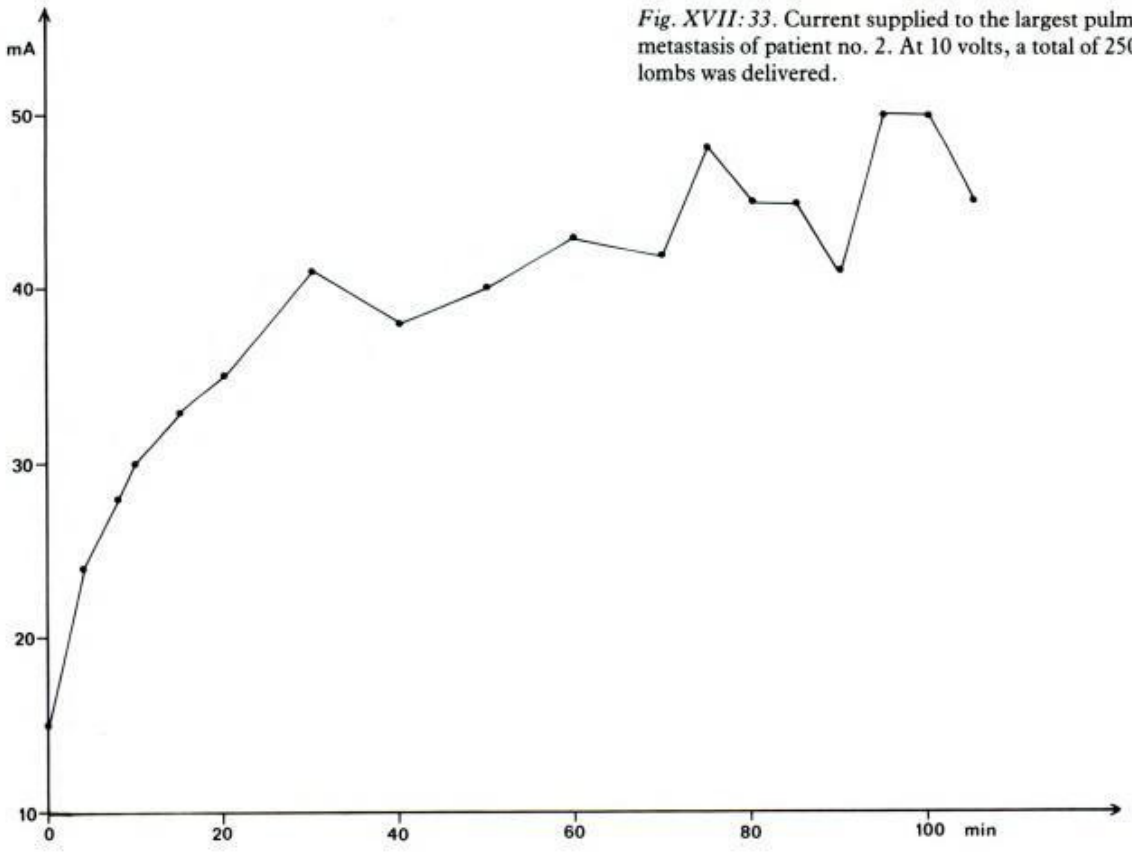

Fig. XVII: 33. Current supplied to the largest pulmonary metastasis of patient no. 2. At 10 volts, a total of 250 coulombs was delivered.

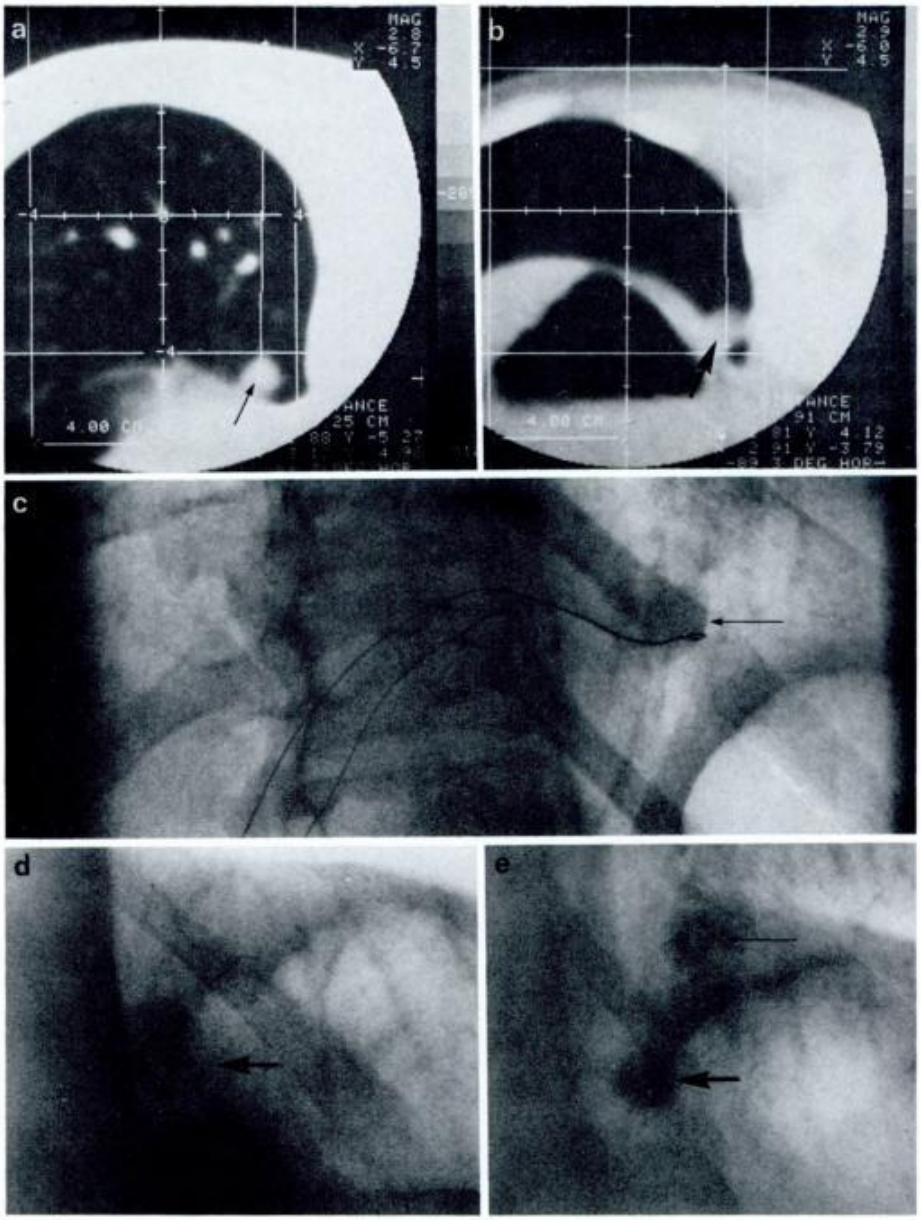

Fig. XVII: 34. Decrease in size of two pulmonary metastases, left lower lobe, patient no. 2, after DC treatment. These two tumours were 2 cm apart in the left lung close to the diaphragm and stomach. Abdominal contents hid them from fluoroscopic view in the lateral projection. Computerized tomography (with patient in prone position) aided planning the direction and depth of implantation of electrodes. (*a*) Computerized tomogram of the smaller, more superior metastasis (thin arrow). (*b*) Computerized tomogram of the larger, more inferior tumour (thick arrow). (*c*) Implanted electrodes for treatment of the smaller tumour. Radiograph, shallow right anterior oblique projection. (*d*) The larger tumour (thick arrow) before treatment. (*e*) Decreased sizes of the more superior tumour (thin arrow) 1 290 days after treatment and the more inferior tumour (thick arrow) 1 020 days after treatment. The centre of the more superior metastasis is now calcified, indicating healing of injured tissue.

13×15×12 mm (II) and 16×19×18 mm (III) respectively, was positioned deep in lung in the costophrenic sulcus, near the diaphragm and gastric fundus. The adjacent abdominal contents obscured fluoroscopic viewing in the lateral projection. The computerized tomograms, however, indicated clearly the sites of the lesions. The most suitable direction and depth for the insertion of each electrode could also be determined in this way. Fig. XVII: 34*c* illustrates the positions of the two electrodes during the treatment of the smaller of the two metastases. The larger tumour (III) is seen before treatment in Fig. XVII: 34*d*. The smaller tumour (II) received 100 coulombs at 10 volts. Its size had decreased slightly and calcium accumulated in its centre 3 years, 6 months after treatment (Fig. XVII: 34*e*). Tumour III received only 65 coulombs at 10 volts but its size also was clearly decreased 2 years, 10 months after treatment (Fig. XVII: 34*e*).

After each treatment the patient was hospitalized only one or two days and then returned to work as a nurse's assistant. She is in good condition and has received no supplementary treatment. To date (after 4 years, 8 months) no new metastases have been observed.

Patient no. 4. A selective effect of the electric field on multiple small tumours is suggested by observations in this patient.

An intrapelvic stromal sarcoma was resected from this woman in 1964 at age 46. Since 1970 she has been treated for diabetes mellitus, systemic hypertension

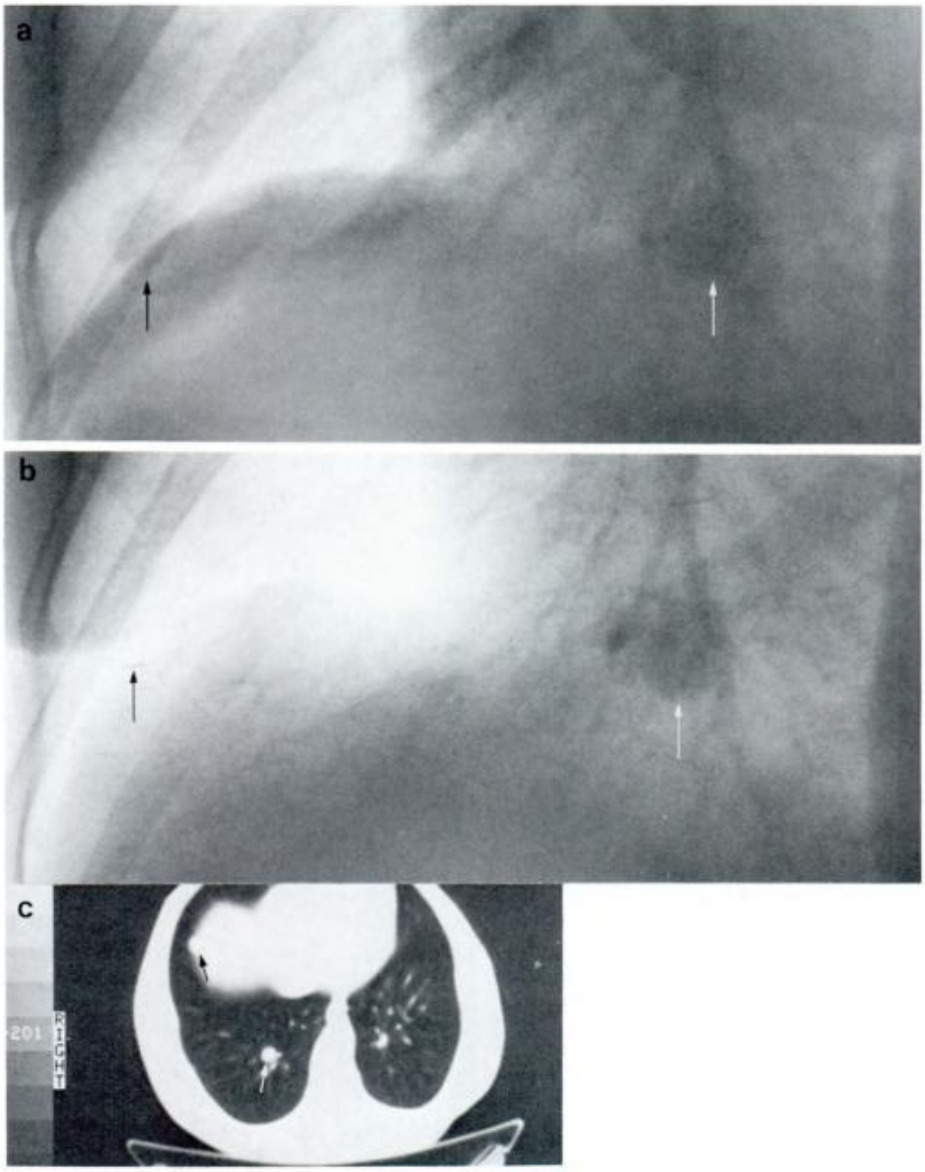

Fig. XVII: 35. Decrease in size of two pulmonary metastases, right lower lobe, patient no. 4, after treatment with direct current. Primary intrapelvic sarcoma. Radiographs, right posterior oblique projection. (*a*) Before treatment, one metastasis is anterolateral (black arrow), one medial (white arrow). The diameter of each tumour is about 1.5 cm. The anterolateral tumour was the first to be treated with direct current (100 coulombs at 10 volts electrode potential). (*b*) 153 days later, the anterolateral tumour has disappeared. A 3 mm piece of platinum electrode (black arrow) shows the previous site of the tumour. 112 days after treatment with direct current (180 coulombs at 10 volts), size of the medially located tumour has decreased slightly. (*c*) Computerized tomogram through the two tumours before treatment. See also Figs. XVII: 38, 40 (electrode implantations).

and atrial fibrillation. In May 1978, two tumours, each approximately 1.5 cm in diameter, were found in the lower lobe of the right lung (Fig. XVII: 35 *a*, *c*). Several 3–4 mm diameter nodules, presumed to be metastases, were also apparent in the posterior basal segment of the right lower lobe (Fig. XVII: 36 *a*).

Before DC treatment of each of the two large tumours, screw needle biopsies were obtained, confirming the diagnosis of metastases from the intrapelvic stromal sarcoma (Fig. XVII: 37).

Fig. XVII: 38 *a* illustrates an electrode implanted in the more anterolateral of the two largest tumours and the screw needle inserted in the tumour for cytologic verification of the diagnosis. Fig. XVII: 38 *b* and *c* shows anteroposterior and lateral photofluorographs of the position of the electrodes in the tumour and in the pulmonary parenchyma before treatment.

DC treatment was performed under local anaesthesia after preliminary medication with 10 mg Valium® and 5 mg morphine-scopolamine. The anterolateral tumour received 100 coulombs at 10 volts. Fig. XVII: 39 presents the relationship of current to time in this treatment. The discontinuities in the curve indicate that the treatment was interrupted twice, each time because the patient complained of sudden pain. The pain is presumed to have been caused when the flow of current was interrupted by gas produced around the electrodes. Other than the moderate discomfort produced by these interruptions of current, the patient had no complaints. When the electrodes were pulled out, one small piece of the tumour electrode broke off and remained in the tumour. A small pneumothorax was also produced but the air resorbed spontaneously in two days.

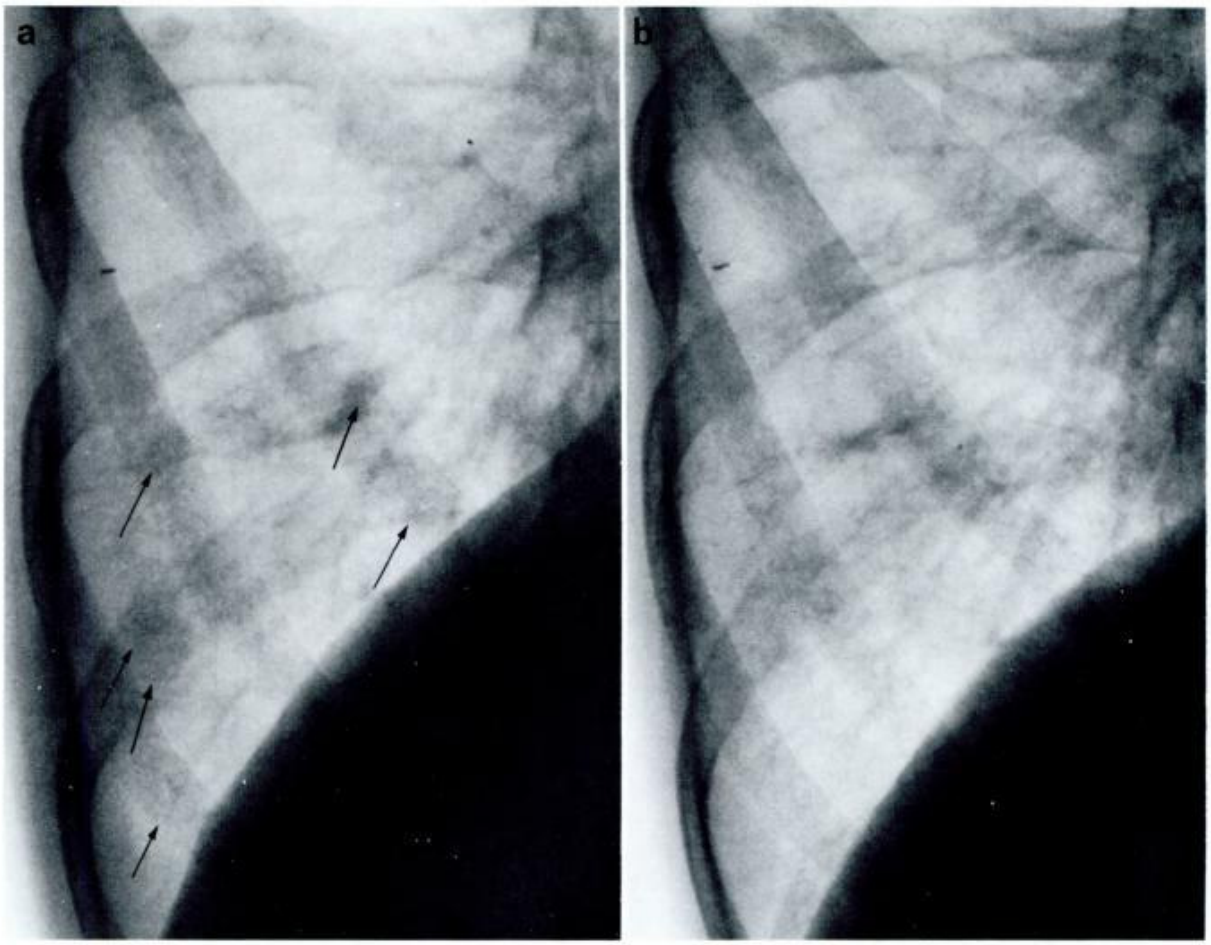

Fig. XVII:36. Decrease in size of small pulmonary nodules (arrows), lateral basal segment, right lower lobe, patient no. 4, after large metastases in the same lobe were treated with direct current. Radiographs, shallow right anterior oblique projection. (*a*) Before treatment. (*b*) Four months later. Several of the small lesions have disappeared or diminished in size.

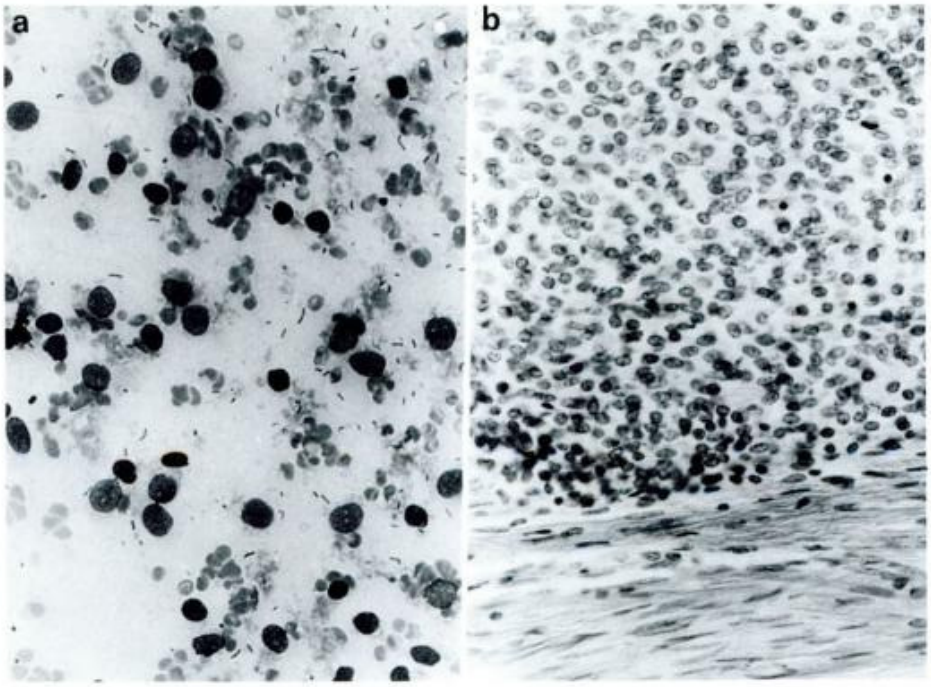

Fig. XVII:37. Sarcomatous tissue from lung and pelvis, patient no. 4. (*a*) Cytologic specimen from metastatic tumour, medially situated in the right lower lobe. (*b*) Histologic section, primary pelvic sarcoma. The cellular material is comparable from each of the two lesions.

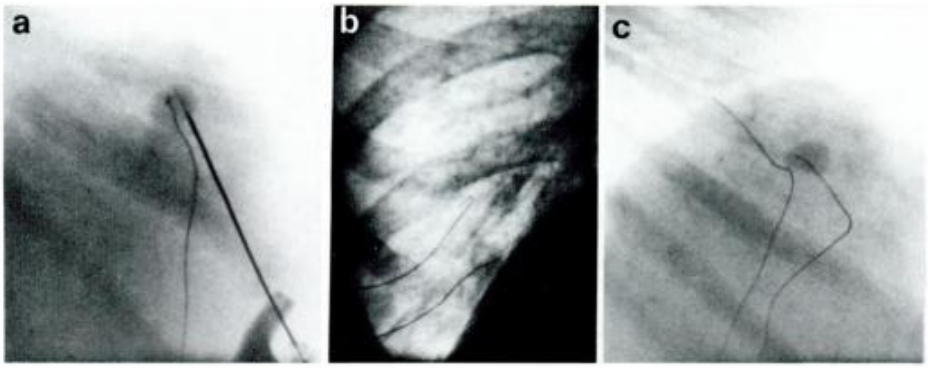

Fig. XVII: 38. Direct current treatment of anterolateral basal pulmonary metastasis, patient no. 4. (*a*) Percutaneous electrode for treatment (wire on left) with screw needle, and sampling of cellular material to confirm the presumptive diagnosis of metastatic sarcoma. (*b*) Anteroposterior, and (*c*) lateral photofluorographs of electrodes in tumour and in nearby pulmonary parenchyma.

In this patient the first treated tumour rapidly decreased in size. Five months after treatment the tumour could no longer be identified. As seen in Fig. XVII: 35 *b*, no tumour remained at its previous site, as indicated by the remaining piece of the electrode. Radiologically, no scar tissue is evident in the lung at the sites of the electrodes.

The position of the electrodes implanted for DC treatment of the posterior basal tumour is also shown in the radiographs in Fig. XVII: 40 *a*, *b*. A computerized tomogram (Fig. XVII: 40 *c*) shows the reactions in the lung about 30 minutes after treatment of this tumour. The arrow points to a small cavity in the tumour, the dotted line a larger cavity at the site of the previous position of the cathode. Haziness in the cathodic area is caused by electroosmotically collected tissue fluid ("B" zone effect). Gas produced around electrodes is always more extensive around the cathode than the anode. This tumour was given 180 coulombs at 10 volts electrode potential. Despite treatment with a dose nearly twice that given the anterolateral metastasis, the medial basal tumour decreased to a size only somewhat smaller than before treatment (right tumour, white arrows in Fig. XVII: 35 *a*, *b*). Neither of the treated lung tumours showed any sign of recurrence during the observation period (485 and 444 days). The patient died from recurrence of her primary intrapelvic sarcoma and brain metastases.

The behaviour of the two tumours of patients no. 2 and 4 requires some comments. In patient no. 2 a more rapid and prominent decrease of the slightly larger tumour (III) occurred after 65 coulombs than of the smaller tumour (II) after 100 coulombs (Table XVII: 2). In patient no. 4, the lateral basal tumour disappeared after 100 coulombs, while the size of the posteromedial basal tumour decreased only slightly after 180 coulombs. These discrepancies between amount of current and effect on tumour size have been interpreted as follows:

The growth of a tumour can be stopped permanently when all tumour cells are destroyed. A resorption of devitalized tumour tissue will then take place, which may lead to total or partial disappearance of the tumour. In case an overdose of current is given, the treatment will also interfere with the functions of the surrounding normal tissue. For example, microthrom-

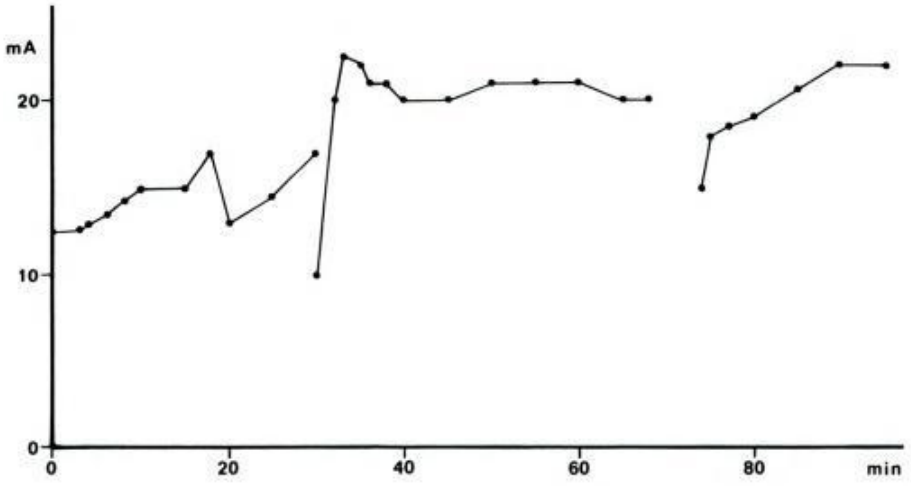

Fig. XVII: 39. Current-time chart, patient no. 4, treatment of the anterolateral metastasis (100 coulombs, 10 volts). Interruptions in the curve indicate the two instances when the patient reported pain, which was presumed to be caused by gas around the electrodes interrupting the flow of current.

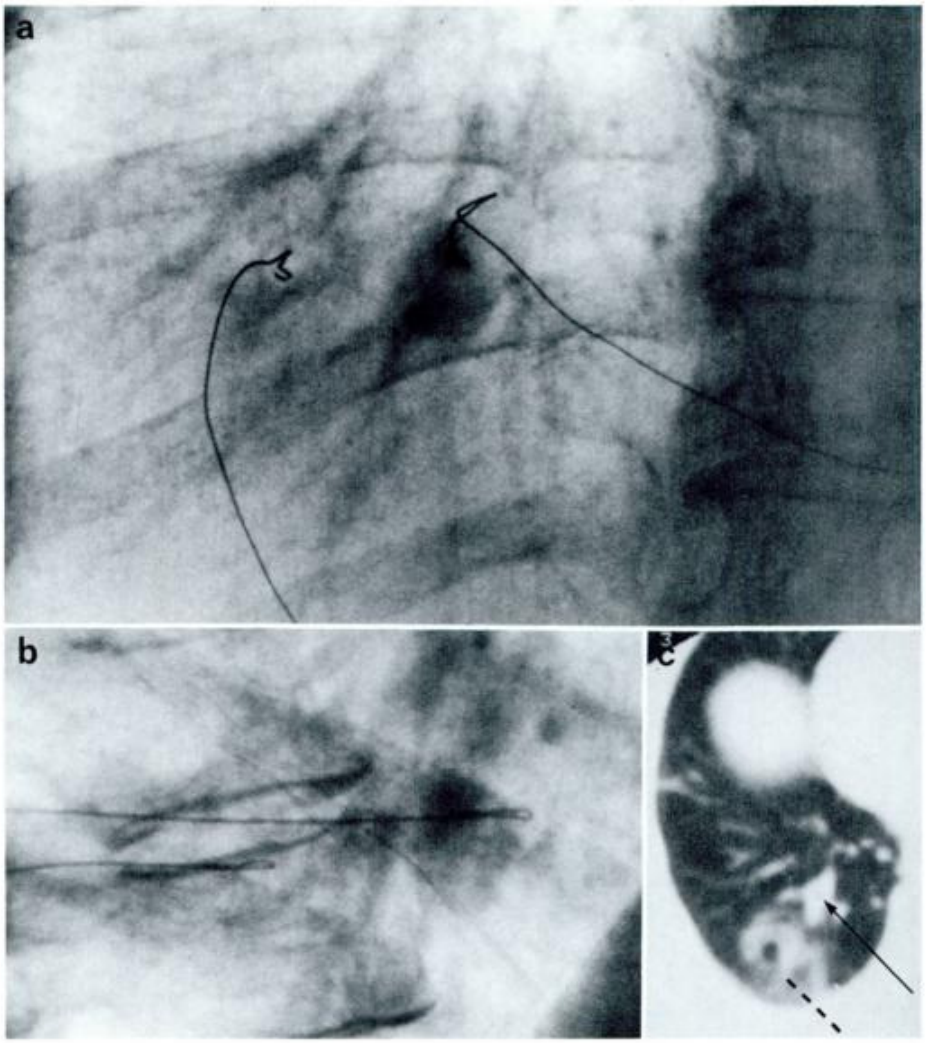

Fig. XVII:40. Direct current treatment of medial basal pulmonary metastasis, patient no. 4, radiographic images. During treatment the cathode was in pulmonary parenchyma posterolateral to the anode in the tumour. Gas has formed around each electrode. (*a*) Anteroposterior, (*b*) lateral projections. (*c*) Computerized tomogram 30 minutes after treatment. Tumour shows small gas bubble (thin arrow). Centre of cathode shows larger cavity surrounded by electroosmotically accumulated oedema (dotted line).

boses and fibrosis may develop, preventing the resorption of destroyed tumour tissue. We then obtain what might be called a *sequestration of destroyed tumour tissue*, which might be an even more reliable effect of the treatment than apparent disappearance of a tumour after treatment. The crucial problem is, however, that it will become difficult to decide whether a slight decrease of a tumour treated with direct current reflects a "safe sequestration" or only partial destruction of tumour tissue, possibly to be followed by later regrowth of the tumour.

Another remarkable finding also developed in patient no. 4. Several of the multiple small nodules in the posterior basal segment of the lower lobe (Fig. XVII: 36*a*) clearly diminished in size after the treatments, as seen in Fig. XVII: 36*b*. It appears, therefore, that a therapeutic effect on tissue may not be limited to the destructive effects on tissue of protons close to the anode. Effects of the electric field may induce sufficient change of the biologic environment to interfere with the living conditions of malignant tissue within the organ but at a distance from the electrodes. This finding is also in agreement with the biologic effects described earlier several centimetres from the anodic and cathodic electrodes. Thus, dehydration, extensive microthromboses and attraction of leukocytes take place around the anode. Around the cathode alkalinity and interstitial oedema are prominent. Large vessels are temporarily occluded, locally impairing the circulation. These biologic field effects as well as the induced changes of ionic composition in the tissue fluids and cells represent, in the view of the author, an interesting and fruitful aspect of treatments with direct current.

Patient no. 10. Chest radiographs (Fig. XVII: 41*a*, *b*) revealed a tumour, 2 cm in diameter, in the middle lobe of the right lung of a 46-year-old woman. One year previously an adenocarcinoma of the left breast had been resected. Needle biopsy of the lung tumour revealed cells which appeared to be of the same type as

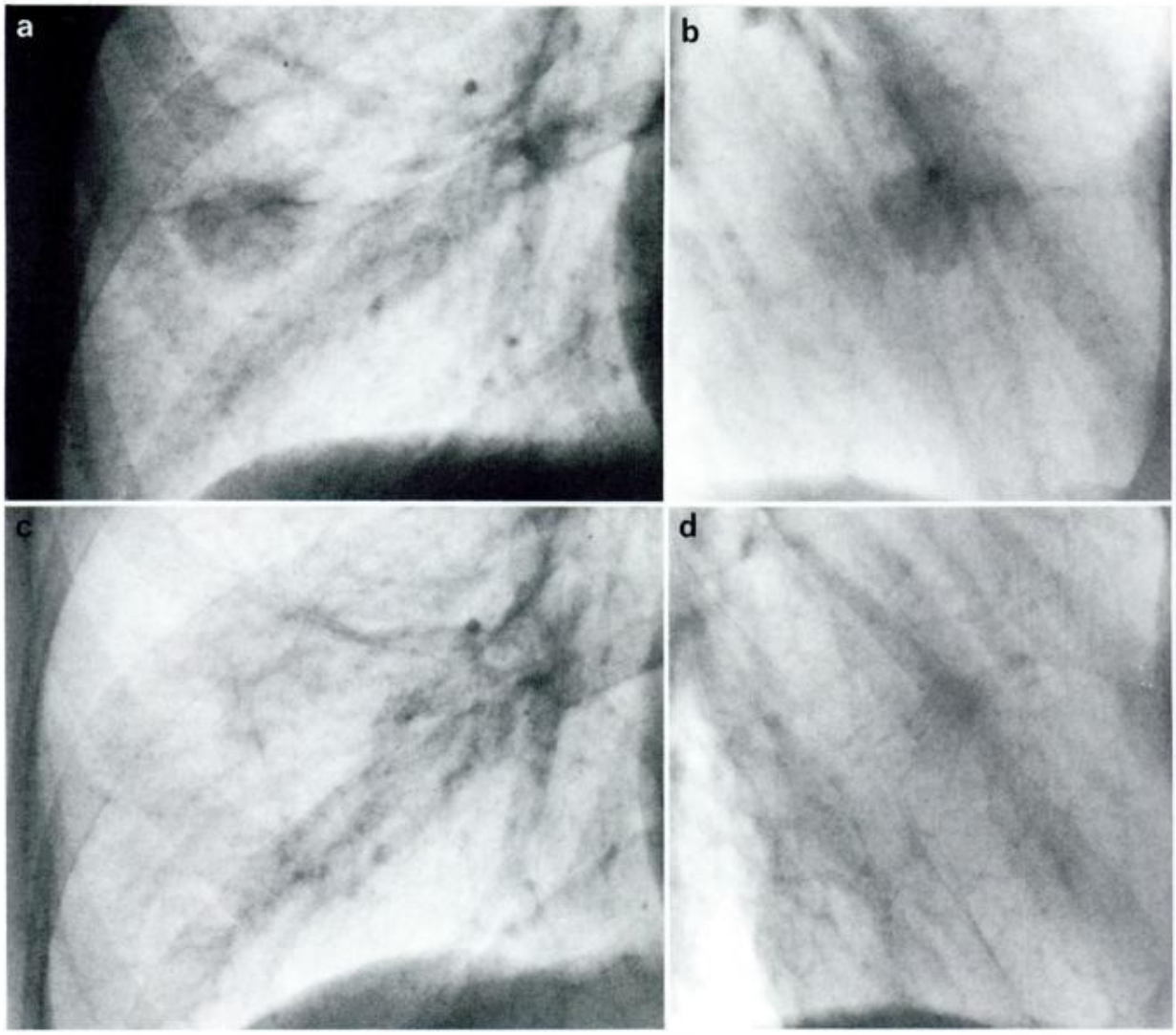

Fig. XVII:41. Decrease in size of a pulmonary metastasis, patient no. 10, after treatment with direct current. Primary adenocarcinoma of breast. Radiographs, (*a*) posteroanterior and (*b*) lateral projections before treatment (190 coulombs at 10 volts). The size of the tumour gradually decreased. Radiographs, (*c*) posteroanterior and (*d*) lateral projections 1 110 days after treatment.

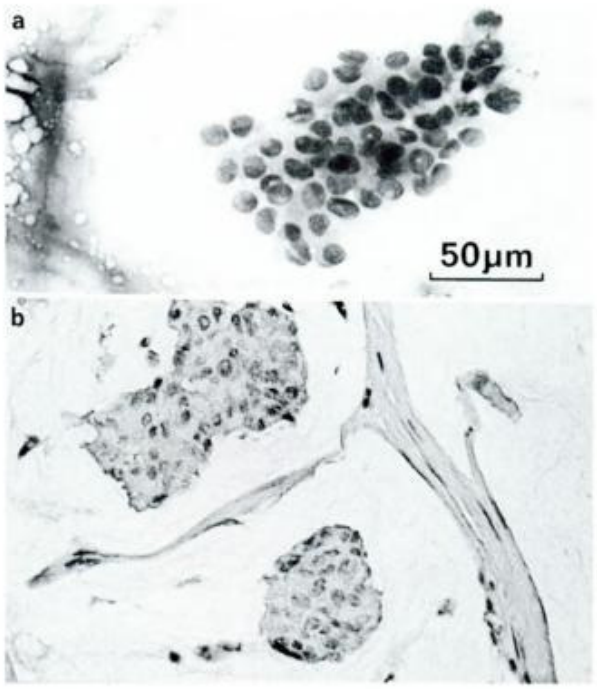

Fig. XVII:42. Patient no. 10. (*a*) Cytologic material from screw needle biopsy of pulmonary metastasis. (*b*) Corresponding histologic tissue section from primary adenocarcinoma of the breast.

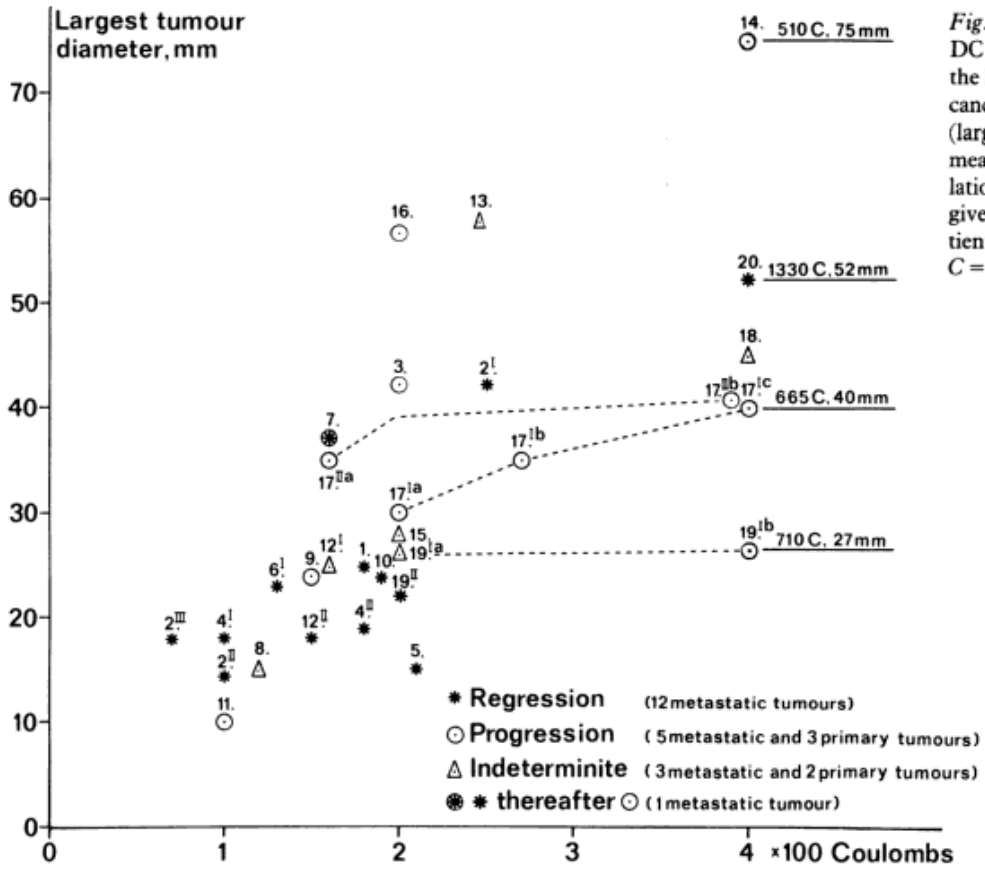

Fig. XVII: 43. Effects of DC treatment of cancers in the lung. Diameter of each cancer before DC treatment (largest radiographically measurable diameter) in relation to quantity of current given. Numbers refer to patients of Table XVII: 2. *C* = coulombs.

the cells from her breast cancer (Fig. XVII: 42). She had no symptoms and was in excellent general condition. Surgical excision of her lung tumour was therefore recommended. The patient refused surgery, radiation and cytostatic therapy but accepted a "slight attempt" with direct current.

The tumour, 24×21×20 mm in diameter, was given 190 coulombs at 10 volts. Gradually the tumour diminished to 9×11×8 mm, 3 years, 1 month after the treatment (Fig. XVII: 41 *c*, *d*). To date (3 years, 8 months after treatment) no metastases are visible in her lungs and she remains free of symptoms.

The actual data on direct current treatment of the series of tumours are surveyed in Fig. XVII: 43, correlating the largest diameter of each cancer at the time of treatment, the amount of current given and the estimated effect on tumour diameter (indicated by symbols). It is obvious that the short observation time does not permit any definitive conclusion about permanent control of the treated tumours. Some conclusions, nevertheless, may be drawn from the results to date.

The first important general comment must be that the majority of the patients were considered as "hopeless", i.e., standard forms of treatment were not appropriate. In spite of their often poor condition, none of the patients has been lost as a result of the treatments. A definitive beneficial effect has been observed in twelve of twenty-one treated metastatic tumours as well as in many neighbouring small tumours in patient no. 4. One metastasis decreased in size during 730 days and then later started to increase in size (patient no. 7). Five metastases have progressed. Observation time is too short to evaluate three of the metastases. Out of five primary cancers no one has so far shown regression. Three have progressed and two are indeterminate because of too short observation time.

Tumours of greatest diameter larger than 30 mm in general did not respond well to treatment, possibly due to too small dose of treatment. The largest tumour to react favourably was the 42 mm diameter sarcoma of patient no. 2. The peripheral site of this tumour probably contributed to this beneficial result. Electroosmotic oedema in the more proximal cathodic field may have interfered with blood circulation and thereby enhanced the possibilities of proton diffusion and migration around the anode.

One relatively small tumour (case no. 11) increased in size after treatment. It was difficult in this patient to keep the anode in the tumour during the treatment. It is therefore likely that the dose delivered to the tumour was too small, as was probably also the case in the other tumours which showed progression. In spite

Table XVII: 2. *Results of treatments with direct current to 26 cancers (21 metastatic, 5 primary) in the lungs of 20 patients*

No.	Patient Age (years)	Primary cancer	Date of treatment Size of pulmonary tumour (mm) M = metastasis P = primary cancer	Voltage (volts)	Coulombs	Position of cathode (Type of anode)	Coulombs per largest diameter (cm) of tumour	Observation time (days) Size of tumour (mm)	Effects of treatment	Comments
1.	H.S. ♀ 66	Adenocarcinoma of ovary Resection 1973 +4 000 rads	M. I 8/6 1978 25×17×17	10–15	180	Pulmonary parenchyma (Type 1)	78	1 350 1×1×1	Regression	Coronary arteriosclerosis, atrial fibrillation and myocardial infarction precluded surgical treatment.
2.	B.K. ♀ 20	Fibroliposarcoma of uterus Resection 1977	M. I 1/6 1978 35×37×42	10	250	Pulmonary parenchyma (Type 1)	60	1 370 20×20×19	Regression	After treatment I, small pleural effusion for two days. After treatment II, minimal haemoptysis.
			M. II 3/8 1978 13×15×12	10	100	Pulmonary parenchyma (Type 1)	71	1 290 12×11×11	Regression	Excellent condition. Resumed her work as nurse assistant.
			M. III 3/5 1979 16×19×18	10	65	Pulmonary parenchyma (Type 1)	36	1 020 10×12×10	Regression	
3.	K.L. ♀ 68	Squamous carcinoma of uterine cervix Resection 1974	M. I 15/8 1978 23×42×36	10	200	Pulmonary parenchyma + pulmonary artery (Type 1)	56	930 49×65×55	Progression	Minimal pneumothorax. Suicide 3 years after treatment. At autopsy multiple small pulmonary metastases.
4.	S.D. ♀ 60	Intrapelvic sarcoma Resection 1964	M. I 18/7 1978 15×18×18	10	100	Pulmonary parenchyma (Type 1)	56	485 15×14×14	Regression	Hypertension. Coronary arteriosclerosis. Diabetes mellitus. Small pneumothorax. Death, 1979, of intracerebral haemorrhage.
			M. II 28/8 1978 16×19×18	10	180	Pulmonary parenchyma (Type 1)	94	444 17×14×14	Regression	
5.	G.P. ♀ 53	Adenocarcinoma of breast Resection 1969	M. I 1/8 1978 15×11×12	10	210	Pulmonary parenchyma (Type 1)	140	1 260 6×14×6	Regression (Indeterminate)	Minimal pneumothorax. Patient received progesterone, so the effect of DC treatment is uncertain.
6.	A.J. ♂ 21	Osteosarcoma Resection 1978	M. I 20/11 1978 23×23×23	10	130	Pulmonary parenchyma (Type 1)	57	50 22×22×20	Regression	Large pneumothorax. Piece of platinum electrode left in lung. Treated tumour I removed surgically but specimen lost. Tumour II not operated. Death from multiple metastases after 60 days.
			M. II (20/11 1978) (25×25×25)	No treatment (control)				(50) (34×34×34)	Progression	
7.	D.J. ♀ 71	Adenocarcinoma of ovary Resection 1974	M. I 25/10 1978 35×37×33	10	160	Pulmonary parenchyma (Type 1)	43	730 22×31×30	Regression	Large pneumothorax. Piece of platinum electrode left in tumour. Coronary arteriosclerosis.
								1 150 50×70×53	Progression	

8.	M.R. ♀ 48	Malignant melanoma resected from skin 1972	M. I	21/11 1978 15×15×15	10	120	Pulmonary parenchyma (Type 2)	80	21 15×15×15 50% destroyed	Indeterminate	Pneumothorax. Death from haemorrhage in cerebral metastasis 3 weeks after treatment.
9.	K.N. ♂ 54	Adenocarcinoma of lung Lobectomy 1978	P. I	9/10 1978 18×24×20	10	150	Pulmonary parenchyma (Type 2)	75	310	Progression	Thickened pleura after lobectomy. Wrong position of anode. Death from multiple metastases. Scar tissue adjacent to treated tumour.
10.	M.L. ♀ 46	Adenocarcinoma of breast Resection 1978	M. I	15/2 1979 24×21×20	10	190	Pulmonary parenchyma (Type 1)	75	1 110 9×11×8	Regression	Small pneumothorax. Pleural drain. Small local bleeding around tumour.
11.	A.S. ♂ 74	Small cell bronchogenic carcinoma	P. I	7/2 1979 10×10×10	10	100	Pulmonary parenchyma (Type 1)	100	1 050 48×45×45	Progression	Diabetes mellitus. Difficulties in keeping anode positioned in tumour. Pleural drain. Local bleeding around tumour. Death from brain metastases.
12.	A.T. ♂ 41	Teratocarcinoma of testis Resection 1977	M. I	5/2 1979 22×25×23	10	160	Pulmonary parenchyma (Type 1)	64	440 Pleural thickening	Indeterminate	Prophylactic pleural drain. Death from multiple metastases.
			M. II	6/3 1979 15×18×15	10	150	Pulmonary artery (Type 1)	83	410 15×17×15	Regression	
13.	N.A. ♂ 76	Squamous cell carcinoma of the oesophagus Resection 1975 + radiation treatment	M. I	7/8 1979 53×53×58	7	245	Aorta (Type 2)	42	180 72×65×53	Progression	Prophylactic pleural drain. Pain in left shoulder. Small pneumothorax. Large central cavity with collapse of tumour. Death from cerebral metastases.
									345 40×48×52	Indeterminate	
14.	K.W. ♂ 70	Squamous cell bronchogenic carcinoma Resection 1977	M. I	23/8 1979 75×65×65	10	510	Aorta (Type 1)	68	840 90×90×85	Progression	Progression after chemotherapy. Small pneumothorax. No pleural drain. Necrotic centre of tumour which progressed also after DC treatment. Death from complicating bronchopneumonias.
15.	Å.H. ♂ 72	Carcinoid tumour of lung	P. I	2/10 1979 27×26×28	10	200	Aorta (Type 2)	71	240 26×26×28	Indeterminate	Emphysema. Prophylactic pleural drain. Death from abuse of alcohol.
16.	E.W. ♂ 54	Poorly differentiated squamous cell carcinoma of lung	P. I	8/10 1979 40×45×57	10	200	Aorta (Type 2)	35	655 65×65×65	Progression	Chronic respiratory insufficiency post poliomyelitis. Bronchial bleeding on removal of electrode. Temporary cardiac arrest, responded to cardiopulmonary resuscitation. Large pleural effusion. Eventual death from local growth of tumour and widespread metastases.

Cont.

Table XVII: 2. *Cont.*

No.	Patient Age (years)	Primary cancer	Date of treatment Size of pulmonary tumour (mm) M = metastasis P = primary cancer	Voltage (volts)	Coulombs	Position of cathode (Type of anode)	Coulombs per largest diameter (cm) of tumour	Observation time (days) Size of tumour (mm)	Effects of treatment	Comments
17.	U.K. ♀ 56	Adenocarcinoma of uterus Resection 1977 + radiation treatment	M. I a 10/10 1979 20×30×17	10	200	Aorta (Type 2)	67	287 35×30×33	Progression	Prophylactic pleural drain. Pleural drain during treatment. Nephrostomy. Stenoses of ureters after radiation treatment. Death from multiple metastases.
			I b 23/7 1980 35×30×33	10	270	Pulmonary artery (Type 2)	77	78 40×28×32	Progression	
			I c 9/10 1980 40×28×32	3.4	665	Pulmonary parenchyma (Type 3)	166	330 65×50×70	Progression	
			M. II a 14/8 1980 33×35×35	10	160	Pulmonary artery (Type 3)	46	90 40×35×35	Progression	
			II b 12/11 1980 40×35×35	1.5–3.5	400	Pulmonary parenchyma (Type 3)	100	300 75×75×70	Progression	
18.	O.S. ♂ 64	Squamous cell bronchogenic carcinoma	P. I 25/9 1979 45×42×43	10	400	Aorta (Type 2)	89		Indeterminate	Arteriosclerosis. Clinically well after treatment. 3 weeks later sudden death, acute myocardial infarction.
19.	S.S. ♂ 58	Adenocarcinoma of rectum Resection 1977	M. I a 16/7 1980 28×22×21	10	200	Pulmonary artery (Type 3)	71	185 28×20×25	Indeterminate	Diabetes mellitus. Pleural thickening post pulmonary tuberculosis.
			I b 21/1 1981 28×20×25	3.4	710	Right subclavian vein (Type 4)	263	400 80×60×75	Progression	
			II 28/10 1981 22×19×18	10	200	Pulmonary parenchyma (Type 2)	91	105 18×12×11	Regression	
20.	A.N. ♀ 61	Carcinoma of uterus stage I grade II	M. I 31/3 1981 40×52×45	5	1 330	Left subclavian vein (Type 4)	333	355 30×42×35	Regression	Anode displaced from tumour for an indeterminate period of time. Actual tumour dose therefore uncertain. Skeletal metastases. Pleural thickening.

of the small material, several observations indicate that different biologic types of cancers may respond differently to DC treatment. Two tumours in patient no. 17 were treated vigorously in comparison with the relatively small dose given to patient no. 2. In the evaluation of the present material, it must be kept in mind that the technique of treatment is still far from optimized. It can be improved and also combined with different other techniques. An electrophoretic attraction of cytostatic agents of suitable charge may be possible, as was shown in principle with Evans blue dye (Chapter XIV, pp. 191–192).

5. Complications

The patients, despite often poor general condition, have usually tolerated direct current treatments very well. Fourteen of the patients have reported moderate pain, which was caused either by location of the anode close to the pleura or by the pleural drainage tube. Local anaesthesia of the pleura and chest wall succeeded in managing these pains. In one patient an irritant cough was probably produced by electrolytic compounds at the surfaces of an electrode, e.g., chlorine at the anode.

Spontaneous interruption of current by gas formed at the electrodes causes intense pain and muscular contractions. The treatment must then be interrupted and the gas allowed to resorb before treatment can be restarted. In this respect electrode Types 3 and 4 are favourable because they contain channels, which allow suction of gas and the injection of solutions, e.g., saline. These aspects are important in attempts to treat large tumours (e.g., over 3 cm in diameter).

Pneumothorax with dyspnoea occurred in some of the patients first treated. Thereafter, a pleural drain was applied before each treatment. In one patient a slowly developing and asymptomatic pneumothorax resulted in displacement of the electrode from the tumour (patient no. 8). In one patient the anode was positioned incorrectly because thickened pleura made its position difficult to determine. Minimal haemoptysis occurred in four patients in connection with the transthoracic positioning of the electrodes. These slight bleedings did not prevent the treatments from being carried out as planned. In actuality, the anode should be kept away from direct contact with large vessels. In the anodic region the tissue dehydrates and vessels thrombose. In the cathodic region a massive collection of interstitial, electroosmotically transferred fluid compresses the vessels. These bioelectric effects all contribute to decreasing the risks of bleeding during treatment.

In one patient with ventilatory insufficiency after poliomyelitis (patient no. 16), major haemoptysis developed when the tumour electrode (one hooked, 0.2 mm thick, platinum electrode, Type 2) was pulled out from a rather centrally located primary carcinoma. Massive bleeding into the bronchus produced transient hypoxaemia and cardiac standstill. Rapid bronchial draining and artificial respiratory assistance quickly restored cardiopulmonary function. The bleeding stopped. The patient recovered and subsequently returned to his work. He died of local recurrence and widespread metastases 1 year, 10 months after the treatment. This episode of local arterial bleeding has been the only serious complication in the present series of patients. How the bleeding happened is difficult to prove, but the following explanation may be offered: the hooked platinum string probably caught a branch of a bronchial artery in the anodic tumour cavity as the electrode was pulled out. The electrode definitely resisted being pulled out. Its distal end was 2.0 cm long, sharply bent as a hook in the tumour. This long length appeared to prevent the hooked end from straightening out during the retraction. Instead, it probably tore a partly injured bronchial artery in the tumour cavity. After this episode the bent part of string-shaped electrodes has been limited to a length of 10 mm. This length permits the string electrode to straighten out rather easily during retraction from a tissue.

In three patients small pieces of a 0.2 mm thick platinum string electrode have broken off, presumably by respiratory movements stressing the material, and then been left behind in the tumour tissue or chest wall. No untoward effects have subsequently developed in any of these patients.

E. DC treatment of lung tumours: discussion and conclusion

Possibilities for treatment of patients with metastatic cancer in the lungs are often very limited (12). In certain cases surgical removal of a solitary metastasis, e.g., hypernephroma, has proven beneficial. When metastases are multiple in a lung or bilateral, surgery is often rejected. Surgery also is commonly rejected in patients with limited cardiopulmonary function or other serious complicating conditions (77).

Radiation therapy is not very effective in most common primary lung cancers, e.g., squamous cell carcinomas, and is generally ineffective for most metastatic tumours (65). A rapid decrease in size of a poorly differentiated tumour after radiation treatment is all too often accompanied by regrowth of the tumour after a short time. Then the tumour is often more insensitive than previously to any attempts at a repeat course of radiation treatment.

Hormonal and cytostatic chemotherapy are occasionally useful. Nonetheless these chemical treatments commonly fail. They also have undesirable side effects.

Other techniques have also previously been introduced in attempts to improve the possibilities of treating lung tumours unsuitable for surgery. For example, the author has tried the following measures: regional perfusion of cytostatic compounds distal to a balloon-occluded pulmonary artery or vein, infusion of cytostatic compounds into intercostal and bronchomediastinal arteries proximal to a balloon-occluded thoracic aorta, selective perfusion of a catheterized bronchial artery, direct injection of cytostatic compounds into the bronchus leading to the region of a tumour and also direct transthoracic injection of such compounds into tumourous tissue after local electrocoagulation of the centre of the tumour (39, 40). Other clinical attempts have been made to improve the effect of radiotherapy by increasing the oxygen content of the tumour tissue (46, 68).

Diathermy is intended to destroy tissue by the generation of heat. This technique can be used with "dry" electrodes in the lung only for treatment of relatively small tumours (less than 1 cm diameter). Regional cooling of tissue by circulating blood and ventilation of lung may interfere with the transmission of heat. The use of liquid-perfused electrodes, as has been shown in this study, improves the possibilities for heat production and heat transmission. Wet electrodes permit coagulation of somewhat larger tumours than do dry electrodes. Electrocoagulation by liquid-perfused electrodes can be made rapidly and relatively simply with tumours less than one cm in diameter. Only occasionally can larger tumours be treated successfully with this technique (Fig. XVII: 5).

The use of direct current for treating tumours offers different and, in some respects, improved possibilities. Therapeutic effects are then induced by anodic liberation of protons as well as by electrophoretic and electroosmotic events, which change the microenvironment of the tissues. Cells and tissues in the electric field thereby undergo a variety of reactions. The electrolytic production of H_2, O_2 and Cl_2 also produce mechanical effects by compression of tissue, an effect more pronounced around the cathode than around the anode.

The ionization of water, which has a high dielectic constant, indicates that the range of compounds which undergo molecular splitting is wide. Biologic molecules with strong internal bonds will require higher electrode voltage than molecules with weak internal bonds, which indicates that the magnitude of applied electrode voltage produces qualitative differences in electrolysis of tissue.

At relatively low voltages, e.g., below 10 volts, ionization effects and transport phenomena are comparably prominent while heat production is comparatively negligible. Nevertheless, coagulation still takes place due to electrochemical precipitation of protein, an effect which also occurs at high voltages. Coagulation appears around the anode as a central grey-white and a surrounding black, dry region. The black anodic zone has the general appearance of dry gangrene and is produced by diffusion and migration of protons. The central grey-white zone is caused by chlorine bleaching the tissue.

Over biologically closed electric circuits (BCEC), several biological effects are encountered. Extensive thrombosis, for instance, is induced as far as several cm out into the tissues surrounding a spontaneously polarizing tumour. Such extensive thrombotic changes are also induced when a tumour undergoes treatment. These changes narrowing the lumens of vessels surrounding a tumour will obviously restrict its blood supply.

An instructive example is the DC-treated patient no. 4, in whom one metastatic tumour, as large as a cherry, disappeared after a dose of 100 coulombs. A second tumour of the same size six weeks later received 180 coulombs under otherwise comparable conditions of treatment. This tumour decreased only slightly in size during the 15 months that followed. Similar results were obtained in patient no. 2. At first glance, these findings do not seem logical, but may be explained in the following way:

If a dose of current is just sufficient to devitalize a tumour, including a "minimum" of capillary thromboses at its periphery, then the resorption of destroyed material from the tumour should proceed relatively rapidly, possibly after a recapillarization of the tissue surrounding the tumour. On delivery of an "overdose" of current, the destructive effects on the capillaries and other components of the tissues around the tumour may become too extensive to allow sufficient recapillarization for ready resorption of devitalized tissue. *A sequestration effect* can then be expected to ensue: a ball of dehydrated, decomposed tumour tissue is formed, which probably best can be regarded as a focus of dry gangrene.

The extensive dystrophic changes in lung tissue around granulomas are a possibly related phenomenon. For example, radiographs of the tuberculous granuloma in Fig. IV: 1 show surrounding dystrophy, which may be explained as a result of intense, spontaneous, focal, electrochemical polarization caused by the tuberculous agent.

The amount of electric energy which is delivered to tissue from an external electric power source is determined by integrating momentary densities of current flow and the duration of the treatment. Considerable ionization and electric transports may therefore ensue

spontaneously, at low densities of current flow over long tissue periods. The size and shape of the electric field will be determined by the sizes, shapes and positions of the electrodes and the conductivity properties of the tissues.

An obvious advantage in DC treatment is placement of the anode in the tumour. Tumour cells are known to possess an excess of fixed electronegative charges on their surfaces. These charges will therefore be attracted inward toward the anode, which is a compelling reason for placing only the electropositive electrode in the tumour.

Another specific effect in DC treatment of tumours is the selective attraction of leukocytes to the region of the anode and the accumulation of leukocytes in vessels which direct the flow of blood toward the cathode. This effect appears probably beneficial for the healing of tumours.

A potentially far-reaching possibility is the concept of delivering via the blood stream an electronegatively charged cytostatic compound during DC treatment. In this way an increased amount of the cytostatic agent might be accumulated in the tumour and in its surrounding tissue, at the same time as undesired general effects could be diminished.

In spite of many differences, both radiation treatment and DC treatment ionize tissue, which may justify some comparisons.

Ionization of tissue in DC treatment is induced from the inside of a tumour. It is therefore far more selective than tissue ionization by external radiation. DC treatment should therefore make it possible to keep the total ionizing dose relatively low. Moreover, in radiation therapy the ionization is "mixed", i.e., nonselective, while DC treatment selectively produces anions and cations and transports them in the electric field. The photon energy in radiation therapy must be high enough to allow removal of electrons from their orbits for a sufficiently long time to prevent them from falling back into their orbits. DC and external radiation treatments might therefore be advantageously combined in the future, leading to a mutual and specific enhancement of the beneficial effects of each.

The observation time of the DC treatments of the cancers here reported is still relatively short, i.e., a few years. Final judgment of the long-term results must necessarily wait. *Preliminary conclusions about the treatments* nevertheless can be made.

1) *DC treatment appears to be a promising method for local therapy of cancer. Beneficial effects have already been obtained with a preliminary technique in 12 of 26 tumours in 20 patients*. The technique is still far from optimized. It depends on many technical and biological variables.

2) The results reported in 1978 of the treatments of 5 patients are still valid (41). It is possible to perform successful DC treatment of metastatic cancers in lungs of patients who have been rejected for surgery, radiotherapy or chemotherapy because of poor general condition, cardiorespiratory insufficiency, diabetes mellitus, multiple locations of pulmonary metastases or failing response to chemotherapy.

3) The treatments are performed under local anaesthesia and are only slightly uncomfortable for the patient. Usually only one treatment is necessary per tumour. Regression then takes place over several months or years. Despite the usually poor condition of the 20 patients, no deaths have occurred as a complication of treatment. One patient, however, had serious haemoptysis and recovered from cardiac arrest; the technique of the procedure was then appropriately revised so that this complication now seems highly unlikely in future treatments.

4) The mode of action of DC treatment of malignant tumours is multifold. Large parts of a tumour, or preferably most of it, should be destroyed by protons liberated from the anodic tumour electrode during the treatment. Because malignant tumour cells possess electronegative surplus charge, they will be attracted to the anodic electrode during treatment, a consideration which should diminish risks of tumour spread. The applied electric field seems selectively to affect neoplastic cells more than normal cells. Clear regression of metastatic pulmonary tumours has been observed radiologically without evidence of corresponding injuries to the surrounding normal tissue. Besides primary destruction of tumour tissue, the electric field induces ionic transports, dehydration around the anode and peritumoural microthromboses. Leukocytes are accumulated around the tumour. These effects, produced by an external power source over tissue electrodes, represent a driven electric system. At the conclusion of the treatment the primary injured tissue will release catabolic energy, which activates BCEC channels as in any healing process. The amount of energy should then be of sufficient magnitude to complete the healing process. For further information on the associated complicated events the reader is referred to preceding chapters of this book.

5) At the present stage of development of the treatment technique, treatment should be limited to tumours peripherally situated in the lung and preferably less than 3 cm in diameter. Further, it seems possible that certain types of cancers might be more suitable for DC treatment than others, as is the case in radiotherapy.

6) Costs of the procedure in terms of material, equipment and duration of hospitalization are low. Much of the expensive equipment and trained personnel are already available in departments of diagnostic radiology. The electrodes and the D.C. Treatment Processor will be available at reasonable cost.

7) This new form of antineoplastic therapy has been performed as a partial simulation and practical consequence of the described mechanism of spontaneous healing outlined in preceding chapters of this book. Our knowledge is still fragmentary concerning the necessary amounts of energy, most suitable electrode potentials and current densities for controlling cancers of different sizes, types and locations. Indiscriminate use of the principle of the outlined healing mechanism may possibly lead to undesirable effects (see Chapter XVI, Section O, P, Q and Chapter XVIII, Section E). Further modifications of the technique may improve its considerable promise as a simple, inexpensive and relatively harmless mode of effective antineoplastic therapy.

References

1. Abramson, H. A., Moyer, L. S., and Gorin, M. H.: Electrophoresis of proteins and the chemistry of cell surfaces. New York, Reinhold Publ. Co., 1942.
2. Anand, B. K., Dua, S., and Schoenberg, K.: Hypothalamic control of food intake in cats and monkeys. J. Physiol. 127: 143, 1955.
3. Andrews, T., and Friedenberg, Z. B.: In vivo bone reactions to varying direct currents. J. Bone Surg. 52A: 600, 1970.
4. Bangham, A. D., Glover, J. C., Hollingshead, S., and Pethica, B. A.: The surface properties of some neoplastic cells. Biochem. J. 84: 513, 1962.
5. Bassett, C. A. L., Pawlick, R. J., and Becker, R. O.: Effects of electrical currents on bone in vivo. Nature 204: 652, 1964.
6. Becker, R. O.: The current status of electrically stimulated bone growth. Onc. J. 2: 35, 1975.
7. Bellamy, D., Hinsall, S., Watson, B., and Blanche, L. A.: Inhibition of the development of Walker 256 carcinoma with a simple metal-plastic implant. Europ. J. Cancer 15: 223, 1979.
8. Berven, E.: Personal communication, 1945.
9. Bolmgren, J., Jacobson, B., and Nordenström, B.: Stereotaxic instrument for needle biopsy of the mamma. Am. J. Roentgenol. 129: 121, 1977.
10. Brighton, C. T., Black, J., and Pollack, S. R.: Electrical properties of bone and cartilage. New York, Grune and Stratton, 1979.
11. Brochet, J.: Cytoplasmic and nuclear structure in relation to metabolic activities. In: Ionizing radiations and cell metabolism. Proc. Ciba Symp. London, Churchill, 1956, p. 3.
12. Cappelen, C., Jr., Efskind, L., and Poppe, E.: Bronchial carcinoma with special regard to the prognosis. Acta path. microbiol. Scand. 51, Suppl. 148: 23, 1961.
13. Carpenter, M. B., Whittier, J. R., and Mettler, F. A.: Analysis of choreoid hyperkinesia in the rhesus monkey. J. Comp. Neurol. 92: 293, 1950.
14. O'Connor, B. T., Currey, J. D., Charlton, H. M., Kirkley, D. R. S., and Woods, C.: Effects of electrical currents on bone in vivo. Nature 222: 162, 1969.
15. Dale, W. M.: Effect of x-rays on aqueous solutions of biologically active compounds. Advanc. Enzymol. 24: 359, 1962.
16. Dunphy, J. E.: Some observations on the natural behavior of cancer in man. New Engl. J. Med. 242: 167, 1950.
17. Errera, M.: The probable role of the cytoplasm in radiobiology. Adv. biol. med. Phys. 12: 333, 1968.
18. Everson, T. C.: Spontaneous regression of cancer. Connecticut Med. 22: 657, 1958.
19. Everson, T. C., and Cole, W. H.: Spontaneous regression of cancer: preliminary report. Ann. Surg. 144: 366, 1956.
20. First World Conference: Spontaneous cancer regression. Medical World News 13: June, 1974.
21. Friedenberg, Z. B., and Brighton, C. T.: Bioelectric potentials in bone. J. Bone Joint Surg. 48A: 915, 1966.
22. Fukada, E., Takamatsu, T., and Yasuda, I.: Callus formation by electret. Japan J. Appl. Physiol. 14: 12, 1975.
23. Gardner, B., Sterling, A., and Brown, J.: Effect of implanted electrodes on tumour metastases in the rat liver. Surgery 62: 361, 1967.
24. Golsinger: Cit. by Horsley, V., and Clarke, R. H.: The structure and functions of the cerebellum examined by a new method. Brain 31: 87, 1908.
25. Göhre, E.: Der zeitliche Ablauf der endostalen Knochenbildung in der Kaninchentibia, hervorgerufen durch Gleichstrom. Dissert., Orthopaed. Klin. d. Freien Univ. Berlin im Oskar-Helene-Heim, 1972.
26. Hagmar, B.: Cell surface charge and metastasis formation. A study on the effect of dextrans and heparin on tumour cells and experimental metastases in a synergeneic murine system. Acta path. microbiol. Scand. (A) 80: 357, 1972.
27. Hagmar, B.: Influence of cell surface changes on the distribution of metastases from intravenously transfused tumour cells. In: Garattini, S., and Franchi, G. (eds.): Chemotherapy of cancer dissimination and metastasis. New York, Raven Press, 1973.
28. Harguindey, S., and Gillis, M.: Experimental and human cancer, pH and spontaneous regressions. Intern. Lab. Nov/Dec: 57, 1979.
29. Hendley, C. D., and Hodes, R.: Effects of lesions on subcortically evoked movement in cat. J. Neurophysiol. 16: 587, 1953.
30. Hetherington, A. W., and Ranson, S. W.: Hypothalamic lesions and adiposity in the rat. Anat. Record. 78: 149, 1940.
31. Horsley, V., and Clarke, R. H.: The structure and functions of the cerebellum examined by a new method. Brain 31: 45, 1908.
32. Iida, H.: Study on dynamic and electric calluses of bone. J. Jap. Orthop. Surg. Soc. 31: 645, 1957.
33. Ingvar, S.: Reaction of cells to the galvanic current in tissue cultures. Proc. Soc. Exper. Biol. Med. 17: 198, 1920.
34. Kaplan, H. S.: DNA-strand scission and loss of viability after x-irradiation of normal and sensitized bacterial cells. Proc. Nat. Acad. Sci. (Wash.) 55: 1442, 1966.
35. Krieg, W. J. S.: Accurate placement of minute lesions in the brains of albino rats. Quart. Bull. Northwest. Univ. Med. Sc. 20: 199, 1946.
36. Lemberg, R., and Legge, M.: Hematin compounds and bile pigments. New York, Interscience Publ. Inc., 1949, p. 166.
37. Liboff, A. R., and Rinaldi, R. A.: (eds.): Conference on electrically mediated growth mechanism in living systems. Ann. N. Y. Acad. Sci. 238, 1974.
38. Loucks, R. B., Weinberg, H., and Smith, M.: The erosion of electrodes by small currents. EEG Clin. Neurophysiol. 11: 823, 1959.
39. Nordenström, B.: Therapeutic roentgenology. Acta Radiol. Diagn. 3: 115, 1965.
40. Nordenström, B.: Electrocoagulation of small lung tumours. In: Potchen, E. J. (ed.): Current concepts in radiology. St. Louis, Mosby, 3: 331, 1977.
41. Nordenström, B.: Preliminary clinical trials of electrophoretic ionization in the treatment of malignant tumors. IRCS Med. Sc. 6: 537, 1978.
42. Nordenström, B., and Holmström, L.: Versatile single and biplane systems for radiologic procedures. In: Anacker, A., Gullotta, U., and Rupp, N. (eds.): Percutaneous biopsy and therapeutic vascular occlusion. Stuttgart, Thieme, 1980, p. 90.
43. Nordenström, B., Svane, G., and Rydén, H.: Breast. In: Zornoza, J. (ed.): Percutaneous needle biopsy. Baltimore/London, Williams and Wilkins, 1980, p. 43.
44. Nordenström, B.: Transthoracic needle biopsy. In: Anacker, H., Gullotta, U., and Rupp, N. (eds.): Percutaneous biopsy and therapeutic vascular occlusion. Stuttgart, Thieme, 1980, p. 11.
45. Nordenström, B.: Mediastinum. In: Zornoza, J. (ed.): Percutaneous needle biopsy. Baltimore/London, Williams and Wilkins, 1980, p. 78.
46. Notter, G., Nordenström, B., Norhagen, Å., and Jakobsson, P. Å.: Kurzzeitfraktionierung bei Bestrahlung von Lungenkarzi-

nomen mit Kobalt 60 bei simultaner Sauerstoffatmung und temporärer Blockierung der Arteria Pulmonalis. Acta Radiol. Ther. Phys. Biol. 4: 494, 1966.
47. Overgaard, J., and Poulsen, H. S.: Effects of hyperthermia and environmental acidity on proteolytic activity in murine ascites tumor cells. J. Natl. Ca. Inst. 58: 1159, 1977.
48. Phillips, J. F.: Transcatheter electrocoagulation of blood vessels. Invest. Radiol. 8: 295, 1973.
49. Quastler, H.: Physiological importance of radiation effects on DNA synthesis. In: Haissinsky, M. (ed.): Chimiques et biologues des radiations. Paris, Masson et Cie, 1963, p. 184.
50. Reis, A.: Die anodische Oxydation als Inaktivator pathogener Substanzen und Prozesse. Klin. Wochenschrift 27/28: 484, 1951.
51. Reis, A., and Henninger, T.: Zerstörung maligner Wachstumsenergie durch anodische Oxydation. Klin. Wochenschrift 1/2: 39, 1951.
52. Rossi-Fanelli, A., Cavaliere, R., Mondovi, B., and Moricca, G.: Selective heat sensitivity of cancer cells. Berlin, Springer, 1977.
53. Samuelsson, L.: Electrolytic destruction of tissue. Dissertation, University of Lund, Sweden, 1980.
54. Samuelsson, L., and Jönsson, L.: Electrolytic destruction of tissue in the normal lung of the pig. Acta Radiol. Diagn. 22: 9, 1981.
55. Samuelsson, L., and Jönsson, L.: Electrolytic destruction of lung tissue. Electrochemical aspects. Acta Radiol. Diagn. 21: 711, 1980.
56. Samuelsson, L., and Olin, T.: Elektrolytisk destruktion av lungvävnad. Hygiea 86: 345, 1977.
57. Samuelsson, L., and Berg, N.: Electrolytic destruction of lung tissue in the rabbit. Acta Radiol. Diagn. 21: 447, 1980.
58. Sawyer, P. N., and Pate, J. W.: Bio-electric phenomena as an etiologic factor in intravascular thrombosis. Am. J. Physiol. 175: 703, 1953.
59. Schanble, M. K., Mutaz, H. B., and Gallick, H. D.: Inhibition of experimental tumor growth in hamsters by small direct currents. Arch. Pathol. Lab. Med. 101: 294, 1977.
60. Sellier, J., and Verger, H.: Recherches expérimentales sur la physiologie de la couche optique. Arch. Physiol. (Paris) 10: 706, 1898.
61. Sellier, J., and Verger, H.: Étude expérimentale des fonctions de la couche optique. Compt. Rend. Soc. Biol. 55: 485, 1903.
62. Shimkin, M. B.: The extent of cancer illness in the United States. Public Health Service, Publ. No. 547, U.S. Government Printing Office, 1958.
63. Smith, J., and Steklin, J. S.: Spontaneous regression of primary malignant melanomas with regional metastases. Cancer 18: 1399, 1965.
64. Smithers, D. W.: Cancer of the breast and menopause. J. Fac. Radiol. 4: 89, 1952.
65. Souders, C. R., and Smedal, M. I.: The selection of the patient with bronchogenic carcinoma for x-ray therapy. Surg. Clin. North Amer. 41: 761, 1961.
66. Srinivasan, S., Cahen, G. L., Jr., and Stoner, G. E.: Electrochemistry in the biomedical sciences. In: Bloom, H., and Gutmann, F. (eds.): Electrochemistry the last thirty and the next thirty years. New York, Plenum Press, 1977, p. 57.
67. Stewart, F. W.: Experiences in spontaneous regression of neoplastic disease in man. Texas Rep. Biol. and Med. 10: 239, 1952.
68. Tableman, W. T., and Cole, A.: Repair of sublethal and oxygen enhancement ratio for low-voltage electron beam irradiation. Radiation Res. 60: 355, 1974.
69. Tafel, J.: In: Bockris, J. O'M., and Dražić, D. M. (eds.): Electro-chemical science. London, Taylor and Francis Ltd., 1972, p. 5.
70. Vassar, P. S.: Electrophoretic mobility of human tumour cells. Nature 197: 1215, 1963.
71. Ward, J. F.: Molecular mechanisms of radiation-induced damage to nucleic acid. In: Lett, J. F., and Adler, H. (eds.): Advances in radiation biology. Academic Press 5: 181, 1975.
72. Whalen, R. E., Starmer, C. F., and McIntosh, H. D.: Electrical hazards associated with cardiac pacemaking. Ann. N. Y. Acad. Sci. 111: 922, 1964.
73. Weigert, M.: Die Förderung der Osteogenese durch inductiven Wechselstrom. Z. Orthop. 107: 362, 1970.
74. Weigert, M., and Müller, J.: Die Beeinflussung der Knochenbruchheilung durch Gleich- und Wechselstrom. Tagung Dt. Ges. Orthop. Traum., Kiel, 1970.
75. Weiss, L., and Zeigel, R.: Cell surface negativity and the binding of positively charged particles. J. Cell Physiol. 77: 1979, 1971.
76. Westermark, N.: The effect of heat upon rat-tumors. Skandinav. Archiv für Physiologie 52–53: 257, 1927/1928.
77. Wiklund, T.: Bronchogenic carcinoma. Doctoral Thesis, Stockholm. Acta Chir. Scand. Suppl. 162, 1961.
78. Yasuda, I.: On the piezoelectric activity on bone. J. Jap. Orthop. Soc. 28: 267, 1954.
79. Yasuda, I.: Electrical callus and callus formation by electret. Clin. Orthop. and Related Res. 124: 53, 1977.
80. Yasuda, I., Noguchi, K., and Satu, T.: Dynamic callus and electric callus. J. Bone Joint Surg. 37A: 1292, 1955.
81. Yoneda, S., Matsuda, M., Shimizu, Y., Goto, H., and Handa, H.: Electrothrombosis of arteriovenous malformations. Neurol. Med. Chir. (Tokyo) 17: 19, 1977.

XVIII.
Afterword: a discussion of principles and consequences of biologically closed electric circuits (BCEC)

A. Structural and functional coordination in biology

Structural organization has long been recognized as a dominating characteristic of biological systems. Many attempts have been made to identify factors which determine structural development. Such attempts have led to theoretical concepts of an extrabiological guiding principle, an "entelechey" according to Driesch (26), the "embryonic field" of Spemann (89) and the "biological field" of Weiss (97). More specific functions have been introduced by Ingvar (43), Lund (54) and Gurwitsch (40) in terms of bioelectric phenomena. For instance, Ingvar showed that external electric fields are capable of orienting growing structures in vitro. This result led Burr and Northrop (19) to formulate an "electrodynamic theory of life" based on interdependence between biologic particles. These correlations, they suggest, depend on interactions between particles and fields at the atomic level. According to this theory, "the pattern or organization of any biological system is established by a complex electrodynamic field, which is in part determined by its atomic physicochemical components and which in part determines the behaviour and orientation of those components". In this theory the characteristic relationships of the elements of any biological system are a function of the field of the system. This theory is built on the basic principles of molecular forces, which evidently must be involved in the structural arrangements of nonorganic as well as organic components. The present work can be regarded as an extension of such a theory. In fact, a combination of superimposed forces over "large" distances and the action of "local" physicochemical forces can be described in terms of biologically closed electric systems.

B. BCEC systems and their physicochemical activation

Nearly the entire content of this book serves one main purpose: to focus attention on the existence and function of an important biological principle, *the biologically closed electric circuit*. To accept this concept will require reviewing actual data in order to overcome an abundance of possible objections. The consequences of the concept appear manifold and useful. They therefore merit some closing considerations.

A simplified expression of the principle follows from the enormous importance of closed electric circuits in modern electronic technology. Is it seriously plausible that biology can "afford to ignore" the exceedingly efficient principle of transporting electric energy over closed circuits? A "yes" to this question means that we continue an unchanged view of biochemical reactions. A "no" means that we must revise extensively our present concepts of conversion of energy in biochemical reactions. The question we have formulated is simple but the answer is difficult and exceedingly important. In the author's opinion, biologically closed electric circuits do exist. Among these circuits, vascular-interstitial closed electric circuits (VICC) represent energy pathways available in all vascularized tissues. The vascular system thereby includes a new essential function. This function is for vessels to serve as electrically conducting "cables" which are capable of connecting different regions of tissue over conducting interstitial fluid.

Arguments will be presented in this discussion that closed circuits other than VICC must also exist. Parts of such closed circuits may consist of different combinations of VICC branches, incretory and excretory ducts of glands and different conducting media. These media may include secretions and collections of electrically conducting fluids, e.g., peritoneal, pleural and cerebrospinal fluid. This prediction is possible as long as at least one insulated and conducting branch, i.e., the vascular branch, is available. It should not be surprising, moreover, if walls of tissues, e.g., glandular ducts, also possess their own relatively insulating properties around their conducting media. The function of BCEC systems also depends closely on the mechanisms of their activation and on the modulating influence the conversion of energy exerts on all biochemical reactions in closed circuits.

This book represents only a slight scratch on a mountain of fascinating problems and possibilities. It should be evident that the future will require a broad multidisciplinary approach to disclose the abundance of morphologic and functional consequences of BCEC systems in health and disease. It is the hope of the author that the efforts presented in this book may serve to attract specialists in different fields to perform extended studies of the many problems and possibilities which the concept offers.

The reader will have found a collection of morphological (radiologic) observations of pulmonary pathology in Chapters II–V. These observations represent important primary data on the existence of BCEC effects. The observed transformations of tissue can not be explained in a conventional way. These observations gave the impetus to the present research. The author's background in diagnostic radiology has in many parts of the work been of advantage. Structural analysis in vivo and in vitro without instrumental interference has been used as a starting point for later experimental studies in vivo and in vitro. Knowledge of this radiologic material is therefore important for explaining and understanding the biokinetic mechanisms described. Structures of the lung have been described and illustrated with indications of the wide range of their appearances. The structures are all components of what are here named the *corona structures*, as their appearance resembles the corona of the sun. Similar structural changes were also looked for in an extrathoracic organ. They were identified around carcinomas of the breast, demonstrating that corona structures are not specific for a particular organ. Prerequisites for their radiographic demonstration have also been described and discussed in Chapter V. The discussion will therefore now continue with emphasis on the underlying biologic principle.

Consider a release of energy for driving reactions over a BCEC. Development of a fluctuating physicochemical potential is a useful concept. Biologic structures are regarded too often as static results of a process of poorly understood development. In reality, all biologic material undergoes continuous modification in an overall recirculating process. Ionic activities are central events in every part of this circle.

Conventional expression of the electrochemical potential of an ionic species is here called *physicochemical potential*. It is a summation of four forces: chemical, volume-pressure, electrical and gravitational. This convention, in the author's view, is insufficient to describe the important interdependence among these four factors. This limitation may be overcome partly by graphical presentation of the physicochemical potential (Fig. XIII: 2). All four participating factors are then seen to depend directly on each other. The magnitude of each factor is also individually variable.

A collection of ions is named an ionar. The introduction of the concept of ergon, i.e., a nonionic energetic compound, is of equal importance for understanding the function of BCEC systems. This importance is particularly apparent when ions and ergons appear in collections, termed ergionars. The ionar-ergonar ratio and concentrations in a closed circuit can be expected to influence its conductivity. The different modes of electric admittance of ions and ergons are of particular importance. The directly available electric energy of ions allows them to react immediately over their electric factor and to migrate in an activated closed circuit. Selective ionic transports are thereby possible and can, moreover, modulate different "local" electrochemical reactions in the circuit. Ergons, on the other hand, carry a balanced charge, which must be activated before it can react over its electric factor. Ergons are consequently unable to migrate in a closed electric circuit, unless they are influenced by a

matrix capable of supporting closed-circuit transport. Such an ergonic transport mechanism can be recognized in electroosmosis (Chapter IX). This mechanism is here also suggested to explain vesicular transports as recognized in, e.g., pinocytosis (Chapter XII). Ergonic transport depends mainly on mechanical and diffusion forces. A kind of selective distribution can nevertheless also be recognized for ergons. Thus, oxygen (an ergon) "saves" its energy in the carrier haemoglobin molecule. Oxygen then is favourably and selectively stored in the myoglobin molecule until local conditions of the muscles permit the activation of the oxygen to ready it for redox reactions. This formulation of the behaviour of an ergon is simply a way to adapt the known relations between oxygen, haemoglobin and myoglobin (45) to the concept of ergonar in BCEC systems.

The electromotive forces driving BCEC systems depend on mixed redox and diffusion potentials. In the experimental models illustrating these assumptions, water and a supporting electrolyte (KCl) were shown as a driven system (electrolysis) and after electrolysis as a self-driving system within a matrix (page 169). Thus, redox reactions of an ergonar (water) begin with the creation of two ionars ($n \cdot OH^-$, $n \cdot H^+$) and two ergonars ($n \cdot H_2$, $n \cdot O_2$). The diffusion potential caused by the ionars may be cancelled by migration of K^+ and Cl^- ions ("local reactions") in the circuit. The ergonars $n \cdot H_2$, $n \cdot O_2$, $n \cdot Cl_2$ remain partly accumulated in the matrix and yet show the capacity to produce a current through the circuit after their activation by metal electrodes. Thus it is possible to illustrate in an experimental model the existence, function and importance of ionars and ergonars in BCEC systems.

The development of diffusion potentials, constituting part of the driving force in BCEC systems, may be modified in many ways in vivo. Diffusion of metabolic reaction products depends on several factors, e.g., ionic concentrations and speeds of mobility. Ionic separation by diffusion, e.g., over charged and uncharged membranes, can further be modified by convection of tissue fluids. These processes can either enhance or level diffusion potentials. Buffering capacity or specific ionic recombinations may further modify these potentials. Pharmacologic induction of functional activity of an organ (e.g., the liver, Fig. VI: 19) was found to induce electrical polarization of the organ (measured as its diffusion potential) vs. its surroundings, here called a physiologic "demand" potential of a BCEC circuit.

Pulmonary malignancies of corresponding size and histologic character sometimes showed an electric polarization but no consistency of polarity or magnitude of electric potential (page 66). This unanticipated finding led to studies which point to tissue injury as mainly responsible for the observed potentials of the lesions. These injury potentials fluctuate and attenuate in relation to surrounding tissue, as was found with spontaneously degrading blood in in vitro experiments (Chapter VII). Once the fact of polarization of tissue is accepted, then attempts to determine "absolute" values of polarization of degrading tumours, without knowing the time-related phase of degradation, are of no or little value. This becomes further evident as local variations of oxygenation of the degrading tissue and the reference tissue should also markedly influence the mixed, total driving potential of the BCEC circuits. Furthermore, BCEC channels can also be expected to contribute (unpredictably) to a continuous levelling of the potential gradients, depending on the variable resistive properties of the circuits. A continuous generation of electric transports over a BCEC might nevertheless lead to considerable transport of material when the driving force is allowed to continue over long time periods, i.e., days, weeks or months. Spontaneously degrading blood under sterile anoxic conditions (Fig. VII: 3) was found to produce in vitro a diffusion potential of about 200 mV. This potential was initially electropositive for some days and associated with acidity. Later on it became electronegative. This continuous fluctuation of polarity, like any spontaneous reaction, will move toward a state of equilibrium. The momentary polarity of a degrading tumour depends on the phase of development of degradation (in relation to the reference tissue) during which the potential is measured.

Early in autolysis, during the electropositive phase of degradation, cells start to die. The rate of cellular death can be presumed to vary according to specific cellular susceptibilities to impaired living conditions. Hydrolytic enzymes, e.g., ribonuclease, phosphatase, cathepsin, etc., are known to be released from lysosomes during autolysis (20, 27). The ensuing reactions drive toward a splitting or decomposition of cells and molecules in energy-liberating, catabolic processes. In the absence of oxygen, protons are liberated as part of the hydrolysis of ATP (Chapter VII). The early formation of a surplus of protons is in turn a special case of liberation of radicals in degrading tissue. In the process of production and dissipation of protons, an initial excess of protons may be regarded as a statistical imbalance in favour of their production.

Enzymatic decomposition of carbohydrates, proteins and fat also is known to produce ionized products. Such spontaneous ionizations of degrading tissue take place over *redox systems* (Chapter XII, XIII). The sequence of ionizations can be anticipated to follow the ionizing energies required for the production of different ions. Ionic recombinations then will be influenced by the ionic physicochemical potentials, mobilities, convection forces and superimposed electrical forces over BCEC channels.

Polarity of a degrading tissue need not change spontaneously only by differences in rates of production and dissipation of different ions. Biologic mechanisms, for example, are known to be capable of driving sequences of reactions, producing in turn large ranges of electric potentials. Such *cascade reactions* (sequential reactions) (46) are well known in the process of spontaneous coagulation of blood. In sum, the present experiments on degrading blood as well as on potentials measured in tumour tissue indicate that a spontaneous injury potential exists and proceeds in a slowly fluctuating and attenuating fashion.

This principle of a spontaneous reaction of two partial functions (E_1 and E_n) producing a resultant function (SE) is illustrated in Fig. XVIII: 1. The normal tissue surrounding an injury also undergoes metabolic fluctuations, representing a physiologic "demand potential". Thus, in Fig. XVIII: 1 the limiting values R+ and R− indicate the range of fluctuating demand potentials of the normal tissues surrounding a local injury.

The fluctuating electrical potential of injured tissue is therefore to be seen as a sum of many changing electric gradients. Furthermore, these gradients will vary between the injured tissue and different parts of the surrounding "reference tissue". Evidently, such circumstances make it difficult to measure definable demand potentials between tissues. Measurements of these varying potentials also depend on size and geometry of the electrodes. Nevertheless, the principle of existence of metabolically changing demand potentials was demonstrated in one organ, the liver (page 63). Their importance as a driving electromotive force of BCEC systems should therefore be evident.

We will now concentrate on the function of BCEC systems in tissue injury and particularly in the redistribution of movable particles around a degrading focus of changing polarity. The transports of material over BCEC channels can be anticipated to follow the fluctuations of the driving forces, even at long distances. These fluctuations should lead to "ebb and flow" sequences of anionic and cationic transports, modified by convection of tissue fluid and characteristics of the tissue matrix, e.g., its "capillarity", density and polarities of fixed charges.

Consider the "simple" example of a local injury, such as a necrotizing process in a tumour (Fig. I: 1). A *physicochemical* potential difference between the injured tissue and the surrounding noninjured tissue is demonstrated by the presence of a fluctuating $\begin{pmatrix} - & + \\ (+) & (-) \end{pmatrix}$ electric potential. The BCEC system, here represented by the vascular-interstitial closed circuit (VICC), contains the conducting blood plasma and interstitial fluid. The insulating properties of the walls of the blood vessels (and also organized components of the tissue matrix) provide relative electrical separation of the circuit from other electrical influences. For the VICC to function as an electrical transport system a minimum of two electrode-equivalent sites, corresponding to two redox interphases, must be found.

The existence of redox reactions in metabolism is well established and needs no discussion. Their locations and distances of electron transport, on the other hand, are appropriate subjects for study (24, 25, 77). For example, wet crystalline haemoglobin has been found to be a conductor of electrons (77). A theory for conduction of electrons in enzyme particles has also been advanced (24). The present studies show that fibrous membranes can easily be produced in tissue

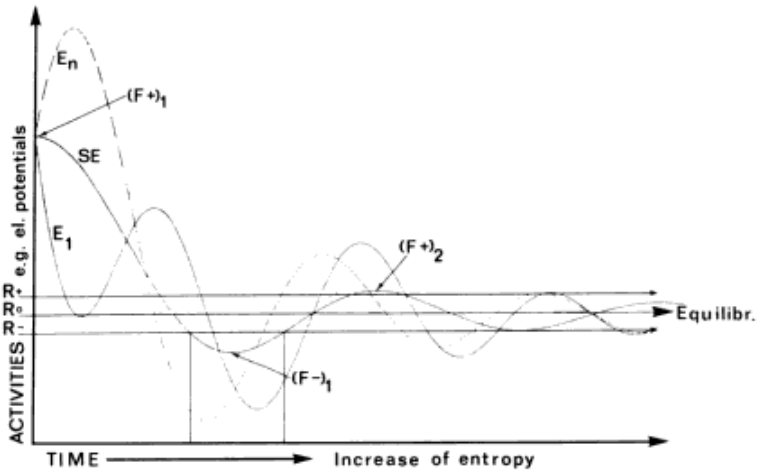

Fig. XVIII: 1. Illustration of fluctuating, attenuating, electric injury potential, comprising a summation of energies (SE) of different ionic collections (ionars, e.g., E_1 and E_n) in relation to the summation of fluctuating physiologic potentials (R+ and R−) of surrounding normal tissue. Entropy of the system increases during healing. $(F+)_1$, $(F-)_1$, $(F+)_2$ represent maxima and minima of fluctuations.

adjacent to platinum electrodes when direct current is led between them. It is therefore possible that fibrous membranes in tissue indicate locations of electrode-equivalent redox steps in closed circuit electric transport in vivo. When current was led in vivo across the surface of a dog liver and spleen (page 133), either electrode-equivalent reactions were produced at the organ surfaces or redox reactions were produced in the vicinity of the organ surface, followed by electrophoretic transport of the reaction products. Whatever the explanation may be, one may here recognize a mechanism, which is capable of explaining development of organ capsules. If future research establishes, as seems possible, a general association between redox reactions and fibrous membranes, then capillary basement membranes should be strongly considered as a product of redox reactions at the nearby endothelial cell membrane.

Further, *a mechanism is described for switching short-distance selective transports to long-distance transports over capillary VICC-channels* (Fig. XII: 30). This mechanism includes field-induced selective contractions of arterial capillaries, apparently leading to regional closure of their endothelial pores. Corresponding venous capillaries are wide permitting, e.g., diapedesis of leukocytes through leaking endothelial pores. In this hypothesis, the capillary basement membrane and the endothelial fibrin film represent products of reactions at the electrode-equivalent sites facing the interstitium and the blood. Intersected reactions and transports in the endothelial cells may be represented in electron micrographs by cytoplasmic vesicles, which might contain ergonic material.

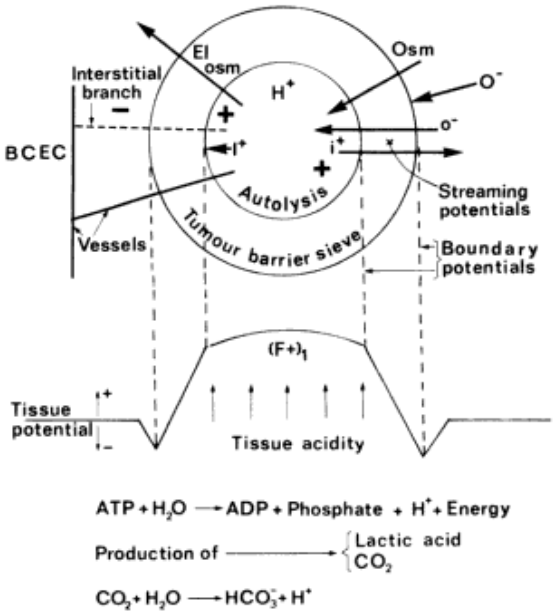

Fig. XVIII: 2. Electropositive, developing polarization (phase $(F+)_1$) of a centrally degrading tumour (lower part). This phase of physicochemical polarization of the tumour is electropositive by enzymatic degradation of cellular material, e.g., by hydrolysis of ATP and glycolysis during hypoxia. Over a BCEC this induces later on (upper part) an electropositive, regressing potential accompanied by electroosmotic outflow (El osm) and osmotic inflow (Osm) of water, net streaming potentials by movement of permeable ions and boundary potentials by deposition of nonpermeable ions at inner and outer surfaces of the tumour barrier. I = inner, nonpermeable ions; O = outer, nonpermeable ions; i = inner, permeable ions; o = outer, permeable ions.

In addition to the experimental studies, indirect evidence pointing to the existence of VICC channels has also been collected in this book. Thus, the structural modifications of tissue in healing of injuries require mechanisms to integrate the various reactions. Direct current applied over tissue can produce elements of tissue healing and all the components of the corona changes which develop spontaneously in lung and breast tissue. Many direct and indirect arguments in this book speak in favour of the existence of BCEC systems. Acceptance of the principle of BCEC systems in tissue leads to the necessity of accepting interpositioned redox steps. We may therefore anticipate that a VICC is constructed roughly as shown in Fig. I: 1, where interpositioned redox steps in tissue healing are suggested to be located in the capillary walls (Fig. XII: 32) and at the interfaces between degrading tissues and thrombotic material on one side and between thrombotic material and blood on the other. These sites should contain the electrode-equivalent functions for closed circuit release of electric energy.

If degrading tissue in the centre of a tumour is connected electrically over a VICC with the surrounding normal tissue, then different boundary phenomena must develop in different parts of the circuit. The peripheral, nonnecrotic part of the tumour will also act as a sieve for closed circuit transport of ions. Ionic transports will be intermittent both to and from the abnormal tissue.

The lower part of Fig. XVIII: 2 represents an electropositive, developing phase $(F+)_1$. This leaves the degrading tumour tissue electropositive in relation to surrounding tissue (upper part), subsequently resulting in selective ionic transport (electropositive, regressing potential), supplementing the one-way mechanical transport of materials in vascular and interstitial channels. A constantly unidirectional gradient of injury potential would be biologically unsuitable, because injured tissue, like any other tissue, needs both anions and cations for its structural development and function. Therefore a series of electropositive and electronegative, developing and regressing, attenuating phases during healing of an injury is a possible (or even necessary) means of adapting the transports to the need for a complete composition of material. Wave-like transformations of energy can be

anticipated as counterreactions after any spontaneous release of biologic energy. As a result, the system should decrease its content of free energy and obtain a higher level of entropy. Evidence also indicates that the main driving force in the healing of injury is delivered by the degrading process itself.

An electronegative, developing phase $(F-)_1$ is illustrated in the lower part of Fig. XVIII: 3. Being the smallest and most mobile ions, protons have been lost more rapidly than anions, e.g., phosphate, which remain behind in the tumour. Combined with differences in the rates of ionic production, the changing concentrations of ions drive the autolyzing tissue in an electronegative direction ($\downarrow\downarrow$) compared to surrounding tissue. In reality, such mechanisms very likely proceed as sequential reactions of several integrated components, similar to the cascade reactions of coagulating blood (Fig. XII: 6). This leaves subsequently the degrading tumour tissue electronegative, regressing in relation to surrounding tissue, resulting in ionic transports as indicated in the upper part of Fig. XVIII: 3. A resulting change of direction of current over a BCEC should then lead to the accumulation of nonpermeable cations at the outer boundary of the tumour barrier and nonpermeable anions at the inner boundary of the tumour barrier.

The presence of VICC will affect ionic transport in the intravascular branches of the circuit as well as in the interstitial branches. A rapid and continuous washout of the arriving ions can be expected in the supplying vessels. Material in the interstitial branches should to some extent be influenced by interstitial convection and lymph flow. It seems likely that material available in the interstitial fluid should be utilized for restructuring in the process of healing.

C. Spontaneous reactions in BCEC systems

1. Healing of injured tissue

The healing of injury is often associated with the development of scar tissue, which may represent a modification of material within a BCEC. At the least, it is easy to produce scar tissue in normal tissue via closed circuit currents between electrodes (Chapter XVI, Sections K, L, M). Fibrosis can regularly be observed around the electrodes of cardiac pacemakers which have been in place for months or years. Fibrotic tissue has electrically insulating properties. When scarring develops around pacemaker electrodes, their function can be seriously disturbed.

2. Production of scar tissue, structural transformation of tissue and cells

Of perhaps greater interest are the *implications of the fibrous tissue produced, even in vitro,* in fat tissue after direct current transforms fat cells and interstitial material (Chapter XVI). The *cathodic type of fibrotic tissue* lacks fibroblasts. The *anodic type* of fibrosis contains many fibroblasts. The anodic fibrous tissue appears as if involved in the development of primitive channels resembling ducts and vessels. Other types of channels are produced in the cathodic field. When produced in vitro *in mammary adipose tissue, the anodic and cathodic types of fibrosis and ductal structures have a striking similarity to the histologic appearance of adenosis, mixed with so-called radial scar tissue* (Chapter XVI,

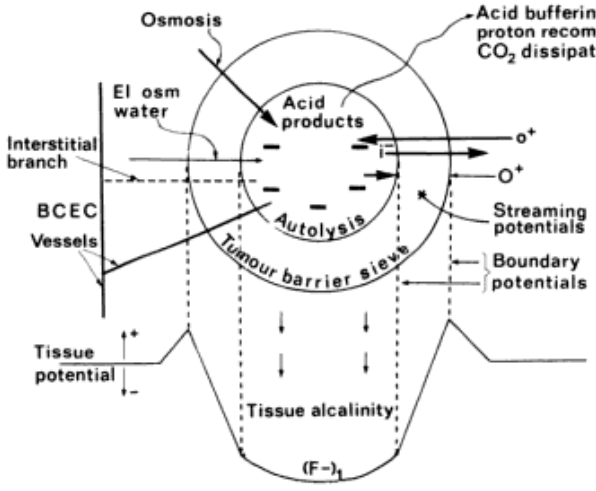

Fig. XVIII: 3. Electronegative, developing polarization (phase $(F-)_1$) of a centrally degrading tumour (lower part). Over a BCEC this induces later on (upper part) an electronegative, regressing potential accompanied by electroosmotic (El osm) and osmotic inflow of water, which becomes balanced by hydrostatic pressure, inflow of permeable cations, outflow of permeable anions, and boundary and streaming potentials. Deposition of nonpermeable ions takes place as a sieve effect at the inner and outer surfaces of the tumour barrier. The change from electropositive (phase $(F+)_1$, see Fig. XVIII: 2) to electronegative (phase $(F-)_1$) polarity is caused by sequential reactions in the degrading tissue coupled to, e.g., differences in ionic mobility, diffusion and migration. *I* = inner, nonpermeable ions; *O* = outer, nonpermeable ions; *i* = inner, permeable ions; *o* = outer, permeable ions.

page 241). Moreover, exposure of normal blood to direct current was found to *transmogrify red blood cells* into monstrous cells and cell complexes (Fig. XIV: 12).

3. Calcifications in tissue

The accumulation of *calcium in injured tissue* is a particularly common and easily recognized manifestation of transport of permeable ions. Deposition of calcium is often seen after traumatic bleeding in skin, muscles, vessels, brain, etc. Calcium is also commonly deposited in tissue after injuries by heat, chemicals and microorganisms.

From the foregoing it may be evident that a tissue injury potential difference is variable and can therefore be characterized as follows: electropositive, developing; electropositive, regressing; electronegative, developing and electronegative, regressing.

Fig. XVIII: 4, lower part, illustrates an electronegative, regressing tissue injury potential profile (dotted line). Permeable cations, such as Ca^{2+} and Mg^{2+}, will then enter the necrotic region, upper part of Fig. XVIII: 4, while permeable anions will leave. The $(F-)_1$ level of potential will become elevated (electronegative regressing phase). Some of the inflowing cations will recombine with available anions, e.g., phosphate. Calcium and magnesium will then eventually precipitate as apatite (*) when the isoelectric levels for these compounds are reached. The events described subsequently drive the reaction of the injured tissue in an electropositive developing phase.

The inflow of calcium over a BCEC leads to the electrical levelling of the previously electronegative region of polarization. In this view, the presence of calcium localized in previously injured tissue should be regarded as the result of a reparative process, rather than as a part of the development of the primary disease. *Calcinosis reparativa* is suggested as an appropriate, pathogenetically descriptive term.

The "profiles" of electric potential shown in Figs. XVIII: 2–4, as well as intermediate stages, have all been encountered in both neoplastic and infectious lung lesions and in breast tumours. These potential profiles were first assumed to depend in some way on the histologic nature of the lesion. It has now become evident that this explanation is unlikely. Instead, the different electric potentials of lesions appear to depend on the development of local degrading processes, which then show fluctuations of their potential in relation to surrounding tissue. This concept of the existence of a fluctuating potential for "pathological" precipitation of calcium (calcinosis reparativa) in tissues was also tested in vitro in experiments to produce *microcalcifications* in adipose tissue (Chapter XVI, Section S, page 259). Unidirectional current produced intracellular matrices which, after reversal of the direction of current, served as targets for precipitation of calcium. The resulting calcified structures histologically appeared the same as microcalcifications in breast tissue.

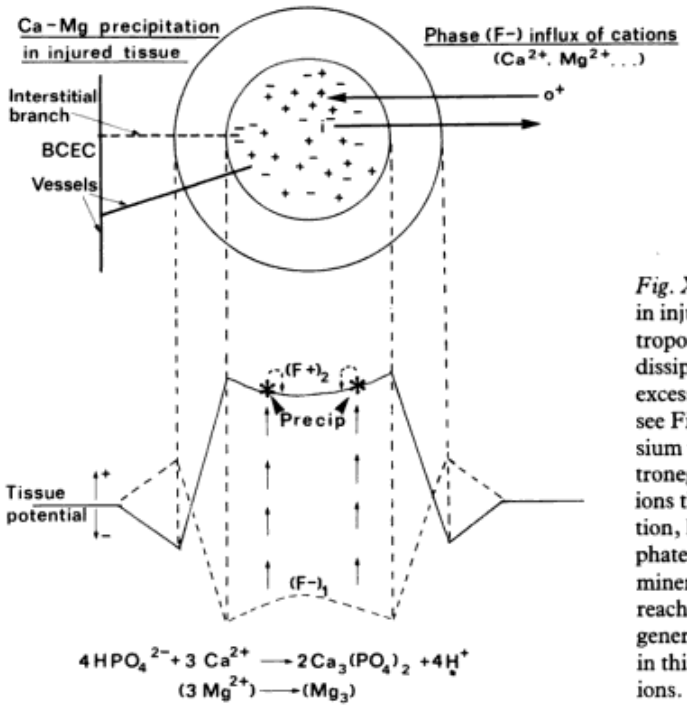

Fig. XVIII: 4. Precipitation of calcium and magnesium salts in injured tissue. The initial phase of degrading tissue is electropositive (phase $(F+)_1$, see Fig. XVIII: 2). After protons dissipate, electronegative ions, e.g., phosphate, remain in excess. The tissue becomes electronegative (phase $(F-)_1$, see Fig. XVIII: 3). Small cations such as calcium and magnesium will migrate over BCEC channels into the necrotic electronegative tissue. Calcium and magnesium and other cations then drive the necrotic tissue in an electropositive direction, leading to phase $(F+)_2$. Calcium-magnesium phosphate and carbonate will precipitate (*) during this phase of mineralization when the appropriate isoelectric levels are reached. It is proposed that apatite, the calcium compound generally found in pathologic tissue calcifications, is created in this way. *i* = inner, permeable ions; *o* = outer, permeable ions.

4. Healing of fractures

The *spontaneous healing of fractures* may proceed by an analogous mechanism. *Initially, callus may be formed during an acid injury phase. Not until the produced matrix turns into an electronegative phase will calcium ions be attracted and precipitate, leading to firm healing of the fracture.* During recent years many attempts have been made to improve healing of fractures by use of electricity (electromagnetic fields, alternating current and direct current) (9, 28, 29, 50, 59, 64, 71, 72, 99). Results have proved rather inconsistent. In the author's opinion, the lack of consistent results derives from a lack of attention to the consideration now apparent, that direct current should be used in simulation of the fluctuating injury potential. In addition, the "extrabiological guiding principle" of applied electrical fields should also in other respects be tailored as closely as possible to existing pathophysiological conditions of spontaneous healing.

5. Electroosmosis

It has become increasingly evident that *electroosmosis* plays an important role in transport of water in tissue. In this mechanism a *BCEC is a prerequisite*, as are narrow interstitial channels lined with fixed charges. Studies of these interstitial channels (Chapter IX, Sections E–H) in normal, freshly excised, dog and human lung tissue, breast fat and mesentery indicated that electroosmotic transport of water proceeds from the electropositive to the electronegative electrode. Observations in vivo in the dog (Chapter XIV, Section L) and also in patients undergoing direct current treatment of tumours in the lung (Chapter XVII) have shown the same direction of displacement of water in tissue between the electrodes. These observations are in complete agreement with the views of Meyer, Weiss and others (57, 98) that probably all cells of vertebrates carry a surplus of fixed negative charges on their surfaces. It is therefore logical that water in intercellular spaces should move from the electropositive to the electronegative part of a BCEC.

Electroosmotic flow of water through a tumour barrier will also be influenced by osmotic and hydrostatic forces. An inward, osmotic flow of water to the degrading tissue will take place due to splitting of molecules in autolysis. Such movements of water will, of course, be modified by hydrostatic pressures as well as by hydrophilic or hydrophobic properties of tissue elements. These factors were therefore particularly studied, leading to descriptions of the biokinetic background of radiographically visible *pleural retraction pockets, lamellae, circular structures, arches and arcades* (Chapter III) in the lung and corresponding structures around breast cancers, including so-called *skin thickening* and *skin retraction* (Chapter XVI).

When a degrading process in a tumour is in an electronegative phase, both osmotic and electroosmotic forces will enhance inflow of water to the electronegative tissue. Such variations of local distribution of water in tissue were studied quantitatively in breast (Chapter XVI, Sections C–F) and experimentally in lung (Chapter IX). See also Chapter XV and Figs. XVIII: 2, 3.

Computerized tomography is an excellent modern tool for studying distribution of water in vivo. Now extensively used in clinical radiologic examinations of the brain, this technique can often disclose *differences of attenuation* between a blood clot, tumour or abscess and the surrounding brain tissue. After some time, e.g., a week or two, the ratio of attenuation between blood clot and surrounding tissue may reverse (13). In the author's opinion, this phenomenon is another example of transport of water (and calcium) over VICC channels.

6. Accumulation of white blood cells

Granulocytes, as well as thrombocytes and erythrocytes, are known to carry a surplus of fixed electronegative charges. These cells should consequently move in a VICC toward anodic tissue. It is therefore logical that granulocytes accumulated extensively around the anode in experiments in which direct current (e.g., 1–2 volts) was applied between one electrode in the tissue and one in a supplying vessel (Fig. XIV: 15). As an injured tissue enters a phase of spontaneous electropositive polarization, the VICC becomes a channelizing mechanism for electrophoretic transport of leukocytes, which accumulate first in small vessels in or near the injured territory and then by diapedesis enter the interstitial tissue. After the polarity of the injured tissue later reverses, leukocytes are already trapped. In vessels, where blood is flowing toward the cathode, granulocytes are selectively retarded and thereby also selectively accumulated. This illustrates how the interaction between mechanical flow and electric field can selectively accumulate charged particles. Experiments on chronically and artificially polarized lung tissue in dogs also revealed that large quantities of lymphocytes accumulate (Chapter XIV, Section I and Chapter XVI, Section U).

This description is an alternative to the so-called chemotactic explanation of accumulation of leukocytes. In fact, no one has been able to define a biokinetic mechanism behind the term chemotaxis. In the view of the author, the many different biologic compounds all said to possess chemotactic properties represent merely agents which polarize tissues. The wide

variation of their chemical constitution is further possible as long as each compound possesses the capability of activating a VICC with energies suitable for electrophoretic migration of leukocytes. Many problems remain to be solved with this new view on accumulation of leukocytes. For example, granulocytes, erythrocytes and thrombocytes all carry different amounts of fixed negative and positive charges in characteristic steric arrangements on their surfaces. Moreover, the mass of each cell, its friction and fluid viscosity, as well as characteristics of the tissue matrix and the strength of the external electric field must be considered.

The massive accumulation of white blood cells that can be obtained around electrodes in in vivo electrophoresis offers possibilities for use in therapy. Modern radiologic techniques permit implantation of electrodes in virtually any organ in a patient. The presumed beneficial effects of granulocytes in various pathologic conditions may be enhanced in this way. A weak current also prevents bacterial growth. It has also been shown (Chapter XIV, Section K) that after intravenous injections a charged compound can accumulate locally around an electrode. The polarity of the compound may, however, be changed during its intravascular passage. Thus, Evans blue dye, which is electronegative, was injected into the aorta of a dog. As current simultaneously passed between mesenteric electrodes, the dye accumulated mainly around the cathode. This finding may indicate that the dye combined after the injection with a compound of surplus electronegative charge. More likely, however, the mechanism of flow and field interaction (described above for leukocytes) caused the accumulation of the dye. Possibilities may exist for electrophoretic accumulation in specific tissues of a wide range of radiopharmaceuticals, cytostatic and antibiotic agents provided with a suitable electric charge.

D. Artificial activation of BCEC systems

Direct current treatment of cancer

The possibility of *treating malignant tumours by means of direct current* merits particular attention. After a careful review of hundreds of cases from the world's medical literature, Everson and Cole (29) came to the conclusion that cancers occasionally do heal spontaneously. The mechanism has seemed obscure but is usually ascribed to spontaneous hormonal or immunologic influences. Theoretically, an additional explanation may now be offered, i.e., the stimulation of BCEC mechanisms sufficiently to heal the tumour in certain fortunate situations. The injury that is the originating stimulus might then include the development of spontaneous necrosis, bleeding or infection inside the tumour. Such degrading processes are common inside a tumour but usually have no obvious effect on continuing growth at the periphery of the tumour. Empyema after thoracotomy for lung cancer, however, has been reported to increase the patient's chances for cure, by mechanisms which have been unclear (79). BCEC mechanisms may explain this association.

If we now assume that in the fortunate patient the degrading process releases sufficient energy to induce the biologic reactions of healing over a VICC system, then the degrading process will indirectly affect the periphery of tumour tissue. The induced changes can then be expected to include altered ionic composition of the tissue fluid, electrophoretic attraction of leukocytes and creation of microthromboses in capillaries. The presence of scar tissue (scirrhous cancers) and microcalcifications, often encountered in association with malignant tumours, may speak in favour of the assumption that such a biologic process of healing over the VICC can take place. Clinical behaviour shows it to be in (almost?) every case insufficient to cause a cancer to heal. Cancer is a progressive disease and develops *progressive injuries*, in contrast to simple injuries such as an incision, which represents a *nonprogressive injury*. Logic should then encourage us to support the tendencies of healing in malignancies, in hopes that healing may become complete. Steps should then be taken to deliver more energy than does the tumour itself to activate the VICC system. The supply of electric energy over implanted electrodes appears to be such a step.

A clinical trial was therefore undertaken by positioning one electrode in the tumour and one in the interstitial or vascular part of the VICC, i.e., about 4–5 cm away from the tumour in the parenchyma or a vessel of the organ. Energy could then be delivered to the tumour in the perspective of strongly activating the biologic healing process. The process also included the creation of an extended local electrochemical injury inside the tumour. These attempts to induce healing by direct current (Chapter XVII) of nonoperable, but relatively small cancers in the lung have shown encouraging results. The technique of treatment can, however, be varied in many ways, so future improvements should be possible.

E. A possible rôle of BCEC in biogenesis, including carcinogenesis

In the author's opinion, endogenous activation of BCEC systems, leading to unidirectional flow of current over long time periods, may lead to modification of cells and tissues. The mechanism involved in cell and tissue modifications demonstrated in Chapters XIV and XVI should function with endogenously generated currents as well as with currents from an external source of power. Strong currents will destroy cells and tissue (Chapter XVII). Weak currents, on the other hand, will more gently create new internal and external environments for cells. The currents will also directly interfere with cellular metabolism and modify structural elements of cells. Damage to structures, e.g., the DNA molecule, is evidently one possible effect of such modifications. Cells subjected to the conditions described can be expected to show variable abilities to survive and to adapt themselves to the new living conditions. Thereby a variety of possibilities should occur for the evolution of normal and pathological populations of cells. A continuous selection of viable, reproducible cells, capable of adapting to environmental factors, which are slowly changing over long time periods, might lead to the development of normal biological tissues. An endogenous activation of BCEC systems in this way should evidently represent an important biogenetic function. The underlying mechanism can, however, also be anticipated to produce a variety of less viable and adaptable cells. Some of these cells may survive, leading to the development of benign or malignant tumours. *In this view the development of neoplastic tissue may depend on the same biologic mechanism as the development of normal tissue.*

A large variety of chemical, physical and biological factors can induce cancer. This capability is not surprising. Many chemicals should have the capability to activate BCEC systems with different magnitudes of energies, either primarily by their own electro-(physico-)chemical potentials or secondarily over a chronic injury polarization. It is therefore possible to understand that *BCEC systems under certain circumstances may function as a common mechanism in carcinogenesis.*

F. Morphogenetic capacity of BCEC systems

Formation of membranes and organ capsules

The *morphogenetic capacity of BCEC systems* should also be discussed briefly with regard to the *development of membranes and organ capsules*. The proposed mechanism anticipates that "fibrotic" material deposits on the surfaces of many organs, e.g., liver and kidney, as a result of their physicochemical polarization in relation to surrounding structures, such as the abdominal wall. In fact, cations and anions may deposit intermittently on their surfaces as a function of normal ionic ebb and flow. *An electric analogue to deposition of material at the surfaces of electrodes* then pertains. The tissues of the intraabdominal organs and the abdominal wall include the function of electrodes, the peritoneal fluid acts as the electrolyte, and the vessels to the organs act as insulated cables connecting the electrodes (Fig. XII: 20). Inside an organ, functional subunits must also polarize against each other. They, too, therefore must possess structural interfaces. For instance, the normal existence of *fasciae* between muscle bundles, *basement membranes* or *fibrous septa* inside an organ in this view may indicate the presence of differences in time of activities or differences of function of adjacent tissues. The apposition of material between two adjoining tissues, e.g., two muscles, should continue until their internal current ceases (during morphogenesis), as is encountered in deposition of polarization products on the surfaces of ordinary electrodes. The fibrous sheaths around the muscles will then serve as electrically insulating media. The insulating capacity of the fibrous sheaths will balance exactly the physiologic demand potentials of the muscles. These considerations are examples of the suggested capability of BCEC systems to contribute to normal structural development.

Further logical consequences can be inferred from acceptance of the principle of BCEC systems.

G. Physiological capacity of BCEC systems

Physiological effects of BCEC systems can be predicted to exist. Thus, any closed electric circuit is not only capable of transporting charges. Various functional effects may take place by release or transformation of energy. Such reactions may occur at sites of change of density of current or as influences by triggering of "local" reactions. With this background it may be appropriate to give an example of the anticipated structure and function of a BCEC which contains ductal conducting branches. In Fig. XVIII: 5 *a* we have positioned two electrodes of metal in rubber bags, which are connected by a vessel containing a valve. One bag is filled with an acid, the other with a base. When the valve is open a current will, of course, flow through the circuit. The bulb may light, representing

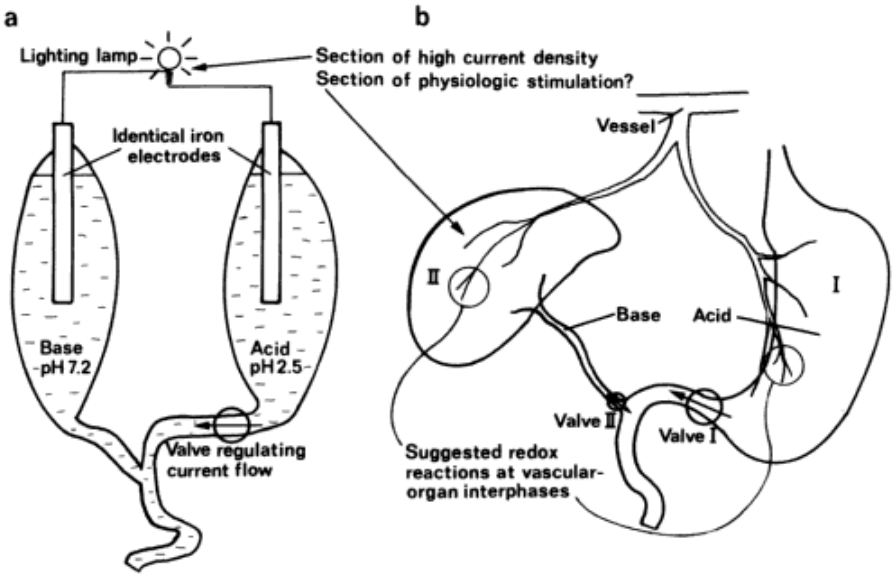

Fig. XVIII: 5. Suggested possible interaction between two organs over Vascular-Ductal Closed Electric Circuits (VDCEC). For explanation, see text.

a section in which the density of current is high. Fig. XVIII: 5 *b* represents a biological analogue of Fig. XVIII: 5 *a*. Two organs are shown, one containing base, the other acid. Valves are also included in the ductal part of the circuit, which is completed by vascular branches to the two organs. When the valves open, ionic transports will be induced in this closed circuit, which may give rise either to undesired or beneficial physiologic effects. Thus, after neurogenic triggering of acid production in organ I, an opening of valves I and II could induce functional activities in organ II over this vascular-ductal closed electric circuit.

H. Acupuncture

The peculiar old Chinese method of *acupuncture* may also relate to the BCEC principle. The author's acquaintance with this method of healing by percutaneous insertions of fine needles is mainly limited to information from periodicals and other literature (48, 59, 90). Recent reports by scientifically trained, western physicians support the idea that acupuncture can not simply be dismissed as psychological hocus-pocus. Beneficial effects are reported in many disorders, including asthma, headache, insomnia, and muscle and joint pains (59). Most dramatic are reports of major surgery, including thoracotomies and laparotomies, performed under anaesthesia by acupuncture. As long as no rational explanation for acupuncture is presented, it is understandable that scientifically trained physicians may be reluctant to use or accept its techniques. The physiological mechanisms involved are probably too complex to be explained in a simple way. The concept presented in this volume that tissues polarize and interconnect via biologically closed electric circuits does, however, offer the possibility of a rational approach toward understanding the mechanism of acupuncture.

Needles introduced under skin can level locally the electric potential of the subcutis. Different parts of this organ in dogs were found to differ in their local quantities of ionic charge (Chapter VI, page 53). Introduced needles were found capable of levelling these differences. However, the levelling by needle was also shown to be reversible as an effect of spontaneous generation of charge. Prolonged levelling of many regions in the subcutis can even markedly reduce subcutaneous potentials to a level at which tissue colloids will then precipitate (75). Such a prolonged and extensive lowering of the electric potential of the subcutis may therefore be dangerous.

The author had the opportunity to attend a demonstration of acupuncture anaesthesia at the International Congress of Cardiology in Tokyo in 1977. Connections like those in the experiments of Chapter VI were used. A grounded external wire connected the introduced needles. One needle was introduced in the skin behind an ear and one in the subcutis of the back of the ipsilateral hand. "Stimulation of the acupuncture points" was then performed through a source of direct current connected with wires to the two needles. The subject reported local sensation of anaesthesia. Apparently separation of ionic charges had been induced between the needles in the electrically interconnecting tissue, which should interfere with its normal function.

Insertion of only one needle is also sometimes used

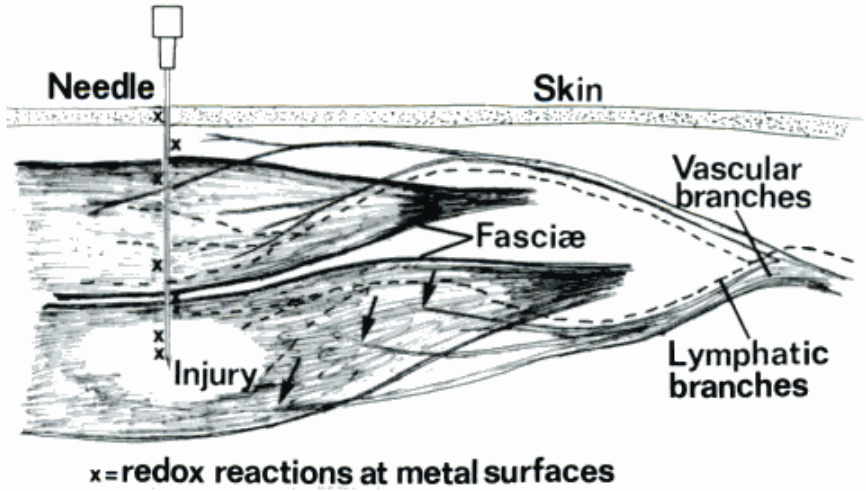

Fig. XVIII: 6. Acupuncture: suggested basic mechanism is illustrated in Figs. XVIII: 6–8.

Two adjoining muscles are separated electrically by their fibrous fasciae. One muscle is injured locally. Secondary effects develop locally around the lesion, e.g., oedema and compression by blood clots (arrows). These effects interfere with the local VICC function of the injured muscle, restricting exchange of materials in the process of healing.

A needle introduced through the skin and normal muscle into the injury will now create new closed circuits, in which the needle connects vascular and interstitial channels in the injured region to corresponding channels in the normal muscle. The new circuits enhance specifically the exchange of ions and transport of water. The driving electromotive forces of the circuits derive from the differences of electric potential between the injured and normal tissues. Redox steps at metal-electrolyte interfaces are indicated by x. The acupuncturist's characteristic twirling of the needle should improve flow of current through the circuits insofar as the twirling movements may loosen any material deposited on the surface of the needle. In case blood vessels are unavailable for BCEC flow, the needle must penetrate normal tissue where interconnecting lymphatic channels are available (possibly equal to an "acupuncture meridian").

An additional way to influence the healing process may be to connect one pole of an electric battery to the needle in the lesion and the other pole to a needle placed in a "meridian" (possibly a lymphatic-interstitial conducting branch) leading to the injured tissue. Closing of this circuit should then correspond to the acupuncturist's "stimulation of the yin and yang of a meridian".

in acupuncture therapy. The principles of BCEC and differences of electric potential in tissues also offer a possible rational explanation for the effects of single needle acupuncture, as follows:

Electrophoretic transports may lead to the development of muscular fasciae by depositing products of polarization on the surfaces of muscle bundles, forming electrically insulating sheaths. Fig. XVIII: 6 shows a locally injured muscle. The injury is healing slowly because available vascular and interstitial channels are functioning inadequately, e.g., by thrombosis, oedema or compression by blood clots. Such interferences apply to diffusion and electrical, matrix-mediated transport of water and other ergons as well as to exchange of ions. The degrading processes of the injury supply the driving force for a VICC, but this energy potential is now inefficient. A metal needle introduced through normal tissues into the injury will create new pathways, more efficient than previously, for exchange of energy and material between the injured and normal tissues. This increased efficiency is possible because the needle connects in parallel all electrically functioning vascular and interstitial branches around the injury. The exchange of material between the injured and surrounding tissues is thereby enhanced.

To facilitate understanding of the proposed explanation of acupuncture, a *self-driving system* (Fig. XVIII: 7 *a–d*) and a *driven system* (Fig. XVIII: 8) will be presented.

In Fig. XVIII: 7 *a*, two metal electrodes (Cu and Zn) are inserted into an electrolyte in two rubber bags (corresponding to the fibrous, electrically insulating fasciae of the muscles in Fig. XVIII: 6). The contents of the bags are connected by a communicating "vessel". Short circuiting of the metals over a cable produces flow of electrons in the metallic part of the circuit and flow of ions in the electrolyte. The potential differences between the metal electrodes and the electrolyte create the driving force.

In Fig. XVIII: 7 *b*, the ionic transports are blocked, as by experimentally clamping the communicating vessels. In Fig. XVIII: 7 *c*, a metal needle is introduced through the two rubber bags, restoring the transport of current in the closed circuit. Redox reactions in this case take place not only at the electrode-electrolyte interfaces but also at the needle-electrolyte interfaces.

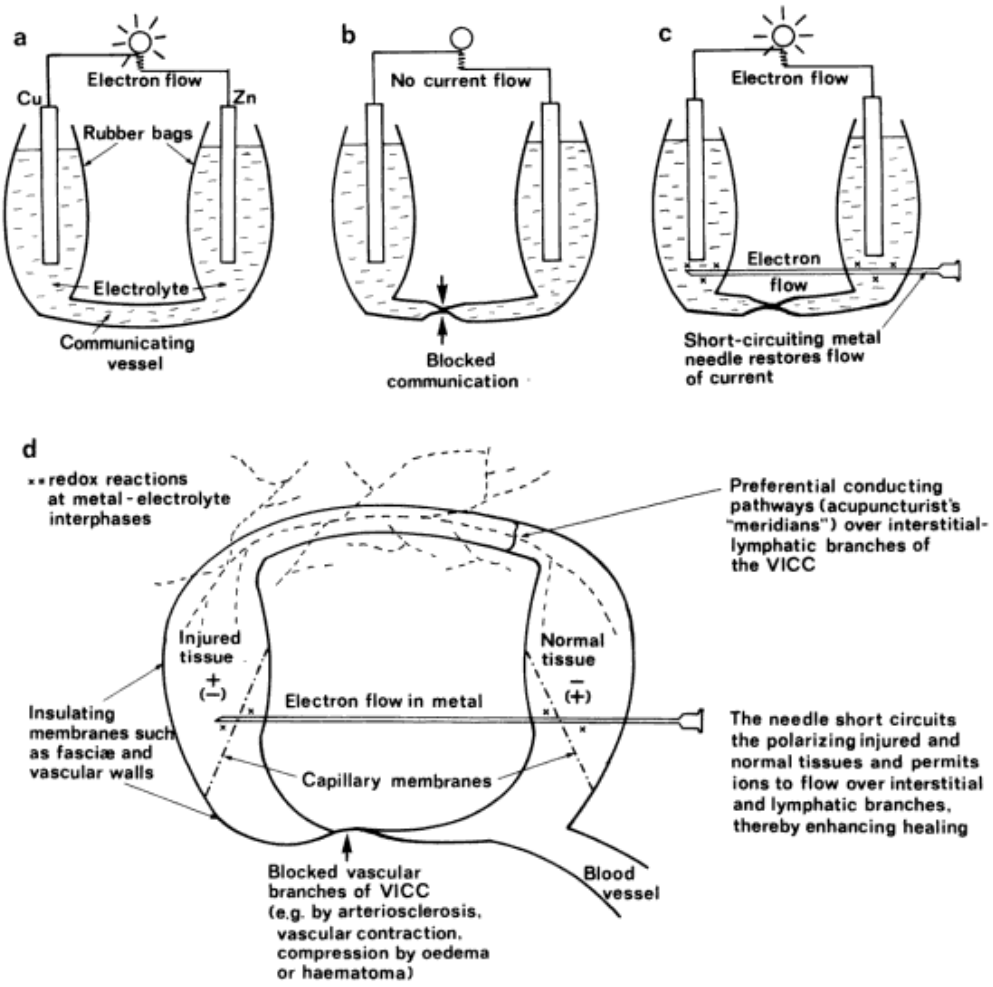

Fig. XVIII:7. Acupuncture: a self-driving electric system, representing the basic principle of the proposed mechanism of acupuncture. (*a*) An analogue of a BCEC system. The energy is delivered by the potential differences across the metal-electrolyte interfaces and is channelized by two conducting branches. (*b*) One branch is blocked, leading to interruption of current flow. (*c*) The closed circuit is restored by the introduction of an "acupuncture needle". Now redox reactions take place at the needle-electrolyte interfaces (x) in addition to reactions at the electrode-electrolyte interfaces (not indicated in the figure). (*d*) A model more close to biologic conditions than *a–c*. The circuit is here activated by fluctuating potential differences between an injured tissue and normal tissue.

Fig. XVIII: 7 *d* more closely approaches conditions in vivo. The driving force is created by the tissue injury potential to the left in relation to the normal potential of the tissue to the right. Interstitial spaces and lymphatics connecting the abnormal and normal regions join somewhere, corresponding to the external cables of Fig. XVIII: 7 *a–c*. Some of these interstitial spaces and lymphatics constitute what is probably a preferential pathway for ions, corresponding to what in acupuncture is called a "meridian". Blood vessels (with their conducting blood plasma and insulating vessel walls) connect both regions of tissue, but are blocked. This prevents closing of the electric circuit. Fig. XVIII: 7 *d* indicates the vascular block, e.g., by arteriosclerosis, contractions of the vessel, or external compression by a haematoma or oedema. After a needle is inserted through the normal muscle into the injured muscle, it is easy to understand that closed circuit ionic transports are restored over the conducting "meridian", resulting in an enhancement of the healing process. The restoration of this self-driving system for ionic transport represents a remarkably simple form of therapy explainable by the principle of BCEC.

A more powerful but less "physiologic" principle is represented by the driven system. It does, however, contain many possibilities still unexplored, particularly apparent in the context of contemporary knowledge of electrochemistry and electronic technology.

The general principle of the driven system is illustrated in Fig. XVIII: 8. The principle, which may be applied in any organ or tissue, is that two needle

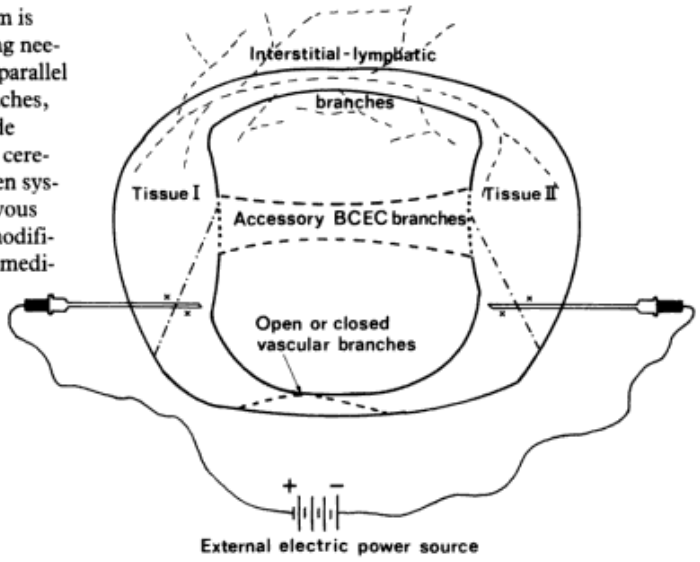

Fig. XVIII: 8. Acupuncture: a driven electrical system is created by an external electric power source connecting needles in Tissues I and II. Current flow is induced over parallel vascular-interstitial branches or accessory BCEC branches, such as ductal channels. The conducting media include blood, intraductal secretions, and pleural, peritoneal, cerebrospinal and interstitial fluids. Self-driving and driven systems should interfere with tissue metabolism and nervous regulation of tissue functions. Associated metabolic modifications and levellings of tissue potentials may explain medical effects of acupuncture.

electrodes connected to an external source of electric power can promote or counteract spontaneous polarization of the two needled regions of tissue. This system permits the driving of ions and ergons (e.g., water) in normal as well as in pathological tissues. The mode of driving the system can be tailored for different purposes. The major practical problem of how best to do it is still unsolved. The total amount of ionic transports can be varied ad libitum. Electrodes can be positioned in any branch of the closed circuit, including in what are here called accessory BCEC branches (e.g., ducts containing secretions, which are electrically conducting), which in Fig. XVIII: 8 are coupled in parallel with VICC (vascular-interstitial closed circuit) branches.

In order to find such accessory BCEC branches and to understand their function, we must first look for different tissue components of relatively low electric conductivity (Table XVIII: 1) and of relatively high conductivity (Table XVIII: 2).

Given this rough separation, which is based on known values of conductivity (Chapter XII), we may recognize tentatively in organs those structural components which possess the capability of creating preferential pathways for closed circuit ionic transports. These preferential pathways connect organs and also regions and cells of organs. Table XVIII: 3 is therefore deliberately incomplete.

Of the various components listed, each will function when at least one single branch of the circuit is vascular. To date, only single components ("x") or combinations ("xx") of arteries, veins and interstitial channels have been studied so far, as indicated in Table XVIII: 3.

Considering acupuncture as principally a way to create or enhance closed circuit transports in tissue, other phenomena, hitherto unexplained, may also become understood. Local anaesthesia in acupuncture, for example, may be induced as a levelling of the electric potential of a tissue. In either a self-driving or a driven system, anaesthesia follows local changes in metabolism, including nervous tissue elements.

Simple electrotechnical analogues imply that a local

Table XVIII: 1. *Tissues and tissue components with electrically "relatively good insulating properties"*

Matrix of cell membranes
Fibrous tissue
Adipose tissue
Hyalin
Air
Matrix of bone
Vessel walls (except capillaries)
Walls of glandular ducts?
Walls of tubular shape, e.g., gastrointestinal and urogenital canals?

Table XVIII: 2. *Biological materials of "relatively good conductivity"*

Intracellular fluid
Interstitial fluid
Blood plasma
Thrombi
Secretions
Peritoneal and pleural fluid
Cerebrospinal fluid
Components providing electrical conduction of nerves
Intraarticular fluid
Urine, gastrointestinal contents
Degrading tissues

Table XVIII: 3. *Structural components with anticipated capability to form pathways of BCEC systems*

(x) indicates components, (xx) combination of components given preliminary exploration in this study

	Interstitial spaces	Lymph vessels	Arteries	Veins	Ducts	Tubes	Bodily cavities	Cerebrospinal spaces	Nerves (axons)
Interstitial spaces	x		xx	xx					see text
Lymph vessels									
Arteries	xx		x	xx					
Veins	xx		xx	x					
Ducts of glands									
Tubes (e.g., gastrointestinal, urogenital)									
Bodily cavities									
Cerebrospinal spaces									
Nerves (axons)	see text								

decrease or increase of transported current may give rise to undesired as well as useful effects. A local change in density of current anywhere in a biologically closed circuit might lead to anaesthesia, or produce pain or other undesired effects far away from the site of the driving force for the closed circuit transports. Clinical considerations which can not simply be understood by the known and accepted mechanism of referred pain might be explained in this way. For example, degenerative alterations in the cervical spine may not only give rise to pain in the distribution of an affected nerve but also to symptoms of local peripheral injury associated with pain, e.g., tenderness to local palpation or active contraction of a muscle or muscles (17).

I. Vesicles in the transmission of nervous impulses

Impulses in nerves represent a particular type of BCEC transport. Thus, closed circuit connections are described between axons and interstitial fluid outside the insulating membrane over Ranvier's nodes (76). Other axonal connections may also be considered. In Chapters XII and XIII, theoretical and experimental analogues have been presented for the formation and transport of vesicles in endothelial cells. This view may also be applied to closed circuit electric transport in nerves and various anticipated communicating outer BCEC branches. Vesicles, which are produced at synaptic stimulation may then represent microergonars or microergionars as a consequence of electrode reactions at nerve-end-plates. The material of vesicles (consisting of an anticipated inactive transmitter precursor) can then be transferred as an electrogenic, matrix-mediated transport or, in the case the precursor is ionic, be transported as hydrated cationic compounds (electropositively charged microergionars) to a second site of electrode reaction leading to the release of the active transmitter substance. Evidently, a continuation of the second, "outer" circuit branch (which may be, e.g., vascular as well as interstitial) has yet to be identified.

This theory of an electrogenic development and transport of an ergonic or ergionic vesicular content for transmission of nerve impulses may be compared with current views on the action of hormones. Thus, hormones are produced in a source organ and transported in an inactive state as the first messenger to a target organ. There, the hormone exerts its specific effects in an activated state over the machinery of the second messenger, as described by Sutherland (91). Compare also the transport of oxygen in a protected ergonic state bound to haemoglobin during transport in the blood stream and bound to myoglobin in muscle (Chapter XIII, page 155).

J. Oral galvanism

After the introduction of amalgams as dental filling materials over 100 years ago, the possible development of galvanic currents in the oral cavity has been discussed from time to time. The symptoms of burning mouth, oral pain or smart, and a taste of metal or salt (18, 92) have been referred to as *oral galvanism*.

The secondary phenomena of oral corrosive processes have also been discussed in terms of local and general biologic reactions (3, 4, 8, 15, 22, 23, 33, 34, 35, 37, 44, 55, 60, 61, 62, 68, 69, 74, 78, 80, 81, 82, 83, 85, 86, 87, 93). Many attempts have been made to explain the symptoms as caused by electrochemical

interaction of metals in the saliva (18, 23, 31, 42, 44, 49, 60, 68, 93). Galvanic currents in the oral cavity have been assumed to develop between relatively anodic and cathodic parts of one metal or on contact between two different restorations and the saliva. As a result of corrosion, different metals or metallic compounds should then appear in the saliva (11, 12, 31, 32, 36, 42, 63, 65, 66, 67, 94) or in the tissues adjacent to amalgam fillings (32, 36, 38, 39, 47, 78, 82, 94). A large number of in vivo studies have been performed of electric potentials between different dental restorations (for references, see Nilner, 1981). Different surfaces of a restoration may present different degrees of polarization, indicating inhomogeneity of the material (11, 12, 47, 49, 51, 56, 65). Potential differences between different restorative materials may gave rise to estimated galvanic currents of a magnitude of 1–36 μA (65). It has been judged that values above 5 μA could possibly explain clinically apparent galvanism. Surprisingly, however, some of the highest values of galvanic current measured were found in a control group of patients without symptoms. In a study of dissolving Ag, Ca, Hg, Sn and Zn in the saliva, no significant differences could be found between patients with symptoms and patients without symptoms in different control groups (65). Studies of this type are important and informative, but illustrate also clearly that the mechanism of oral galvanism is still in many respects unexplained. The possibility of overlying psychological factors has been suggested (38, 39). Neurotoxic effects by retrograde axonal transports of dissolved metal (41) have also been suggested. The mechanism of retrograde axonal transports (30, 84) is also not very well understood. All explanations of oral galvanism have been based on the assumption that an intraoral closed circuit is created when two metals of different electric potential make direct metal-to-metal "electronic" contact (for example, via a silver spoon). The "outer" part of the circuit is created by the electrically conducting saliva. Anodic dissolution of metal will then take place and may in some way produce symptoms. One might then expect that the amounts of dissolved metal in the saliva would correlate with the symptoms of oral galvanism, but no such results have been found. Some of the largest amounts of intraoral galvanic currents were even found in patients without symptoms of galvanism (65).

The principle of BCEC may overcome this dilemma (see also the description of in vivo corrosion, Chapter XII, page 112). As indicated in Fig. XVIII: 8, different branches of BCEC systems may combine with "accessory" or "temporary" conducting biological channels or materials. Thus, in oral galvanism the intraoral ionic conducting branch, formed over the saliva between two electron conductors, may combine with one or several parallel-coupled, biological conducting branches in surrounding tissues. These branches, for instance, may be represented by blood vessels and interstitial channels. Such a circuit is outlined in principle in Fig. XVIII: 9*a*. Its different components represent a set of individual variables. A galvanic current through the circuit can now develop between metals of different electric potential even when these metals are separated by a distance. No direct contact, such as over a silver spoon, is therefore necessary. The interconnecting branch between the metals is created by the saliva.

"Injury reactions" at the interfaces between the gingiva or root canals and the restoration metals provide connections to BCEC channels in the tissues. The "injury reactions" include many different processes which lead to ionization and separation of charges. Examples of such processes are local infection, degrading of tissue or foreign material in the gingival pockets, vascular thrombosis, and local toxic effects of dissolved metal from the restorations (from so-called general corrosion). Each of these processes should lead to closing of the intraoral and the vascular-interstitial channels of the circuit. Coinciding "injury reactions" at two metal-tissue interfaces combined with two metal-saliva interfaces should be sufficient to establish a galvanic current. This system may then be recognized to contain a minimum of four redox sites.

The driving electromotive force of this system need not necessarily be found in the potential difference between relatively anodic and cathodic parts of the metals. Locally degrading processes (injury potentials) adjacent to the metals may also drive the system (see Chapter XII, "complicated corrosion", page 115). Periodontitis or chronic periodontosis of different origins, leading to focal toxic or infectious injuries in the gingival pockets, should be able to induce transport of electric current in the described BCEC without the presence of any metal. The driving electromotive force in such systems may depend on differences in age of two polarizing processes in the circuit (Fig. XVIII: 1). In the case of healthy (noninjured) tissue adjacent to the metals, the biologic circuit is interrupted. Consequently, no current will flow even if the potential difference between the two metals is relatively "large", as was the case in the control subjects reported by Bergman, Ginstrup and Nilner (12). The concept of BCEC makes it therefore possible to explain the seeming inconsistencies between clinical galvanism on one hand and the measured electric potential differences between intraoral metals and amount of dissolved metals in the saliva on the other.

Fig. XVIII: 9*b* illustrates some of the possible biologic reactions adjacent to one of the participating metals of the closed circuit. Thus, redox reactions will take place at one interface against the saliva and at one against the injured tissue. Metal ions may dissolve

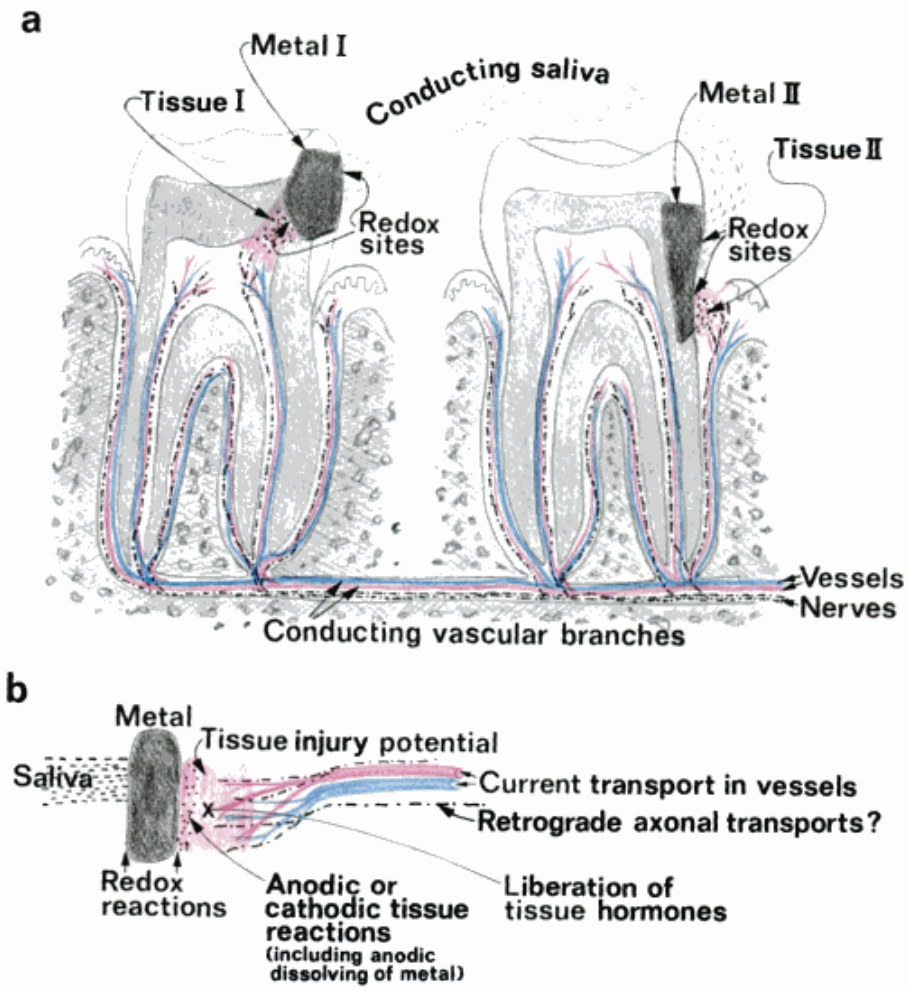

Fig. XVIII:9. Suggested explanation of oral galvanism. (*a*) So-called general corrosion slowly dissolves metal ions, which spread into adjoining tissues and saliva. Toxic injuries induce ionization of tissue. Metals I and II become joined electrically, "externally" by the saliva and "internally" by preferential biologic pathways for current, e.g., vascular and interstitial BCEC branches. A minimum of four redox sites is included in the closed circuit. Differences of potential of metal may deliver the electromotive force. (*b*) The driving force of the closed circuit does not necessarily depend on differences of potential between two filling materials. A slow dissolving of metal, as in general corrosion, may induce toxic changes in tissue. These changes may initiate electric conduction between metal and vascular-interstitial channels and deliver a fluctuating electromotive force. Tissue injuries adjacent to two separate fillings are necessary for closing of the circuit. Injury is enhanced as current flow leads to liberation of tissue hormones, which spread by diffusion, migration in the electric field, tissue convection and possibly as retrograde axonal transports. For further explanation, see text.

when the metal is relatively anodic. Production of cathodic alkalinity and anodic acidity will influence metabolic reactions. Normal and pathological metabolic products will undergo electrophoretic transports. Direct current stimulation of nerve end-plates may directly or indirectly produce pain. Thus, several tissue hormones, e.g., substance P, histamine, serotonin and prostaglandins are known to be involved in inflammatory reactions (14, 70, 96) and may be distributed electrophoretically by the activated closed circuit.

If this proposed explanation of oral galvanism is correct, the conclusion can then be reached that the different causes leading to connection of BCEC branches of the closed circuit are the crucial targets for therapy. One of the difficult causes to treat is then probably the "allergic" reactions of tissue to metals in certain individuals. These reactions may even develop slowly, as in general corrosion at a tissue-metal interface. When the injury reaction is caused by superimposed infection, the condition should be fairly accessible to successful treatment.

K. BCEC systems as receptors for moving external electromagnetic fields

BCEC systems may also represent an important link between the external and internal electric environments of an organism. An abundance of direct and indirect evidence nowadays exists about environmental influence of electromagnetic fields (5, 21, 48) on different biological systems, i.e., plants (7), simple cellular organisms (6, 16), animals and man (48). Strong, moving electromagnetic fields do appear in connection with changes of weather conditions and particularly in certain areas of the world. Thus, the Föhn and the Sirocco winds in Europe are notorious for causing different biologic effects, i.e., headache, hemicrania, epileptic fits, asthma, thromboembolism and joint pain (48). Even the rate of traffic accidents is related statistically to these atmospheric disturbances (95). In experiments with mice it has been shown (88) that 50 Hz alternating fields can be lethal to the animals at sufficiently high intensities. Thus, an exposure of 650 kV/m at 50–500 Hz during 60–120 minutes gave a mortality of 70%–90%.

Associated problems are complex. Beneficial effects of electric fields have been reported. The effect of a 110 V, 60 Hz "household current" on the development of mice (58) showed that mice exposed continuously to the field at about 1 kV/m over one month gained weight more rapidly than the controls. Recently collected data on the possible influences of external man-made and natural electromagnetic fields (48) strongly indicate the importance of environmental electromagnetism in biology. This source of information summarizes the probable minimum safe distance from the path of three-phase high-voltage transmission lines as shown in Table XVIII: 4. Natural electromagnetic fields of different wavelength and strength are always present in the biosphere (2). These fields, like background radiation, probably should be regarded as factors partly responsible for the way biological structures have developed. Nevertheless, situations defined by excessive influence of any one of the natural components which create our environment may lead temporarily to noticeable disturbances (48). This generalization appears also to hold for changes of our external electric environment.

Normal electromagnetic frequencies encountered in the biosphere range from ultralow frequencies (ULF = below 1 Hz) over the whole spectrum of increasing frequencies to cosmic ultraradiation (48). All of these frequencies are natural and therefore likely to be of importance in some way for biology. The ULF, ELF (extremely low frequencies up to 300 Hz) and VLF (very low frequencies up to 300 kHz) are the most easy to regard as influencing biologic functions because normal bioelectrical events often take place in these frequency regions (10). Striking similarities can, for example, be found between alpha and delta waves of human EEG records and some of the natural electromagnetic waves in our environment (1). It is therefore understandable why certain biologic reactions are suspected to be induced by strong manmade or natural electric fields. These should then in some way induce interferences with the electric events of the nervous system. The mechanism of interference is, however, still unknown.

Table XVIII: 4. *Minimum safe distances from the center line of high-voltage transmission lines (48)*

Operating voltage	Distance from the right-of-way: Field intensity <50 V/m (undoubtedly safe)	Field intensity <150 V/m (probably safe)	Field intensity <5 kV/m (probably dangerous)
380 kV	180–250 m	100–140 m	15–20 m (tower height >50 m)
220 kV	140–180 m	75–90 m	6–10 m (tower height >30 m)
100 kV	80–120 m	45–60 m	–
50 kV	50–70 m	34–45 m	–

From a physical point of view, the existence of closed circuit pathways for current in a biologic medium provides a prerequisite for the development of induction currents when such systems are exposed to varying external electromagnetic fields. *An acceptance of BCEC systems leads to the necessary conclusion that these systems should act as receptors for moving external electromagnetic fields.* As indicated earlier (Table XVIII: 3), different combinations of closed circuit branches may create BCEC systems. Axonal transports as part of a closed circuit mechanism, yet to be explored, might constitute a primary target for induction of current. The need for nutritional supply to nervous tissue by vascular-interstitial transports makes it, however, also possible to explain interferences of nervous functions by moving electromagnetic fields, as a secondary effect from induction of currents in VICC branches. Arterioles and arterial capillaries were also found to react selectively with contractions in scattered regions of dog mesentery exposed to electric fields (Chapter XII). The often expressed assumption that the pericyte apparatus of capillaries are likely to be involved in the mechanism of capillary contractions

Table XVIII: 5. *Penetration depth in cm (attenuation to 1/e) of high-frequency electromagnetic waves in various tissues at typical frequency values. After Presman (73)*

	Frequency (MHz)							
Tissue	100	200	400	1 000	3 000	10 000	24 000	35 000
Thin bone	22.90	20.66	18.73	11.90	9.924	0.34	0.145	0.073
Brain	3.56	4.132	2.072	1.933	0.476	0.168	0.075	0.0378
Lens of eye	9.42	4.39	4.23	2.915	0.500	0.174	0.0706	0.0378
Living body	2.17	1.69	1.41	1.23	0.535	0.195	0.045	0.0314
Fat	20.45	12.53	8.52	6.42	2.45	1.1	0.342	–
Muscle	3.451	2.32	1.84	1.456	–	0.314	–	–
Whole blood	2.86	2.15	1.787	1.40	0.78	0.148	0.0598	0.0272
Skin	3.765	2.78	2.18	1.638	0.646	0.189	0.0722	–

now comes into the picture. Their scattered presence in capillary walls indicates that they may be involved in the mechanism of field induced regional capillary contractions.

Values for the depth of penetration of high-frequency electromagnetic waves (73) are presented in Table XVIII: 5. In this Table the depth of penetration refers to the depth in the material at which the amplitude of the wave has fallen to the $1/e$ part of the initial amplitude ($e=2.72$, the base of the natural logarithm).

The penetration of electromagnetic waves increases with decreasing frequency. The penetration of ULF, ELF and VLF waves in biologic material is therefore of considerable interest (53). Shielding of an electric field is usually obtained by means of a device such as a Faraday cage. An irregular or slowly varying magnetic field is far more penetrating and requires shielding especially made for magnetic fields. Some relative values of shielding efficiency of various objects to electric and magnetic fields at 10 kHz frequency (52) appear in Table XVIII: 6.

Table XVIII: 6. *Shielding efficiency of various objects with respect to an electric (E) and magnetic (H) field. After Ludwig (50)*

	Permeability	
Object	E_i/E_e (%)	H_i/H_e(%)
Faraday cage ($r=50$ cm), mesh wire of iron material ($d=0.1$ cm), mesh size 3 cm	0.5	65
Faraday cage as above, mesh size 0.3 cm	<0.1	10
Volkswagen	1.0	50
Sheet-iron garage	<0.1	50
Steel bungalow	<0.1	8
Steel-reinforced concrete bunker (wall thickness 60 cm)	<<0.1	0.1
Sleeping bag with copper lining	<0.1	90

These considerations on possible interactions between moving external electric and magnetic fields and BCEC systems conclude this book.

Concluding remarks

The author has attempted several times to prepare the information of this book as a series of separate articles. These attempts have, to a large extent, been discouraging. One reason is that working nowadays across established specialities is extremely difficult, not to say dangerous. Each section is in itself probably of limited interest. Only when the different pieces of information are put together do the contours of an important biologic mechanism become evident. Thus, the main purpose of this book is to introduce the concept of biologically closed electric circuits (BCEC) and some examples of their functional and morphogenetic role in normal and pathological conditions. BCEC systems should be regarded as an additional circulatory system for selective transports and modulation of biochemical reactions within the circuits. Of necessity, this book is presented as a survey of the seemingly simple principle of BCEC systems. The principle, nevertheless, is capable of offering new possibilities toward explaining biologic problems. Even some conditions which from a traditional medical standpoint have been regarded as more or less obscure may be explained. The existence of preferential pathways for closed circuit transports in tissue leads to further logical consequences which have been only slightly suggested in this book.

It is the hope of the author that the material presented will encourage scientists of different specialities to continue this work. The various aspects of BCEC systems will require interdisciplinary cooperation if improved and truly deep understanding of its manifold possibilities is to be attained.

References

1. Adey, W. R.: Introduction: Effects of electromagnetic radiation on the nervous system. Ann. N.Y. Acad. Sci. 247: 15, 1975.
2. Altmann, G.: Die physiologische Wirkung elektrischer Felder auf Tiere. Verh. Dtsch. Zool. Ges. Wien 11: 360, 1962.
3. Angmar-Månsson, B., Omnell, K.-Å., and Rud, J.: Root fractures due to corrosion. I. Metallurgical aspects. Odontol. Revy 20: 244, 1968.
4. Arvidson, K., and Johansson, G.: Galvanic series of some dental alloys. Scand. J. Dent. Res. 85: 485, 1977.
5. Asanova, T., and Rakov, A.: Health condition of workers exposed to an electrical field of 400–500 kV open distributing installations. Labor Hyg. Occup. Dis. 5: 50, 1966 (Engl. transl.).
6. Bach, S.: Changes in macromolecules produced by alternating electric fields. Dig. Int. Conf. Med. Electron. 21: 1, 1961.
7. Bachmann, C. H., and Reichmanis, M.: Some effects of high electrical fields on barley growth. Int. J. Biometeorol. 17: 253, 1973.
8. Banoczy, J., Roed-Petersen, B., Pindborg, J. J., and Inovay, J.: Clinical and histologic studies on electrogalvanically induced oral white lesions. Oral. Surg. 48: 319, 1979.
9. Bassett, C. A. L., Pawluk, R. J., and Pilla, A. A.: Acceleration of fracture repair by electromagnetic fields: a surgically noninvasive method. Ann. N.Y. Acad. Sci. 238: 242, 1974.
10. Bawin, S. M., Gavalas-Midici, R., and Adey, W. R.: Effects of electric fields on specific brain rhythms. Symposium and workshop on the effects of low frequency magnetic and electric fields on biological communication processes at the 6th annual meeting of the Neuroelectric Society. Vol. 6, 1973.
11. Bergman, B., Bergman, M., and Söremark, R.: Dissolution and uptake of cadmium from dental gold solder implants. Scand. J. Dent. Res. 85: 623, 1977.
12. Bergman, M., Ginstrup, O., and Nilner, K.: Potential and polarization measurements in vivo of oral galvanism. Scand. J. Dent. Res. 86: 135, 1978.
13. Bergström, M., Ericson, K., Levander, B., Svendsen, P., and Larsson, S.: Variation with time of the attenuation values of intracranial hematomas. J. Comput. Ass. Tomography 1: 57, 1977.
14. Bergström, S., and Samuelsson, B.: The prostaglandins. Endeavour 27: 109, 1968.
15. Björn, H.: Electrical excitation of teeth and its application to dentistry. Sven. Tandlaek. Tidskr. 39 Suppl., 1946.
16. Blakemore, R.: Magnetostatic bacteria. Science 190: 377, 1975.
17. Breig, A.: Adverse mechanical tension in the central nervous system. Stockholm, Almqvist & Wiksell International, 1978.
18. Bujas, Z.: Electrical taste. In: Beidler, L. M. (ed.): Handbook of sensory physiology 4. Chemical senses, 2. Berlin, Springer, 1971, p. 180.
19. Burr, H. S., and Northrop, F. S. C.: The electro-dynamic theory of life. Quart. Rev. Biol. 10: 322, 1935.
20. Cameron, G. R., and Spector, W. G.: The chemistry of the injured cell. Springfield, Ill., C. C. Thomas Publ., 1961.
21. Chalmers, J. A.: Atmospheric electricity. 2nd ed. Oxford, Pergamon Press, 1967.
22. Charpy, M. J.: Eczémas de sensibilisation à divers produits absorbés par la muqueuse buccale. Bull. Soc. Franc. Derm. Syph. 59: 338, 1952.
23. Chase, H. S.: Oral electricity. Dent. Cosmos 21: 205, 1879.
24. Cope, F. W.: A theory of enzyme kinetics based on electron conduction through the enzymatic particles, with application to cytochrome oxidases and to free radical decay in melanin. Arch. Biochem. Biophys. 103: 352, 1963.
25. Cope, F. W.: A kinetic theory of electron and ion transport in particulate and membranous systems, with applications to the cytochrome oxidase, melanin free radical, and pyruvate carboxylase reactions and to control of enzymes by hormones and radiation. In: King, T. O., Mason, H. S. and Morrison, M. (eds.): Oxidases and related redox systems. New York, J. Wiley and Sons, 1965, p. 51.
26. Driesch, H.: The science and philosophy of the organism. London, 1908.
27. De Duve, C., and Beaufay, H.: Tissue fractionation studies. 10. Influence of ischaemia on the state of some bone enzymes in rat liver. Biochem. J. 73: 610, 1959.
28. Edds, M. V., Jr., and Sweeny, P. R.: Chemical and morphological differentiation of the basement lamella. In: Rudnick, D. (ed.): Synthesis of molecular and cellular structure. Society for the Study of Development and Growth, Symposium 19. New York, Ronald Press, 1960, p. 111.
29. Everson, T. C., and Cole, W. H.: Spontaneous regression of cancers. Am. Surgeon 144: 366, 1956.
30. Edström, A., and Hansson, M.: Retrograde axonal transport of proteins in vitro in frog sciatic nerves. Brain Res. 61: 311, 1973.
31. von Frauenhofer, J. A., and Staheli, P. J.: Gold-amalgam galvanic cells. Br. Dent. J. 132: 357, 1972.
32. Fredén, H., Helldén, L., and Milleding, P.: Mercury content in gingival tissues adjacent to amalgam fillings. Odontol. Revy 25: 207, 1974.
33. Frykholm, K. O.: Stomatitis electrogalvanica. Acta Derm. Venereol. 41: 422, 1961.
34. Frykholm, K. O., Frithiof, L., Fernström, Å. I. B., Moberger, G., Blohm, S. G., and Björn, E.: Allergy to copper derived from dental alloys as a possible cause of oral lesions of lichen planus. Acta Derm. Venereol. 49: 268, 1969.
35. Frykholm, K. O., and Hedegård, B.: Fall av elektrokemisk korrosion i munhålan. Sven. Tandlaek. Tidskr. 61: 435, 1968 (in Swedish).
36. Fusayama, T., Katayori, T., and Nomoto, S.: Corrosion of gold and amalgam placed in contact with each other. J. Dent. Res. 42: 1183, 1963.
37. Gasser, F.: Nebenwirkungen zahnärztlicher Behandlungsstoffe. Fortsch. Med. 86: 441, 1968.
38. Glantz, P.-O., Björlin, G., and Sundström, B.: Tissue reaction to some dental implant materials. An *in vivo* study in white rats. Odontol. Revy 26: 231, 1975.
39. Glantz, P. O., Bergman, M., Sjölund, B., and Nilner, K.: Oral galvanism – ett elektrokemiskt fenomen. Läkartidningen 78: 3467, 1981 (in Swedish).
40. Gurwitsch, A.: Über den Begriff des embryonalen Feldes. Roux Arch., LI, 1922.
41. Hansson, M.: Oral galvanism—ett neurotaxiskt fenomen? Läkartidningen 47: 4240, 1981 (in Swedish).
42. Holland, R. I.: Galvanic currents between gold and amalgam. Scand. J. Dent. Res. 88: 269, 1980.
43. Ingvar, S.: Reaction of cells to galvanic current in tissue cultures. Proc. Soc. Exp. Biol. and Med. 17: 198, 1920.
44. Inovay, J., and Banoczy, J.: The role of electrical potential differences in the etiology of chronic diseases of the oral mucosa. J. Dent. Res. 40: 884, 1961.
45. Jalonen, J.: Oxygen transport in the blood. Ann. Clin. Res. 13: 39, 1981.
46. Jordan, J.: In: Pilla, A. A. (ed.): Proceedings of a workshop in bioelectrochemistry, Princeton, New Jersey, Oct. 10–14, 1971, p. 102. National Science Foundation, Washington, D.C. and ESB Inc. Technology Center, Yardley, Pennsylvania.
47. Klötzer, W. T.: Die Reaktion der Gingiva im Kontakt mit zahnärztlichen materialen. Dtsch. Zahnaerztl. Z. 28: 1181, 1973.
48. König, H. L., Krueger, A. P., Lang, S., and Sönning, W.: Biologic effects of environmental electromagnetism. New York/Heidelberg/Berlin, Springer, 1981.
49. Lain, E. S., and Caughron, G. S.: Electrogalvanic phenomena of the oral cavity caused by dissimilar metallic restorations. J. Am. Dent. Assoc. 23: 1641, 1936.
50. Liboff, A. R., and Rinaldi, R. A. (eds.): Electrically mediated mechanisms in living systems. Ann. N.Y. Acad. Sci. 238: 1, 1974.
51. Lukas, D. G.: Über die Messung von Spannung und Kurzschlussströmen an zahnärztlichen Metallen. Dtsch. Zahnaerztl. Z. 28: 394, 1973.
52. Ludwig, H. W.: Wirkung einer nächtlichen Abschirmung der elektrischen Feldstärke bei Rheumatikern. Arch. Meteorol. Geophys. Bioklimatol. (B) 21: 305, 1973.
53. Ludwig, H. W.: Shielding effect of materials in the ULF, ELF and VLF region. Int. J. Biometeorol. 17: 207, 1973.
54. Lund, E. J.: Experimental control of organic polarity by the

electric current. II. The normal electrical polarity of Obelia. A proof of inexistence. Jour. Exp. Zool. 36: 477, 1922.
55. Marxkors, R.: Electrochemische Vorgänge an metallischen Fremdstoffen in der Mundhöhle. D. D. Z. 19: 419, 1965.
56. Maschinski, G.: Potentialmessungen an Metallen in der Mundhöhle. Zahnaerztl. Prax. 21: 28, 1970.
57. Meyer, K. H., and Bernfeld, R.: La perméabilité des membranes. IX. La perméabilité ionique des membranes inhomogènes. Helv. Chim. Acta 28: 980, 1945.
58. Moos, W. S., Schmitz, R., and Clark, R. K.: The effects of electric fields on mouse weights. Int. J. Biometeorol. Suppl. 11: 321, 1967.
59. Moss, L.: Acupuncture and you. Secaucus, New Jersey, Citadel Press, Inc., 1971.
60. Mumford, J. M.: Electrolytic action in the mouth and its relationship to pain. J. Dent. Res. 36: 632, 1957.
61. Mumford, J. M.: Pain due to galvanism. Br. Dent. J. 108: 299, 1960.
62. Mumford, J. M., and Björn, H.: Problems in electric pulp-testing and dental algesimetry. Int. Dent. J. 12: 161, 1962.
63. Möller, B.: Reaction of the human dental pulp to silver amalgam restorations. Swed. Dent. J. 2: 93, 1978.
64. Nadol, J. B., Jr., Gibbins, J. R., and Porter, K. R.: A reinterpretation of the structure and development of the basement lamella: an ordered array of collagen in fish skin. Dev. Biol. 20: 304, 1969.
65. Nilner, K.: Studies of electrochemical action in the oral cavity. Swedish Dental Journal, Suppl. 9, 1981.
66. Nilner, K., Glantz, P.-O., Ryge, G., and Sundberg, H.: Oral galvanic action after treatment with extensive metallic restorations. Acta Odontol. Scand. 1981. In press.
67. Nilner, K., Glantz, P.-O., and Zöger, B.: On intraoral potential and polarization measurements of metallic restorations. Acta Odontol. Scand. 1981. In press.
68. Nilsson, B.: Taste perception in the human palate. Umeå university odontological dissertations no. 9, Umeå, Sweden, 1978.
69. Nordenström, B.: Circuits électriques biologiquement fermés, leur signification dans les transformations structurales dans le cancer du sein. Presented at the 1st International Course on Radiodiagnosis of the Breast. Montpellier, France, March 24–27, 1981.
70. Pernow, B.: Substance P: Its distribution, pharmacological actions and possible physiological role in sensory neurons. Clin. Phys. 1: 235, 1981.
71. Pierce, G. B., Jr., Beals, T. F., Ram, J. S., and Midgley, A. R., Jr.: Basement membranes. IV. Epithelial origin and immunologic cross reactions. Am. J. Pathol. 45: 929, 1964.
72. Porter, K. R.: Morphogenesis of connective tissue. In: Stephens, C. A. L., Jr., and Stanfield, A. B. (eds.): Cellular concepts in rheumatoid arthritis. Springfield, Ill., C. C. Thomas Publ., 1966, p. 6–40.
73. Presman, A. S.: Akzeleration und elektromagnetische Felder der Biosphäre. Mod. Med. 2: 224, 1972.
74. Reinhard, M. C., and Solomon, H. A.: Electrical currents from dental metals as an etiologic factor in oral cancer. Am. J. Cancer. 22: 606, 1934.
75. Riddick, T. M.: Control of colloid stability through zeta potential. New York, Zeta-Meter Inc., 1968.
76. Robertson, A.: The input message. Science Journal 3: 60, 1967.
77. Rosenberg, B.: Some problems in the electrical conductivity of proteins. In: King, T. E., Mason, H. S., and Morrison, M. (eds.): Oxidases and related redox systems. New York, J. Wiley and Sons, 1965, p. 72.
78. Rost, A.: Amalgamschäden. Zahnaerztl. Prax. 27: 475, 1976.
79. Ruckdeschel, J. C., Codish, S. D., Stranahan, A.,: Postoperative empyema improves survivial in lung cancer. New Engl. J. Med. 287: 1013, 1972.
80. Rud, J., and Omnell, K.-Å.: Root fractures due to corrosion. Diagnostic aspects. Scand. J. Dent. Res. 78: 397, 1970.
81. Sarkar, N. K., and Greener, E. H.: *In vitro* corrosion resistance of new dental alloys. Biomat. Med. Dev. Art. Org. 1: 121, 1973.
82. Sandrik, J. L., Greener, E. H., and Wragg, L. E.: Tissue reactions and in vivo corrosion of ferrous alloy implants. In: Korostoff, E. (ed.): Research in dental & medical materials. New York, Plenum Press, 1969.
83. Schriever, W., and Diamond, L. E.: Electromotive forces and electric currents caused by metallic dental fillings. J. Dent. Res. 31: 205, 1952.
84. Sharma, R. P., and Obersteiner, E. J.: Metals and neurotaxic effects: cytotoxicity of selected metallic compounds on chick ganglia cultures. J. Comp. Pathol. 91: 235, 1981.
85. Solomon, H. A., and Reinhard, M. C.: Electric phenomena from dental metals. Dent. Surv. 12: 23, 1933.
86. Solomon, H. A., Reinhard, M. C., and Goodale, H. I.: The possibility of precancerous and cancerous oral lesions from electrical causes. Dent. Dig. 39: 142, 1933.
87. Solomon, H. A., Reinhard, M. C., and Goltz, H. L.: Salivary influence on galvanism. Dent. Items. 60: 1047, 1938.
88. Solovév, N. A.: Action of a high-voltage electric field of 59–2 000 Hz on white mice and drosophila. Proceedings of conference on labor hygiene and the biological action of radiofrequency electro-magnetic fields. Moscow, 1963, p. 91.
89. Spemann, H.: Organizers in animal behaviour. Proc. Royal Soc. London, Ser. B, 102: 177, 1927.
90. Stux, G., Stiller, N., Pothmann, R., and Jayasuriya, A.: Lehrbuch der klinischen Akupunktur. Berlin, Heidelberg, New York, Springer Verlag, 1980.
91. Sutherland, E. W.: Studies on the mechanism of hormone action. Science 177: 401, 1972.
92. Söremark, R., Ingels, O., Plett, H., and Samsahl, K.: Influence of some dental restorations on the concentrations of inorganic constituents of the saliva. Acta Odontol. Scand. 20: 215, 1962.
93. Takahasi, S.: Electrochemical processes in oral tissues. Int. Dent. J. 18: 823, 1968.
94. Till, T., and Wagner, G.: Untersuchungen zur Löslichkeit der Bestandteile von Amalgamfüllungen während des Kau- und Trinkaktes. I. Teil. Z. W. R. 82: 945, 1973.
95. Tromp, S. W.: Medical biometeorology. Amsterdam, Elsevier, 1963.
96. Uvnäs, B.: Histamine storage and release. Fed. Proc. 33: 2172, 1974.
97. Weiss, P.: Morphodynamische Feldtheorie und Genetik. Verb. des V. Intr. Kongr. für Vererbungswissenschaft. Berlin, 1927.
98. Weiss, L.: The cell periphery, metastasis and other contact phenomena. Amsterdam, North Holland Publ. Co., 1967, p. 17.
99. Yasuda, I.: Mechanical and electrical callus. Ann. N.Y. Acad. Sci. 238: 457, 1974.

GLOSSARY

As a multidisciplinary work, this volume contains a broad vocabulary. This glossary is designed specifically to define the terms used in this book, including basic vocabulary which may be outside any particular reader's areas of expertise.

This glossary has been prepared by John H. M. Austin, M.D., in association with the author.

* New term, introduced by the author.

Abbreviations:

adj. adjective	n. noun
Anat. anatomy	*Phys.* physics
Biol. biology	pl. plural
Chem. chemistry	*Radiol.* radiology
Elec. electric term	sing. singular
L. Latin	v. verb
Med. medicine	

absorption coefficient, n. *Radiol.* A numerical measure of a material's ability to block the passage of x-rays through it, expressed as the ratio of the quantity of exiting x-rays to the quantity of entering x-rays.

acetylcholine, n. *Chem.* A choline ester which generates biologic actions.

adenocarcinoma, n. *Med.* Epithelial cancer characterized by glandlike organization of cells.

adenoid, adj. *Med.* Glandlike.

adenoma, n. *Med.* An epithelial neoplasm of glandlike structure, usually benign.

adenosis, n. *Med.* The formation of glands or glandlike structures.

adrenal glands, n. *Anat.* Paired ductless glands adjacent to the kidneys. The adrenal glands produce hormones which regulate metabolic functions, e.g., water, glucose and electrolyte balance, as well as hormones, e.g., epinephrine, which evoke cardiovascular pressure responses.

adventitia, n. *Anat.* The outer layer of a vessel.

alloy, n. *Chem.* A substance having metallic properties and composed of two or more chemical elements of which at least one is an elemental metal.

alveolus, n. (*-li*, pl.) *Anat.* Any one of the air sacs in the human lungs. – *alveolar*, adj.

amniotic fluid, n. *Anat.* Serous intrauterine fluid in which an embryo or fetus is immersed.

amyloid, n. *Med.* Abnormal, polymerized, insoluble proteins or protein-polysaccharide complexes of characteristic fibrillar structure.

anaphoresis, n. *Elec.* Movement of colloid particles toward the anode in an electric field. – *anaphoretic*, adj.

anaplastic, adj. *Med.* Characterized by lack of structural and functional differentiation. Descriptive of neoplasms which tend clinically to be rapidly progressive.

angiogenesis, n. *Biol.* Formation of vessels.

angiography, n. *Radiol.* Study of the lumens of blood vessels by the intravascular injection of a contrast medium. – *angiographic*, adj.

anion, n. *Phys.* A negatively charged ion. – *anionic*, adj.

anode, n. *Elec.* Positive electric pole. – *anodic*, adj.

anoxic, adj. *Chem.* 1. Without oxygen. 2. Characterized by levels of oxygen too low to sustain physiologic function.

anterior, adj. *Anat.* Pertaining to the front. Opposite of posterior.

anterolateral, adj. *Anat.* Anterior and lateral.

anteroposterior, adj. *Radiol.* Referring to the direction of movement of the x-ray beam through the subject, i.e., from anterior to posterior.

apatite, n. *Chem.* A complex mineral containing calcium+magnesium phosphate and variable amounts of organic materials.

apex, n. *Anat.* The top or highest point. – *apical*, adj. – *apices*, pl.

**arches* and *archades*, n. *Radiol.* Structural elements, which have developed under the influence of an inhomogeneous electric field at the interphase between "A" and "B"-zone.

areola, n. *Anat.* 1. A circular region of different colour from a central structure which it surrounds. 2. The darkened ring of skin around a nipple.

**arteriocapillaries*, n. *Anat.* Proximal part of the capillary bed, which contracts when exposed to an electric field. See also *venocapillaries*.

arteriography, n. *Radiol.* Procedure of injecting a contrast medium into a vessel and observing by means of x-rays the structure of vessels and the pattern of flow through them. – *arteriographic*, adj.

arteriole, n. *Anat.* A very small arterial branch, usually just proximal to a capillary.

arteriovenous, adj. *Anat.* Directly connecting the lumens of an artery and a vein, without intervening capillaries.

aseptic, adj. *Med.* Noninfectious.

aspiration needle biopsy, n. *Med.* Removal of tissue by aspiration through a needle, which is usually passed through locally anaesthetized skin and, for lung tumours, guided via fluoroscopic monitoring into the mass.

atelectasis, n. *Med.* Airlessness and decreased volume in all or part of a lung.

atrophy, n. *Med.* Wasting away or decreased size, secondary to malnutrition or disease. – *atrophic*, adj.

attenuation, n. Thinning, weakening, decreasing.

autolysis, n. *Chem.* Chemical destruction of tissues or cells by the action of their own enzymes.

axon, n. *Anat.* The elongated, conducting part of a nerve cell. – *axonal*, adj.

**"A" zone*, n. *Radiol.* Zone of lowered x-ray attenuation of tissue, appearing as a halo around a tumour or granuloma. An "A" zone is often but not always synonymous with *a hydropenic zone*, i.e., depleted of tissue water.

basement membrane, n. *Anat.* A thin, noncellular partition lying under internal surfaces covered by epithelium or endothelium.

benign, adj. *Med.* Not malignant; favourable for recovery.

biogalvanic, adj. *Elec.* Pertaining to the ability of a biological system to generate direct current.

birefringent, adj. *Phys.* Doubly refractive.

bronchial vessels, n. *Anat.* Arteries arising from the aorta and supplying blood to the bronchi. Inside the lungs the bronchial veins empty into the pulmonary venous network.

bronchography, n. *Radiol.* Study of the structure of the bronchial tree, performed by filling the bronchi with a contrast medium.

Brownian movement, n. *Phys.* Spontaneous, irregular movements of molecules or colloidal particles suspended in liquid. The movements are caused by fluctuations in the molecular impacts to which each particle is subjected. Discovered in 1827 by Dr. Robert Brown, a Scottish botanist.

**"B" zone*, n. *Radiol.* Zone of increased x-ray attenuation of tissue outside an "A" zone. A "B" zone is often synonymous with an *hydropic zone* of local oedema.

calcinosis, n. *Med.* A condition characterized by focal calcification.

**calcinosis reparativa*, n. *Med.* After injury, deposition of calcium in a tissue is part of the healing process, not a disease *per se*.

calciolytic, adj. *Med.* Characterized by removing calcium.

callus, n. *Med.* Substance exuded around fragments of fractured bone.

capacitance, n. *Elec.* Electric capacity; the amount of charge stored on an isolated conductor per unit change in its potential. The electrical capacitance $C=\frac{Q}{\Delta V}$, where Q = the electric charge and ΔV = the potential difference. – *capacitative*, adj.

capacitor, n. *Elec.* A conductor which holds or stores electric charge.

capillary, n. *Anat.* 1. Any one of the smallest blood vessels which connect the smallest arteries and veins. Tissues receive blood-borne oxygen and nutrients through the walls of capillaries. 2. Any slender channel.

catabolism, n. *Biol.* Destructive process in which living cells convert complex substances into simpler compounds. – *catabolic*, adj.

cataphoresis, n. *Elec.* The migration of an electropositive compound (cation) toward the cathode. – *cataphoretic*, adj.

catheter, n. *Med.* A long, thin tube inserted inside a bodily channel for diagnostic or therapeutic purposes. – *catheterize*, v.

cathode, n. *Elec.* Negative electric pole. – *cathodic*, adj.

cation, n. *Phys.* A positively charged ion. – *cationic*, adj.

cavitation, n. *Med.* The formation of an abnormal space or spaces containing gas. – *cavitated*, adj.

cerebrospinal fluid, n. *Anat.* The fluid in which the brain and spinal cord are immersed.

cerebrum, n. *Anat.* The largest portion of the brain in man. – *cerebral*, adj.

chemisorption, n. *Phys.* Chemical adsorption.

chemotaxis, n. *Biol.* Movement of cells, especially leukocytes, assumed to be induced by chemical compounds. – *chemotactic*, adj.

chemotherapy, n. *Med.* Treatment with chemical agents; commonly used in particular reference to antineoplastic agents.

cicatrix, n. *Med.* Scar.

cineradiography, n. *Radiol.* The exposure of x-ray film in rapid sequence (e.g., 50 frames per sec).

**circular structures*, n. *Radiol.* Structural components of the corona complex.

coeliac axis, n. *Anat.* The first major intraabdominal branch of the aorta, sending arterial blood to the liver, spleen, stomach and duodenum.

collagen, n. *Anat.* A protein and major supportive constituent of connective tissue.

colloid, n. *Chem.* A state of matter in which very small particles are finely dispersed throughout another substance. Usually, the range of diameters of colloid particles varies between 10Å and 10^3Å.

conductance, n. *Elec.* Reciprocal of resistance.

connective tissue, n. *Anat.* The supporting and binding tissue of various structures of the body.

contrast, n. *Radiol.* 1. The property of distinctly different degrees of film or screen activation as a function of the different tissues or substances through which x-rays pass. Conventional diagnostic radiology derives information from five levels of contrast. In increasing order of opacity, these levels are gas, fat, water, calcium and heavy metal. 2. Abbreviation for contrast medium, which is a substance placed in the body, usually by injection into a tubular organ and which absorbs a distinctly different quantity of x-rays than do the surrounding tissues.

**corona complex*, n. *Radiol.* The combination of *corona structures* resulting from electrophoretic transport between an injured tissue and surrounding tissue.

corona maligna, n. *Radiol.* Crownlike radiating structures at the periphery of a tumour formerly and erroneously believed to be a sign of malignancy. A term which should be discarded.

corona radiata, n. *Anat.* 1. The radiating crown of projection fibres which pass from the internal capsule to every part of the cerebral cortex. 2. A layer of columnar follicular cells which remain attached to the ovum.

**corona structures*, n. *Radiol.* Radiating fibrous structures, "A" and "B" zones, arcades and circular displacements of tissue elements around a lesion.

**corona transformation*, n. *Phys.* The biologic process by which corona structures develop around a lesion.

coronary artery, n. *Anat.* One of the arteries supplying blood to the muscle of the heart.

corpuscle, n. *Anat.* A small body, cell or part of a cell forming a distinct part of an organism. – *corpuscular*, adj.

cortex, n. *Anat.* The outer layer of an organ. – *cortical*, adj.

costophrenic, adj. *Anat.* Pertaining to the junction of the diaphragm and the inside of the thoracic cage.

cranial, adj. *Anat.* Toward the head (cranium).

craniocaudal, adj. *Radiol.* Pertaining to an x-ray beam directed through the breast in a superior to inferior direction.

crenation, n. *Biol.* Notching or scalloping.

cytoplasm, n. *Med.* Cellular protoplasm exclusive of the nucleus.

cytostatic, adj. *Med.* Capable of killing or checking the growth of cells, usually as used in antineoplastic chemotherapy.

degenerative, adj. *Med.* Very slowly deteriorating.

**demand potential*, n. *Phys.* Physicochemical difference between substance metabolism (anabolism) plus energy metabolism (catabolism) of a normal or pathological tissue and surrounding tissue. Demand potentials in normal metabolism deliver energy for selective transports over BCEC channels as a participatory mechanism maintaining homeostasis.

dendrite, n. *Anat.* Arboriform, branching extension. – *dendritic*, adj.

dense, adj. *Radiol.* 1. Characterized by a relatively high absorption coefficient. 2. Relatively opaque, said of portions of the radiographic image corresponding to regions of high absorption coefficient in the object or subject exposed to radiographic x-rays.

densitometry, n. *Radiol.* Measurement on an exposed and processed radiograph of the extent of blackening of the film.

diapedesis, n. *Med.* The outward passage of blood cells from the lumen through the intact wall of a capillary. – *diapedetic*, adj.

diathermia, n. *Med.* Generation of heat by means of tissues resisting the passage of electric current at high frequency. Dielectric heating.

dielectric, adj. & n. *Elec.* Insulating material, nonconducting. The electrons of a dielectric are tightly bound to their parent atoms. No material is a perfect insulator, but any substance whose conductivity is extremely small is properly considered to be a dielectric. Dielectrics have the property of molecular polarizability, i.e., application of an electric field may shift the negative and positive charges within a molecule. The effects of polarizability are generally observed only in the absence of appreciable conductivity.

dipole, n. *Elec.* A pair of equal and opposite charges separated by a fixed distance. When induced by another dipole, known as a *dipole-induced dipole*.

dispersion, n. *Chem.* The distribution and incorporation of small particles or molecules of one substance in another medium.

distal, adj. *Anat.* Distant from the site of attachment; remote. Opposite of proximal.

Donnan equilibrium, n. *Phys.* The balanced conditions across a membrane between two solutions which differ in ionic constituents and for which the membrane is permeable only to some of the ions in the solution. An irregular distribution of ions between the solution is present, causing electrical potential between the two sides of the membrane. The two solutions differ in hydrostatic and osmotic pressures.

dorsal, adj. *Anat.* 1. Pertaining to the back. 2. More toward the back than a structure of reference.

duct, n. *Anat.* A tubular passage through which secretions flow. – *ductal*, adj.

dystrophy, n. *Med.* Abnormal development caused by deficient nutrition. – *dystrophic*, adj.

edge enhancement, n. *Phys. 1.* Visual phenomenon in which borders of objects appear intensified because of normal neural inhibitions within the perceiving eye. *Elec. 2.* Local increase of intensity of an electric field.

effective focus, n. *Radiol.* The size of the focal spot of an x-ray tube as observed in the direction of the central x-ray beam.

efferent, n. *Anat.* Away from the brain, referring to the direction of nervous impulses.

elastin, n. *Chem.* The characteristic protein component of elastic tissue.

electret, n. *Phys.* A permanently polarized dielectric, i.e., its molecules are polar and aligned like the molecules in a bar magnet.

electrocardiogram, n. *Med.* A tracing of cardiac electrical activity.

electrocoagulation, n. *Med.* Coagulation produced by electric current passing between two terminals.

electroosmosis, n. *Biol.* Electric transport of water. – *electroosmotic*, adj.

electrophoresis, n. (*-scs*, pl.) *Elec.* The movement of ions, molecules or particles suspended in a fluid and under the action of an applied electric current. – *electrophoretic*, adj.

electrostriction, n. *Phys.* Change in size of a dielectric when polarized by an external field.

embolus, n. *Med.* A plug which passes through the circulation until it lodges in a vessel too small to permit further passage of the plug. The plug is characteristically a thrombus, but may be air or a foreign body.

emphysema, n. *Med.* 1. Disease of the lungs characterized by destruction of alveoli and by abnormal enlargement of distal air spaces. 2. Increased quantity of air per unit volume of lung, without necessarily associated destruction of pulmonary tissue. – *emphysematous*, adj.

endergonic, adj. *Chem.* Referring to a reaction which accumulates energy.

endogenous, adj. *Biol.* Developing or originating within an organism.

endothelium, n. *Anat.* A layer of cells lining the inner surface of the circulatory system. – *endothelial*, adj.

enthalpy, n. *Phys.* Heat content. A fundamental thermodynamic function, along with internal energy, entropy and free energy.

entropy, n. *Phys.* A measure of the unavailable energy in a thermodynamic system. Increase in entropy means a loss of available energy.

epinephrine, n. *Med.* An active chemical, secreted by the adrenal medulla and a powerful cardiovascular stimulant (increased blood pressure and cardiac output).

epithelium, n. *Anat.* The cellular covering layer of the skin and mucous membranes.

equilibrium, n. *Phys.* State of balance; a condition in which opposing forces exactly counter each other. See *Donnan equilibrium*.

**ergon*, n. *Elec.* Nonionic molecule. Symbol ⁎△ – *ergonic*, adj.

**ergonar*, n. *Elec.* Collection of ergons, $n \times$ ⁎△

**ergionar*, n. *Elec.* Collection of ionic and nonionic molecules. – *ergionic*, adj.

erythema, n. *Med.* Redness of the skin, caused by dilated and congested capillaries.

erythrocyte, n. *Anat.* Red blood corpuscle. Its characteristic molecule is haemoglobin, which has a marked affinity for oxygen. Its characteristic function is to circulate oxygen to all parts of the body.

exergonic, adj. *Chem.* Referring to a reaction which releases energy.

exoendothelial space, n. *Anat.* The minute space between the periphery of an endothelial cell and its basement membrane.

exogenous, adj. *Biol.* Produced outside the organism.

extravasation, n. *Med.* Passage of material, e.g., blood, from a vessel into surrounding tissue.

extravascular, adj. *Anat.* Outside a vessel or vessels.

fascia, n. (*-ae*, pl.) *Anat.* A sheet or band of connective tissue enclosing a tissue or tissues.

femoral, adj. *Anat.* Of or pertaining to the femur.

femur, n. *Anat.* Thighbone; the bone of the upper leg. The proximal end of the femur contains a ball-shaped head, joined by a somewhat narrow neck to the main shaft of the bone. Distal to the neck of the femur are two bony projections, called the greater and lesser trochanters, to which muscles from the trunk and pelvis attach.

fibrillation, n. *Med.* Spontaneous contraction of individual muscle fibres, without unified control through a motor nerve.

fibrin, n. *Chem.* A protein essential in blood clotting.

fribroadenoma, n. *Med.* A benign neoplasm common in the female breast, containing glandular and scar-like elements.

fibroadenosis, n. *Med.* A benign nodular condition of the breast, containing fibrous and glandlike elements.

fibroblast, n. *Anat.* A cellular structure in connective tissues.

fibroliposarcoma, n. *Med.* A malignant neoplasm of connective tissue origin containing fibrous and fatty elements.

fibrosis, n. *Med.* Scar tissue.

fluoroscopy, n. *Radiol.* Continuous radiologic imaging on a fluorescent screen. When two perpendicular x-ray beams are employed, fluoroscopy is referred to as biplane. – *fluoroscopic*, adj.

fundus, n. *Anat.* The part opposite the aperture of a hollow organ.

galvanic, adj. *Elec.* Pertaining to direct electric current.

gangrene, n. *Med.* Extensive necrosis of tissue. Dry gangrene follows occlusion of the artery supplying a tissue.

gastric, adj. *Anat.* Pertaining to the stomach.

Gibbs free energy, n. *Phys.* An important thermodynamic concept defined for a chemical reaction G=H-TS, where H=enthalpy, T=temperature (K) and S=entropy.

glucagon, n. *Chem.* A pancreatic polypeptide which acts on the liver to increase the concentration of glucose in the blood.

gram-negative, adj. *Med.* Losing stain in Gram's method of preparation of bacteria for microscopic analysis.

granulation tissue, n. *Med.* Vascularized connective tissue formed early in the course of wound healing.

granulocyte, n. *Med.* A cell containing granules, especially a leukocyte.

granuloma, n. *Med.* A mass of connective tissue formed as part of a healing process, e.g., in tuberculosis.

guide wire, n. *Radiol.* A metal wire temporarily placed inside an angiographic catheter, used to assist in guiding the catheter into specific vessels.

haem, n. *Chem.* The insoluble, nonprotein, ferroprotoporphyrin constituent of haemoglobin.

haematocrit, n. *Med.* The ratio of the volume of red cells to the total volume of a sample of blood.

haematoma, n. *Med.* An abnormal collection of extravascular blood.

haematin, n. *Chem.* The insoluble, nonprotein, iron-containing constituent of haemoglobin. The iron has been oxidized to the ferric state.

haemin, n. *Chem.* The crystalline chloride form of haematin.

haemoglobin, n. *Chem.* The oxygen-carrying red pigment in red blood cells.

haemoptysis, n. *Med.* Expectoration of blood from the lungs.

haemostat, n. *Med.* A surgical instrument for clamping a vessel so that blood flow is arrested.

hamartoma, n. *Med.* A noncancerous mass composed of disorganized elements of the tissue in which the mass arises. In the lung the mass is characteristically peripheral, well circumscribed and slightly lobulated.

hemicrania, n. *Med.* Migraine headache.

heparin, n. *Chem.* An anticoagulant, mucopolysaccharide acid which occurs in various tissues but is most abundant in the liver.

hepatic, adj. *Anat.* Referring to the liver.

hilum, n. *Anat.* That part of an organ in which the channels to it enter. Usually used in reference to the lung, kidney or spleen. – *hilar*, adj.

histamine, n. *Chem.* A potent capillary dilator found in many tissues.

histiocyte, n. *Med.* Phagocytic interstitial cell.

histochemistry, n. *Chem.* The cytologic study of biochemical substances. – *histochemical*, adj.

histology, n. *Anat.* Anatomy of tissue, particularly minute structure as revealed by microscopic analysis. – *histologic*, adj.

homeostasis, n. *Biol.* A tendency to uniformity and stability in an organism, resulting from biologic adjustments to changes in the environment.

hyalin, n. *Med.* A translucent dystrophic protein.

hyaline, adj. *Med.* Transparent or nearly transparent; glassy. – *hyalinization*, n.

hydrion, n. *Chem.* Hydrogen ion.

hydrolase, n. *Chem.* Hydrolytic enzyme.

hydrolysis, n. *Chem.* Chemical splitting caused by incorporation of water, which also splits. – *hydrolytic*, adj.

hydropenic, adj. *Phys.* Deficient in content of water.

hydrophilic, adj. *Phys.* Readily adsorbing water.

hydrophobic, adj. *Phys.* Rejecting the adsorption of water.

hydropic, adj. *Phys.* Excessive in content of water.

hydrostatic, adj. *Phys.* Pertaining to a liquid in a state of equilibrium.

hypernephroma, n. *Med.* Carcinoma of the kidney.

hypoxia, n. *Med.* Low oxygen content. – *hypoxic*, adj.

image intensifier, n. *Radiol.* Electronic device which amplifies a fluoroscopic image approximately 4 000 times and permits immediate viewing of the image without needing to darken the fluoroscopic room.

implant *Med.* 1. v. To insert a material into the body. 2. n. Material inserted into the body.

inert, adj. *Phys.* Without active properties.

inferior, adj. *Anat.* Lower; situated or directed below.

inferior vena cava, n. *Anat.* The large vein into which venous blood from the lower extremities, pelvis and abdomen flows; it empties into the right atrium of the heart.

**infiltrated strands*, n. pl. *Radiol.* Coarse radiating structures in relation to a pulmonary mass in

emphysematous or fibrotic lung. The shapes and directions of the structures are at least partly determined by the local extension of emphysema or fibrosis. See also *lamellae*.

injury potential, n. *Elec*. A specific *demand potential* based on dominating catabolic liberation of energy for exchange of ions and transformation of material within BCEC in the process of healing.

in situ. *L*. In its original or natural position.

intercostal, adj. *Anat*. Between ribs.

interstitial, adj. *Anat*. In general, pertaining to or situated in the interstices of a tissue, i.e., extracellular. In the lung, pertaining to or situated in the compartment of loose connective tissues which contains the conducting airways, blood vessels, lymphatics and nerves, and which does not exchange gas.

intima, n. *Anat*. The innermost lining of a blood vessel. – *intimal*, adj.

in vitro *L*. In glass; not in living organism.

in vivo *L*. In a living organism.

**ionar*, n. *Elec*. Collection of ions. $n \times \triangle$. *Unit:* ion. Symbol $\triangle$.

iontophoresis, n. *Med*. Therapeutic introduction into the body of ions of soluble salts, by means of electric current. – *iontophoretic*, adj.

ipsilateral, adj. *Anat*. On the same side, with reference to the midline.

ischaemia, n. *Med*. Local and temporary deficiency of blood, usually secondary to transient arterial narrowing. – *ischaemic*, adj.

isoelectric, adj. *Elec*. Possessing the same electric potential.

juxtatumoural, adj. *Med*. Situated near or next to a tumour.

karyolysis, n. *Med*. Dissolution of the nucleus of a cell.

lake, v. To lose haemoglobin out of erythrocytes.

**lamella*, n. sing. (*-ae*, pl.) *Radiol*. Coarse, asymmetrical, dense, linear or bandlike structure adjacent to a mass, which is partly collapsed by local necrosis.

laparotomy, n. *Med*. Surgical incision and exploration of the abdomen.

lateral, adj. *Anat*. 1. Pertaining to a side. 2. Situated nearer or directed toward a side; far to the side from the median plane. *Radiol*. 3. Pertaining to a radiographic exposure in which the central beam enters a side of the subject and exits the other side, i.e., an exposure which is perpendicular to frontal or posteroanterior projections. – *laterally*, adv.

leukocyte, n. *Anat*. White blood corpuscle. The most mobile cells of defense, leukocytes exit from the blood stream to help initiate healing at sites of injury or abnormality. The VICC appear to be part of the mechanism of this process.

lingula, n. *Anat*. The anterior and inferior part of the left upper lobe of the lung, so named because of its resemblance to the shape of a tongue.

lipiodol, n. *Radiol*. An iodized oil used as an opaque contrast medium.

liquefaction, n. *Biol*. To change into liquid.

liquid junction potential, n. *Elec*. Potential difference in a liquid arising from differences in speed of diffusion of ions.

lumen, n. (*lumina*, pl.) *Anat*. The channel or passage-way of a tube.

lymphatic channels or *vessels*, n. pl. *Anat*. The network of thin-walled channels through which excess extracellular fluid and proteins are removed from most sites of the body and returned as lymph to reenter the circulating plasma of blood. Cancers commonly spread through lymphatic channels.

lymphocyte, n. *Anat*. A type of white blood cell involved in immune reactions.

lymphoedema, n. *Med*. Swelling of a tissue by excess lymph.

lymphoma, n. *Med*. A cancer of the lymphatic system, usually arising in a lymph node or nodes.

lysis, n. *Med*. Destruction, often of cells or cellular components. – *lytic*, adj.

lysosome, n. *Biol*. A very small, intracytoplasmic body containing lytic enzymes, usually hydrolytic.

macrophage, n. *Anat*. A mononuclear phagocyte which has no fixed position within a tissue.

macroscopic, adj. *Phys*. Visible with the unaided eye.

malignant, adj. *Med*. 1. Tending to lead to death. 2. Cancerous. – *malignancy*, n.

mammogram, n. *Radiol*. Developed radiographs showing results of mammography.

mammography, n. *Radiol*. Radiographic examination of the breast. – *mammographic*, adj.

margination, n. *Med*. Adherance of leukocytes to endothelium, as an early stage in acute inflammation.

mastectomy, n. *Med*. Surgical removal of a breast.

mastitis, n. *Med*. Inflammation of a breast.

matrix, n. *Biol*. Enveloping material which gives form to its contents.

media, n. *Anat*. The middle of the three layers of an arterial wall.

medial, adj. *Anat*. Situated toward the midline. – *medially*, adv.

mediastinum, n. *Anat*. The tissues in the middle of the thorax between the medial surfaces of each pleural cavity. – *mediastinal*, adj.

medium (contrast), n. (*-ia*, pl.) — *Radiol.* Material of radiopacity differing from that of the structure in which it is placed for diagnostic purposes, e.g., injection of a radiopaque contrast medium into a blood vessel opacifies the lumen of the vessel.

medullary, adj. — *Med.* Pertaining to a carcinoma of the breast in which carcinomatous cells predominate and secondarily induced fibrosis is minimal; opposite of scirrhous carcinoma, around which fibrosis is extensive. On clinical examination a medullary carcinoma is soft and circumscribed, a scirrhous carcinoma firm and poorly marginated.

melanoma, n. — *Med.* Epithelial cancer characterized by pigment-containing cells.

mesenchyme, n. — *Biol.* Embryonic connective tissue from which the body's connective tissues, blood vessels and lymphatic system form. – *mesenchymal*, adj.

mesentery, n. — *Anat.* The membranes around the intestine, attaching it to the posterior abdominal wall.

metabolism, n. — *Chem.* The physicochemical processes of living cells. – *metabolic*, adj.

metastasis, n. — *Med.* Spread of disease, usually cancer, from the originating to a distant tissue. – *metastatic*, adj.

microcalcification, n. — *Radiol.* Punctate calcifications in cancers of the breast.

mitochondria, n. — *Anat.* Intracytoplasmic small structures which oxidize sugars and other nutrients, thereby providing energy for various intracellular functions.

mitogenic, adj. — *Chem.* Inducing mitosis.

mole, n. — *Chem.* A mass equal to the molecular weight of the species in grams; contains Avogadro's number of molecules.

monocyte, n. — *Anat.* A large mononuclear leukocyte.

morbidity, n. — *Med.* The condition of being diseased.

morphogenesis, n. — *Biol.* The development of structure. – *morphogenetic*, adj.

morphology, n. — *Biol.* The science of organic structure. – *morphologic*, adj.

mucous membrane, n. — *Anat.* The membrane lining the channels of the body which communicate with external air, e.g., the mouth.

mycetoma, n. — *Med.* A fungal tumour.

myo-, prefix. — *Anat.* Referring to muscle.

myocardium, n. — *Anat.* The muscle of the heart. – *myocardial*, adj.

myoglobin, n. — *Chem.* A haem-globin molecule in muscle. Its affinity for oxygen exceeds that of haemoglobin.

myosarcoma, n. — *Med.* A sarcoma of muscular origin.

necropsy, n. — *Med.* A postmortem anatomic examination; autopsy.

necrosis, n. — *Med.* Death of tissue. – *necrotic*, adj. – *necrotizing*, adj.

neoplasm, n. — *Med.* An abnormal new growth, which may be benign or malignant. – *neoplastic*, adj.

neovascularity, n. — *Anat.* The state or process of developing new blood vessels.

neurilemmoma, n. — *Med.* A neoplasm originating in the sheath of a peripheral nerve.

neuron, n. — *Anat.* Nerve cell.

Nitella, n. — *Biol.* An elongated, unicellular alga commonly found in fresh water.

nodule, n. — *Radiol.* A discrete unit of abnormal tissue, usually round and less than about 3 cm in diameter. – *nodular*, adj.

oat cell carcinoma, n. — *Med.* A type of primary carcinoma of the lung, characterized microscopically by small cells shaped like oats.

oblique, adj. — *Anat.* 1. Inclined. *Radiol.* 2. Referring to an x-ray beam which enters the body in a direction other than perpendicular to the front, back or side. The aspect of the subject adjacent to the part of the radiographic system which records the image determines the name of the oblique projection, e.g., "left anterior oblique projection" means the left anterolateral aspect of the subject is adjacent to the recording apparatus.

oedema, n. — *Med.* Accumulation of excess serous fluid in intercellular tissue spaces. – *oedematous*, adj.

oestrogen, n. — *Chem.* The group of chemical substances, normally produced by the ovaries, which cause the menstrual cycle and female secondary sexual characteristics, e.g., distribution of subcutaneous adipose tissue. – *oestrogenic*, adj.

omentum, n. — *Anat.* Portions of the peritoneum connecting the stomach to adjacent organs.

orthostatic, adj. — *Med.* Referring to or caused by the erect position.

osmosis, n. — *Phys.* Diffusion through a semipermeable membrane, tending to equalize concentrations of solvents on each side of the membrane.

osteosarcoma, n. — *Med.* A primary cancer of bone.

ovary, n. — *Anat.* The paired, ova-containing, female sexual gland.

overpotential, n. — *Elec.* The change of potential difference necessary to cause a net current to pass between electrodes in a solution.

palpate, v. — *Med.* To examine by touch. – *palpable*, adj.

parathyroid, n. — *Anat.* Any one of four small glands located near the thyroid and which produce hormones that regulate metabolism of calcium and phosphorus.

parenchyma, n. — *Anat.* The functional and structural elements characteristic of an organ, as opposed to its framework, or stroma.

pathognomonic, adj. *Med.* Characteristic of a specific disease or pathologic condition; diagnostic.

percutaneous, adj. *Med.* Through the skin. – *percutaneously*, adv.

perfusion, n. *Med.* The act of spreading over or through something, as blood through an organ's blood vessels.

pericyte, n. *Anat.* A cell found along capillaries. It has long processes and is believed to be involved in contraction.

perifocal, adj. *Radiol.* Around a central site.

periodontitis, n. *Med.* Inflammation of tissues around a tooth.

periodontosis, n. *Med.* Degeneration of tissues around a tooth.

peritoneum, n. *Anat.* The transparent membrane which lines the abdominal cavity and encloses the digestive viscera. – *peritoneal*, adj.

peritumoural, adj. *Med.* Around a tumour.

perspex, n. A translucent, radiolucent, plastic material.

phagocyte, n. *Biol.* A cell which ingests microorganisms, other foreign particles and organic debris.

phagocytosis, n. *Biol.* The engulfing by phagocytes of microorganisms, foreign particles, cells and cellular debris.

phrenic, adj. *Anat.* Of or pertaining to the diaphragm.

physiologic saline solution, n. *Chem.* An isotonic solution of sodium chloride in purified water (0.9 per cent).

piezoelectricity, n. *Elec.* Pressure-electricity, especially as produced in crystalline substances such as quartz.

pinocytosis, n. *Elec.* Transport of fluids across endothelial cells by tiny vesicles. – *pinocytotic*, adj.

plasma, n. *Anat.* The noncellular fluid portion of blood or lymph.

pleomorphic, adj. *Anat.* Containing different forms, e.g., a carcinoma characterized histologically by both squamous and adenomatous features.

pleura, n. (*-ae*, pl.) *Anat.* The membrane which lines the inside of the thorax (parietal pleura) and surface of the lungs (visceral pleura), completely enclosing a normally small and fluid-filled space called the pleural cavity.

pneumonectomy, n. *Med.* Surgical removal of a lung.

pneumothorax, n. *Med.* Air or other gas in the pleural cavity.

posterior, adj. *Anat.* Pertaining to the backside. Opposite of anterior.

posteroanterior, adj. *Radiol.* Pertaining to an x-ray beam which enters the backside and exits through the front of a subject.

posterolateral, adj. *Anat.* Posterior and lateral.

postmortem, adj., adv. *Biol.* After death.

protamine, n. *Chem.* A strongly basic protein which neutralizes the effects of heparin.

proteolytic, adj. *Med.* Causing breakdown of proteins.

proximal, adj. *Anat.* Near the site of attachment. Opposite of distal.

pyknosis, n. *Anat.* Shrinking and condensation of the nucleus of a cell.

pylorus, n. *Anat.* The opening between stomach and duodenum.

radiolucent, adj. *Radiol.* 1. Permitting the passage of x-rays. 2. Permitting the passage of many, but not all, incident x-rays. 3. Appearing predominantly black on a standard radiograph. – *radiolucency*, n.

radiopaque, adj. *Radiol.* 1. Not permitting the passage of x-rays. 2. Appearing predominantly white on a standard radiograph. – *radiopacity*, n.

reticulum, n. *Anat.* A network, especially in the cytoplasm of cells. – *reticular*, adj.

**retraction oedema*, n. *Radiol.* Fluid accumulation within a zone of lowered turgor pressure due to retracting scar tissue.

**retraction pocket*, n. *Radiol.* Funnel-shaped indentation of the surface of the lung, produced by contraction of fibrous strands in the lung parenchyma.

retro-, prefix. *Anat.* Located posterior to.

Ringer's solution, n. *Chem.* A solution resembling blood serum in its constituent salts.

saline solution, 0.9%, n. *Chem.* The "physiologic" concentration of sodium chloride in normal mammalian plasma and extracellular, extravascular tissues.

sarcoma, n. *Med.* A cancer, usually highly malignant, of connective tissue origin.

scirrhous, adj. *Med.* Hard; containing a predominance of scar or connective tissue. See *medullary*.

sclerosing, adj. *Med.* 1. Causing or undergoing hardening. 2. Increasing in quantity of scar or connective tissue.

segment, n. *Anat.* A major anatomic subdivision. In the lungs, each lobe is supplied by a single bronchus; the next bronchial divisions define the bronchopulmonary segments, which number between 2 and 5 per lobe.

Seldinger technique, n. *Med.* Percutaneous insertion of a catheter in the lumen of a vessel by a 5-stage procedure: a needle is placed into the lumen of the vessel, a wire is passed through the needle into the lumen, the needle is removed, a catheter is placed over the wire into the lumen, and the wire is removed.

semolina, n. *Biol.* The large hard parts of wheat grains which remain in the sifting of fine flour. The grains are grossly visible, dielectric corpuscles.

serotonin, n. *Chem.* 5-hydroxytryptamine, a potent regulator of local vascular calibre.

serum, n. *Biol.* The clear portion of an animal liquid, especially of blood after coagulation occurs.

shellac, n. *Chem.* An insulating resin, applied to a surface as a thin liquid layer which then solidifies.

silicosis, n. *Med.* Pulmonary fibrosis caused by inhalation of dust containing silicon dioxide; usually a disease of stone miners, sandblasters and foundry workers.

skin thickening, n. *Radiol.* Radiopaque part of the skin adjacent to a breast cancer. Such thickening of skin is pathogenetically synonymous with a hydropic zone in the lung (see also "*B*" *zone*).

spiculated, adj. *Radiol.* Characterized by pointed projections.

spicule, n. *Anat.* A needle-like projection.

spirochaete, n. *Med.* A spiral-shaped bacterium, including those causing syphilis.

squamous, adj. *Anat.* Flat, platelike. Squamous epithelial cells form the lining of the lumina of the tracheobronchial tree.

stasis, n. *Med.* A stopping of normal flow of a bodily fluid.

stellate, n. Shaped like a star.

stereoradiography, n. *Radiol.* Radiography performed from two sites equidistant from the object and separated by the interpupillary distance. When the resultant radiographs are observed in a stereoscopic viewer, the images fuse and appear three-dimensional.

stereotaxic, adj. *Radiol.* Movement of an instrument, e.g., biopsy needle, under stereoradiographic control.

steric, adj. *Phys.* Referring to spacial distribution.

stoma, n. (*stomata*, pl.) *Anat.* A minute opening or pore on a cellular surface or between cells.

striae, n., pl. *Med.* 1. Lines. 2. Narrow, bandlike structures. – *striated*, adj.

stroma, n. *Anat.* The supporting framework of an organ, as opposed to its parenchyma. – *stromal*, adj.

subcutaneous, adj. *Anat.* Beneath the skin.

subcutis, n. *Anat.* Tissue immediately beneath the skin.

sulcus, n. *Anat.* Groove, furrow; e.g., the costophrenic sulcus is the groove between the chest wall and insertions of the domed diaphragm, posteriorly defining the most inferior positions of the lungs.

superior, adj. *Anat.* Elevated; higher, upper; toward the head as opposed to toward the feet. – *superiorly*, adv.

superolateral, adj. *Anat.* Situated or directed both superiorly and laterally.

supradiaphragmatic, adj. *Anat.* Situated immediately superior to the diaphragm.

systemic, adj. *Med.* 1. Pertaining to the body as a whole. 2. Pertaining to circulation of blood from the left ventricle to the entire body and returning to the right atrium, as opposed to the pulmonary circulation of blood between the right ventricle and left atrium.

teratocarcinoma, n. *Med.* A neoplasm containing both teratomatous and carcinomatous components.

teratoma, n. *Med.* A neoplasm containing various differentiated structures such as bone, cartilage, skin, and brain.

thoracotomy, n. *Med.* Surgical incision of the thoracic cage.

thrombectomy, n. *Med.* Surgical removal of a thrombus.

thrombocyte, n. *Anat.* Platelet; important for coagulation, one of many minute anuclear bodies in blood.

thromboembolus, n. (*-i*, pl.) *Med.* A blood clot which detaches from its site of formation and is carried by the flow of blood to a distant site, usually obstructing flow through the blood vessel at that site.

thrombose, v. *Med.* To form a thrombus; to clot.

thrombosis, n. (*-es*, pl.) *Med.* Formation or presence of a thrombus.

thrombus, n. (*-i*, pl.) *Med.* Intravascular clot of coagulated blood which remains at the site of formation.

thymoma, n. *Med.* Epithelial neoplasm of the thymus.

tomogram, n. *Radiol.* A radiograph of a layer of the body.

tomography, n. *Radiol.* A radiographic technique imaging a plane of the body. – *tomographic*, adj.

trabeculae, n. pl. *Anat.* Beams of connective tissue. In bone, the mineralized matrix of the marrow.

transmogrify, v. To transform into something grotesque or surprising.

transthoracic, adj. *Med.* Through the chest wall.

trochanter, n. *Anat.* See *femur*.

tuberculoma, n. *Med.* A tuberculous mass, approximately spherical and well demarcated from surrounding tissue.

unilateral, adj. *Anat.* On one side.

vasa vasorum, n. pl. *Anat.* The small vessels which supply the walls of larger blood vessels.

vascularized, adj. *Anat.* Supplied with vessels. – *vascularization*, n.

vasoconstriction, n. *Med.* Narrowing of vessels secondary to contraction of muscle in their walls.

**venocapillaries*, n. *Anat.* Distal part of the capillary bed, which dilates when exposed to an electric field. See also *arteriocapillaries*.

venule, n. *Anat.* A very small vein, just distal to a capillary.

vesicle, n. *Anat.* A minute, intracytoplasmic, spherical collection of fluid.

viscus, n. (*viscera*, pl.) *Anat.* Any organ in the chest, abdomen or pelvis. See also *pleura*. – *visceral*, adj.

xeroradiograph, n. *Radiol.* A radiograph obtained by a process in which x-rays affect not a photographic film, but an aluminium plate coated with selenium.

zeta potential, n. *Phys.* Electrostatic potential corresponding to the potential drop across the diffuse part of the electric double layer close to a charged interface.

SYMBOLS AND UNITS

Symbol	*Name*	*SI-unit*
Å	Ångström	10^{-10} m
°C	degree Celsius	273.15 K
C	coulomb	1C=1As
$cal_{thermochem}$	thermochemical calorie	4.184 J
D_{co_2}	diffusion coefficient of CO_2	0.16×10^{-4} m^2s^{-1}
D_{o_2}	diffusion coefficient of O_2	0.20×10^{-4} m^2s^{-1}
D_w	diffusion coefficient of water vapor	0.25×10^{-4} m^2s^{-1}
dyn	dyne	10^{-5} N
dyn·cm	dyne×centimetre	10^{-7} J
eV	electron volt	1.602×10^{-19} J
erg	erg	10^{-7} J
F	farad	$1F=1CV^{-1}$
F	Faraday	9.6487×10^{4} $Cmol^{-1}$
G	Gibbs' free energy	
ΔG	Gibbs' free energy change	
ΔG°	Gibbs' standard free energy change	
ΔG°′	Maximal Gibbs' standard free energy change	
H_{sub}	heat of sublimation of water	2.845 Jkg^{-1} at −10°C 2.833 Jkg^{-1} at −5°C 2.824 Jkg^{-1} at 0°C

Symbol	*Name*	*SI-unit*
H_{vap}	heat of vaporization of water	2.490 Jkg^{-1} at 0°C 2.469 Jkg^{-1} at 10°C 2.348 Jkg^{-1} at 20°C 2.435 Jkg^{-1} at 25°C 2.427 Jkg^{-1} at 30°C 2.402 Jkg^{-1} at 40°C 2.377 Jkg^{-1} at 50°C 2.155 Jkg^{-1} at 100°C
Hz	hertz	1Hz=1 cycle s^{-1}
J	joule	1J=1Nm
K	kelvin	0K=−273.15°C
μm	micron	10^{-6} m
N	newton	1N=1kg m s^{-2}
N_A	Avogadro constant	6.0222×10^{-23} m^{-1}
Pa	pascal	1Pa=1Nm^{-2}= 0.102 mmH_2O
R	gas constant	8.3143 $Jm^{-1}K^{-1}$
$\bar{V}_w$	partial molal of water	18.048×10^{-6} m^3mol^{-1} at 20°C
W	watt	$1W=1Js^{-1}$
ϱ_w	density of water	0.9999×10^{-3} kgm^{-3} at 0°C 1.0000×10^{-3} kgm^{-3} at 4°C 0.9997×10^{-3} kgm^{-3} at 10°C 0.9982×10^{-3} kgm^{-3} at 20°C 0.9957×10^{-3} kgm^{-3} at 30°C 0.9923×10^{-3} kgm^{-3} at 40°C
σ	Stefan-Boltzmann constant	5.6696×10^{-8} $Vm^{-2}K^{-4}$
⚠	ion	
*⚠	ergon	

ABBREVIATIONS

A	adenine
ACP	acyl carrier protein
ACTH	adrenocorticotropic hormone
ADP	adenosine diphosphate
Ala	alanine
AMP	adenosine monophosphate
cAMP	cyclic AMP adenosine 3′, 5′-cyclic monophosphate
Arg	arginine
Asn	asparagine
Asp	aspartate
ATP	adenosine triphosphate
ATPase	adenosine triphosphatase
BCEC	*biologically closed electric circuits
CDP	cytidine diphosphate
CMP	cytidine monophosphate
CoA	coenzyme A
CoQ	coenzyme Q (ubiquinone)
CTP	cytidine triphosphate
Cys	cysteine
DNA	deoxyribonucleic acid
DNP	dinitrophenyl
DPN^+	see NAD, NAD^+
DPNH	see NADH
ecg	electrocardiogram
FAD	flavin adenine dinucleotide (oxidized form)
$FADH_2$	reduced form of flavin adenine dinucleotide
FMN	flavin mononucleotide (oxidized form)
$FMNH_2$	flavin mononucleotide (reduced form)
G	guanine
GDP	guanosine diphosphate
Gln	glutamine
Glu	glutamate
Gly	glycine
GMP	guanosine monophosphate
GTP	guanosine triphosphate
Hb	haemoglobin
HbCO	carbon monoxide haemoglobin
HbO_2	oxyhaemoglobin
His	histidine
Ile	isoleucine
i.m.	intramuscular
j	subscript for species *j*
Leu	leucine
Lys	lysine
M	molar (moles/litre)
Mb	myoglobin
MbO_2	oxymyoglobin
Met	methionine
MetHb	methaemoglobin
NAD, NAD^+	nicotinamide adenine dinucleotide (oxidized form)
NADH	nicotinamide adenine dinucleotide (reduced form)
$NADH_2$	reduced form of nicotinamide adenine dinucleotide
NADP, $NADP^+$	nicotinamide adenine dinucleotide phosphate (oxidized form)
NADPH	nicotinamide adenine dinucleotide phosphate (reduced form)
$NADPH_2$	reduced form of nicotinamide adenine dinucleotide phosphate
NHE	normal hydrogen electrode
Phe	phenylalanine
Pro	proline
redox	reduction and oxidation
RNA	ribonucleic acid
mRNA	messenger RNA
rRNA	ribosomal RNA
tRNA	transfer RNA
RNase	ribonuclease
TAF	"tumour-angiogenetic factor"
Val	valine
VDCEC	*vascular-ductal closed electric circuit.
VICC	*vascular-interstitial closed circuit or circuits
w	subscript for water

INDEX

F

G

H

I